PART II

GAUGE FIELDS IN SUPERFLUID HELIUM

Illa quidem debent e levibus atque rutundis
esse magis, fluvido quae corpore liquida constant.
Namque papaveris haustus item facilis quod aquarum;
nec retinentur enim inter se glomeramina quaeque
et perculsus item proclive volubilis exstat.

(But things that liquid and of fluid substance
Must consist rather of smooth round atoms,
For several globules do not hold together.
And you may scoop up poppy seeds as easily
As water, which will also, if you spill it,
Glide away with as ready a downward flow.)

Lucretius, *De Rerum Natura*, Rome, 57 B.C.

SUPERFLUIDITY

The simplest physical system for which a gauge theory of stresses and defects can be developed is superfluid ^{4}He. It possesses precisely the properties described in the Introduction: there exists an ordered ground state at zero temperature. Small disturbances introduce soft long-range excitations which are observable as sound waves. Stronger disturbances, for instance, the rotation of the container of the superfluid, lead to the formation of vortex lines which may be viewed as line-like defects. Moreover there exists a critical temperature at which a phase transition takes place leading to the disappearance of the superfluid state.

The purpose of this second part is to demonstrate that superfluid phase transition may be understood as an infinite growth and proliferation of vortex lines. We will start with a brief résumé of the well-known properties of this system.

1.1. BASIC PROPERTIES

Liquid ^{4}He is an exceptional liquid. It does not become solid when cooled down to absolute zero temperature at atmospheric pressure. Instead, at a temperature $T_c = 2.18$ K, called the λ point, it undergoes a second-order phase transition below which it becomes superfluid (see Fig. 1.1 for the phase diagram). This was first discovered experimentally by Kapitza

in 1937, who observed that the liquid can run through narrow capillaries without friction.

Soon afterwards Landau gave the first explanation of this phenomenon. He observed that due to the low atomic mass, the de Broglie wavelength corresponding to the thermal motion

$$\lambda = 2\pi\hbar(2Mk_B T)^{-1/2}$$

becomes, at T_c,

$$\lambda \sim 2\pi \times 1.05 \times 10^{-27}\,\text{erg sec} \times \left[8 \times 1.68 \times 10^{-24}\,\text{gm} \right.$$

$$\left. \times 1.4 \times 10^{-16}\frac{\text{erg}}{\text{K}} \times 2.18\,\text{K} \right]^{-1/2}$$

$$\sim 10\,\text{Å}. \tag{1.1}$$

Since the density is $\rho_0 \sim 0.145\,\text{g/cm}^3$, the average spacing of the atoms is

$$a = \sqrt[3]{\frac{M}{\rho_0}} = \sqrt[3]{\frac{4 \times 1.68 \times 10^{-24}\,\text{g}}{0.145\,\text{g/cm}^3}} \sim 3.59\,\text{Å}. \tag{1.2}$$

Hence, at T_c, several atoms lie within each other's de Broglie wave-
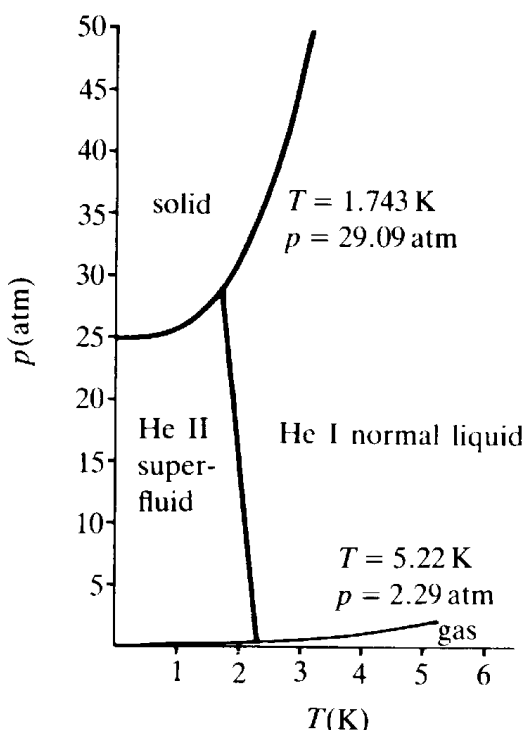
FIG. 1.1   Phase diagram of ^{4}He. At atmospheric pressure, ^{4}He remains liquid down to zero temperature.

length. This gives them the possibility of acting as a coherent quantum state, called a Bose condensate.

Such a condensate can form even in a free Bose gas. There, the chemical potential is determined from the density via $[\varepsilon \equiv \mathbf{p}^2/(2M)]$

$$\rho_0 = \frac{M}{V} \sum_{\mathbf{p}} \frac{1}{e^{-(\mathbf{p}^2/2M - \mu)/k_B T} - 1} \approx \frac{M^{5/2}}{\sqrt{2}\,\pi^2\hbar^3} \int_0^\infty \frac{d\varepsilon\,\sqrt{\varepsilon}}{e^{(\varepsilon-\mu)/k_B T} - 1}. \qquad (1.3)$$

This equation has a solution only for $\mu < 0$. But on lowering the temperature, μ approaches zero from below and hits it at a critical temperature T_c given by[a]

$$\rho_0 = \frac{M}{4\pi^2\hbar^3}(2Mk_B T)^{3/2} \int_0^\infty \frac{dz\,\sqrt{z}}{e^z - 1} = 2\pi M\frac{1}{\lambda^3} \cdot 2.3148. \qquad (1.4)$$

This equation tells us that in a free Bose gas, condensation occurs if the de Broglie wavelength λ exceeds $\lambda_c \approx 2.44$ times the atomic spacing a.

The critical temperature is

$$T_c = \frac{2\pi^2\hbar^2}{k_B M\lambda_c^2} = 3.31\frac{\hbar^2}{Ma^2}\frac{1}{k_B}. \qquad (1.5a)$$

Thus, if ^{4}He were a non-interacting gas, it would condense at

$$T_c \sim 3.07\,\text{K}. \qquad (1.5b)$$

Due to the strong atomic repulsion, however, the transition is shifted down to 2.18 K. Below T_c, the chemical potential μ of the free Bose gas vanishes identically and Eq. (1.4) gives a density

$$\rho_n = \rho_0(T/T_c)^{3/2}. \qquad (1.6a)$$

This is smaller than the total density ρ_0 of ^{4}He atoms. Thus, a number of atoms have disappeared from the integral, namely, those corresponding to

---

[a]The integral is evaluated using the formula $\int_0^\infty \frac{dx}{x}x^\mu\frac{1}{e^x \mp 1} = \Gamma(\mu)\zeta(\mu)\left\{\begin{array}{c}1\\1-2^{1-\mu}\end{array}\right\}$, where $\zeta(z)$ is Riemann's zeta-function $\equiv \sum_{n=1}^\infty n^{-z}$. For $\mu = 3/2$, $\Gamma(3/2)\zeta(3/2) = (\sqrt{\pi}/2)2.6120 = 2.3148$.

$$\rho_s \equiv \rho - \rho_n. \tag{1.6b}$$

It is easy to see how this has happened: Going back to the summation formula in momentum space in Eq. (1.3) we note that for $\mu = 0$, the particle occupation number diverges at $\mathbf{p} = 0$. Therefore, the standard replacement $\Sigma_{\mathbf{p}} \rightarrow V \int (d^3 p/(2\pi\hbar)^3) = (M^{3/2}/\sqrt{2}\pi^2\hbar^3) \int d\varepsilon$ is no longer applicable. Only if we go to a finite volume and treat the density of particles at zero momentum separately, is it the case. This is precisely the density ρ_s.

The particles in the zero momentum state are called the *Bose condensate*. In infinite volume, they can be excited very weakly and become the carriers of the superflow. Hence they are referred to as the *superfluid part* of the liquid. The $\mathbf{p} \neq 0$ particles form the *normal part*. The superfluid part of a free Bose gas is shown in Fig. 1.2 where it is compared with the experimental curve.

1.2. FIELD DESCRIPTION OF SUPERFLUID PHASE TRANSITION

In a weak coupling approximation, the phenomenon of superfluid phase transition can be studied within a second quantized boson field theory. This was done in 1961 by L.P. Pitaevskii, who tried to follow as far as possible the field theoretic description of another phenomenon, namely that of superconductivity. In the case of superconductivity, field theory had been highly successful. In 1950, Ginzburg and Landau proposed field equations which gave an excellent description of thermal and magnetic phenomena in superconductors. We shall come back to these later in this chapter when commenting on historical developments. In the present context, let us follow directly Pitaevskii's approach.

Approximating the short-range repulsion by a δ-function, the energy density of a field of ^{4}He atoms has the form
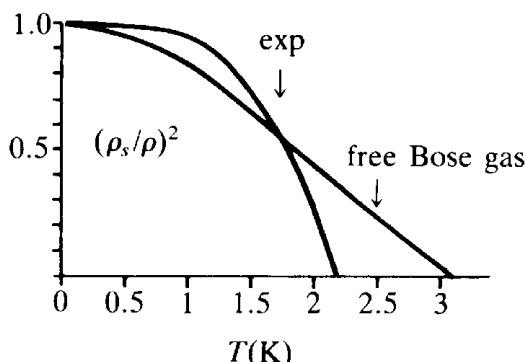

FIG. 1.2. The superfluid density ($=$ density of ^{4}He atoms in the free Bose gas condensate) in comparison with the experimental curve.

$$e(\mathbf{x}) = \frac{\hbar^2}{2M}|\nabla\psi|^2 - \mu|\psi|^2 + \frac{V}{2}|\psi|^4, \tag{1.7}$$

where the chemical potential μ vanishes close to T_c as

$$-\mu \sim \mu_0\left(\frac{T}{T_c} - 1\right). \tag{1.8}$$

This energy is appropriate only for the very low momentum particles which take part in the condensation process, i.e., those particles which form the superfluid phase of the liquid. A full description of the normal phase would require an accurate inclusion of the interatomic potential.

The partition function of the superfluid phase is

$$Z = e^{-F/T} = \int \mathscr{D}\psi\, \mathscr{D}\psi^\dagger\, e^{-(1/T)\int d^3x\, e(\mathbf{x})}. \tag{1.9}$$

The mean-field approximation consists in neglecting the fluctuations and identifying the extremum of the energy functional $E[\psi] \equiv \int d^3x\, e(\mathbf{x})$ with the free energy, i.e., the free energy is given by

$$F \approx E[\psi] = \int d^3x\, e(\mathbf{x}) \equiv \int d^3x\left[\frac{\hbar^2}{2M}|\nabla\psi|^2 - \mu|\psi|^2 + \frac{V}{2}|\psi|^4\right] \tag{1.10}$$

and this quantity is to be evaluated at the extremal value of the field configuration $\psi(\mathbf{x})$. For $T > T_c$, the extremum lies at $\psi \equiv 0$ so that the free energy vanishes identically. In the sense of Chapter 5, Part I, the free energy is then the effective energy of the ψ field theory.

The important property of the free energy is that due to the presence of the repulsive interaction, the path integral (1.9) is well defined also for temperatures below T_c. For these temperatures, the fluctuations around the field origin $\psi = 0$ destabilize. Nevertheless, the positive quartic energy term guarantees the convergence of the path integral. The fluctuations are, however, no longer centered about the field origin. The energy is now minimal at

$$\psi = |\psi_0|\, e^{i\gamma} = \sqrt{\frac{-\mu_0\left(\dfrac{T}{T_c} - 1\right)}{V}}\, e^{i\gamma}, \tag{1.11}$$

where γ is an arbitrary constant angle. At that minimum, the value of the free energy density is

$$f_c = -\frac{1}{2V}\mu_0^2\left(\frac{T}{T_c}-1\right)^2 \equiv -f_0\left(\frac{T}{T_c}-1\right)^2. \tag{1.12}$$

This value is called the *condensation energy density*.

Piecing this solution together with $f \equiv 0$ for $T < T_c$, we can calculate the densities of the *internal energy*

$$u = f - T\frac{\partial}{\partial T}f = \left\{ \begin{array}{c} 0 \\ -f_0\left[\left(\frac{T}{T_c}-1\right)^2 - 2\frac{T}{T_c}\left(\frac{T}{T_c}-1\right)\right] \end{array} \right\} \text{for} \left\{ \begin{array}{c} T > T_c, \\ T < T_c, \end{array} \right. \tag{1.13}$$

and of the *entropy*

$$s = -\frac{\partial f}{\partial T} = \left\{ \begin{array}{ll} 0 & T > T_c, \\ 2\frac{f_0}{T_c}\left(\frac{T}{T_c}-1\right) & T < T_c. \end{array} \right. \tag{1.14}$$

As a consequence, the *specific heat* exhibits a jump at T_c:

$$c = T\frac{\partial s}{\partial T} = \left\{ \begin{array}{ll} 0 & T > T_c, \\ 2\frac{f_0}{T_c}\frac{T}{T_c} & T < T_c, \end{array} \right. \tag{1.15}$$

reflecting a second order phase transition of the superfluid. The thermodynamic functions are plotted in Fig. 1.3 ($\beta_c \equiv 1/T_c$).


$$V = -\mu|\psi|^2 + \frac{V}{4}|\psi|^4$$
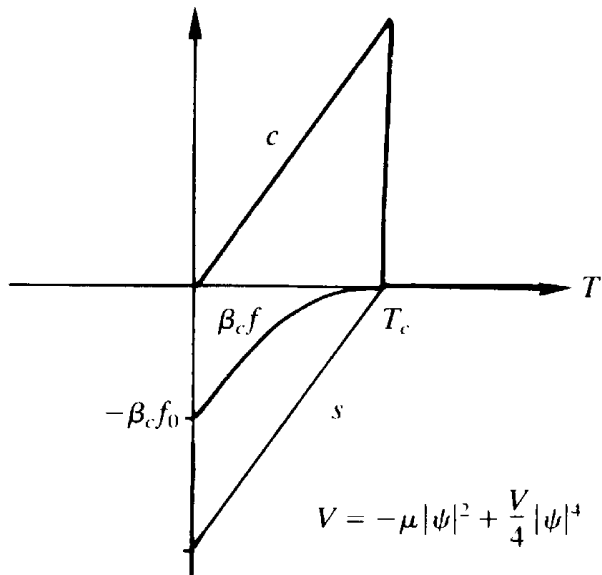
FIG. 1.3. The thermodynamic free *energy density* f, *entropy* s, and *specific heat* c within Pitaevskii's mean field description of superfluid ^{4}He.

When comparing the T dependence of the specific heat (1.15) as shown in Fig. 1.3 with that of the superfluid transition as shown in Fig. 1.4 (for completeness we have also plotted the results for the free Bose gas) we find bad agreement with experiment: while c of (1.15) behaves linearly below the phase transition temperature, the experimental curve diverges logarithmically at $T = T_c$. The discrepancy can be attributed to fluctuations. We see that these must be significant in order to produce such large modifications.

Superfluid ^{4}He has been studied with great accuracy both experimentally and theoretically. It has become one of the most accurate applications of both low temperature technology and ψ^4 field theory.
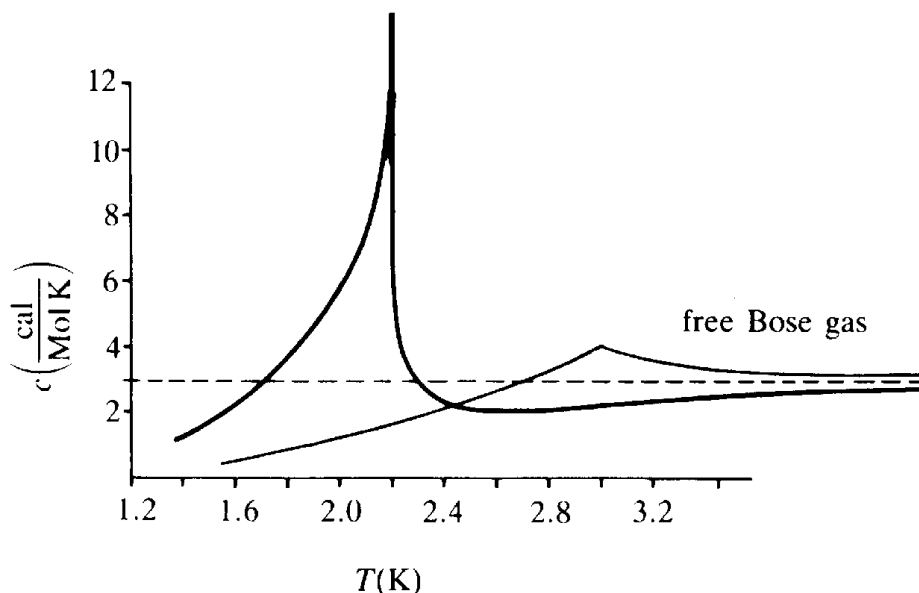
For constant ψ, the field ψ is referred to as an *order parameter* of the superfluid. If ψ has spatial variations, it will be called an *order field*. The order field has different propagation characteristics depending on whether the system is in the normal or the superfluid phase.

In the normal phase, for $T > T_c$, the ground state is given by $|\psi| = 0$. Small fluctuations around this are governed by the quadratic part of $e(\mathbf{x})$ which is

$$e(\mathbf{x}) \sim \frac{\hbar^2}{2M} |\nabla \psi|^2 - \mu |\psi|^2. \qquad (1.16)$$

Let us write this as

FIG. 1.4.   The experimental specific heat compared with that for the free Bose gas.

$$e(\mathbf{x}) \sim \frac{\hbar^2}{2M}(|\nabla\psi|^2 + m^2|\psi|^2), \tag{1.17}$$

where

$$m^2 = -\mu\frac{2M}{\hbar^2} > 0 \tag{1.18}$$

may be considered as the mass parameter of the ψ field. The field equation reads

$$(-\nabla^2 + m^2)\,\psi(\mathbf{x}) = 0. \tag{1.19}$$

This is actually two decoupled equations, one for the real part of ψ, say ψ_1, and one for the imaginary part, say ψ_2. These two components behave in a completely symmetrical way.

Consider a small point-like disturbance placed in the system. This amounts to adding a source term $\propto \delta(\mathbf{x})$ on the right-hand side of the field equation. The solution is given by

$$\psi(\mathbf{x}) \propto \int \frac{d^3k}{(2\pi)^3}e^{i\mathbf{k}\cdot\mathbf{x}}\frac{1}{k^2 + m^2} = \frac{1}{2\pi^2|\mathbf{x}|}\int_0^\infty \frac{dk^2}{k^2 + m^2}\sin k|\mathbf{x}| = \frac{1}{4\pi|\mathbf{x}|}e^{-m|\mathbf{x}|}. \tag{1.20}$$

Thus, at a radius of

$$\xi(T) = \frac{1}{m} = \frac{1}{\sqrt{\dfrac{T}{T_c} - 1}}\sqrt{\frac{\hbar^2}{2M\mu_0}} \tag{1.21}$$

around the disturbance, the field has practically returned to its ground state value. This length parameter ξ is called the *healing* or *coherence length*.

In the superfluid phase, for $T < T_c$, the situation is quite different. In order to simplify the equations, let us renormalize the field and replace ψ by $\sqrt{\mu/\hbar^2}\,\psi$. If we also introduce a coupling constant

$$g \equiv 2V\left(\frac{M}{\hbar^2}\right)^2 \tag{1.22}$$

the energy takes the form

$$E = \int d^3x\, e(\mathbf{x}) = \int d^3x \left\{ \frac{1}{2}|\nabla\psi|^2 + \frac{m^2}{2}|\psi|^2 + \frac{g}{4}|\psi|^4 \right\}, \qquad (1.23)$$

which is just of the type discussed in Section 1.5 of Part I.

For $T < T_c$, $m^2 < 0$, the ground state is given by

$$\psi_0 = \sqrt{-\frac{m^2}{g}}\, e^{i\gamma_0}, \qquad (1.24)$$

where γ_0 is an arbitrary phase angle. The arbitrariness of γ_0 is a consequence of the invariance of the energy under phase rotations:

$$\psi(\mathbf{x}) \rightarrow e^{i\alpha}\,\psi(\mathbf{x}). \qquad (1.25)$$

The important point about the superfluid phase is now that the system always has to choose one fixed value of γ_0 when minimizing the energy. Thus the ground state is not invariant under the symmetry transformations (1.25). The phase transition has destroyed the symmetry of the energy. One speaks of a *spontaneous symmetry breakdown*. This symmetry breakdown manifests itself in the asymmetric way in which the two field degrees of freedom react to an external point-like disturbance. Unlike the normal phase, in which the real and imaginary parts of the field have the same behavior [see (1.20)], there is now only one component which has a finite coherence length. The other has an infinite range. It is this infinite-range mode which plays a central role in the further discussion.

In order to study the field behavior in the superfluid phase it is useful to rewrite the field $\psi(\mathbf{x})$ in terms of polar coordinates as follows:

$$\psi(\mathbf{x}) = \rho(\mathbf{x})e^{i\gamma(\mathbf{x})}.$$

We may then split the field into its ground state value plus its fluctuations in a simple manner:

$$\rho(\mathbf{x}) = \rho_0 + \rho'(\mathbf{x}) = \sqrt{-\frac{m^2}{g}} + \rho'(\mathbf{x}),$$

$$\gamma(\mathbf{x}) = \gamma_0 + \gamma'(\mathbf{x}). \qquad (1.26)$$

Inserting these into (1.23), the fluctuating energy reads

$$E = \int d^3x \left\{ \frac{1}{2}[(\nabla\rho)^2 + \rho^2(\nabla\gamma)^2] + \frac{m^2}{2}\rho^2 + \frac{g}{4}\rho^4 \right\}$$

$$= Vf_c + \int d^3x \left\{ \frac{1}{2}[(\nabla\rho')^2 - 2m^2\rho'^2] + \frac{g}{4}(4\rho_0\rho'^3 + \rho'^4) \right.$$

$$\left. + \frac{\rho_0^2}{2}(\nabla\gamma')^2 + \left(\rho_0\rho' + \frac{\rho'^2}{2}\right)(\nabla\gamma')^2 \right\}. \tag{1.27}$$

This representation displays clearly the two different fluctuation modes:

1. There are *size fluctuations* which, if sufficiently small, are controlled by

$$e_{\text{size}} = \frac{1}{2}[(\nabla\rho')^2 + (-2m^2)\rho'^2], \tag{1.28}$$

i.e., their coherence length is given by (compare (1.17), (1.21))

$$\xi_{\text{size}}(T) = \frac{1}{\sqrt{2|m^2|}} = \frac{1}{\sqrt{2}} \frac{1}{\sqrt{1 - \frac{T}{T_c}}} \sqrt{\frac{\hbar^2}{2M\mu_0}}. \tag{1.29}$$

At the same distance from T_c, the size fluctuations in the ordered phase have a range which is smaller than the common range of ψ_1 and ψ_2 in the normal phase by a factor $\sqrt{2}$.

2. There are *phase fluctuations* which, if they are sufficiently small, have a free energy

$$e_{\text{phase}} = \frac{\rho_0^2}{2}(\nabla\gamma')^2. \tag{1.30}$$

These are massless modes. Their coherence length is infinite [compare (1.17), (1.21)].

As mentioned above, the appearance of long-range fluctuations is a very general feature of condensed phases. It occurs in all phase transitions in which a continuous symmetry of the field energy [here (1.25)] is spontaneously broken. The underlying mechanism was discovered by Nambu and further investigated by Goldstone and for this reason the associated long-range modes are called *Nambu–Goldstone bosons*. Here we shall not present the argument for the general case but

rather rephrase the present situation in a way that can easily be generalized to more complicated symmetries.

Let us display the effective potential
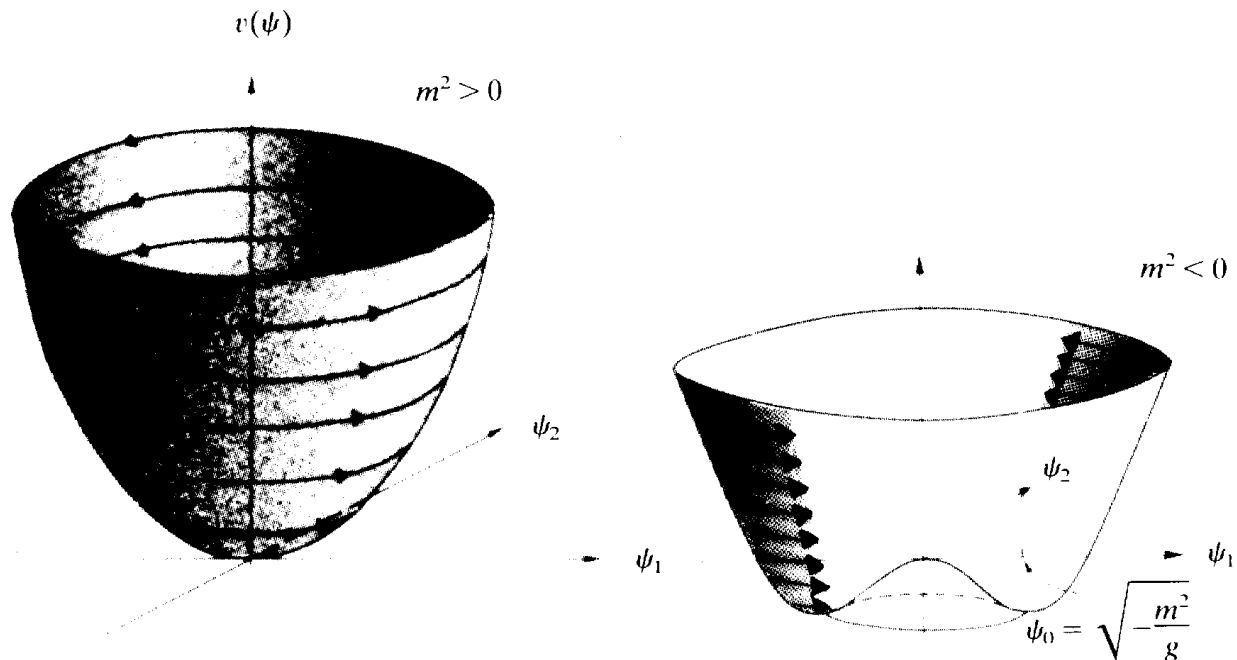
$$v = \frac{m^2}{2}|\psi|^2 + \frac{g}{4}|\psi|^4 \tag{1.31}$$

as shown on Fig. 1.5 over the ψ_1, ψ_2 plane. For $m^2 > 0$ it forms a convex slightly distorted paraboloid. For $m^2 < 0$ it looks like the bottom of a champagne bottle. Both forms are rotationally invariant around the v axis.

For $m^2 > 0$, there is a minimum at the field origin. For $m^2 < 0$, on the other hand, there is a whole circle of degenerate minima, all of fixed radius $|\psi_0|$. The system has to choose one of these minima since it wants to have the smallest possible condensation energy. The circle of degeneracy is a consequence of the symmetry under phase rotations. For more general continuous symmetries the circle is replaced by a multidimensional surface, each point of which represents a possible ground state of the system.

Consider now the fluctuations. For $m^2 > 0$, these are completely symmetric. The curvature of the potential is the same in all directions. The fluctuations in each direction have to run "uphill," implying a finite

FIG. 1.5. The effective potential of the superfluid as a function of the order parameter $\psi = \psi_1 + i\psi_2$ for $T > T_c$ $(m^2 > 0)$ and $T < T_c$ $(m^2 < 0)$. The arrows indicate the invariance under phase rotations $\psi \rightarrow e^{i\alpha}\psi$.

coherence length for all modes. For $m^2 < 0$, on the other hand, we see in Fig. 1.5 that only the radial fluctuations have to run "uphill." Only these acquire a finite coherence length. The orthogonal fluctuations which run azimuthally along the valley of degeneracy are only suppressed by the gradient energy (1.30). Thus they have zero energy in the long-wavelength limit. In this limit, they approach a symmetry transformation of the form $\psi_0 \rightarrow e^{i\gamma'}\psi_0$ with $\gamma' \rightarrow$ const. This is the general feature of all Nambu–Goldstone modes.

Let us study the physics of these modes in more detail.

1.3. NAMBU–GOLDSTONE MODES AND SUPERFLUID VELOCITY

For very low temperatures, the size fluctuations can be neglected, due to their high energy. Only the phase fluctuations — the Nambu–Goldstone modes — are relevant. It is useful to write their bending energy in the following form:

$$E = \int d^3x\, e(\mathbf{x}) = \int d^3x\, \frac{\rho_s}{2}\, \mathbf{v}_s^2 \tag{1.32}$$

where in the normalization of $(1.16)^b$

$$\rho_s = M|\psi|^2 \tag{1.33}$$

and

$$\mathbf{v}_s = \frac{\hbar}{M}\nabla\gamma(\mathbf{x}). \tag{1.34}$$

The quantity $\mathbf{v}_s$ has a direct physical meaning. Because of the general quantum mechanical correspondence rule, the velocity of a particle $\mathbf{v} = \mathbf{p}/M = (\hbar/M)\mathbf{k}$ is obtained by applying the differential operator $-i(\hbar/M)\nabla$ to the wave function $\psi = e^{i\gamma(\mathbf{x})}|\psi|$. Hence $\mathbf{v}_s = (\hbar/M)\nabla\gamma(\mathbf{x})$ describes the velocity with which the condensate moves through space. With this identification, the energy (1.32) has the typical hydrodynamic form $(\rho_s/2)\mathbf{v}_s^2$. This implies that the quanity ρ_s can be considered as the

---

[b]The superfluid density ρ_s is not to be confused with the size of the order parameter ρ_0 for which we have also used the greek letter ρ [compare Eqs. (1.32), (1.30)].

density of the superfluid component of the liquid, i.e., as the superfluid density.

Extremizing the field energy (1.32) leads to the condition of maximal smoothness of phase configurations; they have to satisfy Poisson's wave equation

$$\nabla^2 \gamma(\mathbf{x}) = 0. \tag{1.35}$$

For the superfluid velocity $\mathbf{v}_s$ this implies that its divergence vanishes

$$\nabla \cdot \mathbf{v}_s = 0. \tag{1.36}$$

1.4. STRAIGHT VORTEX LINE

Even though size fluctuations require much more energy than phase fluctuations, they nevertheless play an important role in understanding the properties of the superfluid. In particular, they are necessary for the existence of the vortex lines observed in the laboratory. A straight vortex line can be obtained as a cylindrical solution to the field equation

$$-\frac{\hbar^2}{2M} \nabla^2 \psi - \mu \psi + V|\psi|^2 \psi = 0, \tag{1.37}$$

which minimizes the energy (1.7).

Decomposing ψ into its polar components, $\psi = \rho e^{i\gamma}$, the real and imaginary parts of this equation read

$$\left[-\frac{\hbar^2}{2M} (\nabla^2 - (\nabla \gamma)^2) + (-\mu + V\rho^2) \right] \rho = 0 \tag{1.38}$$

and

$$\partial_i (\rho^2 \partial_i \gamma) = 0. \tag{1.39}$$

The latter equation is simply the statement of current conservation, $\partial_i (\psi^* (\overleftrightarrow{\partial}_i / 2i) \psi) = 0$. It can be solved by a purely circular flow in which ρ depends on the distance r from the cylindrical axis and the phase γ is an integral mutliple of the azimuthal angle in space, $\theta = \tan^{-1}(x_2/x_1)$, i.e., $\gamma = n\theta$. Then, (1.38) reduces to the radial differential equation

$$-\frac{\hbar^2}{2M}\left(\partial_r^2 + \frac{1}{r}\partial_r - \frac{n^2}{2}\right)\rho + V(\rho^2 - \rho_0^2)\rho = 0, \tag{1.40}$$

where $\rho_0 = |\psi_0| = \sqrt{-\mu_0(T/T_c - 1)/V}$ [compare (1.11)].

In order to solve this equation it is convenient to go to reduced quantities $\bar{r}$, $\bar{\rho}$ which measure the distance r in units of the coherence length

$$\xi = \sqrt{2}\,\xi_{\text{size}} = \sqrt{\frac{\hbar^2}{2M}\frac{1}{\mu_0}}\,\frac{1}{\sqrt{1 - \frac{T}{T_c}}} \tag{1.41}$$

and the size of the order parameter ρ in units of ρ_0, i.e., we introduce

$$\bar{x} = x/\xi, \quad \bar{r} = r/\xi, \tag{1.42}$$

$$\bar{\rho} = \rho/\rho_0. \tag{1.43}$$

Then (1.40) takes the form

$$\left[-\left(\partial_{\bar{r}}^2 + \frac{1}{r}\partial_{\bar{r}} - \frac{n^2}{\bar{r}^2}\right) + (\bar{\rho}^2 - 1)\right]\bar{\rho}(\bar{r}) = 0. \tag{1.44}$$

For small $\bar{r} \ll 1$, this is dominated by the first three terms which amount to a differential equation of the Bessel type for $\bar{\rho}(\bar{r})$. Thus, close to the origin, the solution is

$$\bar{\rho}(\bar{r}) = A_n J_n(\bar{r}) \propto \bar{r}^n. \tag{1.45}$$

Multiplying this with the phase factor

$$e^{in\gamma} = e^{in\tan^{-1}(x_2/x_1)}, \tag{1.46}$$

we see that the complex field $\psi(x)$ has the following small $|x|$ behavior

$$\psi(x) \propto \bar{r}^n e^{in\tan^{-1}(x_2/x_1)} = (x_1 + ix_2)^n, \tag{1.47}$$

which corresponds to a zero of n-th order in the complex mapping $x_1 + ix_2 \to \psi$.

For large $\bar{r} \gg 1$, $\bar{\rho}(\bar{r})$ approaches the asymptotic value $\bar{\rho} = 1$. In fact, from (1.44) we can extract the $1/\bar{r}$ expansion,

$$\bar{\rho}_n(\bar{r}) = 1 - \frac{n^2}{2\bar{r}^2} - \left(n^2 + \frac{1}{8}n^4 \right) \frac{1}{\bar{r}^4} - \left(8 + 2n^2 + \frac{1}{16}n^4 \right) \frac{n}{\bar{r}^6} - O\left(\frac{1}{\bar{r}^8} \right). \quad (1.48)$$

Integrating the differential equation numerically inward, we find the solution displayed on Fig. 1.6.

Let us now study the energy of these vortex lines. The calculation can be simplified by using an argument analogous to that employed in deriving the virial theorem: if $\psi(\mathbf{x})$ is the solution of the differential equation (1.37), the rescaled solution

$$\psi_\delta(\mathbf{x}) \equiv e^\delta \cdot \psi(\mathbf{x}) \quad (1.49)$$
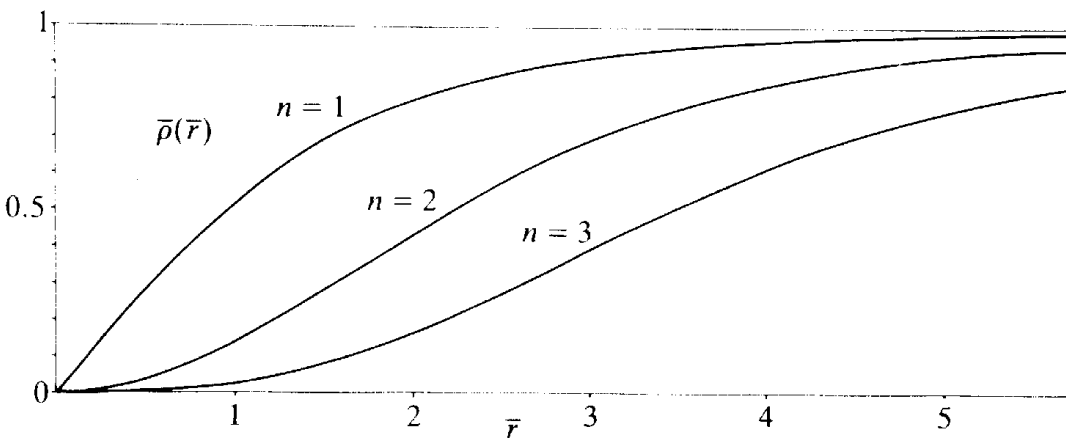
must extremize the energy for $\delta = 0$. But inserting (1.49) into (1.23), we calculate

$$E = \int d^3x \left[\frac{1}{2}e^{2\delta}|\nabla\psi|^2 + e^{2\delta}\frac{m^2}{2}|\psi|^2 + \frac{g}{4}e^{4\delta}|\psi|^4 \right]. \quad (1.50)$$

Setting the derivative with respect to δ equal to zero gives at $\delta = 0$

$$\int d^3x \left[\frac{1}{2}|\nabla\psi|^2 + \frac{1}{2}m^2|\psi|^2 + \frac{g}{2}|\psi|^4 \right] = 0. \quad (1.51)$$

FIG. 1.6.   The order parameter $\bar{\rho} = |\psi|/|\psi_0|$ around a vortex line of strength $n = 1, 2, 3, \ldots$ as a function of the reduced distance $\bar{r} = r/\xi$, where r is the distance from the axis and ξ the healing length.

Subtracting this from (1.50) for $\delta = 0$ we see that the energy of a solution of the field equation is simply given by

$$E = \frac{-g}{4} \int d^3x \, |\psi|^4. \tag{1.52}$$

Most of this energy is due to the asymptotic value $\psi \rightarrow \psi_0$, where it is equal to the condensation energy [see (1.12)]. Subtracting this background energy from E we find the *additional energy* of the vortex line as

$$E_r = \frac{-g}{4} \int d^3x (|\psi|^4 - |\psi_0|^4).$$

In terms of the natural units introduced in (1.42) and (1.43), this is simply

$$E_r = -f_c \xi^3 \int d^3\bar{x} (1 - \bar{\rho}^4(\mathbf{x})). \tag{1.53}$$

Going over to cylindrical coordinates $\bar{r}$, θ, z, the integral becomes, for a length L along the z-direction,

$$2\pi \bar{L} \int_0^\infty d\bar{r}\bar{r}[1 - \bar{\rho}^4(\bar{r})]. \tag{1.54}$$

Before inserting the numerical solutions for $\bar{\rho}(\bar{r})$ shown in Fig. 1.6 we note that due to the factor $\bar{r}$, the additional energy comes mainly from the large $\bar{r}$ regime, i.e., the far zone. In fact, if we insert the leading asymptotic behavior (1.48), we obtain an integral

$$4\pi n^2 L \int^\infty d\bar{r}/\bar{r}, \tag{1.55}$$

which diverges logarithmically for large $\bar{r}$. An immediate conclusion is that a single vortex line can have a finite energy only in a finite container. If this container is cylindrical of radius R, the integral no longer diverges at the upper end but behaves like $4\pi n^2 L \log(R/\xi)$.

Consider now the small $\bar{r}$ behavior. From (1.45) we see that close to the origin, $\bar{\rho}(\bar{r})$ behaves like $\bar{r}^n$. Hence, $1 - \bar{\rho}^4 \approx 1$ and the energy of a thin cylindrical section of radius r grows like r^2. For increasing r, the rate of growth rapidly slows down and settles at the asymptotic rate $4\pi n^2 L$

× $\log(\bar{r}/\xi)$, where ξ is the coherence length. The proper inclusion of the non-asymptotic behavior gives simply a finite correction to the asymptotic energy and the energy of a vortex line in a container of radius R becomes $4\pi n^2 L[\log(R/\xi) + c]$. This is the same result we would have obtained had we replaced the integrand $\bar{r}(1 - \bar{\rho}^4(\bar{r}))$ by the asymptotic form $2n^2/\bar{r}$ and integrated from a radius $r_0 = \xi e^{-c}$ to R.

The precise numerical evaluation of the differential equation (1.44) and the integral (1.54) shows that for the lowest vortex line, c has the value

$$c = 0.385.$$

Hence the energy of the vortex line per unit length becomes

$$\frac{E_v}{L} = f_c \xi^2 4\pi n^2 (\log{(R/\xi)} + 0.385). \tag{1.56}$$

The logarithmic divergence of the energy has a simple physical meaning. In order to see this let us calculate the energy once more, but using the original expression (1.23), i.e. without invoking the virial theorem. It reads, for the radial solutions,

$$E_v = f_c \xi^2 L 4\pi \int d\bar{r}\,\bar{r}\left\{(\partial_{\bar{r}}\bar{\rho})^2 + \frac{1}{2}(1 - \bar{\rho}^2)^2 + \frac{n^2}{\bar{r}^2}\bar{\rho}^2\right\}. \tag{1.57}$$

The first two pieces are rapidly converging. Thus the energy of the far zone resides completely in the last term

$$\frac{n^2}{\bar{r}^2}\bar{\rho}^2 \approx \frac{n^2}{\bar{r}^2}.$$

This energy is a consequence of the angular behavior of the condensate phase $\gamma = n \tan^{-1}(x_2/x_1)$ around a vortex line. In fact, the term (1.58) is entirely due to the *azimuthal part* of the gradient energy $(\hbar^2/2M^2)\rho_s(\nabla\gamma)^2$, i.e., the term which describes the *Nambu–Goldstone modes*. This is not surprising. We have seen in the general discussion of (1.30) that the *long range properties* of the system are determined by the Nambu–Goldstone modes. A phase which behaves like $\gamma = n \tan^{-1}(x_2/x_1)$ can be viewed as a coherent pile-up of these modes and this determines the total energy.

The dominance of the energy carried by the phase gradient can also be

described in a different and more physical way. In the last section we identified the gradient $(\hbar/M)\nabla\gamma$ with the superfluid velocity. For the vortex line at hand, the superfluid velocity is found, far away from the line, to be

$$\mathbf{v}_s = \frac{\hbar}{M}n\nabla\tan^{-1}\left(\frac{x_2}{x_1}\right) = \frac{\hbar}{M}\frac{n}{r^2}(-x_2, x_1, 0) = \frac{\hbar}{M}n\frac{1}{r}\mathbf{e}_\phi, \qquad (1.58)$$

where $\mathbf{e}_\phi$ is the unit vector in azimuthal direction. Thus, around every vortex line, there is a circular flow of the superfluid whose velocity decreases like the inverse distance from the line. The hydrodynamic energy density of this flow is

$$e(\mathbf{x}) = \frac{\rho_s}{2}\mathbf{v}_s^2 = \frac{\rho_s}{2}\frac{\hbar^2}{M^2}\frac{n^2}{r^2}. \qquad (1.59)$$

This is precisely the dominant third Nambu–Goldstone term in the energy integral (1.57). Thus the energy of the vortex line is indeed mainly due to the hydrodynamic energy of the superflow around the line.

For the major part of the volume, the hydrodynamic limit (1.58), (1.59) gives an excellent approximation. Only in the neighborhood of the line, i.e., for small radii $r \lesssim \xi$, the energy density differs from (1.59) due to gradients in the size of the field $|\psi|$. It is therefore suggestive to *idealize* the superfluid and *assume* the validity of the pure gradient energy density

$$e = \frac{\rho_s}{2}\mathbf{v}_s^2 = \frac{\sigma}{2}(\nabla\gamma)^2, \qquad \sigma \equiv \rho_s\frac{\hbar^2}{M^2}, \qquad (1.60)$$

everywhere in space.

The deviations from this law, which become significant only very close to a vortex line, i.e., at distances of the order of the coherence length ξ, are treated *approximately* by simply cutting off the energy integration at a radius ξ away from a vortex line. In other words, we pretend as though there were no superflow at all within the thin tubes of radius ξ, with a sudden onset of idealized flow outside ξ, moving with the limiting velocity (1.58).

Although the internal part of the thin tube carries no superflow, it nevertheless carries rotational energy. Within the present approximation, this energy is associated with the number 0.385 in (1.56). This piece will be called the *core energy*. The core energy has a physical interpretation.

At distances smaller than the coherence length, the different parts of the liquid can no longer slip past each other freely. Hence the core of a vortex line is expected to rotate roughly like a solid rod, rather than with the diverging velocity $v_s \sim 1/r$. Indeed, if we use the approximation

$$v_s \propto n \begin{cases} \dfrac{1}{r}, & r > \xi, \\[2ex] \dfrac{r}{\xi^2}, & r \le \xi, \end{cases} \qquad (1.61)$$

for a line of vortex strength n, the energy density does behave like r^2, for small r, as observed before. Moreover, the energy integration gives

$$n^2 \left[\int_1^{R/\xi} d\bar{r}/\bar{r} + \int_0^1 d\bar{r}\,\bar{r}^3 \right] = n^2 [\log(R/\xi) + 0.25],$$

and we see that the number for the core energy, 0.25, emerges with the right order of magnitude.

To complete our discussion of the hydrodynamic picture, let us calculate the circulation of the superfluid velocity field around the vortex lines:

$$\kappa \equiv \oint_B dx_i\, v_{s_i} = \frac{\hbar}{M} n \oint_B dx_i\, \partial_i \gamma = \frac{\hbar}{M} 2\pi n = n\frac{h}{M} = n\kappa_1. \qquad (1.62)$$

This integral is the same for any size and shape of the circuit B around the vortex line. Thus the circulation is quantized and always appears in multiplets of $\kappa_1 = h/M \approx 10^{-3}\,\mathrm{cm^2/sec}$. The number n is called *vortex strength*.

The integral (1.62) can be transformed into a surface integral, via Stokes' theorem:

$$\int_{S^B} dx_1\, dx_2 (\partial_1 v_{s2} - \partial_2 v_{s1}) = \frac{\hbar}{M} 2\pi n, \qquad (1.63a)$$

where S^B is some surface spanned by the circuit B in (1.62). This integral is the same for any size and shape of S^B. From this result we conclude that the third component of the curl of $\mathbf{v}_s$ must vanish everywhere except at the origin. There it must have a singularity of such a strength that the two-dimensional integral gives the correct vortex strength. Hence

$$\nabla \times \mathbf{v}_s = \frac{\hbar}{M} 2\pi n \, \delta^{(2)}(\mathbf{x}_\perp) \, \hat{\mathbf{z}},$$ (1.63b)

where $\hat{\mathbf{z}}$ is the unit vector along the z-axis and $\mathbf{x}_\perp \equiv (x_1, x_2)$ are the coordinates orthogonal to the vortex line.

If the nonlinearities of the field equation are taken into account, the $\delta^{(2)}$-function is really smeared out over a circle whose radius is of order ξ. As an example, let us replace $1/r^2$ in (1.59) by $1/(r^2 + \varepsilon^2)$. Then the rotation of the superfluid velocity becomes

$$\nabla \times \mathbf{v}_s = \frac{\hbar}{M} n \frac{2\varepsilon^2}{(r^2 + \varepsilon^2)^2} \hat{\mathbf{z}}.$$ (1.64)

The right-hand side is non-zero only within a small radius $r \lesssim \varepsilon$, where it diverges with the total strength

$$\int d^2x \frac{2\varepsilon^2}{(r^2 + \varepsilon^2)^2} = 2\pi\varepsilon^2 \int_0^\infty dr \frac{2r}{(r^2 + \varepsilon^2)^2} = 2\pi.$$

This shows that (1.64) is, indeed, a smeared out version of the δ-function relation (1.63).

Because of their rotational properties, vortex lines can be generated experimentally by rotating a vessel with an angular velocity Ω. Initially, the lack of friction will cause the superfluid part of the liquid to remain at rest. This situation cannot, however, persist forever since it is not in a state of thermal equilibrium. After some time, vortex lines form on the walls which migrate into the liquid and distribute evenly. This goes on until their total number is such that the rotational Helmholtz free energy

$$F_\Omega = F - \mathbf{\Omega} \cdot \mathbf{L} \approx \int d^3x \left(\frac{\rho_s}{2} \mathbf{v}_s^2 - \mathbf{\Omega} \cdot \mathbf{x} \times \rho_s \mathbf{v}_s \right)$$ (1.65)

is minimal. This equilibration process has been observed in the laboratory and has even been photographed directly using the property that vortex lines trap ions which can be accelerated against a photographic plate. Integrating (1.65) with $\mathbf{v}_s$ from (1.58), we find that in a cylindrical vessel of radius R, the first vortex line $n = 1$ appears at a critical angular velocity

$$\Omega_c = \frac{\kappa_1}{\pi R^2} \log \frac{R}{\xi}$$ (1.66)

and settles on the axis of rotation. It is useful to observe that the vortex lines of higher n are all unstable. Since the energy increases quadratically with n, it is favorable for a single line of higher n to decay into n lines of unit strength each. When generating vortex lines by stirring a vessel, one may nevertheless be able to create, for a short time, such an unstable line, and to observe its decay.

1.5.   VORTEX LINES OF ARBITRARY SHAPE, VORTEX DENSITY

We saw in the last section that the total energy of a single vortex line can be split into a contribution from the far zone $r > \xi$, which contains most of the energy and which is dominated by the superflow around the lines, and another from the near zone $r \le \xi$, which carries a certain core energy. This splitting is very useful when it comes to studying ensembles of vortex lines. For such an ensemble, the solution of the full nonlinear differential equation is certainly impossible. Nevertheless, as long as the line spacing is large compared to the thickness ξ of the core, we can still calculate their energy quite accurately. The superflow energy in most of the volume is governed by the simple hydrodynamic expression (1.60)

$$e = \frac{\rho_s}{2} v_s^2 = \frac{\sigma}{2} (\nabla \gamma)^2,$$

and the total core energy depends practically only on the total length of all the lines. In this way, the problem linearizes. The nonlinearities of the field equations are approximately parametrized by the geometric shapes of the vortex lines.

Let us see how lines of arbitrary shape can be characterized. In the last section we showed that the energy of a vortex line is dominated by the behavior of the phase angle γ. But γ is a cyclic variable, periodic in 2π. The values γ and $\gamma + 2\pi n$ are indistinguishable. A vortex line takes advantage of this property. Along a closed loop surrounding the line, $\gamma(\mathbf{x})$ runs from one value to a different but physically indistinguishable value $\gamma + 2\pi n$.

The number n has a fundamental mathematical significance. It is a *topological quantum number*. The solution of (1.58)

$$\gamma = n \tan^{-1} \frac{x_2}{x_1} \tag{1.67}$$

represents a mapping from the azimuthal angle of space onto the phase angle of the order field. Both variables are periodic and equivalent to a circle. Thus, (1.67) is a continuous mapping from a circle onto a circle. The set of all such mappings can be decomposed into equivalence classes characterized by the integer topological quantum number n called *winding number*, which counts how many times the second circle is encircled by the first. It is obvious from Fig. 1.7 that there is no continuous way of removing a winding without leaving the circular space. This topological property is so general that it does not depend on whether the vortex line is straight or curved.

Analytically, we can easily convince ourselves that this topological property is measured by the circuit integral (1.62). This can therefore be used to characterize a closed vortex line of *any* shape. Let us first show that the integral $\oint d\gamma$ must be the same for any circuit integral enclosing the vortex line as a simple consequence of Stokes' theorem. Indeed, if we take the difference between two such integrals

$$\oint_{B_2} d\gamma - \oint_{B_1} d\gamma = \int_{B_2 - B_1} dx_i \partial_i \gamma, \qquad (1.68)$$

it can be transformed into a surface integral over the cylinder spanned by the two circuits (see Fig. 1.8)
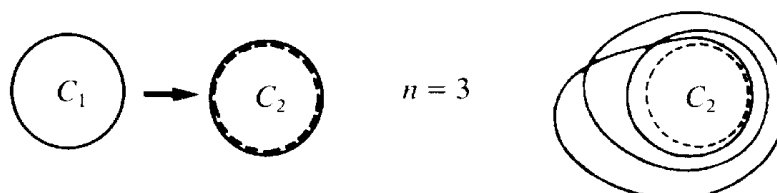
$$\int_{B_2 - B_1} dx_i \partial_i \gamma = \int_{S^B} dS_k \, \varepsilon_{kij} \partial_i \partial_j \gamma. \qquad (1.69)$$

But away from the vortex line, $\gamma(\mathbf{x})$ is a smooth function and the derivatives in front of it commute. Hence $\oint_B d\gamma$ is indeed a constant.

When applying Stokes' theorem to the integral

$$\oint_B d\gamma = 2\pi n \qquad (1.70)$$

FIG. 1.7. Mappings from a circle onto a circle. These can be classified by the winding number n. The example here corresponds to $n = 3$.

itself, we find

$$\int_{S^B} dS_k \, \varepsilon_{kij} \, \partial_i \, \partial_j \, \gamma = 2\pi n, \tag{1.71}$$

where S^B is the surface spanned by the circuit B. This holds for arbitrary circuits enclosing the line.

From this equation we can conclude that at the vortex lines, the differentiations no longer commute and there must be a $\delta^{(2)}$-function singularity of such a strength as to render the surface integral equal to $2\pi n$. For a straight line along the z-axis, we had found in Eq. (1.63) that

$$\int_{S^B} dx_1 \, dx_2 (\partial_1 \partial_2 - \partial_2 \partial_1) \, \gamma(\mathbf{x}) = 2\pi n, \tag{1.72}$$
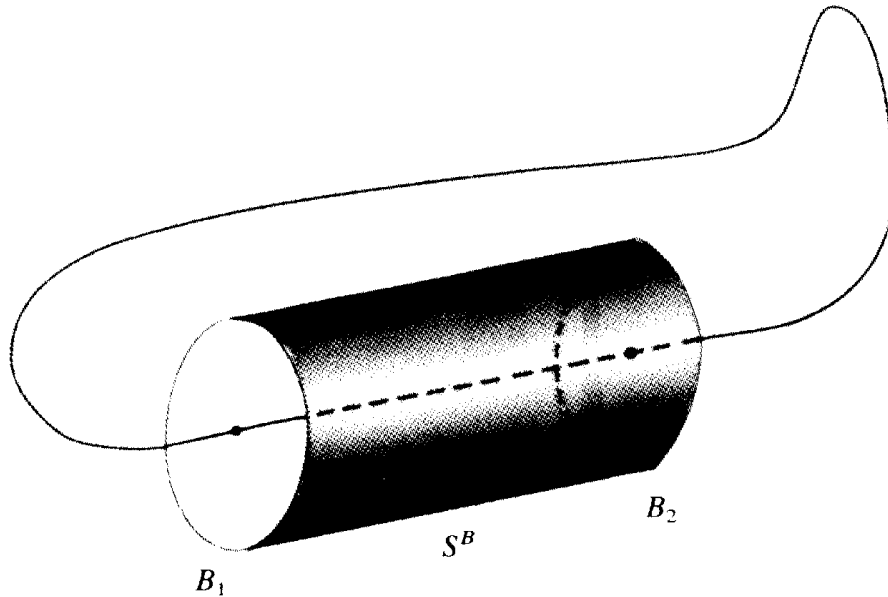
which implied that

$$(\partial_1 \partial_2 - \partial_2 \partial_1) \, \gamma(\mathbf{x}) = 2\pi n \, \delta^{(2)}(\mathbf{x}_\perp).$$

From Eq. (1.71) we now extract a generalization of this property to lines of arbitrary shape: first we observe that for a straight line pointing along any arbitrary axis $k = 1, 2, 3$, we can define the *vortex density*

$$\alpha_k(\mathbf{x}) \equiv \varepsilon_{kij} \, \partial_i \, \partial_j \, \gamma(\mathbf{x}) \tag{1.73}$$

FIG. 1.8. Geometry associated with the proof that the integral $\oint_B d\gamma$ is a constant, using Stokes' theorem and the smoothness of γ on the cylindrical surface S^B.

and find that it is equal to

$$\alpha_k(\mathbf{x}) = 2\pi n \, \delta_k^{(2)}(\mathbf{x}_\perp),\tag{1.74}$$

where the $\delta^{(2)}$-function on the right-hand side refers to the two components transverse to the k-axis. This can be written more conveniently as

$$\delta_k^{(2)}(\mathbf{x}_\perp) \equiv \int_{-\infty}^{\infty} dx_k \, \delta^{(3)}(\mathbf{x}),\tag{1.75}$$

where the integral runs along the line. The generalization of this formula to lines of arbitrary shape is now simple. Let L be any closed curve and $\bar{\mathbf{x}}(s)$ its parametrization. Then we define a transverse δ-function of this line as follows:

$$\delta_k(L) \equiv \int ds \, \frac{d\bar{x}_k(s)}{ds} \delta^{(3)}(\mathbf{x} - \bar{\mathbf{x}}(s)) \equiv \int_L d\bar{x}_k \, \delta^{(3)}(\mathbf{x} - \bar{\mathbf{x}}(s)).\tag{1.76}$$

A more explicit notation would be $\delta(\mathbf{x}; L)$, but we omit $\mathbf{x}$ for brevity. This has the property that the integral over a surface S pierced by L under an angle α is (see Fig. 1.9)

$$\int_S dS_k \, \delta_k(L) = \int ds \int_S dS_k \, \frac{d\bar{x}_k(s)}{ds} \delta^{(3)}(\mathbf{x} - \bar{\mathbf{x}}(s))$$

$$= \int_S dS_k \int_L d\bar{x}_k \, \delta^{(3)}(\mathbf{x} - \bar{\mathbf{x}}) = \cos \alpha.\tag{1.77}$$
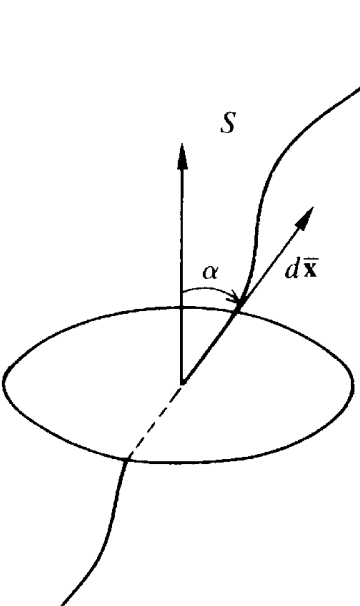
FIG. 1.9. This figure illustrates the integration of a δ-function along a line, $\delta_i(L)$, performed in Eq. (1.77).

Notice that the δ-function is sensitive to the orientation of the line L, which is defined via the direction in which the integral $\int ds$ runs along L. The integral (1.77) would give -1 if the surface S was pierced in the opposite normal direction.

Now, the property (1.77) of $\delta_k(L)$ is just what is needed to solve (1.71); namely,

$$\alpha_k(\mathbf{x}) \equiv \varepsilon_{kij}\, \partial_i\, \partial_j\, \gamma(\mathbf{x}) = 2\pi n\, \delta_k(L). \qquad (1.78)$$

At this point it is useful to recall that in the theory of differential equations, the commutation property of the derivatives in front of γ, i.e.,

$$(\partial_i\, \partial_j - \partial_j\, \partial_i)\, \gamma(\mathbf{x}) = 0 \qquad (1.79)$$

is referred to as the *integrability condition*. Functions which satisfy (1.79) can be defined uniquely through all space [see (I.3.8)]. According to (1.78), the phase angle $\gamma(\mathbf{x})$ violates this condition along the line L and from our earlier discussion it is clear that this is a manifestation of the multivaluedness of $\gamma(\mathbf{x})$.

Stokes' theorem has another important consequence: no vortex line can ever end inside the superfluid. It must either be closed or run to infinity along two different directions (in which case we shall also say that it is "closed at infinity"). This statement is proved quite simply by *reductio ad absurdum*, by assuming that there is an end. Then, enclosing the end by a sphere (see Fig. 1.10), the integral encircling the line $\oint d\gamma$, would give $2\pi n$ while it would simultaneously be equal to a surface integral over the sphere, which in turn vanishes, since there $\gamma(\mathbf{x})$ satisfies the integrability condition. Hence there can be no end.

We shall now demonstrate that this result can also be phrased in a differential way as the statement

$$\partial_k\, \alpha_k(\mathbf{x}) = \varepsilon_{kij}\, \partial_k\, \partial_i\, \partial_j\, \gamma = 0, \qquad (1.80)$$
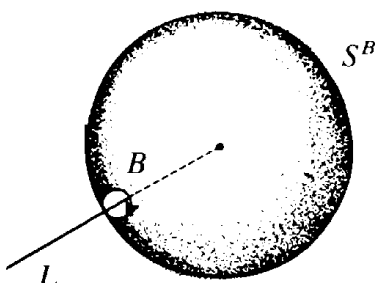

FIG. 1.10. Illustration of the proof that vortex lines can never end.

which means that the vortex density is a divergenceless quantity. In terms of the superfluid velocity $\mathbf{v}_s$ this amounts to

$$\partial_k \, \alpha_k(\mathbf{x}) = \varepsilon_{kij} \, \partial_k \, \partial_i v_{s_j} = 0. \tag{1.81}$$

But this is just an *integrability condition for* $\mathbf{v}_s$ everywhere in space.

In order to prove (1.80) and (1.81) we use (1.78) and show that the function $\delta_k(L)$ for endless vortex lines satisfies the divergence condition

$$\partial_k \, \delta_k(L) = 0. \tag{1.82}$$

Suppose that the line L had open ends and were to connect an initial point, say x_i, with a final point, say x_f. Then we would find

$$\partial_k \, \delta_k(L) = \int_{x_i}^{x_f} d\bar{x}_k \, \partial_k \, \delta^{(3)}(\mathbf{x} - \bar{\mathbf{x}}(s)) = \int_{s_i}^{s_f} ds \, \frac{d\bar{x}_k}{ds} \, \partial_k \, \delta^{(3)}(\mathbf{x} - \bar{\mathbf{x}}(s))$$

$$= -\int_{s_i}^{s_f} ds \, \frac{d\bar{x}_k}{ds} \frac{\partial}{\partial \bar{x}_k} \, \delta^{(3)}(\mathbf{x} - \bar{\mathbf{x}}(s)) = -\int_{s_i}^{s_f} ds \, \frac{d}{ds} \, \delta^{(3)}(\mathbf{x} - \bar{\mathbf{x}}(s))$$

$$= \delta^{(3)}(\mathbf{x} - \mathbf{x}_i) - \delta^{(3)}(\mathbf{x} - \mathbf{x}_f). \tag{1.83}$$

But closed lines have either $\mathbf{x}_i = \mathbf{x}_j$ or both points lie at infinity. In both instances (1.82) is true.

1.6. BRANCHING VORTEX LINES

Up to now we have considered a single line of arbitrary shape. In the last section we mentioned that lines of higher vortex strength can decay into those of lower strength. Such a decay may start at some place of the vortex line ripping it apart in a zipper-like fashion (see Fig. 1.11). It is an
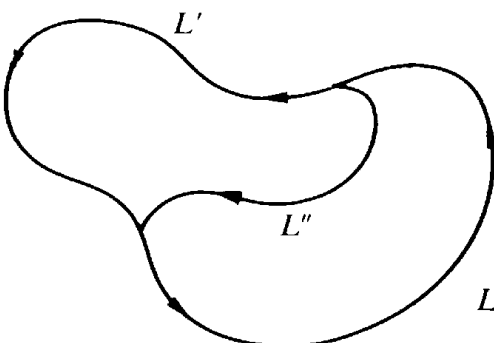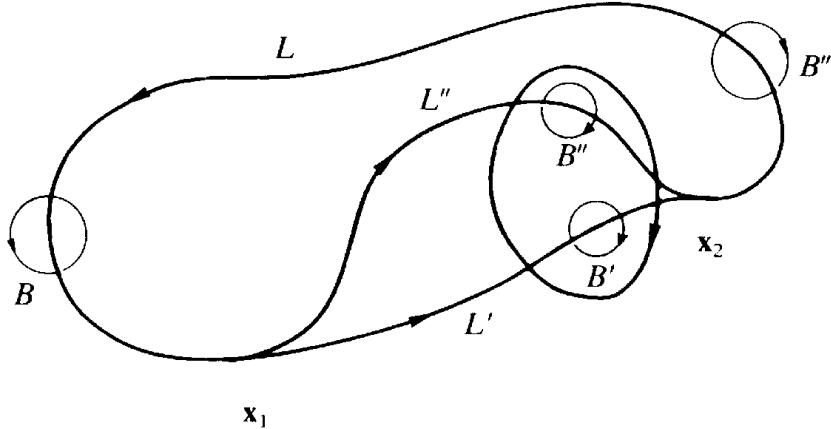

L   FIG. 1.11.   Illustration of the fact that vortex lines can branch off each other.

FIG. 1.12.   Illustration of the conservation law of the winding numbers for branching vortex lines.

immediate consequence of Stokes' theorem that the vortex strengths are always conserved. For a line L that splits into L' and L'', the respective strengths have to satisfy

$$n = n' + n'', \tag{1.84}$$

if they are defined in such a way that the circuits B, B', B'' encircle the oriented lines L, L', L'' in the positive sense (see Fig. 1.12). Notice that the assignment of an orientation to the lines is completely arbitrary as long as we allow for positive and negative vortex strengths n. Only the product $n \, dx_i$ is an invariant. For example, we can reverse the orientation of the line L''. Then the strength of L'' is $-n''$ and we would interprete Fig. 1.8 as line L' splitting into L'' and L. The strength-conservation law would then read

$$n' = n + (-n'')$$

which is the same as (1.84).

It is useful to generalize the $\delta_k(L)$-function to such branching configurations and define

$$\delta_k(L, L', L'') \equiv n \, \delta_k(L) + n' \, \delta_k(L') + n'' \, \delta_k(L'') \tag{1.85}$$

with

$$\alpha_k(x) = 2\pi \, \delta_k(L, L', L'') \tag{1.86}$$

denoting the density of the vortex lines which would appear on the right-

hand side of the differential equation (1.78). The three δ-functions in (1.86) are associated with open lines connecting initial and final points of L, L', L'', respectively. The integrability condition for $\mathbf{v}_s$ implies that any vortex density $\alpha_k(\mathbf{x})$ has to be divergenceless, as in the case of a single line (1.82). Indeed, if the branch points are denoted by $\mathbf{x}_1$ and $\mathbf{x}_2$ [see Fig. (1.12)], we find, using (1.83),

$$
\begin{aligned}
\partial_k \, \delta_k(L, \; L', \; L'') & \\
&= n[\delta^{(3)}(\mathbf{x} - \mathbf{x}_2) - \delta^{(3)}(\mathbf{x} - \mathbf{x}_1)] + n'[\delta^{(3)}(\mathbf{x} - \mathbf{x}_1) - \delta^{(3)}(\mathbf{x} - \mathbf{x}_2)] \\
&\quad + n''[\delta^{(3)}(\mathbf{x} - \mathbf{x}_1) - \delta^{(3)}(\mathbf{x} - \mathbf{x}_2)]
\end{aligned}
$$

and this vanishes since the n's satisfy the conservation law (1.84), i.e.,

$$
\partial_k \, \alpha_k(\mathbf{x}) = 0. \tag{1.87}
$$

1.7. HYDRODYNAMIC ENERGY OF VORTEX LINES

An arbitrary ensemble of vortex lines gives rise to a complicated super-flow configuration. Let us calculate the hydrodynamic energy of this flow which is given by

$$
E = \int d^3x \frac{\rho_s}{2} \mathbf{v}_s^2 = \int d^3x \frac{\sigma}{2} (\nabla \gamma)^2. \tag{1.88}
$$

Minimizing the energy shows that the phase field $\gamma(\mathbf{x})$ satisfies the Euler-Lagrange equation

$$
-\nabla^2 \gamma = 0, \tag{1.89}
$$

which expresses the incompressibility of superflow, i.e.,

$$
\partial_i v_{si} = 0. \tag{1.90}
$$

From the discussion in the last chapter we know that an arbitrary line configuration L gives rise to singularities in the circulation described by the vortex density

$$
\alpha_k(\mathbf{x}) = \frac{M}{\hbar} (\nabla \times \mathbf{v}_s)_k = 2\pi n \, \delta_k(L). \tag{1.91}
$$

Equations (1.90) and (1.91) are familiar from magnetostatics when $\mathbf{v}_s$ is regarded as $\mathbf{B}$. They govern the magnetic field $\mathbf{B}$ carried by an ensemble of current loops along L. The corresponding equations are (in rationalized cgs units as employed by Heaviside and Lorentz)

$$\partial_i B_i = 0, \quad (\nabla \times \mathbf{B})_k = \mu j_k = \mu \frac{I}{c} \delta_k(L), \tag{1.92}$$

where μ is the magnetic permeability, L an oriented closed loop, and I is the current flowing along L. The divergence property of the δ-function is now an expression of *Kirchhoff's law* which says that the current is conserved along the loop.

The calculation of the magnetic field configurations associated with such equations is well known. In magnetostatics this is done for arbitrary current densities $\mathbf{j}(\mathbf{x})$ which are conserved

$$\partial_k j_k(\mathbf{x}) = 0 \tag{1.93}$$

and it is easy to write down the solution of the general equation

$$(\nabla \times \mathbf{B})_k = \frac{\mu}{c} j_k(\mathbf{x}). \tag{1.94}$$

For this it is important to take advantage of the vanishing divergence of the magnetic field, which in magnetostatics implies the absence of magnetic monopoles, and write it as a curl of another vector field, called the *vector potential* $\mathbf{A}$:

$$B_i = \varepsilon_{ijk} \, \partial_j A_k. \tag{1.95}$$

Recall that this way of rewriting B_i is not unambiguous. There is a whole class of vector potentials which gives the same magnetic field since the relation (1.95) is invariant under the *local gauge transformations*

$$A_k(\mathbf{x}) \rightarrow A_k(\mathbf{x}) + \partial_k \Lambda(\mathbf{x}), \tag{1.96}$$

where $\Lambda(\mathbf{x})$ is an arbitrary function which is smooth enough to satisfy the integrability condition

$$(\partial_i \partial_j - \partial_j \partial_i) \Lambda(\mathbf{x}) = 0. \tag{1.97}$$

If we insert (1.95) into (1.94) we find that this takes the form

$$\nabla \times (\nabla \times \mathbf{A}) = -\nabla^2 \mathbf{A} + \nabla(\nabla \cdot \mathbf{A}) = \frac{\mu}{c}\mathbf{j}(\mathbf{x}). \qquad (1.98)$$

This equation is simplified by making use of the gauge freedom and choosing a function $\Lambda(\mathbf{x})$ such that the gauge transformed vector potential $A_k + \partial_k \Lambda$ has no divergence, i.e. it satisfies the transversality condition

$$\partial_k A_k(\mathbf{x}) = 0. \qquad (1.99)$$

In magnetostatics, such a field $A_k(\mathbf{x})$ is said to be in the *transverse gauge*. As long as $A_k(\mathbf{x})$ is an integrable function, this choice is always possible.

In order to verify this statement we define the *Coulomb Green function*:

$$G^c(\mathbf{x}, \mathbf{x}') = G^c(\mathbf{x} - \mathbf{x}') \equiv \int \frac{d^3k}{(2\pi)^3} e^{i\mathbf{k}\cdot(\mathbf{x} - \mathbf{x}')}\frac{1}{\mathbf{k}^2}. \qquad (1.100)$$

It solves the potential equation

$$-\nabla^2 G^c(\mathbf{x} - \mathbf{x}') = \delta^{(3)}(\mathbf{x} - \mathbf{x}'), \qquad (1.101)$$

so that G^c can formally be written as

$$G^c = -(\nabla^2)^{-1}, \qquad (1.102)$$

where the inverse is understood in the functional sense, as always when dealing with differential operators. Then, if we choose

$$\Lambda(\mathbf{x}) = -(\nabla^2)^{-1}\partial_i A_i(\mathbf{x}), \qquad (1.103)$$

we see that $A_i(x) + \partial_i \Lambda(\mathbf{x})$ has, indeed, the Coulomb gauge (1.99). In this gauge, the equation (1.98) becomes simply

$$-\nabla^2 A_k(\mathbf{x}) = \frac{\mu}{c}j_k(\mathbf{x}). \qquad (1.104)$$

But this is solved by

$$A_k(\mathbf{x}) = -\frac{\mu}{c}(\nabla^2)^{-1} j_k(\mathbf{x}) = \frac{\mu}{c}\int d^3x'\, G^c(\mathbf{x} - \mathbf{x}') j_k(\mathbf{x}'). \quad (1.105)$$

For the specific current density (1.92) with line currents flowing along the loops L, formula (1.105) reads

$$A_k(\mathbf{x}) = \frac{\mu I}{c}\int d^3x'\, G^c(\mathbf{x} - \mathbf{x})\, \delta_k(L)$$

$$= \frac{\mu I}{c}\int d^3x'\int ds \frac{dx_k}{ds} G^c(\mathbf{x} - \mathbf{x}')\, \delta^{(3)}(\mathbf{x}' - \mathbf{x}(s))$$

$$= \frac{\mu I}{c}\oint_L dx'_k\, G^c(\mathbf{x} - \mathbf{x}'). \quad (1.106)$$

Now, the Coulomb Green function is explicitly,

$$G^c(\mathbf{x} - \mathbf{x}') = \frac{1}{4\pi R}, \quad (1.107)$$

where $R = |\mathbf{x} - \mathbf{x}'|$ is the relative distance between $\mathbf{x}$ and $\mathbf{x}'$. This brings (1.105) and (1.106) to the simple forms

$$A_k(\mathbf{x}) = \frac{\mu}{4\pi c}\int d^3x' \frac{1}{R} j_k(\mathbf{x}'), \quad (1.108)$$

$$A_k(\mathbf{x}) = \frac{\mu I}{4\pi c}\oint_L dx'_k \frac{1}{R}. \quad (1.109)$$

The Coulomb gauge (1.99) on the left-hand side is assured by current conservation (1.93) on the right-hand side.

It is worth recalling that due to current conservation, the left-hand side of Eq. (1.94) states that

$$\varepsilon_{ijk}\,\partial_i\,\partial_j\, B_k = 0,$$

which is equivalent to the statement that the *magnetic field satisfies the integrability condition*, which is a necessary physical requirement for the magnetic field to be a physical observable. It cannot be multivalued (as γ can), not even in a multiply connected domain of space.

Given the A_k field from (1.109) we can now calculate the magnetic field strength as follows:

$$B_i(\mathbf{x}) = \varepsilon_{ijk}\,\partial_i A_k(\mathbf{x}) = \frac{\mu I}{4\pi c}\,\varepsilon_{ijk} \oint_L dx'_k\,\partial_i \frac{1}{R} = -\frac{\mu I}{4\pi c}\,\varepsilon_{ijk} \oint_L dx'_k\,R_j/R^3,$$

(1.110)

where $R_j \equiv x_j - x'_j$ is the distance vector pointing from the line element to $\mathbf{x}$. Since the superflow configuration of vortex lines follows the same equations [recall (1.90)–(1.92)], except that $\mu I/c$ is replaced by $(\hbar/M)2\pi n \equiv \kappa_n$ [recall (1.63)], Eq. (1.110) gives directly the superfluid velocity field of a vortex line of strength n:

$$v_{si}(\mathbf{x}) = \frac{\kappa_n}{4\pi}\,\varepsilon_{ijk} \oint_L dx'_k\,\partial_j \frac{1}{R} = -\frac{\kappa_n}{4\pi}\,\varepsilon_{ijk} \oint_L dx'_k\,R_j/R^3.$$

(1.111)

For an ensemble of lines, L_1, L_2, L_3, ... with strengths n_1, n_2, n_3, ..., the resulting velocity is simply the sum of the individual terms.

In principle, we can now calculate the flow energy from the formula

$$E = \int d^3x\,\frac{1}{2}\rho_s\,v_s^2.$$

(1.112)

In the magnetic case we are used to calculating

$$E = \int d^3x\,\frac{1}{2\mu}B_i^2.$$

(1.113)

This is done by writing one of the $\mathbf{B}$ fields as $(\nabla \times \mathbf{A})$ and performing a partial integration as follows:

$$E = \frac{1}{2\mu} \int d^3x\,\varepsilon_{ijk}(\partial_j A_k)\,B_i$$

$$= \frac{-1}{2\mu} \int d^3x\,A_k\,\varepsilon_{kij}\,\partial_j B_i = \frac{1}{2\mu} \int d^3x\,\mathbf{A}\cdot\nabla \times (\nabla \times \mathbf{A}).$$

(1.114)

With (1.98) this becomes

$$E = \frac{1}{2c} \int d^3x\,A_k(\mathbf{x})j_k(\mathbf{x})$$

(1.115)

and, inserting (1.108), one finds

$$E = \frac{\mu}{2} \frac{1}{4\pi c^2} \int d^3x\, d^3x'\, j(\mathbf{x}) \frac{1}{R} j(\mathbf{x}').$$ (1.116)

If L is an ensemble of lines $L^{(i)}$ with currents $I^{(i)}$ this can be written as

$$E = \frac{\mu}{2} \sum_{i,j} \frac{I^{(i)} I^{(j)}}{4\pi c^2} \oint_{L^{(i)}} dx^{(i)} \oint_{L^{(j)}} dx^{(j)} \frac{1}{R^{(ij)}},$$ (1.117)

where $R^{(ij)} = |\mathbf{x}^{(i)} - \mathbf{x}^{(j)}|$. This is the well-known *Biot–Savart law*.

This result can be translated directly to the superflow energy E by exchanging $\mu I^{(i)}/c \rightarrow (\hbar/M) 2\pi n^{(i)} = \kappa^{(i)}$ and $\mu \rightarrow 1/\rho_s$. Hence (1.117) becomes

$$E = \frac{\rho_s}{2} \sum_{i,j} \frac{\kappa^{(i)} \kappa^{(j)}}{4\pi} \oint_{L^{(i)}} dx^{(i)} \oint_{L^{(j)}} dx^{(j)} \frac{1}{R^{(ij)}}.$$ (1.118)

This law has the consequence that parallel vortex lines of like strength repel each other (since increasing R lowers the energy). Notice that even though the field energy has the same form as (1.117), the forces are *opposite* to the magnetic case where parallel currents attract each other.
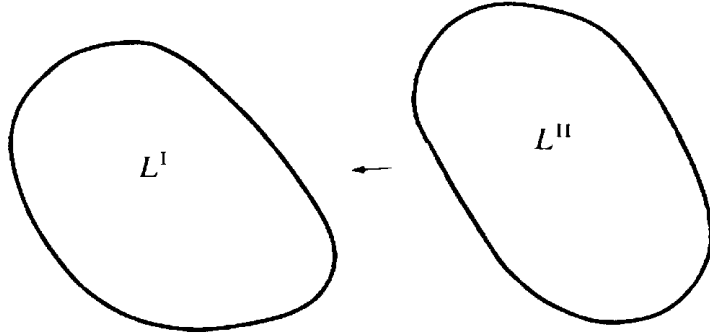
The difference cannot be explained with purely magnetostatic considerations. It is rooted in *electromagnetism*, namely, in the fact that a change in the magnetic field gives rise to an electric field $\mathbf{E}$ which satisfies

$$\partial_t \mathbf{B} = -\nabla \times \mathbf{E}.$$ (1.119)

This induced electric field changes the current and therefore the field energy. An elementary consideration shows that induction simply reverses the sign of the forces between current loops: Consider, for example, a pair of parallel current loops L^{I} and L^{II} at some distance apart (see Fig. 1.13). Anchor L^{I} at a fixed position and move L^{II} towards L^{I}. This increases the magnetic field energy. If the currents are held fixed, work has to be done against the field energy which increases by the amount

$$\delta E = \frac{I^{II}}{c} \oint_{L^{II}} dx_i\, \delta A_i^{I},$$ (1.120)

FIG. 1.13.   Two current loops illustrating the sign reversal of the magnetic field energy due to induction.

where δA^{I} is the magnetic potential along L^{II} coming from L^{I}. Using Stokes' theorem, this line integral can be rewritten in terms of the change of the magnetic flux $\Phi^{\mathrm{I}} = \int_{S^{\mathrm{II}}} dS_k\, B_k^{\mathrm{I}}$ through L^{II}, i.e.,

$$\delta E = \frac{I^{\mathrm{II}}}{c}\,\delta\Phi^{\mathrm{I}}. \qquad (1.121)$$

Because of the interchangeability of the roles of the two loops, we can also write

$$\delta E = \frac{I^{\mathrm{I}}}{c}\,\delta\Phi^{\mathrm{II}}, \qquad (1.122)$$

or

$$\delta E = \frac{1}{2c}\left(I^{\mathrm{II}}\,\delta\Phi^{\mathrm{I}} + I^{\mathrm{I}}\,\delta\Phi^{\mathrm{II}}\right). \qquad (1.123)$$

This δE is, however, not the total energy change of the system. Even if the operation is done arbitrarily slowly there is always a finite rate $(\delta/\delta t)\,\Phi^{\mathrm{I}}$ at which the flux changes, which can be written as

$$\frac{\delta}{\delta t}\Phi^{\mathrm{I}} = \int_{S^{\mathrm{II}}} dS_k\,\frac{\partial B}{\partial t}. \qquad (1.124)$$

But, according to the induction law (1.119), this rate of change is accompanied by an electric field $\mathbf{E}$ which satisfies

$$\frac{\delta\Phi^{\mathrm{I}}}{\delta t} = -\int_{S^{\mathrm{II}}} dS_k(\nabla \times \mathbf{E})_k, \qquad (1.125)$$

which by Stokes' theorem is equal to the integral $-\oint_{L^{II}} dx_i E_i$. This amounts to a voltage around the loop which is opposed to the current direction. Therefore it slows the current down and this energy decreases by:

$$\frac{\delta E^{II}}{\delta t} = -\frac{I^{II}}{c}\frac{\delta \Phi^I}{\delta t} = \frac{1}{c}\frac{I^{II}}{c}\oint_{L^{II}} dx_i E_i, \qquad (1.126)$$

where we have used (1.120), (1.124) and Stokes' theorem. Now, the same decrease takes place in the loop L^I due to the rate of change of the flux coming from L^{II}:

$$\frac{\delta E^I}{\delta t} = -\frac{I^I}{c}\frac{\delta \Phi^{II}}{\delta t}. \qquad (1.127)$$

It follows that the amount of change in the induced energy inside the loops, within an arbitrary time interval δt, is just twice as big and of opposite sign as the amount of increase in magnetic field energy when the currents were held fixed. The final configuration with the two parallel loops brought closer to each other carries smaller currents and therefore a smaller field energy than the initial one. Formally, the factor two has its origin in the quadratic appearance of the currents in the field energy

$$E = \frac{\mu}{2}\frac{1}{4\pi c^2}\int d^3x\, d^3x'\, \mathbf{j(x)} \cdot \mathbf{j(x')}\frac{1}{R}. \qquad (1.128)$$

Symbolically the operation just performed is an application of the chain rule of differentiation

$$\delta E = \frac{\mu}{2}\frac{1}{4\pi c^2}\left[\int d^3x\, d^3x'\, \mathbf{j(x)} \cdot \mathbf{j(x')}\,\delta\frac{1}{R} + 2\int d^3x\, d^3x'\,\delta\mathbf{j(x)} \cdot \mathbf{j(x')}\frac{1}{R}\right]. \qquad (1.129)$$

The first step symbolizes the change of distances at fixed currents, the second the change of the currents due to induction. The law of induction makes the second integral equal but opposite in sign to the first, so that

$$\delta E = -\frac{\mu}{2}\frac{1}{4\pi c^2}\int d^3x\, d^3x'\, \mathbf{j(x)} \cdot \mathbf{j(x')}\,\delta\frac{1}{R}. \qquad (1.130)$$

This is the origin for the attraction between parallel current loops. In

contrast to this, loops of vortex lines are *not* subject to the law of induction and for them only the first piece in (1.129) is present,

$$\delta E = \frac{\rho_s}{2} \frac{\kappa^{\mathrm{I}} \kappa^{\mathrm{II}}}{4\pi} \oint_{L^{\mathrm{I}}} dx_i \oint_{L^{\mathrm{II}}} dx_i' \delta \frac{1}{R} \cdot \tag{1.131}$$

This explains why parallel loops repel each other.

1.8.   VECTOR POTENTIAL VERSUS PHASE ANGLE

In the last section we used the analogy of the superfluid velocity with the magnetic field and found a straightforward solution for superflow configurations of vortex lines and the associated energies. In view of the applications to come it is worthwhile to present an alternative discussion of the same problem which makes more direct use of the phase variable γ rather than the velocity variable $\mathbf{v}_s$.

In terms of γ the energy is [recall (1.60)]

$$E = \frac{\sigma}{2} \int d^3x (\partial_i \gamma)^2 \tag{1.132}$$

with $\alpha = \rho_s (\hbar/M)^2$. We now define a conjugate variable b_i by

$$b_i = \frac{\delta E}{\delta \partial_i \gamma} = \sigma \partial_i \gamma, \tag{1.133a}$$

which is proportional to the superflow velocity

$$b_i = \rho_s \frac{\hbar}{M} v_{si}. \tag{1.133b}$$

The Euler–Lagrange equation is just the Poisson differential equation

$$\nabla^2 \gamma(\mathbf{x}) = 0, \tag{1.134}$$

or, in terms of b_i

$$\partial_i b_i(\mathbf{x}) = 0. \tag{1.135}$$

Changes of $\gamma(\mathbf{x})$ introduce changes in the field energy,

$$\delta E = \int d^3x\, b_i(\mathbf{x})\, \delta\partial_i\, \gamma(\mathbf{x}).\tag{1.136}$$

Consider now a current loop along L^{II} with a field b_i^{II}, say. Suppose we introduce into this field another loop along L^{I}. The change in energy can be written as

$$\delta E^{\mathrm{I\,II}} = \int d^3x\, b_i^{\mathrm{II}}\, \delta\partial_i\, \gamma^{\mathrm{I}} = \int d^3x\, b_i^{\mathrm{II}}\, \partial_i\, \delta\gamma^{\mathrm{I}}.\tag{1.137}$$

Because of the vanishing divergence of b_i this is equal to

$$\delta E^{\mathrm{I\,II}} = \int d^3x\, \partial_i(b_i^{\mathrm{II}}\, \delta\gamma^{\mathrm{I}}).\tag{1.138}$$

This expression looks ready for an application of Gauss's law by which it can be transformed into a surface integral of the form

$$\int dS_i(b_i^{\mathrm{II}}\, \delta\gamma^{\mathrm{I}}).\tag{1.139}$$

In doing this we must, however, be careful since the variable $\delta\gamma^{\mathrm{I}}$ is multivalued. The derivative $\partial_i\,\delta\gamma^{\mathrm{I}}$ in (1.137) is free of ambiguities so that (1.138) is well defined. The integral (1.139), on the other hand, does contain the multivalued field $\gamma(\mathbf{x})$ itself. In order to do the integral we have to specify $\gamma(\mathbf{x})$ in a unique way. For example, a straight vortex line along the z-axis has a phase angle

$$\gamma(\mathbf{x}) = n \tan^{-1} x_2/x_1,\tag{1.140}$$

where the arctangent is a multivalued function.

A possible specification would be to take the principal value of the arctangent. In this case γ acquires a discontinuity along the negative x_1 semi-axis $x_2 = 0$, $x_1 < 0$, where it jumps from π to $-\pi$. Close to the x_1 axis γ has the form

$$\gamma(\mathbf{x}) \approx \pi n\Theta(-x_1)(\Theta(x_2) - \Theta(-x_2)),\tag{1.141}$$

where

$$\Theta(x) = \begin{cases} 1 & x > 0, \\ 0 & x \leq 0, \end{cases} \tag{1.142}$$

is the Heaviside step function. Since $\partial_x \Theta(x) = \delta(x)$, the derivative of $\gamma(\mathbf{x})$ has a δ-function singularity:

$$\partial_1 \gamma(\mathbf{x}) \approx -\pi n \delta(x_1)(\Theta(x_2) - \Theta(-x_2)),$$

$$\partial_2 \gamma(\mathbf{x}) \approx 2\pi n \Theta(-x_1) \delta(x_2). \tag{1.143}$$

Notice, that since this singular $\gamma(\mathbf{x})$ is single valued, it is now also integrable in the entire space: $(\partial_1 \partial_2 - \partial_2 \partial_1) \gamma(\mathbf{x}) = 0$. This contrasts with the smooth derivatives of (1.140), i.e.,

$$\partial_1 \gamma(\mathbf{x}) = -nx_2/(x_1^2 + x_2^2), \quad \partial_2 \gamma(\mathbf{x}) = nx_1/(x_1^2 + x_2^2)$$

[recall (1.58)], which satisfy $(\partial_1 \partial_2 - \partial_2 \partial_1) \gamma(\mathbf{x}) = 2\pi n \, \delta^\perp(\mathbf{x}_\perp)$. The singularity (1.143) amounts to an infinite superflow velocity $v_{si} \propto b_i$ concentrated on the semi-axis $x_2 = 0$, $x_1 < 0$ and pointing in the x_2 direction. This is clearly an unphysical property brought about merely by making $\gamma(\mathbf{x})$ single valued. This unphysical property is stressed by the fact that the singularity moves to other places when choosing another prescription for making $\gamma(\mathbf{x})$ single valued. Nothing forces us to take the principle value. For example, we could let $\gamma(\mathbf{x})$ jump from 2π to 0 when x crosses the positive semi-axis $x_2 = 0$, $x_1 > 0$. It is obvious that the same type of freedom exists if the vortex does not form a straight line but an arbitrary loop. Then the singular plane becomes a surface spanned by the loop and it is this surface which can be placed anywhere in space as long as its border is attached to the loop (see Fig. 1.14).

Given such a singular surface, the energy formula (1.139) can obviously be applied only after having excluded this surface from the integral. We therefore enclose the surface by a very flat ellipsoid and call one side of its surface S^+, the other S^- in such a way that following the oriented boundary line L in the positive sense, the right-handed circuit integral $\oint d\gamma$ begins at S^+ and ends at S^- (see Fig. 1.15). The volume integral covers only the space outside this ellipsoid. Correspondingly, when applying Stokes' theorem and going from (1.138) to (1.139), the surface integral runs over the surface of this restricted space which consists of the surface at infinity, S^∞ and the half surfaces S^+, S^- of the ellipsoid where

FIG. 1.14. The surface S associated with a vortex line L, where the phase angle jumps by 2π. Notice that S can be moved freely around in space since it is not associated with a physically observable quantity, except for its fixed boundary at L.

$v_{si} \propto \partial_i \gamma$

vortex line

$\gamma = 0$

S $\dfrac{0}{2\pi}$ $\dfrac{0}{2\pi}$ $\dfrac{\gamma = 0}{2\pi}$

$\dfrac{0}{2\pi}$

$\oint d\gamma = 2\pi$

L
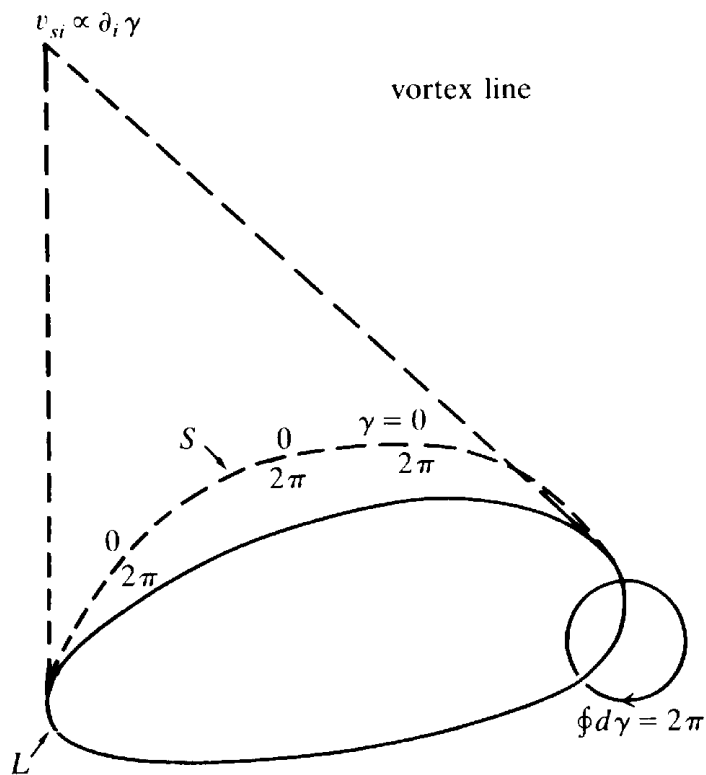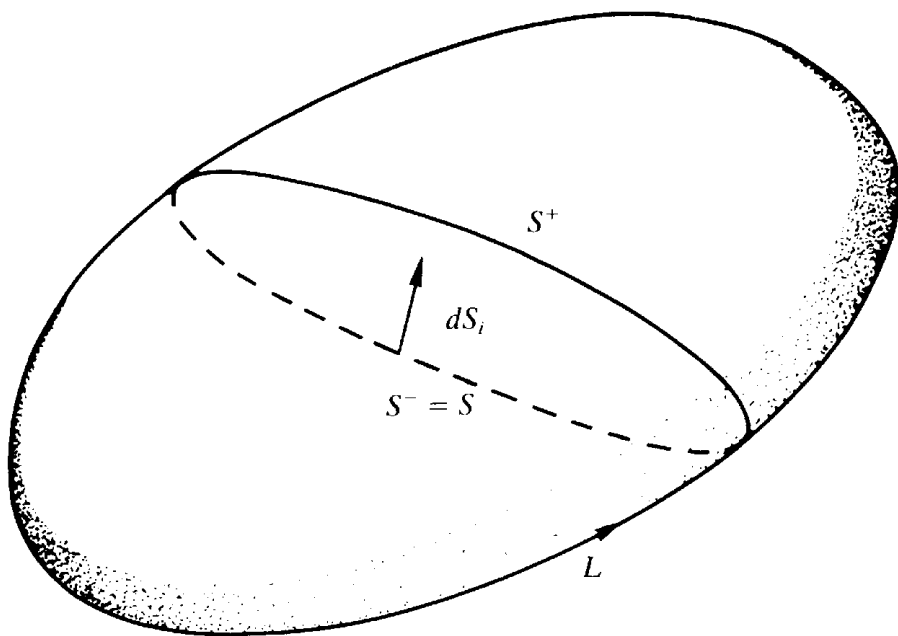
FIG. 1.15. Geometry for the calculation of the energy of a vortex line in the superflow of another. The flat ellipsoid encloses the surface S across which γ jumps by 2π.

S^+

dS_i

$S^- = S$

L

the normal vectors point inward. The first integral vanishes. The second integral can easily be evaluated. If we imagine decreasing the thickness of the ellipsoid to zero, the field b_i^{II} will be the same on both half surfaces S^+ and S^- so that we can rewrite (1.139) in the form

$$\int_{S^-} dS_i\, b_i^{II} (\gamma_{S^-} - \gamma_{S^+}).$$ (1.144)

The discontinuity of the phase variable is, however, determined by the vortex structure,

$$\gamma_{S^-} - \gamma_{S^+} = 2\pi n^I.$$ (1.145)

Hence we find

$$E^{I,\,II} = 2\pi n^I \int_{S^-} dS_i\, b_i^{II}.$$ (1.146)

This is an integral over the half surface S^- which is practically the same as the singular surface S. Since the surface is a mathematical artifact, and only the boundary, the vortex line, is a physical object, this integral should depend only on the shape of the boundary. Indeed, it does, due to the vanishing divergence of the b_i field. This makes it possible to introduce a vector potential **a** via

$$\mathbf{b} = \nabla \times \mathbf{a},$$ (1.147)

after which one can use Stokes' theorem and rewrite (1.146) as a contour integral over the boundary L^I of S:

$$E^{I,\,II} = 2\pi n^I \oint_{L^I} dx_k\, a_k^{II}.$$ (1.148)

In this way we have arrived at a *local coupling* of the vortex line L^I to the vector potential of the vortex line L^{II}. The decomposition is gauge invariant and so is the local coupling (1.148). Indeed, replacing $a_i(\mathbf{x})$ by a gauge transformed vector potential

$$a_k(\mathbf{x}) + \partial_k \Lambda(\mathbf{x}),$$

this brings about a change in energy

$$\oint_{L'} dx_k \, \partial_k \Lambda(\mathbf{x}) = \int d^3x \, \delta_k(L) \, \partial_k \Lambda(\mathbf{x}) = -\int d^3x \, \partial_k \, \delta_k(L) \Lambda(\mathbf{x}),$$

$$(1.149)$$

and this vanishes for closed lines [recall (1.82)]. It is the basic virtue of gauge fields to make couplings to unphysical surfaces local and depend only on the physical boundary.

Let us now see how the vector potential $\mathbf{a}^{ll}(\mathbf{x})$ can be calculated making use only of the phase variable $\gamma(\mathbf{x})$. Consider a vortex loop along L. What we have to do is solve the Poisson field equation (1.134), $\nabla^2 \gamma = 0$, in the presence of this loop. For this we make again $\gamma(\mathbf{x})$ single valued by choosing a singular surface S across which γ jumps by $2\pi n$. Enclosing the surface S by a thin ellipsoid, the space has a total surface S^x, S^+, S^-. We can then use Green's theorem to calculate the solution to the Poisson equation for arbitrary boundary values

$$\gamma(\mathbf{x}) = \frac{1}{4\pi} \int_S dS'_k \left(\frac{1}{R} \partial'_k \gamma - \gamma \partial'_k \frac{1}{R} \right).$$

$$(1.150)$$

Recall how this theorem is derived: One considers Gauss' law for a vector field

$$\int_V d^3x \, \partial_i V_k = \int_S dS_i V_k,$$

$$(1.151)$$

and applies this to the vectors

$$V_k^{(1)}(\mathbf{x}') = \gamma(\mathbf{x}') \, \partial'_k \, G^c(\mathbf{x}' - \mathbf{x}),$$

$$V_k^{(2)}(\mathbf{x}') = \partial'_k \, \gamma(\mathbf{x}') \, G^c(\mathbf{x}' - \mathbf{x}),$$

$$(1.152)$$

where $G^c(\mathbf{x} - \mathbf{x}')$ is the Green function for the Poisson equation

$$-\nabla^2 G^c(\mathbf{x} - \mathbf{x}') = \delta^{(3)}(\mathbf{x} - \mathbf{x}'),$$

$$(1.153)$$

i.e., $G^c(\mathbf{x} - \mathbf{x}')$ is the Coulomb Green function (1.107), $1/(4\pi R)$. We find

$$\int_V d^3x' \, \partial'_k(\gamma(\mathbf{x}') \, \partial'_k \, G^c(\mathbf{x}' - \mathbf{x})) = \int_S dS'_k \, \gamma(\mathbf{x}') \, \partial'_k \, G^c(\mathbf{x}' - \mathbf{x}),$$

$$\int_V d^3x' \, \partial'_k(\partial'_k \, \gamma(\mathbf{x}') \, G^c(\mathbf{x}' - \mathbf{x})) = \int_S dS'_k \, \partial'_k \, \gamma(\mathbf{x}') \, G^c(\mathbf{x}' - \mathbf{x}). \quad (1.154)$$

Subtracting the equations from each other we find

$$
\int_V d^3x' (\gamma(\mathbf{x}') \nabla'^2 G^c(\mathbf{x}' - \mathbf{x}') - (\nabla'^2 \gamma(\mathbf{x}'))G^c(\mathbf{x}' - \mathbf{x}))
$$

$$
= \int_S dS'_k (\gamma(\mathbf{x}') \partial'_k G^c(\mathbf{x}' - \mathbf{x}) - (\partial'_k \gamma(\mathbf{x}')) G^c(\mathbf{x}' - \mathbf{x})). \quad (1.155)
$$

Inserting here (1.153), (1.134) and the explicit form of G^c does indeed lead to equation (1.150).

This equation can now be integrated over S^∞, S^+, S^-. The contribution of S^∞ vanishes. That over the ellipsoid $S^+ + S^-$ can be calculated by going only over $S \equiv S^-$ and replacing the integrand by its discontinuity across the thin ellipsoid. Now, the derivative of γ is the physical superflow velocity which has no discontinuity. The angle γ itself does, however, jump by $2\pi n$. Therefore we find

$$
\gamma(\mathbf{x}) = -\frac{2\pi n}{4\pi} \int_S dS'_k \, \partial'_k \frac{1}{R} = \frac{2\pi n}{4\pi} \Omega(\mathbf{x}), \quad (1.156)
$$

where

$$
\Omega(\mathbf{x}) = -\int_S dS'_k \, \partial'_k \frac{1}{R} = \int_S dS'_k \, R_k / R^3. \quad (1.157)
$$
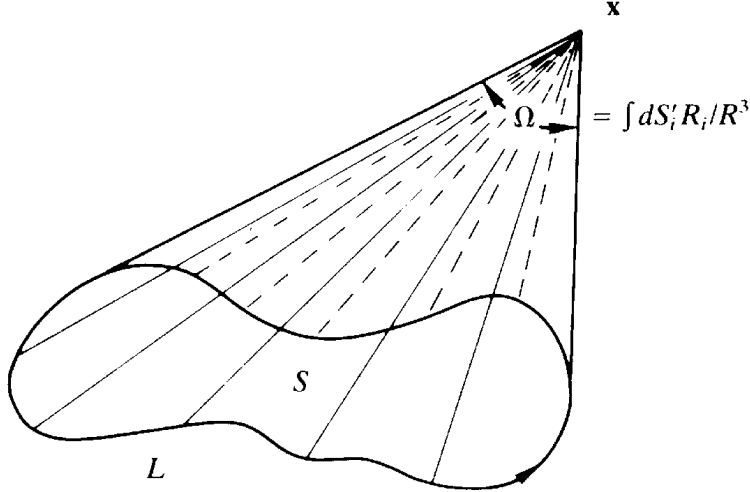
This quantity has a simple geometric meaning. The scalar product $dS'_k R_k / R$ is the projection of the surface element along the direction $R_k = (x - x')_k$. When dividing this quantity by R^2 it becomes the infinitesimal solid angle under which dS_k appears to an observer at $\mathbf{x}$. Hence Ω is the total solid angle spanned by the surface S (see Fig. 1.16). When crossing the surface S from the negative to the positive side, Ω jumps by 4π and γ jumps by $2\pi n$, as it should.

From (1.133b), the quantity b_i is proportional to the superfluid velocity and can be calculated:

$$
b_i = \sigma \frac{2\pi n}{4\pi} \int_S dS'_k \, \partial_i (R_k / R^3). \quad (1.158)
$$

Since $\partial_k (R_k / R^3) = \delta^{(3)}(\mathbf{x} - \mathbf{x})$, this can also be written as

FIG. 1.16. Illustration of the total solid angle under which a vortex loop is seen from the point **x**. (R_i denotes the components of the vector from the point **x** to the surface element dS'_i.)

$$b_i = \sigma \frac{2\pi n}{4\pi} \left[\int_S (dS'_k \, \partial_i R_k / R^3 - dS'_i \partial_k R_k / R^3) + \int_S dS'_i \, \delta^{(3)}(\mathbf{x} - \mathbf{x}') \right].$$

Using Stokes' theorem in the form $\int_L dx_j \, \varepsilon_{jki} = \int_S (dS_k \, \partial_i - dS_i \, \partial_k)$, this becomes

$$b_i(\mathbf{x}) = \sigma \frac{2\pi n}{4\pi} \oint_L dx_j \, \varepsilon_{jki} R_k / R^3 + \sigma \frac{2\pi n}{4\pi} \int dS'_i \, \delta^{(3)}(\mathbf{x} - \mathbf{x}'). \qquad (1.159)$$

which can be rewritten as

$$b_i(\mathbf{x}) = \varepsilon_{ijk} \, \partial_j a_k - \sigma \frac{2\pi n}{4\pi} \int_S dS'_i \, \delta^{(3)}(\mathbf{x} - \mathbf{x}'), \qquad (1.160)$$

with

$$a_k = \sigma \frac{2\pi n}{4\pi} \oint_L dx_k \frac{1}{R}. \qquad (1.161)$$

The second piece in (1.160) is the unphysical, singular part of b_i caused by making $\gamma(\mathbf{x})$ single valued. It is not really present in the superflow and must be dropped. The first piece gives the superflow around a vortex loop. With $L = L^{II}$, $n = n^{II}$, a_k may be inserted into formula (1.147), (1.148) and we obtain the interaction energy

$$E^{\mathrm{I\,II}} = \sigma \frac{2\pi n^{\mathrm{I}} 2\pi n^{\mathrm{II}}}{4\pi} \int_{L^{\mathrm{I}}} d\mathbf{x}^{\mathrm{I}} \cdot \int_{L^{\mathrm{II}}} d\mathbf{x}^{\mathrm{II}} \frac{1}{R} \cdot \qquad (1.162)$$

This formula can be generalized to an arbitrary ensemble of vortex lines:

$$E = \frac{\sigma}{2} \sum_{i,j} \frac{2\pi n^{(i)} 2\pi n^{(j)}}{4\pi} \oint_{L^{(i)}} d\mathbf{x}^{(i)} \cdot \oint_{L^{(j)}} d\mathbf{x}^{(j)} \frac{1}{R^{(ij)}}, \qquad (1.163)$$

and agrees with formula (1.131) which we derived earlier. When evaluating this expression for a given ensemble of lines one should note that the ideal superflow exists only at a distance $r \gtrsim \xi$ from each vortex line. This will therefore imply certain cutoffs in the integrals. We also should remember that the hydrodynamic energy is not the total energy but has to be supplemented by the core energy.

The cutoff procedure can be defined best by formulating the interaction energy in terms of volume integrals over vortex densities. In magnetism we stated the Biot–Savart law for arbitrary continuous current densities $\mathbf{j}(\mathbf{x})$ in the form

$$E = \frac{\mu}{2} \frac{1}{4\pi c^2} \int d^3x \, d^3x' \, \mathbf{j}(\mathbf{x}) \cdot \mathbf{j}(\mathbf{x}') \frac{1}{R} \cdot \qquad (1.164)$$

We can formally do the same thing and use the vortex density introduced in Eq. (1.73), which depends only on the positions of the vortex lines, i.e.,

$$\alpha_k(\mathbf{x}) = \sum_i 2\pi n^{(i)} \delta_k(L^{(i)}).$$

Then the energy becomes

$$E = \frac{\sigma}{2} \frac{1}{4\pi} \int d^3x \, d^3x' \, \alpha_k(\mathbf{x}) \alpha_k(\mathbf{x}') \frac{1}{R} \cdot \qquad (1.165)$$

If we now soften the δ-functions along the vortex lines in the manner discussed above in the context of Eq. (1.64), the volume integrations will receive the proper cutoffs due to the finite core radii of the lines.

NOTES AND REFERENCES

Superfluidity was discovered by
R. Ya. Kapitza, *Nature* **141** (1937) 74, *JETP* **11** (1941) 1, *JETP* **11** (1941) 581.
 The first theoretical explanation was given by
L.D. Landau, *JETP* **11** (1941) 592.
 Details are found in the textbook
L.D. Landau and E.M. Lifshitz, *Statistical Mechanics* (Pergamon Press, New York, 1958).
 For Pitaevskii's approach, see
L.P. Pitaevskii, *JETP* **13** (1961) 451.
 The superfluid density and specific heat of ^{4}He are given in
W.M. Fairbank and C.F. Keller, *Nat'l. Bur. St. Misc. Publ.* **273**, (1966).
 For the Nambu–Goldstone mechanism see any textbook in quantum field theory. The original papers are by
Y. Nambu and F. Jona-Lasinio, *Phys. Rev.* **122** (1961) 345,
J. Goldstone, *Nuovo Cimento* **19** (1961) 154,
J. Goldstone, A. Salam and S. Weinberg, *Phys. Rev.* **127** (1962) 965.
 Vortex lines in rotating superfluid ^{4}He have been photographed by
G.A. Williams, R.E. Packard, *Phys. Rev. Lett.* **33** (1974) 280,
G.B. Hess, W.H. Fairbank, *Phys. Rev. Lett.* **19** (1967) 216,
R.E. Packard, and T.M. Sanders, *Phy. Rev.* **A6** (1972) 799,
K. De Conde, G.A. Williams, R.E. Packard, *Phys. Rev. Lett.* **33** (1974) 683.
 A general review on vortex lines was given by
A.L. Fetter, in *The Physics of Liquid and Solid He, Part I*, eds. K.H. Bennemann and J.B. Ketterson (J. Wiley, New York, 1976).

GRAND CANONICAL ENSEMBLES OF INTERACTING VORTEX LINES

2.1. DISORDER FIELDS FOR VORTEX LINES

In the last chapter we argued that the energy of an ensemble of vortex lines can be calculated approximately as long as their average spacing is sufficiently large compared to their thickness. The energy decomposes into a hydrodynamic piece governed by the ideal superflow expression $(1/2)\rho_s v_s^2$ and a core piece proportional to the length of the lines. The hydrodynamic piece has the same form as the Biot-Savart magnetic energy of a system of current loops. The core energy can be written, for N lines, in the approximate form

$$E_{\text{core}} = e_c \sum_{i=1}^{N} \int_{L^{(i)}} ds^{(i)}, \qquad (2.1)$$

where $ds^{(i)}$ is the length parameter along the line $L^{(i)}$ and $e_c \approx f_c \xi^2 4\pi n^2 \cdot 0.385$ the core energy per unit length [see (1.56)].

We can now easily set up the partition function for this ensemble. It reads

$$Z = \sum_N \frac{1}{N!} \sum_{\{L\}} \exp\left\{ -\frac{1}{T}\left[\frac{\rho_s}{2} \sum_{i,j} \frac{\kappa^{(i)}\kappa^{(j)}}{4\pi} \int ds^{(i)}\, ds^{(j)}/R + e_c \sum_i \int ds^{(i)} \right] \right\}, \qquad (2.2)$$

where $\Sigma_{\{L\}}$ stands symbolically for the sum over all line configurations. The factor $1/N!$ is necessary since the lines are all indistinguishable. For simplicity, we shall assume that the lines are completely random.

Suppose, for the moment, that there is no hydrodynamic energy. Then we can take advantage of the results derived in Part I, according to which the statistical mechanics of random lines can be formulated in terms of a complex disorder field theory. We had shown that the partition function of random lines is given by a path integral of the type

$$Z = \int \mathcal{D} \varphi \, \mathcal{D} \varphi^{\dagger} \, e^{-\int d^3 x [(1/2)|\nabla \varphi|^2 + (m^2/2)|\varphi|^2 + (g/4)|\varphi|^4]} \tag{2.3}$$

[recall Eqs. (6.266), (6.291) of Part I]. The mass term

$$m^2 = \left(\frac{\varepsilon}{T} - \log 2D \right) \frac{2D}{a^2}$$

can be interpreted directly in terms of the energy per link ε, and a is the length of a link. The vortex lines we want to study have a thickness $\xi =$ coherence length. Hence we shall identify a with ξ. The energy per link is then equal to $\varepsilon = e_c a = e_c \xi$, i.e.,

$$\varepsilon \approx f_c \xi^2 4 \pi n^2 \cdot 0.385.$$

The coupling constant g describes the steric repulsion between the vortex lines when they come close to each other. Such a repulsion arises in the superfluid as follows: According to Section 1.6 a vortex line of higher strength always decays into two of lower strength since the hydrodynamic energy increases quadratically with n. The same dependence holds approximately also for the core energy due to the velocity behavior (1.61), according to which the core can be considered roughly as a region of solid rotation and such a rotational energy increases with the square of its angular velocity which, in turn, is proportional to n. Now, the increase of the line energy with n^2 prevents them from lying on top of each other. After all, $(|n_1| + |n_2|)^2$ is always larger than $n_1^2 + n_2^2$. The differences of the energies $\propto [(|n_1| + |n_2|)^2 - (n_1^2 + n_2^2)]$ is responsible for the steric repulsion as described by the coupling constant g. Numerical values of g will be determined later. They are not of interest at the moment. Also, we shall neglect in this discussion multi-vortex interactions in which several vortex lines meet at the same place, and which would produce

higher $|\varphi|^n$ terms in the disorder field energy. We shall later see how these are included.

Notice that the disorder field theory is invariant under global phase transformations:

$$\varphi(\mathbf{x}) \rightarrow e^{i\gamma}\varphi(\mathbf{x}).$$

It is well known that this property is what guarantees the conservation of the current

$$\partial_i j_i(\mathbf{x}) = \partial_i \left(\frac{1}{2i} \varphi^\dagger \overleftrightarrow{\partial_i} \varphi(\mathbf{x}) \right) = 0. \qquad (2.4)$$

This is the disorder field version of the conservation law (1.87) for the vortex density. The conservation law ensures that vortex lines never end and that branching lines conserve the vortex strength [recall the discussion in Section 1.6].

2.2. THERMODYNAMIC QUANTITIES

Let us now calculate the thermodynamic quantities of this disorder field theory at the mean field level. This can be done in complete analogy with the order field theory of the superfluid (1.10). The only difference is that the mass term becomes negative as the temperature *increases above* the critical temperature $T_c = e_c/\log(2D)$. There, the disorder field has a non-vanishing expectation value

$$|\varphi_0|^2 = -\frac{m_0^2}{g}\left(\frac{T_c}{T} - 1\right)$$

in contrast to the order fields $|\psi_0|^2 \propto -(T/T_c - 1)$ for $T < T_c$ in (1.11). The free energy at this field value is

$$\beta f = -\frac{m_0^4}{4g}\left(\frac{T_c}{T} - 1\right)^2,$$

which will be referred to as the mean field condensation energy of the dislocation lines. Just as in (1.12) we define a quantity $f_0 = (m_0^4/4g)\,T_c$ and write

$$\beta f = \begin{cases} 0 & T \leq T_c , \cdot \\ -\beta_c f_0 \left(\dfrac{T_c}{T} - 1\right)^2 & T > T_c . \end{cases} \qquad (2.5a)$$

Differentiation with respect to β gives the internal energy and entropy:

$$u = -\frac{\partial}{\partial \beta}(-\beta f) = -2f_0 \left(\frac{\beta}{\beta_c} - 1\right), \qquad (2.5b)$$
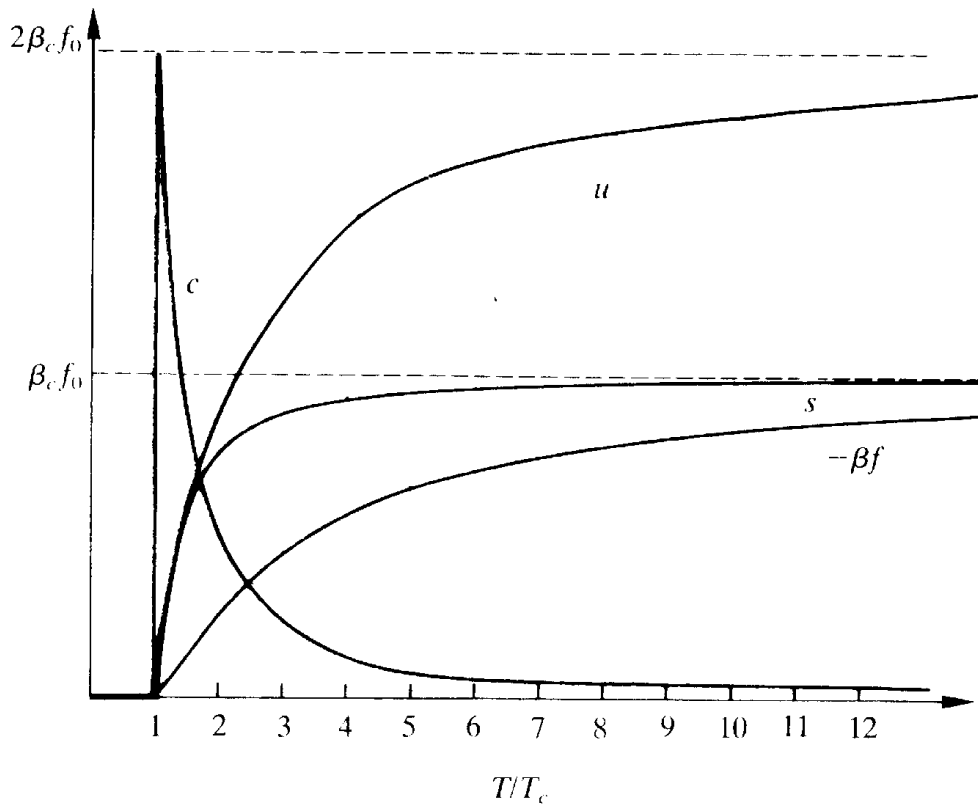
$$s = -\frac{\partial}{\partial T} f = -\left(1 - \beta \frac{\partial}{\partial \beta}\right)\beta f = -2\beta_c f_0 \left(\frac{\beta}{\beta_c} - 1\right)\left[1 + \frac{1}{2}\left(\frac{\beta}{\beta_c} - 1\right)\right]. \tag{2.5c}$$

From this follows the specific heat per volume,

$$c = T\frac{\partial}{\partial T} s = -\beta \frac{\partial}{\partial \beta} s = 2\beta f_0 \left[1 + \left(\frac{\beta}{\beta_c} - 1\right)\right] = \frac{2f_0 \beta^2}{\beta_c}. \qquad (2.5d)$$

The thermodynamic functions are plotted schematically on Fig. 2.1. The

FIG. 2.1.   The thermodynamic functions of the disorder-field theory (2.3) at the mean field level. In contrast to the order field theory (1.10), whose thermodynamic functions were shown in Fig. 1.3, disorder sets in *above* T_c.

behavior is similar to that of the mean field approximation for super-fluid helium, in Fig. 1.3, except that the temperature axis is reversed and the entropy *increases* as T moves *above* T_c, as a consequence of the proliferation of the dislocation lines.

2.3. NAMBU–GOLDSTONE MODES OF THE DISORDER FIELD

We already saw that the complex disorder field theory is trivially symmetric under the global phase transformations $\varphi(\mathbf{x}) \to e^{i\gamma}\varphi(\mathbf{x})$. As a consequence, the disordered phase must possess long-range Nambu–Goldstone modes associated with spatial modulations of the phase of the disorder parameter. Indeed, splitting φ into a radial and an azimuthal part, i.e.,

$$\varphi(\mathbf{x}) \equiv e^{i\gamma(\mathbf{x})}\rho(\mathbf{x}),$$

with a real field $\rho(\mathbf{x})$, the energy density reads

$$-\beta e = \frac{1}{2}(\nabla\gamma)^2\rho^2 + \frac{1}{2}(\nabla\rho)^2 + \frac{m^2}{2}\rho^2 + \frac{g}{4}\rho^4.$$

For $T > T_c$, $m^2 < 0$, where ρ fluctuates around the mean value $\rho_0 = \sqrt{-m^2/g}$, the derivative term for γ is $-(m^2/g)(1/2)(\nabla\gamma)^2$, displaying the long-range properties of the γ field just as in the order-field discussion leading to (1.30).

The question now arises as to the physical nature of these modes. The answer is easily found if we remember that, in the order field theory the current $j_i = (1/2i)\,\varphi^{\dagger}\overleftrightarrow{\partial_i}\varphi \approx \rho_0^2\partial_i\gamma$ represented the superflow. Consequently, the disorder version of this, $j_i = (1/2i)\,\varphi^{\dagger}\,\partial_i\,\varphi \approx \rho_0^2\partial_i\gamma$, must represent the defect flow, i.e., it contains the information on how the defect lines "run" through the system as a function of their length parameter s.

2.4. INCLUSION OF HYDRODYNAMIC FORCES

Let us now include the long-range forces between the vortex lines. According to Chapter 6, Part I, the Biot–Savart type energy (2.2) for a given set of vortex lines can be described by a fluctuating vector potential via the partition function

$$Z = \int \mathcal{D}A\,\Phi[\mathbf{A}]\,e^{-(1/T)\int d^3x[(1/2\rho_s)(\nabla\times\mathbf{A})^2 + i\sum_{i=1}^{N}\kappa^{(i)}\oint dx_i^{(i)}A_i]},$$ (2.6)

where $\Phi[\mathbf{A}]$ is one of the many possible gauge-fixing factors [see Part I Eqs. (3.31, 3.32, 3.35)]. This follows directly from comparing Eq. (6.186) of Part I with (2.2), leading to the identification $\mu = \rho_s$, $I^{(i)} = \kappa^{(i)}$ (after having used (6.188) of Part I). Indeed, integrating the $A_i(\mathbf{x})$ fluctuations out according to the general rules of Chapter 3, Part I, we recover the long-range hydrodynamic part of (2.2).

It is now a simple matter to introduce the same hydrodynamic forces into the grand canonical ensemble of vortex lines. All we have to do is couple the vector potential minimally into the disorder field theory of this ensemble in the way described in Chapter 6 of Part I. In this way we obtain the partition function

$$Z = \int \mathcal{D}A_i\,\Phi[\mathbf{A}]\int \mathcal{D}\varphi\,\mathcal{D}\varphi^\dagger\,e^{-\beta E[\varphi,\,\varphi^\dagger,\,\mathbf{A}]},$$ (2.7a)

where the energy can be written in the form

$$\beta E[\varphi,\mathbf{A}] = \frac{1}{2}(\nabla\times\mathbf{A})^2 + \frac{1}{2}|(\nabla - iq\mathbf{A})\varphi|^2 + \frac{m^2}{2}|\varphi|^2 + \frac{g}{4}|\varphi|^4.$$ (2.7b)

This is a gauge theory of a complex scalar field and we had studied it before. In order to make the notation as simple as possible, we find it convenient to replace the gauge field $\mathbf{A}$ by $\sqrt{T\rho_s}\,\mathbf{A}$. In this way the coupling to the φ field becomes

$$q = \sqrt{\frac{\rho_s}{T}}\kappa_1 = \sqrt{\frac{\rho_s}{T}}\frac{\hbar}{M}2\pi.$$ (2.8)

Only the fundamental lines of lowest vortex strength need to be summed since all other lines of higher strength $\kappa_n = n\kappa_1$ are contained in the sum in (2.7) by superposition of fundamental lines. Notice that the coupling to the gauge field $A_i(\mathbf{x})$ extends the global invariances under phase transformations (2.5) to the local gauge invariance

$$\varphi(\mathbf{x}) \to e^{iq\Lambda(\mathbf{x})}\varphi(\mathbf{x}),$$

$$A_i(\mathbf{x}) \to A_i(\mathbf{x}) + \partial_i \Lambda(\mathbf{x}).$$ (2.9)

The important point to realize now is that the energy (2.7b) has the same form as that used by Ginzburg and Landau in the theory of superconductivity. For this reason, the partition function (2.7) has become one of the best studied field theories in many-body physics. Before we analyze the way in which it describes the vortex lines in superfluid ^{4}He it is worthwhile to pause for a moment in the main development and recall the most important properties of this theory within the context of superconductivity. After this it will be quite easy to translate the results to the superfluid case.

NOTES AND REFERENCES

The statistical role of vortex lines was recognized by
R.P. Feynman, *Prog. Low Temp. Phys.* **1** (1955) 17,
E. Byckling, *Ann. Phys.* **32** (1965) 367,
V.N. Popov, *JETP* **37** (1973) 341,
F.W. Wiegel, *Physics* **65** (1973) 321, *Phys. Reports* **16** (1975) 58 and *Introduction to Path Integral Methods in Physics and Polymer Science* (World Scientific, Singapore, 1986).
Disorder fields for interacting vortex lines were introduced and studied in
H. Kleinert, *Lett. Nuovo Cimento* **34** (1982) 464, *Phys. Lett.* **89A** (1982) 294, *Phys. Lett.* **91A** (1982) 295, *Lett. Nuovo Cimento* **34** (1982) 209, *Phys. Lett.* **93A** (1982) 86.
    Similar considerations are possible for dislocation lines in other systems; for Smectic A liquid crystals, see for instance,
H. Kleinert, *J. Phys.* (Paris) **44** (1983) 353,
and for magnetic superconductors,
H. Kleinert, *Phys. Lett.* **90A** (1982) 259,
for pion condensates,
H. Kleinert, *Lett. Nuovo Cimento* **34** (1982) 103, and lectures presented at the 1983 Conference on *High Energy Nuclear Physics* at Lake Balaton, Hungary (Budapest University Press, Budapest, 1983).

GINZBURG–LANDAU THEORY OF SUPERCONDUCTIVITY

3.1. LONDON EQUATIONS

Superconductivity is a macroscopic quantum phenomenon occurring at low temperatures, of the order of a few degrees Kelvin. It was discovered in 1911 by Kamerlingh Onnes, three years after he had succeeded in liquefying ^{4}He. This feat allowed him to study the properties of many materials in the temperature range from 14 K down to 1 K. When measuring the electric resistance of mercury, he found that below 4 K it abruptly dropped to zero. An electric current in a closed mercury ring would circle around for a very long time without observable decay. Lifetimes of 10^5 years have been seen experimentally. Thus the conductivity is really "super," and the current behaves in very much the same way as a single electron moving around an atomic nucleus.

In 1933 Meissner and Ochsenfeld observed an important magnetic property of superconductors: they are perfect diamagnets, i.e., they cannot be penetrated by a magnetic field. Such fields can enter only a very thin surface layer, decaying exponentially as $e^{-x/\lambda}$ where λ is the so-called *penetration depth* which is of the order of a few hundred Angströms (see Fig. 3.1).

A phenomenological description of the magnetic phenomena was given by the brothers E. London and F. London in 1935. They assumed that a

certain fraction of electrons is able to form a permanent electric current $\mathbf{j}_s = n_s e \mathbf{v}_s$ with a number density n_s and velocity $\mathbf{v}_s$ so that their energy is

$$E = \frac{m}{2} \int d^3x \, n_s \, \mathbf{v}_s^2 = \frac{m}{2} \int d^3x \, \frac{1}{n_s e^2} \mathbf{j}_s^2. \tag{3.1}$$

Such a permanent current is coupled to a magnetic field via Ampère's law

$$\nabla \times \mathbf{H} = \frac{1}{c} \mathbf{j}_s.$$

From this they found the total energy of the system:

$$E = \frac{1}{2} \int d^3x \, [\mathbf{H}^2 + n_s m v_s^2] = \frac{1}{2} \int d^3x \, [\mathbf{H}^2 + \lambda^2 (\nabla \times \mathbf{H})^2], \tag{3.2}$$

where $\lambda = [mc^2/n_s e^2]^{1/2}$ has the dimension of length.

At the mean field level, this can be extremized to give the field equation
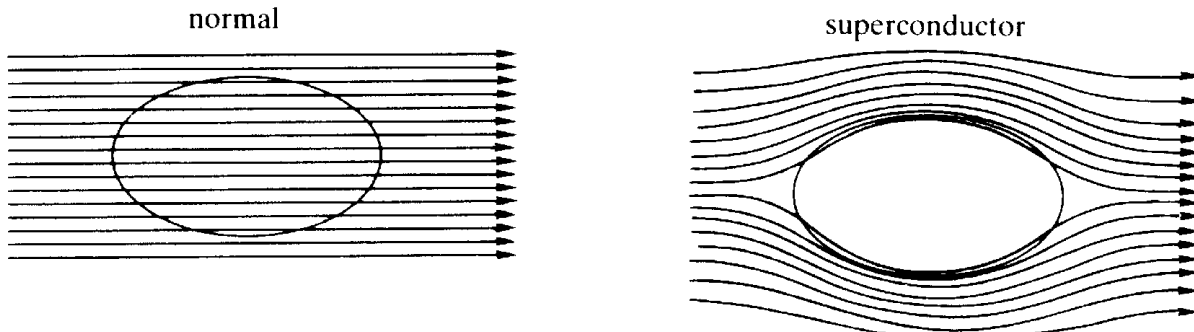
$$\mathbf{H} + \lambda^2 \nabla \times (\nabla \times \mathbf{H}) = 0, \tag{3.3}$$

or also, since $\mathbf{H}$ is divergenceless

$$\mathbf{H} - \lambda^2 \nabla^2 \mathbf{H} = 0. \tag{3.4}$$

This is solved by an exponential $e^{-x/\lambda}$ and explains the finite penetration depth of a magnetic field inside the superconductor. Equation (3.3) is the *first London equation* which can also be stated in the form

FIG. 3.1. The explusion of the magnetic field lines driving the superconducting phase transition (Meissner effect). In the superconductor the field lines have only a finite penetration depth, due to the non-zero value of the order parameter.

normal   superconductor

$$\nabla \times \mathbf{j}_s = -\frac{c}{\lambda^2} \mathbf{H}. \tag{3.5}$$

The observation that the permanent current moves just as a single free electron in the vacuum led the London brothers to the second equation

$$\frac{m}{e} \frac{\partial}{\partial t} \mathbf{j}_s = e n_s \mathbf{E}. \tag{3.6}$$

This equation states that the momentum change of the permanent current is equal to the electric force. It turns out that this equation is not completely independent of the first one. Indeed, its curl reads

$$\frac{m}{e} \frac{\partial}{\partial t} \nabla \times \mathbf{j}_s = e n_s \nabla \times \mathbf{E}. \tag{3.7}$$

By the law of induction,

$$\nabla \times \mathbf{E} = -\frac{1}{c} \frac{\partial}{\partial t} \mathbf{H}; \tag{3.8}$$

so that (3.7) is just the time derivative of the first London equation in the form (3.5).

3.2. ORDER PARAMETER

The thermodynamic understanding began in 1934 when Gorter and Casimir introduced the concept of an order parameter to describe the permanent currents. We had defined an order parameter before in the context of Pitaevskii's description of superfluidity. It was mentioned there that this concept really arose in the attempt to describe a superconductor. In modern notation, what Gorter and Casimir did was to introduce a quantity, nowadays denoted by $|\psi|^2$, which is proportional to the density ρ_s of superconductive electrons, and to postulate that *close* to the transition temperature T_c, at which superconductivity sets in, the free energy is described by

$$f \approx \frac{m^2}{2} |\psi|^2 + \frac{g}{4} |\psi|^4, \tag{3.9}$$

where the parameter m^2 contains the temperature dependence in the form $m^2 \approx m_0^2(T/T_c - 1)$. This is exactly the same expression as that discussed in Section 1.2 in the context of superfluidity, and so we see that for $T = T_c$, a second order phase transition takes place, with the free energy behaving quadratically in $(T/T_c - 1)$, the entropy linearly, and the specific heat jumping upwards when cooling through T_c.

In the superconductor, these characteristics agree with experiment perfectly, much better than the case for superfluid ^{4}He, where fluctuation corrections are rather large. The reason for this will become apparent soon.

3.3. ORDER FIELD

A few years after Gorter and Casimir introduced the order parameter, Landau realized that it is possible to study long wavelength variations of an order parameter by introducing an *order field* $\psi(\mathbf{x})$ and adding to the free energy a gradient energy leading to a fluctuating energy functional

$$E[\psi] = \int d^3x \, e(\mathbf{x}) = \int d^3x \left(\frac{1}{2} |\nabla \psi|^2 + \frac{m^2}{2} |\psi|^2 + \frac{g}{4} |\psi|^4 \right). \quad (3.10)$$

The factor beside the gradient energy can be chosen to be unity by an appropriate renormalization of the ψ field, the mass m, and the coupling g.

As in the case of superfluid ^{4}He [see Eqs. (1.21), (1.29)] the gradient energy gives rise to a finite coherence length, which in the normal phase is

$$\xi(T) = \frac{1}{\sqrt{m^2}} = \frac{1}{\sqrt{m_0^2 \left(\dfrac{T}{T_c} - 1 \right)}}. \quad (3.11)$$

In the superconductive phase there are two coherence lengths, a finite one for the size fluctuations and an infinite one for the phase fluctuations, the long-range Nambu–Goldstone bosons [recall (1.29), (1.30)]

$$\xi_{\text{size}}(T) = \frac{1}{\sqrt{2m^2}} = \frac{1}{\sqrt{2m_0^2 \left(1 - \dfrac{T}{T_c} \right)}}, \quad (3.12)$$

$$\xi_{\text{phase}}(T) = \infty. \quad (3.13)$$

An important point noticed by Landau was that the mean field behavior of a system in the immediate neighborhood of a second order phase transition was determined entirely by an expansion of the free energy in an order field of the type (3.10). In principle, the energy could depend on many more powers of an order field and of the higher gradients of it. However, due to the fact that at the critical temperature, the order parameter goes to zero and the coherence length goes to infinity, all the higher terms are irrelevant to the critical behavior and to the approach to the critical point.

This can be seen as follows. Consider an expansion of the free energy in the form (3.10) and suppose that there are such higher terms — either with more derivatives, say $|\nabla^2 \psi|^2$, or with more powers of ψ, say $|\nabla \psi|^2 |\psi|^2$ or $|\psi|^6$. For $T < T_c$ let us renormalize the fields and divide them by the ground state value $|\psi_0| = -m^2/g$ i.e., introduce renormalized fields $\bar{\psi} = \psi/|\psi_0|$. Let us also rescale the spatial variables by $\sqrt{2}$ times the size coherence length (3.12) and introduce the dimensionless variables $\bar{x} = x/(\sqrt{2}\,\xi)$. Then the free energy density (3.10) becomes

$$e = \frac{(m^2)^2}{g}\left(\frac{1}{2}|\bar{\nabla}\bar{\psi}|^2 - \frac{1}{2}|\bar{\psi}|^2 + \frac{1}{4}|\bar{\psi}|^4\right).$$

(3.14)

The second and third term inside the parentheses are of order unity. So is the gradient term for such fields which vary sizeably over a coherence length. The factor in front is proportional to the condensate energy density $f_c = (m^2)^2/4g$ and behaves quadratically in $(1 - T/T_c)$. Consider now any of the higher corrections. If it involves one more power in ψ, this amounts to an additional factor $\sqrt{-m^2/g}\,\bar{\psi}$. Since $\bar{\psi}$ is of order unity, this decreases by an additional power of $(1 - T/T_c)^{1/2}$ for $T \to T_c$ and can therefore be neglected. If the correction involves one gradient more, the ∂_i terms can be rewritten as $\sqrt{-m^2}\,\bar{\partial}_i$ so that it amounts also to a power $(1 - T/T_c)^{1/2}$ for field configurations which vary sizeably over a coherence length. Thus, at the mean field level, both higher powers and higher gradient terms produce corrections which are at most of the order $(1 - T/T_c)^{1/2}$ and can be neglected in the expression for the free energy close to the critical temperature. If fluctuations are taken into account, it can be shown that the higher terms are still negligible as far as the critical behavior is concerned. They merely influence the size of the thermodynamic quantities, not the critical indices.

We can therefore conclude that whatever the functional form of the free energy, when expressed in terms of an order parameter ψ, the critical behavior of the system can be studied via an expansion in powers of

$|\psi|^2$ up to $|\psi|^4$ while keeping only the lowest gradient term $|\nabla \psi|^2$. Such an expansion will be referred to as *Landau expansion* of the free energy.

Far below T_c, the Landau expansion becomes invalid. The order parameter is then governed by a rather complicated potential energy. Whatever its precise shape, it has the property that size fluctuations are strongly suppressed in comparison with the phase fluctuations. These are dominated, for long wavelengths, by the lowest gradient, and can again be written in the form of a hydrodynamic energy

$$e = \tfrac{1}{2} \rho_s \, \mathbf{v}_s^2,$$

where $\mathbf{v}_s$ is proportional to the gradient of the phase $\partial_i \gamma$ of the field ψ and may be interpreted as the velocity of the superfluid electrons. This hydrodynamic energy has exactly the form (3.1) postulated by the London brothers.

3.4. GINZBURG–LANDAU ENERGY

It took 13 more years before Ginzburg and Landau realized that the London combination of superflow and magnetism could also be accomplished within the order field theory. What they did was couple the vector potential of magnetism with the energy (3.10) in a gauge invariant way, thus arriving at

$$e(\mathbf{x}) = \frac{1}{2} |(\nabla - iq\mathbf{A}) \psi|^2 + \frac{m^2}{2} |\psi|^2 + \frac{g}{4} |\psi|^4 + \frac{1}{2} (\nabla \times \mathbf{A})^2. \qquad (3.15)$$

The microscopic interpretation of this expression became possible only after the theoretical breakthrough in 1957 by Bardeen, Cooper, and Schrieffer. They found that due to the electric polarization caused by an electron in a crystal, pairs of electrons are attracted to each other. For the active electrons close to the Fermi surface the attraction could overcome the Coulomb repulsion (since this is rather small for such electrons, typically $\sim e^2 p_F/\hbar$). There exists a temperature T_c below which the electrons can form bound states, called *Cooper pairs*. The binding energy is observable as a gap $|\Delta|$ in the electron spectrum which changes the free particle spectrum from

$$E \sim \frac{\mathbf{p}^2}{2m} - \mu$$

near the Fermi surface μ to

$$E \sim \sqrt{\left(\frac{\mathbf{p}^2}{2m} - \mu\right)^2 + |\Delta|^2} \qquad (3.16)$$

Since the Cooper pairs form a gas of bosons, the permanent current postulated by the Londons turned out to be the superflow of this Bose gas.

3.5. GORKOV'S DERIVATION

Based on this understanding, a microscopic derivation of the Ginzburg–Landau free energy was given in 1959 by Gorkov using Green function techniques. He found an approximate expression for the free energy density in terms of the expectation of the composite field of two electrons of opposite spin, $\langle \psi_\uparrow (\mathbf{x}) \psi_\downarrow (\mathbf{x}) \rangle$, a complex quantity, which he denoted by[a] $\Delta(\mathbf{x})$:

$$f(\mathbf{x}) = N(0) \left\{ \xi_0^2 \left| \left(\nabla - i\frac{2e}{\hbar c} \mathbf{A} \right) \Delta \right|^2 + \left(\frac{T}{T_c} - 1 \right) |\Delta|^2 + 3\frac{\xi_0^2}{\hbar^2 v_F^2} |\Delta|^4 \right\}. \qquad (3.17)$$

Here,

$$N(0) = \frac{mp_F}{2\pi^2\hbar^3} = \frac{1}{4\pi^2} \frac{1}{k_B T_F} \left(\frac{p_F}{\hbar} \right)^3 \qquad (3.18)$$

is the density of states at the Fermi surface, p_F the Fermi momentum, $T_F = p_F^2/(2mk_B)$ the Fermi temperature, and

$$\xi_0 = \sqrt{\frac{7\xi(3)}{48\pi^2}} \hbar \frac{p_F/m}{k_B T_c} \sim 0.13 \frac{\hbar p_F/m}{k_B T_c} \sim 0.26 \frac{T_F}{T_c} \frac{\hbar}{p_F}, \qquad (3.19)$$

a length scale. The ratio p_F/m is the Fermi velocity v_F which is typically of the order $10^8(\text{cm/sec})(\sim c/300)$ and $\xi(3) = \sum_{n=1}^{\infty} \frac{1}{n^3} \sim 1.2021$. A compari-

---

[a]Actually, $\Delta(\mathbf{x}) = \lambda \langle \psi_\uparrow (\mathbf{x}) \psi_\downarrow (\mathbf{x}) \rangle$, where $H_{\text{int}} = -(\lambda/2) \psi_\alpha^\dagger \psi_\alpha \psi_\beta^\dagger \psi_\beta$ is the short range approximation to the phonon induced attraction between the electrons.

son with the Ginzburg–Landau energy (3.10), at the mean field level, leads to the identification[b]

$$\psi = \sqrt{2N(0)}\,\xi_0\,\Delta, \quad m^2 = \frac{1}{\xi_0^2}\left(\frac{T}{T_c} - 1\right), \quad g = \frac{3}{N(0)\hbar^2 v_F^2 \xi_0^2}.$$

$$(3.20)$$

Hence ξ_0 sets the scale for the coherence length which is

$$\xi(T) = \xi_0 \frac{1}{\sqrt{\dfrac{T}{T_c} - 1}} \qquad T > T_c,$$

$$\xi_{\text{size}}(T) = \xi_0 \frac{1}{\sqrt{2\left(1 - \dfrac{T}{T_c}\right)}} \qquad T < T_c. \qquad (3.21)$$

With the critical temperature of the order of 1 to 10 K, the Fermi temperature of the order 10^4 to 10^5 K, and the Fermi momentum of the order $\hbar/\text{Å}$, this leads to an extremely large length scale for the coherence length, i.e.

$$\xi_0 \sim 10^4\,\text{Å}.$$

The condensation energy density of the superconductor is given by

$$f_0 = \frac{m^4}{4g} = \frac{1}{4\xi_0^4}\frac{(k_B T_c)^2 \xi_0^4}{3 \cdot \dfrac{7\xi(3)}{48\pi^2}} N(0)\left(1 - \frac{T}{T_c}\right)^2$$

$$= \frac{1}{7\xi(3)}\left(\frac{p_F}{\hbar}\right)^3 \frac{T_c}{T_F} k_B T_c \left(1 - \frac{T}{T_c}\right)^2, \qquad (3.22\text{a})$$

which is of the order

$$f_0 \approx 10^{-4} k_B \cdot 1\,\text{K}/\text{Å}^3 \left(1 - \frac{T}{T_c}\right)^2 \approx 10^4\,\text{erg/cm}^3\left(1 - \frac{T}{T_c}\right)^2. \qquad (3.22\text{b})$$

[b]Notice that the dimensions of ψ, $N(0)$, Δ, g are (energy/length)$^{1/2}$, energy$^{-1} \cdot$length^{-3}, energy, and (energy$\cdot$length)$^{-1}$, respectively.

In order to obtain a better idea of the interaction strength, it is useful to go to natural units and employ ξ_0 and $k_B T_c$ as length and energy scales. Then, taking $\sqrt{k_B T_c/\xi_0}$ out of ψ and A, and ξ_0 out of x (i.e., $\psi_{new} = \sqrt{\xi_0/k_B T_c}\,\psi$, $A_{new} = \sqrt{\xi_0/k_B T_c}\,A$, $x_{new} = x/\xi_0$) we arrive at the dimensionless mean field expression

$$\frac{1}{k_B T_c} F = F_{red} = \int d^3x \left\{ \frac{1}{2} |(\nabla - iq\mathbf{A})\,\psi|^2 \right.$$

$$\left. + \frac{1}{2}\left(\frac{T}{T_c} - 1\right)|\psi|^2 + \frac{g}{4}|\psi|^4 + \frac{1}{2}(\nabla \times \mathbf{A})^2 \right\}. \qquad (3.23)$$

Here the couplings g and q are dimensionless

$$g = \frac{3\xi_0 k_B T_c}{N(0)\hbar^2 v_F^2 \xi_0^2} = \frac{3}{2}\pi^2 \sqrt{\frac{7\xi(3)}{48\pi^2}}^{-1}\left(\frac{T_c}{T_F}\right)^2 \sim 111.08\left(\frac{T_c}{T_F}\right)^2,$$

$$q = \frac{2e}{\hbar c}\sqrt{k_B T_c \xi_0} = 2\sqrt{4\pi\alpha\frac{v_F}{c}\sqrt{\frac{7\xi(3)}{48\pi^2}}} \sim 2.59\sqrt{\alpha\frac{v_F}{c}}, \qquad (3.24)$$

where $\alpha = (e^2/4\pi)/\hbar c = 1/137$ is the fine structure constant. Since $T_c/T_F \sim 10^{-4}$ and $\alpha(v_F/c) \sim 10^{-4}$, both couplings are extremely small, i.e., $g \sim 10^{-6}$, $q \sim 10^{-2}$.

Gorkov's original derivation was valid only for perfect crystals. In dirty materials, the mean free path of the electron has a finite value, say ℓ. In that case, the length scale ξ_0^2 in front of the gradient term of (3.18) receives a correction factor

$$r = \frac{\sum_{n=1}^{\infty} \frac{1}{(2n+1)^2}\left(2n + 1 + \frac{\xi_0}{2\pi \cdot 0.18\ell}\right)^{-1}}{\sum_{n=1}^{\infty} \frac{1}{(2n+1)^3}}, \qquad (3.25)$$

with the other terms remaining the same. For $\ell = \infty$, this is equal to 1. In very dirty materials, however, $\ell \ll \xi_0$ and r becomes $\sim 0.18(\ell/\xi_0)$ which can be quite small. If $\xi_0' = r^{1/2}\xi_0$ is used as a new length scale and $\sqrt{r^{1/2}\xi_0/k_B T_c}$ is taken out of the fields, instead of $\sqrt{\xi_0/k_B T}$, the correction factor r changes the constants in the reduced energy as follows:

$$g \to g\, r^{-3/2},$$

$$q \to q\, r^{1/4}. \tag{3.26}$$

Notice that the condensation energy density

$$\frac{f_c}{k_B T_c} = \frac{1}{\xi_0^3} \frac{\left(1 - \dfrac{T}{T_c}\right)^2}{4g}$$

is unchanged since ξ_0 and g are modified by r in precisely opposite ways. This is the content of a theorem by Abrikosov ("dirt does not change the global thermodynamics of the superconductor").

3.6. GINZBURG–LANDAU EQUATIONS

In the light of the discussion in Chapter 1, Part I, the Ginzburg–Landau free energy has to be understood as an effective energy to be minimized in the field variables. This minimization leads to the Ginzburg–Landau equations [using the reduced free energy (3.23)]

$$\left[-(\nabla - iq\mathbf{A})^2 + \left(\frac{T}{T_c} - 1\right) + g|\psi|^2 \right] \psi(\mathbf{x}) = 0, \tag{3.27}$$

$$\nabla \times \nabla \times \mathbf{A} = q\mathbf{j}, \tag{3.28}$$

with the current

$$\mathbf{j} = \frac{1}{2i} \{\psi^\dagger(\nabla - iq\mathbf{A})\,\psi - [(\nabla - iq\mathbf{A})\,\psi]^\dagger\,\psi\} = \frac{1}{2i}\psi^\dagger \overset{\leftrightarrow}{\nabla}\psi - q\mathbf{A}\,\psi^\dagger\psi. \tag{3.29}$$

By (3.27), the current is necessarily conserved:

$$\nabla \cdot \mathbf{j} = 0. \tag{3.30}$$

This is a consequence of the gauge invariance of the free energy. In order to see how the field equation for ψ achieves this, it is useful to observe a simple product rule for differentiating a complex expression in terms of covariant derivatives:

$$\nabla(a^\dagger b) = (\nabla a^\dagger) b + a^\dagger (\nabla b)$$

$$= (\nabla + iq\mathbf{A}) a^\dagger b + a^\dagger (\nabla - iq\mathbf{A}) b = (\mathbf{D}a)^\dagger b + a^\dagger \mathbf{D}b. \qquad (3.31)$$

Thus in each factor we may directly replace the ordinary derivative ∇ by the covariant one $\mathbf{D} = \nabla - iq\mathbf{A}$. Applying this rule to (3.30), we see that

$$\nabla \cdot \mathbf{j} = \frac{1}{2i}\{(\mathbf{D}\psi)^\dagger (\mathbf{D}\psi) + \psi^\dagger \mathbf{D}^2 \psi - (\mathbf{D}\psi)^\dagger (\mathbf{D}\psi) - (\mathbf{D}^2\psi)^\dagger \psi\}$$

$$= \frac{1}{2i}\{\psi^\dagger \mathbf{D}^2 \psi - (\mathbf{D}^2\psi)^\dagger \psi\}, \qquad (3.32)$$

which vanishes indeed, thanks to the field equation (3.27).

The Ginzburg–Landau equations are manifestly invariant under the gauge transformations

$$\mathbf{A}(\mathbf{x}) \to \mathbf{A}(\mathbf{x}) + \nabla \Lambda(\mathbf{x}),$$

$$\psi(\mathbf{x}) \to e^{iq\Lambda(\mathbf{x})} \psi(\mathbf{x}). \qquad (3.33)$$

This can be used to transform away the phase of the ψ field. If we parametrize it in the form $\psi(\mathbf{x}) = e^{i\gamma(\mathbf{x})}\rho(\mathbf{x})$, we may choose $q\Lambda(\mathbf{x}) = -\gamma(\mathbf{x})$ and the field equations become

$$[-(\nabla - iq\mathbf{A})^2 + \tau + g\rho^2(\mathbf{x})]\rho(\mathbf{x}) = 0, \qquad (3.34)$$

$$\nabla \times \nabla \times \mathbf{A} = q\mathbf{j} = -q^2\rho^2(\mathbf{x})\mathbf{A}(\mathbf{x}), \qquad (3.35)$$

where we have set $\tau = T/T_c - 1$, for brevity. Separating real and imaginary parts, the first equation decomposes into an equation for ρ, namely

$$(-\nabla^2 + q^2 A^2 + \tau + g\rho^2)\rho = 0, \qquad (3.36)$$

and another one for $\mathbf{A}$

$$(\partial_i A_i)\rho + 2A_i(\partial_i \rho) = 0. \qquad (3.37)$$

The latter is automatically true, due to Eq. (3.35), which ensures current conservation $(\nabla \cdot \mathbf{j} = -q\nabla \cdot (\rho^2 \mathbf{A}) = 0)$.

It is useful to write down the free energy in this gauge

$$\frac{F}{k_B T_c} = F_{\text{red}} = \int d^3x \left\{ \frac{1}{2}(\nabla\rho)^2 + \frac{\tau}{2}\rho^2 + \frac{g}{4}\rho^4 + \frac{1}{2}q^2\rho^2 A^2 + \frac{1}{2}(\nabla \times A)^2 \right\}.$$

(3.38)

Its Euler–Lagrange equations are (3.35) and (3.36). As a first step toward comparing these equations with experiment let us see whether they lead to the London equations in the superconductive phase. Looking at (3.38) we see that for $\tau \ll 0$, the size of the order parameter ρ is frozen at the minimum $\rho_0 \equiv \sqrt{-\tau/g}$. Therefore we can neglect ρ fluctuations (i.e., $\partial_i\rho \equiv 0$) and are left only with the field equation

$$\nabla \times \nabla \times A = qj = \frac{q^2\tau}{g}A,$$

(3.39)

where current conservation implies $\partial_i A_i = 0$. Thus, in this limit, the gauge $\psi = $ real coincides with the transverse gauge. Taking the curl of this equation and setting $H = \nabla \times A$ we find

$$\nabla \times \nabla \times H = \frac{q^2\tau}{g}H,$$

(3.40)

which is precisely the first London equation (3.3) with

$$\lambda = \sqrt{\frac{g}{q^2}}\frac{1}{\sqrt{-\tau}}$$

(3.41)

(where we recall that this equation expresses λ in terms of the natural length scale $\rho^{1/2}\xi_0$).

Not only the first, but also the second London equation follows directly from (3.39). When taking the time derivative of the current we find

$$\partial_t j = \frac{q\tau}{g}\dot{A}.$$

(3.42)

But in the transverse gauge where $\partial_i A_i = 0$, a neutral system has $A_0 = 0$ so that $\dot{A}$ coincides with the electric field $E = \dot{A} + \partial_i A_0$ caused by the currents. If q is taken to be the charge $-2e$ of the Cooper pairs and $-qj$

and $-\tau/g$ are identified with the supercurrent $\mathbf{j}_s$ and $n_s e/(4m)$, respectively, then (3.42) does indeed agree with (3.6).

The agreement with the London equations ensures that the Ginzburg–Landau equations explain the Meissner effect. But they contain much more information. They predict a large variety of space dependent thermodynamic and magnetic properties of superconductors in the neighborhood of the critical temperature. We shall now discuss a few of these which will be relevant for later purposes.

3.7. CRITICAL MAGNETIC FIELD

The Ginzburg–Landau equations explain the existence of a critical external magnetic field $\mathbf{H}_c$ at which the Meissner effect breaks down and the field invades into the superconductor, thereby destroying the supercurrent. This is most easily derived by studying the magnetic enthalpy, i.e., by considering the energy density

$$f_H = f - \mathbf{H} \cdot \mathbf{H}^{\text{ext}}. \tag{3.43}$$

We can then see that for $H^{\text{ext}} < H_c = (1/\sqrt{2})\,|\tau|/\sqrt{g}$ the enthalpy f_H is minimized by $\rho_0 = \sqrt{-\tau/g}$, $\mathbf{A} = 0$ with a minimal density

$$f_H = -\tfrac{1}{4}\tau^2/g = f_c. \tag{3.44}$$

For $H^{\text{ext}} > H_c$, however, the minimum is given by $\rho = 0$, $H = H^{\text{ext}}$ with

$$f_H = -\frac{(\mathbf{H}^{\text{ext}})^2}{2}. \tag{3.45}$$

Since the order parameter vanishes, this state is no longer superconductive.

For $H^{\text{ext}} = H_c$ the system can be in either state. In cgs units, the critical field is given by $(H_c^{\text{cgs}})^2/2 = f_c$ so that its order of magnitude lies, according to (3.22), in the range of a few gauss.

The interesting consequence of the Ginzburg–Landau equations is that it is also possible to have both states in one and the same sample separated by domain walls. This *mixed state* is experimentally of particular importance and deserves some discussion.

3.8. THE TWO LENGTH SCALES AND TYPE I VERSUS TYPE II SUPERCONDUCTIVITY

According to (3.21), the ρ fluctuations $\delta\rho = \rho - \sqrt{-\tau/g}$ have a coherence length

$$\xi_{\text{size}}(T) = \frac{1}{\sqrt{-2\tau}}.$$ (3.46)

This was derived in detail in the context of superfluid ^{4}He [recall (1.29)]. Comparing with (3.41) we find that the ratio of penetration depth and coherence length is

$$\frac{\lambda}{\sqrt{2}\,\xi_{\text{size}}} = \sqrt{\frac{g}{q^2}}.$$ (3.47)

This ratio is commonly denoted by κ. For $\kappa > 1/\sqrt{2}$ or $< 1/\sqrt{2}$, the magnetic penetration depth is larger or smaller than the coherence length of the order parameter. These two cases are called type II ($\kappa > 1/\sqrt{2}$) and type I ($\kappa < 1/\sqrt{2}$) superconductivity.

From Eq. (3.24) we see that the free energy (3.17) is associated with

$$\kappa \equiv \frac{\lambda}{\sqrt{2}\,\xi_{\text{size}}} = 4.06\,\frac{1}{\sqrt{\alpha\dfrac{v_F}{c}}}\,\frac{T_c}{T_F},$$ (3.48)

which is of the order of 1/100. Thus, a clean superconductor is usually of type-I.

In a dirty superconductor the result is modified by a factor r^{-1} from Eq. (3.26). Hence impurities can bring κ into the type II zone. In aluminium, for instance, 0.1% of impurities are sufficient to achieve this.

Let us now study types of domain walls between normal and superconductive materials; they differ significantly for the two types of superconductors. It will be convenient to go to a further reduced field variable $\hat{\rho} = \kappa/\sqrt{-\tau/g}$ which, in the superconductive state, fluctuates around unity instead of $\rho_0 = \sqrt{-\tau/g}$. Similarly we shall define a reduced vector potential $\hat{A} = A/(\kappa\sqrt{-\tau/g})$ and measure lengths in units of the temperature dependent coherence length $r^{1/2}\xi_0/\sqrt{-\tau}$, rather than $r^{1/2}\xi_0$. Then the free energies (3.23) and (3.38) become, for $\tau < 0$,

$$\hat{F}_{\text{red}} = \frac{g}{\tau^2} F_{\text{red}} = \int d^3x \left\{ \frac{1}{2} |(\nabla - i\mathbf{A})\psi|^2 - \frac{1}{2} |\psi|^2 + \frac{1}{4} |\psi|^4 + \frac{\kappa^2}{2} (\nabla \times \mathbf{A})^2 \right\}$$

$$F_{\text{red}} = \int d^3x \left\{ \frac{1}{2} (\nabla \rho)^2 - \frac{1}{2} \rho^2 + \frac{1}{4} \rho^4 + \frac{1}{2} (\rho^2 \mathbf{A}^2 + \kappa^2 (\nabla \times \mathbf{A})^2) \right\},$$

$$(3.49)$$

where we have dropped the hats on top of the fields, for notational convenience. Correspondingly, the current is

$$j_i = \frac{1}{2i} \psi^\dagger \overleftrightarrow{\partial_i} \psi - A_i |\psi|^2 = -\rho^2 A_i.$$

$$(3.50)$$

We shall also define a reduced magnetic field

$$\mathbf{H} \equiv \kappa \nabla \times \mathbf{A},$$

$$(3.51)$$

such that the magnetic field energy takes the usual form $H^2/2$ and the critical magnetic field H_c is equal to $1/\sqrt{2}$. In these units, the field equations read simply

$$(-\nabla^2 + \mathbf{A}^2 - 1 + \rho^2)\rho(\mathbf{x}) = 0,$$

$$(3.52)$$

$$\kappa^2 \nabla \times (\nabla \times \mathbf{A}) = \kappa \nabla \times \mathbf{H} = -\rho^2 \mathbf{A}.$$

$$(3.53)$$

They can be solved for an H and a ρ field varying, say, along the x-direction with $\mathbf{H}$ pointing in the y-direction. Accordingly, we choose a potential along the z-direction

$$\mathbf{A}(\mathbf{x}) = (0, 0, -A(x)),$$

so that [with $' \equiv \partial_x$]

$$H(x) = \kappa A'(x).$$

The field equations are

$$-\rho''(x) + A^2\rho(x) = \rho(x) - \rho^3(x),$$

$$(3.54)$$

$$\kappa^2 A''(x) = \kappa H'(x) = \rho^2 A(x).$$

$$(3.55)$$

Differentiating the second equation, it reduces to an equation for the magnetic field

$$\rho^2 H = \kappa^2(H'' - 2H'\rho'/\rho) = \kappa^2\rho^2\left(\frac{1}{\rho^2}H'\right)'. \tag{3.56}$$

In the first equation we can eliminate A in favor of the magnetic field by writing the second equation as

$$A = \kappa^2 A''/\rho^2 = \kappa H'/\rho^2 \tag{3.57}$$

so that

$$-\rho'' + \kappa^2 H'^2/\rho^3 = \rho - \rho^3. \tag{3.58}$$

Now we observe that for the value $\kappa = 1/\sqrt{2}$, where magnetic and size fluctuations have equal length scales, these equations become particularly simple. For, if we make a trial ansatz

$$H = \frac{1}{\sqrt{2}}(1 - \rho^2) \tag{3.59}$$

and insert it into Eq. (3.56), this takes the form

$$\frac{1}{\sqrt{2}}(1 - \rho^2)\rho^2 = -\frac{1}{\sqrt{2}}(\rho\rho'' - \rho'^2). \tag{3.60}$$

But this happens to coincide with the second field equation (3.58). Moreover, introducing $\sigma = 2\log\rho$ we see that (3.60) reduces to a differential equation of the Liouville type

$$\frac{\sigma''}{2} = e^\sigma - 1. \tag{3.61}$$

This can be integrated to yield

$$\frac{\sigma'^2}{4} = e^\sigma - 1 - \sigma,$$

or

$$x = \frac{1}{2}\int_{-1}^{\sigma} \frac{ds'}{\sqrt{e^s - 1 - s}}. \tag{3.62}$$

From this we see that for $x \to -\infty$, σ goes to zero (i.e., $\rho \to 1$) like $e^{x/\sqrt{2}}$ (so that $\rho \sim \exp((1/2)e^{x/\sqrt{2}}) \to 1$).

For $x \to -\infty$, there is superconductive order and no magnetic field; for $x \to \infty$ there is no order. $\rho = 0$, and the critical magnetic field $H = H_c = 1/\sqrt{2}$. The important point about a domain wall for $\kappa = 1/\sqrt{2}$ is that in an external magnetic field $H^{\text{ext}} = 1/\sqrt{2}$, it can be formed without any cost in energy. In order to see this we calculate, in reduced units, the magnetic enthalpy (for any κ)

$$\widehat{F}_H = \widehat{F}_{\text{red}} - HH^{\text{ext}}$$

$$= \int d^3x \left\{ \frac{1}{2}(\nabla\rho)^2 - \frac{1}{2}\rho^2 + \frac{1}{4}\rho^4 + \frac{1}{2}(\rho^2\mathbf{A}^2 + \mathbf{H}^2) - \mathbf{H}\cdot\mathbf{H}^{\text{ext}} \right\}. \quad (3.63)$$

Inserting the field equations (3.52) and subtracting off the condensation energy $\widehat{F}_c = -(1/4)\int d^3x$, this can be rewritten as

$$\widehat{F}_H - \widehat{F}_c = \int d^3x \left\{ \frac{1}{4}(1 - \rho^4) + \frac{1}{2}\mathbf{H}^2 - \mathbf{H}\cdot\mathbf{H}^{\text{ext}} \right\}. \quad (3.64)$$

This is the additional energy of a domain wall. At the critical field strength $H^{\text{ext}} = H_c = 1/\sqrt{2}$ pointing in the y-direction it becomes
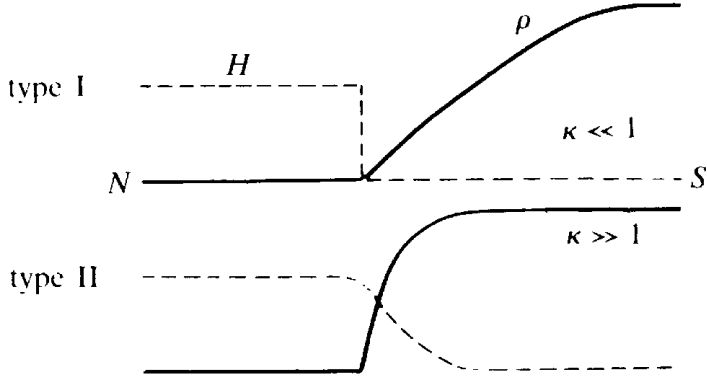
$$\widehat{F}_H - \widehat{F}_c = \frac{1}{2} \int d^3x \left\{ -\frac{\rho^4}{2} + \left(H - \frac{1}{\sqrt{2}} \right)^2 \right\}. \quad (3.65)$$

Inserting $\kappa = 1/\sqrt{2}$ into Eq. (3.59) we indeed obtain zero. For $\kappa = 1/\sqrt{2}$, a domain wall costs no energy.

Assuming that the wall energy is a monotonic function of κ, we expect the regions $\kappa > 1/\sqrt{2}$ and $\kappa < 1/\sqrt{2}$ to have wall energies of the opposite sign. Indeed, a numerical discussion of the different equations confirms this expectation. The solutions to the field equations are shown in Fig. 3.2. Inserting them into (3.65) shows that the energy $\widehat{F}_H - \widehat{F}_c$ is positive for $\kappa < 1/\sqrt{2}$ and negative for $\kappa > 1/\sqrt{2}$. Hence we can conclude that type I superconductors prefer a uniform state, type II superconductors a mixed state.

Actually, the planar domain walls calculated above are not the most energetically favorable way of forming a mixed state. A much better configuration is given by a bundle of magnetic vortex lines. In order to see this, let us study the properties of a solution corresponding to a single vortex line.

FIG. 3.2. The spatial variation of the order parameter ρ and magnetic field H in the neighborhood of a planar domain wall between the normal and superconductive phases. The magnetic field points parallel to the wall.

3.9.   SINGLE VORTEX LINE AND CRITICAL FIELD H_{c_1}

In a type II superconductor, the mixed state begins to form for much lower fields than the critical magnetic field $H_c = 1/\sqrt{2}$. The reason lies in the fact that there exists a solution in which only a very small magnetic flux invades into the superconductor, namely, the flux

$$\Phi_0 = \frac{ch}{2e} \approx 2 \times 10^{-7} \text{ gauss} \cdot \text{cm}^2. \tag{3.66}$$

This solution has the form of a vortex line. Such a vortex line may be considered as a line-like defect in this uniform superconductive state. In this respect, it is a relative of a vortex line in superfluid ^{4}He. The two are however, objects with quite different physical properties, as we shall now see.

Suppose the system is in the superconductive state without an external voltage so that there is no current j. Let us introduce a vortex line along the z-axis. Then we can use the current formula (3.50) to find from it the vector potential,

$$A_i = -\frac{j_i}{|\psi|^2} + \frac{1}{2i} \frac{1}{|\psi|^2} \psi^* \overleftrightarrow{\partial_i} \psi. \tag{3.67}$$

Far away from the vortex line, the state is undisturbed, i.e., j vanishes and we have the relation

$$A_i = \frac{1}{2i} \frac{1}{|\psi|^2} \psi^* \overleftrightarrow{\partial_i} \psi.$$

In a polar decomposition, $\psi(\mathbf{x}) = \rho(\mathbf{x})e^{i\gamma(\mathbf{x})}$, the derivative of $\rho(\mathbf{x})$ cancels and $A_i(\mathbf{x})$ depends only on the phase of the order parameter,

$$A_i(\mathbf{x}) = \partial_i \gamma(\mathbf{x}).\tag{3.68}$$

Here we can establish contact with the discussion in superfluid ^{4}He. There the superflow velocity was proportional to the gradient of a phase angle variable γ. The periodicity of γ led to the quantization rule that, when taking the integral over $d\gamma(\mathbf{x})$ along a closed circuit around the vortex line it had to be an integral multiple of 2π. The same rule now applies here:

$$\oint_B d\gamma(\mathbf{x}) = \oint_B dx_i \partial_i \gamma(\mathbf{x}) = 2\pi n.\tag{3.69}$$

By Stokes' theorem, this is equal to the magnetic flux through the area of the circuit [recall $H = \kappa(\nabla \times \mathbf{A})$ in natural units; see (3.51)]

$$\Phi = \int_{S_B} dS_k H_k = \kappa \int dS_k \varepsilon_{k\ell m} \partial_\ell A_m = \kappa \oint_B dx_k A_k = 2\pi n\kappa.\tag{3.70}$$

This holds in natural units. The quantization condition in cgs units follows by applying the same argument to the original current associated with the energy (3.17) $j \propto (1/i) \Delta^\dagger \overleftrightarrow{\partial}_i \Delta - (2e/\hbar c) A_i |\Delta|^2$ which leads to

$$\Phi = n \Phi_0,$$

with Φ_0 given by (3.66).[c]

Notice that when performing the circuit integral along a circle close to the vortex axis, the angular integral $\oint dx_i \partial_i \gamma$ still has to be $2\pi n$. But then the current no longer vanishes, and we find the quantization rule

$$\oint_B dx_i \left(A_i + \frac{j_i}{|\psi|^2} \right) = 2\pi n,\tag{3.71}$$

---

[c]Less directly we can calculate $\Phi^{cgs} = \oint dx_k A_k^{cgs}$ from (3.70) as follows: from $A^{cgs} = \sqrt{k_B T_c/\xi_0} \sqrt{-\tau/g} \kappa A$ and $x^{cgs}/x = \xi_0/\sqrt{-\tau}$ we see that $\Phi^{cgs} = \sqrt{\xi_0 k_B T_c}(1/q)\int dx_k A_k = \sqrt{\xi_0 k_B T_c} 2\pi n/q = n(ch/2e)$, since from (3.24), $q = (2e/\pi c)\sqrt{k_B T_c \xi_0}$.

or

$$\Phi = -\frac{1}{|\psi|^2} \oint_B dx_i j_i + 2\pi n \kappa. \tag{3.72}$$

This shows that through the smaller circuit there is less flux, part of the $2\pi n \kappa$ is compensated by the magnetic field of the supercurrent flowing around the vortex line.

Quantitatively, we can deduce the properties of a vortex line by solving the field equations (3.52), (3.53) in cylindrical coordinates. Inserting the second into the first equation, we find

$$-\frac{1}{r}\frac{d}{dr}r\frac{d\rho}{dr} + \frac{\kappa^2}{\rho^3}\left(\frac{d}{dr}H\right)^2 - (1 - \rho^2)\rho = 0. \tag{3.73}$$

Forming the curl of the second gives the cylindrical analogue of (3.56), i.e.,

$$H = \kappa^2 \frac{1}{r}\frac{d}{dr}\frac{r}{\rho^2}\frac{d}{dr}H. \tag{3.74}$$

For $r \to \infty$ we have the boundary condition $\rho = 1$, $H = 0$ (superconductive state with Meissner effect) and $\mathbf{j} = 0$ (no current). Since $\mathbf{j} \propto \nabla \times \mathbf{H}$ [see (3.39)], the last condition amounts to

$$H'(r) = 0, \quad r \to \infty. \tag{3.75}$$

In cylindrical coordinates, flux quantization can be written in the form

$$\Phi = 2\pi \int_0^\infty dr\, r H = 2\pi n \kappa. \tag{3.76}$$

Inserting Eq. (3.74) into this result gives

$$\Phi = 2\pi \kappa^2 \left[\frac{r}{\rho^2}H'\right]_0^\infty = -2\pi \kappa^2 \left[\frac{r}{\rho^2}H'\right]_{r=0}, \tag{3.77}$$

so that the quantization condition turns into a boundary condition at the origin:

$$H' \to -\rho^2 \frac{n}{\kappa} \frac{1}{r}, \quad r \to 0. \tag{3.78}$$

Inserting this condition into (3.73) we see that close to the origin $\rho(r)$ satisfies the equation

$$-\frac{1}{r}\frac{d}{dr} r \frac{d}{dr}\rho(r) + \frac{n^2}{r^2}\rho - (1 - \rho^2)\rho \sim 0,$$

which amounts to a behavior

$$\rho(r) = c_n \left(\frac{r}{\kappa}\right)^n + O(r^{n+1}). \tag{3.79}$$

Putting this back into (3.78) we have

$$H(r) = H(0) - \frac{c_n^2}{2\kappa}\left(\frac{r}{\kappa}\right)^{2n} + O(r^{2n+1}). \tag{3.80}$$

For large r, where $\rho \to 1$, Eq. (3.74) is solved by the modified Bessel function K_0, with some factor α, namely[d]

$$H(r) \to \alpha K_0\left(\frac{r}{\kappa}\right), \quad r \to \infty \tag{3.81}$$

For large $\kappa \gg 1/\sqrt{2}$ (i.e., deep type II) ρ goes rapidly to 1 as compared to the length scale over which H changes (which is κ). Therefore, the behavior (3.81) holds very close to the origin. We can determine α by matching (3.81) to (3.78) and find (since $K_0' = -K_1 \sim -1/r$)

$$\alpha \approx \frac{n}{\kappa}. \tag{3.82}$$

In general, $H(r)$ and $\rho(r)$ have to be found numerically. A typical solution for $n = 1$ is shown in Fig. 3.3 for $\kappa = 10$. The energy of a vortex line can be calculated by using (3.49). Inserting the equations of motion,

[d]For very large r this has the limit $\sqrt{\pi\kappa/2r}\,e^{-r/\kappa}$.

and subtracting the condensation energy $\widehat{F}_c = -(1/4)\int d^3x$ gives [compare (3.64)]

$$\widehat{F}_{\text{vort}} = \widehat{F}_{\text{red}} - \widehat{F}_c = \frac{1}{2}\int d^3x\left\{\frac{1}{2}(1-\rho^4) + \mathbf{H}^2\right\}. \qquad (3.83)$$

For $\kappa \gg 1/\sqrt{2}$, we may neglect the small radius $r \lesssim 1$, over which ρ increases quickly from zero to its asymptotic value $\rho = 1$. Beyond $r \gtrsim 1$ but for $r \lesssim \kappa$, H is given by (3.81). Inserting this into (3.73) with (3.79), we find

$$\rho(r) \sim 1 - \frac{n^2}{2r^2}. \qquad (3.84)$$

For the region $1 \lesssim r \lesssim \kappa$ this gives for the energy per length unit

$$\frac{1}{L}\widehat{F}_{\text{vort}} = \frac{1}{2}2\pi\int_1^\kappa dr\,r\left\{\frac{1}{2}(1-\rho^4) + H^2\right\} = \pi n^2\int_1^\kappa dr\,r\left\{\frac{1}{r^2} + \frac{1}{\kappa^2}K_0^2\left(\frac{r}{\kappa}\right)\right\}. \qquad (3.85)$$

For $\kappa \to \infty$, the second integral goes towards a constant [since $\int_0^\infty dx\,x\,K_0^2(x) = \frac{1}{2}$]. The first integral, however, has a logarithmic divergence so that we find

$$\frac{1}{L}\widehat{F}_{\text{vort}} \approx \pi n^2[\log\kappa + \text{const.}]. \qquad (3.86)$$

A more careful estimate gives $\pi n^2(\log\kappa + 0.08)$.

Let us now see at which external magnetic field such a vortex line can form. For this we consider again the magnetic enthalpy (3.64) and subtract from $(1/L)\widehat{F}_{\text{vort}}$ the magnetic $\widehat{F}_{\text{vort}}/L$ coupling HH^{ext} so that, per length unit,

$$\frac{1}{L}\widehat{F}_H = \pi n^2(\log\kappa + 0.08) - 2\pi\int_0^\infty dr\,r\,HH^{\text{ext}}. \qquad (3.87)$$

But the integral over H is simply the flux quantum (3.70) associated with the vortex line, i.e.,

$$\frac{1}{L}\widehat{F}_H = \pi n^2 (\log \kappa + 0.08) - 2\pi n \kappa H^{\text{ext}}. \tag{3.88}$$

When this drops below zero, a vortex line invades the superconductor along the z-axis. The associated critical magnetic field is

$$H_{c_1} = \frac{n}{2}(\log \kappa + 0.08)/\kappa. \tag{3.89}$$

FIG. 3.3.   The order parameter ρ and the magnetic field H for an $n = 1$ vortex line in a deep type II superconductor with $\kappa = 10$.
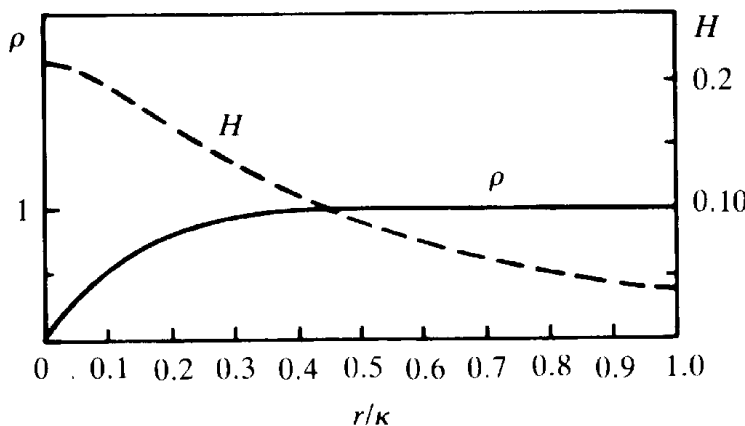
FIG. 3.4.   The critical field H_{c_1} at which a vortex line of strength n forms when it first invades a type II superconductor as a function of the parameter κ. The dotted line indicates the asymptotic result $(1/2\kappa)\log \kappa$ of Eq. (3.89). The magnetic field H_{c_1} is measured in units of $\sqrt{2}H_c$ where H_c is the magnetic field at which the magnetic energy equals the condensation energy.
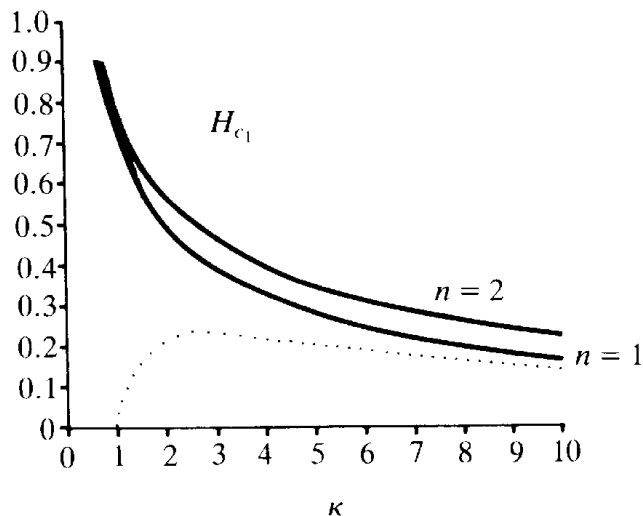
TABLE 3.1. The different critical magnetic fields in gauss for various impurities.

material	H_c	H_{c_1}	H_{c_2}	T_c/K
Pb	550	550	550	4.2
0.85 Pb, 0.15 Ir	650	250	3040	4.2
0.75 Pb, 0.25 In	570	200	3500	4.2
0.70 Pb, 0.30 Tl	430	145	2920	4.2
0.976 Pb, 0.024 Hg	580	340	1460	4.2
0.912 Pb, 0.088 Bi	675	245	3250	4.2
Nb	1608	1300	2680	4.2
0.5 Nb, 0.5 Ta	252	—	1470	5.6

For large κ this field can be quite small. The asymptotic result is compared with a numerical solution of the differential equation for $n = 1$, 2, 3, . . . in Fig. 3.4. For a comparison with experiment one expresses this field in terms of the critical magnetic field $H_c = 1/\sqrt{2}$ and measures the ratio

$$\frac{H_{c_1}}{H_c} = \frac{n}{\sqrt{2}\,\kappa}(\log \kappa + 0.08).$$

(3.90)

As an example, pure lead is a type I superconductor with $H_{c_1} = H_c \cong 550$ gauss. An admixture of 15% Iridium or 30% Thallium brings H_c up to 650 or 430, and H_{c_1} down to 250 or 145, respectively (see Table 3.1).

3.10.   THE FIELD H_{c_2} WHEN SUPERCONDUCTIVITY IS DESTROYED

As the field increases above H_{c_1}, more and more vortex lines invade the superconductor. For $H \sim H_c$, they form a hexagonal array as shown in Fig. 3.5. If the field increases even more, the superconductive regions separating the vortex lines become thinner and thinner until, finally, the whole material is filled with the magnetic field, and superconductivity is destroyed. The field where this happens is denoted by H_{c_2}. Its value can be estimated quite simply following Abrikosov. He noticed that close to H_{c_2}, the order parameter is so small that the nonlinear terms can be forgotten, and the Ginzburg–Landau equation reads
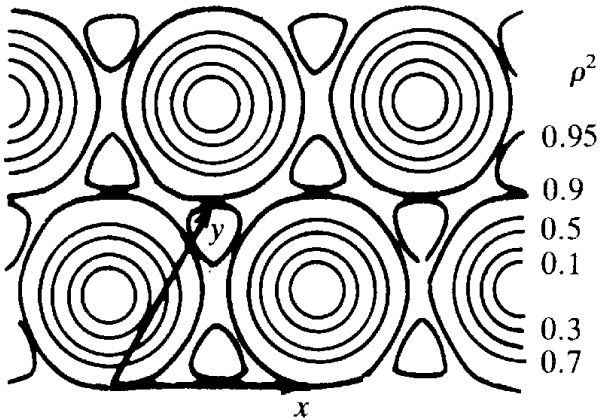
FIG. 3.5. The spatial distribution magnetization of the order parameter $\rho(\mathbf{x})$ in a typical mixed state in which the vortex lines form a hexagonal lattice (from W.M. Kleiner *et al.*, see References).

$$\left[\left(\frac{1}{i}\nabla - \mathbf{A}\right)^2 - 1\right]\psi(\mathbf{x}) = 0. \tag{3.91}$$

For H along the z direction one may choose

$$\mathbf{A}(\mathbf{x}) = \left(0, \frac{1}{\kappa}Hx, 0\right) \tag{3.92}$$

and the following equation emerges:

$$\left[-\partial_x^2 - \left(-i\,\partial_y - \frac{1}{\kappa}Hx\right)^2 - \partial_z^2 - 1\right]\psi(\mathbf{x}) = 0. \tag{3.93}$$

The lowest nontrivial eigenstate is

$$\psi(\mathbf{x}) = \text{const.}\, e^{-(1/\kappa)H(x - p_y\kappa/H)^2/2}\, e^{ip_y y}. \tag{3.94}$$

For this solution to occur, the energy eigenvalue $H/\kappa - 1$ must be negative. This happens for $H < H_{c_2} = \kappa$. In terms of the critical field H_c, H_{c_2} is equal to $H_{c_2} = \sqrt{2}\,\kappa H_c$, i.e., it can be sizeably larger than H_c. As an example, pure lead has $H_{c_2} = H_c = 550$ gauss. The admixture of 15% Indium or 30% Thallium which changes H_c to 650 or 430, increases H_{c_2} to 3040 or 2920 gauss, respectively. The typical behavior of the critical fields H_c, H_{c_1}, H_{c_2} as a function of T is shown in Fig. 3.6.

The invasion of vortex lines becomes apparent from the curve depicted in Fig. 3.7 which shows the behavior of the magnetization curve

$$-M = H^{\text{ext}} - H$$

in a type II superconductor as compared with a type I superconductor.
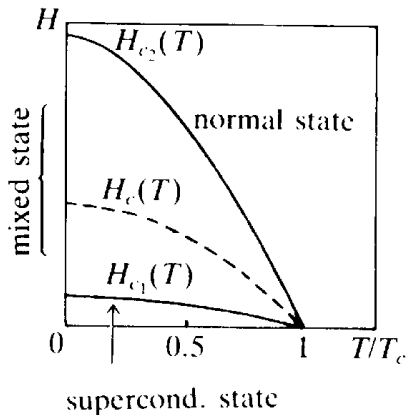
FIG. 3.6. The temperature behavior of the critical magnetic fields of a type II superconductor: H_{c_1} (when the first vortex line invades), H_{c_2} (when superconductivity is destroyed in comparison with the field) and H_c (when the magnetic field energy is equal to the condensation energy).
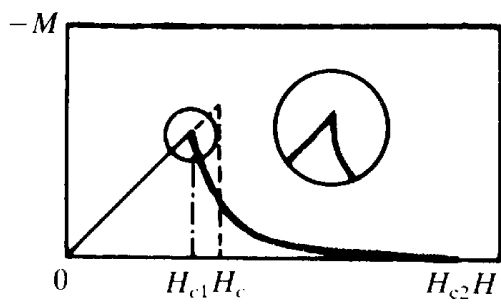
FIG. 3.7. The magnetization curve as a function of the magnetic field H. The dashed curve shows how a type I superconductor would behave.

3.11. FLUCTUATION CORRECTIONS

Gorkov's derivation of the Ginzburg–Landau energy dealt entirely with field expectation values of pairs of electron fields $\langle \psi_\uparrow(\mathbf{x}) \psi_\downarrow(\mathbf{x}) \rangle$. The question arises as to why the agreement with experiment is so perfect, and why no fluctuation corrections are observed. In order to answer this question, let us study the fluctuations. For this we have to consider the field variables in the Ginzburg–Landau energy as fluctuating variables such that the partition function is

$$Z = \int \mathscr{D} A \, \Phi[\mathbf{A}] \int \mathscr{D} \psi \, \mathscr{D} \psi^\dagger \, e^{-(T_c/T) E_{\mathrm{red}}}, \qquad (3.95)$$

where

$$E_{\mathrm{red}} = \int d^3 x \left\{ \frac{1}{2} |(\nabla - iq\mathbf{A}) \psi|^2 + \frac{\tau}{2} |\psi|^2 + \frac{g}{4} |\psi|^4 + \frac{1}{2} (\nabla \times \mathbf{A})^2 \right\} \qquad (3.96)$$

is the reduced Ginzburg–Landau energy (3.23). Since the considerations will only hold slightly below T_c, we can set $T_c = T$ in the Boltzmann factor of (3.95) leaving all the temperature variation to τ. The functional $\Phi[\mathbf{A}]$ is some gauge-fixing factor. In the previous general discussion on

fluctuating gauge fields in Part I, Chapter 3, this factor was chosen in three possible ways (I.3.31), (I.3.32), (I.3.34). The first was the transverse gauge $\Phi[\mathbf{A}] \propto \Pi_x \delta(\partial_i A_i)$. In it the path integral contains four fluctuating fields: the real and imaginary parts of ψ and two transverse components of A_i. In the superconductive phase, none of these three gauges described in Part I, Chapter 3 is convenient. When solving the field equations, we have given preference to a field equation in which the phase γ of the order parameter was absorbed into the vector potential by a gauge transformation [recall (3.36)]. This led to the energy (3.38) which contains the four field variables in the form of one real field ρ and *three* components A_i. It would be desirable to find the proper gauge-fixing factor for these variables. This factor is given by a functional Φ which depends not on the $\mathbf{A}$ field but on the phase variable γ of the ψ field, i.e.,

$$\Phi \equiv \Phi[\gamma] = \prod_x \left(\sqrt{\frac{2\pi}{a^3}} \right) \det(-\nabla^2)^{-1/2} \prod_x \delta(\gamma(\mathbf{x})) \qquad (3.97)$$

(a = lattice spacing).

The equivalence of (3.97) with the transverse gauge (I.3.31) is easily seen. In the latter gauge, the path integral is

$$\int \mathscr{D}^2 A^\perp \, \mathscr{D}\psi \, \mathscr{D}\psi^\dagger. \qquad (3.98)$$

In terms of the size-angle field variables ρ, γ, this is just

$$\int \mathscr{D}^2 A^\perp \, \rho \, \mathscr{D}\rho \, \mathscr{D}\gamma. \qquad (3.99)$$

Let us now perform a gauge transformation [see (3.33)]

$$A_i(\mathbf{x}) \rightarrow A_i(\mathbf{x}) - \frac{1}{q} \partial_i \gamma(\mathbf{x}), \qquad (3.100)$$

which removes the phase of the ψ field. This changes the purely transverse gauge field into another one which has a longitudinal component in momentum space $A^L(\mathbf{k}) = -i \sqrt{\mathbf{k}^2} \, \gamma(\mathbf{k})/q$. Therefore we can replace $\mathscr{D}\gamma$ by $(\Pi_x q)(\det(-\nabla^2))^{-1/2} \mathscr{D} A^L$. This brings (3.99) to the form

$$\left(\prod_x q \right) \det(-\nabla^2)^{-1/2} \int \mathscr{D}^2 A^\perp \, \mathscr{D} A^L \, \rho \, \mathscr{D}\rho. \qquad (3.101)$$

But this is precisely the same as $\int \mathcal{D}A\Phi[\gamma]$ so that (3.97) is in fact the correct gauge-fixing factor. We therefore arrive at the partition function close to T_c,

$$Z = \left(\prod_x q\right) \det(-\nabla^2)^{-1/2} \int \mathcal{D}^3 A\rho \, \mathcal{D}\rho$$

$$\times \exp\left\{-\int d^3x \left[\frac{1}{2}(\nabla\rho)^2 + \frac{\tau}{2}\rho^2 + \frac{g}{4}\rho^4 + \frac{q^2}{2}\rho^2 A^2 + \frac{1}{2}(\nabla \times A)^2\right]\right\}.$$

$$(3.102)$$

This expression can be simplified further. The fluctuations of A^L occur only in the term $(q^2/2)\rho^2 A^2$. Hence we can perform the $\Pi_x(dA^L(\mathbf{k})/\sqrt{2\pi/a^3})$ integrals which gives a factor $\Pi_x(1/\sqrt{2\pi/a^3})$ $\times (\sqrt{2\pi/a^3}/q\rho(\mathbf{x}))$. The size fields $\rho(\mathbf{x})$ in the denominators cancel against those in the integral measure in (3.102) so that the partition function becomes

$$Z = \det(-\nabla^2)^{-1/2} \int \mathcal{D}^2 A^\perp \, \mathcal{D}\rho$$

$$\times \exp\left\{-\int d^3x \left[\frac{1}{2}(\nabla\rho)^2 + \frac{\tau}{2}\rho^2 + \frac{g}{4}\rho^4 + \frac{q^2}{2}\rho^2 A^{\perp 2} + \frac{1}{2}(\nabla \times A^\perp)^2\right]\right\}.$$

$$(3.103)$$

Notice that apart from the factor $\det(-\nabla^2)$ this is the same as the partition function of a real field $\rho(\mathbf{x})$ coupled to the vector potential with the transverse gauge-fixing factor (I.3.31). The factor $\det(-\nabla^2)^{1/2}$ collects the pure gauge fluctuations which in the superconductive phase with $\rho \neq 0$ are decoupled and massless. The form (3.103) will be most convenient in studying fluctuation corrections.

Let us calculate the effective potential energy at the one-loop level. According to the rules in Part I, Chapter 5, this is obtained by adding to the potential energy density of (3.103) the one-loop correction

$$\Delta v = \frac{1}{2}\int \frac{d^3p}{(2\pi)^3}\log(\mathbf{p}^2 + \tau + 3g\rho^2) + 2\frac{1}{2}\int \frac{d^3p}{(2\pi)^3}\log(\mathbf{p}^2 + q^2\rho^2). \qquad (3.104)$$

The first integral collects the size fluctuations, the second the traverse A fluctuations. The factor 2 counts the two transverse degrees of freedom.

Since we are considering the superconductive phase, both fluctuations are short ranged. At the equilibrium point of the mean field theory, $\rho_0 = \sqrt{-\tau/g}$, the ratio of the two length scales is

$$\frac{\lambda}{\xi_{\text{size}}} \equiv \sqrt{2}\,\kappa = \sqrt{2}\ \sqrt{\frac{g}{q^2}},\qquad(3.105)$$

which shows that for $\kappa = 1/\sqrt{2}$ they are equal.

After the one-loop correction, the effective potential energy to be minimized is

$$v(\rho,\ \mathbf{A}) = \frac{\tau}{2}\rho^2 + \frac{g}{4}\rho^4 + \frac{q^2}{2}\rho^2 \mathbf{A}^{\perp^2} + \Delta v,$$

where now ρ and $\mathbf{A}^\perp$ are to be understood as *expectation* values of the fluctuating ρ and $\mathbf{A}^\perp$ fields. The integral can be performed using the formula

$$\int_0^\Lambda dx\, x^2 \log(x^2 + a^2)$$

$$= \frac{1}{3}\left[x^3 \log(x^2 + a^2) - \frac{2}{3}x^3 + 2xa^2 - 2a^3 \tan^{-1}\!\left(\frac{x}{a}\right)\right]_0^\Lambda.\qquad(3.106)$$

In applying (3.106) we have to keep in mind that the description of fluctuations with the Ginzburg–Landau energy is necessarily restricted to long wavelengths, much longer than the length scale $\xi(T)$. Otherwise higher gradient terms would have to be taken into account which would come in with factors $\xi(T)\,\partial$. Therefore, the momentum integrals must be limited to sufficiently small momenta, $|\mathbf{p}| \leqslant \Lambda \ll 1/\xi(T)$. In natural units with $\xi(T) = 1$ in which (3.104) is written, this amounts to $|\mathbf{p}| \ll \Lambda \ll 1$. Thus Λ must be a small number. As long as the system is far away from the critical point this implies that the fluctuation correction (3.104) is of the order Λ^3 which is extremely small compared with the total size of $v(\rho,\ \mathbf{A})$, which is of the order of $-\tau^2/(4g)$. Fluctuations can modify the result only very close to the critical temperature. There the quantities $\tau + 3g\rho^2$, $q^2\rho^2$, which close to the minimum $\rho \sim \sqrt{-\tau/g}$ behave like τ, can become quite small, and the singularity of the logarithms in (3.104) comes into play. The relevant limit in (3.106) is $a^2 \ll \Lambda^2$, which gives

$$\frac{1}{3}\left[\Lambda^3 \log(\Lambda^2 + a^2) - \frac{2}{3}\Lambda^3 + 2\Lambda a^2 - 2a^3 \tan^{-1}\frac{\Lambda}{a} \right]$$

$$\sim \frac{1}{3}\left[\Lambda^3 \log \Lambda^2 - \frac{2}{3}\Lambda^3 + 3\Lambda a^2 - \pi a^3 \right].$$

Inserting this into (3.104) we find

$$\Delta v = \frac{1}{6\pi^2}\left\{ \frac{3}{2}\left(\Lambda^3 \log \Lambda^2 - \frac{2}{3}\Lambda^3 + 3\Lambda\tau \right) + 3\Lambda\left(\frac{3}{2}g\rho^2 + q^2\rho^2 \right) \right.$$

$$\left. - \pi\left(\frac{1}{2}(\tau + 3g\rho^2)^{3/2} + q^3\rho^3 \right) \right\}.$$ (3.107)

The first term represents a small trivial additive constant in the potential. The second term changes the original quadratic terms in the ρ field from $(\tau/2)\rho^2$ to

$$\frac{1}{2}\left[\tau + \frac{\Lambda}{\pi^2}\left(\frac{3}{2}g + q^2 \right) \right]\rho^2.$$ (3.108)

Since $\tau = T/T_c - 1$, this amounts to a small change in the critical temperature, and we can rewrite (3.108) as $(1/2)\tau^{(1)}\rho^2$ with $\tau^{(1)} = (1 - \alpha)(T/T_c^{(1)} - 1)$ and $T_c^{(1)} = T_c(1 - \alpha)$, where $\alpha = (\Lambda/\pi^2) \times ((3/2)g + q^2)$.

The last terms in (3.107) are independent of the momentum cutoff. They are the only terms which change the functional behavior of the potential. Let us first estimate, how close we have to get to the critical temperature in order that these terms are comparable with the mean field potential. At the mean field minimum, the potential is $-\tau^2/(4g)$. The one-loop correction due to size fluctuations, on the other hand, is close to the mean field minimum $\rho_0 = \sqrt{-\tau/g}$ of the order $-(1/6\pi)(1/2)(-2\tau)^{3/2}$. This is negligible compared to $-\tau^2/(4g)$ as long as

$$\tau \gg \tau_G \equiv -\frac{8}{9}\frac{g^2}{\pi^2}.$$ (3.109)

This inequality is called *Ginzburg criterion*, and the temperature range $|\tau| \leq |\tau_G|$ where fluctuations become important is called the *Ginzburg temperature interval*. From the estimates of the coupling g in Eq. (3.24)

we see that in a superconductor of type I, τ_G is extremely small, $\tau_G \sim 10^{-14}$. In a dirty superconductor which is deep type II this can be increased to $\tau_G \sim 10^{-6}$. Still, a temperature resolution of 10^{-6} in a superconductor is impossible to achieve. Thus we conclude that size fluctuations of the order parameter are negligible for all practical purposes.

The Ginzburg interval has a simple intuitive interpretation. It characterizes the temperature $T_G \equiv T_c(1 + \tau_G)$ in which the energy of a typical field fluctuation is of the order of the temperature T_c. A typical fluctuation forms a "field pocket" whose size is the coherence length $\xi = 1/\sqrt{-2\tau}$ (in natural units). The energy of the pocket is obtained by taking the condensation energy density $f_c = -\tau^2/4g$ times the volume of the pocket, i.e., $-(\tau^2/4g)(-2\tau)^{-3/2}$. Fluctuations are important if this energy is smaller than the critical temperature which in the present units is unity. The result is indeed (3.109), apart from a numerical factor.

Consider now the fluctuations of the vector potential. They give a cubic term

$$\Delta v = -\frac{1}{6\pi} q^3 \rho^3. \tag{3.110}$$

Notice that relative to the size fluctuation term, the cubic term is larger or smaller by a factor of the order $\sim q^3/\sqrt{g}^3 = 1/\kappa^3$. Thus in a deep type II superconductor, where $\kappa \gg 1/\sqrt{2}$, the fluctuations of the A field are negligible compared to the size fluctuations which were already shown to be practically irrelevant. Thus only in a deep type I superconductor can we hope to have observable consequences from the A fluctuations. In order to see their influence most clearly, we shall study the effective potential itself:
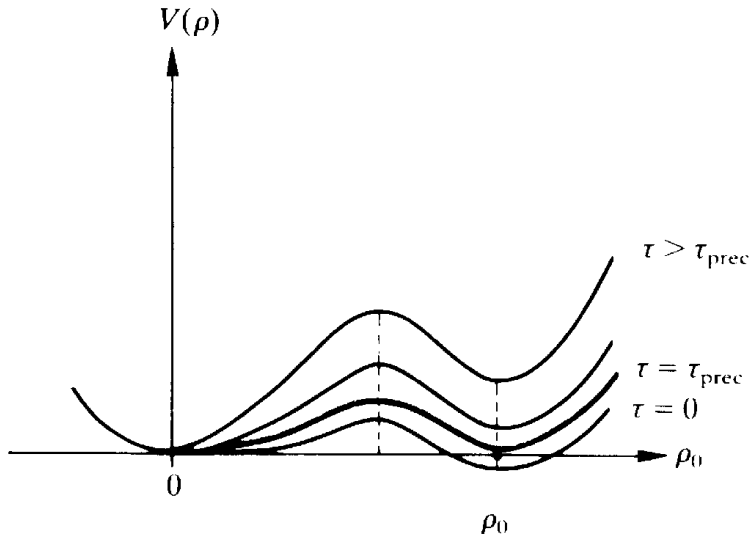
$$v = \frac{\tau}{2}\rho^2 + \frac{g}{4}\rho^4 - \frac{c}{3}\rho^3, \tag{3.111}$$

where we have set $c = q^3/2\pi$ and neglected all the other corrections. The τ parameter is really $\tau^{(1)}$ but we shall drop the superscript, for brevity.

The potential is depicted in Fig. 3.8. The minimum of this potential is obtained from the equation

$$\tau\rho + g\rho^3 - c\rho^2 = 0. \tag{3.112}$$

FIG. 3.8. The first order phase transition generated by a cubic term. For $\tau = \tau_{\mathrm{prec}}$, the order parameter jumps from zero to the non-zero expectation value of the right-hand minimum of the potential curve.

In general, this has two solutions, one at the field origin, and another at

$$\rho_0 = \frac{c}{2g}\left(1 + \sqrt{1 - \frac{4\tau g}{c^2}}\right).$$

(3.113)

The second branch of the square root,

$$\rho_0 = \frac{c}{2g}\left(1 - \sqrt{1 - \frac{4\tau g}{c^2}}\right)$$

(3.114)

gives a maximum. The minimum at ρ_0 appears only for

$$\tau < \frac{c^2}{4g}.$$

(3.115)

The potential at this minimum has the value

$$v(\rho_0) = -\frac{g}{4}\rho_0^3\left(\rho_0 - \frac{2c}{3g}\right).$$

(3.116)

As the temperature is decreased below (3.115), ρ_0 increases, and the minimum (3.116) moves down. For

$$\tau \le \tau_{\mathrm{prec}} = \frac{2c^2}{9g}, \tag{3.117}$$

it reaches the same height as the minimum at the origin (namely zero) and the order parameter ρ_0 makes a jump from the origin to the value $\rho_0 = (2/3)(c/g)$. The corresponding temperature $T_{\mathrm{prec}} = T_c(1 + \tau_{\mathrm{prec}})$ lies above T_c, a fact which is indicated by the subscript prec which stands for "precocious".

A jump in the order parameter is characteristic of a first-order phase transition. Indeed, if we calculate the entropy density

$$s = -\frac{1}{T_c}\frac{\partial}{\partial T}r(\rho_0), \tag{3.118}$$

we find

$$s = -\frac{1}{T_c}\left(\frac{1}{2}\rho_0^2 + \frac{\partial \rho_0}{\partial \tau}\frac{\partial}{\partial \rho_0}r(\rho_0)\right) = -\frac{1}{T_c}\frac{1}{2}\rho_0^2, \tag{3.119}$$

since $(\partial/\partial\rho_0)\,r(\rho_0) = 0$. Therefore, the jump in the order parameter leads to a jump in the entropy,

$$\Delta s = -\frac{1}{T_c}\frac{1}{2}\left(\frac{2}{3}\frac{c}{g}\right)^2. \tag{3.120}$$

This can also be expressed in terms of the precocity τ_{prec} as

$$\Delta s = -\frac{1}{T_c}\frac{\tau_{\mathrm{prec}}^2}{g}, \tag{3.121}$$

which is $4/T_c$ times the mean field condensation energy at the precocious temperature. The size of the precocity can be estimated in the weak coupling limit [recall (3.24)] as

$$\tau_{\mathrm{prec}} = \frac{2}{9}\frac{1}{g}\frac{1}{4\pi^2}q^6 \sim 0.015\left(\frac{T_F}{T_c}\right)^2\left(\alpha\frac{v_F}{c}\right)^3 \sim 10^{-6}. \tag{3.122}$$

Such a small temperature interval is unaccessible, experimentally. For

dirty superconductors there is also a factor $r^3 < 1$ which makes its observation even harder. Notice that the ratio of precocity τ_{prec} and Ginzburg number τ_G is

$$\frac{\tau_{\text{prec}}}{\tau_G} = \frac{\pi^2}{4}\frac{c^2}{g^3} = \frac{1}{16\kappa^6},\qquad(3.123)$$

and that size and $\mathbf{A}^\perp$ fluctuations work against each other. For deep type II materials, size fluctuations dominate over the $\mathbf{A}^\perp$ fluctuations; for type I materials the converse is true.

Equation (3.123) is an important relation. It teaches us that if the superconductor is deep type II, the quantity τ_{prec} will be much smaller than τ_G. This implies that the first-order jump extracted from the effective potential lies completely *inside* the temperature interval wherein size fluctuations cannot be ignored. We must therefore become suspicious of a result whose derivation was based on the assumption that the size of the order parameter $|\psi|$ was approximately constant [see Eq. (3.104)]. The prediction of a first order jump should therefore break down as κ exceeds a certain value, say κ_t. From that value on, the transition should remain continuous. The value κ_t corresponds to a *tricritical* point.

Estimates of the size of κ_t have only recently become possible. The reason is that perturbation theory, even when supported by the power of the renormalization group, was unable to determine this point. Fixing its value requires the knowledge of the fluctuations of vortex lines which can be present in a type II superconductor. Along the center of vortex lines, the order parameter $\rho(\mathbf{x}) = |\psi(\mathbf{x})|$ vanishes. Hence, if the superconductor is filled with a grand canonical ensemble of vortex lines, the fluctuation determinant (3.104) has to be found in the presence of a large number of lines of zeroes of $\rho(\mathbf{x})$. This is a difficult problem. It will be solved later in Chapter 13 by developing a disorder field theory for the ensemble of vortex lines.

What we will find turns out to be physically quite reasonable. If there are no gauge fields, there is a tricritical point when the quartic $|\psi|^4$ coupling constant g changes sign. The presence of gauge fluctuations pushes this point up to a positive value of the order of e^2. If g is much larger than e^2 (i.e., $\kappa \gg 1$) the gauge field plays no role and the system has the same phase transition as the pure $|\psi|^4$ theory itself.

The fluctuation mechanism for changing a second order phase transition into a first order was first proposed in 1973 by Coleman and Weinberg within a four-dimensional Ginzburg–Landau theory. It is there-

fore generally referred to as the Coleman–Weinberg mechanism. A year later the same idea was carried over to three dimensions by Halperin, Lubensky and Ma, suggesting that a physical superconductor should have a first-order transition, albeit with an unobservably small discontinuity. Even though the smallness of the effect makes the prediction of a first-order transition practically irrelevent in superconductors, the question of a qualitative change of the phase transition in the simple gauge theory of the Ginzburg–Landau type is nevertheless of great theoretical interest. One reason lies in the fact that similar field theories appear to be governing the unified description of weak and electromagnetic (and possibly strong) interactions. Such theories determine among other things the history of the early universe. The generation of a first-order transition has been an important ingredient in a recent speculation about an "inflationary universe" in which a great number of universes arises spontaneously out of nothing. As far as we are concerned in this text, the interest in this mechanism is due to the fact that the disorder theory developed before is of the same type and governs the statistical behavior of vortex lines in superfluid ^{4}He. Moreover, as we shall see soon, a similar theory can be used to describe defect lines in other quite different physical systems, for example, dislocation lines in solid crystals, where the melting process is always of the first order, and dislocation lines in smectic A liquid crystals, where the transition is practically always of second order. It will therefore be important to investigate the order of the phase transition in more detail. This will be done in Chapter 10.

3.12. PHASE TRANSITION IN DISORDER FIELD THEORY AND DISORDER VERSION OF THE MEISSNER EFFECT

After this reminder of the Ginzburg–Landau theory we can now return to the point of departure which was the disorder field theory (2.7a), (2.7b) of vortex lines. At the mean field level there was a second order phase transition as the mass term

$$m^2 = \frac{2D}{a^2}\left(\frac{\varepsilon}{T} - \log 2D\right) \tag{3.124}$$

changed sign [recall Section 2.2]. This happened for

$$T \geq T_c = \frac{\varepsilon}{\log 2D}, \tag{3.125}$$

where in constrast to the Ginzburg–Landau theory the mass term becomes negative *above* the critical temperature, rather than below it as a reflection of the *disorder* nature of the φ field. If the temperature *increases* above T_c, disorder proliferates. The proliferation is signaled by the disorder field acquiring a non-zero expectation value

$$|\varphi| = \sqrt{\frac{m^2}{g}} = \sqrt{-\frac{\mu^2}{g}\left(\frac{T_c}{T} - 1\right)}. \tag{3.126}$$

Apart from the change $T/T_c - 1 \to T_c/T - 1$, $\psi \to \varphi$, the disorder field theory (2.7) is completely analogous to the Ginzburg–Landau theory (3.23) so that we will now follow the discussion of the Ginzburg–Landau theory of superconductivity.

An immediate consequence is the existence of a disorder version of the Meissner effect. In the superconductor, this followed from the order field ψ having a ground-state expectation value $\psi_0 \neq 0$ in the ordered state for $T < T_c$. This changed the magnetic field energy from $(1/2\mu)(\nabla \times \mathbf{A})^2$ to

$$\frac{1}{2\mu}(\nabla \times \mathbf{A})^2 + \frac{q^2|\psi|^2}{2}\mathbf{A}^2. \tag{3.127}$$

This was responsible for the experimentally observed finite penetration depth. While in the normal state, magnetic field lines have long range propagation, they cannot invade into the ordered state, except for a small length scale,

$$\lambda = \frac{1}{\sqrt{\mu q^2 |\psi|^2}}. \tag{3.128}$$

Now, in the disorder field theory of vortex lines, we find a completely analogous effect. Here also the vector potential acquires a finite penetration depth, only that this happens now *above* the critical temperature, i.e, in the disordered state. Since the curl of the vector potential is the superfluid velocity this means that *superflow cannot invade into the disordered state* except for a small penetration depth λ.

This is a physically reasonable result. Superflow is a long-range coherent phenomenon of the Bose condensate. The condensation of vortex lines destroys the coherence and thus the superflow. If superflow runs towards a disordered region, it has to flow around it, with streamlines looking just like the magnetic field lines around a superconductive

piece of material shown in Fig. 3.1. Only a thin surface layer can be invaded by superflow.

In addition to this magnetic penetration depth there was, in the superconductor, another length scale, the coherence length of the order field ξ. Recall that for $T > T_c$ there were two field fluctuations, one for the real part and one for the imaginary part of the field with the common coherence length $\xi(T) = 1/\sqrt{m^2}$. This length went to infinity close to the critical temperature. For $T < T_c$, in the ordered state, the two fluctuation modes were split. One of them, the size fluctuations acquired a coherence length $\xi_{\text{size}} = 1/\sqrt{-2m^2}$. This coherence length was observable as the scale over which the order changes substantially at a boundary between the superconductive and normal phases. The other fluctuation mode associated with the phase of the order parameter had no physical relevance since in the presence of a minimally coupled gauge field it corresponded to a gauge degree of freedom of the energy functional.

Let us now see what physical meaning these length scales have in the disorder version of the Ginzburg–Landau theory. Here, the ordered state has the length scale $\xi = 1/\sqrt{m^2}$ for the real and imaginary parts and regulates the range over which the correlation function of a single vortex line $G(\mathbf{x}, \mathbf{y})$ drops to zero. Remember that $P(\mathbf{x}, \mathbf{y}) = (2D/a^2) G(\mathbf{x}, \mathbf{y})$ gives the total number of configurations of a single vortex line, weighted by the proper Boltzmann factor, connecting the points $\mathbf{x}$ and $\mathbf{y}$ [recall Part I, Section 6.5]. Thus ξ is a measure for the average size of a vortex line. At the critical temperature, ξ goes to infinity, i.e., the vortex lines grow infinitely long. Above the critical temperature, the correlation functions separate into a connected piece and disconnected piece. For $|\mathbf{x} - \mathbf{y}| \to \infty$, only the disconnected piece survives, i.e.,

$$G(\mathbf{x}, \mathbf{y}) = \langle \varphi(\mathbf{x})\, \varphi^\dagger(\mathbf{y}) \rangle \to |\varphi|^2. \qquad (3.129)$$

This determines the probability of vortex lines of infinite length since it implies that

$$P(\mathbf{x}, \mathbf{y}) \xrightarrow[|\mathbf{x} - \mathbf{y}| \to \infty]{} \frac{2D}{a^2} |\varphi|^2. \qquad (3.130)$$

In superconductivity, this ratio of the two length scales $\kappa = \lambda/\sqrt{2}\, \xi_{\text{size}}$ was an important parameter which separated type I and type II materials marking the onset of different physical behaviors. It would therefore be interesting to measure λ and ξ_{size} in the superfluid and thus determine the

"type" of the disorder field theory. We shall see later that, theoretically, the ratio κ seems to be slightly larger than $1/\sqrt{2}$, so that the disorder field theory is of type II.

Notice that the description of the superfluid ^{4}He by a Ginzburg–Landau-like theory seems to be an example for which the approximate "derivation" in Section 3.11 of a first order transition due to fluctuations of the gauge field does not appear to hold: The superfluid-normal transition in ^{4}He is one of the best studied second order transitions.

The evidence is not yet conclusive since at the qualitative level established up to this point it is impossible to calculate how large the theoretically expected jump in the order parameter should be, i.e., whether it should be accessible to experiment or not. Only later shall we see that the superfluid is indeed a proper counter example to the above "derivation."

NOTES AND REFERENCES

The important papers on superconductivity are
H.K. Onnes, *Leiden Comm.*, 119b, 122b, 124c (1911),
W. Meissner and R. Ochsenfeld, *Naturwiss.* **21** (1933) 787,
E. London and F. London, *Proc. R. Soc.* **A149** (1935) 71,
C.J. Gorter and H.B. Casimir, *Phys. Z.* **35** (1934) 963,
L.D. Landau, *Phys. Z. Sowjetunion* **11** (1937) 26, 545, reprinted in *The Collected Papers of L.D. Landau*, ed. ter Haar (Gordon & Breach — Pergamon, New York, 1965) p. 193,
V.L. Ginzburg and L.D. Landau, *Zh. Eksperim. i Teor. Fiz.* **20** (1950) 1064,
J. Bardeen, L.N. Cooper and J.R. Schrieffer, *Phys. Rev.* **108** (1957) 1175,
L.P. Gorkov, *Zh. Eksperim. i Teor. Fiz.* **36** (1959) 1918,
L.D. Fadeev and V.N. Popov, *Phys. Lett.* **B25** (1967) 29.
For a rederivation of the Ginzburg–Landau equations and a more detailed discussion of the solutions see
D. Saint-James, E.J. Thomas, & G. Sarma, *Type-II Superconductivity* (Pergamon Press, Oxford, 1969) and
H. Kleinert, *Fortschr. Phys.* **26** (1978) 256.
Vortex lines were investigated by
A.A. Abrikosov, *Sov. Phys. JETP* **5** 1174 (1957),
W.M. Kleiner, L.M. Roth, S.H. Autler, *Phys. Rev.* **A133** (1964) 1226,
L. Kramer, *Phys. Rev.* **B3** (1971) 3821,
L. Jacobs, C. Rebbi, *Phys. Rev.* **B19** (1979) 4486.
Fluctuations were first studied by
V.L. Ginzburg, *Fiz. Twerd. Tela* **2** (1960) 2031 [*Sov. Phys. Solid State* **2** (1961) 1824].
The first-order of the superconductive phase transition was suggested in four dimensions by
S. Coleman and E. Weinberg, *Phys. Rev.* **D7** (1973) 1888;
the three dimensional case was considered by
B.I. Halperin, T.C. Lubensky and S.K. Ma, *Phys. Rev. Lett.* **32** (1974) 292

The κ-dependence of the order of the superconductive transition was estimated in 3 dimensions by

H. Kleinert, *Lett. Nuovo Cimento* **35** (1982) 405, where it was concluded that there exists a tricritical point.

See also a related discussion in four dimensions by

H. Kleinert, *Phys. Lett.* **B128** (1983) 69 and *Phys. Rev. Lett.* **56** (1986) 1441.

The tricritical behaviour suggested by the author was confirmed via Monte Carlo simulations by

J. Bartholomew, *Phys. Rev.* **28** (1983) 5378,

Y. Munehisa, *Phys. Lett.* **155B** (1985) 159.

See also related four-dimensional discussions by

J. Jersák, T. Neuhaus, P.M. Zerwas, *Nucl. Phys.* **B251** [FS13], (1985) 299,

G. Katsoumbas, *Phys. Lett,* **B140** (1984) 379

D. Toussaint, and R. Sugar, *Phys. Rev.* **D32** (1985) 2061,

K. Jansen, J. Jersák, C.B. Lang. G. Vones, T. Neuhaus, *Phys. Lett.* **155B** (1985) 268, *Nucl. Phys.* **B265** (1986) 129.

These results had actually been suggested on the basis of previous studies of $U(1)$ lattice gauge theories which had been shown to be transformable into a Ginzburg–Landau form by H. Kleinert, Erice Lectures 1982, in *Gauge Interactions*, ed. A. Zichichi (Plenum, New York, 1985).

V. Grösch, K. Jansen, J. Jersák, C.B. Lang, T. Neuhaus, C. Rebbi, *Phys. Lett.* **162B** (1985) 171,

J.S. Barber, *Phys. Lett.* **147B** (1984) 330,

R. Gupta, M.A. Novotny, R. Cordery, *Phys. Lett.* **172B** (1986) 86,

Y. Morikawa, A. Iwazaki, *Phys. Lett.* **165B** (1985) 361,

C.B. Lang, *Phys. Rev. Lett.* **57** (1986) 1828, *Nucl. Phys.* **B280** [FS18] (1987) 255,

C.B. Lang, C. Rebbi, *Phys. Rev.* **D35** (1987) 2510,

A.N. Burkitt, *Nucl. Phys.* **B270** [FS16] (1986) 575,

A. Hasenfratz, P. Hasenfratz, *Nucl. Phys.* **B295** [FS21] (1988) 1,

K. Decker, A. Hasenfratz, P. Hasenfratz, *Nucl. Phys,* **B295** [FS21] (1988) 21,

A. Hasenfratz, *Phys. Lett.* **201B** (1988) 492.

See also related questions in

W. Janke and H. Kleinert, *Phys. Rev. Lett.* **S7** (1986) 279, *Nucl. Phys.* **B270** (1986) 399.

The results are relevant even for cosmology where the use of the Ginzburg–Landau-like theories (inflationary universe) has been proposed by

A. Linde, *Rep. Prog. Phys.* **42** (1979) 389 (for a more recent review see *Rep. Prog. Phys.* **47** (1984) 925, by the same author)

and further studied by

A.H. Guth, *Phys. Rev.* **D23** (1981) 347,

A.H. Guth and E. Weinberg, *Nucl. Phys.* **B212** (1983) 321.

For a recent low-brow review see A.H. Guth and P.J. Steinhardt, *Scientific American*, May 1984, 90.

In the smectic-nematic transition of liquid crystals, the disorder field theory can be used to argue for the existence of a tricritical point. This has recently been found experimentally by J. Thoen, M. Maynissen, W. Van Dael, *Phys. Rev. Lett.* **52** (1984) 204.

Notice that Abelian lattice gauge theories in four dimensions can also be shown to be equivalent to a Ginzburg–Landau-like field theory:

H. Kleinert "Hadronization of Quark Theories," Erice Lectures 1976, in *Understanding the Fundamental Constituent of Matter*, ed. A. Zichichi (Plenum Press, New York, 1978).

CHAPTER FOUR

LATTICE MODEL OF
THE SUPERFLUID PHASE TRANSITION

4.1. MOTIVATION

In Chapter 2 we derived, in a continuum approximation, a disorder field theory of the Ginzburg–Landau type. The derivation had a qualitative character to it and several parameters such as the core energy per link and the coupling constant g remained unspecified. Moreover, multi-vortex interactions in which more than two lines meet and separate at one point were ignored. It would be desirable to find a more quantitative and specific access to the disorder field theory of vortex lines, in which all parameters are well defined and calculable, at least in principle, to arbitrary accuracy. Such an access does, indeed, exist. In Part I we saw that a lattice provides a definite way of properly defining all path integrals in a field theory. Therefore we expect that if we want to formulate a well defined theory of vortex lines we should do this on a lattice.

Let us recall here what made our considerations qualitative. It was the fact that the energy of a vortex line was known quantitatively only for a single straight line. For an ensemble of many curved lines we had to make the approximate and not very precise distinction of the two zones, a far zone, for which the size of the order parameter is constant and which is governed by the gradient of the phase of the order parameter, and a near

zone, which has an extra core energy due to the variation of the size of the order parameter. The bending energy in the far zone was very simple and described the superflow around the lines via the hydrodynamic expression

$$E_{\text{hydr}} = \int d^3x\, e = \frac{\rho_s}{2} \int d^3x\, v_s^2 = \frac{\rho_s}{2} \frac{\hbar^2}{M^2} \int d^3x (\nabla \gamma)^2. \qquad (4.1)$$

This was valid everywhere except close to the core of the vortex lines. Close to the core, $(\nabla \gamma)^2$ diverges so that the integral $\int d^3x(\nabla \gamma)^2$ ceases to exist. The infinity is avoided by noting that in the core, the size of the order parameter goes to zero and so does the superfluid part of the liquid as described by the density ρ_s. The core contains mainly the normal liquid and it is this property which makes the core energy finite, thus permitting the physical appearance of vortex lines. In the qualitative discussion it was assumed that for lines of any shape, the core region contributes only a constant core energy per unit length, the shape being irrelevant. This appeared to be a good approximation, at least as long as there were only a few vortex lines around. In this way, the most complicated part of the differential equations for the order parameter of a system of vortex lines disappeared and only the simple potential equation $-\nabla^2\gamma(\mathbf{x}) = 0$ for the far zone remained. We used this to calculate the long range part of the interaction energy. The final partition function of an ensemble of vortex lines did have the correct qualitative behavior. At the mean field level, it had a second order phase transition due to the disorder field acquiring a non-vanishing expectation value. This was interpreted as a signal for the condensation of vortex lines.

While studying the behavior of the thermodynamic functions in Section 2.2 we did not bother about the precise nature of this condensation process. The process could involve a proliferation of short lines or a divergence in length of a few lines, or both. As long as the short range steric interactions between the lines is not specified, we do not know what really happens. As we consider the details of the condensation process we realize that there exists an immediate danger in the field theory previously derived. It may happen that the lines proliferate in such a way that they come to lie within each other's core region. In that case, the derivation of the disorder theory, which was based on a clear separation of a near and a far zone around each line, breaks down. Thus we may wonder whether it still makes sense to apply the disorder field theory beyond the condensation point.

It is obvious, that such a question cannot be answered within the qualitatively derived disorder field theory. We have to go beyond it and find a framework in which it is possible to study ensembles of vortex lines at both, low and high densities. This will now be done for a specific model.

4.2. THE *XY* MODEL

If one had a simple approximate theoretical description of a complicated physical system in a certain limiting situation the question arises whether there does not exist a simplified physical system whose exact treatment leads, in the same limit, precisely to the same theory but which permits going beyond this limit in a well defined way. Such simplified systems serve as *models*. For the system of vortex lines in superfluid ^{4}He which for low temperatures allows for a clear separation into far and near zones, there exists a model known as the classical *planar spin* or the *XY model* in three dimensions.

At low temperatures, this model has the same type of vortex lines as the superfluid. As the temperature is raised the number of lines increases. However, all difficulties associated with a complex field description in the near zone are avoided by using only the phase variables $\gamma(\mathbf{x})$ of $\psi(\mathbf{x})$ and studying them on a lattice of spacing a. The finite lattice spacing has the virtue that the bending energies of the phase variable can no longer diverge. Thus there is no need for an order parameter to vanish in the core of a vortex line and this is why we may assume its size to be frozen throughout the liquid leaving the phase $\gamma(\mathbf{x})$ as the only dynamical variable. In order to be specific, let us assume the space to be a simple cubic lattice with N discrete sites $\mathbf{x}$ and oriented links $\mathbf{i}$ as defined in Eqs. (I.6.1) and (I.6.2), respectively. Let ∇_i be the lattice derivatives, but, unlike those in Eq. (I.6.6), let them be pure differences rather than $1/a$ times the differences, for convenience. Consider now Pitaevskii's energy functional (1.10) on such a simple cubic lattice

$$E = a^3 \sum_{\mathbf{x}} \left\{ \frac{\hbar^2}{2M} \frac{1}{a^2} \sum_i [|\nabla_i \psi|^2 - \mu|\psi|^2 + V|\psi|^4] \right\} . \tag{4.2}$$

If the size of the order parameter is considered to be frozen, this energy becomes

$$E = a \frac{\hbar^2}{2M} |\psi|^2 \sum_{\mathbf{x},i} |\nabla_i e^{i\gamma(\mathbf{x})}|^2 - E_c, \tag{4.3}$$

where E_c is the constant condensation energy $Na(\hbar^2/2M)(\mu^2/4V)$. Omitting this, the energy can be rewritten as

$$E = \frac{\sigma}{2} \sum_{\mathbf{x},i} |\nabla_i e^{i\gamma(\mathbf{x})}|^2 = \frac{\sigma}{2} \sum_{\mathbf{x},i} |e^{i\gamma(\mathbf{x}+\mathbf{i})} - e^{i\gamma(\mathbf{x})}|^2$$

$$= \sigma \sum_{\mathbf{x},i} \left(1 - \cos(\gamma(\mathbf{x}+\mathbf{i}) - \gamma(\mathbf{x})) \right) = \sigma \sum_{\mathbf{x},i} (1 - \cos \nabla_i \gamma(\mathbf{x})). \quad (4.4)$$

The constant σ is equal to $a(\hbar^2/M)|\psi|^2 = a\rho_s(\hbar^2/M^2)$. This is the lattice version of the hydrodynamic energy (4.1), to which it reduces as $a \to 0$. In this limit, $\gamma(\mathbf{x})$ cannot change much from site to site so that $|\nabla_i \gamma| \ll 1$ and $1 - \cos \nabla_i \gamma \sim (\nabla_i \gamma)^2/2 \sim (a^2/2)(\partial_i \gamma)^2$ and hence $E \sim (\rho_s/2)(\hbar^2/M^2) \int d^3x (\partial_i \gamma)^2$.

The advantage of the lattice formulation now becomes apparent. Due to the periodicity of the cosine in (4.4), the phase variable $\gamma(\mathbf{x})$ can jump, from site to site, from $\pi - \varepsilon$ to $-\pi + \varepsilon$, without cost in energy. If such a jump takes place over an entire surface S, energy accumulates close to the boundary of S which acts as a vortex line L, just as in the previously discussed continuum case [see Section 1.8]. Indeed, when going around L, the lattice version of the circuit integral $\oint d\gamma$ is equal to the size of the jump [observe that each $\gamma(\mathbf{x}) \in [-\pi, \pi)$]

$$\sum_{\mathbf{x}} \Delta\gamma(\mathbf{x}) = 2\pi n. \quad (4.5)$$

Unlike the continuum case, the gradient energy of $\gamma(\mathbf{x})$ close to the vortex line remains finite since the lattice gradient is always finite. In this way, the lattice version avoids the need for an order parameter whose size softens the core and prevents the divergence of the core energy. On the lattice, the core size is automatically forced to be larger than the lattice spacing a. The advantage of the lattice model is mainly of a technical nature. Thermodynamic properties can be readily calculated. We shall see that it is easy to determine analytically the limiting behavior for very high and very low temperatures and, by interpolation between the two, one can reach the physically interesting critical regions where the superfluid-normal phase transition takes place. In addition the lattice model can be simulated on a computer, via Monte Carlo techniques. By combining analytical and numerical methods the model can be studied quite reliably.

To be sure, everything that happens far away from the critical region is more a property of the model than of the superfluid. In either limit, $\beta \to \infty$ or $\beta \to 0$, the lattice structure will enter essentially into all results. The superfluid we want to describe, on the other hand, has no lattice structure. Thus we should not expect the model to give reliable physical information for large or small β. Only in the critical regime when all length scales become very large compared to the lattice spacing a, can we expect the properties of the model to become *independent* of the under-lying lattice, i.e., to become universal. If the temperature in superfluid ^{4}He goes to zero, the core size of vortex lines drops to about the interatomic distance of $0.5810\,\text{Å}$ and the superfluid density becomes equal to the total density, $\rho_s \to \rho \sim 3.145\,\text{g/cm}^3$. Even though the model is certainly not valid down to this temperature we shall tentatively adjust the parameters of the lattice model to these values and take

$$a = 3.5810\,\text{Å},$$

$$\sigma = \rho_s \frac{\hbar^2}{M^2} a = 0.145 \frac{\text{g}}{\text{cm}^3} \frac{\hbar^2}{M^2} a = 0.905°\text{K} \sim 1°\text{K}. \tag{4.6}$$

If we agree to measure T in units of σ, the XY model has the partition function

$$Z \equiv e^{-\beta ND} Z' \equiv e^{-\beta ND} \prod_x \left[\int_{-\pi}^{\pi} \frac{d\gamma(x)}{2\pi} \right] e^{\beta \sum_{x,i} \cos \nabla_i \gamma(x)}, \tag{4.7}$$

where $\beta = \sigma/T$ is the inverse temperature in units of $1/\sigma$. In Eq. (4.7) we have found it convenient to define also a slightly modified partition function Z' in which we have removed the constant energy per site and link β so as to remain with a pure cosine exponent. The corresponding free energy and all other thermodynamic quantities derived from Z' will be denoted by a prime.

Let us extract some simple properties of this model. In the limit of zero temperature, only small variations of $\gamma(x)$ are tolerated and Z has the limit

$$Z \to \prod_x \left[\int_{-\pi}^{\pi} \frac{d\gamma(x)}{2\pi} \right] e^{-(\beta/2) \sum_{x,i}(\nabla_i \gamma)^2}$$

$$= \prod_x \left[\frac{1}{\sqrt{2\pi\beta}} \right] \det(-\bar{\nabla} \cdot \nabla)^{-1/2} = \frac{1}{(\sqrt{2\pi\beta \cdot 2D})^N} \det\left(-\frac{\bar{\nabla} \cdot \nabla}{2D} \right)^{-1/2}, \tag{4.8}$$

where N is the total number of lattice sites. The determinant can be rewritten as

$$\exp\left[-\frac{1}{2}\operatorname{tr}\log\left(-\frac{\bar{\nabla}\cdot\nabla}{2D}\right)\right]$$

and has been calculated in (I.6.206b); the result was $\exp((N/2)0.1184)$ for $D = 3$. Thus we obtain the limiting partition function per site, for $D = 3$,

$$z = Z^{1/N} = e^{-(1/2)(\log(2\pi\beta\cdot 2D) - 0.1184)},$$ (4.9)

which amounts to a free energy per site of

$$-\beta f = -\tfrac{1}{2}\log\beta - c,$$ (4.10)

with $c = (1/2)[\log(2\pi\cdot 2D) - 0.1184]$. The internal energy per site is

$$u = -\frac{\partial}{\partial\beta}(-\beta f) = \frac{1}{2\beta} = \frac{T}{2}$$ (4.11)

so that the entropy per site becomes[a]

$$s = -\beta(f - u) = \left(1 - \beta\frac{\partial}{\partial\beta}\right)(-\beta f) = \beta^2\frac{\partial}{\partial\beta}f = -\frac{1}{2}\log\beta - c + \frac{1}{2}.$$ (4.12)

From u we find the specific heat at constant volume per site,

$$c_V = \frac{\partial}{\partial T}u = -\beta^2\frac{\partial}{\partial\beta}u = \frac{1}{2}.$$ (4.13)

These results agree with the Dulong–Petit rules derived for harmonic materials, according to which each degree of freedom contributes an internal energy $T/2$ and a specific heat $1/2$ (in units of k_B). Since, at low temperatures, the phase angle $\gamma(\mathbf{x})$ is a harmonic variable, it qualifies for this rule.

---

[a]The entropy does not vanish at zero temperature, as any proper entropy should, by Nernst's theorem. This is due to the omission of quantum effects (which is permissible in the immediate vicinity of the second order phase transition).

4.3. HIGH TEMPERATURE EXPANSION

For increasing temperatures, the variable $\gamma(\mathbf{x})$ exhibits larger and larger fluctuations. In particular, it can jump from $\pi - \varepsilon$ to $-\pi + \varepsilon$ in a way typical around vortex lines. For high temperatures, the jumps will be randomly distributed and the system will be filled with vortex lines. In this limit, β is so small that we can expand (4.7) as follows

$$Z' = \prod_{\mathbf{x}} \left[\int_{-\pi}^{\pi} \frac{d\gamma(\mathbf{x})}{2\pi} \right] \left(1 + \beta \sum_{\mathbf{x},i} \cos(\gamma(\mathbf{x}+\mathbf{i}) - \gamma(\mathbf{x})) \right.$$

$$\left. + \frac{\beta^2}{2!} \sum_{\substack{\mathbf{x}_1,\mathbf{i}_1 \\ \mathbf{x}_2,\mathbf{i}_2}} \cos(\gamma(\mathbf{x}_1+\mathbf{i}_1) - \gamma(\mathbf{x}_1)) \cos(\gamma(\mathbf{x}_2+\mathbf{i}_2) - \gamma(\mathbf{x}_2)) + \ldots \right).$$

Since the integrals over odd powers of the cosine average out to zero, the result is a power series in β^2. The quadratic term is non-zero only if sites and links are the same. Otherwise there is an unmatched angle $\gamma(\mathbf{x})$ in one of the cosines making its integral zero. Thus we find the lowest terms of the high temperature expansion,

$$Z' = (1 + N\tfrac{3}{4}\beta^2 + \ldots) = \exp[-N(-\tfrac{3}{4}\beta^2 + \ldots)],$$

with

$$f' = f - 3 = -\frac{3}{4}\beta + \ldots, \qquad u' = u - 3 = -3\frac{\beta}{2} + \ldots,$$

$$s' = s = -\frac{3}{4}\beta^2 + \ldots, \qquad c' = c = \frac{3}{2}\beta^2 + \ldots \qquad (4.14)$$

To higher orders, there are many products of cosines to be integrated and it is hard to find all non-zero contributions. There exists, however, a more economical procedure, called *character expansion*.[b] It is based on the well-known Fourier decomposition

$$e^{\beta \cos \gamma} = \sum_{b = -\infty}^{\infty} I_b(\beta) e^{ib\gamma}, \qquad (4.15)$$

---

[b]The name derives from the fact that in the case of non-Abelian group degrees of freedom, a similar expansion is possible in terms of the traces (= characters) of all irreducible representations of the group (which in the present case of a $U(1)$ group are simply $e^{ib\gamma}$).

where the $I_b(\beta)$ are the modified Bessel functions of integer order. Inserting this into (4.7) we obtain

$$Z' = \sum_{\{b_i(\mathbf{x})\}} \left[\prod_{\mathbf{x}} I_{b_i(\mathbf{x})}(\beta)\right] \prod_{\mathbf{x}} \left[\int_{-\pi}^{\pi} \frac{d\gamma(\mathbf{x})}{2\pi}\right] e^{i\Sigma_{\mathbf{x},i} b_i(\mathbf{x}) \nabla_i \gamma(\mathbf{x})}, \qquad (4.16)$$

where the summation symbol $\Sigma_{\{b_i(\mathbf{x})\}}$ denotes the product of sums

$$\prod_{\mathbf{x}} \sum_{b_i(\mathbf{x}) = -\infty}^{\infty}.$$

It is now quite straightforward to integrate out the $\gamma(\mathbf{x})$ variables. For this we observe that the sum in the second exponent can be rewritten as

$$\sum_{\mathbf{x},i} b_i(\mathbf{x}) \nabla_i \gamma(\mathbf{x}) = -\sum_{\mathbf{x},i} (\bar{\nabla}_i b_i(\mathbf{x})) \gamma(\mathbf{x}). \qquad (4.17)$$

This is the lattice version of *integration by parts* which for two arbitrary lattice functions $f(\mathbf{x})$ and $g(\mathbf{x})$ (periodic, or 0 at infinity) goes as follows:

$$\sum_{\mathbf{x}} f^*(\mathbf{x}) \nabla_i g(\mathbf{x})$$

$$= \sum_{\mathbf{x}} f^*(\mathbf{x})(g(\mathbf{x}+\mathbf{i}) - g(\mathbf{x})) = \sum_{\mathbf{x}} (f^*(\mathbf{x}) g(\mathbf{x}+\mathbf{i}) - f^*(\mathbf{x}) g(\mathbf{x}))$$

$$= \sum_{\mathbf{x}} (f^*(\mathbf{x}-\mathbf{i}) g(\mathbf{x}) - f^*(\mathbf{x}) g(\mathbf{x})) = -\sum_{\mathbf{x}} (f^*(\mathbf{x}) - f^*(\mathbf{x}-\mathbf{i})) g(\mathbf{x})$$

$$= -\sum_{\mathbf{x}} (\bar{\nabla}_i f(\mathbf{x}))^* g(\mathbf{x}). \qquad (4.18)$$

Using (4.17), the integrals over $\gamma(\mathbf{x})$ take the form

$$\prod_{\mathbf{x}} \left[\int_{-\pi}^{\pi} \frac{d\gamma(\mathbf{x})}{2\pi}\right] e^{-i\Sigma_{\mathbf{x},i} \bar{\nabla}_i b_i(\mathbf{x}) \gamma(\mathbf{x})}.$$

The factors $\bar{\nabla}_i b_i(\mathbf{x})$ of $\gamma(\mathbf{x})$ are all integers. Therefore, the exponentials are periodic in 2π and the integrals vanish unless $\bar{\nabla}_i b_i(\mathbf{x}) = 0$ at each site $\mathbf{x}$. This brings the partition function to the form

$$Z' = \sum_{\{b_i(\mathbf{x})\}} \delta_{\bar{\nabla}_i b_i, 0} \prod_{\mathbf{x},i} I_{b_i(\mathbf{x})}(\beta), \qquad (4.19a)$$

$$Z' = (I_0(\beta))^{DN} \left[1 + \sum_{\{b_i(\mathbf{x}) \neq 0\}} \delta_{\bar{\nabla}_i b_i, 0} \left(\prod_{\mathbf{x},i} I_{b_i(\mathbf{x})}(\beta)/I_0(\beta) \right) \right], \qquad (4.19b)$$

where we have introduced the notation $\delta_{\bar{\nabla}_i b_i, 0} \equiv \prod_{\mathbf{x}} \delta_{\bar{\nabla}_i b_i(\mathbf{x}), 0}$, for brevity.
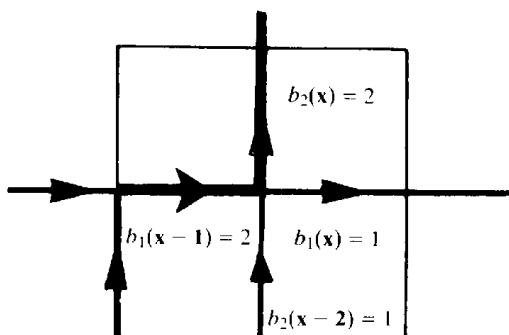
The condition $\bar{\nabla}_i b_i(\mathbf{x}) = 0$ has a simple geometric interpretation. Let us recall that for currents $j_i(\mathbf{x})$ the divergence condition $\partial_i j_i(\mathbf{x}) = 0$ means that streamlines are closed. The condition $\bar{\nabla}_i b_i(\mathbf{x}) = 0$ is the lattice version of this. It implies that if $b_i(\mathbf{x})$ are pictured as integer-valued "currents" flowing from the point $\mathbf{x}$ to $\mathbf{x} + i$ along the link i, then the set of all these "currents" has to form closed loops with "current conservation" at every vertex. We can see this best by looking at the simple case of $D = 2$ dimensions. For the lattice site $\mathbf{x}$, the condition $\bar{\nabla}_i b_i(\mathbf{x})$ means

$$b_1(\mathbf{x}) - b_1(\mathbf{x} - 1) + b_2(\mathbf{x}) - b_2(\mathbf{x} - 2)$$

$$= b_1(\mathbf{x}) + b_2(\mathbf{x}) - b_1(\mathbf{x} - 1) - b_2(\mathbf{x} - 2). \qquad (4.20)$$

The integers $b_1(\mathbf{x})$, $b_2(\mathbf{x})$ are "currents" leaving the point along the positive directions 1 and 2. The integers $b_1(\mathbf{x} - 1)$, $b_2(\mathbf{x} - 2)$ are "currents" which occupy the places to the left and below the point $\mathbf{x}$ and arrive at $\mathbf{x}$ (see Fig. 4.1). The example demonstrates that the "currents" $b_i(\mathbf{x})$ with $\bar{\nabla} \cdot \mathbf{b}(\mathbf{x}) = 0$ are indeed conserved.

We can easily convince ourselves that summing over all $b_i(\mathbf{x})$ under the condition $\bar{\nabla} \cdot \mathbf{b}(\mathbf{x}) = 0$ corresponds to summing over a grand canonical ensemble of all non-backtracking oriented closed chains involving only the fundamental current of strength $|\mathbf{b}| = 1$. The strength $b_i = -1$ is represented by the chain running backwards on the link i. The chains with higher strength $b_i = 2, 3, \ldots$ etc. are obtained by the repeated passage of

FIG. 4.1.   Illustration of the conservation law $\bar{\nabla}_i b_i(\mathbf{x}) = 0$ on the lattice. If the components $b_i(\mathbf{x})$ are pictured as integer-valued directed currents flowing along the link $i(\mathbf{x})$, the total current flowing into each site is zero (Kirchhoff's law).
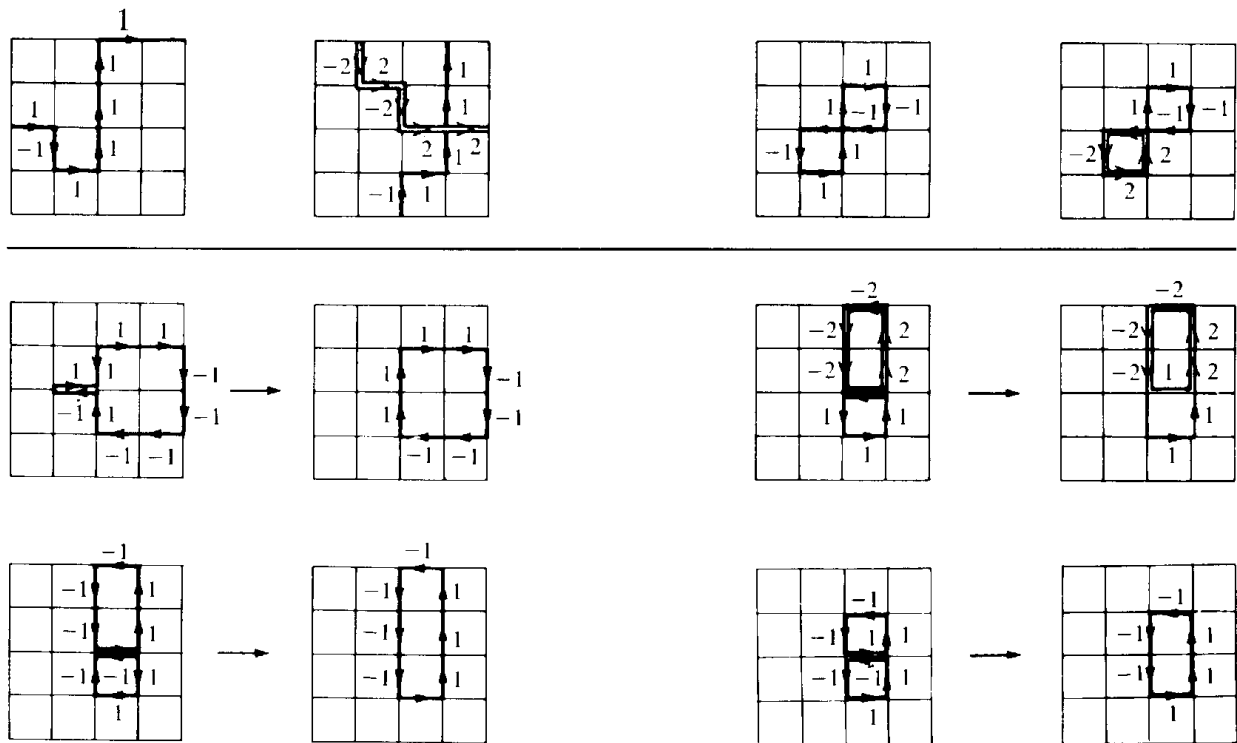
the "fundamental chain" through a given link. By forbidding this "unit valued" chain from backtracking along any link through which it or another chain has run at least once we can make sure that there is no double counting. Otherwise there would be many ways of obtaining the same current strength $b_i(x)$. A few characteristic configurations of these non-backtracking random chains are pictured in the first row of Fig. 4.2. The lower two rows of the figure show forbidden backtracking chains in comparison with those proper chains which they would double count (to their right).

After these observations let us calculate Z' from (4.19). For completeness, we chall consider the general case of D dimensions. To lowest non-trivial order there are only the loops of length 4:

$$\square \begin{pmatrix} D \\ 2 \end{pmatrix}, \quad \square \begin{pmatrix} D \\ 2 \end{pmatrix}, \tag{4.21}$$

They can occur in any of the $\begin{pmatrix} D \\ 2 \end{pmatrix} = D(D-1)/2$ coordinate planes, once for every site, if we assume a large lattice with periodic boundary conditions in each space direction. Hence we find [see Table 4.1]

FIG. 4.2.   Typical non-backtracking random chains contained in the sum $\Sigma_{\{b_i(x)\}}\,\delta_{\bar\nabla_i b_i(x),0}$. The two rows below the line show, on the left-hand side, forbidden backtracking configurations and, on the right-hand side, the proper allowed configurations which they are equivalent to.

$$Z' = (I_0(\beta))^{ND} \left[1 + 2 \left(\frac{I_1(\beta)}{I_0(\beta)} \right)^4 N \binom{D}{2} + \ldots \right]. \qquad (4.22)$$

For the free energy per site this implies

$$-\beta f' = D \log I_0(\beta) + \left(\frac{I_1}{I_0} \right)^4 D(D-1) + \ldots \qquad (4.23)$$

This free energy is correct up to order β^4:

$$-\beta f' = D(\tfrac{1}{4}\beta^2 - \tfrac{1}{64}\beta^4 + \tfrac{1}{16}\beta^4 (D-1) + \ldots)$$
$$= D(\tfrac{1}{4}\beta^2 + \tfrac{1}{16}(D - \tfrac{5}{4})\beta^4 + \ldots). \qquad (4.24)$$

The same loop can also be multiply occupied. This gives a further sum, i.e.,

$$\sum_{n=2}^{\infty} \left(\frac{I_n}{I_0} \right)^4 D(D-1), \quad n \geq 2, \qquad (4.25)$$

in the bracketed quantity in Eq. (4.22). The lowest possibility is $n = 2$ which is of order β^8.

The next larger loop contains six links,
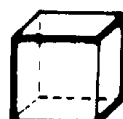
$$\boxed{} 2\binom{D}{2} \qquad (4.26)$$

with both orientations. Here and in the following diagrams we drop the arrows and ignore the orientations during the counting procedure since they merely amount to trivial factors of 2 at the end. The loop (4.26) will occur twice as often as the small loop (4.21) since the second plaquette has two sides to which it can be attached. This gives $2\binom{D}{2}$ (unoriented) loops or a contribution of

$$2N \left(\frac{I_1}{I_0} \right)^6 2\binom{D}{2} \qquad (4.27)$$

to the bracket sum of Z' in (4.22).

The loops of length 6 do not have to be planar. They can be bent such that the two plaquettes lie in two different lattice planes. Their number is determined by observing that they may be considered as running along the edges of a unit cube. In D dimensions, there are $\binom{D}{3}$ ways of forming such a cube at each site with the edges being positively oriented. On each such cube one can place the two plaquettes as often as there are edges, i.e., 12 times:

$$12\binom{D}{3} \tag{4.28}$$

This contributes

$$2N\left(\frac{I_1}{I_0}\right)^6 12\binom{D}{3} \tag{4.29}$$

to the series in brackets in (4.22).

These are not all the diagrams of length 6. It is easy to see that for each of the $\binom{D}{3}$ cubes there are also loops of the type

$$4\binom{D}{3} \tag{4.30}$$
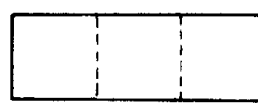
The number 4 is given by the number of diagonals connecting the untouched pairs of corners. This leads to

$$2N\left(\frac{I_1}{I_0}\right)^6 \cdot 4\binom{D}{3} \tag{4.31}$$

in the bracket in Eq. (4.22) [see Table 4.1].

The loops of length 6 can be multiply occupied so that $(I_1/I_0)^6$ has to be replaced by $(I_n/I_0)^6$ with $n \geq 2$. The lowest possibility, $n = 2$, is of order β^{12}.

The loops of length 8 are quite numerous. They may be organized into planar ones and those sticking out into three or four dimensions. The planar ones are easy to count. Their diagrams are

$$2\binom{D}{2} \tag{4.32a}$$

$$\binom{D}{2} \tag{4.32b}$$

$$4\binom{D}{2} \tag{4.32c}$$

The first appears as often as (4.26), twice for each plaquette, due to the two edges along which the first plaquette is extended. Therefore it contributes

$$2N\left(\frac{I_1}{I_0}\right)^8 2\binom{D}{2}. \tag{4.33}$$

The second is symmetric under exchange of x and y directions so that it is unique and the contribution is

$$2N\left(\frac{I_1}{I_0}\right)^8\binom{D}{2}. \tag{4.34}$$

In the third, one of the four plaquettes is omitted, which results in making its contribution appear four times as often as the last one:

$$2N\left(\frac{I_1}{I_0}\right)^8 4\binom{D}{2}. \tag{4.35}$$

The loops of length 8 which extend into a three-dimensional subspace are given separately in Fig. 4.3. The numbers in front of $\binom{D}{3}$ arise as follows.

(a) There are two opposite faces with two occupied edges. For each of these there are two ways of placing the loop. Since there are three ways of counting the opposite faces, one finds the contribution

$$2N\left(\frac{I_1}{I_0}\right)^8 6\binom{D}{3}. \tag{4.36}$$

(b) There is a common factor 3 counting the number of oriented faces

when the second cube is attached to the first. On the combination a loop of length 8 can be placed in four different ways depending on which of the four bottom links are occupied by the loop. This gives a contribution

$$2N\left(\frac{I_1}{I_0}\right)^8 12\binom{D}{3}.\tag{4.37}$$
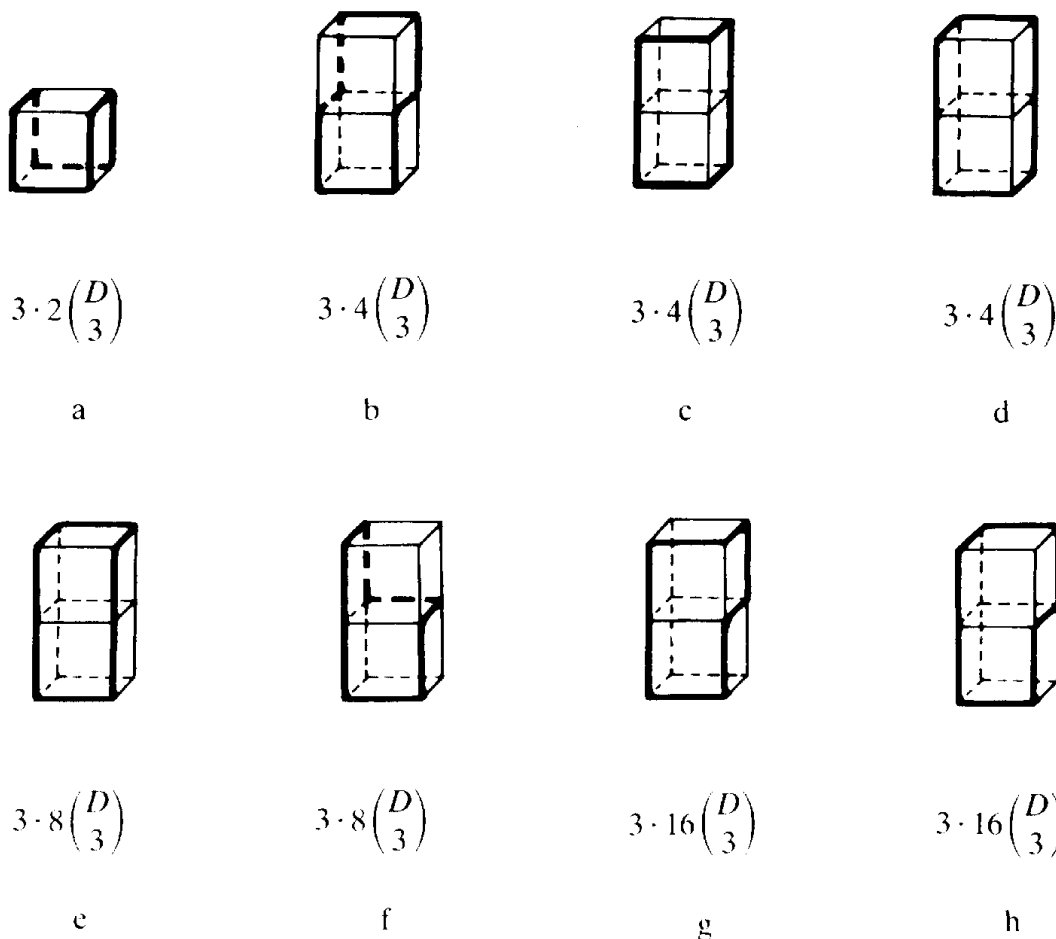
The same holds for (c) and (d). In (e), there are twice as many diagrams as in (b) since there is an additional choice of the top or bottom face to be covered. Thus they contribute

$$2N\left(\frac{I_1}{I_0}\right)^8 24\binom{D}{3}.\tag{4.38}$$

The same contribution arises from diagram (f), where we have four ways of choosing two edges with unoccupied corners and in addition, for each of these, the figure can be drawn topside up or down.

In the diagram (g) there is an extra factor of two since the extra

FIG. 4.3. The loops of length 8 extending into three space dimensions and their number per lattice site (not counting the two orientations).

$$3\cdot2\binom{D}{3}$$

a

$$3\cdot4\binom{D}{3}$$

b

$$3\cdot4\binom{D}{3}$$

c

$$3\cdot4\binom{D}{3}$$

d

$$3\cdot8\binom{D}{3}$$

e

$$3\cdot8\binom{D}{3}$$

f

$$3\cdot16\binom{D}{3}$$

g

$$3\cdot16\binom{D}{3}$$

h

plaquette has two ways of connecting to the long faces. The diagram (h) is a unique modification of (g). Hence, each of these contributes

$$2N\left(\frac{I_1}{I_0}\right)^8 48\left(\frac{D}{3}\right).\qquad(4.39)$$

We now arrive at diagrams which are possible only in a space with more than three dimensions. There, 8 links can be connected to closed loops in such a way that *four* independent space directions are involved. They cover a four-dimensional hypercube whose number is $\left(\begin{array}{c}D\\4\end{array}\right)$. The diagrams are hard to visualize. Let us call the fourth dimension "time." The loops can be grouped into two, which both leave the three-dimensional space, go along one time-like link, run *one* link along a space direction and finally return back into space along a time-like link. Or they run off into the time direction, traverse *two* spatial links, and then return into three-space. There are four ways of picking a time direction. The remaining freedom is rather tedious to describe in words; it will suffice to simply state the results:

 $4 \cdot 72\left(\begin{array}{c}D\\4\end{array}\right),$ $4 \cdot 48\left(\begin{array}{c}D\\4\end{array}\right),$ $4 \cdot 42\left(\begin{array}{c}D\\4\end{array}\right),$

$$(4.39abc)$$

and their contribution to the bracket in (4.22) carries a factor

$$2N\left(\frac{I_1}{I_0}\right)^8.$$

To the same order in $(I_1/I_0)^8$ there are also composite graphs. These can be formed by two elementary plaquettes with $[D(D-1)/2]^2$ $N(N-1)$ ways of arranging them on the lattice. It is useful to separate out all diagrams in which two plaquettes touch each other along one link. If both lie in one and the same plane, this happens the following number of times:

 $N \cdot 2\left(\begin{array}{c}D\\2\end{array}\right)$ $\qquad(4.40)$

[compare (4.26)]. If the plaquettes are taken from two different planes, this happens

$$N \cdot 2 \cdot 12 \binom{D}{3} \tag{4.41}$$

times [compare (4.28)]. The extra factor 2 is due to the possibility of touching all four links in one configuration — there the plaquettes lie on top of each other [one had already been counted before (see (4.25)]. Since the two loops are indistinguishable, we obtain a factor 1/2 and find, for the total number of pairs of plaquettes which do not touch each other at any link, the factor

$$\frac{1}{2}\left\{N^2 \binom{D}{2}^2 - N\left(5\binom{D}{2} + 24\binom{D}{3}\right)\right\}. \tag{4.42}$$

These diagrams give a contribution of

$$4\left(\frac{I_1}{I_0}\right)^8 \frac{1}{2}\left\{N^2 \binom{D}{2}^2 - N\left(5\binom{D}{2} + 24\binom{D}{3}\right)\right\} \tag{4.43}$$

to (4.22). Their orientations now lead to a factor 4 since *each* loop can be traversed in two different directions.

The configurations in which two plaquettes touch each other are now treated separately. There are those of the form (4.26) but with a double current flowing along the common face

$$\tag{4.44}$$

which can occur with two orientations, giving a contribution

$$2\left(\frac{I_1}{I_0}\right)^6 \left(\frac{I_2}{I_0}\right) N 2 \binom{D}{2}. \tag{4.45a}$$

Similarly, there are those of the form (4.28) contributing

$$2\left(\frac{I_1}{I_0}\right)^6 \left(\frac{I_2}{I_0}\right) N 12 \binom{D}{3}. \tag{4.45b}$$
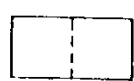
Collecting all terms which contribute up to the order β^8 we have

$$Z' = I_0(\beta)^{ND}[\xi_4 + \xi_6 + \xi_8], \tag{4.46}$$
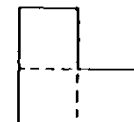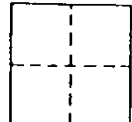
where

$$\xi_4 = 2N\left(\frac{I_1}{I_0}\right)^4\binom{D}{2},$$

$$\tag{4.47}$$
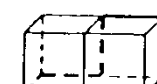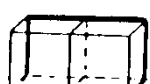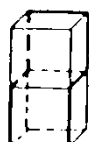
$$\xi_6 = 2N\left(\frac{I_1}{I_0}\right)^6\left[2\binom{D}{2} + (12 + 4)\binom{D}{3}\right],$$
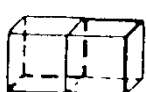
$$\xi_8 = 2N\left(\frac{I_1}{I_0}\right)^8\left\{(2 + 1 + 4)\binom{D}{2}\right.$$
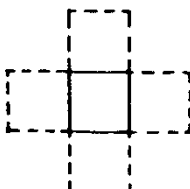
$$+ (6 + 12 + 24 + 12 + 48$$

$$+ 24 + 12 + 48)\binom{D}{3} + (288 + 192$$

$$\left. + 168)\binom{D}{4} + N\left(\left(\binom{D}{2}\right)^2 - \left(5\binom{D}{2} + 24\binom{D}{3}\right)\right)\right\}$$

4. LATTICE MODEL OF SUPERFLUID PHASE TRANSITION

$$+ 2N\left(\frac{I_1}{I_0}\right)^6\left(\frac{I_2}{I_0}\right)\left(2\binom{D}{2} + 12\binom{D}{3}\right) + 2N\left(\frac{I_2}{I_0}\right)^4\binom{D}{2}.$$

$$(4.48)$$

The diagrams of the tenth order are very tedious to count, so we relegate the details to Appendix 4A. The result is

$$\xi_{10} = 2N\left(\frac{I_1}{I_0}\right)^{10}\left[28\binom{D}{2} + 2328\binom{D}{3} + 23136\binom{D}{4} + 47616\binom{D}{5}\right]$$

$$+ 6N\left(\frac{I_1}{I_0}\right)^{10}\left[12\binom{D}{3} + 32\binom{D}{4}\right]$$

$$+ 4N\left(\frac{I_1}{I_0}\right)^{10}\left[N\left(2\binom{D}{2}^2 + 16\binom{D}{2}\binom{D}{3}\right)\right.$$

$$\left. - \left(16\binom{D}{2} + 396\binom{D}{3} + 864\binom{D}{4}\right)\right]$$

$$+ 2N\left(\frac{I_1}{I_0}\right)^8\left(\frac{I_2}{I_0}\right)\left[12\binom{D}{2} + 288\binom{D}{3} + 768\binom{D}{4}\right]$$

$$+ 2N\left(\frac{I_1}{I_0}\right)^6\left(\frac{I_2}{I_0}\right)^2 48\binom{D}{3} + 2N\left(\frac{I_1}{I_0}\right)^4\left(\frac{I_2}{I_0}\right)^3\left[4\binom{D}{2} + 24\binom{D}{3}\right].$$

$$(4.49)$$

In Table 4.1 we marked which graphs occur in the Ising model, which is the XY model with the restriction that the angle γ can have only the two values, zero and π (it coincides with the so-called Z_2 model, to be discussed in detail in Section 10.6). Then the diagrams have no orientation and no link can be occupied twice, while the corners can.

In the literature, the number of single loop configurations of length n were named "lattice constants" by Domb and denoted by p_n. They are listed in Tables 4.2, including lattice symmetries other than those discussed here. The tables also give the number of multiple loop configurations (divided by N) which do not touch each other, either along a link or on a site. They are denoted by $[p_{n1}, p_{n2}]$, $[p_{n1}, p_{n2}, p_{n3}, \ldots]$, $\ldots$ Such configurations are called self-avoiding. As an example of the use of the tables let us look for all loops of length 8 on a square lattice. From Table 4.1 we know that there are 7 simple graphs, namely, the entries

TABLE 4.1. Graphical contributions to the high temperature expansion of the XY and Villain Models. For comparison, also the Ising graphs are counted expanded in powers of $v = \tan\beta$.

		Ising				Orien-tations	XY				Villain power
Graph	Number of graphs per site	$D=2$	$D=3$	$D=4$	power		$D=2$	$D=3$	$D=4$	power	
4.1	$p_4 = \binom{D}{2}$	1	3	6	v^4	2	2	6	12	$\left(\frac{I_1}{I_0}\right)^4$	$\left(\frac{I_1}{I_0}\right)^4$
6.1	$2\binom{D}{2}$	2	6	12	v^6	2	4	12	24	$\left(\frac{I_1}{I_0}\right)^6$	$\left(\frac{I_1}{I_0}\right)^6$
6.2	$12\binom{D}{3}$	—	12	48	v^6	2	—	24	96		
6.3	$4\binom{D}{3}$	—	4	16	v^6	2	—	8	32		
6.1–6.3	$p_6 = 2\binom{D}{2} + 16\binom{D}{3}$	2	22	76	v^6	2	4	44	152	$\left(\frac{I_1}{I_0}\right)^6$	$\left(\frac{I_1}{I_0}\right)^6$
8.1	$2\binom{D}{2}$	2	6	12	v^8	2	4	12	24	$\left(\frac{I_1}{I_0}\right)^8$	$\left(\frac{I_1}{I_0}\right)^8$
8.2	$\binom{D}{2}$	1	3	6		2	2	6	12		
8.3	$4\binom{D}{2}$	4	12	24		2	8	24	48		

						r^8				
8.4	$6\binom{D}{3}$	—	6	24	2	—	12	48
8.5	$12\binom{D}{3}$	—	12	48	2	—	24	96
8.6	$24\binom{D}{3}$	—	24	96	2	—	48	192
8.7	$12\binom{D}{3}$	—	12	48	2	—	24	96
8.8	$48\binom{D}{3}$	—	48	192	2	—	96	384
8.9	$24\binom{D}{3}$	—	24	96	2	—	48	192
8.10	$12\binom{D}{3}$	—	12	48	2	—	24	96
8.11	$48\binom{D}{3}$	—	48	192	2	—	96	384
8.12	$288\binom{D}{4}$	—	—	288	2	—	—	576
8.13	$192\binom{D}{4}$	—	—	192	2	—	—	384

TABLE 4.1. continued

Graph	Number of graphs per site	Ising D=2	Ising D=3	Ising D=4	Ising power	Orien-tations	XY D=2	XY D=3	XY D=4	XY power	Villain power
8.14	$168\binom{D}{4}$	—	—	168	r^8	2	—	—	336	$\left(\frac{I_1}{I_0}\right)^8$	$\left(\frac{I_1}{I_0}\right)^8$
8.1–8.14	$p_8 = 7\binom{D}{2} + 186\binom{D}{3} + 648\binom{D}{4}$	7	207	1434	r^8	2	14	414	2868	$\left(\frac{I_1}{I_0}\right)^8$	$\left(\frac{I_1}{I_0}\right)^8$
8.15	$\frac{N}{2}\binom{D}{2}^2 - \left(\frac{5}{2}\binom{D}{2} + 12\binom{D}{3}\right)$	−2.5	−19.5	−63	r^8	4	−10	−78	−252		
Total Ising = 8.1 − 8.15	$\frac{N}{2}\binom{D}{2}^2 + \frac{9}{2}\binom{D}{2} + 174\binom{D}{3} + 648\binom{D}{4}$	4.5	187.5	1371	v^8						
8.16	$2\binom{D}{2}$	—	—	—	—	2	4	12	24	$\left(\frac{I_1}{I_0}\right)^6\frac{I_2}{I_0}$	$\left(\frac{I_1}{I_0}\right)^{10}$

	$\left(\frac{I_1}{I_0}\right)^{16}$	$\left(\frac{I_1}{I_0}\right)^{8}$ $\left(\frac{I_1}{I_0}\right)^{10}$	$\left(\frac{I_1}{I_0}\right)^{16}$	$\left(\frac{I_1}{I_0}\right)^{10}$	
	$\left(\frac{I_2}{I_0}\right)^{4}$	$\left(\frac{I_1}{I_0}\right)^{8}$ $\left(\frac{I_1}{I_0}\right)^{6}\frac{I_2}{I_0}$	$\left(\frac{I_2}{I_0}\right)^{4}$	$\left(\frac{I_1}{I_0}\right)^{10}$	

8.17	96	24	—	2	—	—	—	—	$12\binom{D}{3}$
8.18	12	6	2	2	—	—	—	—	$\binom{D}{2}$
Total XY $= 8.1 - 8.15$									(orientations included) $2N\binom{D}{2}^2 + 4\binom{D}{2} + 324\binom{D}{3} + 1296\binom{D}{4}$
$+ 8.16 - 8.17$	2616 / 120	336 / 36	4 / 4						$4\binom{D}{2} + 24\binom{D}{3}$
$+ 8.18$	12	6	2						$2\binom{D}{2}$
10.1	24	12	4	2	v^{10}	12	6	2	$2\binom{D}{2}$
10.2	24	12	4	2		12	6	2	$2\binom{D}{2}$
10.3	96	48	16	2		48	24	8	$8\binom{D}{2}$

TABLE 4.1. continued

Graph	Number of graphs per site	Ising D=2	Ising D=3	Ising D=4	Ising power	Orientations	XY D=2	XY D=3	XY D=4	XY power	Villain power
10.4	$4\binom{D}{2}$	4	12	24		2	8	24	48	$\left(\dfrac{I_1}{I_0}\right)^{10}$	$\left(\dfrac{I_1}{I_0}\right)^{10}$
10.5	$8\binom{D}{2}$	8	24	48		2	16	48	96		
10.6	$4\binom{D}{2}$	4	12	24		2	8	24	48		
10.1–10.6	$28\binom{D}{2}$	28	84	168	v^{10}	2	56	168	336		
10.7 (decagons involving 3 dimensions)	$2328\binom{D}{3}$	—	2328	9312	v^{10}	2	—	4656	18624		
10.8 (decagons involving 4 dimensions)	$23136\binom{D}{4}$	—	—	23136	v^{10}	2	—	—	46272		
10.9 (decagons involving 5 dimensions)	$47616\binom{D}{5}$	—	—	—	v^{10}	2	—	—	—		
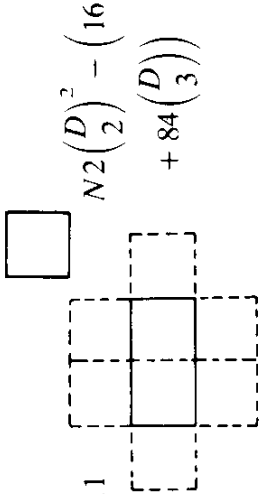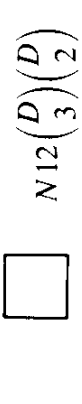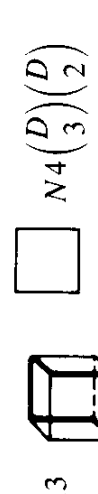
	p									$\left(\dfrac{I_2}{I_0}\right)^{10}$
										$\left(\dfrac{I_1}{I_0}\right)^{10}$
10.1–10.9	$p_{10} = 28\binom{D}{2} + 2328\binom{D}{3} + 23136\binom{D}{4} + 47616\binom{D}{5}$	28	2412	32448	v^{10}	2	56	4824	64896	
10.10	$12\binom{D}{3} + 32\binom{D}{4}$	—	12	68	v^{10}	6	—	72	408	
10.11	$N2\left(\binom{D}{2}^2 - \left(16\binom{D}{2} + 84\binom{D}{3}\right)\right)$	−16	−132	−432		4	−64	−528	−1728	
10.12	$N12\binom{D}{3}\binom{D}{2} - \left(240\binom{D}{3} + 672\binom{D}{4}\right)$	−240	−1392	−4128	v^{10}	4	−960	−5568	−16512	
10.13	$N4\binom{D}{3}\binom{D}{2} - \left(72\binom{D}{3} + 192\binom{D}{4}\right)$	−72	−408	−1200		4	−288	−1632	−4800	$\left(\dfrac{I_1}{I_0}\right)^{16}$
10.14	$4\binom{D}{2}$	—	—	—		2	8	24	48	$\left(\dfrac{I_1}{I_0}\right)^{4}\left(\dfrac{I_2}{I_0}\right)^{3}$

TABLE 4.1. continued

Graph	Number of graphs per site	Ising D=2	D=3	D=4	power	Orientations	XY D=2	D=3	D=4	power	Villain power
10.15	$24\binom{D}{3}$	—	—	—	—	2	—	48	192	$\left(\frac{I_1}{I_0}\right)^4\left(\frac{I_2}{I_0}\right)^3$	$\left(\frac{I_1}{I_0}\right)^{16}$
10.16	$24\binom{D}{3}$	—	—	—	—	2	—	48	192	$\left(\frac{I_1}{I_0}\right)^6\left(\frac{I_2}{I_0}\right)^2$	$\left(\frac{I_1}{I_0}\right)^{14}$
10.17	$24\binom{D}{3}$	—	—	—	—	2	—	48	192		
10.18	$4\binom{D}{2}$	—	—	—	—	2	8	24	48	$\left(\frac{I_1}{I_0}\right)^8\left(\frac{I_2}{I_0}\right)$	$\left(\frac{I_1}{I_0}\right)^{12}$
10.19	$8\binom{D}{2}$	—	—	—	—	2	16	48	96		
10.20–10.27 (= 4(8.4) + 2(8.5) + 2(8.6) + 0(8.7) + 2(8.8) + 2(8.9) + 0(8.10) + 1(8.11))	$288\binom{D}{3}$	—	—	—	—	2	—	576	2304		
10.28–10.30 (= 2(8.12) + 1(8.13) + 0(8.14))	$768\binom{D}{4}$	—	—	—	—	2	—	—	1536	$\left(\frac{I_1}{I_0}\right)^8\left(\frac{I_2}{I_0}\right)$	$\left(\frac{I_1}{I_0}\right)^{12}$

Total Ising = 10.1 – 10.13

$$12\binom{D}{2} + 1944\binom{D}{3} + 22304\binom{D}{4} + 47616\binom{D}{5} + N\left(2\binom{D}{2}\right)^2 + 16\left(\binom{D}{3}\binom{D}{2}\right)$$

Total XY = 10.1 – 10.13 (2 orientations included)

$$-8\binom{D}{2} + 3144\binom{D}{3} + 43008\binom{D}{4} + 95232\binom{D}{5} + 4N\left(2\binom{D}{2}\right)^2 + 16\binom{D}{3}\binom{D}{2}$$

+ 10.14 – 10.19

$$8\binom{D}{2} + 48\binom{D}{3}$$

+ 10.16 – 10.17

$$96\binom{D}{3}$$

+ 10.18 – 10.30

$$24\binom{D}{2} + 576\binom{D}{3} + 1536\binom{D}{4}$$

				Factor	Factor
12	1980	30152	v^{10}		
	—				
-8	3120	55536		$\left(\dfrac{I_1}{I_0}\right)^{10}$	$\left(\dfrac{I_1}{I_0}\right)^{10}$
8	72	240	—	$\left(\dfrac{I_1}{I_0}\right)^{16}$	$\left(\dfrac{I_1}{I_0}\right)^{4}\left(\dfrac{I_2}{I_0}\right)^{3}$
—	96	384	—	$\left(\dfrac{I_1}{I_0}\right)^{14}$	$\left(\dfrac{I_1}{I_0}\right)^{6}\left(\dfrac{I_2}{I_0}\right)^{2}$
24	648	3984	—	$\left(\dfrac{I_1}{I_0}\right)^{12}$	$\left(\dfrac{I_1}{I_0}\right)^{8}\left(\dfrac{I_2}{I_0}\right)$

8.1–8.3 (the entries 8.4–8.12 come in only in higher dimensions). This number 7 is found in Table 4.2a as the lattice constant p_8. We now have to add the graphs composed of two loops of length 4. From Table 4.1 entry 8.15 [or from Eq. (4.42)] we know that their number is $(1/2) N^2 - 4 \cdot 5 N$. This number comes from all N^2 positions minus $4 \cdot N$ touching each other along one link minus N lying on top of each other. The same number

TABLE 4.2a. The lattice constants p_n = numbers of self-avoiding loops of length n (see C. Domb and M.F. Sykes cited in the in Notes and References) in 3 and 2 dimensions.

		fcc	bcc	sc	sq	t
p_3	△	8	—	—	—	2
p_4	□	33	12	3	1	3
p_5	◇	168	—	—	—	6
p_6	⬠	970	148	22	2	15
p_7	⬡	6168	—	—	—	42
p_8	○	42069	2736	207	7	123
p_9	○	301376	—	—	—	380
p_{10}	○	2241420	61896	2412	28	1212
p_{11}		17173224	—	—	—	3966
p_{12}		134806948	1579324	31754	124	13265
p_{13}		1079802216	—	—	—	45144
p_{14}		8789329080	43702920	452640	588	155955

TABLE 4.2b. $[p_3, p_3] = N p_3^2/2 - (p_{6c} + p_{5a} + p_3/2)$.

		fcc	bcc	sc	sq	t
p_{6c}	⋈	204	—	—	—	9
p_{5a}	⬚	36	—	—	—	3
p_3	△	8	—	—	—	2
$[p_3, p_3]$		$32N$ -244				$2N$ -13

TABLE 4.2c. $[p_3, p_4] = Np_3p_4 - (p_{7e} + 3p_{7g} + p_{6b} + 2p_{5a})$.

		fcc	bcc	sc	sq	t
p_{7e}		2040	—	—	—	30
p_{7g}		24	—	—	—	—
p_{6b}		384	—	—	—	12
p_{5a}		36	—	—	—	3
p_3		8	—	—	—	2
p_4		33	12	3	1	3
$[p_3, p_4]$		264N −2568				6N −48

TABLE 4.2d. $[p_3, p_5] = Np_3p_5 - (p_{8g} + 2p_{8s} + p_{7b} + p_{7c} + p_{6b})$.

		fcc	bcc	sc	sq	t
p_{8g}		12096	—	—	—	66
p_{8s}		384	—	—	—	—
p_{7b}		2400	—	—	—	30
p_{7c}		192	—	—	—	6
p_{6b}		384	—	—	—	12
p_3		8	—	—	—	2
p_5		168	—	—	—	6
$[p_3, p_5]$		1344N −15840				12N −114

TABLE 4.2e. $[p_4, p_4] = Np_4^2/2 - (p_{8h} + 3p_{8r} + p_{8s} + p_{7a} + p_{7c} + 3p_{6a} + 3p_{6d} + p_4/2)$.

|		fcc	bcc	sc	sq	t
p_{8h}		4968	618	30	2	24
p_{8r}		9	3	—	—	—
p_{8s}		384	—	—	—	—
p_{7a}		966	192	18	2	12
p_{7c}		192	—	—	—	6
p_{6a}		36	12	—	—	—
p_{6b}		2	—	—	—	—
p_4		33	12	3	1	3
$[p_4, p_4]$		1089/2N −6667.5	72N −861	9/2N −49.5	1/2N −4.5	9/2N −43.5

TABLE 4.2f. $[p_3, p_6] = Np_3p_6 - (p_{9a} + 2p_{9e} + p_{9f} + p_{9g} + p_{8a} + p_{8e} + p_{7b})$.

|		fcc	bcc	sc	sq	t
p_{9a}		79920	—	—	—	180
p_{9e}		2352	—	—	—	—
p_{9f}		1848	—	—	—	—
p_{9g}		160	—	—	—	2
p_{8a}		16464	—	—	—	96
p_{8e}		2016	—	—	—	24
p_{7b}		2400	—	—	—	30
p_3		8	—	—	—	2
p_6		970	148	22	2	15
$[p_3, p_6]$		7760N − 107512				30N − 332

TABLE 4.2g. $[p_4, p_5] = Np_4p_5 - (p_{9b} + p_{9e} + 2p_{9f} + 3p_{9g} + 3p_{9h} + p_{8b} + p_{8e} + 2p_{8p} + 2p_{8q} + 2p_{7f} + 2p_{7h} + p_{6b})$.

		fcc	bcc	sc	sq	t
p_{9b}		58032	—	—	—	102
p_{9e}		2352	—	—	—	—
p_{9f}		1848	—	—	—	—
p_{9g}		160	—	—	—	2
p_{9h}		192	—	—	—	—
p_{8b}		11616	—	—	—	60
p_{8e}		2016	—	—	—	24
p_{8p}		528	—	—	—	—

TABLE 4.2g. continued

		fcc	bcc	sc	sq	t
p_{8q}		24	—	—	—	—
p_{7f}		600	—	—	—	—
p_{7h}		48	—	—	—	—
p_{6b}		384	—	—	—	12
$[p_4, p_5]$		$5544N$ -81552				-204 $18N$

TABLE 4.2h. $[p_3, p_3, p_3] = N^2 p_3^3/6 - N(p_{6c}p_3 + p_{5a}p_3 + p_3^2/2) + (p_{9c} + 2p_{9d} + 2p_{9g} + 2p_{8l} + p_{8m} + 2p_{8q} + 2p_{7c} + 2p_{7g} + 2p_{6c} + 8p_{6d} + 2p_{5a} + p_3/3)$.

		fcc	bcc	sc	sq	t
p_{9c}		6432	—	—	—	48
p_{9d}		744	—	—	—	2
p_{9g}		160	—	—	—	2
p_{8l}		1032	—	—	—	12
p_{8m}		1176	—	—	—	18
p_{8q}		24	—	—	—	—
p_{7c}		192	—	—	—	6
p_{7g}		24	—	—	—	—
p_{6c}		204	—	—	—	9
p_{6d}		2	—	—	—	—
p_{5a}		36	—	—	—	3
p_3		8	—	—	—	2
$[p_3, p_3, p_3]$		$256/3N^2$ $-1952N$ $+12458\frac{2}{3}$				$4/3N^2$ $-26N$ $+134\frac{2}{3}$

TABLE 4.2i. $[p_3, p_{6c}] = Np_3p_{6c} - (2p_{9c} + 3p_{9d} + 3p_{9g} + 2p_{8l} + p_{8m} + 2p_{8q} + p_{7c} + 2p_{6c})$.

		fcc	bcc	sc	sq	t
p_{9c}		6432	—	—	—	48
p_{9d}		744	—	—	—	2
p_{9g}		160	—	—	—	2
p_{8l}		1032	—	—	—	12
p_{8m}		1176	—	—	—	18
p_{8q}		24	—	—	—	0
p_{7c}		192	—	—	—	6
p_{6c}		204	—	—	—	9
$[p_3, p_{6c}]$		1632N -19464				18N -174

TABLE 4.2j. $[p_4, p_6] = Np_4p_6 - (p_{10a} + 2p_{10b} + 3p_{10c} + p_{9k} + 2p_{9m} + 2p_{8c} + 2p_{8l} + 2p_{7a})$.

		fcc	bcc	sc	sq	t
p_{10a}		19584	576	8		
p_{10b}		304	12	0		
p_{10c}		120	0	0		
p_{9k}		6576	324	12		
p_{9m}		456	0	0		

TABLE 4.2j.   continued

	fcc	bcc	sc	sq	t
p_{8c}		480	24	0	
p_{8t}		24	0	0	
p_{7a}		192	18	2	
p_4		12	3	1	
p_6		148	22	2	
$[p_4, p_6]$		1776N	66N	2N	
		−29736	−1020	−24	

(divided by N) is found from Table 4.2e by taking the self-avoiding composite graphs $[p_4, p_4] = (1/2)N - 4 \cdot 5$ but with the number p_{8h} erased from the explicit decomposition

$$[p_4, p_4] = \tfrac{1}{2}Np_4^2 - (p_{8h} + 3p_{8r} + p_{8s} + p_{7a} + p_{7c} + 3p_{6a} + 3p_{6d} + \tfrac{1}{2}p_4),$$

since the graphs touching each other at a corner are already included in entry 8.20 of Table 4.1.

As another example consider the graphs of tenth order. The touching configurations to be subtracted follow from the graphs[c] 10.11–10.13 of Table 4.1 which give the number

$$\binom{D}{2}\left[N\binom{D}{2} - \left(8\binom{D}{2} + 84\binom{D}{3}\right)\right].$$

For $D = 2$ or 3, this number can again be recovered from Tables 4.2. We merely have to take $p_{10} + [p_4, p_6]$ but drop the graph p_{10a} in $[p_4, p_6]$, where two loops touch each other at a corner.

Tables 4.2 are of direct use in applications to ensembles of polymer rings of any length since these form self-avoiding loops.

[c]Notice that, initially, one might think there are only half as many touching plaquette configurations as there are such box graphs; but this is compensated for by a factor 2, since the two orientations of the plaquettes in the box correspond to different graphs.

In Table 4.3 we have given the different numbers with which self-avoiding loops contribute to the free energy of such a loop ensemble Note that f only contains connected graphs. The free energy of polymers is obtained by multiplying each number by the Boltzmann factor $e^{-(\varepsilon/T)n}$ (the fugacity of the loop) where ε is the energy per link, and summing over all n.

Let us now return to the XY model. Having obtained Z', we want to calculate the free energy $-\beta f'$. The expansion of Z' has the form

$$
Z' = (I_0(\beta))^{ND}\left[1 + \xi_4\left(\frac{I_1}{I_0}\right)^4 + \xi_6\left(\frac{I_1}{I_0}\right)^6 \right.
$$

$$
+ \xi_8^{(1)}\left(\frac{I_1}{I_0}\right)^8 + \xi_8^{(2)}\left(\frac{I_1}{I_0}\right)^6\frac{I_2}{I_0} + \xi_8^{(3)}\left(\frac{I_2}{I_0}\right)^4
$$

$$
\left. + \xi_{10}^{(1)}\left(\frac{I_1}{I_0}\right)^{10} + \xi_{10}^{(2)}\left(\frac{I_1}{I_0}\right)^8\frac{I_2}{I_0} + \xi_{10}^{(3)}\left(\frac{I_1}{I_0}\right)^6\left(\frac{I_2}{I_0}\right)^2 + \xi_{10}^{(4)}\left(\frac{I_1}{I_0}\right)^4\left(\frac{I_2}{I_0}\right)^3 \right].
$$

$$
(4.50)
$$

Taking the logarithm and dividing by N we find for the free energy the similar expansion

$$
-\beta f' = D\log I_0(\beta) + f_4\left(\frac{I_1}{I_0}\right)^4 + f_6\left(\frac{I_1}{I_0}\right)^6
$$

$$
+ \left(f_8^{(1)}\left(\frac{I_1}{I_0}\right)^8 + f_8^{(2)}\left(\frac{I_1}{I_0}\right)^6\frac{I_2}{I_0} + f_8^{(3)}\left(\frac{I_2}{I_0}\right)^4 \right)
$$

$$
+ \left(f_{10}^{(1)}\left(\frac{I_1}{I_0}\right)^{10} + f_{10}^{(2)}\left(\frac{I_1}{I_0}\right)^8\frac{I_2}{I_0} + f_{10}^{(3)}\left(\frac{I_1}{I_0}\right)^6\left(\frac{I_2}{I_0}\right)^2 + f_{10}^{(4)}\left(\frac{I_1}{I_0}\right)^4\left(\frac{I_2}{I_0}\right)^3 \right) + \ldots
$$

$$
(4.51)
$$

TABLE 4.3. Coefficients of the free energy fugacity expansion of an ensemble of polymer rings for a simple cubic lattice, $-\beta f = \Sigma f_n v^n$, where $v \equiv e^{-\varepsilon/k_B T}$ is the fugacity of a single chain element. The coefficients f_n are expressed in terms of the lattice constants of Tables 4.2 a–j, where $[p_{n1}, p_{n2}, \ldots]_c$ denotes the connected part of the diagrams in Table 4.2b. For example, $[p_3, p_3]_c = -(p_{6c} + p_{5a} + p_3/3)$ (see Table 4.2b).

$$
\begin{aligned}
&f_3 = p_3, \qquad f_4 = p_4 \\
&f_5 = p_5, \qquad f_6 = p_6 + [p_3, p_3]_c, \\
&f_7 = p_7 + [p_3, p_4]_c, \qquad f_8 = p_8 + [p_3, p_5]_c \\
&f_9 = p_9 + [p_3, p_6]_c + [p_4, p_5]_c + [p_3, p_3, p_3]_c \\
&f_{10} = p_{10} + [p_4, p_6]_c
\end{aligned}
$$

with the f_i's given by the ξ_i's at $N = 1$:

$$f_4 = \xi_4, \quad f_6 = \xi_6, \quad f_8^{(1)} = \xi_8^{(1)} - \tfrac{1}{2}\xi_4^2,$$

$$f_8^{(2),(3)} = \xi_8^{(2),(3)}, \quad f_{10}^{(1)} = \xi_{10}^{(1)} - \xi_4\xi_6, \quad f_{10}^{(2),(3),(4)} = \xi_{10}^{(2),(3),(4)}. \quad (4.52)$$

They are listed in Table 4.1.

Notice that the quadratic pieces N^2 in ξ_8 cancel precisely, resulting in an energy strictly proportional to N. Collecting the different contributions in (4.51) gives the result as shown in Table 4.5. It is most compactly written in terms of binomial coefficients:

$$f_{2n}^{(\ell)} = \sum_{k=0}^{n} c_k^{(\ell)} \binom{n}{k}, \quad (4.53)$$

since the numbers $c_k^{(\ell)}$ are directly related to different graphs of the high temperature expansion. In the literature one often finds $f_{2n}^{(\ell)}$ as polynomials of D which we have added for easier comparison, using the coefficients given in Table 4.4. The high temperature expansion is plotted in Figs. 4.4, 4.5. Notice that in going to (4.51) we have omitted all powers of Bessel functions whose indices add up to more than 10, since those are modified by higher order graphs in Z and therefore can not be trusted. For some purposes it is useful to write the result in the form of a power series. The easiest way to achieve this is by using $(I_1/I_0)(\beta)$ as an expansion parameter. Then only a few higher order terms require a re-expansion. Using the series

TABLE 4.4. The polynomial expansion of the binomial coefficients.

	D	D^2	D^3	D^4	D^5
$\binom{D}{2}$	$-\dfrac{1}{2}$	$\dfrac{1}{2}$	0	0	0
$\binom{D}{3}$	$\dfrac{1}{3}$	$-\dfrac{1}{2}$	$\dfrac{1}{6}$	0	0
$\binom{D}{4}$	$-\dfrac{1}{4}$	$\dfrac{11}{24}$	$-\dfrac{1}{4}$	$\dfrac{1}{24}$	0
$\binom{D}{5}$	$\dfrac{1}{5}$	$-\dfrac{5}{12}$	$\dfrac{7}{24}$	$-\dfrac{1}{12}$	$\dfrac{1}{120}$

TABLE 4.5. The D dependence of the coefficients $f_{2n}^{(\ell)}$ of the free energy as defined in the expansion (4.52). The first entries are $c_{n,k}^{\ell}$, the second $d_{n,k}^{(\ell)}$ with $f_{2n}^{(\ell)} = \sum_{k=2}^{n} c_{n,k}^{(\ell)} \binom{D}{k} = \sum_{k=0}^{n} d_{n,k}^{(\ell)} D^k$. The last four columns give directly $f_{2n}^{(\ell)}$ for $D = 2, 3, 4, 5$, respectively. The expressions Q_n stand for the quotients $I_n(\beta)/I_0(\beta)$.

		$\binom{D}{2}$	$\binom{D}{3}$	$\binom{D}{4}$	$\binom{D}{5}$	D	D^2	D^3	D^4	D^5	$D=2$	$D=3$	$D=4$	$D=5$
f_4	Q_1^4	2	0	0	0	-1	1				2	6	12	20
f_6	Q_1^6	4	32	0	0	$\dfrac{26}{3}$	-14	$\dfrac{16}{3}$			4	44	152	360
$f_8^{(1)}$	Q_1^8	4	324	1296	0	-218	434	-270	54		4	336	2616	9760
$f_8^{(2)}$	$Q_1^6 Q_2$	4	24	0	0	6	-10	4			4	36	120	280
$f_8^{(3)}$	Q_2^4	2	0	0	0	-1	1				2	6	12	20
$f_{10}^{(1)}$	Q_1^{10}	-8	3144	43008	95232	$\dfrac{46732}{5}$	-21544	17548	-6144	$\dfrac{3968}{5}$	-8	3120	55536	341632
$f_{10}^{(2)}$	$Q_1^8 Q_2$	24	576	1536	0	-204	428	-288	64		24	648	3984	13680
$f_{10}^{(3)}$	$Q_1^6 Q_2^2$	0	96	0	0	32	-48	16			0	69	384	960
$f_{10}^{(4)}$	$Q_1^4 Q_2^3$	8	48	0	0	12	-20	8			8	72	240	560

$$I_0(\beta) = 1 + \frac{1}{1!^2}\left(\frac{\beta}{2}\right)^2 + \frac{1}{2!^2}\left(\frac{\beta}{2}\right)^4 + \ldots,$$

$$I_1(\beta) = \left(\frac{\beta}{2}\right)\left(1 + \frac{1}{2!}\left(\frac{\beta}{2}\right)^2 + \frac{1}{3!2!}\left(\frac{\beta}{2}\right)^4 + \frac{1}{4!3!}\left(\frac{\beta}{2}\right)^6 + \ldots\right),$$

$$I_2(\beta) = \left(\frac{\beta}{2}\right)^2\left(\frac{1}{2!} + \frac{1}{3!1!}\left(\frac{\beta}{2}\right)^2 + \frac{1}{4!2!}\left(\frac{\beta}{2}\right)^6 + \ldots\right), \qquad (4.54)$$

we see that

$$\frac{I_2}{I_0} = \frac{1}{2}\left(\frac{I_1}{I_0}\right)^2 + \frac{1}{6}\left(\frac{I_1}{I_0}\right)^4 + \frac{5}{48}\left(\frac{I_1}{I_0}\right)^6 + \ldots,$$

FIG. 4.4.   The high-temperature expansion of the free energy of the $D = 3$ XY model. The dashed lines are due to the two loops which make up most of the energy up to the critical point $\beta_c \sim 0.45$, $T_c^{MF}/T_c \sim 1.35$. The other curves (mean field plus loop) will be derived and explained in the next chapter. The circles are obtained from integrating the Monte Carlo data for the internal energy numerically.
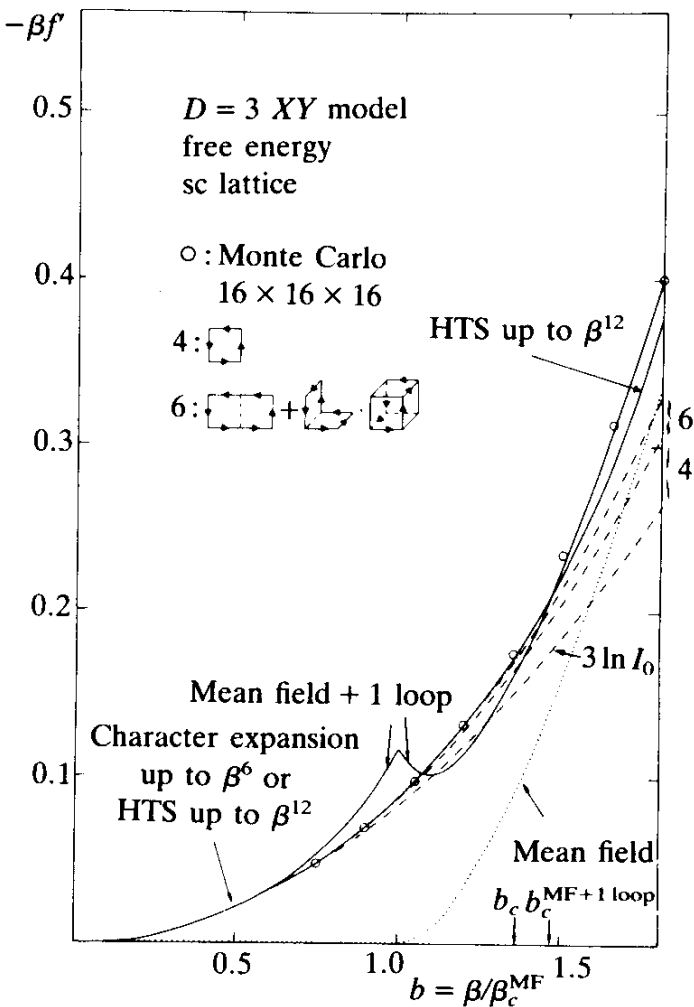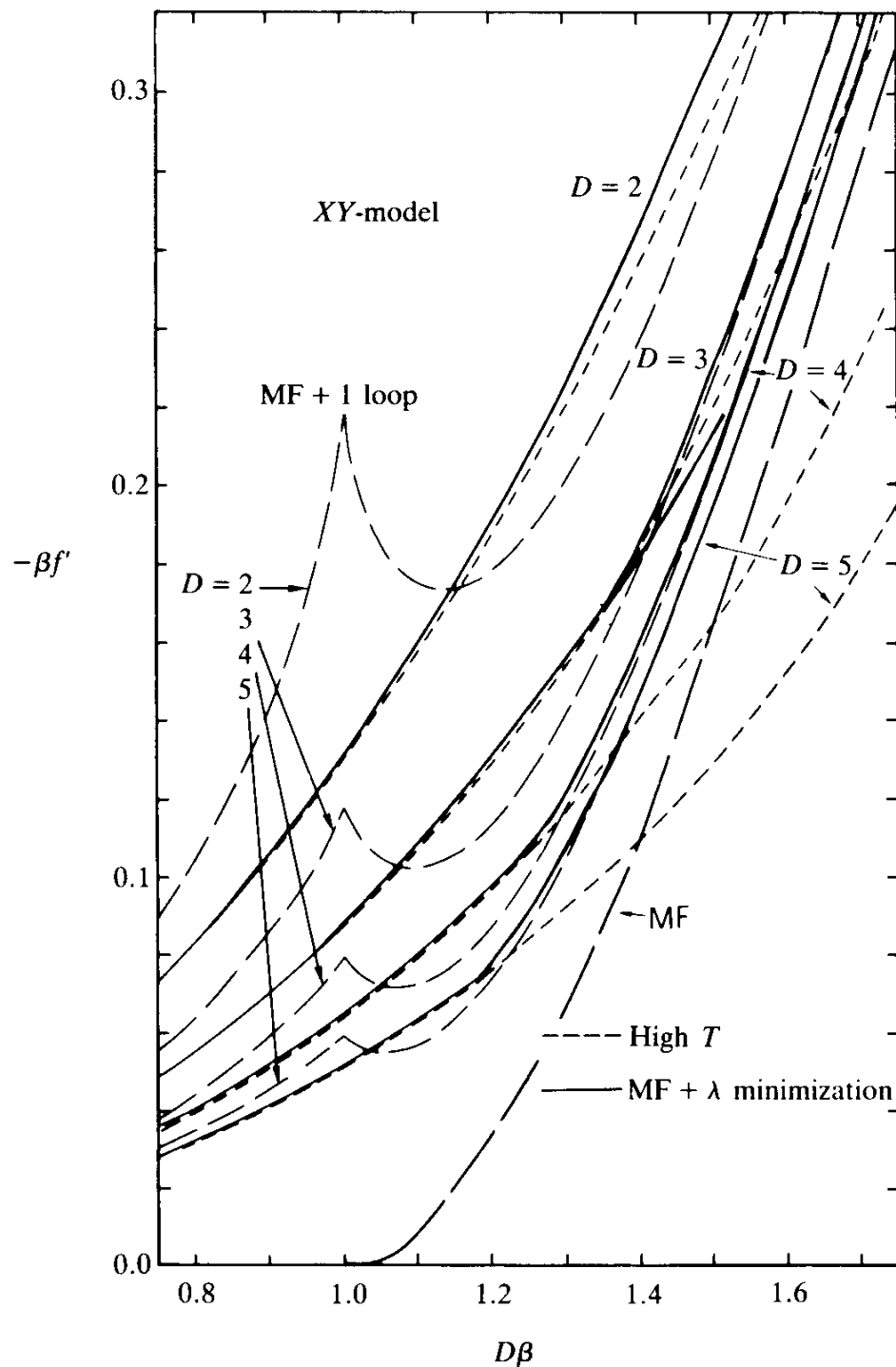
FIG. 4.5. The same curves as in Fig. 4.4 plotted for various dimensions. We see that for $D \to \infty$ the mean field curves become exact. In addition, there are solid curves (λ minimization) which will be discussed later on in Section 5.7.

XY-model

MF + 1 loop

$D = 2$

$D = 2$
3
4
5

$D = 3$

$D = 4$

$D = 5$

$-\beta f'$

MF

- - - - High T

——— MF + λ minimization

$D\beta$

0.3

0.2

0.1

0.0

0.8   1.0   1.2   1.4   1.6

and obtain the power series

$$-\beta f' = D \log I_0(\beta) + \sum_{n=4,6,\ldots} h_n \left(\frac{I_1}{I_0}\right)^n. \tag{4.55}$$

The coefficients h_n are given in Table 4.6. In the literature, the results are often stated as a power series in β:

$$-\beta f' = \sum_{n=2}^{\infty} g_n \left(\frac{\beta}{2}\right)^n. \tag{4.56a}$$

It is quite tedious to put (4.52) into this form. In Table 4.7 we have listed the required re-expansions of the different terms in the series (4.52). Work is aided by Table 4.8. Inserting the content of Table 4.4 leads to the coefficients g as listed in Table 4.9.

In the literature, one sometimes finds the series

$$-\beta f' = D \log I_0(\beta) + \sum_{n=2,4,6} \tilde{g}_n \left(\frac{\beta}{2}\right)^n. \tag{4.56b}$$

The alternative expansions of the free energy are shown explicitly for $D = 2$ and $D = 3$ dimensions in Tables 4.10–4.11.

In two dimensions it is possible to count also the graphs of length 12 and one finds, for the free energy, the additional terms $[Q_i \equiv I_i(\beta)/I_0(\beta)]$

$$-\beta f^{(12)} = \{-57\tfrac{1}{3}Q_1^{12} + 60Q_1^{10}Q_2 + 44Q_1^8Q_2^2$$

$$+ 24Q_1^6Q_2^3 - 20Q_1^6Q_2^3 + 8Q_1^3Q_2^3Q_3 + 2Q_3^4\} \binom{D}{2}. \tag{4.57}$$

Using the expansions in Table 4.7, this leads to an additional row in Tables 4.10–4.14 for $D = 2$. The expansion (4.56a) can be used to obtain directly the internal energy

$$u' = -\frac{\partial}{\partial \beta}(-\beta f') = -\sum_{n=2}^{\infty} g_n \frac{n}{2} \left(\frac{\beta}{2}\right)^{n-1}, \tag{4.58a}$$

TABLE 4.6. The D dependence of the coefficients of the free energy of the XY model in the expansion $-\beta f = D \log I_0(\beta) + \Sigma_n h_n (I_1(\beta)/I_0(\beta))^n$.

	$\binom{D}{2}$	$\binom{D}{3}$	$\binom{D}{4}$	$\binom{D}{5}$	D	D^2	D^3	D^4	D^5	$D=2$	$D=3$	$D=4$	$D=5$
h_4	2	0	0	0	-1	1	0	0	0	2	6	12	20
h_6	4	32	0	0	$\frac{26}{3}$	-14	$\frac{16}{3}$	0	0	4	44	152	360
h_8	$\frac{49}{8}$	336	1296	0	$-\frac{3441}{16}$	$\frac{6865}{16}$	-268	54	0	$\frac{49}{8}$	$\frac{2835}{8}$	$\frac{10707}{4}$	$\frac{39605}{4}$
h_{10}	$\frac{35}{6}$	3466	43776	95232	$\frac{555289}{60}$	$-\frac{256153}{12}$	$\frac{52229}{3}$	-6112	$\frac{3968}{5}$	$\frac{35}{6}$	$\frac{6967}{2}$	57675	$\frac{1046491}{3}$

TABLE 4.7. Re-expansion of the different terms in $-\beta f$ into a power series $\Sigma_{n=2,4,6,\ldots} g_n (\beta/2)^n$.

	D: $\log I_0$	f_4: $\left(\frac{I_1}{I_0}\right)^4$	f_6: $\left(\frac{I_1}{I_0}\right)^6$	$f_8^{(1)}$: $\left(\frac{I_1}{I_0}\right)^8$	$f_8^{(2)}$: $\left(\frac{I_1}{I_0}\right)^6\left(\frac{I_2}{I_0}\right)$	$f_8^{(3)}$: $\left(\frac{I_1}{I_0}\right)^4$	$f_{10}^{(1)}$: $\left(\frac{I_1}{I_0}\right)^{10}$	$f_{10}^{(2)}$: $\left(\frac{I_1}{I_0}\right)^8\left(\frac{I_2}{I_0}\right)$	$f_{10}^{(3)}$: $\left(\frac{I_1}{I_0}\right)^6\left(\frac{I_2}{I_0}\right)^2$	$f_{10}^{(4)}$: $\left(\frac{I_1}{I_0}\right)^4\left(\frac{I_2}{I_0}\right)^3$
g_2	1	0	0	0	0	0	0	0	0	0
g_4	$-\frac{1}{4}$	1	0	0	0	0	0	0	0	0
g_6	$\frac{1}{9}$	-2	1	0	0	0	0	0	0	0
g_8	$-\frac{11}{3 \cdot 2}$	$\frac{17}{6}$	-3	1	$\frac{1}{2}$	$\frac{1}{2^4}$	0	0	0	0
g_{10}	$\frac{19}{5^2 \cdot 3 \cdot 2^3}$	$-\frac{41}{12}$	$\frac{23}{4}$	-4	$-\frac{11}{6}$	$-\frac{1}{6}$	1	$\frac{1}{2}$	$\frac{1}{4}$	$\frac{1}{8}$
g_{12}	$-\frac{11 \cdot 43}{5 \cdot 3^4 \cdot 2^6}$	$\frac{299}{5 \cdot 2^4}$	$-\frac{71}{8}$	$\frac{29}{3}$	$\frac{197}{48}$	$\frac{9}{2^5}$	-5	$-\frac{7}{3}$	$-\frac{13}{12}$	$-\frac{1}{2}$

TABLE 4.8. Expansion of Bessel functions and powers thereof into a power series $\sum_{n=0}^{\infty} q_n (\beta/2)^n$.

$Q(\beta)$	q_0	q_1	q_2	q_3	q_4	q_5	q_6	q_7	q_8	q_9	q_{10}	q_{11}	q_{12}
I_0	1	—	1	—	$\frac{1}{2!2!}$	—	$\frac{1}{3!3!}$	—	$\frac{1}{4!4!}$	—	$\frac{1}{5!5!}$	—	$\frac{1}{6!6!}$
I_1	—	$\frac{1}{0!1!}$	—	$\frac{1}{1!2!}$	—	$\frac{1}{2!3!}$	—	$\frac{1}{3!4!}$	—	$\frac{1}{4!5!}$	—	$\frac{1}{5!6!}$	—
I_2	—	—	$\frac{1}{0!2!}$	—	$\frac{1}{1!3!}$	—	$\frac{1}{2!4!}$	—	$\frac{1}{3!5!}$	—	$\frac{1}{4!6!}$	—	$\frac{1}{5!7!}$
I_3	—	—	—	$\frac{1}{0!3!}$	—	$\frac{1}{1!4!}$	—	$\frac{1}{2!5!}$	—	$\frac{1}{3!6!}$	—	$\frac{1}{4!7!}$	—
$\ln I_0$	—	—	1	—	$\frac{-1}{2^2}$	—	$\frac{1}{3^2}$	—	$\frac{-11}{3\cdot 2^6}$	—	$\frac{19}{5^2\cdot 3\cdot 2^3}$	—	$\frac{-473}{5\cdot 3^4\cdot 2^6}$
I_0^{-1}	1	—	-1	—	$\frac{3}{4}$	—	$\frac{-19}{3^2\cdot 2^2}$	—	$\frac{211}{3^2\cdot 2^6}$	—	$\frac{-1217}{5^2\cdot 3\cdot 2^6}$	—	$\frac{30307}{5^2\cdot 3^3\cdot 2^8}$
$\frac{I_1}{I_0}$	—	1	—	$\frac{-1}{2}$	—	$\frac{1}{3}$	—	$\frac{-11}{3\cdot 2^4}$	—	$\frac{19}{5\cdot 3\cdot 2^3}$	—	$\frac{-473}{5\cdot 3^3\cdot 2^5}$	—
$\left(\frac{I_1}{I_0}\right)^2$	—	—	1	—	-1	—	$\frac{11}{3\cdot 2^2}$	—	$\frac{-19}{3\cdot 2^3}$	—	$\frac{473}{5\cdot 3^2\cdot 2^4}$	—	$\frac{-229}{3^3\cdot 2^4}$
$\left(\frac{I_1}{I_0}\right)^3$	—	—	—	1	—	$\frac{-3}{2}$	—	$\frac{7}{4}$	—	$\frac{-29}{2^4}$	—	$\frac{419}{5\cdot 3\cdot 2^4}$	—
$\frac{I_2}{I_0}$	—	—	$\frac{1}{2}$	—	$\frac{-1}{3}$	—	$\frac{11}{3\cdot 2^4}$	—	$\frac{-19}{5\cdot 3\cdot 2^3}$	—	$\frac{473}{5\cdot 3^3\cdot 2^5}$	—	$\frac{-229}{7\cdot 3^3\cdot 2^4}$
$\left(\frac{I_2}{I_0}\right)^2$	—	—	—	—	$\frac{1}{4}$	—	$\frac{-1}{3}$	—	$\frac{49}{3^2\cdot 2^4}$	—	$\frac{-14}{5\cdot 3^2}$	—	$\frac{7\cdot 1321}{5\cdot 3^3\cdot 2^8}$
$\left(\frac{I_2}{I_0}\right)^3$	—	—	—	—	—	—	$\frac{1}{8}$	—	$\frac{-1}{4}$	—	$\frac{5\cdot 13}{3\cdot 2^6}$	—	$\frac{-1663}{5\cdot 3^2\cdot 2^4}$
$\frac{I_3}{I_0}$	—	—	—	$\frac{1}{6}$	—	$\frac{-1}{8}$	—	$\frac{7}{5\cdot 2^4}$	—	$\frac{-131}{5\cdot 3^3\cdot 2^4}$	—	$\frac{47}{7\cdot 5\cdot 2^5}$	—

and the specific heat

$$c = \beta_0^2 \frac{\partial^2}{\partial \beta^2}(-\beta f') = \sum_{n=2}^{\infty} g_n n(n-1)\left(\frac{\beta}{2}\right)^n.$$ (4.58b)

For some purposes it is useful to know these quantities also in alternative expansions and we have listed them in Tables 4.11, 4.12.

For comparison, we also list the corresponding expansions for other lattice geometries in Tables 4.13, 4.14. The corresponding expansion coefficients of the susceptibility $\chi(\beta)$ will be given later in Table 9.1, where this quantity will be introduced and discussed in more detail.

The expansions for u' and c have the advantage that they can be compared directly with Monte Carlo simulations of the model. For this, one lets a large computer sweep step-by-step many times through a lattice, choosing at each site the variable $\gamma(\mathbf{x})$ according to the Boltzmann distribution of the interaction energies with the next neighbours. After, say, 5000 sweeps, the system has usually come to an equilibrium and one may apply 5000 more sweeps to measure all thermodynamic quantities one is interested in, for instance, the average interaction energy per site

$$\frac{1}{N}\left\langle \sum_{\mathbf{x},i} \cos \nabla_i \gamma \right\rangle,$$

which is the same as $-u'$ or the correlations of the interaction energy

$$\frac{1}{N}\left[\left\langle \sum_{\mathbf{x},i} \cos \nabla_i \gamma(\mathbf{x}) \sum_{\mathbf{x},j} \cos \nabla_j \gamma(\mathbf{x}') \right\rangle - \left\langle \sum_{\mathbf{x},i} \cos \nabla_i \gamma \right\rangle^2 \right],$$

which gives the specific heat as $(1/\beta^2)c$. This follows directly from the defining relations

$$u' = -\frac{1}{Z'}\frac{\partial}{\partial \beta}Z',$$

$$c = -\beta^2 \frac{\partial}{\partial \beta}u' = \beta^2 \left[\frac{1}{Z'}\frac{\partial^2}{\partial \beta}Z' - \left(\frac{1}{Z'}\frac{\partial}{\partial \beta}Z'\right)^2\right].$$

TABLE 4.9. Coefficients of the expansion $-\beta f'_{XY} = \Sigma g_n (\beta/2)^n$ [see Eq. 4.56a)].

	$\binom{D}{1}$	$\binom{D}{2}$	$\binom{D}{3}$	$\binom{D}{4}$	$\binom{D}{5}$	D	D^2	D^3	D^4	D^5	$D=2$	$D=3$	$D=4$	$D=5$
g_2	1					1					2	3	4	5
g_4	$-\frac{1}{4}$	2				$-\frac{5}{4}$	1				$1\frac{1}{2}$	$5\frac{1}{4}$	11	$18\frac{3}{4}$
g_6	$\frac{1}{9}$	0	32			$10\frac{7}{9}$	-16	$5\frac{1}{3}$			$\frac{2}{9}$	$32\frac{1}{3}$	$128\frac{4}{9}$	$320\frac{5}{9}$
g_8	$\frac{-11}{3\cdot 2^6}$	$\frac{-5}{24}$	240	1296		$-243\frac{61}{64}=\frac{-15613}{64}$	$473\frac{43}{48}=\frac{22747}{48}$	-284	54		$\frac{-31}{96}$	$239\frac{13}{64}=\frac{15309}{64}$	$2254\frac{25}{48}=\frac{108217}{48}$	$8878\frac{43}{64}=\frac{568235}{64}$
g_{10}	$\frac{19}{5^2\cdot 3\cdot 2^3}$	$\frac{-5}{2}$	2306	38592	95232	$\frac{6101009}{600}$	$\frac{-92585}{4}$	$\frac{55537}{3}$	-6328	$\frac{3968}{5}$	$\frac{-731}{300}$	$\frac{459719}{200}$	$\frac{717019}{150}$	$\frac{37347259}{120}$
g_{12}	$\frac{-473}{5\cdot 3^4\cdot 2^6}$	$-6\frac{2371}{5\cdot 3^4\cdot 2^3}$									$-6\frac{3319}{4320}$	25322.7		

TABLE 4.10. Alternative expansions of the free energy for the XY model.

$-\beta f'$	$D = 2$			$D = 3$		
	$x = I_1/I_0$	$x = \beta/2$	$x = \beta/2$	$x = I_1/I_0$	$x = \beta/2$	$x = \beta/2$
$\log I_0$	2	2	—	3	3	—
x^2	—	—	2	—	—	3
x^4	2	2	$1\frac{1}{2}$	6	6	$5\frac{1}{4}$
x^6	4	0	$\frac{2}{9}$	44	32	$32\frac{1}{3}$
x^8	$6\frac{1}{8}$	$-\frac{5}{24}$	$-\frac{31}{96}$	$354\frac{3}{8}$	$239\frac{3}{8}$	$239\frac{13}{64}$
x^{10}	$5\frac{5}{6}$	$-2\frac{1}{2}$	$-2\frac{131}{300}$	$3483\frac{1}{2}$	$2298\frac{1}{2}$	$2298\frac{119}{200}$
x^{12}	$-8\frac{485}{648}$	$-6\frac{2371}{3240}$	$-6\frac{3319}{4320}$	39682.75466	25322.80466	25322.74991

TABLE 4.11. Alternative expansions of the internal energy for the XY model.

$-u'$	$D = 2$			$D = 3$		
	$x = I_1/I_0$	$x = \beta/2$	$x = \beta/2$	$x = I_1/I_0$	$x = \beta/2$	$x = \beta/2$
I_1/I_0	—	2	—	—	3	—
x	2	—	2	3	—	3
x^3	4	4	3	12	12	$10\frac{1}{2}$
x^5	6	0	$\frac{2}{3}$	114	96	97
x^7	$7\frac{1}{6}$	$-\frac{5}{6}$	$-1\frac{7}{24}$	$1221\frac{1}{2}$	$957\frac{1}{2}$	$956\frac{13}{16}$
x^9	$-5\frac{1}{6}$	$-12\frac{1}{2}$	$-12\frac{11}{60}$	$15314\frac{1}{2}$	$11492\frac{1}{2}$	$11492\frac{39}{40}$
x^{11}	$-90\frac{161}{270}$	$-40\frac{211}{540}$	$-40\frac{439}{720}$	2122212.113	151936.8280	151936.4995

TABLE 4.12. Alternative expansions for the specific heat of XY model.

$\dfrac{c}{\left(\frac{\beta}{2}\right)^2}$	$D = 2$		$D = 3$	
	$x = I_1/I_0$	$x = \beta/2$	$x = I_1/I_0$	$x = \beta/2$
x^0	4	4	6	6
x^2	18	18	63	63
x^4	$24\frac{2}{3}$	$6\frac{2}{3}$	1033	970
x^6	$14\frac{3}{4}$	$-18\frac{1}{12}$	$15403\frac{5}{8}$	13395
x^8	$-230\frac{31}{45}$	$-219\frac{3}{10}$	$250207\frac{7}{15}$	$206873\frac{11}{20}$
x^{10}	$-1828\frac{1143}{2160}$	$-893\frac{149}{360}$	4258350.040	3342602.989

TABLE 4.13. Internal energy of the XY model in different lattices. $-u' = \sum\limits_{n=1}^{\infty} v_n Q_1^n$, $Q_1 = I_1(\beta)/I_0(\beta)$.

n	fcc	bcc	sc ($D = 3$)	sc ($D = 2$)	hex ($D = 2$)
			v_n		
1	6	4	3	2	3
2	24	—	—	—	6
3	132	48	12	4	12
4	804	—	—	—	21
5	5256	816	114	6	$34\frac{1}{2}$
6	36502	—	—	—	$50\frac{1}{2}$
7	$266017\frac{1}{2}$	17594	$1221\frac{1}{2}$	$7\frac{1}{6}$	$50\frac{3}{4}$
8	$2010172\frac{5}{6}$	—	—	—	$-60\frac{7}{24}$
9		438846	$15314\frac{1}{2}$	$-5\frac{1}{6}$	
10		—	—		—
11				$-90\frac{161}{270}$	

TABLE 4.14. The specific heat of the XY model in different lattices: $c = \sum\limits_{n=2}^{x} c_n \left(\frac{\beta}{2}\right)^n$.

n	fcc	bcc	sc ($D = 3$)	sc ($D = 2$)	hex ($D = 2$)
			c_n		
2	12	8	6	4	6
3	96	—	—	—	24
4	774	276	63	18	63
5	6240	—	—	—	120
6	506007	$7453\frac{1}{3}$	970	$6\frac{2}{3}$	175
7	418992	—	—	—	168
8	$3543499\frac{3}{4}$	$218919\frac{1}{6}$	$13395\frac{3}{8}$	$-18\frac{1}{12}$	$-212\frac{5}{8}$
9	$30466813\frac{1}{3}$	—	—	—	$-2512\frac{2}{3}$
10			$206873\frac{11}{20}$	$-219\frac{3}{10}$	-12387.075
11		—	—		-46926.000
12				$-893\frac{149}{360}$	

TABLE 4.15.   Monte Carlo data for the XY model in 3 dimensions on a $16 \times 16 \times 16$ s.c. lattice. The angle γ is approximated by 16 values between 0 and 2 ("Z (16) approximation"). There were 5000 sweeps for equilibriation and a further 5000 sweeps for measurement (W. Janke and H. Kleinert, unpublished).

β	u	c	$\langle \cos \gamma \rangle$	β	u	c	$\langle \cos \gamma \rangle$
2.0000	0.2622	0.5610	0.9363	1.0500	0.5302	0.6639	0.8695
1.9500	0.2691	0.5350	0.9350	1.0000	0.5606	0.6732	0.8618
1.9000	0.2768	0.5602	0.9330	0.9500	0.5957	0.6771	0.8531
1.8500	0.2846	0.5444	0.9312	0.9000	0.6363	0.6999	0.8422
1.8000	0.2929	0.5643	0.9290	0.8500	0.6831	0.7262	0.8305
1.7500	0.3020	0.5605	0.9268	0.8000	0.7374	0.7843	0.8160
1.7000	0.3113	0.5598	0.9245	0.7500	0.8035	0.8265	0.7985
1.6500	0.3216	0.5750	0.9221	0.7000	0.8851	0.8948	0.7764
1.6000	0.3324	0.5737	0.9193	0.6500	0.9874	1.0031	0.7475
1.5500	0.3439	0.5702	0.9164	0.6000	1.1217	1.1346	0.7075
1.5000	0.3563	0.5512	0.9135	0.5500	1.3053	1.2995	0.6474
1.4500	0.3695	0.5760	0.9102	0.5000	1.5731	1.6889	0.5445
1.4000	0.3839	0.6016	0.9064	0.4500	2.0250	2.0333	0.2122
1.3500	0.3998	0.6110	0.9027	0.4000	2.2589	0.4914	0.0559
1.3000	0.4167	0.6061	0.8980	0.3500	2.3955	0.2951	0.0363
1.2500	0.4350	0.6087	0.8935	0.3000	2.5044	0.1900	0.0290
1.2000	0.4553	0.6351	0.8887	0.2500	2.6013	0.1152	0.0238
1.1500	0.4774	0.6167	0.8830	0.2000	2.6888	0.0681	0.0206
1.1000	0.5021	0.6140	0.8773	0.1500	2.7697	0.0367	0.0181
				0.1000	2.8489	0.0157	0.0163
				0.0500	2.9246	0.0038	0.0152
				0.0000	3.0002	0.0000	0.0138

The measurements are done successively for increasing temperatures and then back to low temperature (see Table 4.15). This is referred to as a *thermal cycle*. Such Monte Carlo simulations have been performed for the XY model by many researchers and are now a standard exercise in statistical mechanics.

In Table 4.15 we have listed the results found on a $16 \times 16 \times 16$ lattice via $5000 + 5000$ equilibrium and measurement sweeps, respectively, as explained above. The continuous variable $\gamma \in [0, 2\pi]$ was approximated by the 16 discrete values $(2\pi/16)n$, $n = 0, \ldots, 15$. This will be referred to as the "Z_{16} approximation." In Figs. 4.6–4.8 we compare the high temperature expansions (4.58) of u' and c with the Monte Carlo data of Table 4.15. For small β, the agreement is excellent. Close to the critical point $\beta_c \sim 0.45$, this is no longer the case, in particular for the specific heat.

FIG. 4.6. Comparison of the internal energy from the high temperature expansion with Monte Carlo data obtained on a 16^3 lattice. The model was updated 5000 times for equilibriation and, after that, 5000 times more for the measurement $\Sigma_i \cos \nabla_i \gamma$. The low temperature curves will be derived and explained in the next chapter.
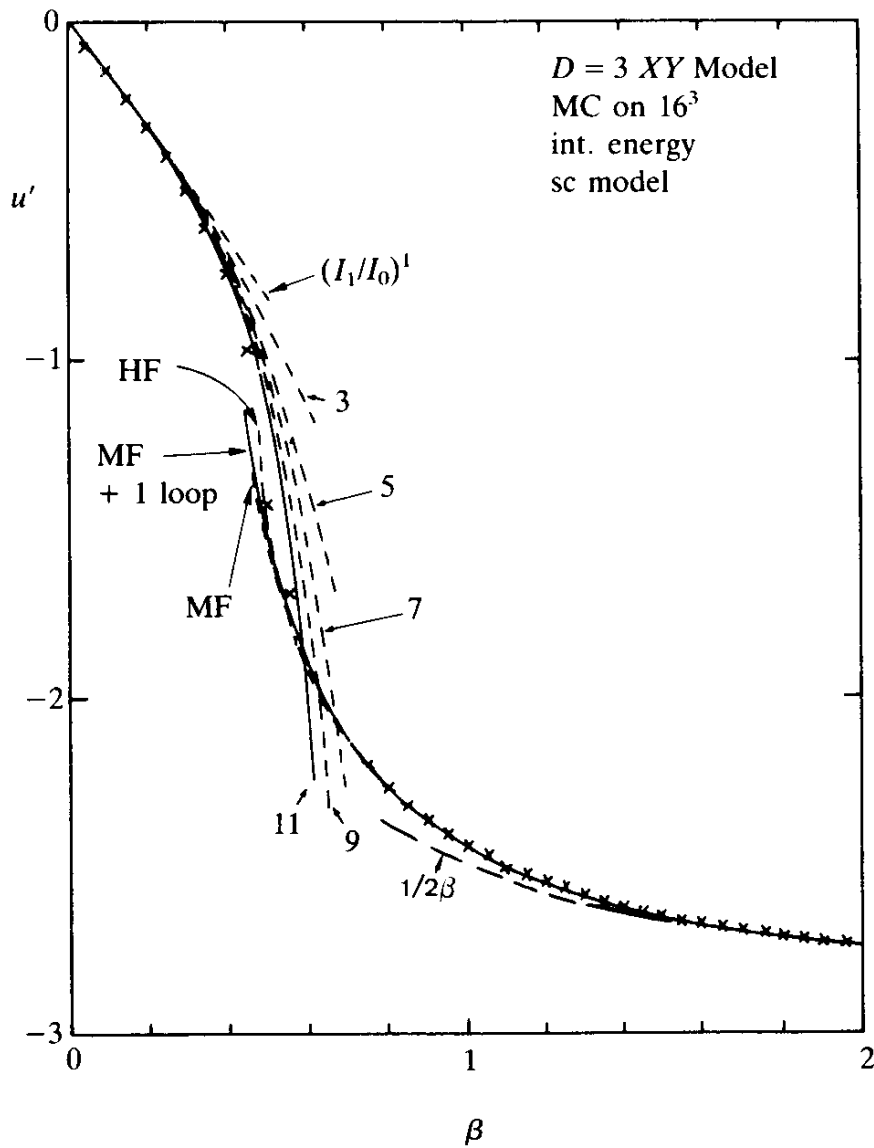

FIG. 4.7. Comparison of specific heat from the high temperature expansion with Monte Carlo data, obtained on a 16^3 lattice. The number of sweeps is the same as those in Fig. 4.6.
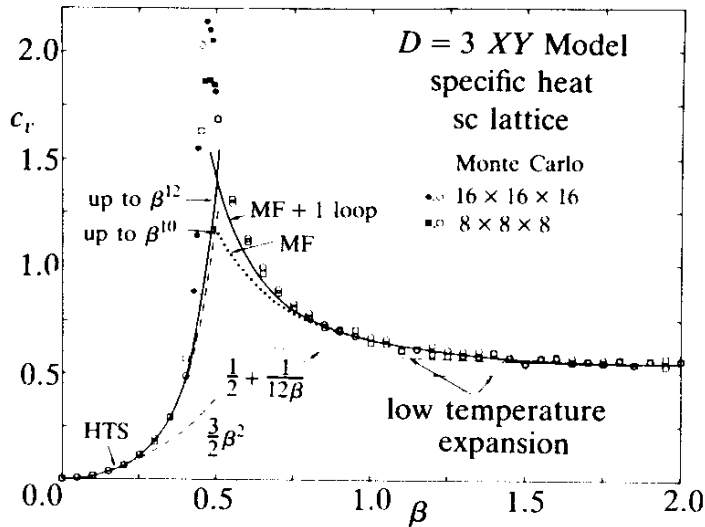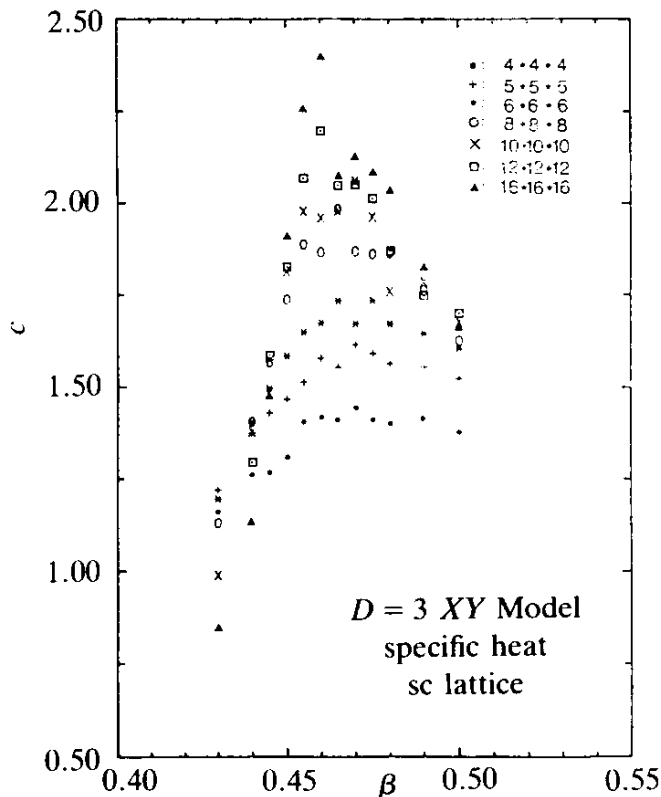
FIG. 4.8. Finite size effects in the critical regime of the specific heat. From this figure one can extract the critical index v (or $\alpha = 2 - vD$). The maximum behaves like $L^{2/v-D}$, the position of the peak like $L^{-\alpha/v}$ ($L = N^{1/2}$) (W. Janke, H. Kleinert, unpublished).

4.4. PHYSICAL INTERPRETATION

The graphs occurring in the high temperature expansion (4.51) have a simple physical interpretation. As we shall understand better later on, the closed lines of integer $b_i(\mathbf{x})$ fields are direct pictures of closed stream lines of superflow. At high temperatures, the system is in the normal state. It performs fluctuations into the superfluid state, occasionally creating small rings of superflow. Close to the critical point these rings become larger and larger and, at the transition point, they grow infinitely long.

It is important to realize that large rings with fundamental strength $b_i = 1$ are much more important than small rings with higher strength which can practically be neglected as compared with the large ones (even in the close vicinity of T_c). For $T > T_c$, the loops proliferate and fill the entire system with superflow. The expansion in powers of β breaks down at T_c.

4.5. ESTIMATE OF CRITICAL PROPERTIES
VIA THE RATIO TEST

Mathematically, the breakdown of the strong coupling series has a simple reason. In a finite system, the partition function is a polynomial of a high degree in β.[d] In the complex β plane, this has as many zeroes as its degree. A close study of the position of the zeroes reveals that they approach the real β in the form of two sequences from above and below. In the thermodynamic limit of an infinite system, the points of the sequences are spaced infinitesimally close to each other and form a continuous line. The ends of the two-line pinch the β axis. When taking the logarithm of Z and forming $-\beta f'$, this line of zeroes becomes a line of singularities.

The qualitative way in which such a singularity appears in the free energy has been known for a long time from the experimental study of second order phase transitions. The specific heat of a system behaves close to the critical temperature like

$$c \sim (\beta - \beta_c)^{-\alpha}, \tag{4.59}$$

or equivalently, like $(\beta^2 - \beta_c^2)^{-\alpha}$. The power α is called the *critical index* of the specific heat. Such a singularity implies that by expanding c into a strong coupling series in powers of β^2 the large order coefficients of this series will behave like

$$c \sim \sum_n \binom{-\alpha}{n} \left(\frac{\beta^2}{\beta_c^2}\right)^n.$$

For the ratios R_n of two successive large order coefficients this implies the following limit:

$$R_n = \frac{1}{\beta_c^2} \binom{-\alpha}{n} \Big/ \binom{-\alpha}{n-1}$$

$$= \frac{1}{\beta_c^2} \frac{\alpha(\alpha+1)\dots(\alpha+n-1)}{n!} \Big/ \frac{\alpha(\alpha+1)\dots(\alpha+n-2)}{(n-1)!}$$

$$= \frac{1}{\beta_c^2} \frac{\alpha+n-1}{n} \rightarrow T_c^2 \left(1 + \frac{\alpha-1}{n} + O\left(\frac{1}{n^2}\right)\right), \tag{4.60}$$

---

[d]This follows directly from (4.7).

or, for the square root of the ratios

$$\sqrt{R_n} \to T_c \left(1 + \frac{\alpha - 1}{2n} + O\left(\frac{1}{n^2}\right) \right). \tag{4.61}$$

If a strong coupling series is known up to sufficient high order in β^2, this can be used to estimate the critical temperature T_c as well as the critical index α. One simply has to plot $\sqrt{R_n}$ against $1/n$ and read off T_c from the extrapolated intercept. This procedure is called the "ratio test." From the slope, $-(\alpha - 1/2) T_c$, the critical index α is extracted.

For the XY model we can use the results summarized the Table 4.9. and write down the expansion in $D = 3$ dimensions,

$$-\beta f = 3 \left(\frac{\beta}{2}\right)^2 + \frac{21}{4}\left(\frac{\beta}{2}\right)^4 + \frac{97}{3}\left(\frac{\beta}{2}\right)^6 + \frac{7 \cdot 3^7}{2^6}\left(\frac{\beta}{2}\right)^8 + 2298\textsf{\textrm{\textit{\i}}}.5949 \left(\frac{\beta}{2}\right)^{10}. \tag{4.62}$$

Differentiation leads to the series for the specific heat

$$c = \beta^2 \frac{\partial^2}{\partial \beta^2}(-\beta f) = 3 \cdot 2 \left(\frac{\beta}{2}\right)^2 + \frac{21}{4} \cdot 4 \cdot 3 \left(\frac{\beta}{2}\right)^4 + \frac{97}{3} \cdot 6 \cdot 5 \left(\frac{\beta}{2}\right)^6$$
$$+ \frac{7 \cdot 3^7}{2^6} 8 \cdot 7 \left(\frac{\beta}{2}\right)^8 + 2298.5949 \cdot 10 \cdot 9 \left(\frac{\beta}{2}\right)^{10}. \tag{4.63}$$

This gives the ratios

$$R_2 = 2.6248, \quad R_3 = 3.8494, \quad R_4 = 3.4525, \quad R_5 = 3.8608, \tag{4.64}$$

or

$$\sqrt{R_2} = 1.62012, \quad \sqrt{R_3} = 1.96201, \quad \sqrt{R_4} = 1.85809, \quad \sqrt{R_5} = 1.96489. \tag{4.65}$$

If we plot these against $1/n$ in Fig 4.9 we see that the ratios tend toward a point somewhere above $\sqrt{R_n} \sim 2.1$, but the convergence is still rather bad. An improvement comes from the β^{12} value which was found by a computer search of non-backtracking loops,

FIG. 4.9.   Ratio tests of the expansion coefficients of the specific heat in powers of $(\beta/2)^2$ for the determination of T_c. The ratios are taken from Eqs. (4.65), (4.67), (4.75).
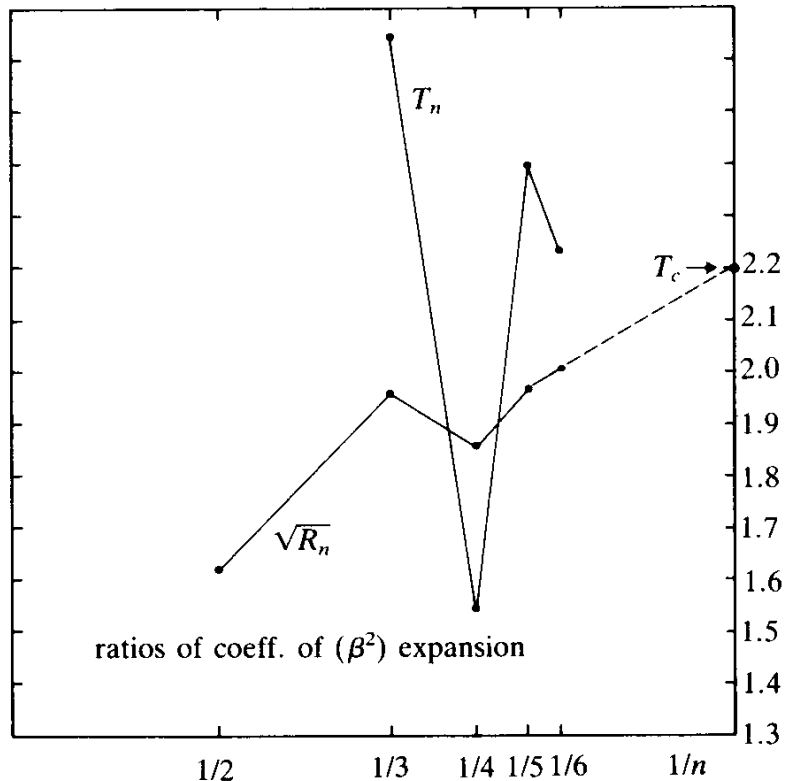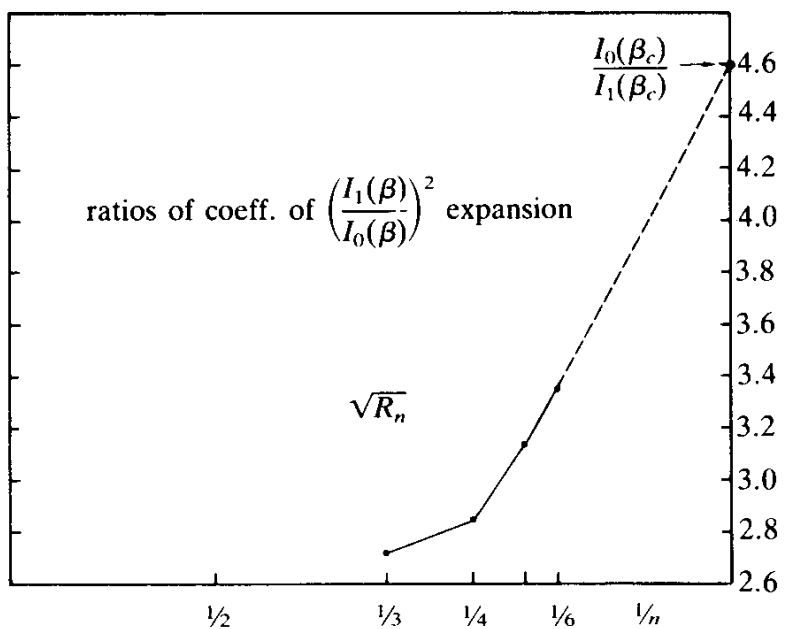

FIG. 4.10.   Ratio test in an expansion of the free energy in powers of $I_1(\beta)/I_0(\beta)$ for the determination of $I_1(\beta_c)/I_0(\beta_c)$ at the critical point β_c.

$$-\beta f = 25322.74991 \left(\frac{\beta}{2}\right)^{12},$$

(4.66)

provides for one more ratio,

$$R_6 = 4.0394, \quad \sqrt{R_6} = 2.00982.$$

(4.67)

By giving most weight to the last two ratios, we extrapolate the result

$$T_c \sim 2.2.$$

(4.68)

From the slope of the last piece we read off

$$\frac{\alpha - 1}{2} T_c = -\frac{0.6}{0.5}$$

$$\alpha \sim -0.1.$$

(4.69)

This agrees well with Monte Carlo simulations of the model XY which give

$$T_c \sim 1/0.45 \sim 2.22, \quad \alpha \sim 0.$$

(4.70)

Comparing these results with superfluid ^{4}He we see that the critical temperature itself agrees reasonably well with that of the λ point. The smallness of the critical index α explains the observation of an almost logarithmic divergence of the specific heat[c]

---

[c]The critical behaviour (4.71) for $T > T_c$ and for $T < T_c$ leads to

$$c_s \sim -A \log|\tau| - \tfrac{1}{2} r A \operatorname{sgn} \tau + b.$$

The original measurements gave

$$A \sim \tfrac{1}{2}(A_{T<T_c} + A_{T>T_c}) = 1.3 \pm 0.02, \quad b = 0.6828,$$

$$r = \frac{A_{T<T_c} - A_{T>T_c}}{A_{T<T_c} + A_{T>T_c}} \frac{1}{\alpha} \sim \left(1 - \frac{A_{T>T_c}}{A_{T<T_c}}\right)\frac{1}{\alpha} \sim 4.4.$$

$$c \sim \frac{A}{\alpha}\left(1 + \alpha \log\left|\frac{T}{T_c} - 1\right| + \ldots\right). \tag{4.71}$$

A precise experimental determination of the critical behavior by Ahlers (of the Notes and References at the end of the chapter) yields, at saturated vapour pressure (see Figs. 4.11a, b)

$$c_s \sim \frac{A}{\alpha}|\tau|^{-\alpha}[1 + \delta|\tau|^{0.5}] + B, \tag{4.72}$$

where $\tau \equiv T/T_c - 1$ and

$$\alpha = -0.026 \pm 0.004,$$

$$\frac{A_{T>T_c}}{A_{T<T_c}} = 1.112 \pm 0.022, \quad A = \frac{1}{2}(A_{T<T_c} + A_{T>T_c}) \approx 1.3 \pm 0.02$$

$$\frac{\delta_{T>T_c}}{\delta_{T<T_c}} = 1.29 \pm 0.25, \quad \delta \sim \frac{1}{2}(\delta_{T<T_c} + \delta_{T>T_c}) \approx 4.0 \tag{4.73}$$

Incidentally, the value of α can be used, together with the scaling relation, $v = (2 - \alpha)/D$, to predict the critical behavior of the superfluid density near T_c, which is parametrized by

$$\frac{\rho_s}{\rho} = b\left(1 - \frac{T}{T_c}\right)^v. \tag{4.74}$$
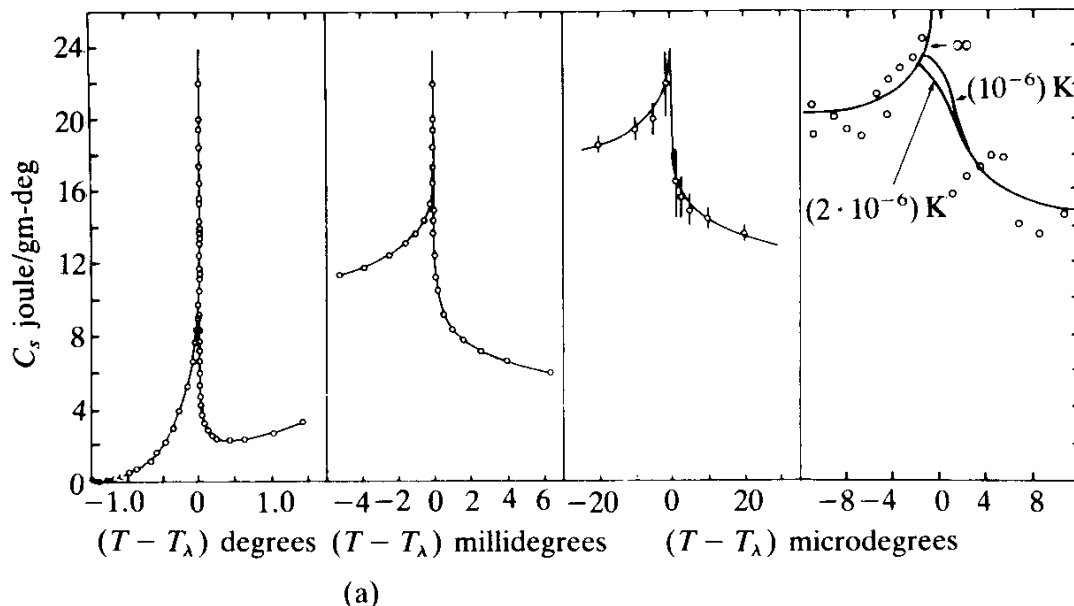
Using the above value of $\alpha = -0.026 \pm 0.004$ one predicts $v = 0.6753 \pm 0.003$. The best direct fit to the experimental data to be shown later in Figs. 5.3, 5.5 on the other hand, gives $v = 0.6749 \pm 0.0007$ in very good agreement with the scaling prediction.

In principle, the limiting form (4.61) can be used to extract directly the following sequences
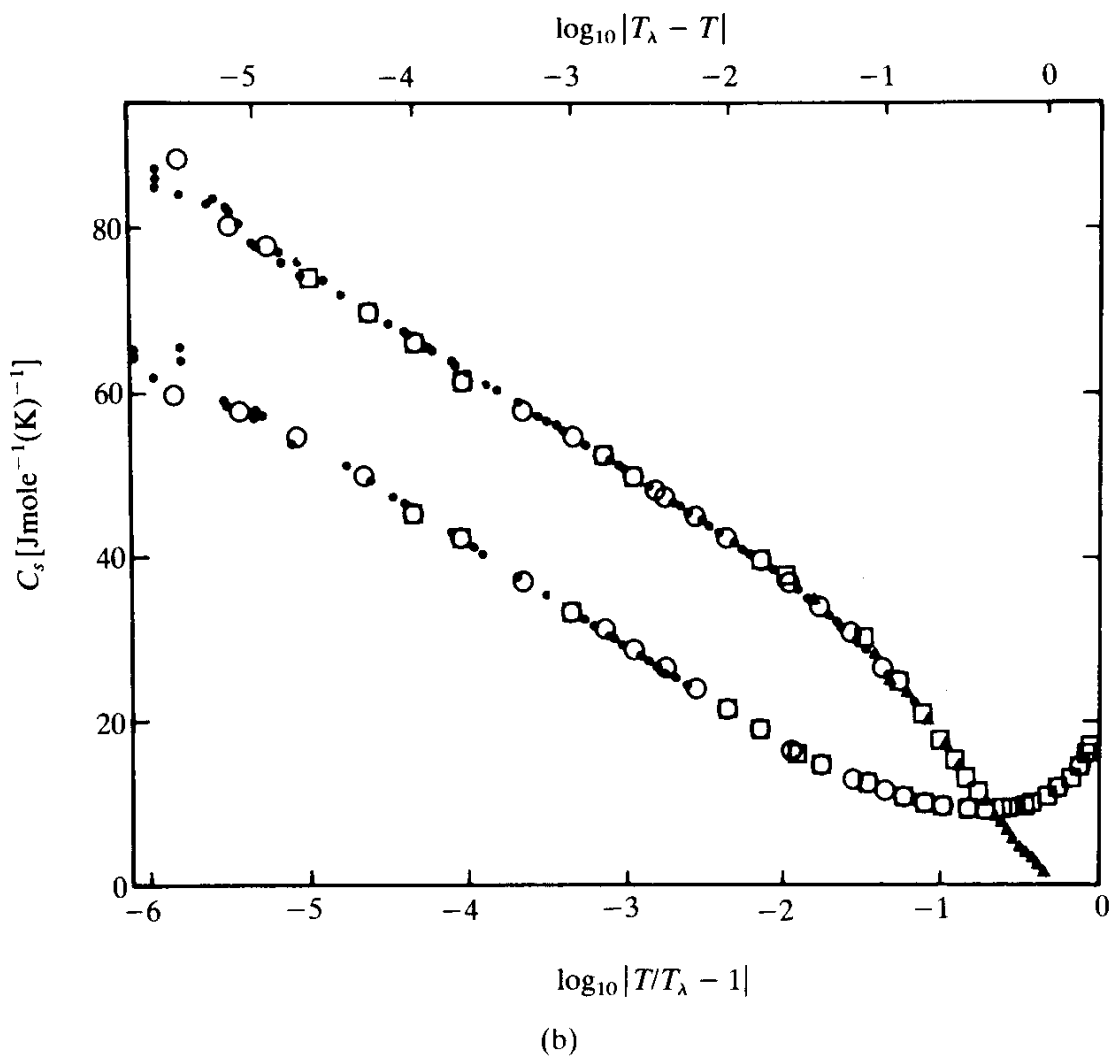
$$T_n = n\sqrt{R_n} - (n - 1)\sqrt{R_{n-1}}, \tag{4.75a}$$

and

FIG. 4.11.   The experimental specific heat of Fairbank *et. al* (a) and Ahlers (b) (see Notes and References).

(a)

(b)

$$\alpha_n = 1 + \frac{2(\sqrt{R_n} - \sqrt{R_{n-1}})\bigg/\left(\dfrac{1}{n} - \dfrac{1}{n-1}\right)}{n\sqrt{R_n} - (n-1)\sqrt{R_{n-1}}}$$

$$= 1 - 2\frac{(\sqrt{R_n/R_{n-1}} - 1)}{\dfrac{1}{n-1}\sqrt{\dfrac{R_n}{R_{n-1}}} - \dfrac{1}{n}}, \qquad (4.75b)$$

which have to converge against T_c and α, respectively. If only a few ratios are known, however, this method is not very useful. If we plot the numbers

$$T_3 = 2.646, \quad T_4 = 1.546, \quad T_5 = 2.392, \quad T_6 = 2.234, \qquad (4.76)$$

against $1/n$, we see in Fig. 4.9 that these form a zig-zag curve; it is hard to deduce an accurate limiting value from this. Similarly, the numbers α_n possess strong oscillations

$$\alpha_3 = -0.55, \quad \alpha_4 = 2.61, \quad \alpha_5 = -0.78, \quad \alpha_6 = -0.2, \qquad (4.77)$$

and are not very useful for practical purposes either.

In the previous section we saw that there exists a more natural power series for the free energy, namely, that in powers of $I_1(\beta)/I_0(\beta)$:

$$-\beta f = 3\log I_0(\beta) + 6\left(\frac{I_1}{I_0}\right)^4 + 44\left(\frac{I_1}{I_0}\right)^6 + \frac{2835}{8}\left(\frac{I_1}{I_0}\right)^8 + \frac{6967}{2}\left(\frac{I_1}{I_0}\right)^{10} + \ldots \qquad (4.78)$$

From the $(\beta/2)^{12}$ term (4.66) we can recover (via Table 4.12) one more coefficient

$$39682.75466\left(\frac{I_1}{I_0}\right)^{12}.$$

In order to extract from this a specific heat behaving like $(\beta - \beta_c)^{-\alpha}$, the free energy has to be singular, like

$$-\beta f \sim (\beta - \beta_c)^{2-\alpha}, \tag{4.79}$$

or

$$-\beta f \sim \left(\left(\frac{I_1(\beta)}{I_0(\beta)}\right)^2 - \left(\frac{I_1(\beta_c)}{I_1(\beta_c)}\right)^2\right)^{2-\alpha}. \tag{4.80}$$

When expanded in powers of $(I_1/I_0)^2$, this implies that the ratios R_n of the coefficients of $-\beta f$ have to behave, for large n, like

$$\sqrt{R_n} \sim \left(\frac{I_1(\beta_c)}{I_0(\beta_c)}\right)\left(1 + \frac{\alpha - 3}{2n} + O\left(\frac{1}{n^2}\right)\right). \tag{4.81}$$

From (4.78), (4.79) we find

$$\sqrt{R_3} = \sqrt{\frac{44}{6}} = 2.708, \quad \sqrt{R_4} = \sqrt{\frac{2835}{8 \cdot 44}} = 2.838,$$

$$\sqrt{R_5} = \sqrt{\frac{6967 \cdot 4}{2835}} = 3.135. \tag{4.82}$$

When plotted against $1/n$ in Fig. 4.5, the last two ratios tend linearly to the value $I_0(\beta_c)/I_1(\beta_c) \approx 4.6$ which corresponds to[f] $\beta_c \sim 0.45$ or $T_c \sim 2.22$, in good agreement with the previous estimate. The slope is ~ 7 so that

$$\frac{\alpha - 3}{2} \sim -\frac{6}{4.6},$$

or

$$\alpha \sim -0.04,$$

---

[f]For going back and forth between $I_1(\beta)/I_0(\beta)$ and β in the regime $\beta \in (0.4, 0.5)$ one can use the approximation $I_1(\beta)/I_0(\beta) \sim 0.196 + 0.464(\beta - 0.4)$, $\beta \sim 0.4 + (I_1/I_0 - 0.196)/0.464$ with an error of 10^{-3}.

which is again small and has the right sign. The smoother behavior of R_n as a function of $1/n$ indicates that $x = I_1(\beta)/I_0(\beta)$ is, indeed, a better expansion parameter than β. (An even better determination of β_c is possible using the high temperature expansion of the magnetic susceptibility of the XY model which will be discussed later in Section 9.5.)

APPENDIX 4A: GRAPHS OF ORDER β^{10}

Let us neglect the two possible orientations and organize the graphs according to how many dimensions they occupy in space. The numbers in front refer to the numbers under which the graphs are listed in Table 5.1.

1.   *Simple planar graphs*: They are easy to count

$$10.1 \quad \square\square = 2\binom{D}{2} N, \qquad 10.2 \quad \square\square\square = 2\binom{D}{2} N,$$

$$10.3 \quad \square\square\square = 4 \cdot 2\binom{D}{2} N, \qquad 10.4 \quad \square\square = 2 \cdot 2\binom{D}{2} N,$$

$$10.5 \quad \square\square\square = 4 \cdot 2\binom{D}{2} N, \qquad 10.6 \quad \square\square = 2 \cdot 2\binom{D}{2} N.$$

As explained previously, $\binom{D}{2}$ accounts for the number of ways of choosing two out of D dimensions in which to place the graph. Then there are 2 ways of placing the long axis of the graphs. If a graph is asymptotic with respect to one or both of the axes, there is an extra factor of 2 or 4. Altogether there are

$$28\binom{D}{2} N$$

planar graphs of order 10.

2. *Simple three- to five- dimensional graphs.* A computer search by Fisher and Gaunt (see the Notes and References at the end of the chapter) gives the total number of

$$\left(2328\binom{D}{2} + 23136\binom{D}{4} + 47616\binom{D}{5}\right)N$$
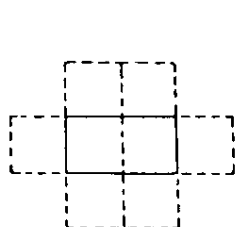
simple graphs in 3, 4 and 5 dimensions, respectively (the numbers 10.7–10.9 in Table 4.1).

3. *Exceptional simple graphs of 3 and 4 dimensions.* Three loops around a single plaquette can meet at a single link

There are $\left[12\binom{D}{3} + 32\binom{D}{4}\right]N$ configurations of this type. The three plaquettes can lie in two or three different coordinate planes (if they all lie in the same plane they will be counted separately in 10.14 as a graph with doubly occupied links). In the case of two coordinate planes, the graph 10.10 can be thought of as arising from the graph 8.5 by shifting one loop to the opposite face. This is why their number is the same $(= 12)$. The number 12 arises from the $\binom{3}{2}$ ways of selecting two planes out of three dimensions, times 2 for the ways the two sides the second loop touch the first, times 2 for the possibility of letting the third loop point up or down. In four dimensions, this is replaced by 4 times 4 for attaching the second loop, since it must point up or down, times 2 for attaching the third loop, again pointing in two directions (of the fourth dimension).

4. *Disconnected graphs.* The order 10 can be reached by combining graphs of order 6 and 4 in the following ways

10.11   10.12   10.13

where the subgraph of order six is planar, two- or three-dimensional and has multiplicities 2, 12, 4 (see 6.1, 6.2, 6.3 in Table 4.1). Hence there are $2\binom{D}{2}^2 N^2$, $12\binom{D}{2}\binom{D}{3}N^2$, $4\binom{D}{3}\binom{D}{2}N^2$ combinations, where 2, 12, 4 are the multiplicities of the first subgraph.

From these we have to subtract those which touch at edges (touching on corners is allowed). Obviously, there are 8 ways of placing the second loop on top or around the first loop. Hence we have to subtract $2 \cdot 8\binom{D}{2}$ graphs. In addition, there are $2 \cdot 6(D-2)$ graphs where the simple plaquette points into a third dimension and $2(D-2)$ graphs of the type 10.10. Altogether we have

$$2N\left[N\binom{D}{2}^2 - \left(8\binom{D}{2} + 84\binom{D}{3}\right)\right],$$
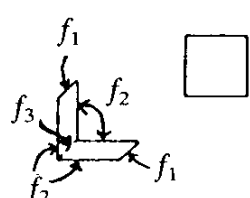
of type 10.11. For 10.12, the result is

$$12N\left[N\binom{D}{3}\binom{D}{2} - \left(20\binom{D}{3} + 56\binom{D}{4}\right)\right].$$

In order to verify the subtracted number of forbidden graphs, call it f; we write

$$f = 2 + f_1 + f_2 + f_3,$$

where 2 denotes the two possibilities of letting the second loop fall on top of one of the two others and the numbers $f_{1,2,3}$ are those configurations whose second loop touches the others along the following edges:
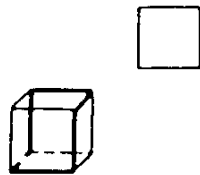
Obviously we have

$$f_1 = 2(1 + 2(D - 2)), \quad f_2 = 2(5 + 2 \cdot 2(D - 3)), \quad f_3 = 2 + 2(D - 3).$$

In (10.13), finally, we find

$$4N\left[\binom{D}{3}\binom{D}{2} - \left(18\binom{D}{3} + 48\binom{D}{4}\right)\right].$$

If f denotes again the subtracted number, it can be written as $f = 6 + f_1$

where 6 is the number of faces on top of which the second loop is forbidden from falling upon and f_1 is the number of ways of attaching the second loop to one of the edges, i.e.,

$$f_1 = 6(2 + 2(D - 3)).$$

If orientations are included, all graphs carry a factor 4 except for the graph 10.10 which carries a factor 6.

While counting the disconnected graphs we can check once more the number of exceptional graphs 10.10 in Table 4.1. Graphs of this type arose counting the omitted graphs in 10.11 and 10.12, the following number of times

$$\left[12\binom{D}{3}\left(2 + 2(D - 3) + 2\binom{D}{2}2(D - 2)\right)\right]N = \left[36\binom{D}{3} + 96\binom{D}{4}\right]N.$$

But since the additional plaquette is indistinguishable from the others, i.e.,

the three graphs are always identical, which gives the correct number

$$\left[12\binom{D}{3} + 32\binom{D}{4}\right]$$ N, as stated above. If orientations are included, all

graphs receive the factor 2 × 2 = 4, except 10.10, for which the factor is 6 as can easily be seen by drawing all possible fluxes

5. *Graphs with currents of flux 2*. These graphs are easy to count since they are identical in shape to simpler graphs of lower order and carry a factor accounting for the number of ways in which they can be joined by a flux two bridge. First, there are planar octogons with a single flux 2 bridge across one of the links. The $D = 2$ octogons 8.1 and 8.3 result in the diagrams

10.18 $4\binom{D}{2}N$

10.19 $8\binom{D}{2}N$

Similarly, we can place a flux 2 bridge in the $D = 3$ and $D = 4$ octogons and find $288\binom{D}{3}N + 764\binom{D}{4}N$ graphs. Then there are two types of

graphs with two links of flux 2:

$$10.16 \quad \boxed{\text{(cube graph)}} = 2 \cdot \#6.2$$
$$= 24\binom{D}{3} \cdot N$$

$$10.17 \quad \boxed{\text{(cube graph)}} = 6 \cdot \#6.3$$
$$= 24\binom{D}{3} \cdot N$$

and two more types of graphs with three links of flux 2:

$$10.14 \quad \boxed{\text{(graph)}} = 2 \cdot \#6.1$$
$$= 4\binom{D}{2} \cdot N$$

$$10.15 \quad \boxed{\text{(cube graph)}} = 2 \cdot \#6.2$$
$$= 24\binom{D}{3} \cdot N$$

The total contribution to the partition function is given in Eq. (4.49).

Counting the graphs of twelfth order is extremely tedious. We refer to the thesis of W. Janke (Free University, Berlin, 1988) for details.

NOTES AND REFERENCES

A general review of high temperature expansions is found in
J.M. Drouffe and J.B. Zuber, *Phys. Reports* **102** (1984) 1,

R. Balian, J.M. Drouffe, C. Itzykson, *Phys. Rev.* **D11** (1975) 2098, 2104; *ibid.* **D19** (1979) 2514. (*Erratum*) (note: the twelfth order term is incorrect).

The graphical analysis of the *XY* model (in two dimensions up to $I_1(I_0)^{12}$) and for self-avoiding polymer rings can be found in
W. Janke, Freie Univ. Berlin, Thesis, 1985,
who also gives the Monte Carlo data. See also
H. Kleinert, W. Miller, *Phys. Rev. Lett.* **56** (1986) 11, *Phys. Rev.* **D38** (1988) 1239.
The high temperature expansion of the 3 D *XY* model on a s.c. lattice was calculated up to β^{12} by
M. Ferer, M.A. Moore, M. Wortis, *Phys. Rev. Lett.* **B8** (1973) 5205.
The lattice constants p_n were systematized by
C. Domb and M.F. Sykes, *Phil. Mag.* **2** (1957) 733
and tabulated by
C. Domb, *Adv. Phys.* **9** (1960) 149, 345.
The present state of affairs is found in
M.F. Sykes, D.L. Hunter, D.S. McKenzie, B.R. Heap, *J. Phys.* **A5** (1972) 661,
M.F. Sykes, D.S. McKenzie, M.G. Watts, J.L. Martin, *J. Phys.* **A5** (1974) 661,
for b.c.c. up to $n = 16$, for s.c. up to $n = 20$, for the square lattice up to $n = 26$, and for the triangular lattice up to $n = 18$. The series was carried for the square lattice up to $n = 38$ by
I.G. Enting, *J. Phys.* **A13** (1980) 3713.
The f.c.c. numbers can also be taken from an expansion for arbitrary $O(N)$ spins in
D.S. English, D.L. Hunter, C. Domb, *J. Phys.* **A12** (1979) 2111,
if one inserts in their formulas $d = 0$ (after correcting in their $n = 11$ result the number 2321 270 341 832, i.e., the last three digits 832 should read 632).
See also:
M.E. Fisher and D.F. Gaunt, *Phys. Rev.* **133** (1964) A224,
M.F. Sykes, J.L. Martin, D.L. Hunter, *Proc. Roy. Phys. Soc.* **91** (1967) 671,
A.J. Guttmann, G.S. Joyce, *J. Phys.* **C6** (1973) 2691.
  Susceptibility expansions are given by
R.G. Bowers and G.S. Joyce, *Phys. Rev. Lett.* **19** (1967) 630;
see also
M.A. Moore, *Phys. Rev. Lett.* **23** (1969) 861,
W.J. Camp and J.P. van Dyke, *J. Phys.* **C8** (1975), 336,
M. Ferer, M.J. Velgakis, *Phys. Rev.* **B27** (1983) 314.
  For the zeroes in the partition function see
C.N. Yang and T.D. Lee, *Phys. Rev.* **87** (1952) 404, 410,
M.E. Fisher, in *Lectures in Theoretical Physics*, Vol VIC (Univ. of Colorado Press, Boulder, 1965) p. 1,
R.B. Pearson, *Phys. Rev.* **B26** (1982) 6285,
C. Itzykson, R.B. Pearson, J. B. Zuber, *Nucl. Phys.* **B220** (F98) (1983) 415,
B. Derrida, L. De Seze, C. Itzykson, *J. Stat. Phys.* **33** (1983) 559.
The critical behaviour of the specific heat in superfluid ^{4}He was measured by
W.M. Fairbank, M.J. Buckingham, C.F. Keller as reviewed by W.M. Fairbank and C.F. Keller, in *Proceedings 1965 Washington Conf. on Critical Phenomena*, ed. M.S. Green and J.V. Sengers *Nat'l. Bur. Stand. Misc. Publ.* **273** (1966) 71.
More accurate data are given in
G. Ahlers, *Phys. Rev.* **A3** (1971) 696.
See also G. Ahlers' lecture, in *1978 Erice Conference on Low Temperature Physics*, ed. J. Ruvalds and T. Regge (North Holland, Amsterdam, 1978),
T.H. McCoy, L.H. Graf, *Phys. Lett.* **A58** (1972) 287,

K.H. Mueller, G. Ahlers, F. Pobell, *Phys. Rev.* **B14** (1976) 2096,
J.A. Lipa and T.C.P. Chiu, *Phys. Rev. Lett.* 51 (1983) 2291.
A rather complete theoretical discussion is found in
M. Barmatz, P.C. Hohenberg, A. Kornblit, *Phys. Rev.* **B12** (1975) 1947.

CHAPTER FIVE

MEAN FIELD METHODS FOR LATTICE MODELS

While the high temperature expansion is quite accurate in describing almost the entire high temperature phase (except in the immediate vicinity of the critical point), it fails completely in the low temperature phase. Other methods are therefore needed in order to complete our understanding of the model. The most prominent among them is based on the mean field theory plus fluctuation corrections.

5.1. VARIATIONAL ESTIMATES OF THERMODYNAMIC PROPERTIES

The mean field approximation to the lattice partition function is useful for finding rough estimates for thermodynamic properties. This approximation can be derived from the Peierls–Jensen inequality which states: given an arbitrary positive functional integration measure, let $\langle s \rangle$ denote the average of a functional with respect to this measure. Then

$$\langle e^{-s} \rangle \geq e^{-\langle s \rangle}.$$ (5.1)

This inequality is a simple consequence of the convexity of the exponential. For functions of real variables, say γ, a convex function is defined by the property that

409

$$f\left(\frac{\gamma_1 + \gamma_2}{2}\right) \leq \frac{f(\gamma_1) + f(\gamma_2)}{2}, \qquad (5.2)$$

i.e., the value of a function evaluated somewhere between any two fixed points is lower than the average of the values of the function at the two fixed points. By applying this property repeatedly it can be shown to be equivalent to the requirement

$$f(\mu_1 \gamma_1 + \mu_2 \gamma_2) \leq \mu_1 f(\gamma_1) + \mu_2 f(\gamma_2), \qquad (5.3)$$

where μ_1, μ_2 are arbitrary positive numbers which add up to unity (i.e., $\mu_1 + \mu_2 = 1$); clearly, γ_1, γ_2 can also be replaced by an arbitrary function $h(\gamma_1)$, $h(\gamma_2)$, so that we have

$$f(\mu_1 h(\gamma_1) + \mu_2 h(\gamma_2)) \leq \mu_1 f(h(\gamma_1)) + \mu_2 f(h(\gamma_2)). \qquad (5.4)$$

This, in turn, can be generalized to

$$f\left(\int d\mu(\gamma) h(\gamma)\right) \leq \int d\mu(\gamma) f(h(\gamma)) \qquad (5.5)$$

with $\int d\gamma \mu(\gamma) = 1$ and even further to the case that h is a functional of an x dependent function $\gamma(x)$, i.e.,

$$f\left(\int \mathscr{D}\mu[\gamma] h[\gamma]\right) \leq \int \mathscr{D}\mu[\gamma] f(h[\gamma]). \qquad (5.6)$$

where $\int \mathscr{D}\gamma\mu[\gamma] = 1$. This implies (5.1)

Consider now the partition function of the XY model:

$$Z' = \prod_x \left[\int_{-\pi}^{+\pi} \frac{d\gamma(x)}{2\pi}\right] e^{-\beta E'[\gamma]} = \prod_x \left[\int_{-\pi}^{+\pi} \frac{d\gamma(x)}{2\pi}\right] e^{\beta \Sigma_{x,i} \cos \nabla_i \gamma(x)}. \qquad (5.7)$$

The idea is to set up a variational method using a trial partition function which can easily be evaluated and optimized via the inequality (5.6). A simple ansatz involving only a single free variational parameter α is given by

$$Z_0(\alpha) = \prod_x \left[\int_{-\pi}^{+\pi} \frac{d\gamma(x)}{2\pi}\right] e^{-\beta E_0[\gamma]} \equiv \prod_x \left[\int_{-\pi}^{\pi} \frac{d\gamma(x)}{2\pi}\right] e^{\alpha \Sigma_x \cos \gamma(x)}. \qquad (5.8)$$

The parameter $\alpha \neq 0$ gives a preference to a zero phase angle. It plays a role similar to the mean magnetic field in a ferromagnet which tries to align the local magnetization. The ansatz (5.8) has the virtue that the different sites are decoupled. Therefore, the integrations can be done easily with the result

$$Z_0 = \prod_x I_0(\alpha) = e^{N \log I_0(\alpha)} \equiv e^{-\beta F_0}. \tag{5.9}$$

The point is now that we can identify

$$\int \mathscr{D}\mu \equiv \prod_x \int d\mu(\mathbf{x}) \equiv \frac{1}{Z_0} \prod_x \left[\int_{-\pi}^{\pi} \frac{d\gamma(\mathbf{x})}{2\pi} \right] e^{\alpha \Sigma_x \cos \gamma(\mathbf{x})} \tag{5.10}$$

as a positive normalized measure to be used in the Peierls–Jensen inequality (5.6). Let us denote the expectation calculated with this measure by $\langle \ \rangle_0$. Then we can write

$$Z = Z_0 \prod_x \left[\int d\mu(\mathbf{x}) \right] e^{\beta \Sigma_{x,i} \cos \nabla_i \gamma(\mathbf{x}) - \alpha \Sigma_x \cos \gamma(\mathbf{x})}$$

$$= Z_0 \prod_x \left[\int d\mu(\mathbf{x}) \right] e^{-\beta(E'[\gamma] - E_0[\gamma])} = Z_0 \langle e^{-\beta(E'[\gamma] - E_0[\gamma])} \rangle_0. \tag{5.11}$$

Applying (5.1) to this, we obtain the inequality

$$Z \geq Z_0 e^{-\beta \langle E'[\gamma] - E_0[\gamma] \rangle_0}. \tag{5.12}$$

For the free energy this amounts to the bound

$$-\beta F' \geq -\beta F_0 - \beta \langle E'[\gamma] - E_0[\gamma] \rangle_0. \tag{5.13}$$

Let us calculate the expectation value of the right-hand side. By definition, it is given by the integral

$$-\beta \langle E'[\gamma] - E_0[\gamma] \rangle$$

$$= \prod_x \left[\int d\mu(\mathbf{x}) \right] \left(\beta \sum_{x,i} \cos \nabla_i \gamma(\mathbf{x}) - \alpha \sum_x \cos \gamma(\mathbf{x}) \right)$$

$$= \frac{1}{Z_0} \prod_x \left[\int_{-\pi}^{+\pi} \frac{d\gamma(\mathbf{x})}{2\pi} \right] e^{\alpha \Sigma_x \cos \gamma(\mathbf{x})} \left(\beta \sum_{x,i} \cos \nabla_i \gamma(\mathbf{x}) - \alpha \sum_x \cos \gamma(\mathbf{x}) \right).$$

$$\tag{5.14}$$

But this expectation value is easy to evaluate after writing

$$\cos \nabla_i \gamma(\mathbf{x}) = \cos(\gamma(\mathbf{x} + \mathbf{i}) - \gamma(\mathbf{x}))$$

$$= \cos \gamma(\mathbf{x} + \mathbf{i}) \cos \gamma(\mathbf{x}) + \sin \gamma(\mathbf{x} + \mathbf{i}) \sin \gamma(\mathbf{x}). \quad (5.15)$$

The $\sin \gamma$ terms do not contribute, since they are odd functions of γ so that the right-hand side can be expressed completely in terms of the expectation of $\cos \gamma$, which we shall call u:[a]

$$\langle \cos \gamma \rangle_0 = \frac{\displaystyle\int_{-\pi}^{\pi} \frac{d\gamma}{2\pi} e^{\alpha \cos \gamma} \cos \gamma}{\displaystyle\int_{-\pi}^{\pi} \frac{d\gamma}{2\pi} e^{\alpha \cos \gamma}} = \frac{\dfrac{\partial}{\partial \alpha} I_0(\alpha)}{I_0(\alpha)} = \frac{I_1(\alpha)}{I_0(\alpha)} \equiv u. \quad (5.16)$$

Thus we find

$$-\beta \langle E'[\gamma] - E_0[\gamma] \rangle_0 = N(\beta D u^2 - \alpha u). \quad (5.17)$$

Inserting this result, together with (5.9), into (5.13), we find that the free energy per site f' is bounded from above by

$$-\beta f' \geq \log I_0(\alpha) + \beta D u^2 - \alpha u \quad (5.18a)$$

$$= \log I_0(\alpha) + \beta D \left(\frac{I_1(\alpha)}{I_0(\alpha)}\right)^2 - \alpha \frac{I_1(\alpha)}{I_0(\alpha)}. \quad (5.18b)$$

This inequality holds for an arbitrary "mean magnetic field" α. By minimizing the right-hand side we can optimize the bound. Differentiation with respect to α yields

$$\frac{I_1}{I_0} + \beta D \left(\frac{2 I_1 I_1'}{I_0^2} - 2 \frac{I_1^3}{I_0^3}\right) - \alpha \left(\frac{I_1'}{I_0} - \frac{I_1^2}{I_0^2}\right) - \frac{I_1}{I_0} = 0,$$

which amounts to the equation

---

[a]This is not to be confused with the internal energy density, for which we use the same letter u, for historic reasons.

$$\alpha = 2D\beta u = 2D\beta \frac{I_1(\alpha)}{I_0(\alpha)}.$$ (5.19)

For this value of the magnetic field, the free energy per site is bounded by

$$-\beta f' \geq -\frac{1}{4\beta D}\alpha^2 + \log I_0(\alpha) \equiv -\beta f'^{MF}$$ (5.20)

Since α plays the role of a *mean* magnetic field, the bound on the right-hand side is referred to as the *mean field free energy*, as indicated by the superscript MF. The right-hand side corresponds to an internal energy

$$u'^{MF} = -\frac{\partial}{\partial\beta}(-\beta f'^{MF}) = -Du^2 = -\frac{\alpha^2}{4D\beta^2}$$ (5.21a)

(the derivatives $\partial\alpha/\partial\beta$ do not contribute since $-\beta f'^{MF}$ is extremal in α), to an entropy

$$s'^{MF} = -\beta(f'^{MF} - u'^{MF}) = \log I_0(\alpha)$$ (5.21b)

and to a specific heat

$$c^{MF} = -\beta^2\frac{\partial u'^{MF}}{\partial\beta} = 2D\beta^2 u\frac{\partial u}{\partial\beta}.$$ (5.21c)

Using the field equation $2D\beta u = \alpha$, $u = I_1(\alpha)/I_0(\alpha)$ we find

$$\frac{\partial u}{\partial\beta} = -\frac{u}{\beta}\frac{1 - u^2 - \dfrac{1}{2D\beta}}{1 - u^2 - \dfrac{1}{D\beta}}$$ (5.21d)

so that[b]

---

[b]Later in Eqs. (5.60) and (5.67) we will find that the mass of the fluctuations of the order parameter is $M^2/2D = -(1 - u^2 - 1/D\beta)/(1 - u^2 - 1/2D\beta)$ so that $c^{MF} = 2D\beta u^2 \times (M^2/2D)^{-1}$.

$$c^{MF} = -2D\beta u^2 \frac{1 - u^2 - \dfrac{1}{2D\beta}}{1 - u^2 - \dfrac{1}{D\beta}}.$$ (5.21e)

Notice that the inequality (5.18a) is also valid if the right-hand side is considered as a function of two independent variables α and u. Then minimization of f' in α gives (5.16), the maximization in u gives (5.20). The condition (5.20) can be solved graphically (see Fig. 5.1).[c] To do this we plot the function $I_1(\alpha)/I_0(\alpha)$ and search for the intersection of this graph with a straight line through the origin with slope $1/2D\beta$. For small β (i.e., high T), the solution is $\alpha = 0$. For large β (i.e., small T), there is a non-trivial solution which can be estimated using the asymptotic form of the Bessel functions,

$$I_n(\alpha) \sim \frac{e^\alpha}{\sqrt{2\pi\alpha}} \left\{ 1 - \frac{n^2 - \frac{1}{4}}{2\alpha} + \frac{1}{2!} \frac{(n^2 - \frac{1}{4})(n^2 - \frac{9}{4})}{(2\alpha)^2} \right.$$
$$\left. - \frac{1}{3!} \frac{(n^2 - \frac{1}{4})(n^2 - \frac{9}{4})(n^2 - \frac{25}{4})}{(2\alpha)^3} + \ldots \right\},$$ (5.22)

so

$$u = \frac{I_1(\alpha)}{I_0(\alpha)} \sim 1 - \frac{1}{2\alpha} - \frac{1}{8\alpha^2} - \frac{1}{8\alpha^3} - \ldots$$ (5.23)

and

$$\alpha = 2D\beta u = 2D\beta \left(1 - \frac{1}{2\alpha} - \frac{1}{8\alpha^2} - \frac{1}{8\alpha^3} - \ldots \right)$$
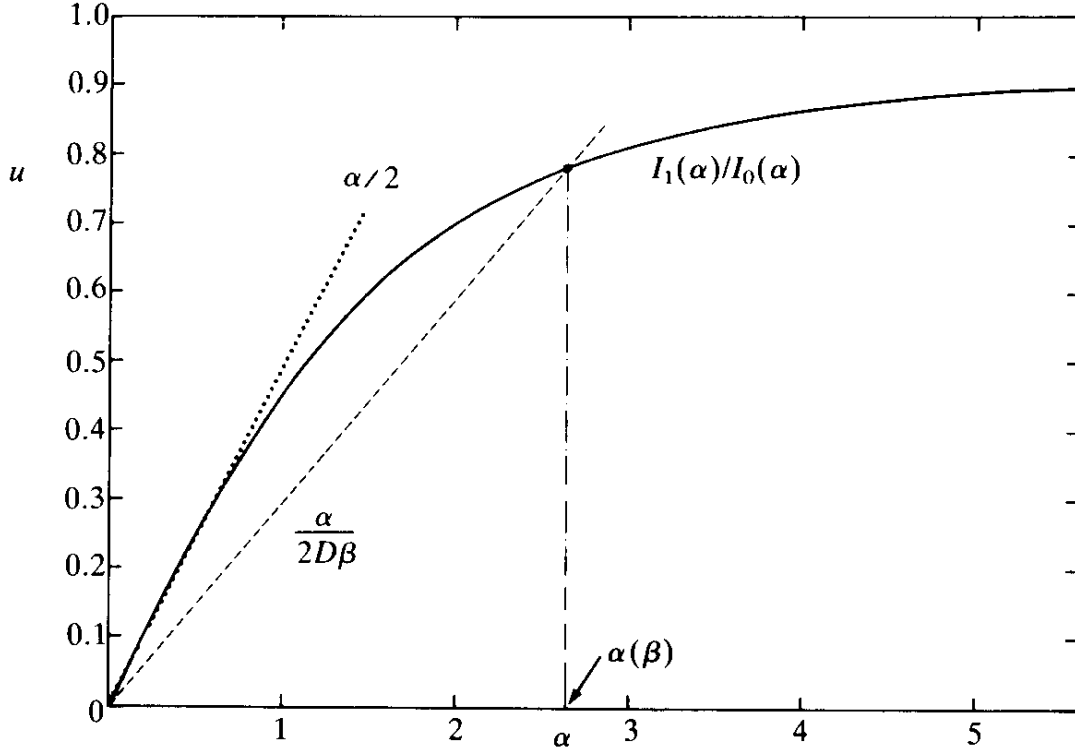
has the large β limit

$$\alpha = 2D\beta u = 2D\beta \left(1 - \frac{1}{2(2D\beta)} - \frac{3}{8(2D\beta)^2} - \frac{9}{16(2D\beta)^3} - \ldots \right).$$ (5.24)

Inserting this limit into (5.20) expanded for large α,

[c]In practice one does not really have to use this graphical method but takes, in the low temperature phase, a table for $I_1(\alpha)/I_0(\alpha)$ and calculates from this $\beta(\alpha) = (\alpha/2D)[I_0(\alpha)/I_1(\alpha)]$.

FIG. 5.1.   The graphical solution of the mean field equation $\alpha/2D\beta = I_1(\alpha)/I_0(\alpha)$ [see Eq. (5.19)] via the intersection of the straight line $\alpha/2D\beta$ with the curve $I_1(\alpha)/I_0(\alpha)$. The phase transition occurs at $D\beta_c^{MF} = 1$ (dotted line).

$$-\beta f' \geq -\beta f'^{MF} = -\frac{1}{4\beta D}\alpha^2 + \alpha - \frac{1}{2}\log 2\pi\alpha + \frac{1}{8\alpha} + \frac{1}{16\alpha^2} + O\left(\frac{1}{\alpha^3}\right),$$
$$(5.25)$$

we see that the bound has the large β limit

$$-\beta f' \geq \beta f'^{MF} = D\beta - \frac{1}{2}\log(2\pi \cdot 2D\beta) + \frac{1}{4(2D\beta)} + \frac{3}{16(2D\beta)^2} + O\left(\frac{1}{\beta^3}\right).$$
$$(5.26)$$

From Eqs. (5.21) we find the other thermodynamic functions,

$$u'^{MF} = -\frac{\partial}{\partial\beta}(-\beta f'^{MF}) = -Du^2$$

$$= D\left(1 + \frac{1}{2D\beta} + \frac{1}{2(2D\beta)^2} + \frac{3}{4(2D\beta)^3} + \dots\right),$$

$$s^{MF} = -\frac{1}{2}\log(2\pi 2D\beta) + \frac{1}{2} + \frac{1}{2(2D\beta)} + \frac{9}{16(2D\beta)^2} + \dots,$$

$$c^{MF} = \frac{1}{2} + \frac{1}{2(2D\beta)} + \frac{9}{8(2D\beta)^2} + \dots.$$
$$(5.27)$$

The leading $1/\beta$ behavior agrees with the large β limit behavior calculated before in (4.9)–(4.13), so that the Dulong-Petit rule is satisfied (recall $-\beta f' \equiv D\beta - \beta f$). The thermodynamic functions $-\beta f'^{MF}$, u'^{MF}, c^{MF} are shown in Figs. 4.6–4.8, where they are compared with the high temperature expansion and with the Monte Carlo data, which are available for $u = D + u'$ and c. The non-zero solution for α first becomes possible when the straight line comes to lie tangential to $I_1(\alpha)/I_0(\alpha)$ at the origin. Since these functions have the power series expansions

$$I_0(\alpha) = 1 + \frac{1}{1!^2}\frac{\alpha^2}{4} + \frac{1}{2!^2}\left(\frac{\alpha^2}{4}\right)^2 + \ldots,$$

$$I_1(\alpha) = \frac{\alpha}{2}\left(1 + \frac{1}{1!2!}\frac{\alpha^2}{4} + \frac{1}{2!3!}\left(\frac{\alpha^2}{4}\right)^2 + \ldots\right),$$

$$\frac{I_1(\alpha)}{I_0(\alpha)} = \frac{\alpha}{2} - \frac{1}{2}\left(\frac{\alpha}{2}\right)^3 + \frac{1}{3}\left(\frac{\alpha}{2}\right)^5 + \ldots, \tag{5.28}$$

(recall Table 4.8) the behavior at the origin is $I_1(\alpha)/I_0(\alpha) \sim \alpha/2$ and the temperature T_c^{MF} is given by

$$T_c^{MF} = D = 3. \tag{5.29}$$

This temperature disagrees considerably with T_c of Eq. (4.70) so that the mean field approximation will need corrections.

In the neighborhood of T_c^{MF}, we find, from (5.19) and (5.28), that

$$\alpha = \frac{T_c^{MF}}{T}\alpha\left(1 - \frac{1}{8}\alpha^2 + \frac{1}{48}\alpha^4 + \ldots\right),$$

which is solved by

$$\alpha \sim \sqrt{8}\sqrt{1 - \frac{T}{T_c^{MF}}}\left(1 + \frac{2}{3}\left(1 - \frac{T}{T_c^{MF}}\right) + \ldots\right). \tag{5.30}$$

This is the typical temperature behavior of the magnetization in a ferromagnet near (but not too close to) the Curie point. The energy near this point follows from inserting (5.30) into (5.21). Expanding the logarithm in powers of α we find, in the neighborhood of T_c, the *Landau approximation*

$$\beta f' \gtrsim \frac{1}{4}\left(\frac{1}{\beta D} - 1\right)\alpha^2 + \frac{1}{64}\alpha^4, \qquad (5.31)$$

which is minimal for $\alpha = \sqrt{8}\sqrt{1 - T/T_c^{MF}}$. Thus, close to the critical temperature T_c^{MF}, f'^{MF} behaves as

$$\beta f'^{MF} \gtrsim -\left(1 - \frac{T}{T_c^{MF}}\right)^2. \qquad (5.32)$$

This quadratic behavior in $(1 - T/T_c^{MF})$ was found before for the energy (1.10) and corresponds to a second order phase transition with an internal energy, entropy, and specific heat per site (compare (1.15))

$$\frac{u'^{MF}}{T_c^{MF}} = \begin{cases} 0 \\ -2\left(\dfrac{T}{T_c^{MF}}\right)^2\left(1 - \dfrac{T}{T_c^{MF}}\right) \end{cases} \quad \text{for} \begin{cases} T \geq T_c^{MF} \\ T < T_c^{MF} \end{cases},$$

$$s'^{MF} = -\frac{\partial f'^{MF}}{\partial T} = \begin{cases} 0 \\ -2\left(1 - \dfrac{T}{T_c^{MF}}\right) + 3\left(1 - \dfrac{T}{T_c^{MF}}\right)^2 \end{cases} \quad \text{for} \begin{cases} T \geq T_c^{MF} \\ T < T_c^{MF} \end{cases},$$

$$c^{MF} = T\frac{\partial s'^{MF}}{\partial T} = \begin{cases} 0 \\ 2\left(\dfrac{T}{T_c^{MF}}\right)^2 - 4\dfrac{T}{T_c^{MF}}\left(1 - \dfrac{T}{T_c^{MF}}\right) \end{cases} \quad \text{for} \begin{cases} T \geq T_c^{MF} \\ T < T_c^{MF} \end{cases},$$

$$(5.33)$$

which agree with the results (1.15) close to T_c^{MF}.

5.2. EQUIVALENT FIELD FORMULATION OF THE XY MODEL

Since the lowest approximation to the critical temperature gives a result which is too large by about 24%, the question arises whether there exists a systematic way of improving the variational estimate. This is indeed the case. By means of some simple manipulations it is possible to express the partition function in terms of a new complex field $\psi(x)$. The resulting field theory can be treated with the perturbation techniques of Part I giving higher order free energies with increasing accuracy. The lowest mean field approximation agrees precisely with the variational energy. Fortunately, it will turn out that above the transition temperature the one-

loop correction is sufficient to provide reasonably accurate free and internal energies. For the specific heat, however, the approximation will be insufficient. Even many higher loop corrections will not help since some important fluctuations are missed out by the mean-field-plus-one-loop correction approach. These are the vortex lines which must be calculated in another way.

Let us see how the complex field theory is derived. Our starting point is the partition function of the XY model (4.7). In the exponent, we again split the $\cos \nabla_i \gamma(\mathbf{x})$ term as in (5.15), i.e.,

$$\cos \nabla_i \gamma(\mathbf{x}) = \cos(\gamma(\mathbf{x} + \mathbf{i}) - \gamma(\mathbf{x}))$$

$$= \cos \gamma(\mathbf{x} + \mathbf{i}) \cos \gamma(\mathbf{x}) + \sin \gamma(\mathbf{x} + \mathbf{i}) \sin \gamma(\mathbf{x}). \quad (5.34)$$

Introducing a two-component unit vector

$$U_a(\mathbf{x}) = (\cos \gamma(\mathbf{x}), \ \sin \gamma(\mathbf{x})), \quad (5.35)$$

this can be cast as

$$U_a(\mathbf{x}) \, U_a(\mathbf{x} + \mathbf{i}) = U_a(\mathbf{x})(U_a(\mathbf{x}) + U_a(\mathbf{x} + \mathbf{i}) - U_a(\mathbf{x}))$$

$$= U_a(\mathbf{x})(1 + \nabla_i) \, U_a(\mathbf{x}). \quad (5.36)$$

Summing this over $\mathbf{x}$, the lattice gradient term can be rewritten as follows:

$$\sum_{\mathbf{x}} U_a(\mathbf{x}) \nabla_i U_a(\mathbf{x})$$

$$= -\sum_{\mathbf{x}} U_a(\mathbf{x}) \, \bar{\nabla}_i U_a(\mathbf{x}) = \frac{1}{2} \sum_{\mathbf{x}} U_a(\mathbf{x})(\nabla_i - \bar{\nabla}_i) \, U_a(\mathbf{x})$$

$$= \frac{1}{2} \sum_{\mathbf{x}} U_a(\mathbf{x})(U_a(\mathbf{x} + \mathbf{i}) - U_a(\mathbf{x})) + \frac{1}{2} \sum_{\mathbf{x}} U_a(\mathbf{x})(U_a(\mathbf{x} - \mathbf{i}) - U_a(\mathbf{x}))$$

$$= \frac{1}{2} \sum_{\mathbf{x}} \{ U_a(\mathbf{x}) U_a(\mathbf{x} + \mathbf{i}) - U_a(\mathbf{x})^2 \} + \frac{1}{2} \sum_{\mathbf{x}} \{ U_a(\mathbf{x} - \mathbf{i}) U_a(\mathbf{x}) - U_a(\mathbf{x})^2 \}$$

$$= \frac{1}{2} \sum_{\mathbf{x}} U_a(\mathbf{x})[U_a(\mathbf{x} + \mathbf{i}) - U_a(\mathbf{x}) - U_a(\mathbf{x}) + U_a(\mathbf{x} - \mathbf{i})]. \quad (5.37)$$

But the last expression is recognized as [recall Eq. (1.6.11) for $a = 1$]

$$\frac{1}{2}\sum_{\mathbf{x}} U_a(\mathbf{x})\,\bar{\nabla}_i \nabla_i\, U_a(\mathbf{x}) \quad (i \text{ fixed}). \tag{5.38}$$

Hence the partition function (4.7) of the XY model can be rewritten in the following form

$$Z \equiv e^{-\beta ND}\,Z' \equiv e^{-\beta ND}\prod_{\mathbf{x}}\left[\int_{-\pi}^{+\pi}\frac{d\gamma(\mathbf{x})}{2\pi}\right]e^{D\beta\Sigma_{\mathbf{x}} U_a(\mathbf{x})(1+\bar{\nabla}_i\nabla_i/2D)U_a(\mathbf{x})}, \tag{5.39}$$

where repeated link indices imply summation (Einstein's convention). We would like to find an alternative expression for this Z which somehow makes use of the trial partition function $Z_0(\alpha)$ discussed in the last section.

This is indeed possible. Let us denote, for a moment, the lattice differential operator between the U_a's by

$$\mathscr{D} = 1 + \frac{\bar{\nabla}_i \nabla_i}{2D}. \tag{5.40}$$

Now we introduce two real fluctuating fields $\psi_1(\mathbf{x})$, $\psi_2(\mathbf{x})$ as well as two additional fields $\widehat{\psi}_1(\mathbf{x})$, $\widehat{\psi}_2(\mathbf{x})$ which are related to the above by the square root of the operator $\mathscr{D}$

$$\widehat{\psi}_a(\mathbf{x}) \equiv (\mathscr{D}^{1/2}\psi_a)(\mathbf{x}) = \sum_{\mathbf{y}}\mathscr{D}^{1/2}(\mathbf{x},\mathbf{y})\,\psi_a(\mathbf{y}). \tag{5.41a}$$

The length of the $\widehat{\psi}_a(\mathbf{x})$ fields is now identified with $\alpha(\mathbf{x})$, i.e.,

$$\alpha(\mathbf{x}) = (\widehat{\psi}_1^2(\mathbf{x}) + \widehat{\psi}_2^2(\mathbf{x}))^{1/2}. \tag{5.41b}$$

We then show that Z may be rewritten exactly as a Gaussian average of the trial partition function $Z_0(\alpha(\mathbf{x}))$, when integrated over all $\psi_1(\mathbf{x})$, $\psi_2(\mathbf{x})$ fluctuations as follows:

$$Z' = \prod_{\mathbf{x}}\left[\int_{-\infty}^{+\infty}\frac{d\psi_1(\mathbf{x})\,d\psi_2(\mathbf{x})}{(\sqrt{4\pi\beta D})^2}\right]e^{-(1/4\beta D)\Sigma_{\mathbf{x}}\psi_a^2(\mathbf{x})}Z_0(\alpha(\mathbf{x})). \tag{5.42}$$

The proof is straightforward. We simply insert the explicit integral representation

$$Z_0(\alpha) = [I_0(\alpha)]^N = \left[\int_{+\pi}^{+\pi}\frac{d\gamma}{2\pi}\exp(\widehat{\psi}_1 U_1 + \widehat{\psi}_2 U_2)\right]^N$$

and write

$$Z' = \prod_{\mathbf{x}} \left[\int_{-\infty}^{+\infty} \frac{d\psi_1(\mathbf{x})\, d\psi_2(\mathbf{x})}{(\sqrt{4\pi\beta D})^2} \right] \prod_{\mathbf{x}} \left[\int_{-\pi}^{+\pi} \frac{d\gamma(\mathbf{x})}{2\pi} \right] e^{-(1/4\beta D)\Sigma_{\mathbf{x}}\psi_a^2 \,+\, \Sigma_{\mathbf{x}}(\hat{\psi}_1 U_1 + \hat{\psi}_2 U_2)}.$$

Performing a quadratic completion in the exponent and integrating out the Gaussian integrals over ψ_1, ψ_2 we recover (5.39). It should be noted that the additional fields $\hat{\psi}_a(\mathbf{x})$ are not real. Indeed, when calculating these fields in (5.41) we had to take the square root of the operator $\mathscr{D}(\mathbf{x}, \mathbf{y})$. This is defined in momentum space as follows:

$$\hat{\psi}_a(\mathbf{x}) \equiv (\mathscr{D}^{1/2}\psi_a)(\mathbf{x}) \equiv \int_{-\pi}^{\pi} \frac{d^D k}{(2\pi)^D} \sqrt{1 - \frac{\overline{K}_i K_i}{2D}}\, \psi_a(\mathbf{k})\, e^{i\mathbf{k}\cdot\mathbf{x}}. \tag{5.43}$$

Inserting the explicit expression (6.39) of Part I for K_i, $\overline{K}_i$, the square root reads $\sqrt{(1/D)\Sigma_i \cos k_i a}$ and we see that within the Brillouin zone $|k_i| \leq \pi/a$, the argument has as many positive as negative eigenvalues. For the negative eigenvalues we shall choose the *positive* imaginary square root, say. For these eigenvalues, the Fourier components of $\hat{\psi}_a(\mathbf{x})$ satisfy the condition

$$\hat{\psi}_a(\mathbf{k}) = i\,\sqrt{\left(\frac{1}{D}\sum_i \cos k_i a\right)}\, \psi_a(\mathbf{k}) = -\left(i\,\sqrt{\left(\frac{1}{D}\sum_i \cos k_i a\right)}\, \psi_a(-\mathbf{k}) \right)^*$$

$$= -(\hat{\psi}_a(-\mathbf{k}))^*,$$

so that $\hat{\psi}_a(\mathbf{k}) = \int (d^D k/(2\pi)^D)\, \hat{\psi}_a(\mathbf{k})\, e^{i\mathbf{k}\cdot\mathbf{x}}$ is not real. This is of no consequence since the only relevant property of $\hat{\psi}_a(\mathbf{x})$ is that

$$\sum_{\mathbf{x}} \hat{\psi}_a(\mathbf{x})^2 = \sum_{\mathbf{x}} (\mathscr{D}^{1/2}\psi_a)^2 = \int \frac{d^D k}{(2\pi)^D}\, \hat{\psi}_a(-\mathbf{k})\, \hat{\psi}_a(\mathbf{k})$$

$$= \int \frac{d^D k}{(2\pi)^D}\, \psi_a(-\mathbf{k}) \left[\frac{1}{D}\sum_i \cos k_i a \right] \psi_a(\mathbf{k})$$

$$= \sum_{\mathbf{x},\mathbf{y}} \psi(\mathbf{x})\, \mathscr{D}(\mathbf{x}, \mathbf{y})\, \psi(\mathbf{y}),$$

which ensures that (5.39) and (5.42) are equivalent. The new partition

function (5.42) can be interpreted as the theory of a fluctuating complex field $\psi = \psi_1 + i\psi_2$,

$$Z' = \int \frac{\mathscr{D}\psi\,\mathscr{D}\psi^\dagger}{\sqrt{4\pi\beta D^2}}\, e^{-\beta E'[\psi,\,\psi^\dagger]}, \tag{5.44a}$$

with an energy

$$\beta E'[\psi,\,\psi^\dagger] = \sum_\mathbf{x}\left\{\frac{1}{4\beta D}|\psi|^2 - \log I_0(\alpha)\right\}. \tag{5.44b}$$

For a constant mean field, $|\psi|$ is equal to $|\widehat{\psi}| = \alpha$ so that this energy is precisely the same as the mean field energy (5.20). The partition function (5.44a) allows going beyond this approximation by specifying all fluctuations around the mean field. This is what we wanted to achieve.

The result is remarkable also in another sense. Recall that the XY model had been derived from an extrapolation of the Pitaevskii theory which involved a complex field down to zero temperature. In that limit, the *size* of the order parameter was assumed to be completely *frozen* such that only *phase* fluctuations could occur. Now, after some functional manipulation, we have been able to rewrite this XY model once more as a complex field theory. It contains again *phase* and *size* fluctuations. Indeed, if we study the field $\psi(\mathbf{x})$ close to T_c, we can expand the energy *à la* Landau keeping only terms up to ψ^4 and $|\nabla\psi|^2$.

Since[d] $\log I_0(z) = (1/4)z^2 - (1/64)z^4 + \ldots$ this gives

$$\beta E' = \sum_\mathbf{x}\left\{\frac{1}{4\beta D}|\psi|^2 - \frac{1}{4}((\mathscr{D}^{1/2}\psi_1)^2 + (\mathscr{D}^{1/2}\psi_2)^2)\right.$$

$$\left. + \frac{1}{64}((\mathscr{D}^{1/2}\psi_1)^2 + (\mathscr{D}^{1/2}\psi_2)^2)^2\right\} + \ldots$$

$$= \sum_\mathbf{x}\left\{\frac{1}{8D}(\nabla_i\psi)^\dagger\nabla_i\psi + \frac{1}{4}\left(\frac{1}{\beta D} - 1\right)|\psi|^2 + \frac{1}{64}|\psi|^4\right\} + \ldots \tag{5.45}$$

This is precisely a lattice version of the Pitaevskii energy (1.10) if

---

[d]See Table 4.8.

we identify ψ with $(4D\hbar^2/2M)^{1/2}\psi$. The chemical potential and the $(V/2)|\psi|^4$ interaction are now determined as $\mu = -(D/a^2)(\hbar^2/2M) \times ((1/\beta D) - 1)$ and $V = (1/2)(D^2/a)(\hbar^2/2M)^2$, respectively.

For $T \lesssim T_c^{MF}$, the system is in the ordered phase, the size of the order parameter ψ being given by

$$|\psi| \approx \sqrt{8}\left(1 - \frac{T}{T_c^{MF}}\right)^{1/2}, \quad T \approx T_c^{MF} \tag{5.46}$$

Moreover, setting $\psi = |\psi|e^{i\gamma}$ we see that the phase fluctuations are governed by the bending energy

$$E = \frac{\sigma}{2}\sum_x (\nabla_i \gamma)^2 \tag{5.47}$$

with

$$\sigma = \frac{|\psi|^2}{4\beta D} \simeq 2\left(1 - \frac{T}{T_c^{MF}}\right), \quad T \simeq T_c^{MF} \tag{5.48}$$

Since we are working in natural energy units where $\sigma(T = 0) = 1$ this really means

$$\frac{\sigma(T)}{\sigma(0)} \approx 2\left(1 - \frac{T}{T_c^{MF}}\right), \quad T \simeq T_c^{MF} \tag{5.49}$$

Recalling the definition of the superfluid density,

$$E = \int d^3x \frac{\rho_s}{2}v_s^2 = \frac{1}{2}\rho_s\frac{\hbar^2}{M^2}a\sum_{x,i} (\nabla_i \gamma)^2,$$

and Eq. (4.6), we conclude that close to the phase transition, the superfluid density is given by

$$\frac{\rho_s}{\rho} = 2\left(1 - \frac{T}{T_c^{MF}}\right), \quad T \simeq T_c^{MF} \tag{5.50}$$

Experimentally this is not quite true as we have seen before in Eq. (4.74). The most precise measurements by Ahlers et al. (see Fig. 5.5) show that

$$\frac{\rho_s}{\rho} = b\tau^{0.6749}(1 + a\tau^{1/2}),$$ (5.51)

where τ measures the temperature distance from the critical point

$$\tau \equiv 1 - \frac{T}{T_c},$$

and the parameters b, a are

$$b = 2.396 - 0.0288p, \quad a = 0.6514 - 0.04548p,$$

depending slightly on the pressure p (measured in atmospheres). Thus, the overall factor in (5.50) has roughly the correct size. There is, however, a considerably discrepancy in the power of τ. This can be explained by fluctuation corrections, using well-known renormalization group techniques (see the last reference given in Chapter 4 for the theoretical work). The size fluctuations have a coherence length (in units of a)

$$\xi_{\text{size}} \simeq \frac{1}{\sqrt{4D\left(1 - \frac{T}{T_c^{\text{MF}}}\right)}}, \quad T \simeq T_c^{\text{MF}}$$ (5.52)

This length scale governs the thickness of vortex lines which grows to infinity close to the critical temperature.

The partition function (5.44) can be used to study the temperature behaviour of the field fluctuations of the XY model for all temperatures. This will be done in the next section.

5.3. FLUCTUATION MODES

We have observed before the important advantage of the new partition function (5.44). It permits studying fluctuation corrections to the mean field solutions. Let ψ be a constant background field of minimal energy at arbitrary temperature T. Then $|\psi| = \sqrt{\psi_a^2}$ satisfies

$$|\psi| = 2D\beta\frac{I_1(|\psi|)}{I_0(|\psi|)},$$ (5.53)

which is precisely the mean field equation (5.19) solved before. Inserting this solution into (5.44b) we also find the mean field energy derived before as an upper bound to the exact energy. In order to study the fluctuations we now follow the general rules developed in Part I, Chapter 4. We replace the field $\psi_a(\mathbf{x})$ by $\psi_a + \delta\psi_a(\mathbf{x})$ in the energy functional (5.44b), where ψ_a is the constant mean field and expand up to quadratic order in $\delta\psi_a(\mathbf{x})$. The linear term vanishes due to (5.53). Since ψ_a is constant, $\widehat{\psi}_a(\mathbf{x})$ has the fluctuations

$$\widehat{\psi}_a(\mathbf{x}) = \psi_a + \sqrt{1 + \frac{\bar{\nabla}_i\nabla_i}{2D}}\,\delta\psi_a(\mathbf{x}). \tag{5.54}$$

We find

$$\beta E' = \beta E'[\psi_a, \psi_a^\dagger] + \frac{1}{4\beta D}\sum_{\mathbf{x}} \delta\psi_a(\mathbf{x})\,\delta\psi_a(\mathbf{x})$$

$$-\frac{1}{2}\frac{\partial^2}{\partial\psi_a\,\partial\psi_b}F(\psi^2)\sum_{\mathbf{x}}\delta\psi_a(\mathbf{x})\left[\left(1 + \frac{\bar{\nabla}_i\nabla_i}{2D}\right)\delta\psi_b(\mathbf{x})\right], \tag{5.55}$$

where we have used the abbreviation $[\psi^2 \equiv \psi_a^2 \equiv \psi_1^2 + \psi_2^2]$

$$F(\psi^2) \equiv \log I_0(\sqrt{\psi_a^2}). \tag{5.56}$$

The derivatives can be split into a longitudinal part and a transverse part[c] to the background field ψ_a as

$$\frac{\partial^2}{\partial\psi_a\,\partial\psi_b}F(\psi^2) = \frac{\partial}{\partial\psi_a}(F'2\psi_b) = \delta_{ab}2F'(\psi^2) + 4F''(\psi^2)\,\psi_a\psi_b$$

$$= \left(\delta_{ab} - \frac{\psi_a\psi_b}{\psi_c^2}\right)2F' + \frac{\psi_a\psi_b}{\psi_c^2}(2F' + 4F''\psi_c^2).$$

This gives the fluctuation energy

$$\beta\delta^2E' = \sum_{\mathbf{x}}\delta\psi_a^t(\mathbf{x})\left\{\left[\frac{1}{4\beta D} - F'(\psi^2)\left(1 + \frac{\bar{\nabla}_i\nabla_i}{2D}\right)\right]\delta\psi_a^t\right\}(\mathbf{x}) \tag{5.57}$$

$$+ \sum_{\mathbf{x}}\delta\psi_a^\ell(\mathbf{x})\left\{\left[\frac{1}{4\beta D} - (F'(\psi^2) + 2F''(\psi^2)\,\psi^2)\left(1 + \frac{\bar{\nabla}_i\nabla_i}{2D}\right)\right]\delta\psi_b^\ell\right\}(\mathbf{x}),$$

[c]The background field ψ_a is considered as a two-component vector in some internal space and "longitudinal" and "transverse" mean parallel and orthogonal to this vector, respectively.

where $\delta \psi_a^t(\mathbf{x}) = (\delta_{ab} - (\psi_a \psi_b / \psi^2)) \delta \psi_b(\mathbf{x})$ and $\delta \psi_a^\ell(\mathbf{x}) = (\psi_a \psi_b / \psi^2) \delta \psi_b(\mathbf{x})$ are the longitudinal and transverse projections of the ψ_a fluctuations (in the two-dimensional ψ_a space).

Consider now the ordered phase. Then $F'(\psi^2)$ is fixed by the field equations (5.53) to satisfy

$$F'(\psi^2) = \frac{1}{2|\psi|} \frac{d}{d|\psi|} F = \frac{1}{2|\psi|} \frac{I_1(|\psi|)}{I_0(|\psi|)} = \frac{1}{4D\beta},$$

so that the transverse part is simplified to

$$\frac{1}{4\beta D} \sum_{\mathbf{x}} \delta \psi_a^t(\mathbf{x}) \left[\left(-\frac{\bar{\nabla}_i \nabla_i}{2D} \right) \delta \psi_a^t \right] (\mathbf{x}). \tag{5.58}$$

For the longitudinal part we observe that

$$2F'(\psi^2) + 4F''(\psi^2) \psi^2 = \frac{d^2 F}{d|\psi|^2}$$

and obtain the fluctuation energy

$$\frac{1}{4\beta D} \sum_{\mathbf{x}} \delta \psi_a^\ell(\mathbf{x}) \left\{ \left[1 - 2\beta D \frac{d^2 F}{d|\psi|^2} \left(1 + \frac{\bar{\nabla}_i \nabla_i}{2D} \right) \right] \delta \psi_a^\ell \right\} (\mathbf{x}). \tag{5.59}$$

Let us introduce the parameter

$$\frac{m^2}{2D} \equiv \left(1 - 2\beta D \frac{d^2 F}{d|\psi|^2} \right) = 1 - 2\beta D \left(\frac{I_1(|\psi|)}{I_0(|\psi|)} \right)'$$

$$= 1 - 2\beta D \left(1 - \frac{1}{|\psi|} \frac{I_1(\beta)}{I_0(\beta)} - \left(\frac{I_1(\beta)}{I_0(\beta)} \right)^2 \right) = 2 - 2\beta D(1 - u^2), \tag{5.60}$$

where we have used $I_1' = I_0 - I_1/|\psi|$. Then (5.59) becomes

$$\frac{1}{4\beta D} \sum_{\mathbf{x}} \delta \psi_a^\ell \left[\frac{m^2}{2D} + \left(1 - \frac{m^2}{2D} \right) \left(-\frac{\bar{\nabla}_i \nabla_i}{2D} \right) \right] \delta \psi_a^\ell. \tag{5.61}$$

In complex field notation, $\psi(\mathbf{x}) = |\psi(\mathbf{x})| e^{i\gamma(\mathbf{x})}$, the transverse fluctuations are just those in the phase of the order parameter,

$$|\delta\psi'| \simeq |\psi|\, \delta\gamma(\mathbf{x}).$$ (5.62)

They are the Goldstone modes of the system with energy [see (5.58)]

$$E = \frac{1}{8\beta^2 D^2}|\psi|^2 \sum_{\mathbf{x}} (\nabla_i \delta\gamma)^2.$$ (5.63)

Thus we see that the parameter $\sigma(T)$ which controls the stiffness of the phase angle, and which at zero temperature was normalized to

$$\sigma(0) = a\rho \frac{\hbar^2}{2M}\frac{1}{1\,\mathrm{K}} \sim 1,$$ (5.64)

[recall Eq. (4.6)] has the temperature dependence

$$\sigma(T) = \frac{1}{4\beta^2 D^2}|\psi|^2.$$ (5.65)

Without the special normalization (5.64), this is really just the ratio $\sigma(T)/\sigma(0)$. As a check we verify that in the limit of zero temperature the ratio $\sigma(T)/\sigma(0)$ tends to 1, due to (5.24), as it should. Close to T_c, ρ_s/ρ reduces to $2(1 - T/T_c^{\mathrm{MF}})$ as found before in (5.50). The result (5.65) gives the superfluid density of the XY model for all temperatures in the mean field approximation (see Fig. 5.2):

$$\frac{\rho_s(T)}{\rho} = \frac{1}{4\beta^2 D^2}|\psi|^2.$$ (5.66)
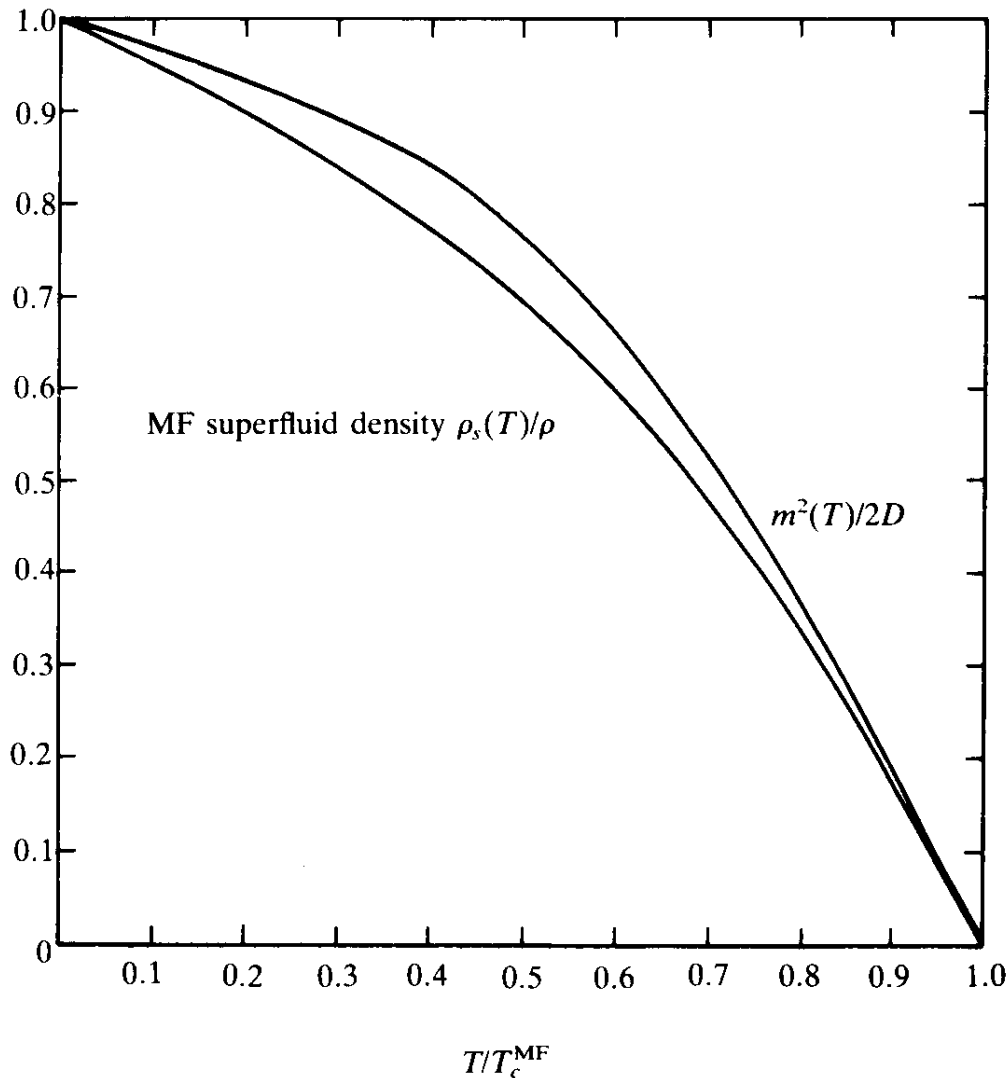
This agrees reasonably well with experiment if the critical temperature is adjusted to the experimental value (see Fig. 1.2). Close to T_c, however there is significant disagreement since fluctuation corrections are very strong (see Figs. 5.3, 5.4, 5.5).

Let us now look at the size fluctuations. From (5.61) we see that their range is given by the inverse of the mass (in units of a)

$$\xi_{\mathrm{size}}^{-1} \equiv M = \left(\frac{m^2}{1 - \frac{m^2}{2D}}\right)^{1/2}.$$ (5.67)

The temperature dependence of $m^2/2D$ is shown in Fig. 5.2. In the $T \to 0$ limit, $m^2/2D \to 1 - 1/4D\beta - 3/16D^2\beta^2$ so that $M^2/2D$ diverges like

FIG. 5.2. The superfluid density in the mean field approximation. The same coordinate system is used to display the temperature behaviour of the mass parameter m^2 calculated in Eq. (5.60).

$4D/T(1 - D/T - \ldots)$. For $T \gtrsim T_c$, on the other hand, we can calculate from (5.60):

$$\frac{m^2}{2D} = 2 - 2\beta D \left(1 - \frac{I_1^2}{I_0^2}\right)$$

$$\approx 2\left(1 - \frac{T_c^{MF}}{T}\right) + 2\frac{T_c^{MF}}{T} \cdot \frac{1}{4}|\psi|^2 \approx 2\left(1 - \frac{T}{T_c^{MF}}\right),$$

so that

$$M \sim \sqrt{4D\left(1 - \frac{T}{T_c^{MF}}\right)} \qquad\qquad (5.68)$$
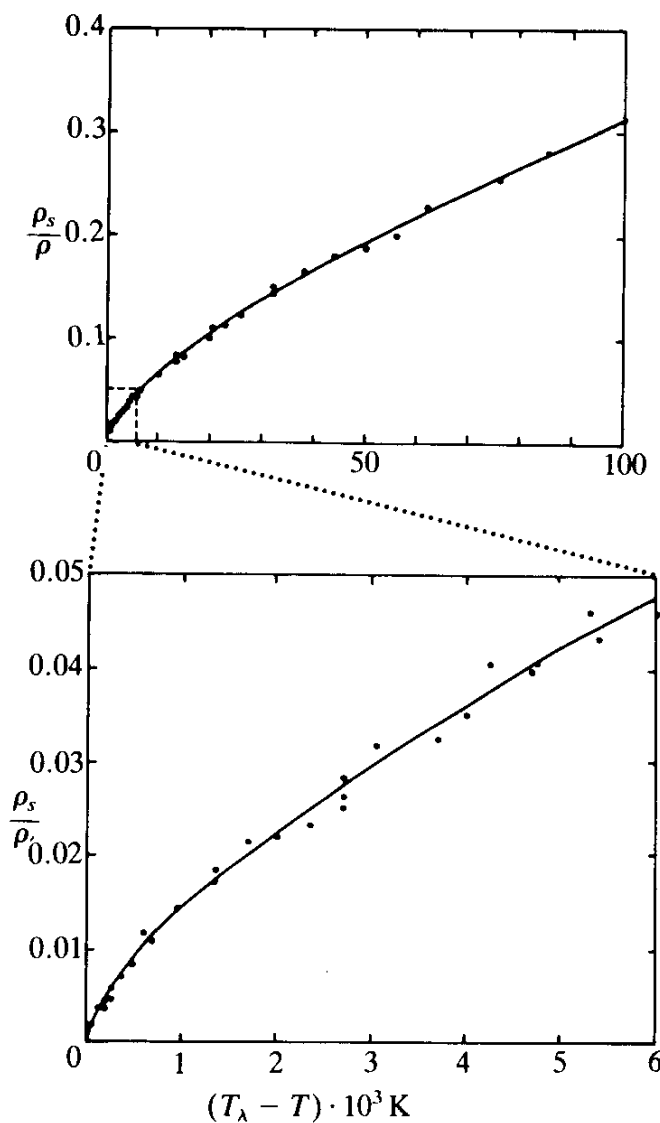
FIG. 5.3. The deviation of the experimental superfluid density from the linear behaviour predicted by mean field theory very close to the λ-transition. Notice that the curves look the same on two different scales. The data are from J.R. Clow and J.D. Reppy, cited in the Notes and References. The solid curve is $\rho_s/\rho = 1.438(T_c - T)^{2/3}$, where T is measured in K. The mean field line $\rho_s/\rho = 2(1 - T/T_c) \approx 0.92 \times (T_C - T)/K$ lies too low ($T_\lambda = T_c$).

in agreement with (5.52). Notice that the divergence at zero temperature implies the absence of size fluctuations in this limit (one says that they are "frozen"). Thus the complex field theory leads back to the XY model we started out with, for which the only degree of freedom was the phase angle $\gamma(\mathbf{x})$.

We now turn to the fluctuations around the trivial mean field solution $\psi_a = 0$ for $T > T_c^{MF}$. Then

$$F'(\psi_a^2)|_{\psi_a=0} = \frac{1}{2|\psi|} \frac{I_1(|\psi|)}{I_0(|\psi|)}\Bigg|_{|\psi|=0} = \frac{1}{4}$$

and

$$[2F'(\psi_a^2) + 4F''(\psi_a^2)\,\psi_a^2]|_{\psi_a=0} = \frac{d^2F}{d|\psi|^2}\Bigg|_{|\psi|=0} = \left(\frac{I_1(|\psi|)}{I_0(|\psi|)}\right)' = \frac{1}{2}.$$

FIG.5.4. The experimental superfluid density in a double logarithmic plot and the extraction of the critical power $\rho_s \sim \tau^{0.67}$. The data points are from I. Rudnik (○) J.R. Clow and J.D. Reppy (●) and from D.G. Dash, R.O. Taylor (△) (all cited in the Notes and References).
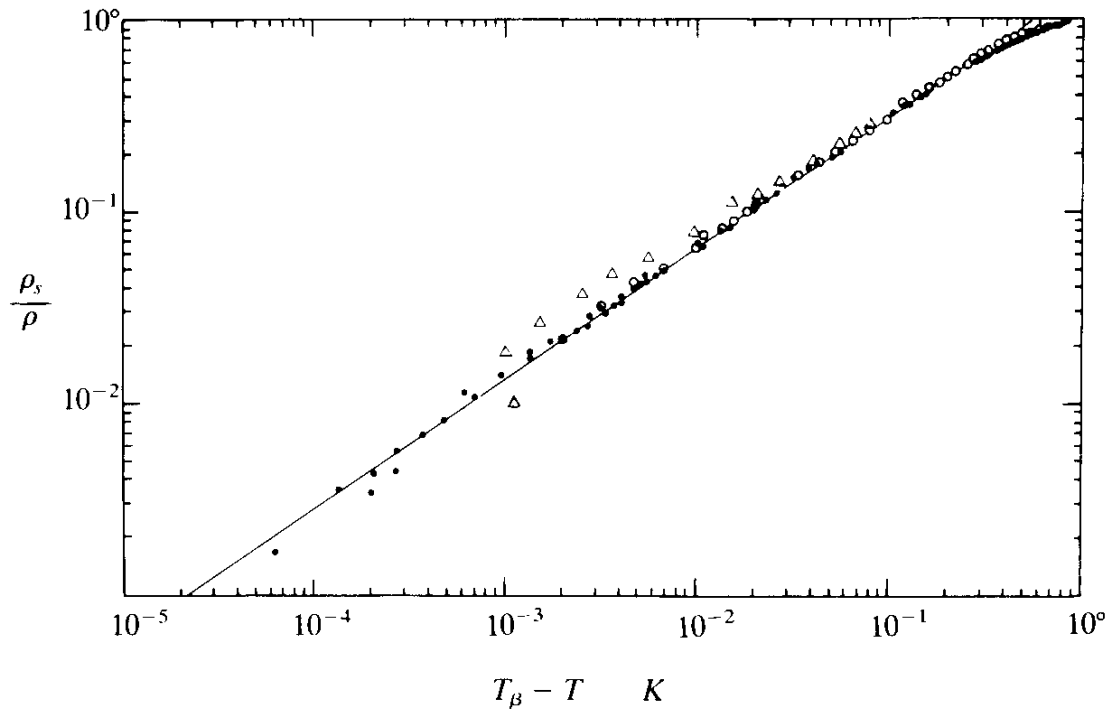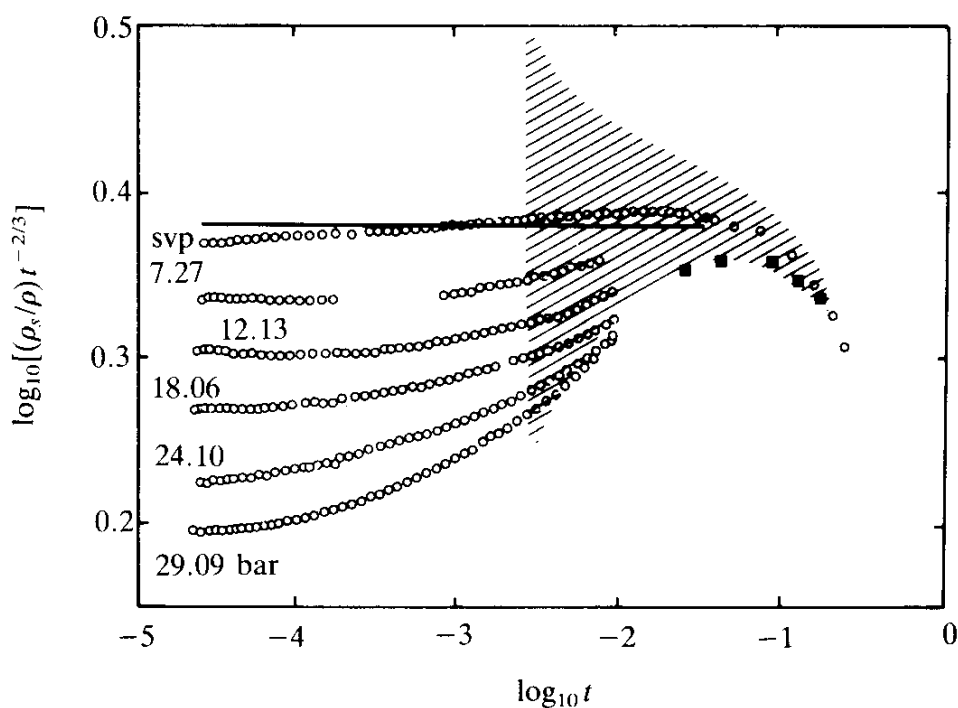
FIG. 5.5. The high accuracy study of ρ_s/ρ by Greywall and Ahlers (1972) at different pressures as a function of $t = 1 - T/T_c$. The squares are from 253 bar studies of V.P. Peshkov, K.N. Zinov'eva. The solid line represents best fit to vapor pressure data of Tyson (1968), shaded area is obtained from data of Romer and Duffy (1969) (all cited in the Notes and References).

The fluctuation energy is

$$\beta\delta^2 E' = \frac{1}{4\beta D}\sum_{\mathbf{x}}\delta\psi_a(\mathbf{x})\left(1 - \beta D\left(1 + \frac{\bar{\nabla}\nabla}{2D}\right)\right)\delta\psi_a(\mathbf{x}) \qquad (5.69)$$

corresponding to two modes of the form (5.61) with $m^2/2D = 1 - \beta D$. Thus both longitudinal and transverse modes have the same mass:

$$\frac{m^2}{2D} = \frac{\dfrac{m^2}{2D}}{1 - \dfrac{m^2}{2D}} = \frac{1}{\beta D} - 1 = \frac{T}{T_c^{\mathrm{MF}}} - 1.$$

5.4. ONE-LOOP CORRECTION TO THE MEAN-FIELD ENERGY

Having analyzed the quadratic fluctuations it is quite easy to calculate the additional energy due to these modes. As explained in Chapter 4, Part I, all we have to do is integrate out the quadratic $\delta\psi(\mathbf{x})$ fields. This gives

$$-\beta f^{1\,\mathrm{loop}} = -\frac{1}{2}\left\{\mathrm{tr}\log\left(-\frac{\bar{\nabla}\cdot\nabla}{2D}\right) + \mathrm{tr}\log\left(\frac{m^2}{2D} + \left(1 - \frac{m^2}{2D}\right)\left(-\frac{\bar{\nabla}\cdot\nabla}{2D}\right)\right)\right\}$$

$$= -\frac{1}{2}\int\frac{d^D k\,a^D}{(2\pi)^D}\log\left(\frac{\bar{\mathbf{K}}\cdot\mathbf{K}}{2D}\right)$$

$$-\frac{1}{2}\int\frac{d^D k\,a^D}{(2\pi)^D}\log\left(\frac{m^2}{2D} + \left(1 - \frac{m^2}{2D}\right)\frac{\bar{\mathbf{K}}\cdot\mathbf{K}}{2D}\right). \qquad (5.70)$$

The first integral contains the fluctuations of the Goldstone modes and has been evaluated numerically in Part I, Eq. (6.207b)

$$-\int\frac{d^D k}{(2\pi)^D}\log\left(1 - \frac{1}{2D}2\sum_{i=1}^{D}\cos k_i\right)$$

$$= \sum_{n=2,4,6,\ldots}^{\infty}\frac{1}{n(2D)^n}H_n = 0.1184 \quad (D = 3). \qquad (5.71\mathrm{a})$$

The second integral contains the massive fluctuations and can be expanded as follows:

$$-\int \frac{d^D k}{(2\pi)^D} \log\left(\frac{m^2}{2D} + \left(1 - \frac{m^2}{2D}\right)\frac{\overline{\mathbf{K}} \cdot \mathbf{K}}{2D}\right)$$

$$= -\int \frac{d^D k}{(2\pi)^D} \log\left(\frac{m^2}{2D} + \left(1 - \frac{m^2}{2D}\right)\left(1 - \frac{1}{2D}2\sum_{i=1}^{D} \cos k_i\right)\right)$$

$$= -\int \frac{d^D k}{(2\pi)^D} \log\left(1 - \left(1 - \frac{m^2}{2D}\right)\frac{1}{2D}2\sum \cos k_i\right)$$

$$= \sum_{n=2,4,6,\ldots}^{\infty} \frac{1}{n(2D)^n}\left(1 - \frac{m^2}{2D}\right)^n H_n$$

$$= \sum_{n=2,4,6,\ldots}^{\infty} \frac{1}{n}\frac{H_n}{(2D + M^2)^n} = \int \frac{d^D k}{(2\pi)^D}\log(M^2 + \overline{\mathbf{K}} \cdot \mathbf{K}) - \log(M^2 + 2D).$$

$$(5.71b)$$

It is plotted in Fig. 5.6 for various dimensions.

For small temperatures we find that

$$\frac{m^2}{2D} = 2 - 2\beta D(1 - u^2) \xrightarrow[\beta \to \infty]{} 1 - \frac{1}{2(2\beta D)} + O\left(\frac{1}{\beta^2}\right)$$
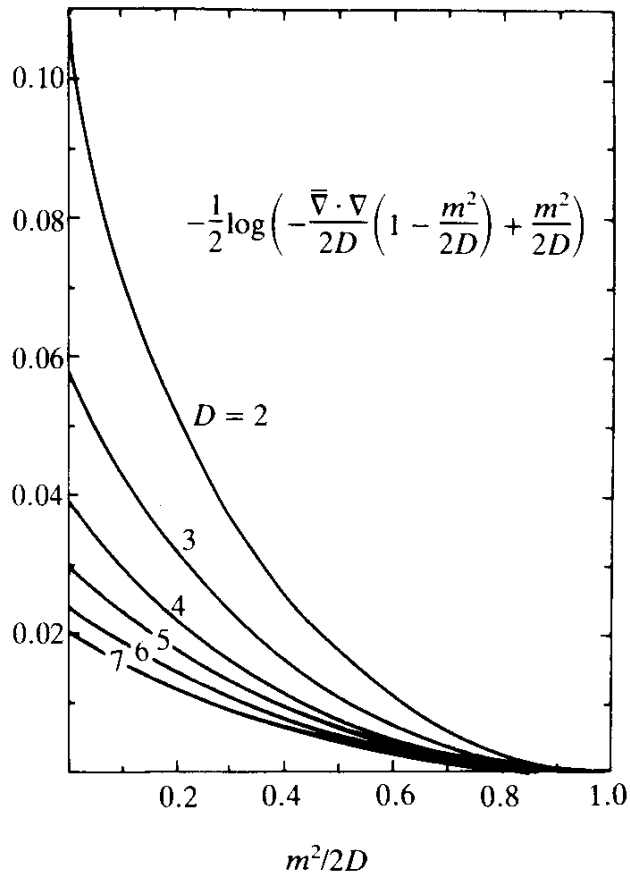

FIG. 5.6. The fluctuation determinant needed for the one-loop correction to the mean field free energy [see Eq. (5.71b)].

[recall (5.23)], so that $-\beta f^{1\,\mathrm{loop}}$ starts out as

$$\frac{0.118}{2} + \frac{1}{2D}\frac{1}{2^4}\frac{1}{(2\beta D)^2} + \cdots$$

and grows very slowly for decreasing β. Thus the massive fluctuations do not contribute to the limiting behaviour of $-\beta f^{1\,\mathrm{loop}}$ which for $T \to 0$ is given by the leading part of (5.26) plus the Goldstone part of (5.70):

$$-\beta f' \to \beta D - \frac{1}{2}\log(2\pi(2\beta D)) + \frac{1}{2}0.1184 + \frac{1}{8\beta D} + O\left(\frac{1}{\beta^2}\right). \tag{5.72}$$

The first three terms represent the free energy per site associated with the free γ fluctuations described by the partition function

$$Z_0' = e^{\beta D}\prod_{\mathbf{x}}\left[\int \frac{d\gamma}{2\pi}\right] e^{-\beta/2\Sigma_{\mathbf{x},i}(\nabla_i\gamma)^2},$$

as they should [recall (4.8) − (4.10)]. The fourth term gives the lowest correction due to the interaction among the Goldstone modes, as we shall see in detail later. At the mean field transition temperature $T_c^{\mathrm{MF}} = 1/\beta_c^{\mathrm{MF}} = D$, the free energy $-\beta f'^{\mathrm{MF}}$ vanishes and $-\beta f'^{\mathrm{MF}+1\,\mathrm{loop}}$ is entirely given by the loop correction. This, in turn, reduce simply to two massless fluctuation trace logs so that we find (compare Figs. 4.4, 4.5)

$$-\beta f'^{\mathrm{MF}+1\,\mathrm{loop}}\big|_{\beta_c^{\mathrm{MF}}} = 0.1184.$$

Let us now turn to the high temperature mean field solution $\psi_a = 0$. Its free energy $-\beta f'^{\mathrm{MF}}$ vanishes for all $\beta < \beta_c^{\mathrm{MF}}$ so that the one-loop corrected $-\beta f'$ is given purely by the trace logs associated with the two degenerate massive fluctuations with $m^2/2D = 1 - \beta D$. Hence $M^2/2D = -1/\beta D - 1$ and

$$-\beta f'^{\mathrm{MF}+1\,\mathrm{loop}} = -\log\left(1 - \beta D - \beta D\frac{\bar{\nabla}\cdot\nabla}{2D}\right). \tag{5.73}$$

For $\beta = \beta_c^{\mathrm{MF}} = 1/D$ this reduces again to 0.1184 and thus joins up continuously with the high β free energy. Because of the easy access through Monte Carlo simulations, let us also give explicitly the internal energy of the one-loop correction.

For $T < T_c^{\mathrm{MF}}$ we differentiate (5.70) and find

$$u^{1\,\text{loop}} = -\frac{\partial}{\partial\beta}(-\beta f^{1\,\text{loop}}) = \frac{1}{2}\frac{\partial(m^2/2D)}{\partial\beta}\frac{1}{1-\frac{m^2}{2D}}\left(\frac{2D}{1-\frac{m^2}{2D}}v_M(0)-1\right),$$

where

$$v_M(0) = \sum_{n=0}^{\infty}\left(1-\frac{m^2}{2D}\right)^{n+1}H_n/(2D)^{n+1} = \sum_{n=0}^{\infty}\frac{H_n}{(2D+M^2)^{n+1}}$$

is the free field correlation function of mass M at $x = 0$. The differentiation of (5.60) gives

$$\frac{\partial(m^2/2D)}{\partial\beta} = -2D(1-u^2) + 4\beta Du\frac{\partial u}{D\beta}$$

and using the field equations $2\beta Du = \alpha$, $u = I_1(\alpha)/I_0(\alpha)$ and $1 - u^2 = (2 - m^2/2D)/2\beta D$ we obtain [the first was given in (5.21d)]

$$\frac{du}{d\beta} = -\frac{u}{\beta}\frac{1-u^2-\frac{1}{2\beta D}}{1-u^2-\frac{1}{\beta D}} = \frac{u}{\beta}\frac{1}{M^2/2D},$$

$$\frac{d\alpha}{d\beta} = -\frac{u}{\beta}\frac{1}{1-u^2-\frac{1}{\beta D}} = \frac{u}{\beta}\frac{2\beta D}{m^2/2D},$$

so that

$$\frac{\partial}{\partial\beta}\frac{m^2}{2D} = -\frac{1}{\beta}\left(2-\frac{m^2}{2D}\right) + 4Du^2\frac{1}{M^2/2D}$$

$$= \frac{1}{m^2/2D}\left[4D\left(1-\frac{m^2}{2D}\right)-\frac{1}{\beta}\left(2-\frac{m^2}{2D}\right)^2\right]$$

and the internal energy becomes

$$u^{1\,\text{loop}} = \frac{1}{2}\frac{1}{m^2/2D}\left[4D - \frac{\left(2-\frac{m^2}{2D}\right)^2}{\beta\left(1-\frac{m^2}{2D}\right)}\right]\left(\frac{2D}{1-\frac{m^2}{2D}}v_M(0)-1\right).$$

As a check we take the limit of low temperatures [recall (5.24)],

$$\frac{m^2}{2D} = 2 - 2\beta D(1 - u^2) = 1 - \frac{1}{2(2\beta D)} - \frac{3}{4(2\beta D)^2} - \ldots,$$

$$\frac{M^2}{2D} = 4\beta D\left(1 - \frac{1}{\beta D} - \ldots\right),$$

$$\frac{2D}{1 - \frac{m^2}{2D}} v_M(0) = 1 + \frac{\left(1 - \frac{m^2}{2D}\right)^2}{(2D)^2} 2D + \ldots = 1 + \frac{1}{2D}\frac{1}{4(2\beta D)^2} + \ldots$$

and find

$$u^{1\,\mathrm{loop}} = \frac{1}{8(2\beta D)^3} + \frac{9}{16(2\beta D)^4} + \ldots,$$

$$c^{1\,\mathrm{loop}} = \frac{1}{D}\left(\frac{3}{16(2\beta D)^2} + \frac{9}{8(2\beta D)^3} + \ldots\right),$$

in agreement with the previously calculated limit of [see (5.26)]

$$-\beta f^{1\,\mathrm{loop}} = \frac{1}{2D}\left(\frac{1}{16}\frac{1}{(2\beta D)^2} + \frac{3}{16(2\beta D)^3} + \ldots\right).$$

In Figs. 4.4, 4.5 we had plotted the mean-field-plus-one-loop approximation to the free energy against β. When approaching the mean field transition point, from high β, it shows an ugly cusp as a reflection of the singularity in the fluctuation determinant for massless modes. For lower temperatures, as the cusp is passed, the mean-field-plus-one-loop curve drops rapidly and approaches correctly the high temperature expansion for $\beta \to 0$.

Since the high temperature expansion is correct to order β^{12} and the omitted β^{14}, β^{16}, ... terms are very small up to $\beta \sim 0.4$, we conclude that the high temperature expansion is the more credible approximation to the free energy up to the neighborhood of the point of transition $\beta_c \sim 0.45$. For very large β, on the other hand, the mean-field-plus-one-loop energy becomes exact, namely,

$$-\beta f^{\mathrm{MF}+1\,\mathrm{loop}} \xrightarrow[\beta \to \infty]{} \beta D - \tfrac{1}{2}\log(2\pi(2\beta D)) - \tfrac{1}{2}0.1184.$$

We can now easily verify that the $1/\beta^2$, $1/\beta^3$, ... corrections to this are rather small above $\beta_c \sim 0.45$. For instance, Eq. (5.72) shows that the $1/\beta^2$ correction makes up only 2% of the leading one-loop term (1/2) 0.1184 and 0.7% of the total $-\beta f'$. This shows that above $\beta \sim 0.5$ the mean-field-plus-one-loop curve should be quite trustworthy.

Thus we are led to identify the point of intersection of the two curves, $\beta_c \sim 0.45$ with the transition point. This value agrees well with the result of Monte Carlo simulations of the XY model in three dimensions, which we extracted before from Fig. 4.8.

The transition from the high temperature curve to the mean-field-plus-one-loop curve is not completely smooth in the slopes. The combined curves describe, therefore a transition which is slightly of first order. From Monte Carlo simulations, we know, however, that it is of second order. Obviously, the approximation is not accurate enough to reproduce the correct order. At first sight it may appear as though the theoretical result could be corrected, in principle, by driving the loop corrections to the mean field approximation to higher and higher orders. This would, indeed, decrease entropy discontinuity at the transition, but only very slowly. It is easily realized that whatever the number of loop corrections are, they are incapable of reproducing contributions to the free energy of the type $e^{-\beta \cdot \mathrm{const}}$. These are not expandable in a power series in $1/\beta$, as the mean-field-plus-loop approach is. They have to be found by other methods. We shall see in the following chapters that they are caused by vortex lines. These have to be identified, counted, and added properly in the partition function. Only then can we hope to obtain a satisfactory description of the phase transitions (see Section 6.2 for the general discussion, Section 7.9 for the specific calculation, and Figs. 11.9, 11.10 for a comparison of the results with Monte Carlo data).

We also plotted in Figs. 4.6 and 4.7 the internal energy and the specific heat from the above formulas together with the corresponding quantities from the high temperature expansion and compared them with Monte Carlo data on a 16^3 lattice. We see that up to the critical point $\beta_c \approx 0.45$ the internal energy follows closely the two theoretical curves from their respective sides. Notice that due to the weak β dependence of the one-loop correction to $-\beta f'$ the correction to $u' = -(\partial/\partial\beta)(-\beta f')$ can practically be neglected. For the specific heat the agreement is satisfactory only on the high temperature side, a considerable piece is missed by the mean-field-plus-one-loop curve. The reason lies again in the omission of terms $e^{-\beta \cdot \mathrm{const}}$ coming from vortex lines. In $-\beta f'$, these terms are rather small numerically since the energies in the exponent are

quite large. This is why the critical point could be determined quite accurately *without* them. When going to the specific heat, however, one has to apply two differentiations with respect to β and this produces a large multiplicative factor const^2. This raises their relative importance so much that they can no longer be neglected. We shall see later in Sections 6.4, 7.9, how the vortex contributions can be calculated.

It is worth pointing out that the mean field free energy as a function of D becomes exact in the limit $D \to \infty$. This can be guessed from the plot of $-\beta f'$ for increasing dimensions as shown in Fig. 4.6. Formally it follows from the fact that the mean field energy depends only on $D\beta$ (and has no further explicit D dependence) while each loop correction is suppressed by a factor $1/2D$ [see Eqs. (5.71)].

Let us conclude this section with the observation that from the path integral over the ψ fields, it is also possible to obtain the strong coupling expansion. For this we have to proceed in the following manner: We must choose the quadratic piece $(1/4\beta D)\sum_x |\psi_a|^2$ in (5.44b) as the "free part" of the total fluctuation energy and consider $-\log I_0(|\alpha|)$ as an interaction. The free field correlation function is

$$\langle \psi_a(\mathbf{x})\, \psi_b(\mathbf{0}) \rangle = 2\beta DN \int \frac{d^D k\, a^D}{(2\pi)^D}\, e^{i\mathbf{k}\cdot\mathbf{x}}\, \delta_{ab} = 2\beta DN\, \delta_{\mathbf{x},0}\,\delta_{ab}.$$

If we now expand $\log I_0(|\alpha|)$ in a power series, we can find a perturbation series just as described in Section 4.3. This converges only as long as the fluctuations are small, which is true for small β, i.e., for high temperatures. If we organize this series in powers of β, the result necessarily coincides with the high temperature series (4.62) given before.

5.5. LOCAL FORMULATION WITH TWO COMPLEX FIELDS

The complex field theory described in the last section has a slightly unappealing feature. The operation $\widehat{\psi} = \mathscr{Q}^{1/2}\psi$ makes the $\log I_0(\alpha)$ term nonlocal. For small fluctuations this was no problem, and locality was reestablished [see the expansion (5.55)]. But for larger fluctuations this is no longer so. It is gratifying to note that there exists a way of reformulating the XY model as a local field theory, albeit at the expense of doubling the number of fields. We now describe this reformulation.

Consider two sets of real two-component fields α_a, u_a. They satisfy the following identity:

$$\int_{-\infty}^{\infty} du_1\, du_2 \int_{-i\infty}^{i\infty} \frac{d\alpha_1\, d\alpha_2}{(2\pi i)^2} e^{-\alpha_a(u_a - U_a)} = \int du_1\, du_2\, \delta^2(u_a - U_a) = 1. \qquad (5.74)$$

Inserting this into (5.39) we can replace U_a in the energy by u_a and arrive at

$$Z' = \prod_{\mathbf{x}} \left[\int_{-\infty}^{\infty} du_1(\mathbf{x})\, du_2(\mathbf{x}) \right] \prod_{\mathbf{x}} \left[\int_{-i\infty}^{i\infty} \frac{d\alpha_1(\mathbf{x})}{2\pi i}\, \frac{d\alpha_2(\mathbf{x})}{2\pi i} \right]$$

$$\times \exp \left\{ D\beta \sum_{\mathbf{x}} u_a(\mathbf{x}) \left(1 + \frac{\overline{\nabla} \cdot \nabla}{2D} \right) u_a(\mathbf{x}) - \sum_{\mathbf{x}} \alpha_a(\mathbf{x}) u_a(\mathbf{x}) + \sum_{\mathbf{x}} F(\alpha(\mathbf{x})) \right\},$$

$$(5.75)$$

where $F(\alpha) = \log I_0(\sqrt{\alpha_a^2})$ collects the interactions $(\alpha^2 \equiv \alpha_a^2 \equiv \alpha_1^2 + \alpha_2^2)$:

$$e^{F[\alpha_a]} = \int_{-\pi}^{\pi} \frac{d\gamma}{2\pi} e^{\alpha_a U_a} = I_0(\sqrt{\alpha_a^2}). \qquad (5.76)$$

In this way, the partition function of the XY model is replaced by a theory of four fluctuating real fields with energy

$$\beta E'[\alpha_a, u_a] = -\sum_{\mathbf{x}} \left[\beta D u_a \left(1 + \frac{\overline{\nabla} \cdot \nabla}{2D} \right) u_a - \alpha_a u_a + \log I_0(\sqrt{\alpha_a^2}) \right]. \qquad (5.77)$$

Of course, the fields α_a, u_a may be combined into two complex fields $\alpha = \alpha_1 + i\alpha_2$, $u = u_1 + i u_2$.

At the mean field level, this theory gives the same result as the old one. For constant mean fields α_a, u_a, the free energy per site is now given by

$$-\beta f' = \beta D u_a^2 - \alpha_a u_a + \log I_0(\sqrt{\alpha_a^2}). \qquad (5.78)$$

This is exactly the expression which was found in Eq. (5.18a) to provide a bound for the free energy. Extremizing f' in u_a and α_a gives the two equations:

$$2\beta D u_a = \alpha_a, \qquad (5.79a)$$

$$u_a = \frac{\alpha_a}{\sqrt{\alpha_a^2}} \frac{I_1(\sqrt{\alpha_a^2})}{I_0(\sqrt{\alpha_a^2})}. \qquad (5.79b)$$

Reinserting (5.79a) into (5.78), the free energy takes the form

$$-\beta f' = -\frac{1}{4\beta D}\alpha_a^2 + \log I_0(\sqrt{\alpha_a^2}), \qquad (5.80)$$

as in (5.20) with a minimum for

$$|\alpha| = 2\beta D\frac{I_1(|\alpha|)}{I_0(|\alpha|)}. \qquad (5.81)$$

This is the same as (5.53) after we identify, for constant fields, α_a with ψ_a [recall Eqs. (5.41b), (5.43)].

Notice that the path integral (5.75) over du_a is really divergent as it stands for the positive eigenvalues of the differential operator $\mathscr{D} = 1 + \bar{\nabla} \cdot \nabla/2D$; only *after* the α_a integration which produces the δ functions (5.74) does it converge. Contact with the previous one-field formulation (5.44) is established by observing that the du_a integrals can be made convergent by rotating, for positive eigenvalues of $\mathscr{D}$, the contours of integration [of $u_a^1(\mathbf{k}) = (u_a(\mathbf{k}) + u_a^*(\mathbf{k}))/2$, $u_a^2(\mathbf{k}) = (u_a(\mathbf{k}) - u_a^*(\mathbf{k}))/2i$] so that they run along the imaginary axis. For the same $\mathbf{k}$ vectors we rotate the $\alpha_a^{1,2}(\mathbf{k})$ integrations into the opposite direction such that they come to run along the real axis. For the zero and negative eigenvalues of $\mathscr{D}$ we leave the integrals as they are.

Performing now the integral over du_a we arrive at

$$Z' = (\det'|\mathscr{D}|)^{-1}\prod_{\mathbf{x}}\left[\int\frac{d\hat{\alpha}_1\,d\hat{\alpha}_2}{\sqrt{4\pi D\beta^2}}\right]e^{-\Sigma\mathbf{x}\{(1/4\beta D)\alpha_a(1\,+\,\bar{\nabla}\cdot\nabla/2D)^{-1}\alpha_a\,-\,\log I_0(\sqrt{\alpha_a^2})\}} \qquad (5.82)$$

where the hat on the integrals over $d\alpha_1$, $d\alpha_2$ indicates that the Fourier components of α_a have to be integrated differently for positive and negative eigenvalues of $\mathscr{D}(\mathbf{k}) = (1/D)\Sigma_i\cos k_i a$. The Fourier components of the zero eigenvalues 1 or $\mathscr{D}(\mathbf{k})$ are frozen since for them, the term $u_a(1 + \bar{\nabla}\cdot\nabla/2D)u_a$ provides no damping and the u integrations give, via the second term in the exponent of (5.75), a δ-function in α. During the u_a integrations each non-zero eigenvalue of $\mathscr{D}(\mathbf{k})$ appears as an inverse factor. The product is denoted by $(\det'|\mathscr{D}|)^{-1}$ with the prime indicating the absence of the zero modes and the bars the absolute values of the eigenvalues. As a check we can change the variables from $\alpha_a(\mathbf{k})$ to $\mathscr{D}^{1/2}\alpha_a(\mathbf{k})$. This cancels the determinant and leads us back to (5.44).

It is instructive to calculate the quadratic fluctuations of the two-com-

ponent fields and compare them with the single field case. Expanding the energy (5.77) around the extremal values (5.79), we find the second variation of the exponent

$$-\frac{1}{2}\sum_{\mathbf{x}}(\delta u_a, \delta\alpha_a)\begin{pmatrix} -2\beta D\left(1+\dfrac{\bar{\nabla}\cdot\nabla}{2D}\right)\delta_{ab} & -i\delta_{ab} \\ -i\delta_{ab} & \dfrac{\partial^2 F(\alpha)}{\partial\alpha_a\partial\alpha_b} \end{pmatrix}\begin{pmatrix}\delta u_b \\ \delta\alpha_b\end{pmatrix}, \quad (5.83)$$

where we have rotated the $\delta\alpha_a$ fluctuations by a phase factor i so as to have $\delta\alpha_a$ run along the real axis. The matrix can be split into a transverse 2×2 part[f]

$$-\frac{1}{2}\sum_{\mathbf{x}}(\delta u', \delta\alpha')\begin{pmatrix} -2\beta D\left(1+\dfrac{\bar{\nabla}\cdot\nabla}{2D}\right) & -i \\ -i & \dfrac{1}{|\alpha|}\dfrac{dF}{d|\alpha|} \end{pmatrix}\begin{pmatrix}\delta u' \\ \delta\alpha'\end{pmatrix} \quad (5.84)$$

and a longitudinal 2×2 part[f]

$$-\frac{1}{2}\sum_{\mathbf{x}}(\delta u^\ell, \delta\alpha^\ell)\begin{pmatrix} -2\beta D\left(1+\dfrac{\bar{\nabla}\cdot\nabla}{2D}\right) & -i \\ -i & \dfrac{d^2 F}{d|\alpha|^2} \end{pmatrix}\begin{pmatrix}\delta u^\ell \\ \delta\alpha^\ell\end{pmatrix} \quad (5.85)$$

Using the field equation $|\alpha| = 2\beta D(I_1(|\alpha|)/I_0(|\alpha|))$ the transverse matrix becomes

$$\begin{pmatrix} -2\beta D\left(1+\dfrac{\bar{\nabla}_i\nabla_i}{2D}\right) & -i \\ -i & \dfrac{1}{2\beta D} \end{pmatrix}. \quad (5.86)$$

Using (5.60), the longitudinal matrix can be cast in the form

$$\begin{pmatrix} -2\beta D\left(1+\dfrac{\bar{\nabla}_i\nabla_i}{2D}\right) & -i \\ -i & \dfrac{1}{2\beta D}\left(1-\dfrac{m^2}{2D}\right) \end{pmatrix}. \quad (5.87)$$

[f]The terms "transverse" and "longitudinal" refer again to the internal index space $a = 1, 2$.

Both matrices can be easily diagonalized in momentum space. Thus integrating out the fluctuations in α and u we find the determinant

$$\det\left(-\frac{\bar{\nabla}\cdot\nabla}{2D}\right)^{-1} \quad \text{and} \quad \det\left(\frac{m^2}{2D} + \left(1 - \frac{m^2}{2D}\right)\left(-\frac{\bar{\nabla}\cdot\nabla}{2D}\right)\right)^{-1},$$

respectively, such that they produce the same fluctuation corrections found previously in (5.70).

5.6. CORRELATION FUNCTIONS OF THE XY MODEL

Let us see how the mean field methods can serve to calculate correlation functions of the XY model. Our starting point is the two-field formulation of the partition function

$$Z'_{XY} \propto \int \mathscr{D}u \, \mathscr{D}u^\dagger \int_{-i\infty}^{i\infty} \frac{\mathscr{D}\alpha \, \mathscr{D}\alpha^\dagger}{(2\pi i)^2} e^{\beta D \sum_x u^\dagger(x)(1 + \bar{\nabla}\cdot\nabla/2D) u(x) - \sum_x \alpha u + \sum_x \log I_0(|\alpha|)}. \tag{5.88}$$

The two-point correlation function is [recall (5.35); $U \equiv U_1 + iU_2$]

$$G(\mathbf{x}', \mathbf{x}'') = \langle e^{i\gamma(\mathbf{x})} e^{-i\gamma(\mathbf{x}'')} \rangle = \langle U(\mathbf{x}') U^\dagger(\mathbf{x}'') \rangle. \tag{5.89}$$

Within the formulation (5.88) this is calculated simply by inserting $u(\mathbf{x}') u^\dagger(\mathbf{x}'')$ into the path integral and dividing the whole expression by Z'_{XY}. Hence $G(\mathbf{x}', \mathbf{x}'')$ coincides with the correlation function of the complex fluctuating field $u(\mathbf{x})$:

$$G(\mathbf{x}', \mathbf{x}'') = \langle u(\mathbf{x}') u^\dagger(\mathbf{x}'') \rangle \tag{5.90}$$

in the field theory (5.88).

In the limit of low temperatures, the field $u(\mathbf{x})$ has an expectation value

$$\langle u(\mathbf{x}) \rangle \equiv u \xrightarrow[\beta \to \infty]{} 1 - \frac{1}{2\alpha} = 1 - \frac{1}{4\beta D}. \tag{5.91}$$

This value becomes visible in $G(\mathbf{x}', \mathbf{x}'')$ when separating the arguments $\mathbf{x}'$, $\mathbf{x}''$ arbitrarily far in which case the correlation function reduces to the disconnected piece

$$G(\mathbf{x}', \mathbf{x}'') \xrightarrow[|\mathbf{x}' - \mathbf{x}''| \to \infty]{} |\langle u(\mathbf{x}) \rangle|^2 = u^2. \tag{5.92}$$

The fact that this limit is non-zero is a signal of the presence of an ordered state. For smaller distances, the connected part shows up. Since the real components have an infinite fluctuation mass, it is the imaginary parts only that show up

$$\langle u(\mathbf{x}') u^\dagger(\mathbf{x}'') \rangle_c \xrightarrow[\beta \to \infty]{} \langle \delta u'(\mathbf{x}') \delta u'(\mathbf{x}'') \rangle_{\beta \to \infty}. \tag{5.93}$$

This correlation function can be read off Eq. (5.84). Inverting the fluctuation matrix written down there and taking the matrix element 1,1 we find

$$\langle \delta u(\mathbf{x}') \delta u^\dagger(\mathbf{x}'') \rangle \xrightarrow[\beta \to \infty]{} \frac{1}{\beta} \frac{1}{-\bar{\nabla} \cdot \nabla}(\mathbf{x}', \mathbf{x}'') = \frac{1}{\beta} v(\mathbf{x}' - \mathbf{x}''). \tag{5.94}$$

To the same order, there is also a one-loop correction to the expectation of u. It is found by extracting the cubic term $\delta\alpha^\ell \delta\alpha'^2$ from $\log I_0(\sqrt{\alpha^2 + 2\alpha \delta\alpha^\ell + \delta\alpha'^2 + \delta\alpha'^2})$:

$$\log I_0 \sim \log I_0(\alpha) + \frac{I_1(\alpha)}{I_0(\alpha)}\left(\delta\alpha^\ell + \frac{1}{2}\frac{\delta\alpha'^2 + \delta\alpha'^2}{\alpha} - \frac{1}{2}\frac{\delta\alpha^\ell(\delta\alpha'^2 + \delta\alpha'^2)}{\alpha^2} \right)$$
$$+ \frac{1}{2!}\left(\frac{I_1(\alpha)}{I_0(\alpha)}\right)'\left(\delta\alpha'^2 + \frac{\delta\alpha^\ell(\delta\alpha'^2 + \delta\alpha'^2)}{\alpha} \right) + \ldots \tag{5.95}$$

Thus $\langle u(\mathbf{x}) \rangle = u + \langle \delta u^\ell(\mathbf{x}) + i\delta u'(\mathbf{x}) \rangle$ receives an additional graphical contribution[g]

$$-i^3\frac{1}{2}\left(\frac{I_1}{I_0} - \left(\frac{I_1}{I_0}\right)'\right)\frac{1}{\alpha}\langle \delta u^\ell(0) \int d^3x\, \delta\alpha^\ell(\mathbf{x}) \rangle \langle \delta\alpha'(\mathbf{x}) \delta\alpha'(\mathbf{x}) \rangle.$$

Inverting the fluctuation matrices (5.87) and (5.86) and using the 1,2 and 2,2 matrix elements respectively gives

$$\langle \delta u^\ell(0) \delta\alpha^\ell(\mathbf{x}) \rangle = -\frac{i}{\dfrac{m^2}{2D} + \left(1 - \dfrac{m^2}{2D}\right)\left(-\dfrac{\bar{\nabla} \cdot \nabla}{2D}\right)}(0, \mathbf{x}),$$

---

[g]Remember that we have rotated the variables $\delta\alpha_a$ such that the fluctuations run along the real axis [see the remarks after (5.83)].

$$\langle \delta a'(\mathbf{x})\, \delta a'(\mathbf{x}) \rangle = \frac{-2\beta D\left(1 + \dfrac{\bar{\nabla} \cdot \nabla}{2D}\right)}{\dfrac{\bar{\nabla} \cdot \nabla}{2D}}(\mathbf{x}, \mathbf{x}) = 2\beta D(1 - 2D\, v_0(\mathbf{0})). \quad (5.96)$$

In the limit of large β, $\alpha \to 2D\beta$, $m^2 \to 2D$, $I_1/I_0 \to 1$, $(I_1/I_0)' \to 0$ and the loop correction to the expectation of $u(\mathbf{x})$ becomes

$$\langle u(\mathbf{x}) \rangle^{1\,\mathrm{loop}} \xrightarrow[\beta \to \infty]{} \frac{1}{2}\frac{1}{2\beta D}(1 - 2D\, v(\mathbf{0})).$$

Combining this with (5.91) we see that $|\langle u(\mathbf{x}) \rangle|^2$ has the large β limit

$$|\langle u(\mathbf{x}) \rangle|^2 \to 1 - \frac{1}{\beta}v(\mathbf{0}).$$

Together with (5.94) this gives

$$G(\mathbf{x}', \mathbf{x}'') = \langle u(\mathbf{x}')\, u^\dagger(\mathbf{x}'') \rangle \xrightarrow[\beta \to \infty]{} |\langle u(\mathbf{x}') \rangle|^2 + \frac{1}{\beta}v(\mathbf{x}' - \mathbf{x}'')$$

$$= 1 + \frac{1}{\beta}(v(\mathbf{x}' - \mathbf{x}'') - v(\mathbf{0})). \quad (5.97)$$

5.7. IMPROVEMENT OF THE MEAN-FIELD-PLUS-ONE-LOOP APPROXIMATION

When looking at the free energy at the mean-field-plus-one-loop level in Fig. 4.7, the strongest deviation from the combination of high and low T expansions is the cusp in the neighbourhood of the mean field critical point $\beta_c^{\mathrm{MF}} = 1/D$. The question arises whether there does not exist a simple improvement of the method which removes this undesirable feature. Indeed, such a method exists! A simple cure comes from realizing that the field theory (5.75) in terms of complex u and α fields is actually invariant under a wide variety of changes of the energy functional. Since the functional integration over $\alpha(\mathbf{x})$ in (5.75) eventually forces $u(\mathbf{x})$ to be of modulus unity, we can add to the field energy any

functional which vanishes for $|u| = 1$ and is arbitrary otherwise. It is obvious that such an addition can change the mean field approximation in an arbitrary way. If loop corrections are included, however, the change will become smaller and smaller and disappear once the corrections are carried to infinite order.

The simplest additional term by which one can remove the cusps in the one-loop corrected free energy is an energy of the form

$$\Delta \beta E = -\beta D(\lambda - 1) \sum_x (u^\dagger u - 1), \tag{5.98}$$

where λ is to be treated like a Lagrange multiplier. In the presence of λ, the mean field equations are

$$2\beta D \lambda u = \alpha, \tag{5.99a}$$

$$u = \frac{I_1(\alpha)}{I_0(\alpha)}, \tag{5.99b}$$

for u and α amounting to a multiplicative renormalization of β to $\beta\lambda$. Minimizing in λ gives the additional mean field equation

$$u^\dagger u = 1.$$

Thus, in order to obtain $|u| \neq 1$ and a non-trivial free energy, λ cannot be treated as a variational parameter. At the one-loop level, however, this is no longer true. Then variations in λ lead to a non-trivial equation for λ and to an essential improvement of the one-loop approximation. The one-loop free energy for a given arbitrary λ is easy to write down,

$$-\beta f = \beta D \lambda u + \left(1 + \frac{\bar{\nabla} \cdot \nabla}{2D\lambda}\right) u - \alpha u + \log I_0(\alpha) - D\beta(\lambda - 1) - \beta f^{1 \, \text{loop}}, \tag{5.100}$$

with

$$-\beta f^{1 \, \text{loop}} = -\frac{1}{2N} \text{tr} \log\left(\frac{m_t^2}{2D} + \left(1 - \frac{m_t^2}{2D}\right)\left(-\frac{\bar{\nabla} \cdot \nabla}{2D\lambda}\right)\right)$$

$$-\frac{1}{2N} \text{tr} \log\left(\frac{m_\ell^2}{2D} + \left(1 - \frac{m_\ell^2}{2D}\right)\left(-\frac{\bar{\nabla} \cdot \nabla}{2D\lambda}\right)\right), \tag{5.101}$$

where the mass parameter m_t^2, m_ℓ^2 of real and imaginary parts of the fields are determined by [compare (5.83)–(5.87)]

$$1 - 2D\beta\lambda\left(1 + \frac{\bar{\nabla}\cdot\nabla}{2D\lambda}\right)\frac{1}{\alpha}F'(\alpha) = \frac{m_t^2}{2D} + \left(1 - \frac{m_t^2}{2D}\right)\left(-\frac{\bar{\nabla}\cdot\nabla}{2D\lambda}\right),$$

$$1 - 2D\beta\lambda\left(1 + \frac{\bar{\nabla}\cdot\nabla}{2D\lambda}\right)F''(\alpha) = \frac{m_\ell^2}{2D} + \left(1 - \frac{m_\ell^2}{2D}\right)\left(-\frac{\bar{\nabla}\cdot\nabla}{2D\lambda}\right), \quad (5.102)$$

with

$$F(\alpha) = \log I_0(\alpha), \quad F'(\alpha) = I_1(\alpha)/I_0(\alpha),$$

$$F''(\alpha) = 1 - \frac{1}{\alpha}\frac{I_1(\alpha)}{I_0(\alpha)} - \left(\frac{I_1(\alpha)}{I_0(\alpha)}\right)^2.$$

Explicitly

$$\frac{m_t^2}{2D} = 1 - 2\beta D\lambda F'(\alpha)/\alpha,$$

$$\frac{m_\ell^2}{2D} = 1 - 2\beta D\lambda F''(\alpha). \quad (5.103)$$

In the hot phase, $u = \alpha = 0$ and the masses are degenerate:

$$\frac{m_t^2}{2D} = \frac{m_\ell^2}{2D} = \frac{m^2}{2D} = 1 - \beta D\lambda. \quad (5.104)$$

In the cold phase, we use (5.99) and see that the transverse mass vanishes as the usual manifestation of the Nambu–Goldstone theorem, i.e.,

$$\frac{m_t^2}{2D} = 0. \quad (5.105)$$

The longitudinal mass is simplified to [compare (5.60) for $\lambda = 1$]

$$\frac{m_\ell^2}{2D} = 2 - 2\beta D\lambda(1 - u^2). \quad (5.106)$$

Let us now determine an optimal value of λ by extremizing (5.100) in λ. By using the field equations (5.99) this gives[h]

$$2\beta D(1 - u^2) = 2\beta D\lambda \, F'(\alpha)/\alpha \frac{\left[\dfrac{1}{\lambda} + \left(1 + \dfrac{\bar{\nabla} \cdot \nabla}{2D\lambda}\right) \dfrac{(F'(\alpha)/\alpha)'}{F'(\alpha)/\alpha} \dfrac{\partial \alpha}{\partial \lambda}\right]}{1 - 2D\beta\lambda\left(1 + \dfrac{\bar{\nabla} \cdot \nabla}{2D\lambda}\right) F'(\alpha)/\alpha}$$

$$+ 2\beta D\lambda \, F''(\alpha) \frac{\left[\dfrac{1}{\lambda} + \left(1 + \dfrac{\bar{\nabla} \cdot \nabla}{2D\lambda}\right) \dfrac{F'''(\alpha)}{F''(\alpha)} \dfrac{\partial \alpha}{\partial \lambda}\right]}{1 - 2D\beta\lambda\left(1 + \dfrac{\bar{\nabla} \cdot \nabla}{2D\lambda}\right) F''(\alpha)}$$

$$= 2D(v_{M_r}(0) + v_{M_i}(0)) - \left[\frac{(F'(\alpha)/\alpha)'}{F'(\alpha)/\alpha}\left(1 - \frac{\alpha}{\beta F'(\alpha)} v_{M_r}(0)\right)\right.$$

$$\left. + \frac{F'''(\alpha)}{F''(\alpha)}\left(1 - \frac{1}{\beta F''(\alpha)} v_{M_i}(0)\right)\right] \frac{\partial \alpha}{\partial \lambda}, \qquad (5.107)$$

where $v_M(0)$ is the lattice Coulomb potential of mass M and

$$\frac{M_r^2}{2D} = \frac{\alpha}{2\beta D F'(\alpha)} - \lambda = \lambda \frac{m_r^2/2D}{1 - m_r^2/2D},$$

$$\frac{M_i^2}{2D} = \frac{1}{2\beta D F''(\alpha)} - \lambda = \lambda \frac{m_i^2/2D}{1 - m_i^2/2D}, \qquad (5.108)$$

are the total masses of the fluctuations of the real and imaginary field components [compare (5.67)].

In the hot phase we can insert $\alpha = u = 0$ and (5.104) into (5.107) and find

$$\beta = 2v_M(0) \qquad (5.109)$$

with

[h]For the sake of maximal symmetry between m_r^2 and m_i^2, we did not insert immediately Eq. (5.104) although we could have done so.

$$\frac{M^2}{2D} = \lambda \frac{m^2/2D}{1 - m^2/2D} = \frac{1}{\beta D} - \lambda. \tag{5.110}$$

In the cold phase, we use (5.99) to calculate $\partial \alpha/\partial \lambda = 2\beta Du$ $(1 - 2\beta D\lambda F''(\alpha))' = -F'(\alpha)/[\alpha(F'(\alpha)/\alpha)']$ and Eq. (5.106) becomes

$$\beta(1 - u^2) = v_0(0) + v_M(0) - \frac{1}{2D}\left[\frac{F''(\alpha) - F'(\alpha)/\alpha}{F'(\alpha)}\left(1 - \frac{\alpha}{\beta F'(\alpha)}v_0(0)\right)\right.$$

$$\left. + \frac{F'''(\alpha)}{F''(\alpha)}\left(1 - \frac{1}{\beta F''(\alpha)}v_M(0)\right)\right]\frac{2\beta Du}{1 - 2\beta D\lambda F''(\alpha)}$$

$$= v_0(0) + v_M(0) + \frac{1}{2D\lambda}(1 - 2D\lambda v_0(0))$$

$$- \frac{F'''(\alpha)}{F''(\alpha)}\left(1 - \frac{1}{\beta F''(\alpha)}v_M(0)\right)\frac{\beta u}{1 - 2\beta D\lambda F''(\alpha)}, \tag{5.111}$$

where M^2 without subscript now denotes the "longitudinal" mass
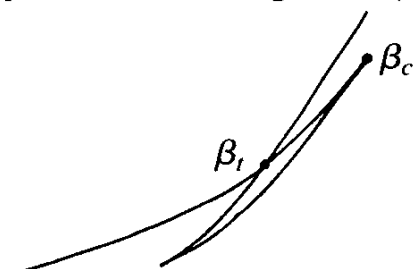
$$\frac{M^2}{2D} \equiv \frac{M_\ell^2}{2D} = -\lambda\frac{2 - 2\beta D\lambda(1 - u^2)}{1 - 2\beta D\lambda(1 - u^2)} = -\lambda - \lambda\frac{1}{1 - 2\beta D(1 - u^2)}. \tag{5.112}$$

For a given α, we find u from (5.99b), then $\beta D\lambda$ from (5.99a) and after that, β from (5.111).

Previously, in Fig. 4.5 we plotted the free energy for $D = 2, 3, 4, 5$ and compared it with the high and low temperature expansions. We now see that the introduction of λ removes the unpleasant cusp and leads to a curve which interpolates quite well between the two expansions. For $D \geq 3$, the two branches of the solutions meet at

$$\beta_c = 2v_0(0). \tag{5.113}$$

This is the temperature at which the fields $u = 0$, $\alpha = 0$ begin to destabilize. For $D \leq 4$ the free energy curve has a small multivalued piece where it describes a loop of the following form (see Fig. 4.5 curve $D = 3$)

Hence the approximation has a first order phase transition and we identify the β value of the transition, β_t, as the point of intersection of the hot and cold branches of the free energy. For $D \geq 4$ the approximation reproduces correctly the second order of the phase transition and Eq. (5.113) is just the approximation to the critical inverse temperature. The value $D = 4$ is usually called the *upper critical dimension*.

For $D = 2$ there exists no low temperature branch since $v_0(0) = \infty$. The high temperature branch, on the other hand, is a rather good approximation to the entire free energy curve. The absence of a phase transition in this approximation is a manifestation of the infinite order of the transition. The value $D = 2$ is usually called the *lower critical dimension*.

Some results are listed in Table 5.1 and compared with Monte Carlo data An important advantage of the λ minimization method is that it allows for a more reliable calculation of the order parameter

$$\langle e^{i\gamma} \rangle = \langle U \rangle, \qquad\qquad (5.114)$$
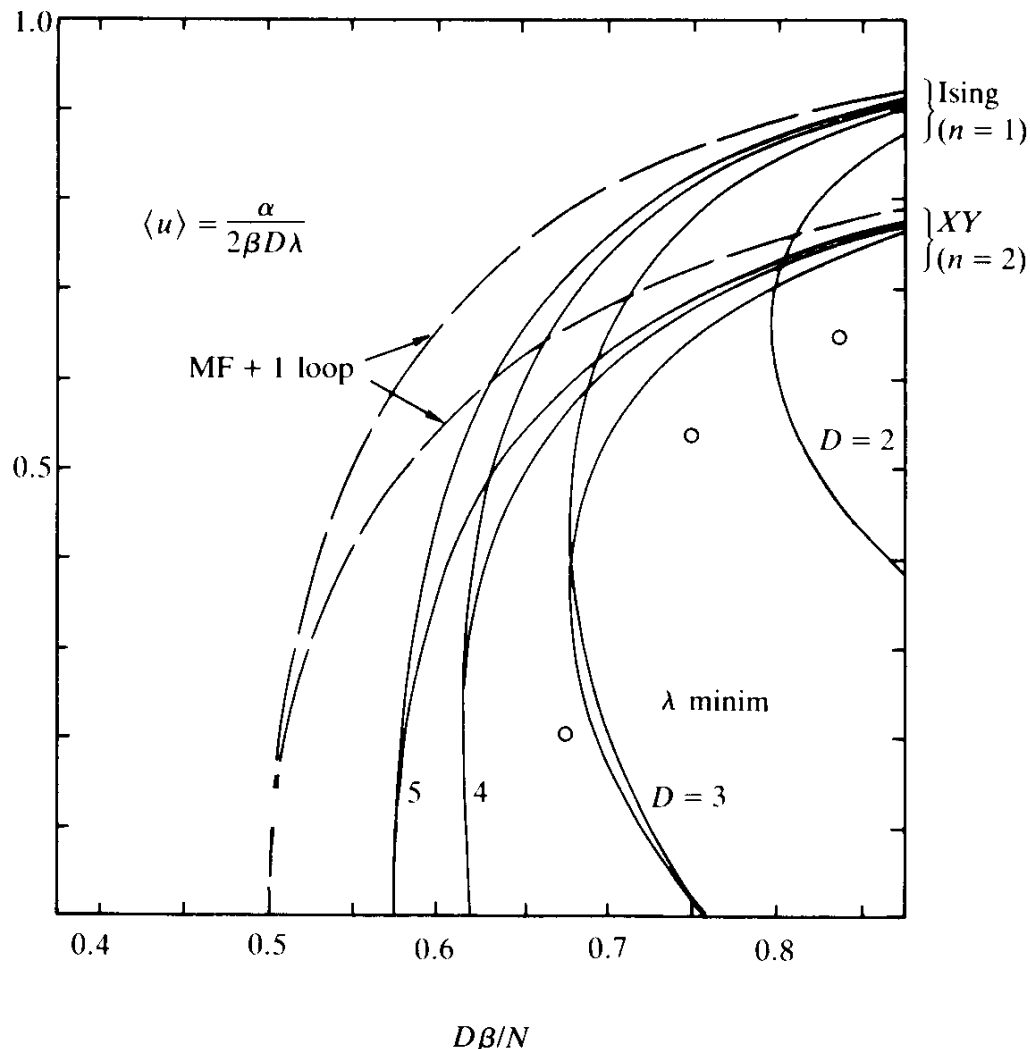
than the mean-field-plus-one-loop corrections. The behavior of the order parameter in the vicinity of the critical point is plotted in Fig. 5.7. A comparison with Monte Carlo data obtained for $D = 3$ on a $16 \times 16 \times 16$ lattice is also shown there. The rather poor agreement of the mean field curve with the Monte Carlo points is improved considerably by the $\lambda \neq 1$ solution. Still, it cannot yet be said to be satisfactory. This is reminiscent

TABLE 5.1.   The point of instability β_c and the transition point β_t of the XY model for the mean-field-plus-one-loop approximation with a λ term. For $D = 3$ ($<$ upper critical dimension) the approximation has a first order transition such that it takes place at $\beta_t < \beta_c$. For $D = 2$ (= lower critical dimension) the approximation has no transition at all and the high temperature branch is the only solution. The third column gives the Monte Carlo values. The succeeding columns show the transition temperatures obtained from the intersection of the high-temperature expansion with the mean-field-plus-one-loop free energy in Fig. 4.5, (column 4), the instability temperatures derived from the effective action of the next section (column 5) [they are solutions of (5.155) and (5.156)], and the values β_c^{GF} are taken from the $1/D$ expansion of Gerber and Fisher, up to $1/D^5$, also quoted in Eq. (5.158) (column 6).

D	β_c		β_t	β_c^{MC}	$\beta_c^{HT, MF1 loop}$	$\beta_c^{eff. ac.}$	β_c^{GF}
2				1.123	0.81		
3	0.5055	$>$	0.4805	0.45	0.47	0.448	0.449
4	0.3098	$>$	0.3085		0.32	0.297	0.299
5	0.2312	$=$	0.2312		0.24	0.227	0.228
∞	$1/2D$	$=$	$1/2D$	$1/2D$		$1/2D$	$1/2D$

of the application of the extremality principle in quantum mechanics. While it is relatively easy to obtain good approximations for the energy, it is very hard to obtain corresponding good ones for the wave functions. The worst property of the theoretical $D = 3$ curve is certainly the unphysical "belly" which reflects the first order of the transition in this approximation. This calls for the development of a more powerful calculation method. The basis for such a method is provided by the effective energy functional, whose general properties were explained in Part I, Chapter 5, and we shall spend the next section applying it to the XY model.

FIG. 5.7.   The order parameter $\langle e^{i\gamma} \rangle = \langle U \rangle$ of the XY model in the critical regime, in the mean-field-plus-one-loop approximation (which plotted against $D\beta$ is independent of D) and after minimizing in the additional parameter λ explained in Section 5.7. The circles are Monte Carlo data on a $16 \times 16 \times 16$ lattice. We see that the λ method removes part of the discrepancy. The $D = 3$ curve still has an unphysical first order "belly." For comparison, we also have drawn the theoretical curves of the Ising model.

$$\langle u \rangle = \frac{\alpha}{2\beta D\lambda}$$

$D\beta/N$

5.8. EFFECTIVE ENERGY APPROACH

A further improvement of free energy and order parameter is possible by applying the mean field method self-consistently, i.e., via the effective energy methods explained in Part I, Chapter 5. The starting point is the field representation of the partition function (5.44a),

$$Z' = \prod_{x,a} \left[\int \frac{d\psi_a}{\sqrt{4\pi\beta D}} \right] e^{-\beta E'[\psi, \psi^*]}, \tag{5.115}$$

with the field energy

$$\beta E'[\psi, \psi^*] = \sum_x \frac{1}{4\beta D} |\psi|^2 - \log I_0(\alpha), \tag{5.116}$$

where α is equal to $\mathcal{D}^{1/2} \psi = \sqrt{1 + \bar{\nabla} \cdot \nabla/2D} \, \psi$. The effective energy is obtained by forming the free correlation function in the presence of a non-vanishing background field $\psi_a = \Psi_a$:

$$G_\Psi^{-1}(x, y)_{ab} = \frac{\delta^2 E}{\delta\psi_a(x)\,\delta\psi_b(y)} \Bigg|_{\psi_a = \Psi_a} \tag{5.117}$$

and calculating all one-particle irreducible graphs involving the vertices

$$V_n^\Psi(x_1, \ldots, x_n)_{a, \ldots a_n} = \beta \frac{\delta^n E}{\delta\psi_{a_1}(x_1) \ldots \delta\psi_{a_n}(x_n)} \Bigg|_{\psi_a = \Psi_a}. \tag{5.118}$$

Since Ψ_a is a constant, the expectation of $\alpha_a(x)$ is also a constant and equal to

$$\langle \alpha_a(x) \rangle \equiv \alpha_a \equiv \Psi_a. \tag{5.119}$$

Just as in the mean field approach we shall split the 2×2 matrix G_Ψ^{-1} into a longitudinal and transverse part, parallel and orthogonal to the field expectation Ψ_a, and write

$$G_\Psi^{-1}(x, y)_{ab} = \beta \frac{\delta^2 E}{\delta\psi_a(x)\,\delta\psi_b(y)} = \frac{1}{2\beta D} \delta_{ab}\,\delta_{x,y} - \sum_z \frac{\delta\alpha_a(x)}{\delta\psi_{a'}(z)} \frac{\delta\alpha_b(y)}{\delta\psi_{b'}(z)} \sigma_{ab}$$

$$= \frac{1}{2\beta D} \delta_{ab}\,\delta_{x,y} - \left(1 + \frac{\bar{\nabla} \cdot \nabla}{2D}\right) \sigma_{ab}, \tag{5.120}$$

where σ_{ab} is the 2×2 matrix

$$\sigma_{ab} = \sigma_t P_{ab}^t + \sigma_\ell P_{ab}^\ell, \tag{5.121}$$

with

$$\sigma_t \equiv \frac{1}{\alpha}\frac{dF}{d\alpha}, \quad \sigma_\ell = \frac{d^2F(\alpha)}{d\alpha^2} \tag{5.122}$$

[recall (5.56)] and the 2×2 projection matrices transverse and longitudinal to Ψ_a defined by

$$P_{ab}^t = \delta_{ab} - \frac{\Psi_a \Psi_b}{\Psi^2}, \tag{5.123}$$

$$P_{ab}^\ell = \frac{\Psi_a \Psi_b}{\Psi^2}. \tag{5.124}$$

If we rewrite G_Ψ^{-1} as

$$G_\Psi^{-1}(\mathbf{x}, \mathbf{y})_{ab} \equiv G_\Psi^{-1}(\mathbf{x}, \mathbf{y})^t P_{ab}^t + G_\Psi^{-1}(\mathbf{x}, \mathbf{y})^\ell P_{ab}^\ell$$

$$= \frac{1}{2\beta D}\left(1 - 2\beta D\,\sigma_t\left(1 + \frac{\overleftarrow{\nabla}\cdot\nabla}{2D}\right)\right) P_{ab}^t$$

$$+ \frac{1}{2\beta D}\left(1 - 2\beta D\,\sigma_\ell\left(1 + \frac{\overleftarrow{\nabla}\cdot\nabla}{2D}\right)\right) P_{ab}^\ell \tag{5.125}$$

and compare with (5.101) we are led to introduce the mass parameters

$$\frac{m_t^2}{2D} = 1 - 2\beta D\,\sigma_t, \tag{5.126}$$

$$\frac{m_\ell^2}{2D} = 1 - 2\beta D\,\sigma_\ell, \tag{5.127}$$

which now depend upon the background field $\Psi = \sqrt{\Psi_a^2}$.

We can now write down directly the self-consistent one-loop correction to the free energy, i.e., the one-loop effective energy, by simply performing the integral over all quadratic fluctuations in Z. This gives

$$-\frac{1}{2N}\mathrm{tr}\,\log(2\beta D\,G_\Psi^{-1}) \tag{5.128}$$

so that the free energy density is, with $b \equiv \beta D$,

$$-\beta f = -\frac{1}{4b}\Psi^2 + \log I_0(\psi) - \frac{1}{2N}\mathrm{tr}\log\left(\frac{m_t^2}{2D} + \left(1 - \frac{m_t^2}{2D}\right)\left(-\frac{\bar{\nabla}\cdot\nabla}{2D}\right)\right)$$

$$-\frac{1}{2N}\mathrm{tr}\log\left(\frac{m_t^2}{2D} + \left(1 - \frac{m_t^2}{2D}\right)\left(-\frac{\bar{\nabla}\cdot\nabla}{2D}\right)\right). \qquad (5.129)$$

Numerically the traces of the logarithm can be calculated via the hopping expansion [recall Eq. (5.71b)]

$$-\frac{1}{N}\mathrm{tr}\log\left(\frac{m^2}{2D} + \left(1 - \frac{m^2}{2D}\right)\left(-\frac{\bar{\nabla}\cdot\nabla}{2D}\right)\right) = \sum_{n=2}^{\infty}\frac{1}{n}\left(1 - \frac{m^2}{2D}\right)^n \frac{H_n}{(2D)^n}, \qquad (5.130)$$

where $H_2 = 2D$, $H_4 = 6D(2D - 1)$, ..., are the number of closed random walks as given in Part I, Tables 6.1 and 6.2.

Consider now the two-loop corrections. The one-particle irreducible diagrams are ∞ and $\ominus$. It will be convenient to define vertices of the α fields

$$\hat{V}_{3\,abc} = \frac{1}{3!}\left[4F''(\alpha)(\alpha_a\,\delta_{bc} + 2\text{ cyclic perm}) + 8F'''(\alpha)\,\alpha_a\,\alpha_b\,\alpha_c\right],$$

$$\hat{V}_{4\,abcd} = \frac{1}{4!}[4F''(\alpha)(\delta_{ab}\,\delta_{cd} + \delta_{ac}\,\delta_{bd} + \delta_{ad}\,\delta_{bc}) + 8F'''(\alpha)$$

$$\times (\alpha_a\,\alpha_b\,\delta_{cd} + \alpha_a\,\alpha_c\,\delta_{bd} + \alpha_a\,\alpha_d\,\delta_{bc} + \alpha_b\,\alpha_c\,\delta_{ad} + \alpha_b\,\alpha_d\,\delta_{ac}$$

$$+ \alpha_c\,\alpha_d\,\delta_{ab}) + 16F''''(\alpha)\,\alpha_a\,\alpha_b\,\alpha_c\,\alpha_d], \qquad (5.131)$$

where primes denote the derivatives of $F(\alpha) = \log I_0(\sqrt{\alpha^2})$ with respect to α^2, i.e., $' = (1/2\alpha)(d/d\alpha)$. If a dot denotes the derivative with respect to α, we have

$$F' = \frac{1}{2\alpha}\dot{F} = \frac{1}{2\alpha}\frac{I_1(\alpha)}{I_0(\alpha)} = \frac{1}{2}\sigma_t$$

$$F'' = \frac{1}{2\alpha}\left(\frac{1}{2\alpha}\dot{F}\right)^{\cdot} = \frac{1}{4\alpha^2}(\ddot{F} - \dot{F}/\alpha) = \frac{1}{4\alpha}\dot{\sigma}_t = \frac{1}{4\alpha^2}(\sigma_t - \sigma_t). \qquad (5.132)$$

$$F''' = -\frac{3}{8\alpha^3}\dot{\sigma}_t + \frac{\dot{\sigma}_t}{8\alpha^3},$$

$$F'''' = \frac{5}{16\alpha^5}\dot{\sigma}_t - \frac{3}{8\alpha^5}\dot{\sigma}_\ell + \frac{1}{16\alpha^4}\ddot{\sigma}_\ell.$$

The correlation functions of the $\alpha_a(\mathbf{x})$ fields differ from those of the $\psi_a(\mathbf{x})$ fields by a factor $\mathscr{D}^{1/2}$ from the right and left, i.e.,

$$\langle \alpha_a(\mathbf{x})\,\alpha_b(\mathbf{y})\rangle = (\mathscr{D}^{1/2}\,G_\Psi\,\mathscr{D}^{1/2})(\mathbf{x},\,\mathbf{y})_{ab} = \left[\left(1 + \frac{\bar{\nabla}\cdot\nabla}{2D}\right)G_\Psi\right](\mathbf{x},\,\mathbf{y})_{ab}$$

(5.133)

Let us call this correlation function $\widehat{G}(\mathbf{x}-\mathbf{y})_{ab}$. Then the two contributions are

$$-\beta f^\infty = \frac{1}{4!}[4F''(\delta_{ab}\,\delta_{cd} + 2\text{ perm}) + 8F'''(\Psi_a\,\Psi_b\,\delta_{cd} + 5\text{ perm})$$

$$+ 16F''''\Psi_a\,\Psi_b\,\Psi_c\,\Psi_d \cdot (\widehat{G}(0)_{ab}\,\widehat{G}\,(0)_{cd} + 2\text{ perm}),\quad (5.134)$$

$$-\beta f^\Theta = \frac{1}{2}\frac{1}{3!^2}\sum_{\mathbf{x}}[4F''(\Psi_a\,\delta_{bc} + 2\text{ perm}) + 8F'''\Psi_a\,\Psi_b\,\Psi_c]$$

$$\times [4F''(\Psi_{a'}\,\delta_{b'c'} + 2\text{ perm}) + 8F'''\Psi_{a'}\,\Psi_{b'}\,\Psi_{c'}]$$

$$\times [\widehat{G}(\mathbf{x})_{aa'}\,\widehat{G}(\mathbf{x})_{bb'}\,\widehat{G}(\mathbf{x})_{cc'} + 5\text{ perm}],\quad (5.135)$$

Introducing the notation $\bar{\widehat{G}}(\mathbf{x}) \equiv \Psi_a\widehat{G}(\mathbf{x})_{ab}\Psi_b$, $\bar{\widehat{G}}^2(\mathbf{x}) = \Psi_a\widehat{G}_{ab}(\mathbf{x})\,\widehat{G}_{bc}(\mathbf{x})\Psi_c$, ... we can write

$$-\beta f^\infty = \frac{1}{4!}\{4F''[3(\text{tr }\widehat{G}(0))^2 + 6\,\text{tr}(\widehat{G}(0))^2]$$

$$+ 8F'''[6\,\text{tr }\widehat{G}(0)\,\bar{\widehat{G}}(0) + 12\bar{\bar{\widehat{G}}}^2(0)] + 16F''''\cdot 3(\bar{\widehat{G}}(0))^2\},(5.136)$$

$$-\beta f^\Theta = \frac{1}{2}\frac{1}{3!^2}\sum_{\mathbf{x}}\{(4F'')^2[18\,\text{tr}(\widehat{G}^2(\mathbf{x}))\,\bar{\widehat{G}}(\mathbf{x}) + 36\bar{\bar{\widehat{G}}}^3(\mathbf{x})]$$

$$+ 36(4F'')(8F''')\bar{\bar{\widehat{G}}}^2(\mathbf{x})\bar{\widehat{G}}(\mathbf{x}) + 6(8F''')^2(\bar{\widehat{G}}(\mathbf{x}))^3\},\quad (5.137)$$

where the trace refers now only to the 2×2 indices of $\widehat{G}(\mathbf{x})_{ab}$.

In order to calculate these energies it is most convenient to use again the hopping expansion in powers of the hopping matrix

$$H(\mathbf{x}, \mathbf{y}) = \sum_{\pm i = 1}^{D} \delta_{\mathbf{x}, \mathbf{y}+\mathbf{i}} = \sum_{\pm i} \nabla_i = 2D + \bar{\nabla} \cdot \nabla = 2DP(\mathbf{x}, \mathbf{y}). \quad (5.138)$$

Then $\widehat{G}(\mathbf{x}, \mathbf{y})_{ab}$ has the expansion [see (5.125)]

$$\widehat{G} = \frac{H}{2D} G_{\Psi} = \beta H (1 - \beta \sigma H)^{-1}{}_{ab} = \beta \sum_{n=0}^{\infty} (\beta \sigma)^n H^{n+1}. \quad (5.139)$$

Remembering that the mean field depends only on $b = \beta D$ and represents the $D \rightarrow \infty$ limit of the theory, we introduce this parameter also here and write

$$\widehat{G} = \frac{b}{D} \sum_{n=0}^{\infty} \left(\frac{b}{D}\sigma\right)^n H^{n+1}. \quad (5.140)$$

This can again be decomposed into transverse and longitudinal parts with respect to the expectation value Ψ_a:

$$\widehat{G} = \widehat{G}^t P^t + \widehat{G}^\ell P^\ell, \quad (5.141)$$

where

$$\widehat{G}^t(\mathbf{x}) = \frac{b}{D} \sum_{n=0}^{\infty} \left(\frac{b}{D}\sigma_t\right)^n H^{n+1}(\mathbf{x}, \mathbf{0}), \quad (5.142)$$

$$\widehat{G}^\ell(\mathbf{x}) = \frac{b}{D} \sum_{n=0}^{\infty} \left(\frac{b}{D}\sigma_\ell\right)^n H^{n+1}(\mathbf{x}, \mathbf{0}). \quad (5.143)$$

In terms of $\widehat{G}^t$, $\widehat{G}^\ell$ we have

$$\operatorname{tr}\widehat{G} = \operatorname{tr}(\widehat{G}^t + \widehat{G}^\ell), \quad \operatorname{tr}\widehat{G}^2 = \operatorname{tr}(\widehat{G}^{t2} + \widehat{G}^{\ell 2}),$$

$$\overline{\widehat{G}} = \Psi^2 \widehat{G}^\ell, \quad \overline{\widehat{G}^2} = \Psi^2 \widehat{G}^{\ell 2}. \quad (5.144)$$

We now observe that higher and higher loop diagrams at fixed $b = \beta D$ are all suppressed by as many powers as there are loops (i.e., the ℓ-loop diagrams by $1/D^\ell$). This follows from the fact that due to the overall factor of $1/D$ in $\widehat{G}$ [see (5.140)], there is such a factor for each internal line. Each space integral on the other hand, gives at most a factor D. This results in a leading behaviour of $1/D$ of loops. Hence we decide to treat

the loop diagrams systematically in a $1/D$ expansion. In $\widehat{G}(0)$ we have to keep only the leading term in $1/D$,

$$\widehat{G}(0)_{ab} = \frac{b^2}{D^2}(\sigma_t P'_{ab} + \sigma_t P^t_{ab})2D + O\left(\frac{1}{D^2}\right),\tag{5.145}$$

where we have used $H^2(0, 0) = 2D$. This gives the approximations

$$\overline{\widehat{G}}(0) = 2\frac{b^2}{D}\sigma_t \Psi^2 + O\left(\frac{1}{D^2}\right), \quad \overline{\widehat{G}^2}(0) = 4\frac{b^2}{D^2}\sigma_t^2 \Psi^2 + O\left(\frac{1}{D^3}\right).\tag{5.146}$$

Hence, up to order $1/D^2$, the diagram ∞ gives in (5.136)

$$-\beta f^{\infty} = \frac{b^4}{2D^2}\{4F''[3\sigma_t^2 + 3\sigma_t^2 + 2\sigma_t\sigma_t]\tag{5.147}$$

$$+ 8F''' \Psi^2[2\sigma_t\sigma_t + 6\sigma_t^2] + 16F'''' \Psi^4 \sigma_t^2\} + O\left(\frac{1}{D^3}\right).\tag{5.148}$$

For the diagrams Θ we truncate

$$\widehat{G}(\mathbf{x}) = \frac{b}{D}H(\mathbf{x}, 0) + \frac{b^2}{D^2}(\sigma_t P' + \sigma_t P')H^2(\mathbf{x}, 0) + \ldots\tag{5.149}$$

Inspection of (5.137) shows that to order $1/D^2$ only the lowest term contributes which is independent of σ_t, σ_t:

$$\text{tr}(\widehat{G}^2(\mathbf{x})) = 2\frac{b^2}{D^2}H(\mathbf{x}, 0), \quad \overline{\widehat{G}}(\mathbf{x}) = \frac{b}{D}\Psi^2 H(\mathbf{x}, 0),$$

$$\overline{\widehat{G}^3}(\mathbf{x}) = \frac{b^3}{D^3}\Psi^4 H(\mathbf{x}, 0), \quad \overline{\widehat{G}^2}(\mathbf{x})\overline{\widehat{G}}(\mathbf{x}) = \frac{b^3}{D^3}\Psi^4 H(\mathbf{x}, 0),$$

$$(\overline{\widehat{G}^3}(\mathbf{x}))^3 = \frac{b^3}{D^2}\Psi^6 H(\mathbf{x}, 0).\tag{5.150}$$

Inserting this into (5.137) we obtain

$$-\beta f^\Theta = \frac{b^3}{6D^2}[12(4F'')^2 \Psi^2 + 6(4F'')(8F''') \Psi^4 + (8F''')^2 \Psi^6] + O\left(\frac{1}{D^3}\right).\tag{5.151}$$

In order to be consistent, we must also truncate the one-loop diagram in the same way. Thus we carry the expansion (5.130) in (5.129) only up to H^4 and use

$$\frac{1}{N}\operatorname{tr}\log\left(\frac{m^2}{2D} + \left(1 - \frac{m^2}{2D}\right)\left(-\frac{\bar{\nabla}\cdot\nabla}{2D}\right)\right)$$

$$= \frac{1}{2}\left(\frac{b}{D}\sigma\right)^2 2D + \frac{1}{4}\left(\frac{b}{D}\sigma\right)^4 12D^2 + O\left(\frac{1}{D^3}\right), \qquad (5.152)$$

where we have replaced $H_4 = 6D(2D - 1)$ by $12D^2$ in order to be consistent in keeping only terms up to order $1/D^2$. The total free energy

$$-\beta f = -\frac{1}{4b}\Psi^2 + \log I_0(\Psi) - \frac{1}{2N}\operatorname{tr}\log(2bG_{\bar{\Psi}}^{-1}) - \beta f^{(0)} - \beta f^{()}$$

$$= -\frac{1}{4b}\Psi^2 + \log I_0(\Psi) + \frac{b^2}{2D}[\sigma_t^2 + \sigma_{\bar{t}}^2] + \frac{b^3}{6D^2}(3\dot{\sigma}_t^2 + \dot{\sigma}_{\bar{t}}^2] + \frac{b^4}{2D^2}$$

$$\times \left\{3\sigma_t^4 + 3\sigma_{\bar{t}}^4 - \frac{4}{\Psi}\sigma_t\dot{\sigma}_t\sigma_t + \frac{3}{\Psi}\sigma_t^2\dot{\sigma}_t + \frac{2}{\Psi}\sigma_t\sigma_t\dot{\sigma}_t + \sigma_{\bar{t}}^2\ddot{\sigma}_t\right\} + O\left(\frac{1}{D^3}\right)$$

(5.153)

must now be minimized in Ψ. The result is plotted in Fig. 5.8.

For small b, the minimum lies at $\Psi = 0$ and is equal to

$$-\beta f = \frac{1}{D}\left(\frac{b}{2}\right)^2 + \frac{1}{D^2}\left(\frac{b}{2}\right)^4 + O\left(\frac{1}{D^3}\right). \qquad (5.154)$$

For large b, there is a nontrivial minimum given by the equation

$$-\beta\Psi_a^{-1}\frac{\partial f}{\partial\Psi_a} = 0 = g_{-1}\frac{1}{b} + g_0 + g_2 b^2 + g_3 b^3 + g_4 b^4, \qquad (5.155)$$
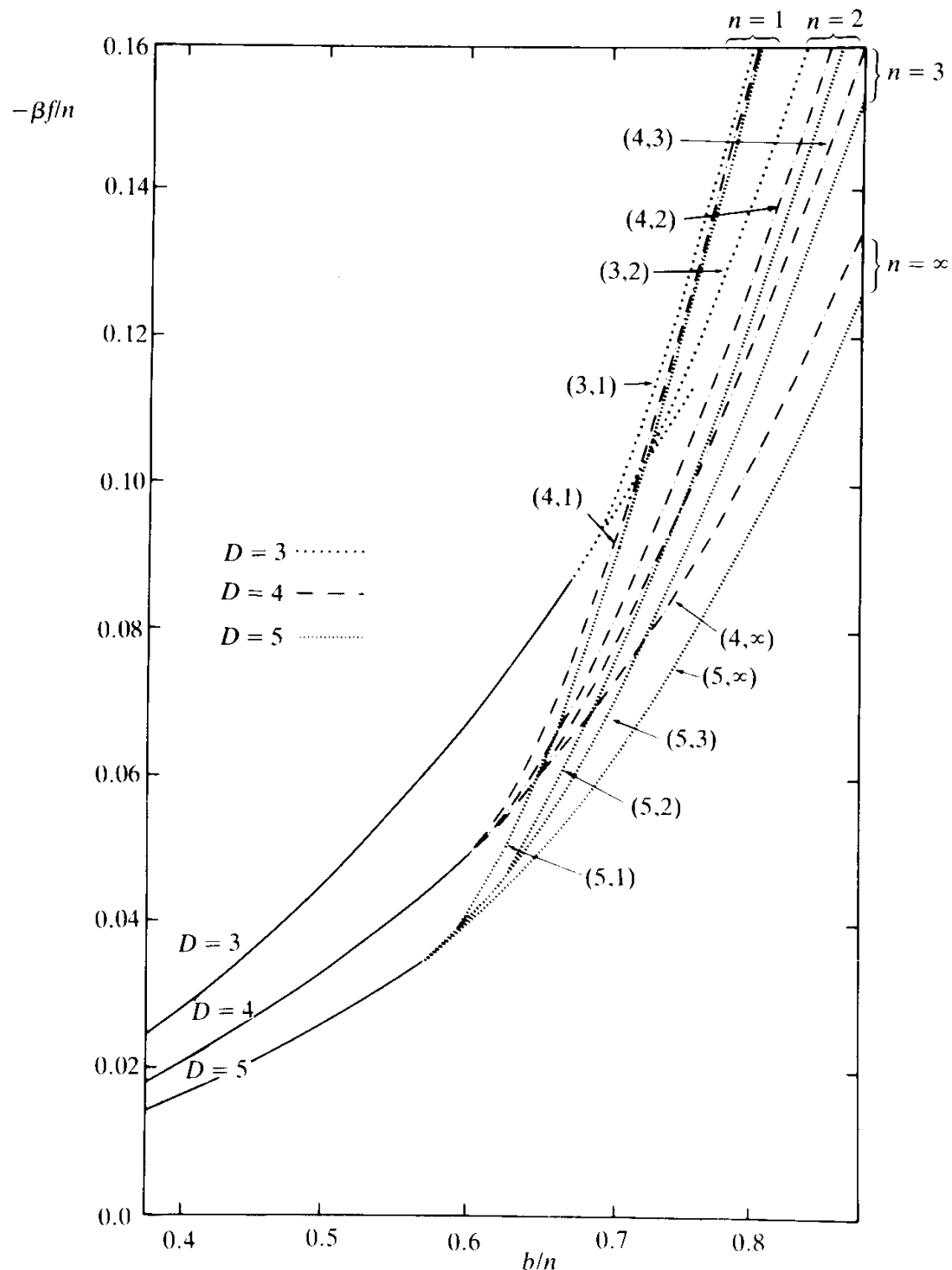
where

$$g_{-1} = -\frac{1}{2}, \quad g_0 = \sigma_t = \dot{F}(\Psi)/\Psi, \quad g_2 = \frac{1}{D\Psi}[\sigma_t\dot{\sigma}_t + \sigma_{\bar{t}}\dot{\sigma}_{\bar{t}}],$$

$$g_3 = \frac{1}{3D^2\Psi}[\dot{\sigma}_{\bar{t}}\ddot{\sigma}_t + \frac{3}{\Psi}\dot{\sigma}_t\dot{\sigma}_t - \frac{6}{\Psi}\dot{\sigma}_t^2],$$

$$g_4 = \frac{1}{2D^2\Psi}[12\sigma_t^3\dot{\sigma}_t + 12\sigma_{\bar{t}}^3\dot{\sigma}_t + \bar{g}_4],$$

FIG. 5.8. The free energy of the $O(n)$ spin model in the effective energy approach up to two loops, where the diagrams are calculated in a $1/D$ expansion up to $1/D^2$. The curves are labeled by (D, n). The XY model has $n = 2$. In the $D = 3$ case, there is a small section where the curve describes a multivalued loop as explained in the text. In a hopping expansion this disappears (Figs. 5.8–5.11 are due to Matsui, Kleinert and Ami).

$$\bar{g}_4 = \frac{2}{\Psi^3} 13\sigma_t\sigma_\ell^2 - \frac{37}{\Psi^3}\sigma_\ell^2\sigma_\ell - \frac{12}{\Psi^2}\sigma_t\sigma_\ell\dot\sigma_\ell + \frac{7}{\Psi^2}\sigma_t^2\dot\sigma_t + \frac{15}{\Psi^3}\sigma_t^3$$

$$- \frac{4}{\Psi^3}\sigma_\ell^3 + \frac{2}{\Psi^2}\sigma_\ell^2\dot\sigma_\ell + \frac{2}{\Psi}\sigma_t\dot\sigma_\ell^2 + \frac{2}{\Psi}\sigma_t\sigma_\ell\ddot\sigma_\ell + \sigma_\ell^2\ddot\sigma_t + 2\sigma_\ell\dot\sigma_\ell\ddot\sigma_\ell.$$

$$(5.156)$$

The critical values of β are those where the solution $\Psi \neq 0$ first appears. They are found by solving the equation (5.155) at $\Psi = 0$, where

$$g_{-1} = -\frac{1}{2}, \quad g_0 = \frac{1}{2}, \quad g_2 = -\frac{1}{4D}, \quad g_3 = \frac{1}{16D^2}, \quad g_4 = 0. \quad (5.157)$$

The result is shown in Table 5.1. Our values of b_c are very close to those found by Gerber and Fisher in a systematic $1/D$ expansion up to order D^{-5}. Those authors treat the more general case of $O(n)$ spins $\beta \sum_{x,i} \sum_{a=1}^{n} s_a(\mathbf{x}) s_a(\mathbf{x} + \mathbf{i})$ with $\sum_{a=1}^{n} s_a^2 = 1$ instead of planar spins and find[i]

$$\frac{b_c}{n} = \frac{1}{2}\left[1 - \frac{1}{2D} - \frac{n+1}{2D^2(n+2)} - \frac{1}{8D^3}\left(3 + \frac{4n}{n+2}\right) - \frac{1}{16D^4} \right.$$

$$\times \left(16 + \frac{(21N+32)}{(n+2)^2} - \frac{2n^2}{(n+2)(n+4)} \right) - \frac{1}{32D^5}$$

$$\left. \times \left(102 + \frac{(129n^2 + 422n + 340)n}{(n+2)^3} - \frac{16n^2}{(n+2)(n+4)} \right) \right]^{-1} + O\left(\frac{1}{D^6}\right).$$

$$(5.158)$$

Going to the planar spin case, i.e., inserting $n = 2$, we find the values shown in the last column of Table 5.1.

The free energy for various dimensions is plotted in Fig. 5.8. For completeness, we have added the curves for the different $O(n)$ models ($n = 1$ Ising, $n = 2$ XY, $n = 3$ Heisenberg, ..., $n = \infty$ spherical).

In Fig. 5.9 we have displayed the case $D = 3$ separately for $n = 1$ and $n = 2$.

Figure 5.10, finally, gives the order parameter $\langle e^{i\gamma}\rangle = \langle U \rangle$ as a function of b.

[i]For the general $O(n)$ effective action see the original paper by T. Matsui, H. Kleinert, S. Ami, cited in the Notes and References. See also Appendix 5A.

FIG. 5.9. The $D = 3$ effective energy (E) of the $O(n)$ model compared with the high temperature $(S = $ strong coupling) and mean-field-plus-one-loop expansion (M). The notation is $(D, n)_{F,S,M}$ respectively. We have not plotted the curves due to λ minimization which would lie only slightly lower than the effective energy curves.
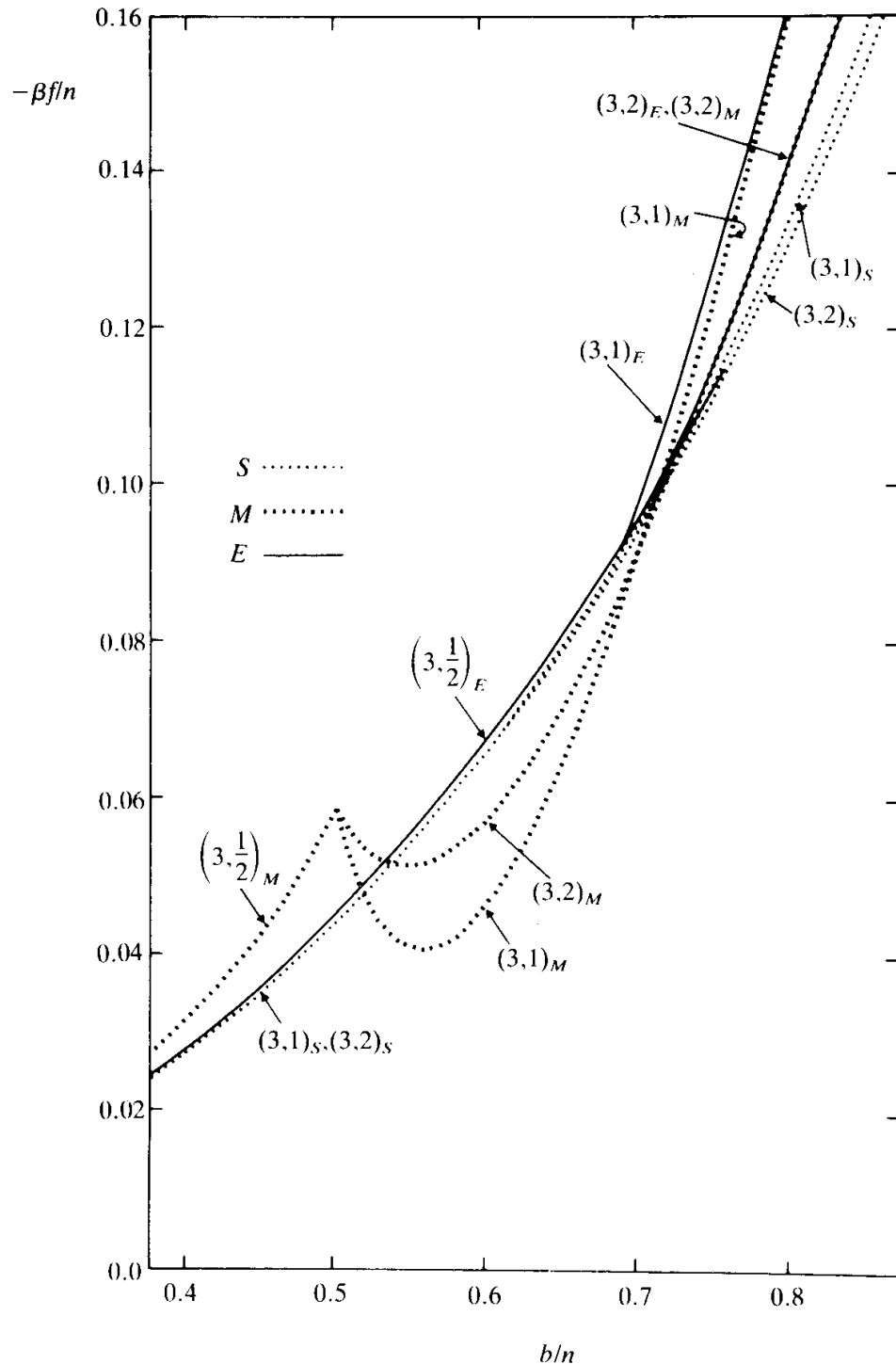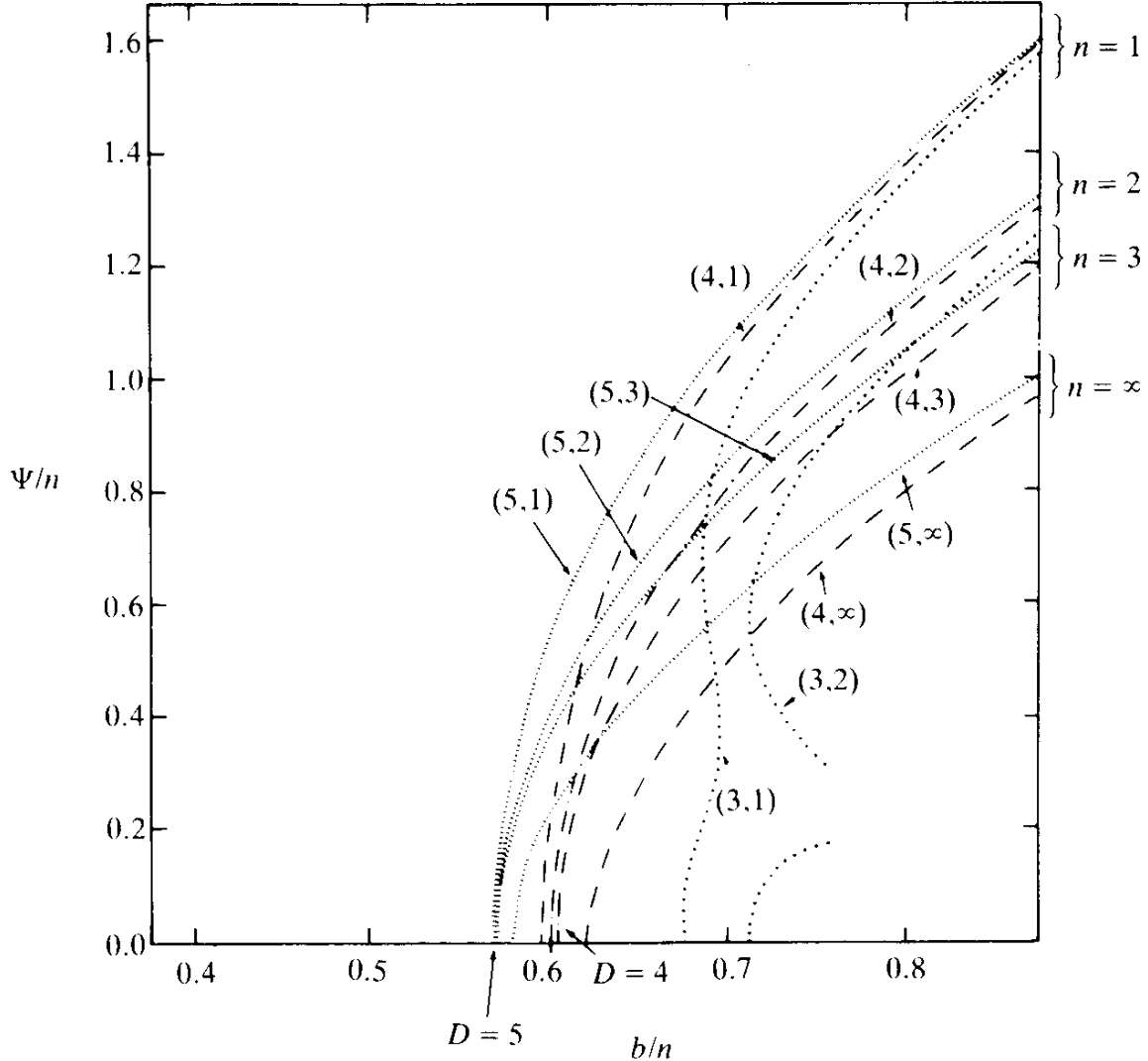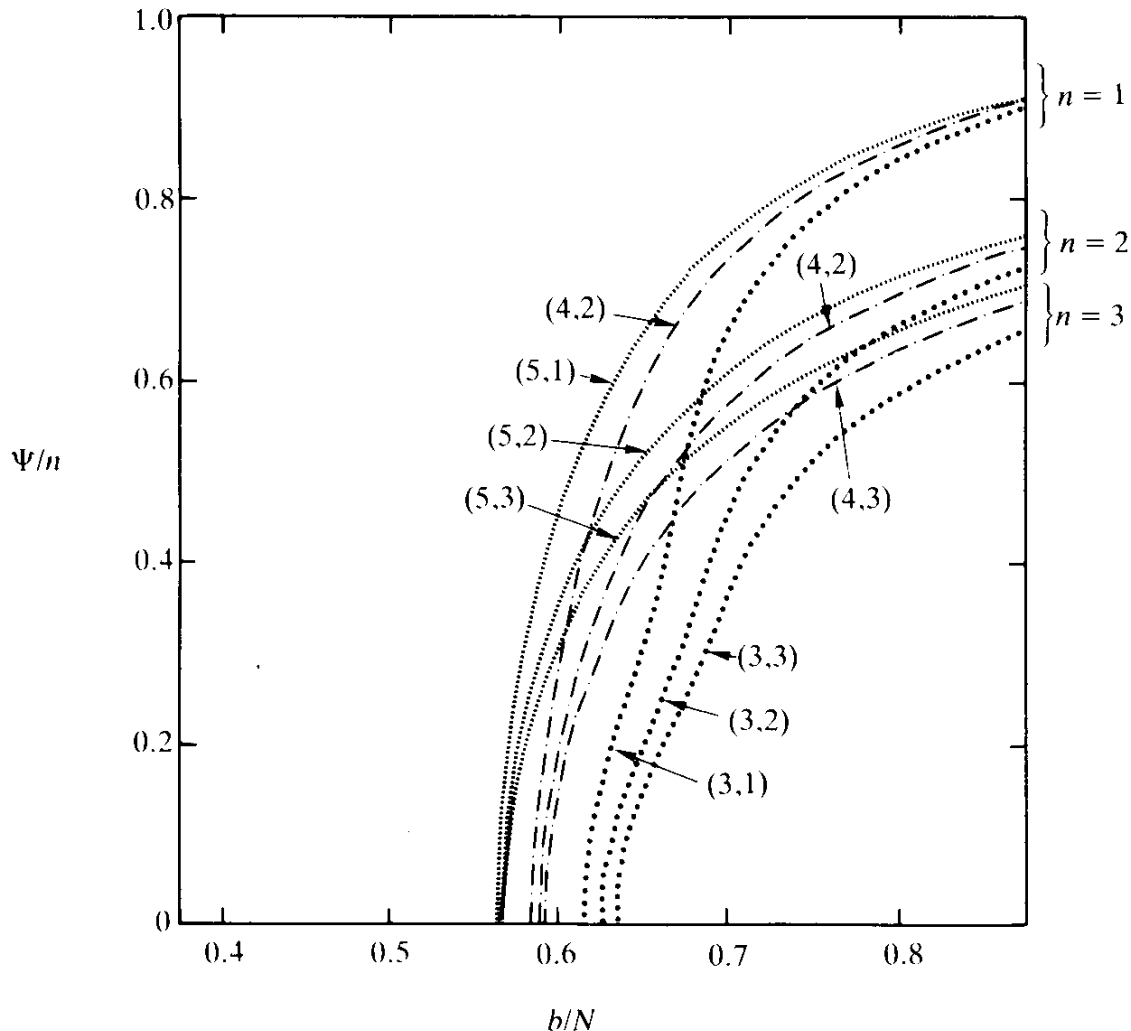
FIG. 5.10. The order parameter $\Psi/n = (2b/n)\langle u \rangle$ in the $O(n)$ spin model for various dimensions and values of n from the two-loop effective emergy (up to second order in $1/D$). For low D and large N the (unphysial) first order, transition shows up in a concave or a missing piece in the solution.

Just as was true for the λ minimization, the present approximation produces a first order transition for $D = 3$. This reflects itself in a multivalued piece of the free energy curve and a corresponding concave piece in the order parameter. This is, certainly, in disagreement with the Monte Carlo data, as shown in Fig. 5.7. There is a simple cure for this desease. All we have to do is change the systematics of our expansion from counting powers of $1/D$ into counting powers of the hopping operator $H(\mathbf{x}, \mathbf{y}) = 2DP(\mathbf{x}, \mathbf{y})$. This is the "hopping expansion" of the two-loop effective energy two-loop. Up to second order, this amounts to using the proper graph number $H_2 = 6D(2D - 1)$ in formula (5.152) rather than the leading term $12D^2$. This gives rise to an extra factor $(1 - 1/2D)$ in the terms

FIG. 5.11.   The order parameter $\Psi/n = (2b/n)\langle u \rangle$ as in Fig. 5.10 but with the two-loop diagrams calculated up to second order in the *hopping expansion*. Now there are only second-order transitions.

$$\frac{b^4}{2D^2}[3\sigma_t^4 + 3\sigma_l^4] \tag{5.159}$$

on the right-hand side of (5.153). It changes (5.154) by an extra term $-(3/2)(1/D^3)(b/2)^4$ and the $g_4 = 0$ value of (5.157) becomes

$$g_4 = \frac{1}{16}\frac{1}{D^3}. \tag{5.160}$$

After these changes, the order parameter is convex (see Fig. 5.11) and the phase transition is of second order, as it should. The agreement with the Monte Carlo data is improved (recall the data points of Fig. 5.9) even though the critical value $\beta_c^{\text{hopp exp}} \approx 0.416$ is somewhat smaller than the true value (≈ 0.453).

With the transition being second order for all dimensions $D = 2$ it becomes possible to study the neighbourhood of the critical point by expanding the free energy *à la* Landau,

$$-\beta f = -\beta f_0 - \frac{1}{2} m^2 \Psi^2 - \frac{g}{4!} \Psi^4 \qquad (5.161)$$

and we find from (5.155) [after the hopping modification (5.159)]

$$m^2 = -\gamma(b - b_c), \quad \gamma = \frac{1}{2b_c^2} - \frac{4b_c}{Dn^3} + \frac{12b_c^2}{D^2 n^4 (n+2)} + \frac{24b_c^3}{D^3 n^5},$$
$$(5.162)$$

$$\frac{g}{4!} = \frac{1}{4n^2(n+2)} - \frac{b_c^2}{2D} \frac{5n+16}{n^4(n+2)^2} + \frac{b_c^3}{D^2} \frac{16}{n^5(n+2)^2}$$

$$+ \frac{b_c^4}{D^2} \frac{7n^2 + 30n + 44}{n^6(n+2)^3} + \frac{b_c^4}{D^3} \frac{3(7n+32)}{2n^6(n+2)^2}. \qquad (5.163)$$

For completeness, the result is written down for all $O(n)$ models and one has to insert $n = 2$ to recover the case of planar spins that we are now considering.

The advantages of the hopping expansion over the $1/D$ expansion in $D = 3$ dimensions have been known in the literature for a long time. The prime example is the $O(n)$ spin model for $n \to \infty$ called the spherical model where the critical temperature is given exactly by

$$\beta_c = v_0(0) \approx 0.252731. \qquad (5.164)$$

In Part I, Chapter 5 we calculated $v_0(0)$ via a hopping expansion. This is a convergent expansion for $D > 2$. If we set $q = 2D$, it has the explicit form [recall Table 6.1, Part I]

$$\beta_c = v_0(0) = \frac{1}{q} + \frac{q}{q^3} + \frac{3q}{q^5}(-1+q) + \frac{5q}{q^7}(8 - 9q + 3q^2)$$

$$+ \frac{35q}{q^9}(-33 + 41q - 18q^2 + 3q^3) + \ldots \qquad (5.165)$$

Thus it is a power series in $1/q$, but with coefficients which depend

themselves on q. If expanded *systematically* in powers of $1/2D = 1/q$, the series would be

$$\beta_c = \frac{1}{q} + \frac{1}{q^2} + \frac{3}{q^3} + \frac{12}{q^4} + \frac{60}{q^5} + \frac{355}{q^6} + \frac{2380}{q^7} + \frac{17430}{q^8} + \frac{134190}{q^9}$$

$$+ \frac{1027656}{q^{10}} + \frac{6922146}{q^{11}} + \frac{21248073}{q^{12}} - \frac{601744143}{q^{13}} - \frac{20802115620}{q^{14}}.$$

$$(5.166)$$

Inserting $D = 4, 5, 6, \ldots$ this series gives quite reliable results. For $D = 3$, however, it gives a *negative* value reflecting the fact that it does not converge at all.

APPENDIX 5A: GENERALIZATION TO CLASSICAL $O(n)$ SPIN MODELS

The mean field formalism developed in this chapter for classical planar spins can easily be generalized to $O(n)$ spin models:

$$Z = \prod_{\mathbf{x}} \left[\int \frac{ds_a(\mathbf{x})}{S_n} \right] e^{\beta \sum_{\mathbf{x},i} \sum_{a=1}^{n} s_a(\mathbf{x}) s_a(\mathbf{x}+i)}, \qquad (5A.1)$$

where a runs from 1 to n, s_a are unit vectors on an n-dimensional sphere, $\int ds_a/S_n$ are the integrals over the surface of the sphere normalized to unity (i.e., $S_n = 2\pi^{n/2}/\Gamma(n/2)$). In such models, all formulas hold as before except that $I_0(\beta)$ is to be replaced by

$$\int \frac{ds_a}{S_n} e^{\alpha_a s_a} = \frac{\Gamma(n/2)}{\alpha^{n/2-1}} I_{n/2-1}(\sqrt{\alpha_a^2}). \qquad (5A.2)$$

Hence the mean field free energy becomes

$$-\beta f'^{\mathrm{MF}} = \beta D u_a^2 - \alpha_a u_a + F(\alpha_a^2), \qquad (5A.3)$$

with $F(\alpha_a^2) = \log(\Gamma(n/2) I_{n/2-1}(\sqrt{\alpha_a^2})/\alpha^{(n/2-1)})$ and the mean field equations are

$$\alpha = 2\beta D u, \qquad (5A.4)$$

$$u = \frac{dF}{d\alpha} = I_{n/2}(\alpha)/I_{n/2-1}(\alpha).$$ (5A.5)

There are now $n - 1$ massless Nambu–Goldstone modes orthogonal to the direction of the ground state fields and the one-loop correction reads

$$-\beta f^{1 \text{ loop}} = -\frac{n-1}{2N} \operatorname{tr} \log\left(-\frac{\bar{\nabla} \cdot \nabla}{2D}\right) - \frac{1}{2N} \operatorname{tr} \log\left(\frac{m^2}{2D} + \left(1 - \frac{m^2}{2D}\right)\left(-\frac{\bar{\nabla} \cdot \nabla}{2D}\right)\right),$$ (5A.6)

where [compare (5.60)]

$$\frac{m^2}{2D} = 1 - 2D\beta \left(\frac{I_{n/2}(\sqrt{\alpha_a^2})}{I_{n/2-1}(\sqrt{\alpha_a^2})}\right)'$$

$$= 1 - 2D\beta\left\{1 - \frac{n^{-1}}{\alpha}\frac{I_{n/2}}{I_{n/2-1}} - \left(\frac{I_{n/2}}{I_{n/2-1}}\right)^2\right\} = n - 2D\beta(1 - u^2).$$ (5A.7)

At the mean-field level, the internal energy is

$$u'^{\text{MF}} = -Du^2.$$ (5A.8)

For the specific heat we have to calculate

$$\frac{\partial u}{\partial \beta} = -\frac{u}{\beta}\frac{1 - u^2 - \frac{n-1}{2\beta D}}{1 - u^2 - \frac{n}{2\beta D}} = \frac{u}{\beta}\frac{1}{M^2/2D},$$ (5A.9)

so that

$$c^{\text{MF}} = 2\beta Du^2/(M^2/2D),$$ (5A.10)

just as before [see (5.21c)]. The one-loop correction to the internal energy is again

$$u^{1 \text{ loop}} = \frac{1}{2}\frac{\partial(m^2/2D)}{\partial \beta}\frac{1}{1 - \frac{m^2}{2D}}\left(\frac{2D}{1 - \frac{m^2}{2D}}v_M(0) - 1\right).$$ (5A.11)

Since

$$\frac{\partial(m^2/2D)}{\partial\beta} = -2D(1 - u^2) + 4\beta Du\frac{\partial u}{\partial\beta}$$

$$= \frac{1}{m^2/2D}\left[4D\left(1 - \frac{m^2}{2D}\right) - \frac{1}{\beta}\left(2 - \frac{m^2}{2D}\right)^2\right] \qquad (5A.12)$$

does not depend on n, we arrive again at Eq. (5.74). The case of $n = 1$ with s_a taking only the values ± 1 is known as the *Ising model*, which shall be discussed again in Section 10.6.

For small α, $I_{n/2}(\alpha) \sim 1/\Gamma((n/2) + 1)(\alpha/2)^{n/2}$, $I_{n/2}/I_{n/2-1} \sim \alpha/n$, and the critical point in the mean-field approximation is given by

$$2\beta_c^{MF}D/n = 1. \qquad (5A.13)$$

From Fig. 4.5 we see that loop corrections must drive this value *upwards* so that we expect the inequality

$$\beta_c > \frac{n}{2D} \qquad (5A.14)$$

to hold. This can be proved rigorously as shown by Simon and by Lieb (cited in the Notes and References).

Aizenman and Simon and Brydges *et. al.* have sharpened this result to

$$\beta_c > \frac{n}{2D}\left[1 - \frac{1}{(n + 2)D}\right]^{-1}, \qquad (5A.15)$$

which is to be compared with the $1/D$ expansion result

$$\beta_c = \frac{n}{2D}\left[1 - \frac{1}{2D} - \frac{2(n + 2) - 2}{(n + 2)(2D)^2} - \cdots\right] \qquad (5A.16)$$

(see Eq. (5.158)).

For general n, the coefficients in (5.157) are $g_{-1} = -1/2$, $g_0 = 1/n$, $g_2 = -2/Dn^3$, $g_3 = 4/D^2n^4(n + 2)$ and the solution of (5.155) agress with (5A.16) up to order $1/D^3$.

NOTES AND REFERENCES

General mean field methods are reviewed in
J.M. Drouffe, J.B. Zuber, *Phys. Reports* **102** (1983) 1,
and by
B. Lautrup, *Saddle Point Methods in Lattice Field Theories*, Lecture Notes, Niels Bohr Institute, 1982.
For a survey article on effective actions in field theory see
H. Kleinert, *Fortschr. Phys.* **30** (1982) 187.
The effective action methods were adapted to $O(n)$ lattice spin models by
T. Matsui, H. Kleinert, S. Ami, *Phys. Lett.* **143B** (1984) 199*.
    Rigorous inequalities on β_c in $O(n)$ models were derived by
B. Simon, *Commun. Math. Phys.* **77** (1980) 11, *J. Stat. Phys.* **22** (1980) 491,
E. Lieb, *Commun. Math. Phys.* **77** (1980) 127,
M. Aizenmann and B. Simon, *Commun. Math. Phys.* **77** (1980) 137, *Phys. Lett.* **76A** (1980) 281,
D. Brydges, J. Fröhlich and T. Spencer, *Commun. Math. Phys.* **83** (1982) 123,
J. Fröhlich, B. Simon and T. Spencer, *Commun. Math. Phys.* **50** (1976) 79.
    Expansions of β_c in powers of $1/D$ were given by
P.R. Gerber and M.E. Fisher, *Phys. Rev.* **B10** (1974) 4697,
M.E. Fisher and D.S. Gaunt, *Phys. Rev.* **133** (1964) A224.
    Measurements on the superfluid density in ^{4}He can be found in
I. Rudnik, in *Quantum Fluids*, eds. N. Wiser and D.J. Amit (Gordon and Breach, New York, 1970) p. 275,
D.G. Dash and R.D. Taylor, *Phys. Rev.* **105** (1965) 7,
J.R. Clow and J.D. Reppy, *Phys. Rev. Lett.* *16*, 887 (1966),
J.A. Tyson and D.H. Douglas, *Phys. Rev. Lett.* **17** (1966) 472,
J.A. Tyson, *Phys. Rev.* **166**, (1968) 166,
R.H. Romers and R.J. Duffy, *Phys. Rev.* **186** (1969) 255.
The most precise determination of Eq. (5.51) was given by
D.S. Greywall and G. Ahlers, *Phys. Rev. Lett.* **28** (1972) 1251,
who also find the pressure dependence as stated in the discussion following Eq., (5.51) and
V.P. Peshkov, K.N. Zinov'eva, *JETP* **18** (1948) 438.

*The curves shown in Figs. 1–3 of that paper for $D = 3$, $N = 2$ in the $1/D$ expansion contain a slight error. The gap equation (19) gives no solution for $\rho \epsilon 1.44$, so that a small part of the unphysical section of the curves is missing. See Figs 5.10–5.11 for the corrected version!

VORTEX LINES IN THE XY MODEL

In the general discussion in Chapter 2 we argued that superfluid ^{4}He should be describable as an ensemble of vortex lines together with their long-range hydrodynamic interactions. Let us now verify this expectation within the XY model.

6.1. INTEGER-VALUED GAUGE FIELDS

Our starting point is the XY model in $D = 3$ dimensions in the form (4.19) which we shall rewrite as follows,

$$Z' = I_0(\beta)^{3N} \sum_{\{b_i(\mathbf{x})\}} \delta_{\bar{\nabla}_i b_i(\mathbf{x}),0} \, e^{-\sum_{\mathbf{x},i} \log(I_{b_i(\mathbf{x})}(\beta)/I_0(\beta))}. \tag{6.1}$$

In Section 4.3, Fig. 4.1, we interpreted the condition $\bar{\nabla}_i b_i(\mathbf{x}) = 0$ geometrically and showed that it enforces "current conservation" of $b_i(\mathbf{x})$ vectors along the links. There is, however, another interpretation which we shall now explore.

In magnetism, we are familiar with the magnetic field having a vanishing divergence, $\partial_i B_i = 0$. This condition implies that magnetic field lines have no sources but always form closed loops. It is customary to

466

satisfy this condition automatically by introducing a vector potential A_i and setting $B_i = \varepsilon_{ijk} \partial_j A_k$. The magnetic field is invariant under the local gauge transformations

$$A_i(\mathbf{x}) \rightarrow A_i(\mathbf{x}) + \partial_i \Lambda(\mathbf{x}). \tag{6.2}$$

Therefore we have the freedom of fixing a gauge, for example,

$$\partial_i A_i(\mathbf{x}) = 0 \quad \text{(transverse gauge)}, \tag{6.3}$$

$$A_3(\mathbf{x}) = 0 \quad \text{(axial gauge)}. \tag{6.4}$$

It is suggestive to try and interprete the vectors $b_i(\mathbf{x})$ as *integer-valued magnetic fields* and generate the closed field lines by an *integer-valued gauge field* $a_\ell(\mathbf{x})$
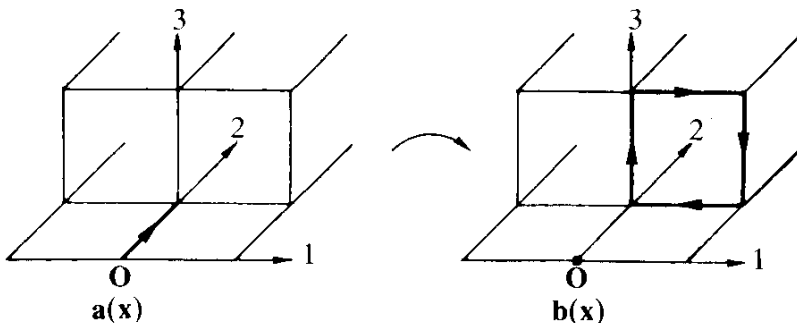
$$b_i(\mathbf{x}) = \varepsilon_{ij\ell} \, \overline{\nabla}_j \, a_\ell(\mathbf{x} - \boldsymbol{\ell}). \tag{6.5}$$

The condition $\overline{\nabla}_i b_i = 0$ follows, as usual, from the antisymmetry of the $\varepsilon_{ij\ell}$ tensor. The right-hand side is a lattice version of the curl operation and will be denoted by $(\overline{\nabla} \times \mathbf{a})_i(\mathbf{x})$. The geometry of this curl operation is illustrated in Fig. 6.1. The shift in the argument of the vector potential by one link is useful since it leads to the invariance of $b_i(\mathbf{x})$ under the following gauge transformation

$$a_\ell(\mathbf{x}) \rightarrow a_\ell(\mathbf{x}) + \nabla_\ell \Lambda(\mathbf{x}). \tag{6.6}$$

Indeed, $a_\ell(\mathbf{x} - \boldsymbol{\ell})$ transforms into $a_\ell(\mathbf{x} - \boldsymbol{\ell}) + \nabla_\ell \Lambda(\mathbf{x} - \boldsymbol{\ell})$ which, due to the identity

FIG. 6.1. Illustration of the lattice curl operation $b_i(\mathbf{x}) = \varepsilon_{ijk} \overline{\nabla}_j a_k (\mathbf{x} - \mathbf{k})$ of Eq. (6.5). An $\mathbf{a}(\mathbf{x})$ field of unit strength on a single link generates a closed loop of unit strength around a plaquette.

$$\nabla_\ell \Lambda(\mathbf{x} - \boldsymbol{\ell}) = \Lambda(\mathbf{x}) - \Lambda(\mathbf{x} - \boldsymbol{\ell}) = \bar{\nabla}_\ell \Lambda(\mathbf{x}), \tag{6.7}$$

implies

$$a_\ell(\mathbf{x} - \boldsymbol{\ell}) \rightarrow a_\ell(\mathbf{x} - \boldsymbol{\ell}) + \bar{\nabla}_\ell \Lambda(\mathbf{x}) \tag{6.8}$$

and the invariance of (6.5) follows from the antisymmetry of the $\varepsilon_{ij\ell}$ tensor.

In order to render the lattice curl relation (6.5) unique, we have to choose a gauge. Unlike the continuum case, however, there is very little freedom in doing this when working with integer fields $a_i(\mathbf{x})$. Consider, for example, the transverse gauge $\bar{\nabla}_\ell a_\ell(\mathbf{x}) = 0$ as a candidate. If the gauge field were continuous it would always be possible to choose this gauge since, if $a_\ell(\mathbf{x})$ did not satisfy $\bar{\nabla}_\ell a_\ell(\mathbf{x}) = 0$, we could always perform a gauge transformation $a_\ell(\mathbf{x}) \rightarrow a'_\ell(\mathbf{x}) = a_\ell(\mathbf{x}) + \nabla_\ell \Lambda(\mathbf{x})$ with

$$\Lambda(\mathbf{x}) = -\frac{1}{\bar{\nabla} \cdot \nabla} \bar{\nabla}_\ell a_\ell(\mathbf{x}), \tag{6.9}$$

such that $\nabla_\ell a'_\ell(\mathbf{x}) = 0$. Here, this is no longer true. For, if we have an integer-valued vector potential $a_\ell(\mathbf{x})$ and if $\Lambda(\mathbf{x})$ is calculated via (6.9), the new field

$$a'_\ell(\mathbf{x}) = a_\ell(\mathbf{x}) + \nabla_\ell \Lambda(\mathbf{x}) \tag{6.10}$$

is no longer integer (even though $\bar{\nabla}_\ell a_\ell(\mathbf{x})$ is) since the lattice Green function applied to an integer source gives in general non-integer numbers (see Part I, Chapter 6, Table 6.9 for $-1/\bar{\nabla} \cdot \nabla$ applied to a source of unit charge at the origin).

This problem does not arise for the axial gauge $a_3(\mathbf{x}) = 0$. If $a_3(\mathbf{x})$ has arbitrary integer values, we can always go to a new vector potential

$$a'_3(\mathbf{x}) = a_3(\mathbf{x}) + \nabla_3 \Lambda(\mathbf{x}), \tag{6.11}$$

which has $a'_3(\mathbf{x}) = 0$, by choosing

$$\Lambda = -\nabla_3^{-1} a_3 \equiv -\sum_{x'_3=0}^{x_3-1} a_3(x_1, x_2, x'_3). \tag{6.12}$$

Since $a_3(\mathbf{x})$ is integer, $\Lambda(\mathbf{x})$ is likewise integer such that $a'_1 = a_1 + \nabla_1 \Lambda$ and $a'_2 = a_2 + \nabla_2 \Lambda$ are also integers.

Certainly, instead of $a_3 = 0$ we can also choose the gauge

$$\mathbf{n} \cdot \mathbf{a}(\mathbf{x}) = 0, \tag{6.13}$$

where $\mathbf{n}$ points in any of the three lattice directions. This is to be contrasted with the axial gauge in the continuum, $\mathbf{n} \cdot \mathbf{A} = 0$, where $\mathbf{n}$ can point into a continuum of spatial directions $\mathbf{n} = (\cos\theta, \sin\theta\cos\varphi, \sin\theta\sin\varphi)$.

The axial condition $a_3(\mathbf{x}) = 0$ is not yet sufficient to fix $a_1(\mathbf{x})$, $a_2(\mathbf{x})$ uniquely in terms of $b_i(\mathbf{x})$. Since

$$b_1 = -\bar{\nabla}_3 a_2(\mathbf{x} - \mathbf{2}), \quad b_2 = \bar{\nabla}_3 a_1(\mathbf{x} - \mathbf{1}), \tag{6.14}$$

$$b_3 = \bar{\nabla}_1 a_2(\mathbf{x} - \mathbf{2}) - \bar{\nabla}_2 a_1(\mathbf{x} - \mathbf{1}), \tag{6.15}$$

we see that we have to specify the boundary condition for $a_2(\mathbf{x})$ and $a_1(\mathbf{x})$. In order to invert the first equation we may choose, for example,

$$a_2(\mathbf{x}_1, \mathbf{x}_2, 0) = 0, \tag{6.16}$$

so that

$$a_2(\mathbf{x}) = -\sum_{x_3' = 0}^{x_3} b_1(x_1, x_2 + 1, x_3'). \tag{6.17}$$

The function $a_1(\mathbf{x})$ cannot, in general, be chosen to satisfy $a_1(x_1, x_2, 0) = 0$, because of the third equation $b_3 = \bar{\nabla}_1 a_2 - \bar{\nabla}_2 a_1$. Instead, we have to solve $b_2 = \bar{\nabla}_3 a_1$ by

$$a_1(\mathbf{x}) = \sum_{x_3' = 0}^{x_3} b_2(x_1 + 1, x_2, x_3') + c(x_1, x_2), \tag{6.18}$$

with an arbitrary integer function $c(x_1, x_2)$, and calculate

$$\bar{\nabla}_1 a_2(\mathbf{x} - \mathbf{2}) - \bar{\nabla}_2 a_1(\mathbf{x} - \mathbf{1}) = \sum_{x_3' = 0}^{x_3} (-\bar{\nabla}_1 b_1 - \bar{\nabla}_2 b_2)(x_1, x_2, x_3') - \bar{\nabla}_2 c(x, x_2)$$

$$= \sum_{x_3' = 0}^{x_3} \bar{\nabla}_3 b_3(x_1, x_2, x_3') - \bar{\nabla}_2 c(x_1, x_2)$$

$$= b_3(x_1, x_2, x_3) - b_3(x_1, x_2, 0) - \bar{\nabla}_2 c(x_1, x_2).$$

$$\tag{6.19}$$

Since this has to be equal to $b_3(x_1, x_2, x_3)$, we must take

$$c(x_1, x_2) = -\sum_{x_2'=0}^{x_2} b_3(x_1, x_2', 0) + d(x_2). \qquad (6.20)$$

The function $d(x_2)$ can be chosen to vanish such that $c(0, x_2) = 0$. Thus we arrive at

$$a_1(\mathbf{x}) = \sum_{x_3'=0}^{x_3} b_2(x_1 + 1, x_2, x_3') - \sum_{x_2'=0}^{x_2} b_3(x_1, x_2', 0). \qquad (6.21)$$

This $a_1(\mathbf{x})$ satisfies the boundary condition

$$a_1(x_1, 0, 0) = 0. \qquad (6.22)$$
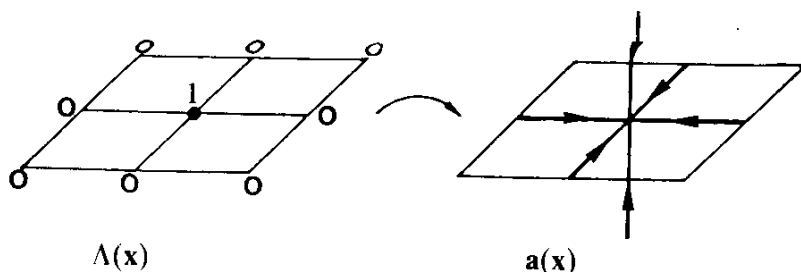
The two conditions, (6.15) and (6.22), specify the $a_3 \equiv 0$ gauge uniquely. This agrees with the obvious fact that we can always add to $a_i(\mathbf{x})$ with $a_3 \equiv 0$ the gradient of an integer function $\Lambda(x_1, x_2)$ to make $a_2(x_1, x_2, 0)$ vanish and, after this, the gradient of a function $\bar{\Lambda}(x_1)$ to also make $a_1(x_1, 0, 0)$ vanish. This completely exhausts the gauge freedom. Geometrically, adding $\nabla_i \Lambda(\mathbf{x})$ amounts to adding a pure source or sink term to the $a_i(\mathbf{x})$ field as illustrated in Fig. 6.2.

With the additional specifications (6.15), (6.22) in mind we can now rewrite the partition function (6.1) as follows:

$$Z' = (I_0(\beta))^{ND} \sum_{\{a_i(\mathbf{x})\}} \delta_{a_3, 0} e^{\sum_{\mathbf{x}, i} \log(I_{(\bar{\nabla} \times \mathbf{a})_i}(\beta)/I_0(\beta))}. \qquad (6.23)$$

It will be convenient to expand the exponent in powers of $(\bar{\nabla} \times \mathbf{a})$. This proceeds in two steps. First, we make use of the representation of the Bessel function,

FIG. 6.2. Illustration of the pure gauge term $a_i(\mathbf{x}) = \nabla_i \Lambda(\mathbf{x})$ with $\Lambda = $ integer which adds to the vector potential a pure "sink" (since $\bar{\nabla} \times \mathbf{a}(\mathbf{x}) = 0$).

$\Lambda(\mathbf{x})$ $\mathbf{a}(\mathbf{x})$

$$I_n(\beta) = \int_{-\pi}^{\pi} \frac{d\gamma}{2\pi} e^{\beta \cos \gamma} \cos n\gamma. \tag{6.24}$$

Expanding this in powers of n gives

$$I_n(\beta) = \sum_{p=0}^{\infty} (-1)^p \frac{n^{2p}}{(2p)!} \int_{-\pi}^{\pi} \frac{d\gamma}{2\pi} e^{\beta \cos \gamma} \gamma^{2p}. \tag{6.25}$$

If we introduce the functions

$$G^{(p)}(\beta) = (-2\beta)^p \frac{1}{I_0(\beta)} \frac{p!}{(2p)!} \int_{-\pi}^{\pi} \frac{d\gamma}{2\pi} e^{\beta \cos \gamma} \gamma^{2p}, \tag{6.26}$$

we arrive at the series

$$\frac{I_n(\beta)}{I_0(\beta)} = \sum_{p=0}^{\infty} \frac{(-1)^p}{(2\beta)^p} \frac{G^{(p)}(\beta)}{p!} (n^2)^p. \tag{6.27}$$

The functions $G^{(p)}(\beta)$ can be calculated explicitly by expanding

$$e^{\beta \cos \gamma} = I_0(\beta) + 2 \sum_{n=1}^{\infty} I_n(\beta) \cos n\gamma, \tag{6.28}$$

so that

$$G^{(p)}(\beta) = (2\beta)^p \frac{p!}{(2p)!} \left[\frac{\pi^{2p}}{2p+1} + 2 \sum_{n=1}^{\infty} \left(\int_{-\pi}^{\pi} \frac{d\gamma}{2\pi} \gamma^{2p} \cos n\gamma \right) \frac{I_n(\beta)}{I_0(\beta)} \right]. \tag{6.29}$$

The integral is given by

$$\int_{-\pi}^{\pi} \frac{d\gamma}{2\pi} \gamma^{2p} \cos n\gamma = \frac{(2p)!}{2\pi} \sum_{k=0}^{2p} \frac{1}{(2p-k)!} \frac{\gamma^{2p-k}}{n^{k+1}} \sin \left(n\gamma + \frac{k\pi}{2} \right) \Bigg|_{-\pi}^{\pi}$$

$$= \frac{(2p)!}{\pi} \sum_{k=1,3}^{2p-1} \frac{(-1)^{n+(k-1)/2}}{(2p-k)!} \frac{\pi^{2p-k}}{n^{k+1}}. \tag{6.30}$$

For $p = 1, 2, 3, \ldots$ this amounts to

$$\int_{-\pi}^{\pi} \frac{d\gamma}{2\pi} \gamma^2 \cos n\gamma = 2\frac{(-1)^n}{n^2},$$

$$\int_{-\pi}^{\pi} \frac{d\gamma}{2\pi} \gamma^4 \cos n\gamma = 4\frac{(-1)^n}{n^2}(\pi^2 - 6/n^2),$$

$$\int_{-\pi}^{\pi} \frac{d\gamma}{2\pi} \gamma^6 \cos n\gamma = 6\frac{(-1)^n}{n^2}(\pi^4 - 20\pi^2/n^2 + 120/n^4), \qquad (6.31)$$

so that

$$G^{(1)}(\beta) = \beta\left[\frac{\pi^2}{3} - 4\sum_{n=1}^{\infty} \frac{(-)^{n-1}}{n^2}\frac{I_n(\beta)}{I_0(\beta)}\right],$$

$$G^{(2)}(\beta) = \frac{\beta^2}{3}\left[\frac{\pi^4}{5} - 8\sum \frac{(-)^{n-1}}{n^2}(\pi^2 - 6/n^2)\frac{I_n(\beta)}{I_0(\beta)}\right],$$

$$G^{(3)}(\beta) = \frac{\beta^3}{15}\left[\frac{\pi^6}{7} - 12\sum_{n=1}^{\infty} \frac{(-)^{n-1}}{n^2}(\pi^4 - 20\pi^2/n^2 + 120/n^4)\frac{I_n(\beta)}{I_0(\beta)}\right],$$

$$\vdots \qquad \qquad \vdots \qquad \qquad \vdots$$

$$G^{(p)}(\beta) = \frac{\beta^p}{(2p-1)!!}\left[\frac{\pi^{2p}}{2p+1} - 4p\sum_{n=1}^{\infty} \frac{(-)^{n-1}}{n^2}\right.$$

$$\left. \times \left(\pi^{2p-2} - \frac{(2p-1)!}{(2p-3)!}\frac{\pi^{2p-4}}{n^2} + \frac{(2p-1)!}{(2p-5)!}\frac{\pi^{2p-6}}{n^4} - \cdots\right)\frac{I_n(\beta)}{I_0(\beta)}.$$

$$(6.32)$$

These expansions converge rapidly for $\beta \ll 1$. In Table 6.1 we have listed a few of them. For $\beta \gg 1$ it is more convenient to extract $G^{(p)}(\beta)$ directly from the large β expansion of the Bessel functions, which reads

$$I_n(\beta) \rightarrow \frac{e^\beta}{\sqrt{2\pi\beta}}\left\{1 + \frac{n^2 - \frac{1}{4}}{(-2\beta)} + \frac{1}{2!}\frac{1}{(-2\beta)^2}\left(n^2 - \frac{1}{4}\right)\left(n^2 - \frac{9}{4}\right)\right.$$

$$\left. + \frac{1}{3!}\frac{1}{(-2\beta)^3}\left(n^2 - \frac{1}{4}\right)\left(n^2 - \frac{9}{4}\right)\left(n^2 - \frac{25}{4}\right) + \cdots\right.$$

$$= I_0(\beta) + n^2\frac{e^\beta}{\sqrt{2\pi\beta}}\left\{-\frac{1}{2\beta} - \frac{1}{2!}\frac{1}{(2\beta)^2}\frac{10}{4} - \frac{1}{3!}\frac{1}{(2\beta)^3}\right.$$

$$\left. \times \left(\frac{1}{4}\frac{9}{4} + \frac{1}{4}\frac{25}{4} + \frac{9}{4}\frac{25}{4}\right) + \cdots\right\} +$$

TABLE 6.1. The coefficients in the cumulant expansion of the magnetic field energy of the *XY* model $\sum_{p=1}^{x} \frac{G_c^{(p)}(\beta)}{p!} \frac{1}{(-2\beta)^p} (\bar{\nabla} \times \mathbf{A})^{2p}$.

β	$G_c^{(1)}(\beta) = G^{(1)}(\beta)$	$G^{(2)}(\beta)$	$G_c^{(2)}(\beta) = G^{(2)} - G^{(1)^2}$
0.1	0.30914	0.05985	−0.0357
0.2	0.57935	0.21978	−0.1159
0.3	0.81221	0.45213	−0.2076
0.4	1.0098	0.73210	−0.2875
0.5	1.1744	1.0381	−0.3411
0.6	1.3089	1.3520	−0.3612
0.7	1.4161	1.6591	−0.3463
0.8	1.4991	1.9480	−0.2993
0.9	1.5608	2.2106	−0.2256
1.0	1.6043	2.4414	−0.1322
1.1	1.6321	2.6374	−0.0264
1.2	1.6470	2.7975	−0.0849
1.3	1.65129	2.9225	−0.1957

$$+ n^4 \frac{e^\beta}{\sqrt{2\pi\beta}} \left\{ \frac{1}{2!(2\beta)^2} + \frac{1}{3!} \frac{1}{(2\beta)^3} \left(\frac{1}{4} + \frac{9}{4} + \frac{25}{4} \right) + \ldots \right\} + \ldots$$

$$= I_0(\beta) \left(1 - \frac{n^2}{2\beta} G^{(1)}(\beta) + \frac{n^4}{2!(2\beta)^2} G^{(2)}(\beta) + \ldots \right). \tag{6.33}$$

The result is tabulated in Table 6.2.

Now we proceed to the second step. For the partition function (6.23) we have to find the power series expansion of the logarithm of the series (6.27). Let us denote its coefficients by $G_c^{(p)}$, i.e.,

$$\log \sum_{p=0}^{\infty} \frac{(-1)^p}{(2\beta)^p} \frac{G^{(p)}(\beta)}{p!} (n^2)^p \equiv \sum_{p=0}^{\infty} \frac{(-1)^p}{(2\beta)^p} \frac{G_c^{(p)}(\beta)}{p!} (n^2)^p. \tag{6.34}$$

Identifying n^2 with j and calling the two series $Z(j)$ and $W(j)$, respectively, we see that $G^{(p)}$ and $G_c^{(p)}$ are related to each other in the same way as the connected and disconnected correlation functions $G^{(n)}$ and $G_c^{(n)}$ are in Part I, Eqs. (4.40), (4.41) which means that the $G_c^{(p)}$'s are the cumulants of the $G^{(p)}$'s [recall Eq. (4.45)]:

$$G_c^{(1)} = G^{(1)},$$
$$G_c^{(2)} = G^{(2)} - G^{(1)2},$$
$$G_c^{(3)} = G^{(3)} - 3G^{(2)} G^{(1)} + 2G^{(1)3}$$
$$G_c^{(4)} = G^{(4)} - 4G^{(3)} G^{(1)} + 12G^{(2)} G^{(1)2} - 3G^{(2)2} - 6G^{(1)4}. \tag{6.35}$$

TABLE 6.2. Large β series for coefficients of the cumulant expansion of magnetic field energy in the XY model.

	1	β^{-1}	β^{-2}	β^{-3}	β^{-4}
$I_0(\beta)e^{-\beta}\sqrt{2\pi\beta}$	1	$\dfrac{1}{2^3}$	$\dfrac{3^2}{2^7}$	$\dfrac{3\cdot 5^2}{2^{10}}$	$\dfrac{3\cdot 5^2\cdot 7^2}{2^{15}}$
$I_0^{-1}(\beta)e^{\beta}\sqrt{2\pi\beta^{-1}}$	1	$-\dfrac{1}{2^3}$	$-\dfrac{7}{2^7}$	$-\dfrac{59}{2^{10}}$	$-\dfrac{23\cdot 131}{2^{15}}$
$G^{(1)}(\beta) = G_c^{(1)}(\beta)$	1	$\dfrac{1}{2}$	$\dfrac{13}{3\cdot 2^3}$	$\dfrac{7}{2^3}$	$\dfrac{1187}{5\cdot 2^7}$
$G^{(2)}(\beta)$	1	$\dfrac{2^2}{3}$	$\dfrac{7}{3}$	$\dfrac{31}{3\cdot 2}$	$\dfrac{1249}{3^2\cdot 5\cdot 2}$
$G^{(3)}(\beta)$	1	$\dfrac{5}{2}$	$\dfrac{7\cdot 37}{5\cdot 2^3}$	$\dfrac{457}{3\cdot 2^3}$	$\dfrac{41^2\cdot 73}{3\cdot 5\cdot 2^7}$
$G_c^{(2)}(\beta)$	0	$\dfrac{1}{3}$	1	$\dfrac{23}{2^3}$	3^2
$G_c^{(3)}(\beta)$	0	0	$\dfrac{3}{5}$	4	$\dfrac{3\cdot 5\cdot 11}{3^3}$

Notice that for large β, the second and third cumulants start out with $G_c^{(2)} \sim 1/(3\beta)$ and $G_c^{(3)} = -3/5\beta^2$ due to a cancellation of the leading terms. With (6.34) we can rewrite the partition function (6.23) in the form

$$Z' = I_0(\beta)^{ND} \sum_{\{a_i(\mathbf{x})\}} \delta_{a_3,0}\, e^{\sum_{\mathbf{x},i}[\sum_p(-1)^p|G_c^{(p)}(\beta)/(2\beta)^p p!](\bar{\nabla}\times\mathbf{a})_i^{2p}}, \qquad (6.36)$$

which will be important in the following discussion.

6.2. VORTEX LINES

The representation (6.36) is the starting point for the introduction of vortex lines. For this purpose, let us recall a very simple formula used in

the theory of diffraction of light behind a fine grating: the amplitude of the diffracted light is obtained from a sum of the phases of the type

$$\sum_{\ell=-\infty}^{\infty} e^{2\pi i \ell A},$$

where $2\pi i A$ is the phase difference between the individual light waves. It leads to a diffraction pattern which consists of a regular array of infinitely sharp maxima

$$\sum_{\ell=-\infty}^{\infty} e^{2\pi i \ell A} = \sum_{a=-\infty}^{\infty} \delta(A - a). \qquad (6.37)$$

This formula is commonly referred to as *Poisson formula*. The sum over infinitely many integers ℓ with the phase $e^{2\pi i A}$ forces the real numbers A to become integers.

Poisson's formula makes it possible to replace a sum over integer vector fields a by an integral over continuous fields at the expense of an extra sum over integers. The fundamental formula to be used is

$$\sum_{a=-\infty}^{\infty} = \int_{-\infty}^{\infty} dA \sum_{\ell=-\infty}^{\infty} e^{2\pi i \ell A},$$

or, more specifically adapted to the sum appearing in (6.36),

$$\sum_{\{a_i(\mathbf{x})\}} \delta_{a_3, 0} = \prod_{\mathbf{x}} \left[\int_{-\infty}^{\infty} dA_1(\mathbf{x}) \, dA_2(\mathbf{x}) \right] \sum_{\{\ell_i(\mathbf{x})\}} \delta_{\ell_3, 0} \, e^{2\pi i \sum_{\mathbf{x}} \ell_i(\mathbf{x}) A_i(\mathbf{x})}. \qquad (6.38)$$

When doing the sum over $\ell_i(\mathbf{x})$ we have to remember that the fields $A_2(x_1, x_2, 0)$ and $A_1(x_1, 0, 0)$ vanish in the gauge $A_3(\mathbf{x}) = 0$ [see (6.15), (6.22)]. Hence the corresponding $\ell_2(x_1, x_2, 0)$, $\ell_1(x_1, 0, 0)$ must be omitted from the sum so as to avoid infinite overall factors. This will tacitly be assumed in writing $\sum_{\{\ell_i(\mathbf{x})\}} \delta_{\ell_3, 0}$.

The vortex line representation of the partition function is now obtained from the observation that since A_3 vanishes, the restriction $\ell_3(\mathbf{x}) = 0$ can be lifted and the two-component integer field $\ell_1(\mathbf{x})$, $\ell_2(\mathbf{x})$ can be extended by a dummy third component $\ell_3(\mathbf{x})$ as long as there is a *unique* assignment of $\ell_3(\mathbf{x})$ for every pair $\ell_1(\mathbf{x})$, $\ell_2(\mathbf{x})$. A particularly attractive

choice is one in which the three vectors $\ell_1(\mathbf{x})$, $\ell_2(\mathbf{x})$, $\ell_3(\mathbf{x})$ are chosen so as to satisfy the divergence condition

$$\bar{\nabla}_i \ell_i(\mathbf{x}) = 0. \tag{6.39}$$

Then the field $\ell_i(\mathbf{x})$ is associated with all unit valued non-backtracking closed loops on the lattice. Formally, all we have to do is define $\ell_3(\mathbf{x})$ by
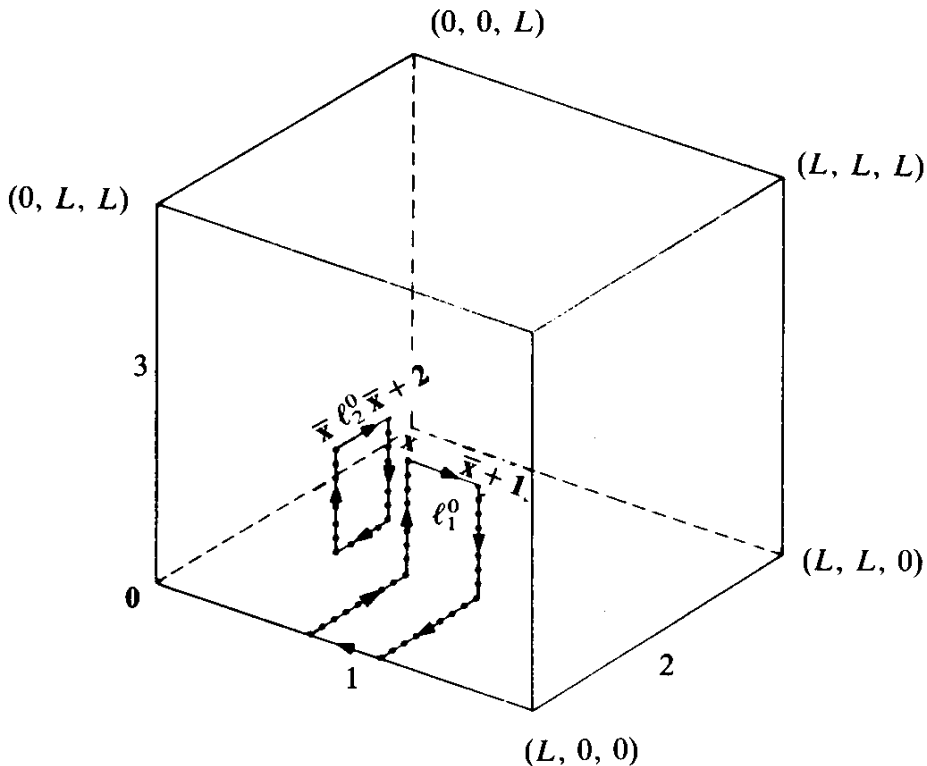
$$\ell_3(\mathbf{x}) = -\frac{1}{\bar{\nabla}_3}(\bar{\nabla}_1 \ell_1(\mathbf{x}) + \bar{\nabla}_2 \ell_2(\mathbf{x})). \tag{6.40}$$

With an appropriate boundary condition this equation yields integer values of $\ell_3(\mathbf{x})$ and the sum (6.38) becomes

$$\sum_{\{a_i(\mathbf{x})\}} \delta_{a_3,0} = \prod_{\mathbf{x}} \left[\int_{-\infty}^{\infty} dA_1(\mathbf{x}) dA_2(\mathbf{x}) \right] \sum_{\{\ell_i(\mathbf{x})\}} \delta_{\nabla_i \ell_i(\mathbf{x}),0} e^{2\pi i \sum_{\mathbf{x}} \ell_i(\mathbf{x}) A_i(\mathbf{x})}. \tag{6.41}$$

In a finite volume, the construction of $\ell_3(\mathbf{x})$ via (6.40) requires some care in order that the loops really close. Let $x_i = 0$, $L(i = 1, \ldots, D)$ be the boundaries of a finite cubic system (see Fig. 6.3) and consider an arbitrary

FIG. 6.3. Illustration of the construction of closed loops $\bar{\nabla}_i \ell_i(\mathbf{x}) = 0$ from a sum over arbitrary line pieces $\ell_1^0(\mathbf{x})$, $\ell_2^0(\mathbf{x})$ in the gauge $A_3 \equiv 0$, $A_2(x_1, x_2, 0) = 0$, $A_1(x_1, 0, 0) = 0$. For details see Eqs. (6.42)–(6.47).

integer $\ell_2^0(\bar{\mathbf{x}})$ sitting on the link 2 emerging from the point $\bar{\mathbf{x}}$ with $\bar{x}_3 \neq 0$ (otherwise $\ell_2^0 = 0$ by assumption). Let us project the end points $\bar{\mathbf{x}}$, $\bar{\mathbf{x}} + 2$ of this link into the plane $x_3 = 0$ and assign, to all links 3 along the lines of the projection, down to the plane $x_3 = 0$, the occupation numbers $\ell_3(\mathbf{x}) = \pm|\ell_2^0(\bar{\mathbf{x}})|$, and to the link 2 in the plane $x_3 = 0$ the number $\ell_2(\mathbf{x}) = -|\ell_2^0(\bar{\mathbf{x}})|$. The orientations are shown in Fig. 6.3. The newly assigned values $\ell_3(\mathbf{x})$, $\ell_2(x_1, x_2, 0)$ do not couple to $A_i(x)$ due to the gauge $A_3 = 0$ and the boundary condition (6.15).

Mathematically, this construction can be described as follows: Let us define, for this particular purpose, the inverse gradients $1/\bar{\nabla}_i$ as the sums

$$\frac{1}{\bar{\nabla}_3} f(\mathbf{x}) \equiv \left(\frac{1}{\bar{\nabla}_3} f\right)(\mathbf{x}) \equiv -\sum_{x_3'=x_3+1}^{L} f(x_1, x_2, x_3'), \qquad (6.42)$$

which satisfy the boundary condition $((1/\bar{\nabla}_3)f)(x_1, x_2, L) = 0, \ldots$. Then defining $\ell_2^0(\mathbf{x}) \equiv \delta_{\mathbf{x},\bar{\mathbf{x}}} \ell_2^0(\bar{\mathbf{x}})$, we form

$$\ell_3(\mathbf{x}) = -\frac{1}{\bar{\nabla}_3} \bar{\nabla}_2 \ell_2^0(\mathbf{x}). \qquad (6.43)$$

This sum creates the string of $\pm\ell_2^0$ along the links on the dotted lines in Fig. 6.3. At the boundary $x_3 = 0$, the ℓ_3's have $\bar{\nabla}_3 \ell_3 \neq 0$, and we can close the loop by taking

$$\ell_2 = -\frac{1}{\bar{\nabla}_2} \bar{\nabla}_3 \ell_3. \qquad (6.44)$$

If the initial link $\ell^0(\bar{\mathbf{x}})$ points along the 1 direction, we can again form the projection down into the $x_3 = 0$ plane via

$$\ell_3 = -\frac{1}{\bar{\nabla}_3} \bar{\nabla}_1 \ell_1^0. \qquad (6.45)$$

But these ℓ_3 vectors have $\bar{\nabla}_3 \ell_3 \neq 0$ with the ends pointing along the 1 direction such that they cannot be closed into a loop without consequences due to (6.15). A further projection onto the 1 axis is necessary with

$$\ell_2 = -\frac{1}{\overline{\nabla}_2} \overline{\nabla}_3 \, \ell_3. \tag{6.46}$$

The end points of this projection lie on the **1** axis and can finally be connected to a loop by

$$\ell_1 = -\frac{1}{\overline{\nabla}_1} \overline{\nabla}_2 \, \ell_2, \tag{6.47}$$

which does not couple to $a_i(\mathbf{x})$, due to (6.22). In this way, we can form closed loops for any choice of $\ell_2^0(\mathbf{x})$ which does not lie on the lower face $(x_1, x_2, 0)$ and of $\ell_1^0(\mathbf{x})$ which does not lie on the x_1 axis. This set of $\ell_1^0(\mathbf{x})$, $\ell_2^0(\mathbf{x})$ values coincides precisely with the set of $\ell(\mathbf{x})$'s contained in the sum $\Sigma_{\{\ell_i(\mathbf{x})\}} \delta_{\ell_3, 0}$. We have therefore proved that this sum is equivalent to a sum over closed loops constructed in the above way.

Sums over integer-valued fields $\ell_i(\mathbf{x})$ with $\overline{\nabla}_i \ell_i(\mathbf{x}) = 0$ have been encountered before in (4.19). There they carried the name $b_i(\mathbf{x})$ and appeared as sums over all non-backtracking closed random chains of superflow of unit strength. In the present context, these closed chains will describe the closed vortex lines of the XY model.

The fact that the integrals (6.41) are asymmetric in $A_1(\mathbf{x})$, $A_2(\mathbf{x})$, $A_3(\mathbf{x})$ and are taken only over $A_1(\mathbf{x})$, $A_2(\mathbf{x})$ has no adverse consequence due to the gauge invariance of the coupling $2\pi i \, \Sigma_{\mathbf{x}} \, \ell_i(\mathbf{x}) A_i(\mathbf{x})$ under

$$A_i(\mathbf{x}) \to A_i(\mathbf{x}) + \nabla_i \Lambda(\mathbf{x}). \tag{6.48}$$

Such an invariance always requires gauge fixing. In the integral (6.41), the gauge-fixing functional is

$$\Phi[A] = \prod_{\mathbf{x}} \delta(A_3(\mathbf{x})) \tag{6.49}$$

and we can write the integration measure as

$$\prod_{\mathbf{x}} \left[\int_{-\infty}^{\infty} dA_1(\mathbf{x}) \, dA_2(\mathbf{x}) \right] = \prod_{\mathbf{x}, i} \left[\int_{-\infty}^{\infty} dA_i(\mathbf{x}) \, \Phi[A] \right]. \tag{6.50}$$

From the general discussion in Part I, Section 3.2 we know that instead of

$\Phi[\mathbf{A}]$ we can use any other gauge-fixing factor as long as it has the same normalization integral

$$\prod_{\mathbf{x}} \left[\int d\Lambda(\mathbf{x}) \right] \Phi[A^{\Lambda}] \tag{6.51}$$

[recall the discussion leading to Eq. (3.39) in Part I]. In the present case this integral has the value

$$\prod_{\mathbf{x}} \left[\int d\Lambda(\mathbf{x}) \right] \Phi[A_3 + \nabla_3 \Lambda] = (\det \nabla_3)^{-1} = \det(-\bar{\nabla}_3 \nabla_3)^{-1/2}. \tag{6.52}$$

The last step follows from the fact that (for $a = 1$)

$$\det \nabla_3 = \prod_{\mathbf{k}} i K_3 = \prod_{\mathbf{k}} (e^{i k_3} - 1) = \prod_{\mathbf{k}} \sqrt{(e^{i k_3} - 1)(e^{-i k_3} - 1)} = \prod_{\mathbf{k}} \sqrt{\bar{K}_3 K_3}. \tag{6.53}$$

This product can be easily calculated. By rewriting it as

$$\det(-\bar{\nabla}_3 \nabla_3) = e^{\sum_k \log \bar{K}_3 K_3} = e^{\int (d^D k/(2\pi)^D) \log(2 - 2\cos k_3)} = e^{\int (dk_3/2\pi) \log(2 - 2\cos k_3)}, \tag{6.54}$$

we see that it is equal to the determinant of $-\bar{\nabla} \cdot \nabla$ in $D = 1$ dimension which, according to Part I, Eq. (6.204), is equal to unity. Hence any gauge-fixing factor is acceptable as long as it satisfies

$$\prod_{\mathbf{x}} \left[\int d\Lambda(\mathbf{x}) \right] \Phi[\mathbf{A}^{\Lambda}] = 1, \tag{6.55}$$

where $\mathbf{A}^{\Lambda}$ is the gauge transformed vector potential $\mathbf{A} + \nabla \Lambda$. As an example, we may choose the gauge $\bar{\nabla} \cdot \mathbf{A}(\mathbf{x}) = 0$. The corresponding gauge-fixing factor satisfying the normalization condition (6.55) is

$$\Phi[\mathbf{A}] = \det(-\bar{\nabla} \cdot \nabla) \prod_{\mathbf{x}} \delta(\bar{\nabla}_i A_i) \tag{6.56}$$

since

$$\sum_{\mathbf{x}} \left[\int d\Lambda(\mathbf{x}) \right] \Phi[\mathbf{A}^\Lambda] = \det(-\bar{\nabla} \cdot \nabla) \prod_{\mathbf{x}} \left[\int d\Lambda(\mathbf{x}) \, \delta(\bar{\nabla} \cdot \mathbf{A} + \bar{\nabla} \cdot \nabla \Lambda(\mathbf{x})) \right] = 1.$$

(6.57)

Thus we have the general identity

$$\sum_{\{a_i(\mathbf{x})\}} \delta_{a_3, 0} = \prod_{\mathbf{x}, i} \left[\int_{-\infty}^{\infty} dA_i(\mathbf{x}) \right] \Phi[\mathbf{A}] \sum_{\{\ell_i(\mathbf{x})\}} \delta_{\bar{\nabla} \cdot \ell, 0} \, e^{2\pi i \Sigma_{\mathbf{x}} \ell_i(\mathbf{x}) A_i(\mathbf{x})}. \quad (6.58)$$

This identity allows us to rewrite the partition function (6.36) in the form

$$Z' = (I_0(\beta))^{3N} \prod_{\mathbf{x}, i} \left[\int_{-\infty}^{\infty} dA_i(\mathbf{x}) \right] \Phi[\mathbf{A}] \, e^{\Sigma_{\mathbf{x}, i} \Sigma_p [G_c^{(p)}(\beta)/(-2\beta)^p p!] (\nabla \times \mathbf{A})_i^{2p}}$$

$$\times \sum_{\{\ell_i(\mathbf{x})\}} \delta_{\bar{\nabla} \cdot \ell, 0} \, e^{2\pi i \Sigma_{\mathbf{x}} \ell_i(\mathbf{x}) A_i(\mathbf{x})}. \quad (6.59)$$

This is the desired vortex line representation of the XY model. In the $p = 1$ term of the first exponent we recognize the superflow energy written in terms of the gauge field $A_i(\mathbf{x})$, just as described in the qualitative discussion earlier in Chapter 2 [recall Eq. (2.6)]. The higher p terms account for the non-linear corrections. They grow important only near the vortices where $b_i(\mathbf{x})$ is large. Recall that in Chapter 2 we had to assume that the vortex lines were far enough separated to allow for a clear identification of a far zone and a near zone, which was parametrized by a core energy. In the present lattice model, the validity of this assumption can be investigated. From what we have learned in Chapter 4 we expect the splitting to be ideally realized at zero temperature where vortex lines are infinitely thin (remember $M \to \infty$ for $T \to 0$ so that the correlation length of the size fluctuations of the order parameter, which governs the thickness of vortex lines becomes infinitely small). Then there are very few vortex lines and the entire crystal consists of the "far zone." There, the approximate description of Chapter 2 becomes exact. Let us study this.

6.3. FORMAL LOW TEMPERATURE LIMIT OF THE VORTEX-LINE REPRESENTATION

In Table 6.2 we listed the low temperature behaviour of the coefficients $G_c^{(p)}(\beta)$ of $(\bar{\nabla} \times \mathbf{A})^{2p}(\mathbf{x})$ as follows

$$G_c^{(1)}(\beta) = 1 + O\left(\frac{1}{\beta}\right), \tag{6.60}$$

$$G_c^{(2)}(\beta) = \frac{1}{3\beta} + O\left(\frac{1}{\beta^2}\right), \tag{6.61}$$

$$G_c^{(3)}(\beta) = -\frac{3}{5\beta^2} + O\left(\frac{1}{\beta^3}\right). \tag{6.62}$$

Hence, formally, the large β limit of the field energy in the exponent of (6.59) is dominated by the first term $-(1/2\beta)(\bar{\nabla} \times \mathbf{A})^2$ and the *XY* model has the limiting low temperature representation

$$Z' \xrightarrow[\beta\to\infty]{} (I_0(\beta))^{ND} \prod_{\mathbf{x},i}\left[\int dA_i(\mathbf{x})\right] \Phi[\mathbf{A}]\, e^{-(1/2\beta)\Sigma_{\mathbf{x}}(\bar{\nabla}\times\mathbf{A})^2} \sum_{\{\ell_i(\mathbf{x})\}} \delta_{\bar{\nabla}_i\ell_i,0}\, e^{2\pi i\Sigma_{\mathbf{x}}\ell_i(\mathbf{x})A_i(\mathbf{x})}. \tag{6.63}$$

This is precisely of the form derived before in Chapter 2 via approximate arguments. The energy $(1/2\beta)(\bar{\nabla} \times \mathbf{A})^2$ is the elastic energy $(\rho_s/2)\, v_s^2$ in the far zone when expressed in a gauge-field representation on the lattice. The coupling to the integer values $\ell_i(\mathbf{x})$ is the minimal gauge invariant coupling to all non-backtracking random loops of unit strength.

In the formal low temperature representation (6.63) it is now possible to integrate out the vector potential using the rules developed before in Part I, Section 3.1. Choosing the gauge factor (6.49) we have to evaluate

$$\prod_{\mathbf{x}}\left[\int_{-\infty}^{\infty} dA_1(\mathbf{x})\, dA_2(\mathbf{x})\right] e^{-(1/2\beta)\Sigma_{\mathbf{x}}(\bar{\nabla}\times\mathbf{A})^2 + 2\pi i\Sigma_{\mathbf{x}}\ell_i(\mathbf{x})A_i(\mathbf{x})} \tag{6.64}$$

with $A_3(\mathbf{x}) \equiv 0$. In momentum space, the gradient energy is equal to

$$\frac{1}{2\beta}\sum_{\mathbf{k}}(\bar{\mathbf{K}}\cdot\mathbf{K}\,\delta_{ij}^{\perp} - K_i^{\perp}\,\bar{K}_j^{\perp})\, A_i^{\perp *}(\mathbf{k})\, A_j^{\perp}(\mathbf{k}), \tag{6.65}$$

where $A_i^{\perp}$ and $K_i^{\perp}$ denote the components in the 1 and 2 directions and $\delta_{ij}^{\perp}$ is the unit matrix in this subspace. The matrix between the $A_i^{\perp}$ fields is inverted by adding and subtracting $\bar{\mathbf{K}}\cdot\mathbf{K}K_i^{\perp}\,\bar{K}_j^{\perp}/\bar{\mathbf{K}}^{\perp}\cdot\mathbf{K}^{\perp})$ and observing that

$$\overline{K} \cdot K \left(\delta_{ij}^{\perp} - \frac{K_i^{\perp} \overline{K}_j^{\perp}}{\overline{K}^{\perp} \cdot K^{\perp}} \right) + (\overline{K} \cdot K - \overline{K}^{\perp} \cdot K^{\perp}) \frac{K_i^{\perp} K_j^{\perp}}{\overline{K}^{\perp} \cdot K^{\perp}} \qquad (6.66)$$

is a decomposition according to the orthogonal 2×2 projection matrices. Thus $\overline{K} \cdot K$ and $\overline{K} \cdot K - \overline{K}^{\perp} \cdot K^{\perp} = \overline{K}_3 K_3$ are the eigenvalues, so that

$$\frac{1}{\overline{K} \cdot K} \left(\delta_{ij} - \frac{K_i^{\perp} \overline{K}_j^{\perp}}{K^{\perp} \cdot \overline{K}^{\perp}} \right) + \frac{1}{K_3 \overline{K}_3} \frac{K_i^{\perp} \overline{K}_j^{\perp}}{K^{\perp} \cdot \overline{K}^{\perp}} = \frac{1}{\overline{K} \cdot K} \left(\delta_{ij} + \frac{1}{\overline{K}_3 K_3} K_i^{\perp} \overline{K}_j^{\perp} \right) \qquad (6.67)$$

is the inverse. After quadratic completion the integral (6.64) becomes

$$(\sqrt{2\pi\beta})^{2N} \det(-\overline{\nabla}_3 \nabla_3)^{-1/2} \det(-\overline{\nabla} \cdot \nabla)^{-1/2}$$

$$\times \sum_{\ell_i(\mathbf{x})} \delta_{\overline{\nabla}_i \ell_i, 0} \, e^{-\beta(4\pi^2/2) \Sigma_k \ell_i^{\perp}(\mathbf{k})^* (1/\overline{K} \cdot K)(\delta_{ij} + (1/\overline{K}_3 K_3) K_i^{\perp} \overline{K}_j^{\perp}) \ell_j^{\perp}(\mathbf{k})} \qquad (6.68)$$

where the product of eigenvalues $K_3 \overline{K}_3$, $\mathbf{K} \cdot \overline{\mathbf{K}}$ give rise to the determinants. Now, the divergence condition for $\ell_i(\mathbf{x})$ reads, in momentum space,

$$\overline{K}_i \ell_i(\mathbf{k}) = 0, \qquad (6.69)$$

or

$$\overline{K}_i^{\perp} \ell_i^{\perp}(\mathbf{k}) = -\overline{K}_3 \ell_3(\mathbf{k}), \qquad (6.70)$$

so that the exponent becomes

$$e^{-\beta(4\pi^2/2) \Sigma_k \ell_i^*(\mathbf{k})(1/\overline{K} \cdot K) \ell_i(\mathbf{k})} = e^{-\beta(4\pi^2/2) \Sigma_{\mathbf{x}, \mathbf{x}'} \ell_i(\mathbf{x}) v(\mathbf{x} - \mathbf{x}') \ell_i(\mathbf{x}')}, \qquad (6.71)$$

where $v(\mathbf{x} - \mathbf{x}') = -(\overline{\nabla} \cdot \nabla)^{-1}(\mathbf{x}, \mathbf{x}')$ is the Coulomb Green function on the lattice. With the determinant of $-\overline{\nabla}_3 \nabla_3$ being equal to unity [see Eq. (I.6.204)], the partition function (6.63) takes the form

$$Z' \xrightarrow[\beta \to \infty]{} I_0(\beta)^{3N} (\sqrt{2\pi\beta})^{2N} \det(-\overline{\nabla} \cdot \nabla)^{-1/2} \sum_{\{\ell_i(\mathbf{x})\}} \delta_{\overline{\nabla}_i \ell_i, 0} e^{-\beta(4\pi^2/2) \Sigma_{\mathbf{x}, \mathbf{x}'} \ell_i(\mathbf{x}) v(\mathbf{x} - \mathbf{x}') \ell_i(\mathbf{x}')}. \qquad (6.72)$$

This is the partition function of a grand canonical ensemble of vortex lines on a lattice just as the one derived previously for the idealized lines

in the continuum. The lattice formulation has brought about the same expression as in the continuum by going to the limit of low temperature in which the separation between vortex lines is very large.

As a check of the normalization factor, let us repeat the calculation with the transverse gauge fixing (6.56):

$$\prod_{\mathbf{x},i}\left[\int dA_i(\mathbf{x})\right]\Phi[\mathbf{A}]\,e^{-(1/2\beta)\Sigma_{\mathbf{x}}(\bar{\nabla}\times\mathbf{A})^2+2\pi i\Sigma_{\mathbf{x}}\,\ell_i(\mathbf{x})\,A_i(\mathbf{x})}. \tag{6.73}$$

Writing with $\varepsilon \approx 0$

$$\prod_{\mathbf{x}}\delta(\bar{\nabla}_i A_i)=\prod_{\mathbf{x}}\frac{1}{\sqrt{2\pi\beta\varepsilon}}\,e^{(1/2\beta\varepsilon)\Sigma_{\mathbf{x}}(\bar{\nabla}\times\mathbf{A})^2}, \tag{6.74}$$

we have in **k**-space

$$\det(-\bar{\nabla}\cdot\nabla)\prod_{\mathbf{x},i}\left[\frac{1}{\sqrt{2\pi\beta\varepsilon}}\int dA_i(\mathbf{x})\right]e^{-(1/2\beta)\Sigma_{\mathbf{k}}A_i^*(\mathbf{k})(\bar{\mathbf{K}}\cdot\mathbf{K}\delta_{ij}-K_i\bar{K}_i+(1/\varepsilon)K_i\bar{K}_j)A_j(\mathbf{k})}$$

$$\times\,e^{2\pi i\Sigma_{\mathbf{k}}\ell_j A_i(\mathbf{k})}. \tag{6.75}$$

The matrix between the fields can be inverted as follows:

$$\left(\bar{\mathbf{K}}\cdot\mathbf{K}\delta_{ij}-K_i\bar{K}_j+\frac{1}{\varepsilon}K_i\bar{K}_j\right)^{-1}=\frac{1}{\bar{\mathbf{K}}\cdot\mathbf{K}}\left(\delta_{ij}-\frac{K_i\bar{K}_j}{\mathbf{K}\cdot\bar{\mathbf{K}}}\right)+\frac{\varepsilon}{\bar{\mathbf{K}}\cdot\mathbf{K}}\frac{K_i\bar{K}_j}{\bar{\mathbf{K}}\cdot\mathbf{K}}, \tag{6.76}$$

so that the integration over the **A(x)** fields gives

$$\det(-\bar{\nabla}\cdot\nabla)\det(-\bar{\nabla}\cdot\nabla)^{-3/2}(\sqrt{2\pi\beta})^{2N}\,e^{-(4\pi^2\beta/2)\Sigma_{\mathbf{k}}\,\ell_i(\mathbf{k})(1/\bar{\mathbf{K}}\cdot\mathbf{K})[\delta_{ij}-(K_i\bar{K}_j/\bar{\mathbf{K}}\cdot\mathbf{K})]\ell_j(\mathbf{k})}. \tag{6.77}$$

This leads again to (6.72) via current conservation $\bar{K}_i\ell_j(\mathbf{k})=0$.

We have in fact been somewhat careless doing these calculations. For one thing, we have proceeded as though the vector potential in the lattice curl (6.5) was $a_k(\mathbf{x})$ rather than $a_k(\mathbf{x}-\mathbf{k})$. Since $a_k(\mathbf{x})$ couples to $\ell_k(\mathbf{x})$, this can be corrected by replacing $\ell_i(\mathbf{x})$ by $\ell_i(\mathbf{x}+\mathbf{i})$ in the final formula (6.72). This, however, does not produce any change due to translational invariance, so that the final result is still correct.

A more severe mistake is the following: when taking the formal limit $\beta \to \infty$ in the field energies (6.59) we assumed that the higher powers in the magnetic field did not matter due to the $1/\beta^n$ prefactors. Unfortunately, this is only true in the absence of vortex lines, where $\sqrt{A^2}$ is of the order β. In the presence of vortex lines, however, this is no longer true. In fact using only the leading term $-(1/2\beta)\sum_x (\bar\nabla \times A)^2$ in (6.59) the average vector potential in the transverse gauge is given by

$$A_i(x) = \beta 2\pi i \frac{1}{-\bar\nabla \cdot \nabla} \ell_i(x)$$

and the mean magnetic field becomes

$$b = \bar\nabla \times A = \beta 2\pi i \frac{1}{-\bar\nabla \cdot \nabla} \bar\nabla \times \ell.$$

Hence, for large β, b grows like β. The lowest $p = 2$ correction is $(1/3\beta^3)\sum_{x,i} b_i^4$ and thus of the same order as the leading term. Far away from the vortex lines, the magnetic fields are small so that the b_i^4, b_i^6, ... terms can certainly be neglected. But a finite core energy of each vortex will escape our attention in the above formal procedure, and the limit $\beta \to \infty$ is not correctly calculated. We shall study this issue in detail in the next section.

Let us end this section by noticing once more, what we have already pointed out in Eq. (I.6.297): were it not for the factor i in the coupling

$$2\pi i \sum_x \ell_i(x) A_i(x) \tag{6.78}$$

the partition function would have been the same as that of the random set of electric current loops with $b_i(x)^2$ being the magnetic field energy. The factor i accounts for the absence of inductive forces in the system of vortex lines which makes the field energy equal to the total energy, as discussed in Section 1.7. Still it will be useful to think of $\ell_i(x)$ as current loops quantized to integer values and of $A_k(x)$ as a magnetic vector potential. The integers $b_i(x)$ can be considered as an integer valued magnetic b-field encircling the quantized current loops. This was the reason for introducing the letter $b_i(x)$ first of all, back in (4.15).

6.4. IMPROVED TREATMENT OF THE LOW TEMPERATURE LIMIT

The question arises as to how we can improve upon the formal limit of the vortex-line representation. For this we go back to the representation (6.23), but re-express the modified Bessel functions via their integral representation so that

$$Z' = \sum_{\{a_1(\mathbf{x}),\, a_2(\mathbf{x})\}} \prod_{\mathbf{x},i} \left[\int \frac{d\gamma_i(\mathbf{x})}{2\pi} \right] e^{\beta \Sigma_{\mathbf{x},i} \cos \gamma_i(\mathbf{x}) + i \Sigma_{\mathbf{x},i} \gamma_i(\mathbf{x})(\bar{\nabla} \times \mathbf{a})_i(\mathbf{x})}. \qquad (6.79)$$

Performing the sum over $a_1(\mathbf{x})$, $a_2(\mathbf{x})$ leads to the conditions

$$\nabla_2 \gamma_3(\mathbf{x}) - \nabla_3 \gamma_2(\mathbf{x}) = 2\pi \ell_1(\mathbf{x}), \quad \nabla_3 \gamma_1(\mathbf{x}) - \nabla_1 \gamma_3(\mathbf{x}) = 2\pi \ell_2(\mathbf{x}), \qquad (6.80)$$

where $\ell_1(\mathbf{x})$, $\ell_2(\mathbf{x})$ are integers. There are two ways of satisfying these uniquely. We may go to the gauge $\gamma_3 = 0$ and find $\gamma_1(\mathbf{x})$ and $\gamma_2(\mathbf{x})$ from

$$\gamma_1^0(\mathbf{x}) = \frac{1}{\nabla_3} 2\pi \ell_2(\mathbf{x}), \quad \gamma_2^0(\mathbf{x}) = -\frac{1}{\nabla_3}(2\pi \ell_2(\mathbf{x}) - \nabla_2 \gamma_1(\mathbf{x})) \qquad (6.81)$$

with the same boundary condition as those for $a_i(\mathbf{x})$ in Section 6.1 [see Eqs. (6.15), (6.22)]. These are integer multiples of 2π. Since they have to lie in the interval $(-\pi, \pi]$, only *one* configuration $\ell_1(\mathbf{x})$, $\ell_2(\mathbf{x})$ is admissible. Given $\gamma_i^0(\mathbf{x})$ we can add a gradient $\nabla_i \gamma'(\mathbf{x})$ without violating (6.80) and the partition function becomes

$$Z' = \prod_{\mathbf{x}} \left[\int_{-\pi}^{\pi} \frac{d\gamma'(\mathbf{x})}{2\pi} \right] \sum_{\{\ell_1(\mathbf{x}),\, \ell_2(\mathbf{x})\}} e^{\beta \Sigma_{\mathbf{x},i} \cos(\gamma_i^0(\mathbf{x}) + \nabla_i \gamma'(\mathbf{x}))}$$

$$= \prod_{\mathbf{x}} \left[\int_{-\pi}^{\pi} \frac{d\gamma'(\mathbf{x})}{2\pi} \right] e^{\beta \Sigma_{\mathbf{x},i} \cos \nabla_i \gamma'}, \qquad (6.82)$$

which is the original form we started out with.

But there is also a second solution. We may choose the transverse gauge for $\gamma_i^0(\mathbf{x})$ and satisfy (6.80) by the noninteger values

$$\gamma_i^0(\mathbf{x}) = 2\pi \frac{1}{-\bar{\nabla} \cdot \nabla} (\bar{\nabla} \times \ell)_i \quad \mathrm{mod}\ 2\pi \qquad (6.83)$$

where "mod 2π" is chosen to bring each $\gamma_i^0(\mathbf{x})$ into the interval $(-\pi, \pi]$. Also here we can add any gradient and have

$$\gamma_i(\mathbf{x}) = \gamma_i^0(\mathbf{x}) + \nabla_i \gamma'(\mathbf{x}). \tag{6.84}$$

The only restriction on γ' is that none of the $\gamma_i(\mathbf{x})$'s moves out of the interval $(-\pi, \pi]$. We shall indicate this condition by a subscript sm for "smooth." In this way, the partition becomes

$$Z' = \prod_{\mathbf{x}} \left[\int \frac{d\gamma_{sm}'(\mathbf{x})}{2\pi} \right] \sum_{\{\ell_i(\mathbf{x})\}} \delta_{\bar{\nabla}_i \ell_i, 0}\, e^{\beta \sum_{\mathbf{x}, i} \cos(\gamma_i^0(\mathbf{x}) + \nabla_i \gamma_{sm}'(\mathbf{x}))}. \tag{6.85}$$

Physically speaking the γ_{sm}' fluctuations should be so smooth that they do not give rise to further vortices. What (6.85) amounts to is an expansion of the XY model into $\gamma(\mathbf{x})$ field configurations due to vortex lines plus their small distortions.

In order to calculate the individual contributions we expand

$$\beta \sum_{\mathbf{x}, i} \cos(\gamma_i^0 + \nabla_i \gamma_{sm}')$$

$$= \beta \sum_{\mathbf{x}, i} \cos \gamma_i^0(\mathbf{x}) \cos \nabla_i \gamma_{sm}' - \sin \gamma_i^0(\mathbf{x}) \sin \nabla_i \gamma_{sm}'$$

$$\approx \beta \sum_{\mathbf{x}, i} \cos \gamma_i^0(\mathbf{x}) - \frac{\beta}{2} \sum_{\mathbf{x}, i} (\cos \gamma_i^0(\mathbf{x})(\nabla_i \gamma_{sm}')^2 + 2 \sin \gamma_i^0(\mathbf{x}) \nabla_i \gamma_{sm}')$$

$$= \beta \sum_{\mathbf{x}, i} \left(\cos \gamma_i^0(\mathbf{x}) + \frac{1}{2} \bar{\nabla}_i \sin \gamma_i^0(\mathbf{x}) \frac{1}{-\bar{\nabla}_\ell \cos \gamma_\ell^0(\mathbf{x}) \nabla_\ell} \bar{\nabla}_j \sin \gamma_j^0(\mathbf{x}) \right)$$

$$- \frac{\beta}{2} \sum_{\mathbf{x}, i} \left(\gamma_{sm}' - \frac{\bar{\nabla}_i \sin \gamma_i^0(\mathbf{x})}{-\bar{\nabla}_\ell \cos \gamma_\ell^0(\mathbf{x}) \nabla_\ell} \right) (-\bar{\nabla}_\ell \cos \gamma_\ell^0(\mathbf{x}) \nabla_\ell)$$

$$\times \left(\gamma_{sm}' - \frac{\bar{\nabla}_j \sin \gamma_j^0(\mathbf{x})}{-\bar{\nabla}_\ell \cos \gamma_\ell^0(\mathbf{x}) \nabla_\ell} \right) \tag{6.86}$$

and find

$$Z \xrightarrow[\beta \text{ large}]{} \frac{e^{3\beta N}}{(\sqrt{2\pi\beta})^N} \det(-\bar{\nabla} \cdot \nabla)^{-1/2} \sum_{\{\ell_i(\mathbf{x})\}} \delta_{\nabla_i \ell_i, 0}\, v[\ell]\, e^{-\beta E[\ell]}, \tag{6.87}$$

where

$$E[\ell] = -\sum_{\mathbf{x}, i} \left(\cos \gamma_i^0(\mathbf{x}) - 1 + \frac{1}{2}\bar{\nabla}_i \sin \gamma_i^0(\mathbf{x}) \frac{1}{-\bar{\nabla}_\ell \cos \gamma_\ell^0(\mathbf{x}) \, \nabla_\ell} \bar{\nabla}_j \sin \gamma_j^0(\mathbf{x}) \right)$$

$$(6.88)$$

is the energy of the vortex configuration and

$$v[\ell] = \det \left(\sum_\ell \bar{\nabla}_\ell \cos \gamma_\ell^0(\mathbf{x}) \, \nabla_\ell \right) \Big/ \det \left(\sum_\ell \bar{\nabla}_\ell \nabla_\ell \right) \equiv e^{S[\ell]}$$

may be interpreted as the entropy factor of the small fluctuations of the vortex lines. Comparing the energy with

$$\frac{4\pi^2}{2} \sum_{\mathbf{x}, \mathbf{x}'} \ell_i(\mathbf{x}) \frac{1}{-\bar{\nabla} \cdot \nabla} \ell_i(\mathbf{x}) \qquad (6.89)$$

of the previous naive approximation (6.72) we see that as far as the far zone of the vortices is concerned, the energies are the same. There $|\gamma_i^0| \ll \pi/2$ so that we can expand

$$E[\ell] \sim \frac{1}{2} \sum_{\mathbf{x}, i} \left(\gamma_i^{02} - \bar{\nabla}_i \gamma_i^0 \frac{1}{-\bar{\nabla} \cdot \nabla} \bar{\nabla}_i \gamma_i^0 \right). \qquad (6.90)$$

Since $\bar{\nabla}_i \gamma_i^0(\mathbf{x}) = 0$, this gives

$$\frac{1}{2} \sum_{\mathbf{x}, i} \gamma_i^{02} = \frac{4\pi^2}{2} \sum_{\mathbf{x}} \left(\frac{1}{-\bar{\nabla} \cdot \nabla} \bar{\nabla} \times \ell \right) \left(\frac{1}{-\bar{\nabla} \cdot \nabla} \bar{\nabla} \times \ell \right) = \frac{4\pi^2}{2} \sum_{\mathbf{x}} \ell_i \frac{1}{-\bar{\nabla} \cdot \nabla} \ell_i,$$

$$(6.91)$$

in agreement with (6.90). In the near zone, however, (6.88) has definitely *less* energy than (6.90). The result shows that the nonlinearities of the cosine change the energy of the ensemble of vortex lines even in the limit of zero temperature.

NOTES AND REFERENCES

Some of the manipulations of this chapter can be found in
R. Savit, *Phys. Rev.* **B17** (1978) 1340.

See also

P.R. Thomas and M. Stone, *Nucl. Phys.* **B144** (1978) 513,

J.V. José, L.P. Kadanoff, S. Kirkpatrick and D.R. Nelson, *Phys. Rev.* **B16** (1977) 1217,

T. Ohta and D. Jasnow, *Phys. Rev.* **B20** (1979) 139 [This paper contains some results which we do not believe to be true, e.g., their Eqs. (2.18), (3.41)].

For two-dimensional considerations, more detail will be given in Chapter 11.

THE VILLAIN APPROXIMATION AND
THE VILLAIN MODEL

7.1. THE VILLAIN APPROXIMATION

In the last section we saw that a proper treatment of the vortex lines of the XY model becomes quite complicated, even for very low temperatures. The reason was the awkward nonlinear form of the energy $\cos \nabla_i \gamma$. In order to overcome this difficulty, Villain, in 1975, proposed a simple approximation to the field energy which is much easier to handle but represents correctly the essential physical properties of the XY model in the vicinity of the phase transition, with only insignificant numerical differences.

Since the simplest physical theories are those for which fluctuations are of the Gaussian form he searched for an approximation of just this form which would be as similar as possible to the Boltzmann factor $e^{\beta \cos \nabla_i \gamma}$. So, he introduced the ansatz

$$e^{\beta \cos \gamma} \approx R_V(\beta) \sum_{n=-\infty}^{\infty} e^{-(\beta_V(\beta)/2)(\gamma - 2\pi n)^2}, \qquad (7.1)$$

in which $e^{\beta \cos \gamma}$ is approximated by a periodic Gaussian with unknown normalization $R_V(\beta)$ and bending energy $\beta_V(\beta)$, both being functions of temperature. For very large β, such an approximation should become

exact since then the γ-fluctuations would be squeezed into the periodic maxima of $\cos\gamma$, i.e., $\gamma_{\text{max},n} = 2\pi n$, with small fluctuations around them,

$$e^{\beta\cos\gamma} \sim e^{\beta} e^{-(\beta/2)(\gamma - 2\pi n)^2},$$

and the same thing can be achieved on the right-hand side of (7.1) by letting $R_V(\beta) \to e^{\beta}$, $\beta_V(\beta) \to \beta$.

If only for this low temperature property, the Villain approximation would have remained of little use. The only really interesting region is the critical region near the phase transition which takes place at the rather small value $\beta_c \approx 0.45$, i.e., at a rather high temperature. It is a fortunate fact that periodic Gaussian happens to approximate the exponential $e^{\beta\cos\gamma}$ not only for large β but also for small β, albeit with a drastic renormalization of $\beta \to \beta_V(\beta)$. Moreover, for small β the approximation is even better than that for large β.

In order to see this second property, let us rewrite the Gaussian integral in the following way. The sum over n can be executed using Poisson's formula (6.37) which forces b to take integer values and leads to the identity

$$\sum_{n=-\infty}^{\infty} e^{-\beta(1/2)(\gamma - 2\pi n)^2} = \sum_{b=-\infty}^{\infty} \frac{1}{\sqrt{2\pi\beta}} e^{-(1/2\beta)b^2 + ib\gamma}. \tag{7.2}$$

This identity is well-known in the mathematical literature, particularly in the theory of the Jacobi theta function. Now, for small β, the right-hand side can be approximated by

$$\frac{1}{\sqrt{2\pi\beta}}(1 + 2e^{-1/2\beta}\cos\gamma + \ldots) \sim \frac{1}{\sqrt{2\pi\beta}}e^{2e^{-1/\beta}\cos\gamma + \ldots}. \tag{7.3}$$

Therefore, Villain found that the potential of the XY model could be written in both limits as

$$e^{\beta\cos\gamma} \to R_V(\beta) \sum_{n=-\infty}^{\infty} e^{-\beta_V(1/2)(\gamma - 2\pi n)^2}, \tag{7.4}$$

where for $\beta \to \infty$, $R_V \to e^{\beta}$, $\beta_V \to \beta$ and for $\beta \to 0$, $R_V \to \sqrt{2\pi\beta_V}$, $\beta_V \to -2\log(\beta/2)$. Faced with these two opposite limits Villain thought that it should be possible to interpolate between them and find an approx-

imation for all β, using an appropriate choices for $R_V(\beta)$, $\beta_V(\beta)$. Expanding both sides of (7.1) in a Fourier series he obtained

$$\sum_{b=-\infty}^{\infty} c_b e^{ib\gamma} \approx \sum_{b=-\infty}^{\infty} d_b e^{ib\gamma} \tag{7.5}$$

and argued that the greatest similarity is reached by equating the lowest two Fourier coefficients

$$c_0 = d_0, \tag{7.6}$$

$$c_{\pm 1} = d_{\pm 1}. \tag{7.7}$$

Now, by (4.15), the coefficients c_b are simply $I_b(\beta)$. The coefficients d_b, on the other hand, are given by

$$d_b = R_V \int_{-\pi}^{\pi} \frac{d\gamma}{2\pi} e^{-ib\gamma} \sum_{n=-\infty}^{\infty} e^{-(\beta_V/2)(\gamma - 2\pi n)^2} \tag{7.8}$$

and can be directly read off (7.2),

$$d_b = R_V \frac{1}{\sqrt{2\pi\beta_V}} e^{-b^2/(2\beta_V)}. \tag{7.9}$$

With this, the two conditions (7.6) and (7.7) determine the parameters of the Villain approximation (7.1) as follows:

$$R_V(\beta) = \sqrt{2\pi\beta_V} I_0(\beta), \tag{7.10}$$

$$\beta_V = -2\log(I_1(\beta)/I_0(\beta))]^{-1}. \tag{7.11}$$

At low temperatures we use the large β expansion

$$\frac{I_1(\beta)}{I_0(\beta)} \equiv 1 - \frac{1}{2\beta} - \frac{1}{8\beta^2} - \frac{1}{8\beta^3} - \frac{5^2}{2^7\beta^4} - \frac{13}{3^5\beta^5} - \ldots, \tag{7.12}$$

and find from the second equation

$$\beta_V = \beta\left(1 - \frac{1}{2\beta} - \frac{5}{3 \cdot 2^3\beta^2} - \frac{7}{3 \cdot 2^3\beta^3} - \frac{13 \cdot 269}{3^2 \cdot 5 \cdot 2^7\beta^4} - \ldots\right); \tag{7.13a}$$

and from the first

$$R(\beta) \xrightarrow[\beta \to \infty]{} e^{\beta} \left(1 - \frac{1}{8\beta} - \frac{37}{3 \cdot 2^7 \beta^2} - \frac{433}{3 \cdot 2^7 \beta^3} - \frac{11 \cdot 13217}{3 \cdot 5 \cdot \beta^4} - \cdots \right). \tag{7.14a}$$

For high temperature, Table 4.8 can be used to calculate

$$\beta_V \xrightarrow[\beta \to 0]{} - \left[2\ln(\beta/2) - \frac{\beta^2}{4} + \frac{5}{3 \cdot 2^6} \beta^4 - \frac{5}{3 \cdot 2^9} \beta^6 + \cdots \right]^{-1} \tag{7.13b}$$

and

$$R_V(\beta) \xrightarrow[\beta \to 0]{} \sqrt{2\pi\beta_V} \left(1 + \frac{\beta^2}{2^2} + \frac{\beta^4}{2^6} + \frac{\beta^6}{3^2 \cdot 2^8} + \cdots \right). \tag{7.14b}$$

Certainly both limits agree with those observed after Eq. (7.4) where the approximation was shown to become exact. The full temperature behaviour of $\beta_V(\beta)$ is plotted in Figs. 7.1, 7.2.
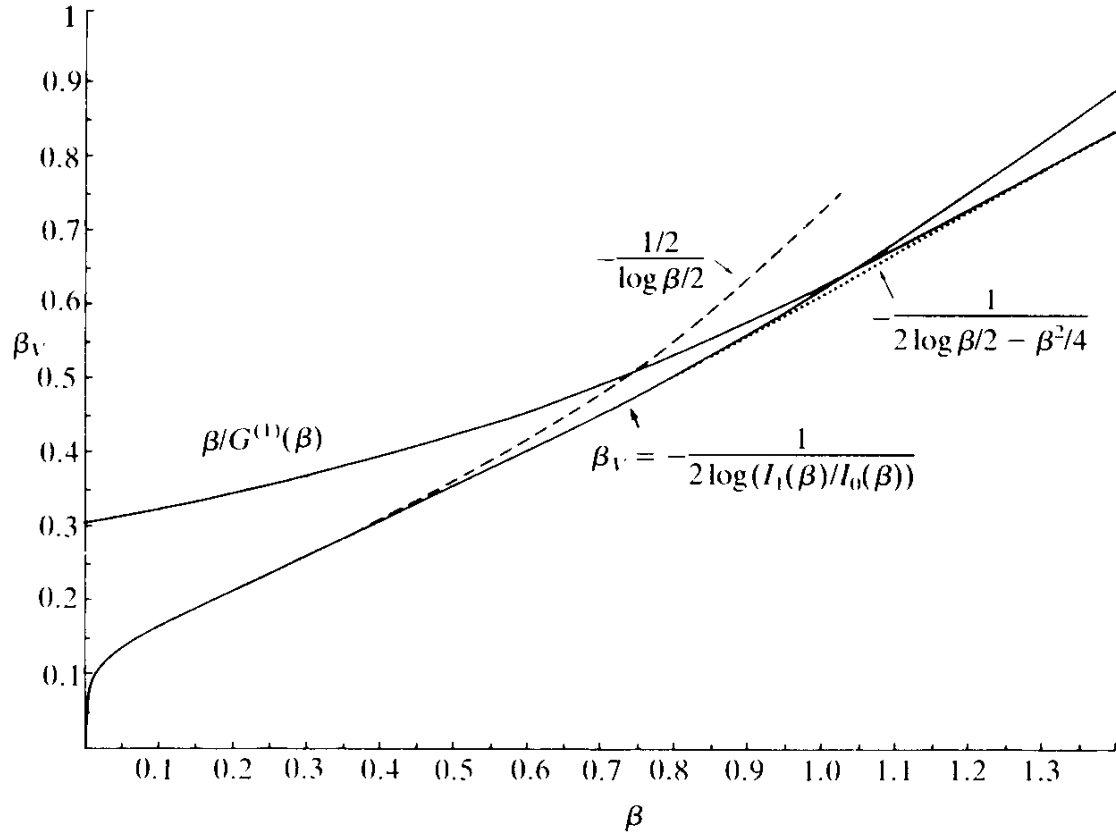
With these functions $\beta_V(\beta)$, $R_V(\beta)$, let us compare the two sides of Eq. (7.1) numerically. In Fig. 7.3 we see that close to the critical temperature of the XY model, $T \sim T_c \sim 2.2$, $\beta \sim \beta_c \sim 0.45$, the two Boltzmann factors are quite similar to each other, with the small β approximation being applicable. The Villain approximation favours slightly larger values of $\gamma = \pi/2$. This can be seen also from the energies themselves which we plotted in Fig. 7.4.

When inserted into the partition function of the XY model, the Villain approximation leads to the partition function

$$Z'_{XY} \approx Z'_V = [R_V(\beta)]^{ND} \prod_{\mathbf{x}} \left[\int \frac{d\gamma(\mathbf{x})}{2\pi} \right] \sum_{\{n_i(\mathbf{x})\}} e^{-(\beta_V/2)\Sigma_x(\nabla_i \gamma - 2\pi n_i)^2}. \tag{7.15}$$

The particular virtue of this expression is its Gaussian form. This permits a direct derivation of the vortex-line representation as follows: An auxiliary field $B_i(\mathbf{x})$ is introduced to linearize the exponent, i.e.,

FIG. 7.1.   Temperature behaviour of Villain's $\beta_V(\beta)$ as a function of the XY model's β. The dotted and dashed lines correspond to the lowest two high temperature approximations. For comparison we have plotted the stiffness $\beta/G^{(1)}(\beta)$ of the XY model which governs the long-range interactions between vortex lines in the formal limit of low temperatures [cf. (6.36) and Table 6.1].
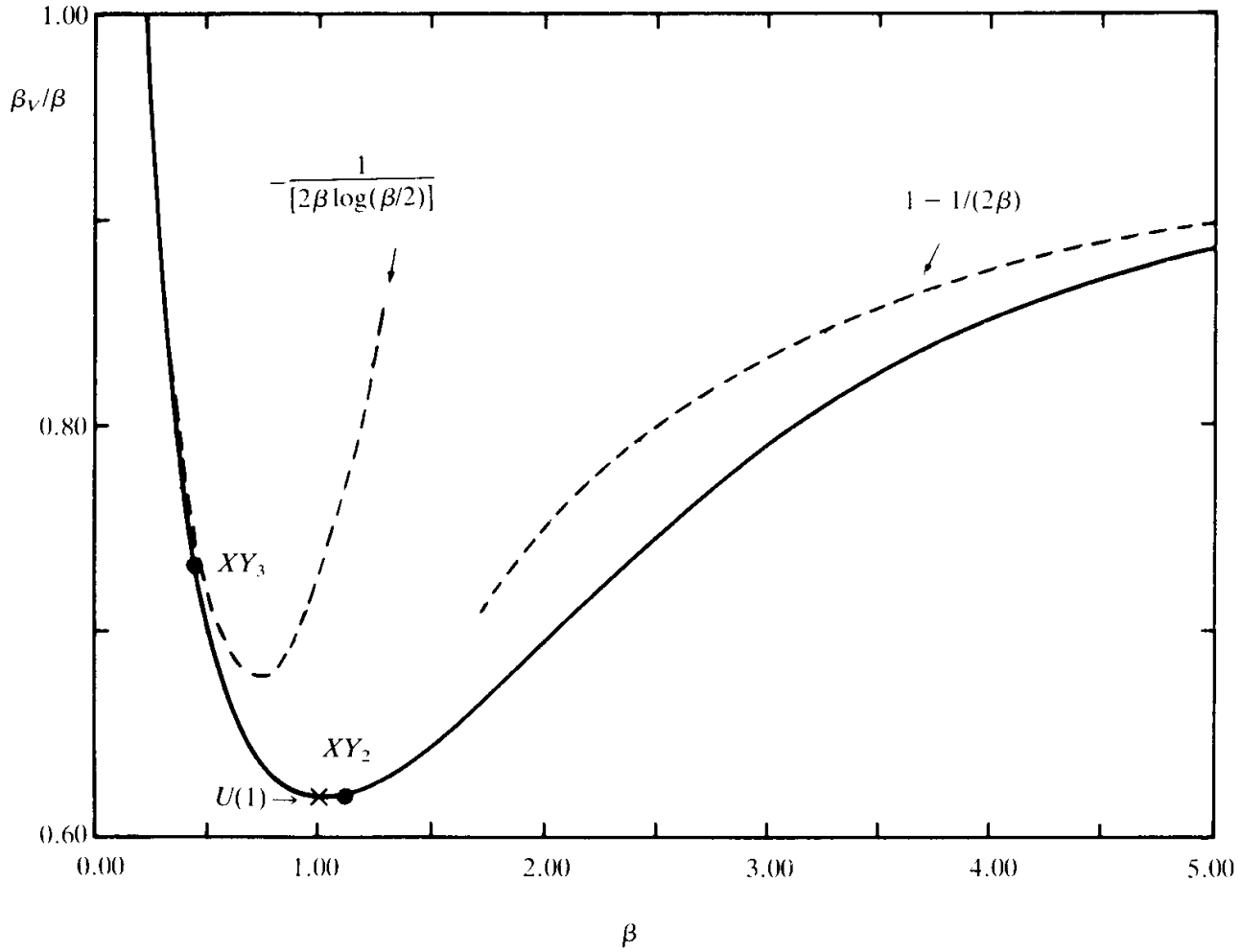

$$Z'_V = R_V^{ND} \prod_{x,i} \left[\int_{-\infty}^{\infty} \frac{dB_i(x)}{\sqrt{2\pi\beta_V}} \right] \prod_x \left[\int_{-\pi}^{\pi} \frac{d\gamma}{2\pi} \right] \sum_{\{n_i(x)\}} e^{-(1/2\beta_V)\Sigma_x B_i(x)^2 + i\Sigma_x B_i(\nabla_i \gamma - 2\pi n_i)}.$$

$$(7.16)$$

The sum over n_i can now be performed using Poisson's formula (6.37). This leads to a sum over δ-functions at each x, i, which squeezes the $B_i(x)$ integrations onto integer values of $b_i(x) = 0$, ± 1, ± 2, ... Hence Z'_V becomes

$$Z'_V = R_V^{ND} \frac{1}{(\sqrt{2\pi\beta_V})^{ND}} \sum_{\{b_i(x)\}} e^{-(1/2\beta_V)\Sigma_x b_i(x)^2} \prod_x \left[\int_{-\pi}^{+\pi} \frac{d\gamma(x)}{2\pi} \right] e^{-i\Sigma_x b_i\nabla_i\gamma}. \quad (7.17)$$

The factor with the $\gamma(x)$ integrals has appeared before in Eq. (4.16) in the derivation of the high temperature expansion of the XY model. The lattice version of partial integration brings the second exponent to the form $i\Sigma_x\bar{\nabla}_i b_i(x)\,\gamma(x)$ whereupon the integrals enforce the constraint

FIG. 7.2.   The ratio β_V/β as a function of β shows clearly the quality and range of validity of the low and high temperature approximations (----) to $\beta_V = -[2\log(I_1(\beta)/I_0(\beta))]^{-1}$. The dots mark the transition points of the $D = 2$ and $D = 3$ XY models (the cross of the $U(1)$ model will be discussed in Section 10.3).
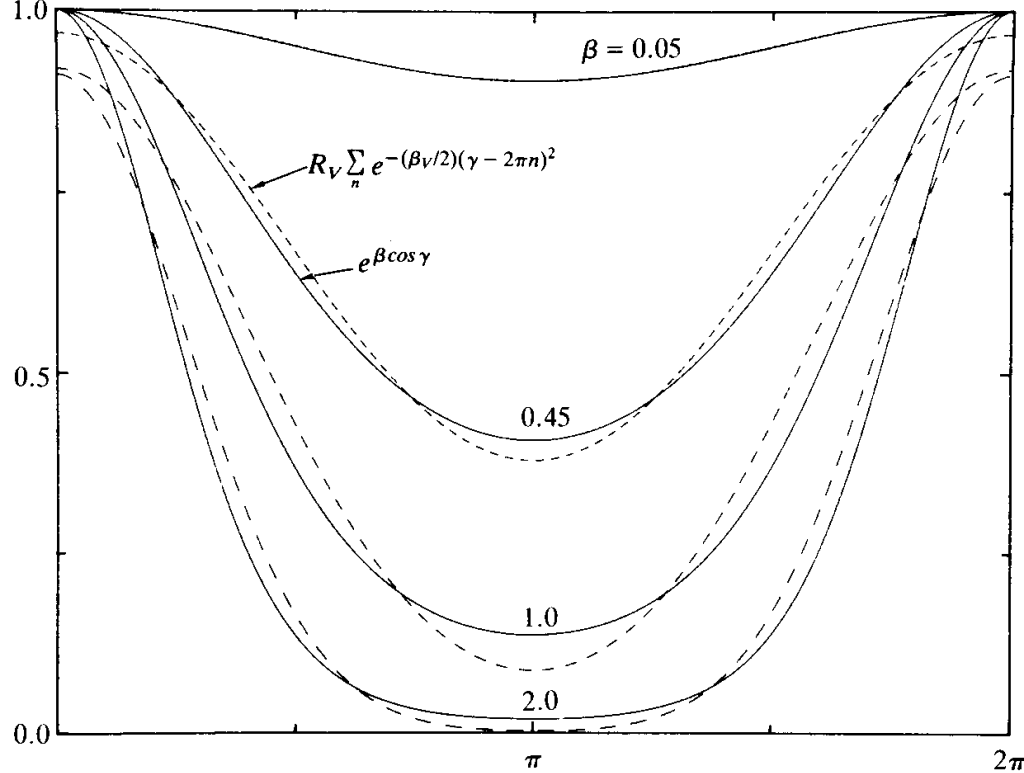
$\nabla_i b_i(x) = 0$ at each $\mathbf{x}$. The integer field $b_i(\mathbf{x})$ consists again of closed non-backtracking random chains of unit strength. In this way, the partition function of the Villain approximation becomes

$$Z'_V = R_V^{ND} \frac{1}{(\sqrt{2\pi\beta_V})^{ND}} \sum_{\{b_i(\mathbf{x})\}} \delta_{\overline{\nabla}_i b_i, 0} \, e^{-(1/2\beta_V)\Sigma_{\mathbf{x}} b_i(\mathbf{x})^2}. \tag{7.18}$$

In $D = 3$ dimensions we can use an integer-valued vector potential in the axial gauge $a_3 = 0$, to rewrite this result as

$$Z'_V = R_V^{3N} \frac{1}{(\sqrt{2\pi\beta_V})^{3N}} \sum_{\{a_i(\mathbf{x})\}} \delta_{a_3, 0} \, e^{-(1/2\beta_V)\Sigma_{\mathbf{x}}(\overline{\nabla} \times \mathbf{a})^2}. \tag{7.19}$$

FIG. 7.3. Boltzmann factor of the XY model in comparison with that of its Villain approximation for $\beta \approx 0.45$ (critical β_c for $D = 3$), $\beta \approx 1$ (close to critical $\beta_c \approx 1.12$ for $D = 2$), $\beta \approx 0.05$ and $\beta \approx 2$, 0, for comparison.

This result may be compared with the previous exact expansion (6.36). Since
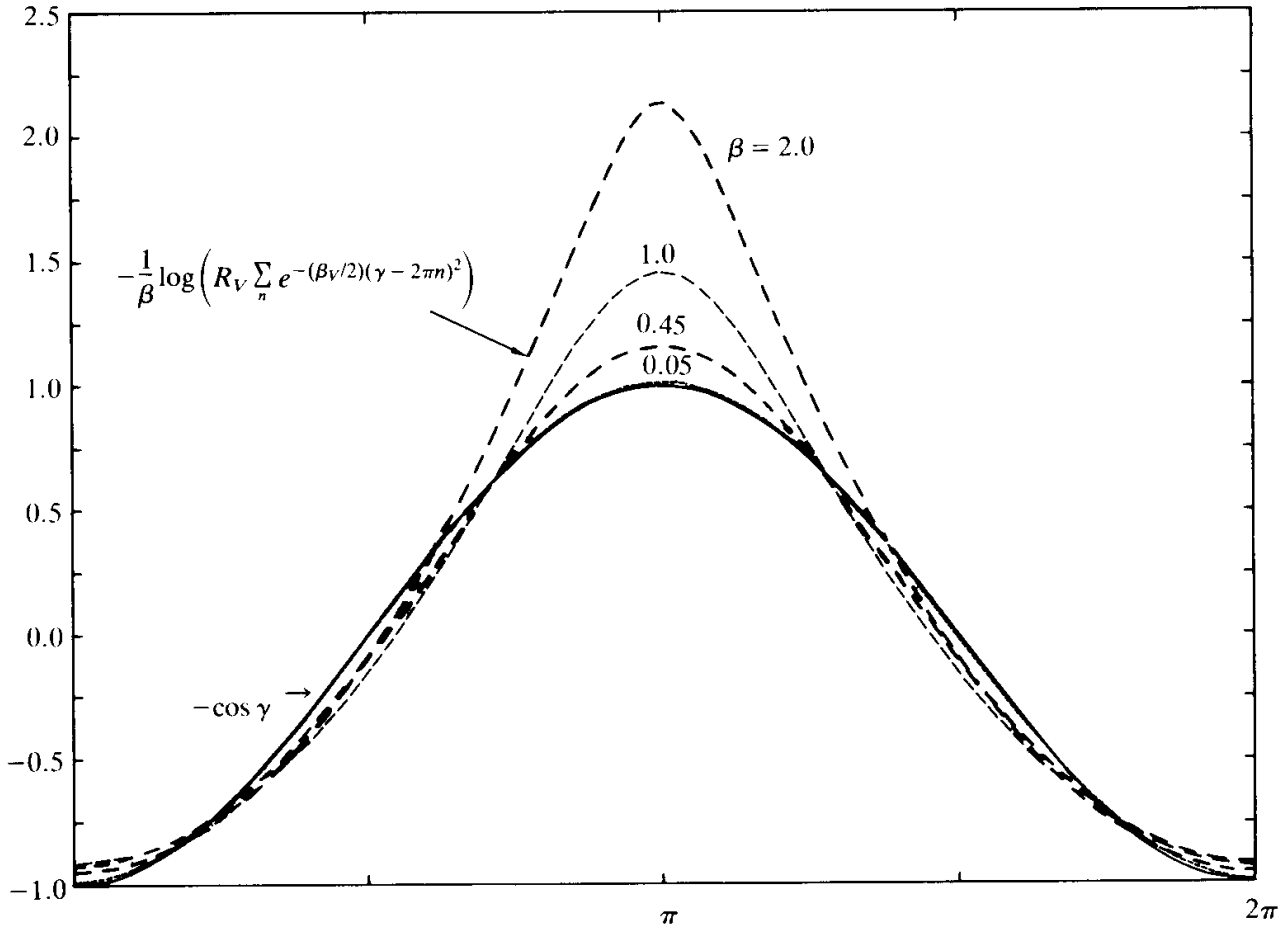
$$R_V \frac{1}{\sqrt{2\pi\beta_V}} = I_0(\beta),\qquad (7.20)$$

we see that the normalization factor is the same. The energy in the exponent of the Villain expression contains only the $p = 1$ part of (6.36) with $G^{(1)}(\beta)/2\beta$ being replaced by $1/2\beta_V$. In Fig. 7.1 where we have plotted $\beta_V(\beta)$, we have also shown $\beta/G^{(1)}(\beta)$, for comparison. For larger temperatures, the curves are quite different since the vortex lines dominate not on the basis of (6.36), which is a low temperature expansion, but due to the approximation $\beta_V \rightarrow -[\log(\beta/2)]^{-1}$.

In order to see this more clearly, consider once more the original partition function (6.23),

$$Z' = \sum_{\{a_i(\mathbf{x})\}} \delta_{a_3,0} \prod_{\mathbf{x},i} I_{(\bar{\nabla}\times\mathbf{a})_i(\mathbf{x})}(\beta).\qquad (7.21)$$

FIG. 7.4. The energy in the approximated Villain Boltzmann factors (----) as compared with the XY model (——).

For small β, the modified Bessel functions possess the threshold behaviour

$$I_b(\beta) \sim \frac{1}{|b|!}\left(\frac{\beta}{2}\right)^{|b|},$$

which can be written as

$$I_b(\beta) \sim \frac{1}{|b|!} e^{\log(\beta/2)|b|}. \tag{7.22}$$

Thus, if β is small, only $n = 0$ and $n = \pm 1$ can contribute to the partition function. For these two values we can replace (7.22) by

$$I_b(\beta) \xrightarrow[\beta \to 0]{} e^{-(1/2)[-2\log(\beta/2)]b^2}, \tag{7.23}$$

and Z' becomes

$$Z' \xrightarrow[\beta \to 0]{} \sum_{\{a_i(\mathbf{x})\}} \delta_{a_3,0} \; e^{-(1/2)[-2\log\beta/2]\sum_\mathbf{x} (\bar{\nabla}\times\mathbf{a})^2}, \tag{7.24}$$

which is precisely the same as (7.19) in the limit $\beta \to 0$. The advantage of the Villain approximation is that the vortex-line representation can now be derived for all temperatures from (7.19) in the same way as we did previously from the limiting form (6.63). The sum over the integer-valued gauge field is now replaced by an integral over a continuous gauge field coupled to the sum of all non-backtracking random loops $\ell_i(\mathbf{x})$ of unit strength,

$$Z_V' = I_0(\beta)^{3N} \prod_{\mathbf{x},i} \left[\int dA_i(\mathbf{x}) \right] \Phi[\mathbf{A}] \, e^{-(1/2\beta_V)\Sigma_\mathbf{x}(\bar{\nabla}\times\mathbf{A})^2} \sum_{\{\ell_i(\mathbf{x})\}} \delta_{\bar{\nabla}_i\ell_i,0} \; e^{2\pi i \Sigma_\mathbf{x}\ell_i(\mathbf{x})A_i(\mathbf{x})}. \tag{7.25}$$

The fluctuations of the vector potential can be integrated just as before with the result

$$Z_V' = I_0(\beta)^{3N}(\sqrt{2\pi\beta_V})^{2N} \det(-\bar{\nabla}\cdot\nabla)^{-1/2}$$

$$\times \sum_{\{\ell_i(\mathbf{x})\}} \delta_{\bar{\nabla}_i\ell_i,0} \; e^{-\beta_V(4\pi^2/2)\Sigma_{\mathbf{x},\mathbf{x}'}\ell_i(\mathbf{x})v(\mathbf{x}-\mathbf{x}')\ell_i(\mathbf{x}')}. \tag{7.26}$$

Comparing this with the limiting forms (6.63), (6.72) of the XY model, we see that the expressions are the same except that β is replaced by $\beta_V(\beta)$ in two places.

In contrast to the limiting formula, the vortex-line representation is now applicable not only in the limit $\beta \to \infty$ but also for small β. In the latter case, $\beta_V \sim -1/(2\log\beta/2)$ and the vortex-line representation (7.25) becomes

$$Z' \xrightarrow[\beta \to 0]{} \prod_{\mathbf{x},i} \int [dA_i(\mathbf{x})] \, \Phi[\mathbf{A}] \, e^{-(1/2)\Sigma_\mathbf{x}[-2\log(\beta/2)](\bar{\nabla}\times\mathbf{A})^2} \sum_{\{\ell_i(\mathbf{x})\}} \delta_{\bar{\nabla}\ell,0} \; e^{2\pi i \Sigma_\mathbf{x}\ell_i(\mathbf{x})A_i(\mathbf{x})}, \tag{7.27}$$

while the sum (7.26) has the limit

$$Z' \xrightarrow[\beta \to 0]{} \det(-\bar{\nabla} \cdot \nabla)^{-1/2}(\sqrt{-\pi/\log(\beta/2)})^{2N}$$

$$\times \sum_{\{\ell_i(\mathbf{x})\}} \delta_{\bar{\nabla}\ell,0}\, e^{-(1/2)(4\pi^2/(-2\log(\beta/2)))\Sigma_{\mathbf{x},\mathbf{x'}}\ell_i(\mathbf{x})r(\mathbf{x}-\mathbf{x'})\ell_i(\mathbf{x'})}. \qquad (7.28)$$

7.2. THE VILLAIN MODEL

We shall now set out to study the accuracy of the Villain approximation. For this, it is useful to drop the normalization factor on the right-hand side of Eq. (7.15) and investigate directly the partition function

$$Z_{VM} \equiv e^{-N\beta_V f_{VM}} = \prod_{\mathbf{x}} \left[\int_{-\pi}^{\pi} \frac{d\gamma(\mathbf{x})}{2\pi} \right] \sum_{\{n_i(\mathbf{x})\}} e^{-(\beta_V/2)\Sigma_{\mathbf{x}}(\nabla_i\gamma - 2\pi n_i)^2}, \qquad (7.29)$$

to be called *Villain model*, in which $\beta_V \equiv 1/T_V$ is considered as the inverse temperature. The Villain model has an internal energy and specific heat on its own,

$$u_{VM} = -\beta_V \frac{\partial}{\partial \beta_V}(-\beta_V f), \qquad (7.30)$$

$$c_{VM} = -\beta_V^2 \frac{\partial}{\partial \beta_V} u_{VM}. \qquad (7.31)$$

If one wants to go back to the corresponding XY model quantities, one has to remember the connection.

$$Z'_{XY}(\beta) \approx Z'_V = R_V(\beta)^{ND} Z_{VM}(\beta_V), \qquad (7.32)$$

so that the free energies of the two models are related by

$$-\beta f'_{XY} \approx -\beta f'_V = D \log R_V(\beta) - \beta_V f_{VM}(\beta_V). \qquad (7.33)$$

Differentiating with respect to β and using

$$\dot{\beta}_V(\beta) \equiv \frac{\partial \beta_V}{\partial \beta} = \frac{1}{2 \left(\dfrac{\log I_1(\beta)}{I_0(\beta)} \right)^2} \frac{I_0(\beta)}{I_1(\beta)} \frac{d}{d\beta} \left(\frac{I_1(\beta)}{I_0(\beta)} \right)$$

$$= -2\beta_V^2 \left(e^{-1/2\beta_V} - e^{1/2\beta_V} + \frac{1}{\beta} \right),$$

$$\dot{R}_V(\beta) \equiv \frac{\partial R_V(\beta)}{\partial \beta} = I_1(\beta)\sqrt{2\pi\beta_V} + I_0(\beta)\frac{1}{2}\sqrt{2\pi\beta_V}\frac{1}{\beta_V}\cdot\frac{\partial \beta_V}{\partial \beta}$$

$$= R_V \left(e^{-1/2\beta_V} + \frac{1}{2}\dot{\beta}_V/\beta_V \right), \tag{7.34}$$

one finds

$$u'_{XY} \sim u'_V = -D\frac{\dot{R}_V}{R_V} + \dot{\beta}_V u_{VM} \tag{7.35}$$

For the specific heat one needs the relations

$$\ddot{\beta}_V(\beta) = 2\dot{\beta}_V^2/\beta_V + 2\beta_V^2 \left[e^{-1/\beta_V} - e^{1/\beta_V} + \frac{1}{\beta}(e^{-1/2\beta_V} + e^{1/2\beta_V}) + \frac{1}{\beta^2} \right],$$

$$\frac{\ddot{R}_V}{R_V} - \frac{\dot{R}_V^2}{R_V^2} = \frac{1}{2}\left[\frac{\ddot{\beta}_V}{\beta_V} - \frac{\dot{\beta}_V^2}{\beta_V^2} \right] + 1 - \frac{1}{\beta}e^{-1/2\beta_V} - e^{-1/\beta_V}. \tag{7.36}$$

These give

$$c_{XY} \sim c_V = \beta^2 D \left(\frac{\ddot{R}_V}{R_V} - \frac{\dot{R}_V^2}{R_V^2} \right) - \beta^2 \ddot{\beta}_V u_{VM} + \beta^2 \frac{\dot{\beta}_V^2}{\beta_V^2} c_{VM}. \tag{7.37}$$

7.3. HIGH AND LOW TEMPERATURE EXPANSIONS OF THE VILLAIN MODEL

We shall now proceed to study the partition function of the Villain model (7.29) in its own right. The results will then be inserted into (7.35) and (7.37) allowing us to make a detailed analysis of the accuracy of the Villain approximation.

From (7.18), (7.26) we know immediately that there are two alternative forms of the partition function:

$$Z_{VM} = \frac{1}{(\sqrt{2\pi\beta_V})^{ND}} \sum_{\{b_i(\mathbf{x})\}} \delta_{\bar{\nabla}_i b_i, 0} \, e^{-(1/2\beta_V)\Sigma_{\mathbf{x}} b_i^2(\mathbf{x})}$$

$$(\triangleq \text{ closed integer magnetic fields}), \qquad (7.38)$$

$$Z_{VM} = \frac{1}{(\sqrt{2\pi\beta_V})^N} \det(-\bar{\nabla}\cdot\nabla)^{-1/2} \sum_{\{\ell_i(\mathbf{x})\}} \delta_{\bar{\nabla}_i \ell_i, 0} \, e^{-(\beta_V/2)4\pi^2\Sigma_{\mathbf{x},\mathbf{x}'} \ell_i(\mathbf{x})v(\mathbf{x}-\mathbf{x}')\ell_i(\mathbf{x})}$$

$$(\triangleq \text{ closed integer vortex lines}). \qquad (7.39)$$

The first one converges fast for low β_V, the second for high β_V. In analogy with the XY model we shall sometimes use the primed quantities defined by

$$Z'_{VM} = e^{\beta_V DN} Z_{VM}.$$

Characteristic of both the high and low temperature expansions of the Villain model is their factorization property,

$$Z_{VM} = Z_{as,\beta_V \to 0} \, Z_{sf}, \qquad (7.40\text{a})$$

$$Z_{VM} = Z_{as,\beta_V \to \infty} \, Z_v, \qquad (7.40\text{b})$$

where

$$Z_{as,\beta_V \to 0} \equiv \frac{1}{(\sqrt{2\pi\beta_V})^{DN}}, \quad Z_{sf} \equiv \sum_{\{b_i(\mathbf{x})\}} \delta_{\bar{\nabla}_i b_i, 0} \, e^{-(1/2\beta_V)\Sigma_{\mathbf{x}} b_i^2(\mathbf{x})}, \qquad (7.41\text{a})$$

$$Z_{as,\beta_V \to \infty} \equiv \frac{1}{(2\pi\beta_V)^{N/2}} \det(-\bar{\nabla}\cdot\nabla)^{-1/2},$$

$$Z_v \equiv \sum_{\{\ell_i(\mathbf{x})\}} \delta_{\bar{\nabla}_i \ell_i, 0} \, e^{-(\beta_V/2)4\pi^2\Sigma_{\mathbf{x},\mathbf{x}'} \ell_i(\mathbf{x})v(\mathbf{x}-\mathbf{x}')\ell(\mathbf{x}')}. \qquad (7.41\text{b})$$
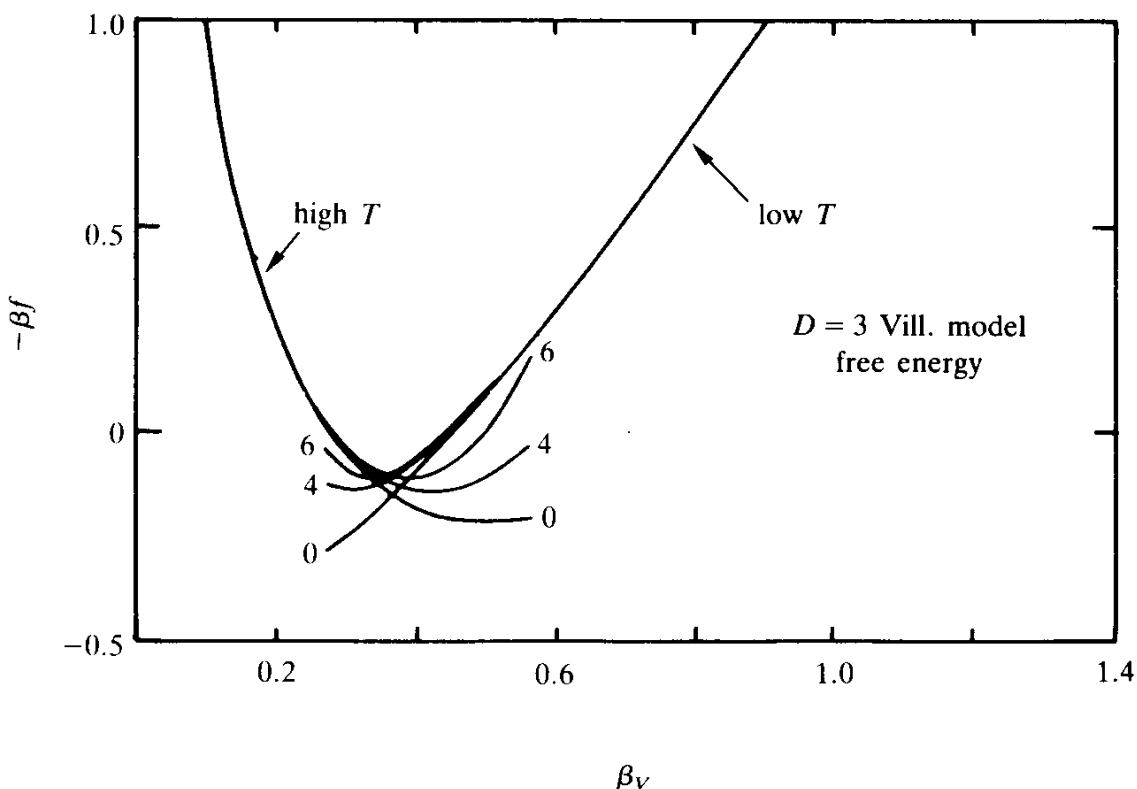
The asymptotic factors $Z_{as,\beta_V \to \infty}$ collect the fluctuations of the long-wavelength fluctuations, the "spin waves" which can be summed *independently* of the vortex lines collected in Z_v. The factor $Z_{as,\beta_V \to 0}$ on the other hand, collects the sums over $n_i(\mathbf{x})$ in (7.29) which, for small β_V, can be approximated as Gaussian integrals. As the temperature $T_V = 1/\beta_V$ is lowered, there are corrections due to closed loops of super-flow described by Z_{sf}.

The factorization (7.40) is a consequence of the purely Gaussian form of the Villain model.

The low β_V expansion is easily performed following the same procedure used in (4.46). Apart from the factor $1/(\sqrt{2\pi\beta_V})^{DN}$, all we have to do is to replace each factor $I_b(\beta)/I_0(\beta)$ by $\exp(-(1/2\beta_V)b^2) = [I_1(\beta)/I_0(\beta)]^{b^2}$ (see also the last column in Table 4.1). This yields

$$
Z_{VM} = \frac{1}{(\sqrt{2\pi\beta_V})^{DN}} \left\{ 1 + N e^{-4/2\beta_V} 2\binom{D}{2} + N e^{-6/2\beta_V} \left[4\binom{D}{2} + 32\binom{D}{3} \right] \right.
$$

$$
+ N e^{-8/2\beta_V} \left[2N\binom{D}{2}^2 + 4\binom{D}{2} + 324\binom{D}{3} + 1296\binom{D}{4} \right]
$$

$$
+ N e^{-10/2\beta_V} \left[2N\left(4\binom{D}{2}^2 + 32\binom{D}{2}\binom{D}{3}\right) - 4\binom{D}{2} \right.
$$

$$
\left. + 3168\binom{D}{3} + 43008\binom{D}{4} + 95232\binom{D}{5} \right] + \dots \right\}, \qquad (7.42a)
$$

FIG. 7.5. Free energy of the $D = 3$ Villain model in the high and low temperature expansions. The curves show the contribution of the different low order loop diagrams (superflow loops for high- and vortex loops for low temperatures). The intersection of the two expansions gives a critical point $\beta_c \approx 0.35$ (compare with the Monte Carlo value of 0.333).
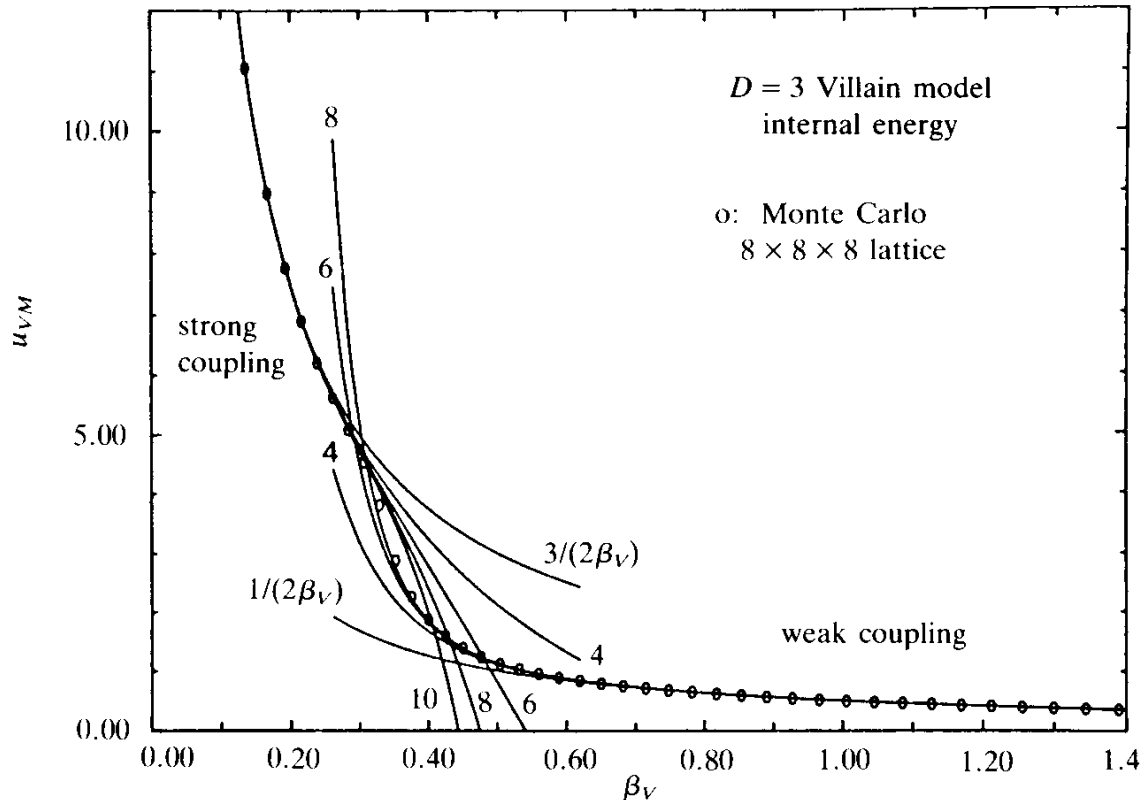
so that in $D = 3$ dimensions

$$-\beta_V f'_{VM} = 3\beta_V - \tfrac{3}{2}\log 2\pi\beta_V + 6e^{-2/\beta_V} + 44e^{-3/\beta_V} + 336e^{-4/\beta_V} + 3156e^{-5/\beta_V}.$$

$$(7.42\text{b})$$

In Fig. 7.5 we have plotted this free energy. The resulting internal energy $u'_{VM} = -(\partial/\partial\beta_V)(-\beta_V f'_{VM})$ and specific heat $c_{VM} = -\beta_V^2(\partial/\partial\beta_V)u'_{VM}$ are shown in Figs. 7.6, 7.7 where they can be compared with Monte Carlo data. The latter topic will be described in more detail in Section 7.4. The agreement is seen to be excellent, in particular for u'_{VM}, up to the critical point $\beta_c \approx 0.333$. For c_{VM}, there are deviations in the immediate vicinity of the critical point, due to the omission of higher loop diagrams.

Let us now turn to the low temperature expansion. Our starting point is the vortex-line representation (7.39). There are again the same closed loop diagrams but, in contrast to (7.38), the different loop diagrams possess different interaction energies depending on their shape. Up to loops of length six, we can immediately write down the expansion in the form,
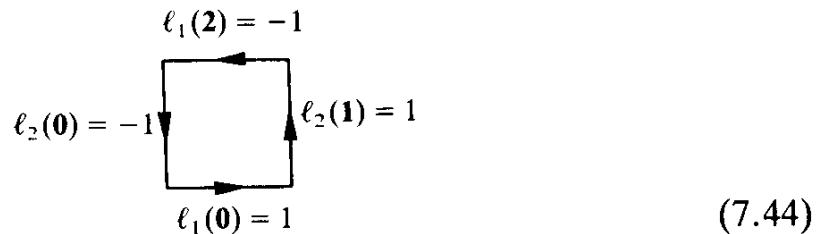
FIG. 7.6.   Internal energy of the $D = 3$ Villain model in the high- and low-temperature expansions. The different curves are explained in the heading of the previous figure. The data points are from a Monte Carlo simulation on an 8^3 lattice (see Table 7.3). The numbers denote the successive terms in the high- and low-temperature expansions. The agreement is excellent.

$$-\beta_V f'_{VM} = 3\beta_V - \tfrac{1}{2}[\log(2\pi\beta_V) + 1.6734] + 6e^{-\beta_V 4\pi^2 V_4}$$

$$+ 12e^{-\beta_V 4\pi^2 V_6} + 24e^{-\beta_V 4\pi^2 V'_6} + 8e^{-\beta_V 4\pi^2 V''_6}. \tag{7.43}$$

Here V_4 is the interaction energy of the diagram $\square$, V_6 that of $\square\!\square$, V'_6 that of ▦ , and V''_6 that of ▦ , etc. (see Table 4.1, entries 4.1, 6.1, 6.2 and 6.3.
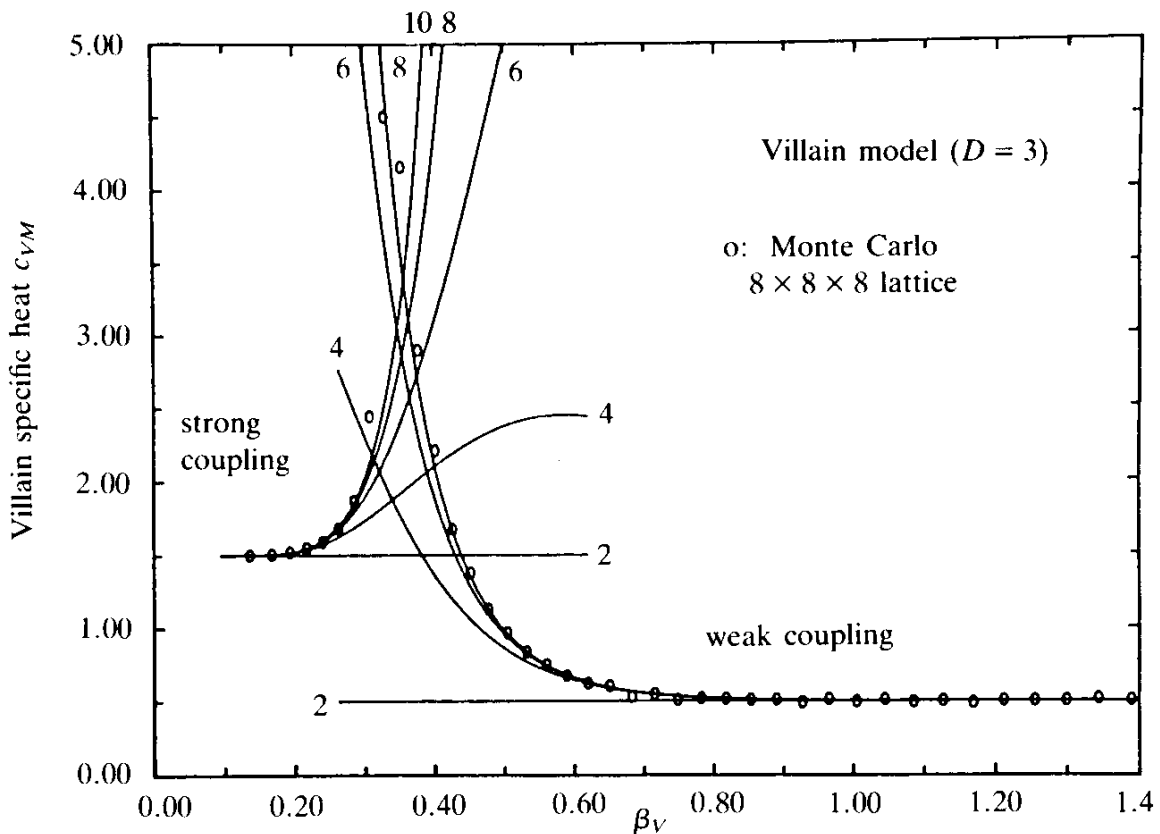
Let us calculate these energies. The smallest loop may be chosen in the xy plane as follows (the bold number ℓ denote link vectors)

$$\ell_1(2) = -1$$

$$\ell_2(0) = -1 \qquad \ell_2(1) = 1$$

$$\ell_1(0) = 1 \tag{7.44}$$

such that its ℓ vectors are

$$\ell(0) = (1, -1, 0), \quad \ell(1) = (0, 1, 0), \quad \ell(2) = (-1, 0, 0). \tag{7.45}$$

FIG. 7.7. Specific heat of the $D = 3$ Villain model as compared with high-T, low-T expansions and Monte Carlo data (same as in Fig. 7.6). We see clearly the transition at $\beta_{V_c} \approx 0.33$.
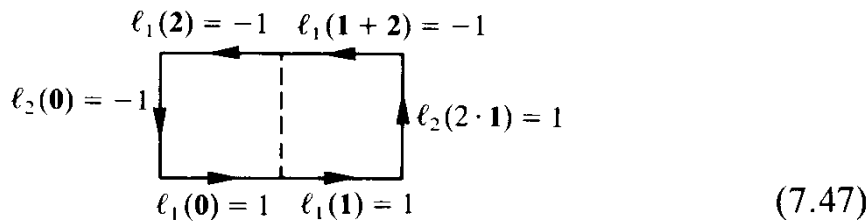
This leads to the interaction energy [recall the values of $v(\mathbf{x})$ listed in Table 6.9 of Part I]

$$V_4 = \tfrac{1}{2}v(0)(\ell^2(0) + \ell^2(1) + \ell^2(2)) + v(1)(\ell(0) \cdot \ell(1) + \ell(0) \cdot \ell(2))$$

$$= 2(v(0) - v(1)) = \tfrac{1}{3}. \tag{7.46}$$

where we have used cubic symmetry to replace $v(2) \to v(1)$.

Of the next larger loops the simplest one is the planar hexagon

$$\tag{7.47}$$

which has the ℓ vectors

$$\ell(0) = (1, -1, 0), \quad \ell(1) = (1, 0, 0), \quad \ell(2 \cdot 1) = (0, 1, 0),$$

$$\ell(2) = (-1, 0, 0), \quad \ell(1 + 2) = (-1, 0, 0), \tag{7.48}$$
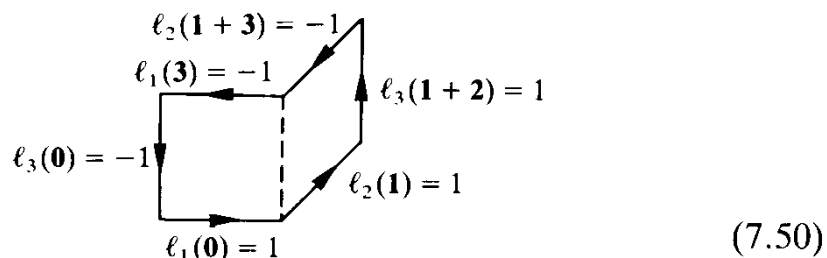
and gives

$$V_6 = \tfrac{1}{2}v(0) \sum \ell^2 + v(1)\,\ell(0) \cdot \ell(1) + v(2)\,\ell(0) \cdot \ell(2 \cdot 1)$$

$$+ v(1)\,\ell(0) \cdot \ell(2) + v(1, 1)\,\ell(0) \cdot \ell(1 + 2) + v(1)\,\ell(1) \cdot \ell(2 \cdot 1)$$

$$+ v(1, 1)\,\ell(1) \cdot \ell(2) + v(1)\,\ell(1) \cdot \ell(1 + 2) + v(1, 2)\,\ell(2 \cdot 1) \cdot \ell(2)$$

$$+ v(1, 1)\,\ell(2 \cdot 1) \cdot \ell(1 + 2) + v(1)\,\ell(2) \cdot \ell(1 + 2)$$

$$= 3 \cdot v(0) - v(2) - 2v(1, 1) \approx 0.6048 \tag{7.49}$$

Here and in the following equations, we employ the notation

$$v(0) \equiv v(0, 0, 0), \quad v(2) \equiv v(2, 0, 0) = v(0, 2, 0) = v(0, 0, 2),$$

$$v(1, 1) \equiv v(1, 1, 0) = v(1, 0, 1) = v(0, 1, 1), \quad \text{etc.}$$

The second larger loop is the bent hexagon

$$\tag{7.50}$$
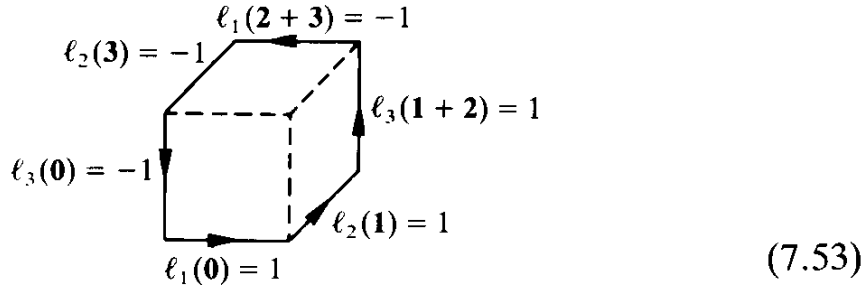
It has the ℓ vectors

$$\ell(0) = (1, 0, -1), \quad \ell(1) = (0, 1, 0), \quad \ell(1 + 2) = (0, 0, 1),$$

$$\ell(3) = (-1, 0, 0), \quad \ell(1 + 3) = (0, -1, 0), \tag{7.51}$$

with the interaction energy

$$V_6' = \tfrac{1}{2}v(0) \sum \ell^2 + (v(1)\,\ell(0) \cdot \ell(1) + v(1, 1)\,\ell(0) \cdot \ell(1 + 2)$$

$$+ v(1)\,\ell(0) \cdot \ell(3) + v(1, 1)\,\ell(0) \cdot \ell(1 + 3))$$

$$+ v(1)\,\ell(1) \cdot \ell(1 + 2) + v(1, 1)\,\ell(1) \cdot \ell(3) + v(1)\,\ell(1) \cdot \ell(1 + 3)$$

$$+ v(1, 1, 1)\,\ell(1 + 2) \cdot \ell(3) + v(1, 1)\,\ell(1 + 2) \cdot \ell(1 + 3)$$

$$+ v(1)\,\ell(3) \cdot \ell(1 + 3)$$

$$= 3v(0) - 2v(1) - v(1, 1)$$

$$= \tfrac{1}{3} + v(0) - v(1, 1) \approx 0.5309. \tag{7.52}$$

The third larger loop is the twisted hexagon

$$\tag{7.53}$$

and has the ℓ vectors

$$\ell(0) = (1, 0, -1), \quad \ell(1) = (0, 1, 0), \quad \ell(1 + 2) = (0, 0, 1),$$

$$\ell(3) = (0, -1, 0), \quad \ell(2 + 3) = (-1, 0, 0), \tag{7.54}$$

which give

$$V_6'' = 3v(0) - 3v(1, 1) \approx 0.5925. \tag{7.55}$$

Hence, to this approximation, the weak coupling expansion of the Villain model is

$$-\beta_V f' = 3\beta_V - \tfrac{1}{2}(\log 2\pi\beta_V + 1.6734) + 6e^{-\beta_V(4\pi^2/3)} + 12e^{-\beta_V 4\pi^2 \cdot 0.6048}$$

$$+ 24e^{-\beta_V 4\pi^2 \cdot 0.5307} + 8e^{-\beta_V 4\pi^2 \cdot 0.5925} + \dots \tag{7.56}$$

Notice that the bent hexagon has the lowest energy, followed by the twisted and then the planar one. The interaction energies are listed in Table 7.1 for all loop diagrams up to length 8.

For higher loop diagrams, the calculation of $-\beta f$ becomes quite tedious, in particular because disconnected diagrams come in and make matters more complicated. Contrary to the high temperature expansion, the total energy is no longer additive in the energy of the constituent loops. Fortunately, except for a few cases, the binding energies are relatively small and they occur always in pairs with opposite signs. For this reason, they cancel approximately and the free energy can be calculated for all practical purposes from the connected graphs alone, just as is the case with the high-temperature expansion. Only the few exceptional graphs with large binding energy require special treatment.

In order to understand these exceptional graphs consider, for example, the disconnected two-loop diagrams of size 4 touching each other at a corner (see the graphs 8.15a, 8.15b in Table 7.1). The individual loops together would have an energy $2 \cdot V_4 = 4(v(0) - \bar{v}(1)) = 2/3$. The binding energy is $B = 2\underline{v}(1) - 4v(1, 1) + 2v(2, 1) \sim 0.0232$. This has to be added to the 2/3 above if the loops are oriented the same way, and subtracted from it in the opposite case. The binding energy is only 3% of the total energy. The strongest binding energy occurs for two loops lying on top of each other. For this it is ± 0.1236 which amounts to 18%.

Let Nv_i be the number of composite graphs of length 8 as shown in entries (8.15a)–(8.15j) of Table 7.1. They can be distinguished according to their relative orientation, half of them having the binding energy added, half of them subtracted. We know that in D dimensions, the sum over all these graphs is given by (4.42), i.e., for $D = 3$, by

$$\frac{N}{2} \sum_i v_i = \frac{N}{2} 2 \cdot 2 \cdot 3(3N - 13), \tag{7.57}$$

where the factor 3 counts the three lattice planes and the factor $2 \cdot 2$ is due to the two possible orientations of each loop. If the relative binding energy is denoted by δ (i.e., $B_i = 2 \cdot V_4 \delta_i$), the two loops contribute to the partition function the amount

$$\frac{N}{2} e^{-\beta v 4\pi^2 (2/3)} \sum_i \frac{1}{2} v_i [e^{-\beta v 4\pi^2 (2/3)\delta_i} + e^{\beta v 4\pi^2 (2/3)\delta_i}]. \tag{7.58}$$

This can be rewritten as

TABLE 7.1. Vortex-line configurations and their superflow energies.
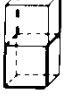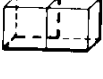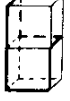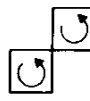
graph	$V = \frac{1}{2} \sum_{x,x'} \ell_i(\mathbf{x})\, v(\mathbf{x}, \mathbf{x}')\, \ell_i(\mathbf{x}')$	numerical value V	binding energy	number per site
4.1		$2v(0) - 2v(1) = \frac{1}{3}$	0.3333	—	$2 \cdot 3$
6.1		$3v(0) - v(2) - 2v(1, 1)$	0.6049	—	$2 \cdot 6$
6.2		$3v(0) - 2v(1) - v(1, 1)$	0.5309	—	$2 \cdot 12$
6.3		$3v(0) - 3v(1, 1)$	0.5926	—	$2 \cdot 4$
8.1		$4v(0) + v(1) - 4v(1, 1) + 2v(2) - 2v(1, 2) - v(3)$	0.8626	—	$2 \cdot 6$
8.2		$4v(0) + 4v(1) - 4v(2) - 4v(1, 2)$	1.0399	—	$2 \cdot 3$
8.3		$4v(0) - 2v(2) - 2v(1, 2)$	0.8533	—	$2 \cdot 6$
8.4		$4v(0) - 6v(1) + 2v(1, 1)$	0.6049	—	$2 \cdot 6$
8.5		$4v(0) - 3v(1) + 2v(1, 1) - 2v(1, 1, 1) - v(1, 2)$	0.7400	—	$2 \cdot 12$
8.6		$4v(0) - v(1) - 2v(1, 1) - v(1, 2)$	0.7785	—	$2 \cdot 24$
8.7		$4v(0) + 2v(1) - 2v(1, 1) - 2v(1,1, 1) - 2v(2)$	0.8997	—	$2 \cdot 12$
8.8		$4v(0) - v(1) - v(1, 1) - v(1, 1, 1) - v(2)$	0.7832	—	$2 \cdot 48$
8.9		$4v(0) - v(1) - 4v(1, 1) + v(1, 1, 1)$	0.7477	—	$2 \cdot 24$
8.10		$4v(0) + 2v(1) - 2v(1, 1) - 2v(1, 1, 1) - 2v(1, 2)$	0.9137	—	$2 \cdot 12$
8.11		$4v(0) - 2v(1, 1) - v(1, 1, 1) - v(1, 2)$	0.7477	—	$2 \cdot 48$
8.15a		$4v(0) - 4v(1) - [2v(1) - 4v(1, 1) + 2v(1, 2)]$	0.6434	-0.0232	$2\left(\frac{3 \cdot 4}{2}\right)$

TABLE 7.1.   continued
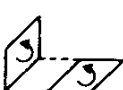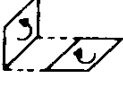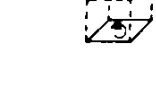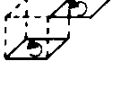
graph	$V = \frac{1}{2} \sum_{x,x'} \ell_i(x)\, v(x,\, x')\, \ell_i(x')$	numerical value V	binding energy	number per site
8.15b	$4v(0) - 4v(1) + [2v(1) - 4v(1,\, 1) + 2v(1,\, 2)]$	0.6899	+0.0232	$2\left(\dfrac{3 \cdot 4}{2}\right)$
8.15c	$4v(0) - 4v(1) - [v(1) - 2v(1,\, 1) + v(1,\, 1,\, 1)]$	0.6474	−0.0193	$2\left(\dfrac{3 \cdot 4 \cdot 4}{2}\right)$
8.15d	$4v(0) - 4v(1) + [v(1) - 2v(1,\, 1) + v(1,\, 1,\, 1)]$	0.6859	+0.0193	$2\left(\dfrac{3 \cdot 4 \cdot 4}{2}\right)$
8.15e	$4v(0) - 4v(1) - [v(1) - 4v(2) + 2v(1,\, 2) + v(3)]$	0.6527	−0.0139	$2\left(\dfrac{3 \cdot 4}{2}\right)$
8.15f	$4v(0) - 4v(1) + [v(1) - 4v(2) + 2v(1,\, 2) + v(3)]$	0.6806	+0.0139	$2\left(\dfrac{3 \cdot 4}{2}\right)$
8.15g	$4v(0) - 4v(1) - [v(1) - v(1,\, 1) - v(2) + v(1,\, 2)]$	0.6428	−0.0239	$2\left(\dfrac{3 \cdot 4 \cdot 2}{2}\right)$
8.15h	$4v(0) - 4v(1) + [v(1) - v(1,\, 1) - v(2) + v(1,\, 2)]$	0.6906	+0.0239	$2\left(\dfrac{3 \cdot 4 \cdot 2}{2}\right)$
8.15i	$4v(0) - 4v(1) + [4v(1) - 4v(1,\, 1)]$	0.7902	0.1235	$2\left(\dfrac{3 \cdot 2}{2}\right)$
8.15j	$4v(0) - 4v(1) - [4v(1) - 4v(1,\, 1)]$	0.5432	−0.1235	$2\left(\dfrac{3 \cdot 2}{2}\right)$
8.15k	$4v(0) - 4v(1) + [4v(2) - 4v(1,\, 2)]$	0.6945	0.0278	$2\left(\dfrac{3 \cdot 2}{2}\right)$
8.15l	$4v(0) - 4v(1) - [4v(2) - 4v(1,\, 2)]$	0.6388	−0.0278	$2\left(\dfrac{3 \cdot 2}{2}\right)$
8.15m	$4v(0) - 4v(1) + [4v(1,\, 1) - v(1) - 2v(1,\, 1,\, 1) - v(1,\, 2)]$	0.6783	0.0116	$2\left(\dfrac{3 \cdot 4 \cdot 4}{2}\right)$
8.15n	$4v(0) - 4v(1) - (4v(1,\, 1) - v(1) - 2v(1,\, 1,\, 1) - v(1,\, 2)]$	0.6551	−0.0116	$2\left(\dfrac{3 \cdot 4 \cdot 2}{2}\right)$

TABLE 7.1. continued

graph	$V = \frac{1}{2} \sum_{x,x'} \ell_i(x) v(x, x') \ell_i(x')$	numerical value V	binding energy	number per site
8.16		$5v(0) - 8v(1) + v(2) + 2v(1, 1)$	0.7284	—	$2 \cdot 6$
8.17		$5v(0) - 6v(1) + v(1, 1)$	0.8025	—	$2 \cdot 12$
8.18		$8v(0) - 8v(1) = \frac{4}{3}$	1.3333	—	$2 \cdot 3$

$$\frac{N}{2} \cdot 12(3N - 13) e^{-\beta_V 4\pi^2(2/3)} + \frac{N}{2} e^{-\beta_V 4\pi^2(2/3)} \sum_i \nu_i \sinh^2\left(\beta_V 4\pi^2 \frac{1}{3}\delta_i\right). \qquad (7.59)$$

When going from Z to the free energy density, the N^2 term cancels and the contribution of these graphs is

$$-\beta f_{\{\square\square\}} = \left[-\frac{1}{2} \cdot 12 \cdot 13 + \frac{1}{2} \sum_i \nu_i \sinh^2\left(\beta_V 4\pi^2 \frac{1}{3}\delta_i\right)\right] e^{-\beta_V 4\pi^2(2/3)}. \qquad (7.60)$$

The first term is what would have been found if the graph energies were purely additive, as they are in the high T expansion. The second term gives the modification due to the binding energy. The only relevant region where the binding effects in the disconnected graphs are observable is close to the critical point. Otherwise they are hidden completely under the first term of the expansion (7.56). Near the critical point, the argument of $\sinh^2(\beta_V 4\pi^2(1/3)\delta_i)$ is about $4.4\delta_i$. Thus, for almost all graphs, where $\delta_i \lesssim 3\%$, $\sinh^2(4.4 \cdot 3\%) \sim 2\%$ and we can ignore the binding energy.

For the explicit calculation it is convenient to pull out the factor 6 which counts the orientations of the first loop and write the free energy in the form
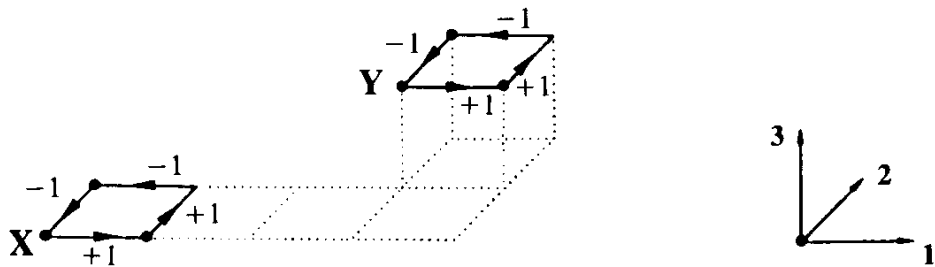
$$-\beta f_{\{\square\square\}} = 6e^{-\beta_V 4\pi^2(2/3)}\left[\sum_{\{\square\square\}} 2\sinh^2\left(\frac{\beta_V}{2} 4\pi^2 B_i\right) - 13\right], \qquad (7.61)$$

where $\sum_{\{\square\square\}}$ denotes a sum over all unoriented configurations of the second loop for a given first loop. The internal energy and the specific heat associated with this sum are
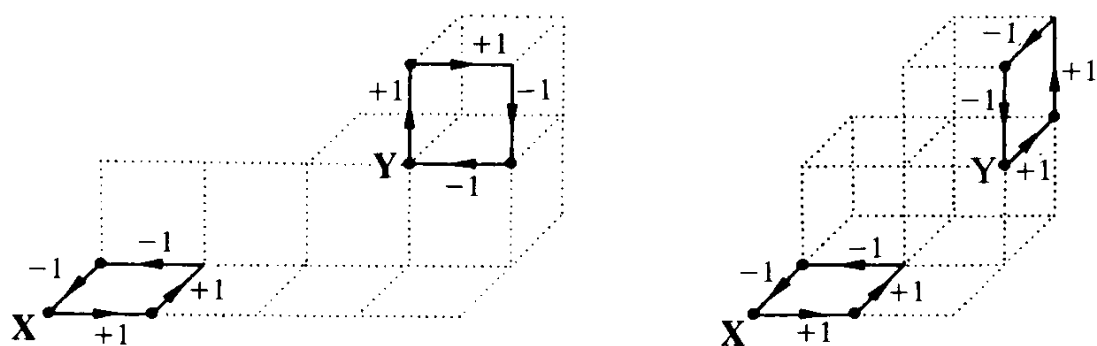
$$u_{\{\square\square\}} = 4\pi^2 \frac{2}{3} \cdot 6 \, e^{-\beta_V 4\pi^2(2/3)}$$

$$\left[\sum_{\{\square\square\}} \left(2\sinh^2\left(\frac{\beta_V}{2} 4\pi^2 B_i\right) - \frac{B_i}{2/3}\sinh(\beta_V 4\pi^2 B_i) \right) - 13 \right], \qquad (7.62)$$

$$c_{\{\square\square\}} = \beta_V^2 \left(4\pi^2 \frac{2}{3} \right)^2 \cdot 6 e^{-\beta_V 4\pi^2(2/3)}$$

$$\left[\sum_{\{\square\square\}} \left(2\sinh^2\left(\frac{\beta_V}{2} 4\pi^2 B_i\right) - \left(\frac{B_i}{2/3}\right)^2 \cosh(\beta_V 4\pi^2 B_i) \right) - 13 \right].$$
$$(7.63)$$

After these general remarks, let us calculate the binding energies systematically. In order to define them uniquely we shall consider two plaquettes associated with the points **X**, **Y** along the 3 positively oriented pairs of links. These belong either to parallel planes, i.e.,

or to orthogonal planes, i.e.,


We now define the loop-loop potential as

$$V(\mathbf{X} - \mathbf{Y}) = \frac{1}{2}\sum_{\mathbf{x},\mathbf{y}} \ell(\mathbf{x})\,v(\mathbf{x} - \mathbf{y})\,\ell(\mathbf{y}).$$

If both loops lie in the 12 plane, the ℓ vectors are given by [see (7.45)]

$$\ell(\mathbf{X}) = (1, -1, 0), \quad \ell(\mathbf{X} + 1) = (0, 1, 0), \quad \ell(\mathbf{X} + 2) = (-1, 0, 0), \quad (7.64)$$

$$\ell(\mathbf{Y}) = (1, -1, 0), \quad \ell(\mathbf{Y} + 1) = (0, 1, 0), \quad \ell(\mathbf{Y} + 2) = (-1, 0, 0), \quad (7.65)$$

from which we find

$$V(\mathbf{X} - \mathbf{Y}) = 2 \cdot 2(v(0) - v(1)) + 2v(\mathbf{X} - \mathbf{Y}) - v(\mathbf{X} - \mathbf{Y} - 1)$$
$$- v(\mathbf{X} - \mathbf{Y} - 2) - v(\mathbf{X} - \mathbf{Y} + 1) + v(\mathbf{V} - \mathbf{Y})$$
$$- v(\mathbf{X} - \mathbf{Y} + 2) + v(\mathbf{X} - \mathbf{Y}). \quad (7.66)$$

Thus we can identify the binding energy as

$$B(\mathbf{X} - \mathbf{Y}) = -(\nabla_1\bar{\nabla}_1 + \nabla_2\bar{\nabla}_2)\, v(\mathbf{X} - \mathbf{Y}). \quad (7.67)$$

If the orientations of the two loops are opposite, the sign changes.

If one loop lies in the 12 and the other in the $\begin{Bmatrix} 23 \\ 13 \end{Bmatrix}$ plane, we have instead

$$\ell(\mathbf{Y}) = \begin{Bmatrix} (0, 1, -1) \\ (1, 0, -1) \end{Bmatrix}, \quad \ell\left(\mathbf{Y} + \begin{Bmatrix} 3 \\ 1 \end{Bmatrix}\right) = (0, 0, 1),$$

$$\ell(\mathbf{Y} + 3) = \begin{Bmatrix} (0, -1, 0) \\ (-1, 0, 0) \end{Bmatrix}, \quad (7.68)$$

and find

$$V(\mathbf{X} - \mathbf{Y}) = 2 \cdot 2(v(0) - v(1)) + \left(\mp v(\mathbf{X} - \mathbf{Y}) \pm v(\mathbf{X} - \mathbf{Y} - 3) \right.$$
$$\left. \pm v\left(\mathbf{X} - \mathbf{Y} + \begin{Bmatrix} 1 \\ 2 \end{Bmatrix}\right) - v\left(\mathbf{X} - \mathbf{Y} - 3 + \begin{Bmatrix} 1 \\ 2 \end{Bmatrix}\right) \right)$$
$$= 2 \cdot 2(v(0) - v(1)) + \begin{Bmatrix} \bar{\nabla}_3\nabla_1 \\ -\bar{\nabla}_3\bar{\nabla}_2 \end{Bmatrix} v(\mathbf{X} - \mathbf{Y}), \quad (7.69)$$

so that the binding energy is

$$B(\mathbf{X} - \mathbf{Y}) = \left\{ \begin{array}{c} \bar{\nabla}_3 \nabla_1 \\ -\bar{\nabla}_3 \nabla_2 \end{array} \right\} v(\mathbf{X} - \mathbf{Y}). \tag{7.70}$$

It turns out that the formulas for the binding energies can be obtained more directly. In the next chapter we shall demonstrate [see Eq. (8.3)] that the closed loops are related to the jump numbers $n_i(\mathbf{x})$ by the lattice curl

$$\ell_i(\mathbf{x}) = (\nabla \times \mathbf{n})_i(\mathbf{x}) = \varepsilon_{ijk} \nabla_j n_k(\mathbf{x} + \mathbf{i}). \tag{7.71}$$

An elementary loop in the 12 plane at $\mathbf{X}$ is given by $n_3(\mathbf{x}) = \delta_{\mathbf{x}-1-2,\mathbf{x}}$. Indeed, if we insert this into (7.71), we find

$$\ell_1(\mathbf{x}) = \nabla_2 n_3(\mathbf{x} + \mathbf{1}) = n_3(\mathbf{x} + \mathbf{1} + \mathbf{2}) - n_3(\mathbf{x} + \mathbf{1}) = \delta_{\mathbf{x},\mathbf{x}} - \delta_{\mathbf{x},\mathbf{x}+2},$$

$$\ell_2(\mathbf{x}) = -\nabla_1 n_3(\mathbf{x} + \mathbf{2}) = -n_3(\mathbf{x} + \mathbf{1} + \mathbf{2}) + n_3(\mathbf{x} + \mathbf{2}) = -\delta_{\mathbf{x},\mathbf{x}} + \delta_{\mathbf{x},\mathbf{x}+1},$$

$$\ell_3(\mathbf{x}) \equiv 0, \tag{7.72}$$

which agrees with (7.64).

Invoking the analogy of vortex loops and current loops, a loop at $\mathbf{X}$ in the ij plane corresponds to a magnetic dipole field $d_k(x)$ with values ± 1 pointing orthogonal to the loop. The jump numbers $n_k(\mathbf{x})$ are related by

$$n_k(\mathbf{x}) = d_k(\mathbf{x} - \mathbf{i} - \mathbf{j}) \quad ijk \text{ cyclic.} \tag{7.73}$$

For loops of higher strength, $n_k \cong d_k$ runs through all integer values.

The numbers $n_k(\mathbf{x}) \cong d_k(\mathbf{x})$ which parametrize directly the positions and orientations of the magnetic dipoles formed by the loops permit a reformulation of an ensemble of vortex lines in terms of elementary vortex *loops* around each plaquette. If we make use of (7.71), we find for their interaction energy the following formula,

$$V(\mathbf{X} - \mathbf{Y}) = \frac{1}{2} \sum_{\mathbf{x},\mathbf{y}} \ell(\mathbf{x}) \cdot v(\mathbf{x} - \mathbf{y}) \ell(\mathbf{y}) = \frac{1}{2} \sum_{\mathbf{x}} (\nabla \times \mathbf{n}) \cdot \frac{1}{-\bar{\nabla} \cdot \nabla} (\nabla \times \mathbf{n})$$

$$= \frac{1}{2} \sum_{\mathbf{x}+\mathbf{i}} \varepsilon_{ik\ell} \nabla_k n_\ell(\mathbf{x} + \mathbf{i}) \left[\frac{1}{-\bar{\nabla} \cdot \nabla} \varepsilon_{ik'\ell'} \nabla_{k'} n_{\ell'} \right] (\mathbf{x} + \mathbf{i})$$

$$= \frac{1}{2} \sum_{\mathbf{x}} \left[\nabla_k n_\ell(\mathbf{x}) \frac{1}{-\bar{\nabla} \cdot \nabla} \nabla_k n_\ell(\mathbf{x}) - \nabla_k n_\ell(\mathbf{x}) \frac{1}{-\bar{\nabla} \cdot \nabla} \nabla_\ell n_k(\mathbf{x}) \right]$$

$$= \frac{1}{2} \sum_{x} n_\ell(\mathbf{x})(-\bar{\nabla} \cdot \nabla \delta_{\ell k} + \nabla_\ell \bar{\nabla}_k) \frac{1}{-\bar{\nabla}\nabla} n_k(\mathbf{x})$$

$$= \frac{1}{2} \sum_{x} n_\ell(\mathbf{x})\left(\delta_{\ell k} - \frac{\nabla_\ell \bar{\nabla}_k}{\bar{\nabla} \cdot \nabla} \right) n_k(\mathbf{x}). \tag{7.74}$$

Inserting (7.73), this becomes

$$V(\mathbf{X} - \mathbf{Y}) = \frac{1}{2} \sum_{x} d_\ell(\mathbf{x})\left(\delta_{\ell k} - \frac{\nabla_\ell \bar{\nabla}_k}{\bar{\nabla} \cdot \nabla} \right) d_k(\mathbf{x}). \tag{7.75}$$
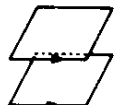
The potential

$$v_{\ell k}(\mathbf{x}) = \delta_{\ell k}\delta_{\mathbf{x},\mathbf{y}} - \frac{\nabla_\ell \bar{\nabla}_k}{\bar{\nabla} \cdot \nabla} = -(\delta_{\ell k}\nabla\bar{\nabla} - \nabla_\ell \bar{\nabla}_k) v(\mathbf{x}) \tag{7.76}$$

is recognized as the lattice version of the usual potential between magnetic dipoles, $\delta_{\ell k}\delta(\mathbf{x}) - (\delta_{\ell k} - 3\hat{x}_\ell \hat{x}_k)/4\pi x^3$.

Notice, however, that the sign is *opposite* the usual sign for dipoles. Two magnetic dipoles on top of each other *attract*. Two loops on top of each other have double superflow velocity and thus four times as much superflow energy. Hence they *repel*. Formally, the reversed sign comes from the factor i in the magnetic coupling $2\pi i \sum_{\mathbf{x}} A_i(\mathbf{x}) \ell_i(\mathbf{x})$ which is absent in magnetism. As shown in Chapter 1, after Eq. (1.119), this absence of i has its root in the induction forces which lie outside purely magnetostatic considerations and are a consequence of electrodynamics. Applying (7.74) to the special cases of two loops in the same or different planes we recover the previous binding energy (7.67), (7.70).
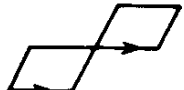
We shall now apply these formulas to two-loop diagrams in close proximity from each other. Two equally oriented loops cannot coincide nor have a common link since otherwise they would be counted as a double loop of type 8.18 in Table 7.1 or as a larger hexagonal single loop of type 6.1. Two oppositely oriented loops cannot lie on top of each other either nor have a common link since otherwise they would annihilate each other or be counted as a graph of the type 8.16 in Table 7.1. So they must lie either spaced by one unit on top of each other or touch each other at a corner. In the first case we find the binding energy

$$B(\mathbf{X}, \mathbf{X} + 3) = -(\nabla_1 \bar{\nabla}_1 + \nabla_2 \bar{\nabla}_2) v(-3)$$

$$= -v(-3 + 1) + 2v(-3) - v(-3 - 1) - v(-3 + 2)$$

$$+ 2v(-3) - v(-3 - 2)$$

$$= 4(v(1) - v(1, 1)) = 0.12349, \tag{7.77}$$

with the opposite sign for opposite orientations (see Table 7.1, graph 8.15i, j). In the second case we find

$$B(X, X + 1 + 2) = -(\nabla_1 \bar{\nabla}_1 + \nabla_2 \bar{\nabla}_2) v(-1 - 2)$$

$$= -v(-2) + 2v(-1 - 2) - v(-2 \cdot 1 - 2)$$

$$- v(-1) + 2v(-1 - 2) - v(-1 - 2 \cdot 2)$$

$$= 4v(1, 1) - 2v(1, 2) - 2v(1) = -0.02323 \tag{7.78}$$

(see Table 7.1, graphs 8.15a, b).

For larger separations we find
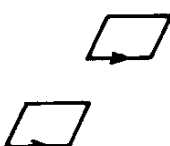
$$B(X, X + 2 \cdot 1) = -v(1) + 4v(2) + 2v(1, 2) + v(3)$$

$$= -0.01392, \tag{7.79}$$

$$B(X, X + 1 + 3) = 4v(1, 1) - v(1) - 2v(1, 1, 1) - v(1, 2)$$

$$= 0.0116, \tag{7.80}$$

$$B(X, X + 2 \cdot 3) = 4v(2) - 4v(1, 2), \tag{7.81}$$

$$= 0.0278$$
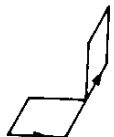
$$B(X, X + 1 + 2 + 3) = 4v(1, 1, 1) - 2v(1, 1, 2)$$

$$- 2v(1, 1) = 0. \tag{7.82}$$

Notice that the binding energy vanishes whenever loops with the same normal vectors are arranged along the space diagonal, since in that instance

$$-\nabla_3 \bar{\nabla}_3 v(\mathbf{x}) = -\nabla_1 \bar{\nabla}_1 v(\mathbf{x}) = -\nabla_2 \bar{\nabla}_2 v(\mathbf{x}) = -\frac{1}{3} \nabla \cdot \bar{\nabla} v(\mathbf{x}) = \delta_{\mathbf{x}, \mathbf{0}}$$

so that $-(\nabla_1 \bar{\nabla}_1 + \nabla_2 \bar{\nabla}_2) v(\mathbf{x}) = 0$ for $\mathbf{x} \neq \mathbf{0}$. The energy (7.82) is of this type since it can be written as $-(v(\mathbf{x} + 1) - 2v(\mathbf{x}) + v(\mathbf{x} - 1) - v(\mathbf{x} + 2) - 2v(\mathbf{x}) + v(\mathbf{x} - 2))$ at $\mathbf{x} = 1 + 2 + 3$.

If the two plaquettes lie in different planes, say 12 and 23, the values of $\mathbf{X}$ and $\mathbf{Y}$ cannot coincide since otherwise the diagram would be counted separately as in graph 6.2 of Table 7.1, if they are oriented the same way; or as in graph 8.17, if they are oriented in the opposite way. Thus the closest configurations are

$$B(\mathbf{X}, \mathbf{X} + 1 + 2) = -\bar{\nabla}_3 \nabla_1 v(-1 - 2)$$

$$= -v(-2) + v(-1 - 2) + v(-2 - 3)$$

$$- v(-1 - 2 - 3)$$

$$= -v(1) + 2v(1, 1) - v(1, 1, 1)$$

$$= -0.0193, \tag{7.83}$$

$$B(\mathbf{X}, \mathbf{X} - 1) = -\bar{\nabla}_3 \nabla_1 v(1)$$

$$= -v(2 \cdot 1) + v(1) + v(2 \cdot 1 - 3) - v(1 - 3)$$

$$= -v(2) + v(1) + v(1, 2) - v(1, 1) = 0.0239. \tag{7.84}$$

Continuing this procedure we find all the binding energies listed in Table 7.1.

Using these binding energies, we can collect the eight most important contributions to $-\beta f_V$ as follows:

$$\sum_{\{\square^\square\}} 2 \sinh^2 \left(\frac{\beta_V}{2} 4\pi^2 B_i \right)$$

$$= 4 \sinh^2 \left(\frac{\beta_V}{2} 4\pi^2 \cdot 0.1235 \right) + 4 \sinh^2 \left(\frac{\beta_V}{2} 4\pi^2 \cdot 0.0278 \right)$$

$$+ 16 \sinh^2 \left(\frac{\beta_V}{2} 4\pi^2 \cdot 0.0239 \right) + 16 \sinh^2 \left(\frac{\beta_V}{2} 4\pi^2 \cdot 0.0239 \right)$$

$$+ 8\sinh^2\left(\frac{\beta_V}{2}4\pi^2 \cdot 0.0232\right) + 32\sinh^2\left(\frac{\beta_V}{2}4\pi^2 \cdot 0.0193\right)$$

$$+ 8\sinh^2\left(\frac{\beta_V}{2}4\pi^2 \cdot 0.0139\right) + 16\sinh^2\left(\frac{\beta_V}{2}4\pi^2 0.0116\right). \qquad (7.85)$$

Notice that the sum converges rapidly[a] since the binding energy decreases like $1/r^3$ with the distance between the elementary loops so that $\Sigma\sinh^2$ behaves like $\int dr(r^2/r^6)$.

Adding the loop graphs 8.1–8.11 of Table 7.1 and (7.61) with (7.85) to the previously calculated free energy (7.56) we obtain the curves shown in Fig. 7.5. From the intersections of the low and high temperature curves, the phase transition is found at

$$\beta_{Vc} \sim 0.35, \quad T_{Vc} \sim 2.84. \qquad (7.86)$$

This is to be compared with a rigorous bound, obtained by Myerson (see the Notes and References at the end of the chapter)

$$T_{Vc} < 3.086, \qquad (7.87)$$

and with the correct transition temperature found by Monte Carlo techniques, to be described in the next section (see the peak in the specific heat in Fig. 7.7)

$$T_{Vc} = \frac{1}{\beta_{Vc}} \approx \frac{1}{0.33} \sim 3.03. \qquad (7.88)$$

Notice that a rather good estimate of the critical point can already be obtained from the lowest approximations to the high and low temperature expansions. The asymptotic partition functions are equal when β_V satisfies

---

[a]For $\beta_V \sim 0.33$, the terms (7.85) together give $3.1976 + 0.1326 + 0.3909 + 0.39094 + 0.1841 + 0.5084 + 0.0658 + 0.0915 = 4.9582$ as compared to the total sum 5.6132.

$$\frac{1}{(\sqrt{2\pi\beta_V})^{DN}} = \frac{1}{(\sqrt{2\pi\beta_V})^N} \det(-\bar{\nabla} \cdot \nabla)^{-1/2}, \qquad (7.89)$$

or

$$-\tfrac{3}{2}\log(2\pi\beta_V) \approx -\tfrac{1}{2}[\log(2\pi\beta_V) + 1.6734]. \qquad (7.90)$$

Hence

$$\beta_{V_c}^0 \approx \frac{1}{2\pi}e^{(1/2)1.6734} \approx 0.3674. \qquad (7.91)$$

This lies only 11% above the correct critical value of $\beta_{V_c} \approx 0.33$. A one-loop correction at low and high temperature moves this to 0.359, since it amounts to a correction factor

$$\exp(6e^{-2/\beta_{V_c}^0} - 6e^{-4\pi^2\beta_{V_c}^0/3}) \sim 1 - 0.022. \qquad (7.92)$$

It is clear from the Fig. 7.5 that for the free energy the exponential suppression of most diagrams is rather strong for each type of expansion.

In Figs. 7.6 and 7.7 we have compared the internal energy and the specific heat also with the numbers obtained from a Monte Carlo simulation of the Villain model. This will be described in detail in the next section. The figures show the importance of larger and larger loops in the immediate vicinity of the transition point β_c, either vortex-loop graphs above β_c or stress-loop graphs below.

Physically, the exponentials in the vortex-loop expansion of the partition function can be interpreted as the Boltzmann factors of a "lattice roton" and its bound states. For the single roton at the transition point we have

$$\beta_V \frac{4\pi^2}{3} \sim 4.3864. \qquad (7.93)$$

This is to be compared with the roton energy in superfluid ^{4}He of

$$E_{\rm rot} = 9.6\,{\rm K}, \qquad (7.94)$$

[Balibar *et al.* (1977)] or, going to the same units as (7.93),

$$\frac{E_{\text{rot}}}{T_c} = \frac{9.6\,\text{K}}{2.18\,\text{K}} = 4.39. \tag{7.95}$$

The agreement with (7.93) is surprisingly good. The lowest two-roton bound state in the model has a binding energy of [see (7.77)]

$$\frac{B}{T_c} \approx \beta_V 4\pi^2 (0.1235) \approx 1.61. \tag{7.96}$$

7.4. MONTE CARLO SIMULATION OF THE VILLAIN MODEL

The Villain model can be simulated via Monte Carlo techniques just as easily as the XY model. At first sight it may appear as though this would be much more time consuming since the partition function,

$$Z_{VM} = \prod_{\mathbf{x}} \left[\int \frac{d\gamma(\mathbf{x})}{2\pi} \right] \sum_{\{n_i(\mathbf{x})\}} e^{-(\beta_V/2)\Sigma_{\mathbf{x},i}(\nabla_i \gamma - 2\pi n_i)^2} \tag{7.97}$$

contains 4 fluctuating variables: $\gamma(\mathbf{x})$ and $n_i(\mathbf{x})$ at each site. Fortunately, this is not true. The integers $n_i(\mathbf{x})$ at different sites are independent such that they can be summed up separately. We introduce an auxiliary potential $V_{\beta_V}(\gamma)$ via

$$e^{-V_{\beta_V}(\gamma)} \equiv \sum_{n} e^{-(\beta_V/2)(\gamma - 2\pi n)^2} \tag{7.98}$$

and see that the partition function can be written as

$$Z_{VM} = \prod_{\mathbf{x}} \left[\int \frac{d\gamma(\mathbf{x})}{2\pi} \right] e^{-\Sigma_{\mathbf{x},i} V_{\beta_V}(\nabla_i \gamma)}. \tag{7.99}$$

This has the same form as Z'_{XY} and thus can be simulated in the same way.

The internal energy is found by differentiation,

$$u_{VM} = -\frac{1}{N} \frac{\partial}{\partial \beta_V} \log Z_{VM} = \frac{1}{N Z_{VM}} \prod_{\mathbf{x}} \left[\int_{-\pi}^{\pi} \frac{d\gamma(\mathbf{x})}{2\pi} \right] \sum_{\mathbf{y},j} \dot{V}_{\beta_V}(\nabla_j \gamma(\mathbf{y})) \, e^{-\Sigma_{\mathbf{x},i} V_{\beta_V}(\nabla_i \gamma)}, \tag{7.100}$$

with the local energy density per link

$$\dot{V}_{\beta_V}(\gamma) \equiv \frac{\partial}{\partial \beta_V} V_{\beta_V}(\gamma) = \frac{1}{2} \frac{\sum\limits_n (\gamma - 2\pi n)^2 e^{-(\beta_V/2)(\gamma - 2\pi n)^2}}{\sum\limits_n e^{-(\beta_V/2)(\gamma - 2\pi n)^2}}. \tag{7.101}$$

Introducing $e \equiv N^{-1} \sum\limits_{\mathbf{x},i} \dot{V}_{\beta_V}(\nabla_i \gamma(\mathbf{x}))$ we have $U_{VM} = \langle e \rangle$.

Similarly, the specific heat of the Villain model is given by

$$c_{VM} = \beta_V^2 \left\{ \frac{1}{N Z_{VM}} \prod_{\mathbf{x}} \left[\int_{-\pi}^{\pi} \frac{d\gamma(\mathbf{x})}{2\pi} \right] \left(\sum_{y,j,k} \dot{V}_{\beta_V}(\nabla_j \gamma(\mathbf{y})) \dot{V}_{\beta_V}(\nabla_k \gamma(\mathbf{0})) \right. \right.$$

$$\left. - \sum_j \ddot{V}_{\beta_V}(\nabla_j \gamma(\mathbf{0})) \right) e^{\sum_{\mathbf{x},i} V_{\beta_V}(\nabla_i \gamma(\mathbf{x}))} \tag{7.102}$$

$$\left. - \frac{1}{N Z_{VM}^2} \left[\prod_{\mathbf{x}} \left[\int_{-\pi}^{\pi} \frac{d\gamma(\mathbf{x})}{2\pi} \right] \sum_{\mathbf{x},j} \dot{V}_{\beta_V}(\nabla_j \gamma(\mathbf{x})) e^{\sum_{\mathbf{x},i} V_{\beta_V}(\nabla_i \gamma(\mathbf{x}))} \right]^2 \right\},$$

We now introduce the function

$$W_{\beta_V}(\gamma) \equiv \frac{\sum\limits_n \frac{1}{4}(\gamma - 2\pi n)^4 e^{-(\beta_V/2)(\gamma - 2\pi n)^2}}{\sum\limits_n e^{-(\beta_V/2)(\gamma - 2\pi n)^2}}, \tag{7.103}$$

which can be tabulated together with V_{β_V}, $\dot{V}_{\beta_V}$. Using $\ddot{V}_{\beta_V} = -W_{\beta_V} + \dot{V}_{\beta_V}^2$, we obtain c_{VM} as the expectation value

$$c_{VM} = \beta_V^2 \left[N(\langle e^2 \rangle - \langle e \rangle^2) + \sum_j [\langle W_{\beta_V}(\nabla_j \gamma(\mathbf{0})) \rangle - \langle \dot{V}_{\beta_V}^2(\nabla_j \gamma(\mathbf{0})) \rangle] \right].$$
$$\tag{7.104}$$

The simulation is now standard. We take, for instance, a $16 \times 16 \times 16$ simple cubic lattice, attach to each lattice point a random set of angles (discretized to say, 16 points) and sweep through the lattice, site by site, updating successively each $\gamma(\mathbf{x})$ according to the probability measure $\exp(-\sum_{\mathbf{x},i} V_{\beta_V}(\nabla_i \gamma(\mathbf{x})))$. We do this a great number of times in order to reach equilibrium. After this we sweep again through the lattice, also a large number of times, and measure each time the expectations of the

functions $e_1 e^2$, $V_{\beta_1}^2(\nabla_i\gamma)$ and $W_{\beta_1}(\nabla_i\gamma)$. The resulting internal energy and specific heat are listed in Table 7.2 and plotted in Figs. 7.6, 7.7, together with the previously calculated analytic results. We see that the loop corrections to the high- and low-temperature limits rapidly approximate the Monte Carlo data. The agreement is excellent even if only a few loop corrections are included, except for the specific heat in the immediate vicinity of the transition point where all loop diagrams become important. The transition point is found to lie at

$$\beta_{V_c} \approx 0.33, \quad T_{V_c} \approx 3.03.$$

In Fig. 7.8 we display a high resolution picture of the peak of the specific heat of Fig. 7.7 which shows the sensitivity to the finite size of the lattice.

7.5. COMPARISON OF THE *XY* MODEL WITH ITS VILLAIN APPROXIMATION

Let us use these Monte Carlo numbers of the Villain model and insert them into formulas (7.35) and (7.37) to find the internal energy and specific heat of the Villain approximation to the *XY* model. These are compared with the Monte Carlo data of the *XY* model in Figs. 7.9, 7.10. In addition, we have taken the high and low temperature series of the Villain model and treated them in the same way.[b] We see that the agreement between the *XY* model and its Villain approximation is excellent only for *low* values of β up to the transition point $\beta_c \approx 0.45$. The location of β_c is almost precisely given by the relation $\beta_V = -[2\log(I_1(\beta)/I_0(\beta))]^{-1}$. In fact, using $\beta_{V_c} \approx 0.33$ we calculate from this $\beta_c \approx 0.45$ (use Fig. 7.2) in excellent agreement with the Monte Carlo value for the *XY* model, $\beta_c \approx 0.454$. In Table 7.2 we have made the same comparison also for $D = 2$ (and for another model called $U(1)$ lattice gauge theory to be discussed in Section 10.2).

Notice that while the quality of the Villain approximation is very good for small β up to the critical point (cf. Fig. 7.11) it is extremely bad for moderately large $\beta \approx 1.5 - 2$. Only for *very* large β does the approximation improve once more and becomes exact for $\beta \to \infty$. One has to go to $\beta \gtrsim 10$ in order for the specific heat to reach the proper Dulong-Petit limit 1/2.

[b]For convenience, we list the expansion coefficients of the free energy in powers of $\exp(-1/(2\beta_V)) = I_1(\beta)/I_0(\beta)$ in Table 7.3.
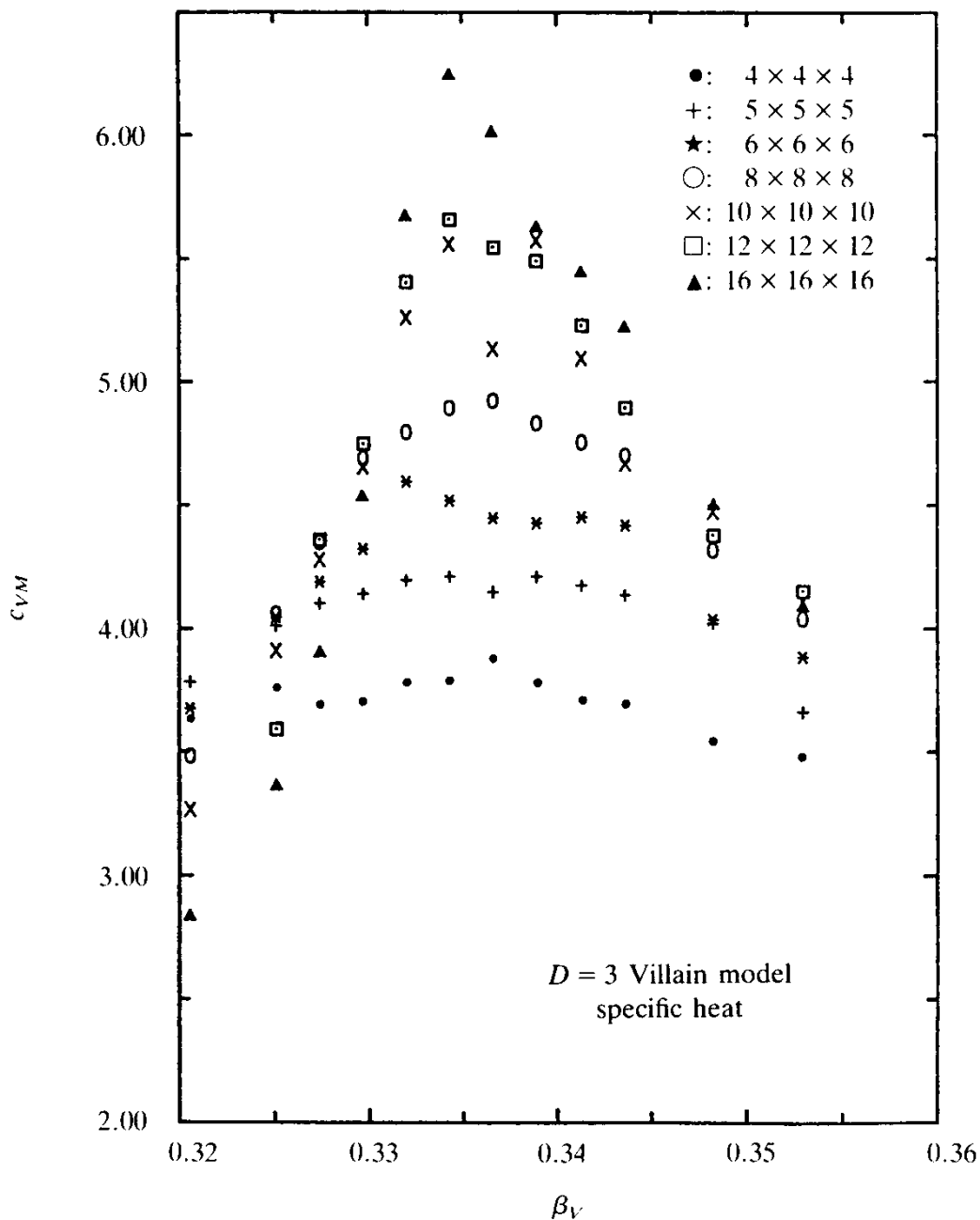
TABLE 7.2 Internal energy and specific heat of the Villain model and the Villain approximation to the $D = 3$ XY model. Monte Carlo data on 16^3 lattice, 5000 equilibriation + 5000 measurement sweeps [$U(1)$ approx. by $Z(16)$]. The data are taken only in the cooling direction. The heating data are practically the same [from W. Janke and H. Kleinert (1986), op. cit. in Notes and References].

β	β_V	u_{VM}(cool)	c_{VM}(cool)	u_V(cool)	c_V(cool)
0.05	0.1355	11.0670	1.5013	2.9246	0.0038
0.10	0.1668	8.9885	1.5074	2.8489	0.0157
0.15	0.1928	7.7672	1.5235	2.7697	0.0367
0.20	0.2167	6.8954	1.5525	2.6888	0.0684
0.25	0.2396	6.2027	1.6087	2.6013	0.1152
0.30	0.2620	5.6121	1.7217	2.5046	0.1885
0.35	0.2844	5.0809	1.8888	2.3962	0.2953
0.40	0.3069	4.5558	2.1890	2.2616	0.4722
0.45	0.3297	3.9164	5.1399	2.0505	1.7353
0.50	0.3529	2.8903	4.0886	1.6352	1.5494
0.55	0.3766	2.2695	2.9248	1.3838	1 2190
0.60	0.4008	1.8661	2.1817	1.2175	1.0072
0.65	0.4257	1.5857	1.7211	1.0974	0.8906
0.70	0.4512	1.3835	1.3768	1.0058	0.8027
0.75	0.4974	1.2315	1.1334	0.9322	0.7490
0.80	0.5044	1.1151	0.9713	0.8712	0.7291
0.85	0.5321	1.0228	0.8232	0.8187	0.7010
0.90	0.5605	0.9477	0.7312	0.7723	0.7023
0.95	0.5898	0.8844	0.6795	0.7300	0.7273
1.00	0.6199	0.8305	0.6569	0.6913	0.7715
1.05	0.6508	0.7846	0.5870	0.6558	0.7605
1.10	0.6826	0.7425	0.5510	0.6216	0.7750
1.15	0.7152	0.7055	0.5376	0.5900	0.8065
1.20	0.7486	0.6718	0.5520	0.5599	0.8650
1.25	0.7829	0.6412	0.5354	0.5316	0.8821
1.30	0.8180	0.6131	0.5213	0.5049	0.8962
1.35	0.8539	0.5866	0.5233	0.4792	0.9259
1.40	0.8907	0.5617	0.5100	0.4546	0.9305
1.45	0.9282	0.5389	0.4967	0.4318	0.9293
1.50	0.9666	0.5174	0.4947	0.4101	0.9390
1.55	1.0057	0.4971	0.4937	0.3894	0.9463
1.60	1.0456	0.4782	0.5048	0.3702	0.9676
1.65	1.0862	0.4605	0.4918	0.3521	0.9484
1.70	1.1276	0.4430	0.5035	0.3345	0.9647
1.75	1.1696	0.4274	0.4940	0.3187	0.9437
1.80	1.2123	0.4123	0.5112	0.3036	0.9630
1.85	1.2557	0.3983	0.4948	0.2898	0.9246
1.90	1.3997	0.3846	0.5176	0.2763	0.9491
1.95	1.3443	0.3718	0.4986	0.2640	0.9015
2.00	1.3894	0.3597	0.5018	0.2525	0.8891

FIG. 7.8.   Resolution of the critical regime of Fig. 7.7 and finite size effects. From these curves one can extract the critical index v as follows ($\alpha = 2 - vD$):

$$c_{\max} = L^{\alpha/v}, \quad \beta_L - \beta_c \sim L^{-1/v},$$

where $L = N^{1/D}$ is the linear size of the system. The figure shows $c_{\max} \sim \log L$. Hence one can conclude that $\alpha \sim 0$.

In Section 7.1 and in much of the standard literature, the quality of the Villain approximation is often inferred from the limit

$$\lim_{\beta \to \infty} e^{\beta \cos \gamma} = \sum_n e^{-(\beta/2)(\gamma - 2\pi n)^2}. \tag{7.105}$$

TABLE 7.3.   Villain approximation of the free energy of the $D = 2$ and $D = 3$ XY model re-expressed directly in terms of powers of $I_1(\beta)/I_0(\beta)$ or $\beta/2$.

$-\beta f_V'$	$D = 2$			$D = 3$		
	$x = I_1/I_0$	$x = \dfrac{\beta}{2}$	$x = \dfrac{\beta}{2}$	$x = I_1/I_0$	$x = \dfrac{\beta}{2}$	$x = \dfrac{\beta}{2}$
$\ln I_0$	2	2	—	3	3	—
x^2	—	—	2	—	—	3
x^4	2	2	$1\frac{1}{2}$	6	6	$5\frac{1}{4}$
x^6	4	0	$\frac{2}{9}$	44	32	$32\frac{1}{3}$
x^8	4	$-2\frac{1}{3}$	$-2\frac{43}{96}$	336	221	$220\frac{53}{64}$
x^{10}	-4	$-3\frac{5}{6}$	$-3\frac{77}{100}$	3156	$2044\frac{1}{2}$	$2044\frac{119}{200}$
x^{12}	$-33\frac{1}{3}$	$-2\frac{83}{120}$	$-2\frac{9437}{12960}$			

This is certainly true since, for large β, all fluctuations of γ are squeezed into the periodic potential valleys and these are trivially the same on both sides. But the approach to this limit is extremely slow so that it is of no practical relevance.
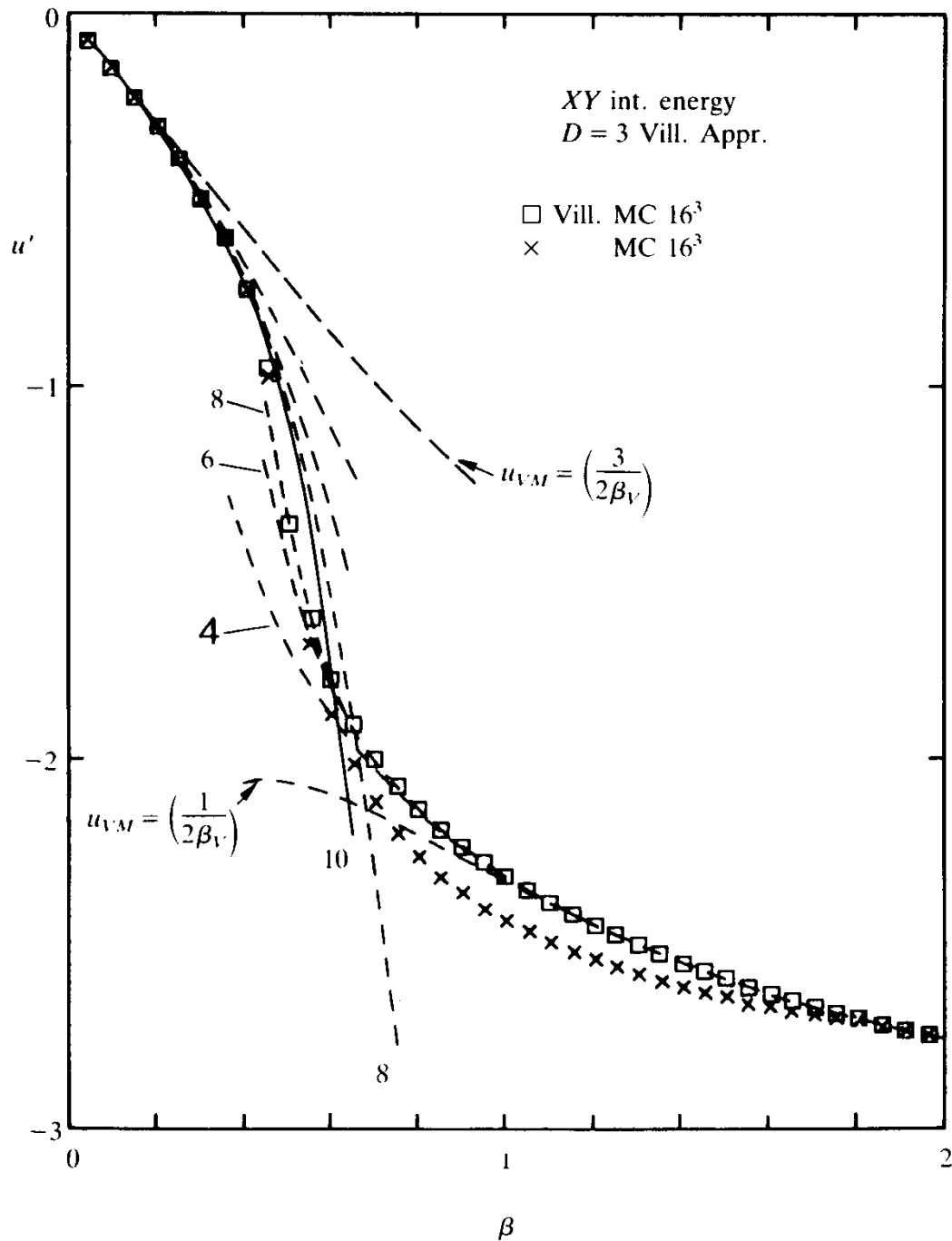
We can see this also analytically using the fact that the low temperature behaviour of internal energy and specific heat in the Villain model are

$$u_{VM} \rightarrow \frac{1}{2\beta_V}, \qquad c_{VM} \rightarrow \frac{1}{2},$$

and that this is true to *all* orders in $1/\beta_V$ (only $e^{-\beta_V \text{const.}}$ terms are omitted). Inserting this into Eqs. (7.35), (7.37) and expanding the coefficient functions in powers of $1/\beta$ (see the Appendix at the end of the Chapter) gives

$$u' \xrightarrow[\beta \to \infty]{} \frac{\dot{\beta}_V}{2\beta_V} - D\frac{\dot{R}}{R}$$

$$\rightarrow -D + \frac{1}{2\beta} + \left(\frac{1}{4} - \frac{D}{8}\right)\frac{1}{\beta^2} + \left(\frac{1}{3} - \frac{5D}{24}\right)\frac{1}{\beta^3} + \left(\frac{39}{64} - \frac{53D}{128}\right)\frac{1}{\beta^4} + \cdots,$$

$$(7.106)$$

FIG. 7.9. Comparison of internal energy of the Villain approximation and of the *XY* model. The stars are Monte Carlo data of the Villain model, transformed to the *XY* quantities via (7.35). The circles are Monte Carlo data of the *XY* model itself. The agreement is excellent up to the phase transition.

$$c \xrightarrow[\beta \to \infty]{} \beta^2 \left(\frac{\dot\beta_V}{\beta_V}\right)^2 \frac{D}{2} - \beta^2 \ddot\beta_V \frac{D}{2\beta_V} + \beta^2 D \left[\frac{\ddot R}{R} - \left(\frac{\dot R}{R}\right)^2\right]$$

$$\to \frac{1}{2} + \left(\frac{1}{2} - \frac{D}{4}\right)\frac{1}{\beta} + \frac{8 - 5D}{8}\frac{1}{\beta^2} + \frac{78 - 53D}{32}\frac{1}{\beta^3} + \dots \qquad (7.107)$$

The plot of this expansion, which is the Villain approximation to the *XY* model to all orders in $1/\beta$ (only vortex terms of the type $e^{-\beta\,\mathrm{const.}}$ are
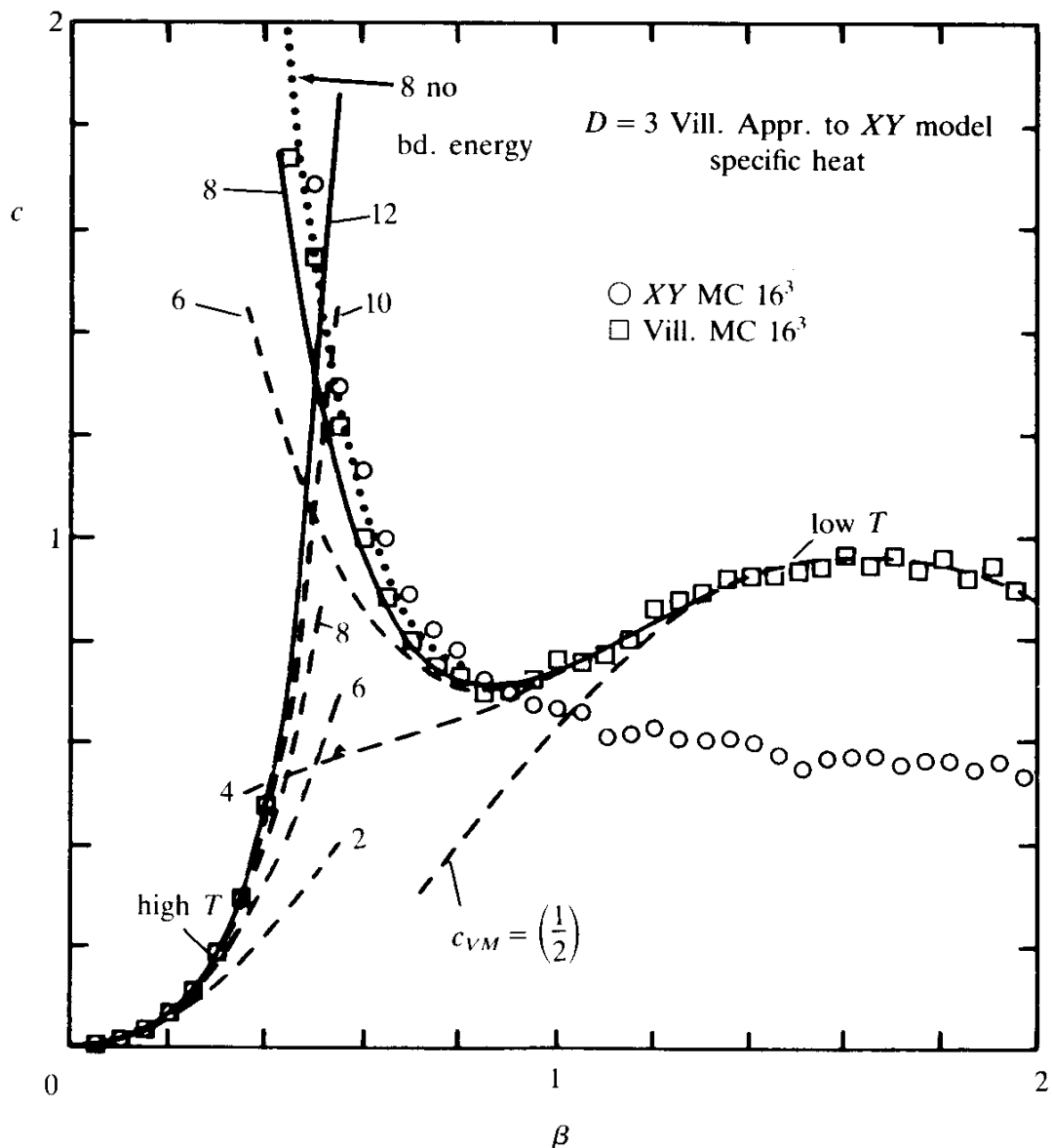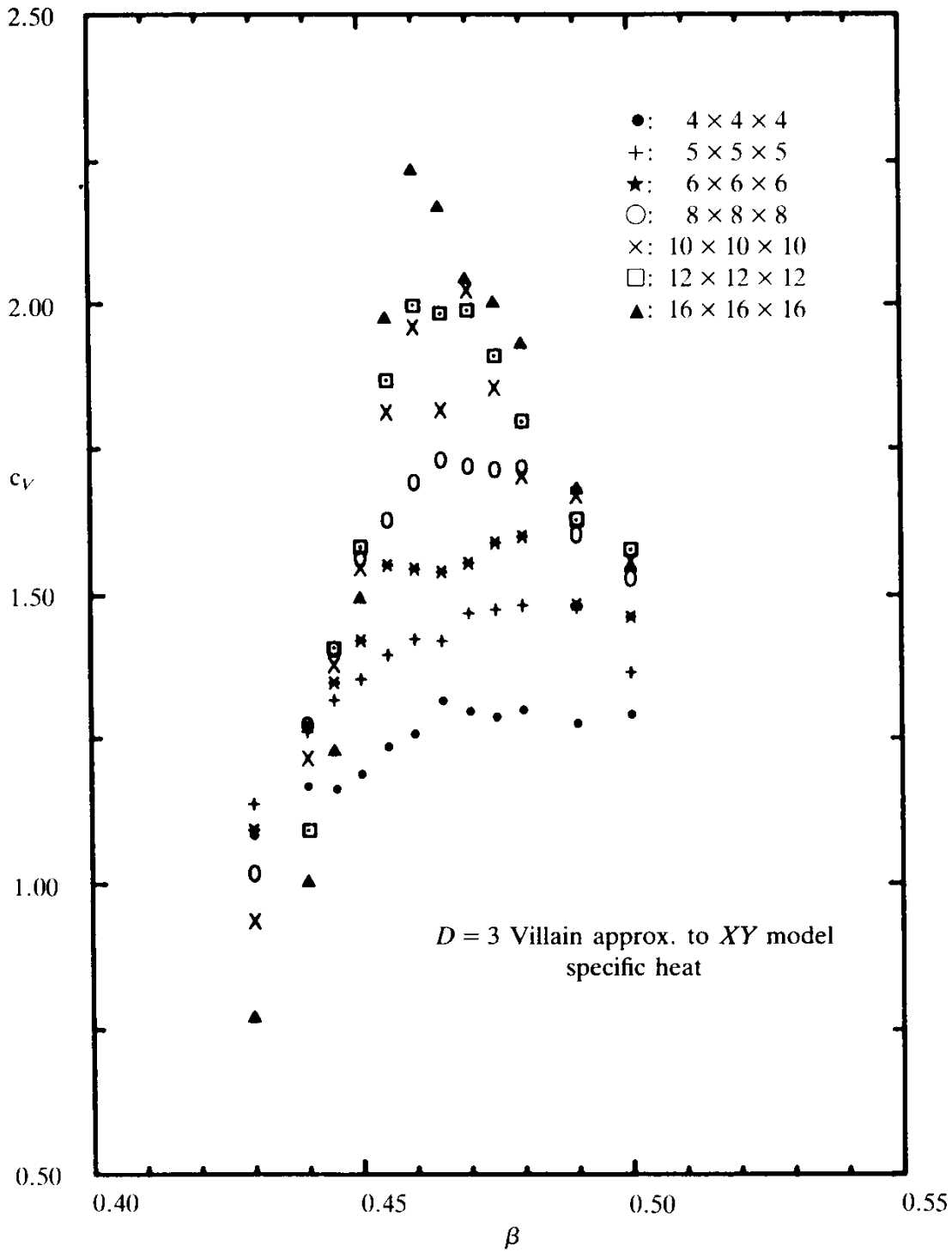
FIG. 7.10. The same data as in Fig. 6.1 but for the specific heat $c \sim c_V$.

TABLE 7.4. Comparison of critical temperatures in the XY model for $D = 2, 3$, and $U(1)$ lattice gauge theory (see Section 10.2 for more details) with the values obtained from the Villain approximation via $\beta_V = -[2\log(I_1(\beta)/I_0(\beta)]^{-1}$. The values are taken from the following references (quoted in the Notes and References): (a) Tobochnik and Chester (1979). MC; Samuel and Yee (1985), MC; (b) Shugard et al. (1978), MC; Villain (1975); (c) Ferer et al. (1973), HTS; (d) Dasgupta and Halperin (1981), MC; (e) Lautrup and Nauenberg (1980), MC; Bhanot (1981), MC; Caldi (1983), MC; (f) De Grand and Toussaint (1980, 1981), MC. MC and HTS indicate results obtained from the Monte Carlo simulation and the high temperature series, respectively.

Model	β_c	β_c (from VA)	β_{Vc}
2D XY	1.19[a]	1.18	0.73[b]
3D XY	0.45[a]	0.45	0.33[d]
4D $U(1)$	1.00[e]	0.99	0.63[f]
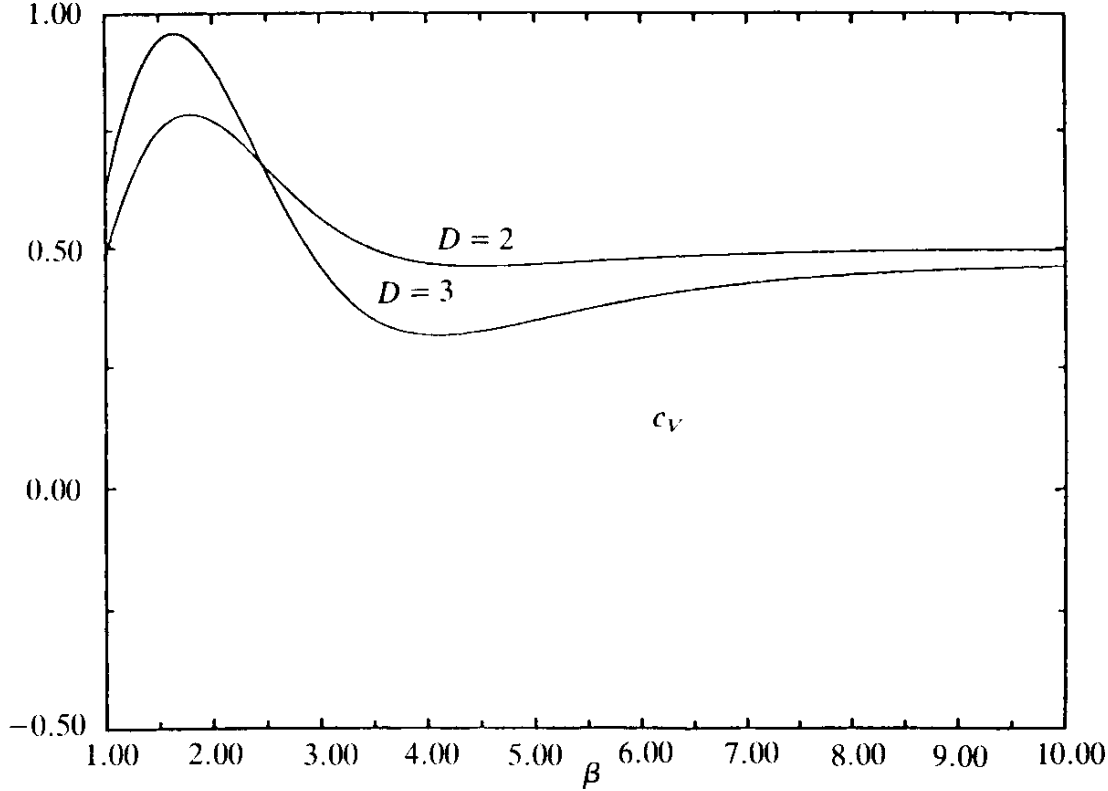
FIG. 7.11. Finite size scaling within the peak of $c \sim c_V$. This is to be compared with Fig. 4.8 for the XY model itself.

Legend:
- ●: $4 \times 4 \times 4$
- +: $5 \times 5 \times 5$
- ★: $6 \times 6 \times 6$
- ○: $8 \times 8 \times 8$
- ×: $10 \times 10 \times 10$
- □: $12 \times 12 \times 12$
- ▲: $16 \times 16 \times 16$

$D = 3$ Villain approx. to XY model specific heat

missing) in Fig. 7.12, shows a completely unphysical peak around $\beta \sim 1.2 - 2$. This is the origin of the disagreement in Figs. 7.10 and 7.11. It is a curious fact that it is the regime of *small* $\beta(\lesssim 1)$ that is really relevant for the study of phase transitions. Fortunately, it is there where the Villain approximation works best.

The excellent quality in the high temperature regime can easily be

FIG. 7.12.   The Villain approximation to the specific heat coming only from the Dulong-Petit limit for $u_{VM} = (1/2)\beta$, $c_{VM} = 1/2$ (neglecting the defect contributions, which in the high β regime on this figure are extremely small). The peak around $\beta \sim 1.5$ is the origin for the failure of the approximation in this regime [compare Fig. 7.10].

understood graphically: Consider the high temperature expansion of the XY model and exchange, in all diagrams in which closed lines appear with double or higher strength, the weight factors $I_{b_i}(\beta)/I_0(\beta)$ by $(I_1(\beta)/I_0(\beta))^{b_i^2}$. Rewrite this further more as

$$e^{-(1/2)[-2\log(I_1(\beta)/I_0(\beta))]b_i^2},$$ (7.108)

or, using $\beta_V = -[2\log(I_1(\beta)/I_0(\beta))]^{-1}$, as $e^{-(1/2\beta_V)b_i^2}$. Then the high temperature series of the XY model becomes,

$$Z_{XY}' \to I_0(\beta)^{3N} \sum_{\{b_i(x)\}} \delta_{\bar{\nabla}_i b_i,0}\, e^{-(1/2\beta_V)\Sigma_x b_i^2(x)}.$$

Comparing this with Eq. (7.25) we see that this is precisely the Villain approximation to the XY model.

The above replacement means that in the Villain model, all vortex loops of unit strength receive the same weight factor, as in the XY model. Those with strength larger than unity, however, receive a different weight factor $(I_1/I_0)^{b_i^2}$ instead of (I_{b_i}/I_0).

How serious is this difference? In the high-temperature expansion, the lowest order in β in which the replacement causes any change is β^8, where one has $\binom{D}{2}$ double loops of length 4 competing with a much larger number of simple loops of length 8. A similar situation holds to order 10, and further on to all higher orders in β. The number of multiple loops is always *much smaller* than that of simple loops of higher length due to the large increase in configurational entropy with length $\sim(2D)L$. This suggests strongly that the phase transition in both the XY and the Villain model is driven by *simple* loops becoming infinitely long rather than by double (and multiple) loops proliferating. If this is so then, since the XY model and its Villain approximation differ only in the numerically irrelevant multiple loops, they should also have the same critical behaviour.

In order for this conclusion to be true we must make sure that the weight factors do not have any anomalous temperature behaviour which overcompensates for the difference in configurational entropy. Let us therefore see what the energetic suppression caused by the weight factors is in the two cases. Near the transition point $\beta_c \approx 0.454$ of the XY model, the loops of strength 2 and 1 have a relative weight $I_2(\beta_c)/I_1(\beta_c) \approx 0.112$. In the Villain approximation with $\beta_{V_c} \approx 0.33$, on the other hand, this relative weight is $e^{-4/(2\beta_{V_c})}/e^{-1/(2\beta_{V_c})} \equiv (I_1(\beta_c)/I_0(\beta_c))^3 \approx 0.0106$. Thus, in both cases, the double loops are really strongly suppressed, in the Villain approximation far more than in the XY model. Seen in another way, it is due to the fact that $\beta_c \approx 0.454$ still lies in the regime where $I_0(\beta) \approx 1$, $I_1(\beta) \approx \beta/2$, $I_2(\beta) \sim \beta^2/8$ so that $I_2(\beta)/I_1(\beta) \sim \beta/4$ while $e^{-4/(2\beta_V)}/e^{-1/(2\beta_V)} \approx (I_1(\beta)/I_0(\beta))^3$ behaves like $\beta^3/8$. This shows explicitly an extra suppression factor of $\beta^2/2$.

In Figure 7.13 we have displayed the vortex loops in an XY model When going through the phase transition at $\beta_c \approx 0.454$ on an $8 \times 8 \times 8$ simple cubic lattice, via Monte Carlo simulations. We see that all vortex loops are of unit strength. The distribution of the different lengths is listed in Table 7.5.

In order to facilate the counting we have plotted the same loop configuration once more in two different views in Fig. 7.14 as they would be seen stereographically by an observer. By looking at the two views with the left and right eye separately one can see the spatial distribution of loops stereoscopically and follow them easily.

The extraction of the loops from the $\gamma(\mathbf{x})$ configurations was done by minimizing for given $\gamma(\mathbf{x})$ the expression $\Sigma_{\mathbf{x}}(\nabla_i\gamma - 2\pi n_i)^2$ in $n_i(\mathbf{x})$ and forming $\boldsymbol{\ell} = \nabla \times \mathbf{n}$. In this way the lines are necessarily closed (since

FIG. 7.13. Monte Carlo illustration of the condensation of vortex lines when going through the phase transition. Notice that the condensate consists mostly of a very long loop of low strength. Observe the periodic boundary condition.
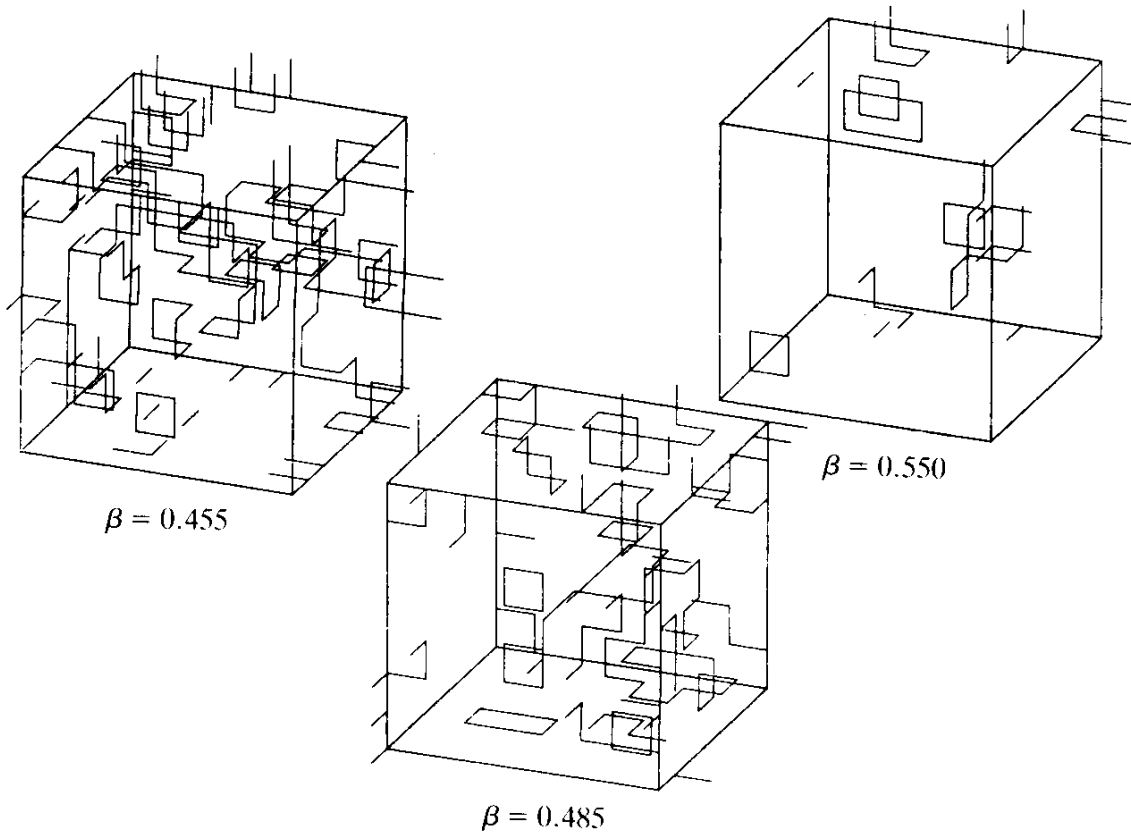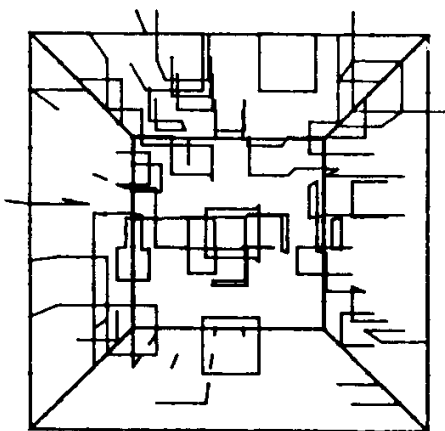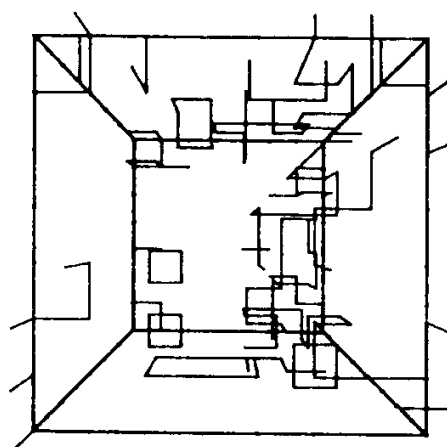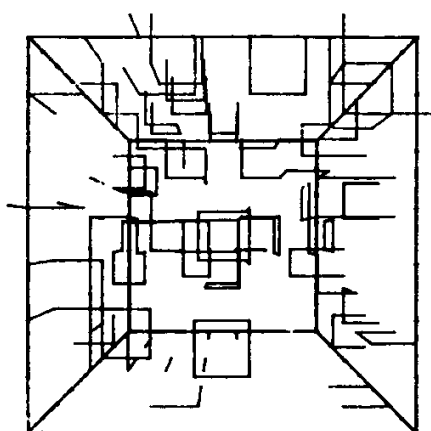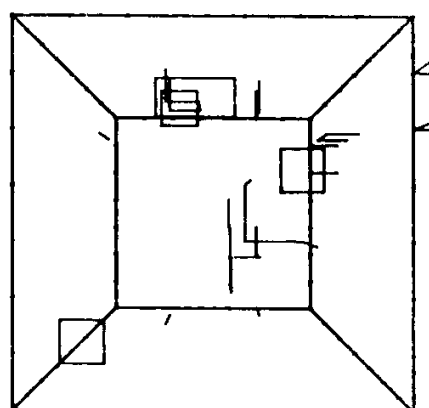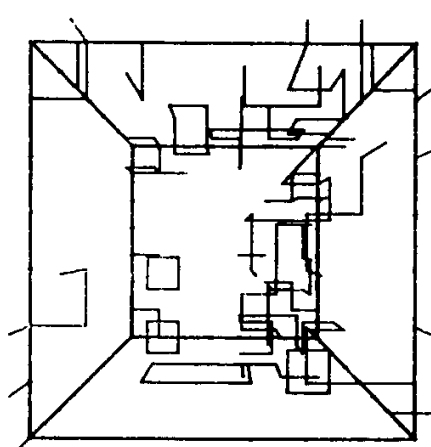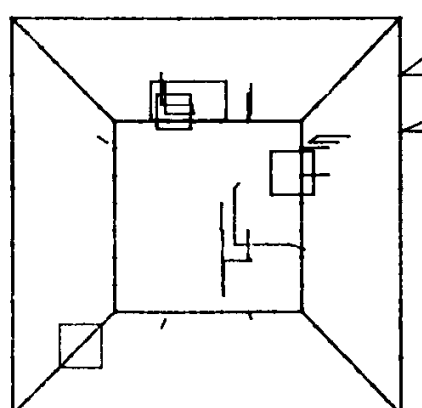
$\beta = 0.455$

$\beta = 0.550$

$\beta = 0.485$

TABLE 7.5. Distribution of loop lengths in Figs. 7.13, 7.14.

$\beta = 0.455$		$\beta = 0.485$		$\beta = 0.550$	
number of loops	length	number of loops	length	number of loops	length
7	4	3	4	5	4
6	6	5	6	2	6
2	8	1	8	1	8
1	10	1	10	1	14
1	128	1	14		
		1	20		
		1	28		
		1	42		

$\nabla \cdot \ell = 0$). That these ℓ configurations may be really identified with the vortex lines will be seen more explicitly in the next chapter. The figures show clearly that the total length in the high temperature phase comes mainly from a few *very long* loops of unit strength.

The above discussion suggests that it is possible to apply the Villain

FIG. 7.14. Stereoscopic view of the three-vortex line configurations of Fig. 7.13. For depth perception view the pictures with prismatic glasses (or bring side-by-side pictures to coincidence by a simple eye exercise).

$\beta = 0.455$

$\beta = 0.485$

$\beta = 0.550$

approximation to other models with an energy different from $\beta \cos(\nabla_i \gamma)$ as long as its vortex loops are the same and the suppression of the double loops is sufficiently strong so that the single loops dominate the critical behaviour. Consider, for example, a modified energy expression,

$$\beta[\cos(\nabla_i \gamma) + \delta \cos(2\nabla_i \gamma) - 1 - \delta]/(1 + 4\delta), \qquad (7.109)$$

which has the same low-temperature behaviour as the XY model since the power series expansion starts with $-(\beta/2)(\nabla_i \gamma)^2$. The high-temperature expansion of such a model can be done just as before except that the modified Bessel functions $I_b(\beta)$ are replaced by the functions

$$I_b^\delta(\beta) = \int_{-\pi}^{\pi} \frac{d\gamma}{2\pi} e^{ib\gamma + \beta(\cos \gamma + \delta \cos 2\gamma)}. \qquad (7.110)$$

The Villain approximation would then read

$$Z^\delta = \prod_x \left[\int_{-\pi}^{\pi} \frac{d\gamma(x)}{2\pi} \right] e^{\beta \Sigma_{x,i}(\cos \nabla_i \gamma + \delta \cos 2\nabla_i \gamma)}$$

$$\approx R_V^\delta(\beta) \prod_x \left[\int_{-\pi}^{\pi} \frac{d\gamma(x)}{2\pi} \right] \sum_{\{n_i(x)\}} e^{-(\beta_V/2)\Sigma(\nabla_i \gamma - 2\pi n_i)^2}, \qquad (7.111)$$

with

$$R_V^\delta(\beta) = I_0^\delta(\beta) \sqrt{2\pi\beta_V}, \qquad (7.112a)$$

and

$$\beta_V = -[2\log(I_1^\delta(\beta)/I_0^\delta(\beta))]^{-1}. \qquad (7.112b)$$

This would ensure that the high-temperature expansions in both cases agree with each other for vortex lines of single strength.

The approximation will be excellent for all those δ for which $I_2^\delta(\beta)/I_1^\delta(\beta)$ remains small up to the critical point β_c. A dangerous value is $\delta = 1/4$. In this case

$$
I_b^\delta(\beta) = \begin{cases}
1 - \dfrac{5}{4}\beta & b = 0, \\[2mm]
\dfrac{\beta}{4} & b = 1, \\[2mm]
\dfrac{\beta}{16} & b = 2, \\[2mm]
O(\beta^2) & b > 2.
\end{cases}
$$

Here the suppression factor is only 1/4 and it remains to be seen by Monte Carlo runs whether this is sufficient to permit the Villain model to have the same critical behavior.

The discussion suggests that there is a value of δ for which the model (7.111) is reproduced most accurately by the Villain approximation, better than the simple $\beta\cos\gamma$ model. For this we require that not only the lines of fundamental strength but also those of strength two have the same Boltzmann weight in both models. This gives the condition

$$
\frac{I_1^\delta(\beta)}{I_0^\delta(\beta)} = e^{-1/2\beta v}, \qquad \frac{I_2^\delta(\beta)}{I_0^\delta(\beta)} = e^{-4/2\beta v}. \tag{7.113}
$$

Assuming that the value of δ is much smaller than 1 up to the phase transition we can solve (7.113) approximately. Expanding (7.110) to lowest order in δ we find

$$
I_0^\delta(\beta) = \int_{-\pi}^{\pi} \frac{d\gamma}{2\pi} e^{\beta\cos\gamma}(1 + \beta\delta\cos 2\gamma) + \ldots
$$

$$
= I_0(\beta) + \beta\delta \int_{-\pi}^{\pi} \frac{d\gamma}{2\pi} e^{\beta\cos\gamma}\cos 2\gamma + \ldots
$$

$$
= I_0(\beta) + \beta\delta \cdot I_2(\beta) + \ldots,
$$

$$
I_1^\delta(\beta) = \int_{-\pi}^{\pi} \frac{d\gamma}{2\pi}\cos\gamma\, e^{\beta\cos\gamma}(1 + \beta\delta\cos 2\gamma) + \ldots
$$

$$
= I_1(\beta) + \frac{\beta\delta}{2} \int_{-\pi}^{\pi} \frac{d\gamma}{2\pi} e^{\beta\cos\gamma}(\cos\gamma + \cos 3\gamma) + \ldots
$$

$$
= I_1(\beta) + \frac{\beta\delta}{2}(I_1(\beta) + I_3(\beta)) + \ldots,
$$

$$I_2^\delta(\beta) = \int_{-\pi}^{\pi} \frac{d\gamma}{2\pi} \cos 2\gamma \, e^{\beta \cos \gamma}(1 + \beta\delta \cos 2\gamma) + \ldots$$

$$= I_2(\beta) + \frac{\beta\delta}{2} \int_{-\pi}^{\pi} \frac{d\gamma}{2\pi} e^{\beta \cos \gamma}(\cos 2\gamma + \cos 4\gamma) + \ldots$$

$$= I_2(\beta) + \frac{\beta\delta}{2}(I_0(\beta) + I_4(\beta)) + \ldots \tag{7.114}$$

Inserting this into (7.113) gives

$$\beta\delta = 2 \frac{(I_1/I_0)^4 - I_2/I_0}{1 + \dfrac{I_4}{I_0} - 2\left(\dfrac{I_2}{I_0}\right)^2 - 4\left[\left(\dfrac{I_1}{I_0}\right)^4\left(1 + \dfrac{I_3}{I_1}\right) - 2\dfrac{I_2}{I_0}\right]} + \ldots \tag{7.115}$$

For a given β we may find δ from (7.115) and then β_V to lowest order in δ from

$$\beta_V^{-1} = -[2\log(I_1^\delta/I_0^\delta)]^{-1} \approx (\beta_V^{-1})^{\delta=0} - \beta\delta\left(1 + \frac{I_3}{I_1} - 2\frac{I_2}{I_0}\right). \tag{7.116}$$
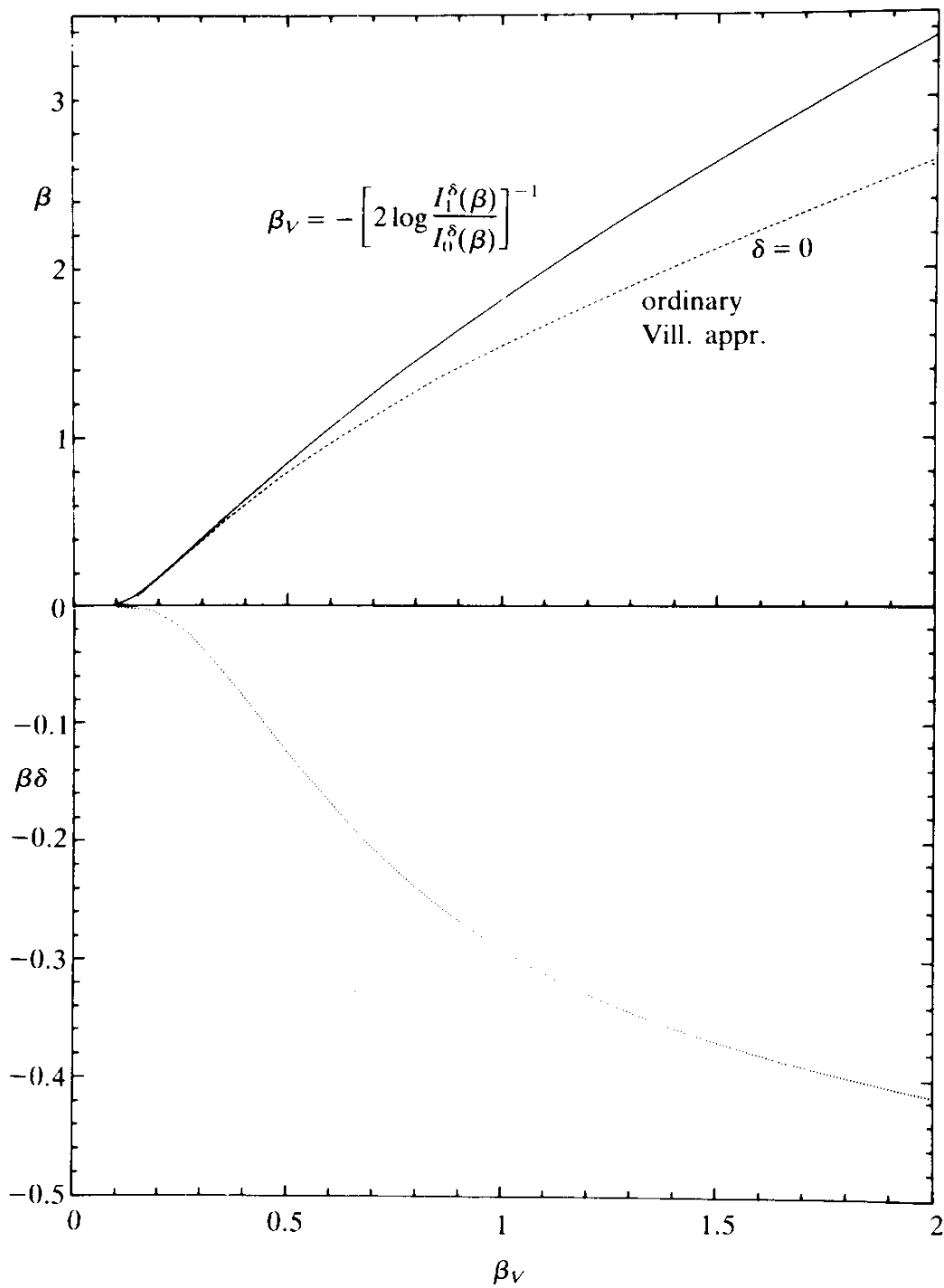
The precise solution to Eqs. (7.113) is shown in Fig. 7.15. In Fig. 7.16 we have displayed also the Boltzmann factors of the two sides of Eq. (7.111) and see that the mixed action model has an almost perfect Villain approximation, as compared with a pure XY model.

In fact, these arguments are too crude to ensure that the Villain approximation and XY model really give the same critical behaviour. We can convince ourselves somewhat more safely that this is true by showing that the approximation can be brought to a field theory which has the same universality class as the XY model. For this we write the expansion (7.17) in the form

$$Z_V' = R_V^{ND} \frac{1}{(\sqrt{2\pi\beta_V})^{ND}} \prod_{\mathbf{x}} \left[\int_{-\pi}^{\pi} \frac{d\gamma(\mathbf{x})}{2\pi}\right] \sum_{\{b_i(\mathbf{x})\}} e^{-(1/2\beta_V)\Sigma_{\mathbf{x}} b_i^2(\mathbf{x})} \cos(b_i \nabla_i \gamma).$$

$$\tag{7.117a}$$

To this expansion we can apply the mean field techniques, in which case we obtain the same type of representation in terms of two complex fields $u(\mathbf{x})$ and $\alpha(\mathbf{x})$ as in the XY model, except that the action $\beta \mathrm{Re} \, \Sigma_{\mathbf{x},i} u^\dagger(\mathbf{x}) u(\mathbf{x} + i)$ is replaced by
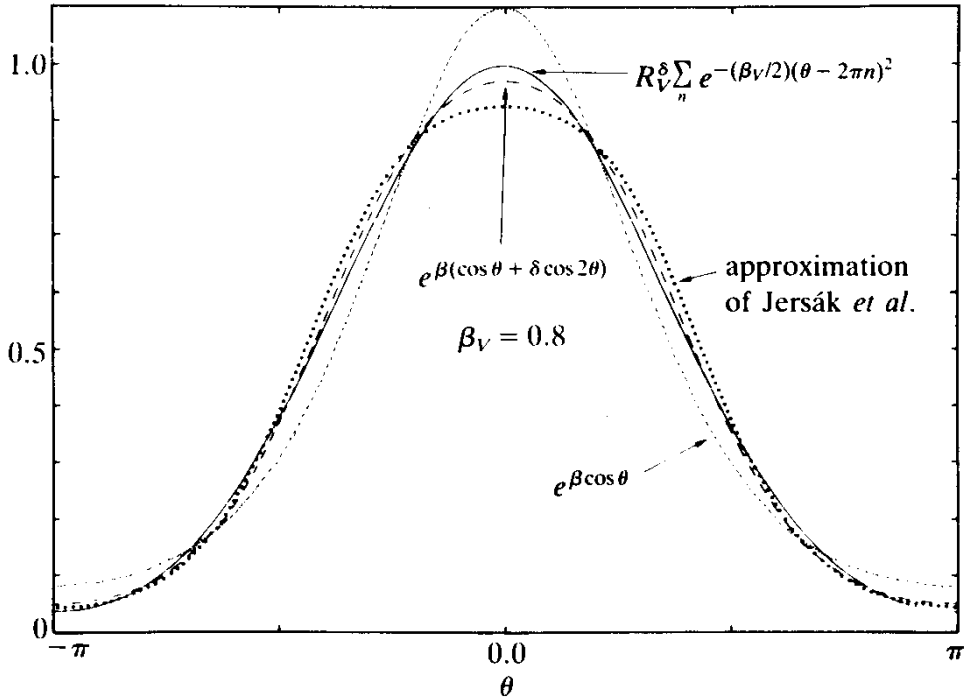
FIG. 7.15.   The parameters β and $\beta\delta$ as functions of β_V for the improved Villain approximation [see Eq. (7.113)].

$$\sum_{\mathbf{x},i} \log\left(1 + \sum_{b \neq 0} e^{-b^2/2\beta_V}\cos(b\nabla_i\gamma(\mathbf{x}))\right)$$

$$= \sum_{\mathbf{x},i} \log\left[\mathrm{Re}\left(1 + \sum_{b=0} e^{-b^2/2\beta_V}(u^\dagger(\mathbf{x})\,u(\mathbf{x}+\mathbf{i}))^b\right)\right]. \quad (7.117\mathrm{b})$$

This differs from the previous field theory only by the presence of higher powers in $u^\dagger(\mathbf{x})\,u(\mathbf{x}+\mathbf{i})$. At the mean field level it is easy to see that such

FIG. 7.16. The Boltzmann factors of the Villain model as compared with that of the mixed action $\beta(\cos\nabla_i\gamma + \beta\cos2\nabla_i\gamma)$ and the ordinary XY action model $\beta\cos\nabla_i\gamma$. The curve is from Janke and Kleinert (1985) and the dotted curve shows another approximation proposed by Jersák (1985).

terms are irrelevant close to T_c. Then, according to renormalization group arguments, they should also be irrelevant to the critical indices, as long as the order of the phase transition is the same. As mentioned above, this need not always be the case. An example is the $U(1)$ lattice gauge theory (to be defined in Section 10.3). More details can be found in recent papers by Janke and the author (1986) cited at the end of this chapter.

Notice that it is, in principle, possible to use (7.117a) and apply to this the mean field plus loop correction techniques. This would, however, be quite inefficient since the Villain approximation can be studied directly via high- and low-temperature graphs. This is precisely its virtue.

7.6. THE XY MODEL VERSUS VILLAIN MODEL OF SUPERFLUIDITY

Since the XY and the Villain models have the same critical behaviour, they can both serve equally well for a study of the superfluid phase transition. The question arises which is the preferable model to use. Both models require the same amount of work in calculating the high-

temperature expansion. In this respect then, there is no distinction between them. On the low temperature side, on the other hand, the XY model seems to have the important advantage of possessing a simple mean field approximation to which it is, in principle, possible to perform loop corrections to arbitrary accuracy.

A closer look teaches us though that this is not really an advantage but more of a burden. However accurately we can perform the loop corrections, they will always yield corrections to the thermodynamic mean field properties of the power type $1/\beta''$. Therefore, they will never be capable of describing the pre-critical vortex proliferation, which behaves like $e^{-\beta \text{const.}}$ and represents the only interesting *model-independent* feature of the XY model. All the $1/\beta$ expansion is able to give is the softening of the harmonic vibrations and their interactions. This is the trivial model dependent part which comes from the specific $\cos \nabla_i \gamma$ form of the energy and the implied nonlinear interactions

$$\sum_{n=}^{\infty} \frac{(-1)^n}{(2n)!} (\nabla_i \gamma)^{2n}.$$

In fact, the mean-field-plus-loop-correction approach may be viewed as an efficient way of summing the perturbation theory of the partition function

$$Z' = \prod_{\mathbf{x}} \left[\int_{-\pi}^{\pi} \frac{d\gamma(\mathbf{x})}{(2\pi)} \right] e^{\beta \Sigma_{\mathbf{x},i} \cos \nabla_i \gamma}$$

$$= e^{\beta D N} \prod_{\mathbf{x}} \left[\int_{-\pi}^{\pi} \frac{d\gamma(\mathbf{x})}{2\pi} \right] e^{-(\beta/2)\Sigma_{\mathbf{x}}(\nabla_i \gamma)^2 + \beta \sum_{n=2}^{\infty} ((-1)^n/(2n)!)(\nabla_i \gamma)^{2n}}. \quad (7.118a)$$

Rescaling the γ variable this becomes

$$Z' = e^{\beta D N} \frac{1}{(\sqrt{2\pi\beta})^N} \prod_{\mathbf{x}} \left[\int_{-\sqrt{\beta}\pi}^{\sqrt{\beta}\pi} \frac{d\gamma'(\mathbf{x})}{2\pi} \right] e^{-(1/2)\Sigma_{\mathbf{x}}(\nabla_i \gamma')^2 + \sum_{n=2}^{\infty} ((-1)^n/(2n)!)(1/\beta^{n-1})(\nabla_i \gamma')^{2n}},$$

$$(7.118b)$$

which shows that Z' has a perturbation expansion in $1/\beta$ in which the higher interaction terms with $n \geq 2$ do appear to order $1/\beta^{n-1}$.

In order to obtain a pure $1/\beta$ series we have to extend the range of the γ' integrations from the interval $(-\sqrt{\beta}\pi, \sqrt{\beta}\pi]$ to $(-\infty, \infty)$. The error which arises in doing this is of the exponential form $e^{-\pi^2\beta/2}$. The easiest way to see this is by considering the correlation function of γ in a simple integral

$$\langle \gamma^2 \rangle = \int_{-\pi}^{\pi} d\gamma\, \gamma^2 e^{-\beta\gamma^2/2} \bigg/ \int_{-\pi}^{\pi} d\gamma\, e^{-\beta\gamma^2/2} = -2\frac{\partial}{\partial\beta} \log \int_{-\pi}^{\pi} d\gamma\, e^{-\beta\gamma^2/2}$$

$$= -2\frac{\partial}{\partial\beta}\log\left[\sqrt{\frac{2\pi}{\beta}}\left(1 - \frac{2}{\sqrt{\pi}}\int_{\pi\sqrt{\beta/2}}^{\infty} d\gamma'\, e^{-(1/2)\gamma'^2}\right)\right]$$

$$= \frac{1}{\beta} - 2\frac{\partial}{\partial\beta}\log[1 - \mathrm{erfc}(\pi\sqrt{\beta/2})].   \tag{7.119}$$

The complementary error function erfc (z) has a large z behaviour $(1/\sqrt{\pi})(1/z)e^{-z^2} = (1/\pi^{3/2}\sqrt{\beta/2})e^{-\pi^2\beta/2}$ so that $\langle\gamma^2\rangle$ behaves, for large β, like

$$\langle\gamma^2\rangle \to \frac{1}{\beta} + 2\frac{\partial}{\partial\beta}\left(\frac{1}{\pi^{3/2}\sqrt{\beta/2}}e^{-\pi^2\beta/2}\right).   \tag{7.120}$$

By extending the range of the γ integrations to infinity we omit the second term. It is precisely such terms that are being missed in a mean field approach with loop corrections for *any* order. The resulting partition function can always be expanded in power series in $1/\beta$ and thus fails to reproduce all terms of the form $e^{-\beta\mathrm{const.}}$ which do not possess such an expansion.

7.7. PERTURBATION EXPANSIONS OF THE *XY* MODEL ($1/\beta$-EXPANSION)

It is instructive to verify the above statement by calculating the *XY* free energy via the perturbation expansion of the partition function (7.118). Since the interaction terms involve only the lattice gradients of γ, the only correlation function needed as a propagator is $\langle \nabla_i \gamma(\mathbf{x}) \nabla_i \gamma(\mathbf{x}')\rangle$. From the free field part $-(\beta/2)\Sigma_{\mathbf{x},i}(\nabla_i\gamma)^2$ this is found to be simply

$$\langle \nabla_i\gamma(\mathbf{x})\nabla_i\gamma(\mathbf{x}')\rangle = \frac{1}{\beta}\nabla_i\nabla_i'\frac{1}{-\bar{\nabla}\cdot\nabla}(\mathbf{x}-\mathbf{x}') = -\frac{1}{\beta}\nabla_i\bar{\nabla}_j\frac{1}{-\bar{\nabla}\cdot\nabla}(\mathbf{x}-\mathbf{x}').   \tag{7.121}$$

For $\mathbf{x} = \mathbf{x}'$ we can use cubic symmetry among the indices i, j and calculate

$$\langle \nabla_i\gamma(\mathbf{x})\nabla_j\gamma(\mathbf{x})\rangle = -\frac{1}{\beta}\nabla_i\bar{\nabla}_j\frac{1}{-\bar{\nabla}\cdot\nabla}(\mathbf{0}) = \frac{\delta_{ij}}{\beta D}.   \tag{7.122}$$

Leaving out all interactions in (7.118), the variables $\gamma(\mathbf{x})$ can be integrated out and we find the partition function

$$Z_0' = e^{\beta DN} \frac{1}{(\sqrt{2\pi\beta})^N} \det(-\bar{\nabla} \cdot \nabla)^{-1/2}, \qquad (7.123)$$

which gives a free energy

$$-\beta f_0' = \beta D - \tfrac{1}{2}\log \sqrt{2\pi\beta} - \tfrac{1}{2}\ell, \qquad (7.124)$$
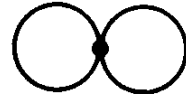
where (recall Table 6.4)

$$\ell = \int \frac{d^D k}{(2\pi)^D} \log(\bar{\mathbf{K}} \cdot \mathbf{K}) = \begin{cases} 1.1664 & D = 2, \\ 1.6734 & D = 3. \end{cases} \qquad (7.125)$$

The lowest correction comes from the interaction

$$\frac{\beta}{4!} \sum_{\mathbf{x},i} (\nabla_i \gamma)^4, \qquad (7.126)$$

which allows for three Wick contractions and gives the two loop contribution to the free energy [recall (2.26) Part I]
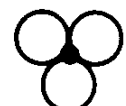
 $\qquad -\beta f^{(2)} = \frac{1}{8} \frac{1}{\beta D}. \qquad (7.127)$

The next correction comes from three sources: First there is the sixth order interaction

$$-\frac{\beta}{6!} \sum_{\mathbf{x},i} (\nabla_i \gamma)^6, \qquad (7.128)$$

whose 15 Wick contractions give the three-loop free energy

 $\qquad -\beta f^{(3)} = -\frac{1}{24} \frac{1}{(\beta D)^2}. \qquad (7.129)$

Second, there are the three-loop graphs coming from contractions between two interactions $(\beta/4!)(\nabla_i \gamma)^4$. These give [recall (2.26) Part I]

$$\frac{1}{2!}\left(\frac{\beta}{4!}\right)^2\left(72\; \bigcirc\!\!\bigcirc\!\!\bigcirc + 24\; \otimes \right).$$ (7.130)

The first graph implies the contractions

$$\sum_{\mathbf{x},\mathbf{y},i,j} \overline{\nabla_i\gamma(\mathbf{x})\,\nabla_i\gamma(\mathbf{x})}\,\overline{\nabla_i\gamma(\mathbf{x})\,\nabla_i\gamma(\mathbf{x})}\,\overline{\nabla_j\gamma(\mathbf{y})\,\nabla_j\gamma(\mathbf{y})}\,\overline{\nabla_j\gamma(\mathbf{y})\,\nabla_j\gamma(\mathbf{y})}$$

$$= \frac{1}{(\beta D)^2}\frac{1}{\beta^2}\sum_{\mathbf{x},\mathbf{y},i,j} - \nabla_i\overline{\nabla}_j v(\mathbf{x}-\mathbf{y}),$$ (7.131)

where $v(\mathbf{x}-\mathbf{y}) = (-\overline{\nabla}\cdot\nabla)^{-1}(\mathbf{x},\mathbf{y})$. But

$$\sum_{\mathbf{x}}\sum_{i,j} -\nabla_i\overline{\nabla}_j v(\mathbf{x}) = \int\frac{d^D k}{(2\pi)^2}\sum_{i,j}\frac{K_i\overline{K}_j\overline{K}_i K_j}{(\overline{\mathbf{K}}\cdot\mathbf{K})^2} = 1,$$ (7.132)

so that the contribution to $-\beta f$ is

$$\frac{1}{2!}\left(\frac{\beta}{4!}\right)^2 72\frac{1}{(\beta D)^2\beta^2} = \frac{1}{16}\frac{1}{(\beta D)^2}.$$ (7.133)

The second graph amounts to the contractions

$$\sum_{\mathbf{x},\mathbf{y},i,j}(\overline{\nabla_i\gamma(\mathbf{x})\,\nabla_j\gamma(\mathbf{y})})^4 = \frac{1}{(\beta D)^4}\sum_{\mathbf{x},\mathbf{y},i,j}(\nabla_i\overline{\nabla}_j v(\mathbf{x}-\mathbf{y}))^4.$$ (7.134)

Since $\nabla_i\overline{\nabla}_j v(\mathbf{x})$ decreases like $(1/|\mathbf{x}|^D)$, this sum is dominated by the $\mathbf{x}=\mathbf{y}$ term, and there by the diagonal one $i=j$. This gives a contribution to $-\beta f$ of

$$\frac{1}{2}\left(\frac{\beta}{4!}\right)^2 4!\,D\frac{1}{(\beta D)^4} = \frac{1}{48D}\frac{1}{(\beta D)^2}.$$ (7.135)

The $\mathbf{x}=\mathbf{y}$ and $i=j$ parts can be shown to make up less than 5% of this. Thus, up to order $1/\beta^2$ we arrive, to a good approximation, at the energies

$$-\beta f' = \beta D - \frac{1}{2}\log(4\pi\beta D) + \frac{1}{8(\beta D)} + \frac{1}{24}\frac{1}{(\beta D)^2} + \frac{1}{48D}\frac{1}{(\beta D)^2},$$ (7.136a)

$$\frac{u'}{D} = -1 + \frac{1}{2\beta D} + \frac{1}{8(\beta D)^2} + \frac{1}{12(\beta D)^3} + \frac{1}{24D}\frac{1}{(\beta D)^3} + \cdots \qquad (7.136b)$$

7.8. HARTREE-FOCK RESUMMATION

It turns out that, due to the cosine form of the energy it is possible to proceed more efficiently and perform a resummation of a certain *infinite* subset of diagrams. Let us recall that according to Wick's theorem the expectation value of a cosine of a harmonic variable, say φ, is given simply by the exponential of the correlation function, i.e.,

$$\langle \cos \varphi \rangle_0 = e^{-(1/2)\langle \varphi^2 \rangle_0}. \qquad (7.137)$$

This follows directly from the integrals

$$\langle \cos \varphi \rangle_0 = \frac{\int d\varphi \, e^{-(a/2)\varphi^2} \cos \varphi}{\int d\varphi \, e^{-(a/2)\varphi^2}} = \frac{\int d\varphi \, e^{-(a/2)\varphi^2} \dfrac{e^{i\varphi} + e^{-i\varphi}}{2i}}{\int d\varphi \, e^{-(a/2)\varphi^2}}$$

$$= \frac{1}{2} \frac{\int d\varphi \left(e^{-(a/2)(\varphi - i/a)^2} + e^{-(a/2)(\varphi + i/a)^2} \right) e^{-1/2a}}{\int d\varphi \, e^{-(a/2)\varphi^2}} = e^{-1/2a}$$

$$\langle \varphi^2 \rangle_0 = \frac{\int d\varphi \, e^{-(a/2)\varphi^2} \varphi^2}{\int d\varphi \, e^{-(a/2)\varphi^2}} = \frac{1}{a}. \qquad (7.138)$$

The formula (7.137) means, graphically, that when doing a perturbation expansion on the left-hand side, the contraction between different φ's in the powers of cosine add up precisely to the series $\Sigma_n(-(1/2)\langle \varphi^2 \rangle_0)^n/n!$.

There exists a simple generalization of this statement: When calculating, in a perturbation expansion, correlation functions of several expressions involving $\cos \varphi$ of a harmonic variable, $\langle \cos \varphi \ldots \cos \varphi \rangle$, the sum of all Feynman graphs can be split into graphs which connect the φ's of one cosine with those of another and graphs which contract the φ's *within* a cosine. It is possible to resum all the latter contractions by writing

$$\cos \varphi = e^{-(1/2)\langle \phi^2 \rangle_0}(1 + :\cos \varphi:) \tag{7.139}$$

where the double dots on the right side mean that, in a perturbation expansion, the powers of φ in $:\cos\varphi: = :\Sigma_n(-)^n(\varphi^{2n}/(2n)!:$ should be contracted only with those in *another* $:\cos \varphi:$. In quantum field theory this prescription is called normal ordering of the field operators.

Let us do such a resummation in the XY model. For this we choose a certain harmonic behavior of the variable, say

$$\langle \nabla_i \gamma(\mathbf{x}) \nabla_i \gamma(\mathbf{x}) \rangle = \frac{1}{\beta^R D}. \tag{7.140}$$

Then we take the energy of the XY model

$$\beta \sum_{\mathbf{x},i} \cos \nabla_i \gamma(\mathbf{x}), \tag{7.141}$$

treat it as we did Eq. (7.129), add and subtract a free-field energy $(\beta^R/2)\Sigma_{\mathbf{x}}(\nabla_i\gamma)^2$ and rewrite the latter, using the double dot definition, as[c]

$$(\nabla_i\gamma)^2 = \langle(\nabla_i\gamma)^2\rangle_0 + :(\nabla_i\gamma)^2: \tag{7.142}$$

By identifying $\beta e^{-\langle(\nabla_i\gamma)^2\rangle_0/2}$ with β^R we obtain the renormalization equation

$$\beta^R = \beta e^{-1/2\beta^R D}. \tag{7.143}$$
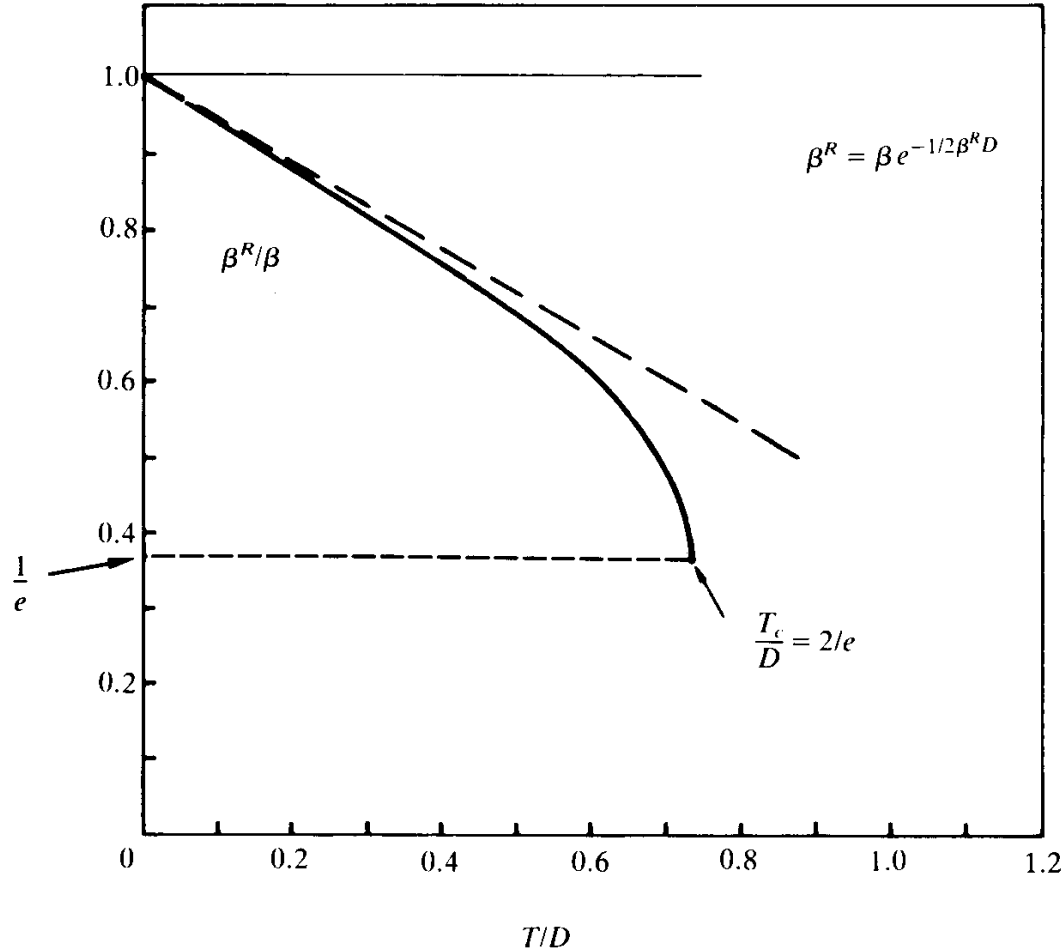
This eliminates all quadratic terms between double dots. It is called the *Hartree-Fock self-consistency equation*. After this, the partition function of the XY model becomes

$$Z'_{XY} \approx e^{-\Sigma_{\mathbf{x},i}\beta^R(1 + \langle\nabla_i^2\gamma\rangle_0/2)} \prod_{\mathbf{x}} \left[\int_{-\pi}^{\pi} \frac{d\gamma(\mathbf{x})}{2\pi} \right] e^{-(\beta^R/2)\Sigma_{\mathbf{x},i}(\nabla_i\gamma)^2 + \beta^R:\Sigma_{\mathbf{x},i}[\cos\nabla_i\gamma + (1/2)(\nabla_i\gamma)^2 - 1]:} \tag{7.144}$$

When plotting the renormalization of the stiffness $\beta^R D$ as a function of T/D (see Fig. 7.17) we see that there exists a solution only for $T/D < 2/e = 0.7358$. Up to this point, the stiffness has softened to $1/e$ of its $T = 0$ value.

[c] This can be derived from (7.139) by replacing φ by $\lambda\varphi$ and expanding both sides in powers of λ^2. The lowest term gives (7.142).

FIG. 7.17. Solution of the self-consistency equation (7.143) for the renormalization of the stiffness β of the XY model (for any dimension D).

$$\beta^R = \beta e^{-1/2\beta^R D}$$

$$\frac{T_c}{D} = 2/e$$

T/D

Up to T_c we use this partition function for a resummed perturbation expansion in which the lines represent the correlation function

$$\langle \nabla_i \gamma(\mathbf{x})\, \nabla_j \gamma(\mathbf{y}) \rangle = -\frac{1}{\beta^R}\, \nabla_i \bar{\nabla}_j v(\mathbf{x} - \mathbf{y}) \qquad (7.145)$$

and the interaction vortices correspond to all higher powers of $:\cos \nabla_i \gamma:$

$$\beta^R \sum_{\mathbf{x},i} \sum_{n=2}^{\infty} \frac{(-1)^n}{(2n)!} : (\nabla_i \gamma)^{2n} : \qquad (7.146)$$

Due to the double dots, there are only Feynman graphs with lines connecting *different* interaction vertices.

To lowest order, the free energy can be read off directly from the exponent in (7.144):

$$-\beta f'^{\mathrm{HF}} = \beta D\, e^{-1/2\beta^R D}\left(1 + \frac{1}{2\beta^R D}\right) - \frac{1}{2}\log(2\pi\beta^R) - \frac{1}{2}\int \frac{d^D k}{(2\pi)^D}\log(\bar{\mathbf{K}}\cdot\mathbf{K})$$

$$= \beta^R D + \frac{1}{2} - \frac{1}{2}\log(2\pi\beta^R) - \frac{1}{2}\int \frac{d^D k}{(2\pi)^D}\log(\bar{\mathbf{K}}\cdot\mathbf{K}). \qquad (7.147)$$

Differentiating the Hartree-Fock equation (7.143) we find

$$\frac{\partial\beta^R}{\partial\beta} = e^{-1/2\beta^R D}\,\frac{1}{1 - \dfrac{1}{2\beta^R D}} = \frac{\beta^R}{\beta}\,\frac{1}{1 - \dfrac{1}{2\beta^R D}}, \qquad (7.148)$$

so that the internal energy becomes

$$u'^{\mathrm{HF}} = -\frac{\partial}{\partial\beta}(-\beta f')^{\mathrm{HF}} = \left(D - \frac{1}{2\beta^R}\right)\frac{\partial\beta^R}{\partial\beta} = -D\frac{\beta^R}{\beta}, \qquad (7.149)$$

and the specific heat

$$c^{\mathrm{HF}} = -\beta^2\frac{\partial}{\partial\beta}u'^{\mathrm{HF}} = \frac{1}{2}\frac{\beta^R}{\beta}\,\frac{1}{1 - \dfrac{1}{2\beta^R D}}. \qquad (7.150)$$

The low temperature expansion of β^R is

$$\beta^R = \frac{1}{t} - \frac{1}{2} - \frac{t}{8} - \frac{t^2}{12} - \cdots, \qquad (7.151)$$

where $t \equiv 1/\beta D = T/D$. Using this we find

$$-\beta f'^{\mathrm{HF}} = \frac{1}{t} - \frac{1}{2}\log(4\pi/t) + \frac{t}{8} + \frac{t^2}{24} - \frac{1}{2}\int \frac{d^D k}{(2\pi)^D}\log(\bar{\mathbf{K}}\cdot\mathbf{K}) + O(t^3),$$

$$\qquad (7.152)$$

$$-\beta u'^{\mathrm{HF}} = t^2\frac{\partial}{\partial t}(-\beta f'^{\mathrm{HF}}) = -1 + \frac{t}{2} + \frac{t^2}{8} + \frac{t^3}{12} + O(t^4), \qquad (7.153)$$

$$c^{\mathrm{HF}} = \frac{\partial}{\partial t}\frac{u'^{\mathrm{HF}}}{D} = \frac{1}{2} + \frac{t}{4} + \frac{t^2}{4} + O(t^3). \qquad (7.154)$$

There are now infinitely many powers of t coming from the infinite subset of graphs summed up exactly in the present procedure.

In contrast to the direct perturbation approach, the first correction comes now from the three-loop graph

$$x \quad \bigotimes \quad y \quad = \frac{1}{2!}\left(\frac{\beta^R}{4!}\right)^2 \sum_{x,y,i,j} (\nabla_i \overline{\gamma(x)} \nabla_j \overline{\gamma(y)})^4, \qquad (7.155)$$

with four legs $-(1/\beta^R)\nabla_i\nabla_j v(\mathbf{x} - \mathbf{y})$ connecting the two different vortices, which is just the term (7.135). With the same approximation we can therefore write

$$-\beta f^{(3)} = \frac{1}{2}\left(\frac{\beta^R}{4!}\right)^2 4! \frac{D}{(\beta^R D)^4} = \frac{1}{48 D} \frac{1}{(\beta^R D)^2}. \qquad (7.156)$$

We can now verify that, up to the order $1/\beta^2$, the self-consistent solution agrees with the direct perturbation expansion (7.136), as it should.

7.9. COMPARISON WITH THE MEAN-FIELD-PLUS-LOOP APPROACH

Let us compare this with the low temperature expansion of the mean field result (5.26)

$$-\beta f'^{MF} = \frac{1}{t} - \frac{1}{2}\log(4\pi/t) + \frac{t}{8} + \frac{3}{64}t^2 + O(t^3). \qquad (7.157)$$

This is a D independent function of the quantity $t = 1/\beta D$. It agrees with the perturbative result up to the order t, apart from the missing constant $-(1/2)(\ell - \log(2D))$. This constant comes from the one-loop correction

$$-\beta f^{1\,\text{loop}} = -\frac{1}{2}\int \frac{d^D k}{(2\pi)^D}\left[\log\left(-\frac{\overline{\mathbf{K}}\cdot\mathbf{K}}{2D}\right) + \log\left(\frac{m^2}{2D} + \left(1 - \frac{m^2}{2D}\right)\frac{\overline{\mathbf{K}}\cdot\mathbf{K}}{2D}\right)\right]$$

$$= -\frac{1}{2}(\ell - \log(2D)) + \frac{1}{2}\sum_{n=2,4,6,\ldots}^{\infty}\left(1 - \frac{m^2}{2D}\right)^n \frac{H_n}{n(2D)^n}, \qquad (7.158)$$

where [recall (5.70), (5.71), (5.60)]

$$\frac{m^2}{2D} = 2 - 2\beta D(1 - u^2).$$ (7.159)

For large β, where $u \sim 1 - 1/2\beta D - 3/32(\beta D)^2 - \ldots$, this has the limit

$$\frac{m^2}{2D} \to 1 - \frac{1}{4\beta D}$$ (7.160)

so that [recall the similar discussion after Eq. (5.71b)]

$$-\beta f^{1\,\mathrm{loop}} \to -\frac{1}{2}(\ell - \log(2D)) + \frac{1}{8 \cdot 16D}\frac{1}{(\beta D)^2}.$$ (7.161)

Comparing (7.157) plus (7.161) with the perturbative result (7.136a) we see that they begin disagreeing with each other at the level of $1/\beta^2$. Quantitatively, however, the disagreement is not severe, since the perturbative result to this order

$$\frac{1}{24(\beta D)^2} + \frac{1}{48D}\frac{1}{(\beta D)^2}$$ (7.162)
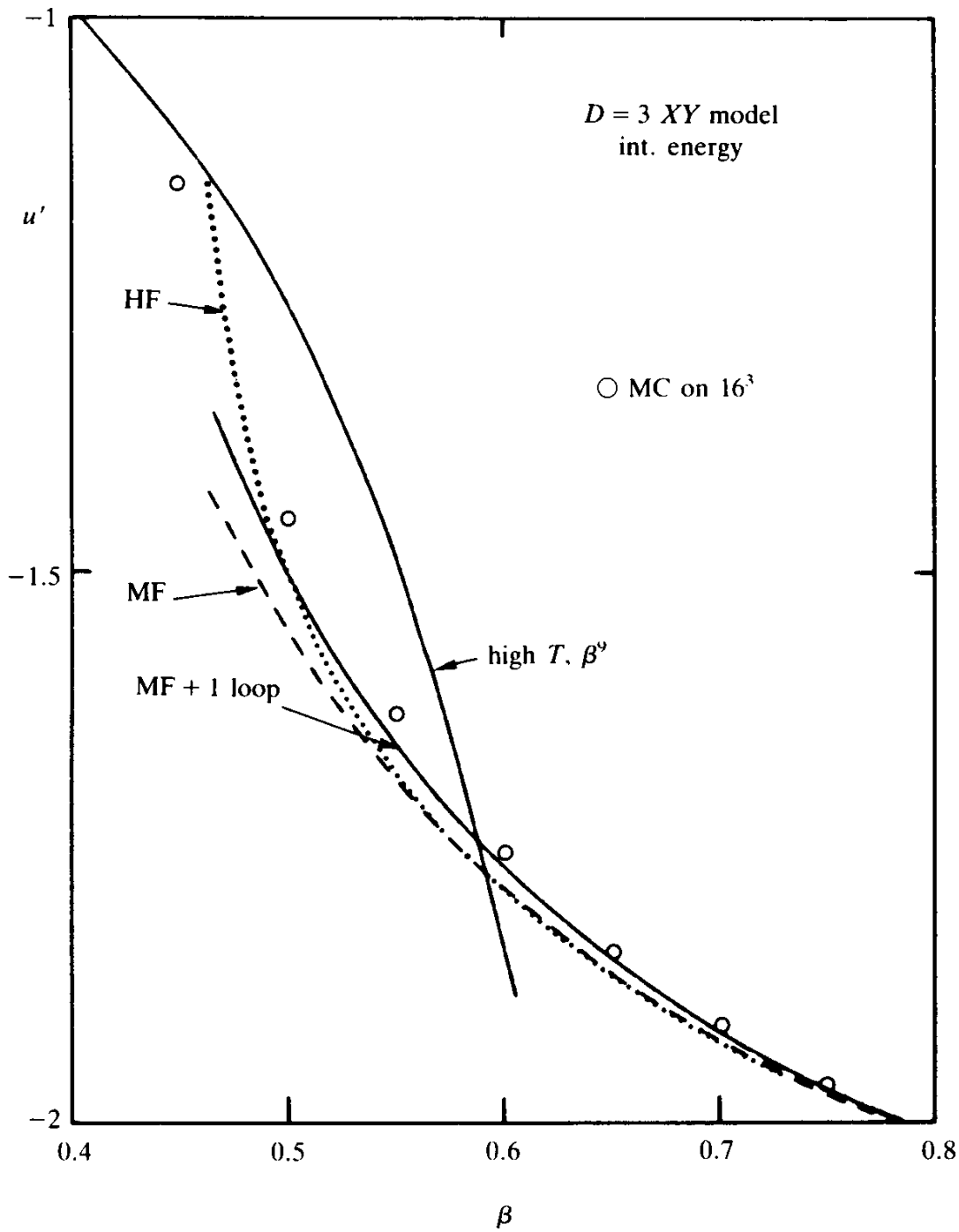
and the corresponding mean-field-plus-one loop term

$$\frac{3}{64(\beta D)^2} + \frac{1}{128D}\frac{1}{(\beta D)^2}$$ (7.163)

are both numerically small up to the phase transition so that their small difference causes an error of a few percent only.

In Figs. 7.18, 7.19 we have plotted the self-consistent internal energy and specific heat and compared them with the mean-field-plus-one-loop curves as well as with Monte Carlo data in the immediate vicinity of the critical point. The good agreement of the theoretical curves with each other demonstrates that the mean-field-plus-one-loop approach is an effective way of resumming infinitely many perturbative diagrams due to the nonlinear interactions in the $\cos \nabla_i \gamma$ energy. Both curves, however fail to give a satisfactory fit to the data in particular for the specific heat. The same comparison will be made once more in the two-dimensional XY model to be discussed in detail in Chapter 11. The corresponding curves will be shown in Figs. 11.9 and 11.10 and the situation will be seen to be much worse than with the three-dimensional case.

FIG. 7.18.   Internal energy of the $D = 3$ XY model as obtained from the self-consistent Hartree-Fock method in comparison with Monte Carlo data of Table 4.17. The agreement is quite good since the internal energy is not very sensitive on the vortex contribution of the type $\exp(-\beta\text{const.})$, which was omitted.

7.10.   VORTEX CORRECTIONS

The important point to realize is that this disagreement would remain even if we could drive the loop corrections to arbitrarily high order. The missing pieces are the vortex lines which behave like $e^{-\beta\text{const.}}$ and such

terms can never be obtained from a power series expansion in T. In order to convince ourselves that this is true we make use of the results of Section 6.4 according to which the vortex corrections to the perturbative partition function are given by a sum similar to the low temperature expansion of the Villain model. We merely have to replace the Boltzmann factors of that expansion [recall (7.39)]

$$e^{-\beta(4\pi^2/2)\sum \ell(x)\cdot v(x-x')\ell(x')}$$
(7.164)

by [recall (6.87)]

$$v[\ell]\,e^{-\beta E[\ell]},$$
(7.165)

where $E[\ell]$ is a modified vortex energy

$$E[\ell] = -\sum_{x,i}\left[\cos\gamma_i^0(x) - 1 + \frac{1}{2}\bar{\nabla}_i\sin\gamma_i^0(x)\frac{1}{-\bar{\nabla}_\ell\cos\gamma_\ell^0(x)\,\nabla_\ell}\bar{\nabla}_i\sin\gamma_i^0(x)\right],$$
(7.166)

and $v[\ell]$ an entropy factor due to the small vibrations of the vortex lines

$$v[\ell] = \det\left(\sum_\ell \bar{\nabla}_\ell\cos\gamma_\ell^0(x)\,\nabla_\ell\right)\bigg/\det\left(\sum_\ell \bar{\nabla}_\ell\nabla_\ell\right).$$
(7.167)

The function $\gamma_i^0(x)$ is the phase configuration around the vortex line

$$\gamma_i^0(x) = 2\pi\frac{1}{-\bar{\nabla}\cdot\nabla}(\bar{\nabla}\times\ell)_i.$$
(7.168)

If the vortex corrections are added to the specific heat shown in Fig. 11.10, we find that a large part of the discrepancy on the *low* temperature shoulder of the peak is removed and the agreement becomes satisfactory.

These results make it quite clear that the essential physics of the phase transition is carried by the vortex lines and not by the perturbative aspects of the nonlinear energy $\cos(\nabla_i\gamma)$ which are accounted for by mean-field methods including loop corrections. The power of these methods concerns only the model dependence and thus physically the least important aspects of the XY model. For example, had we chosen another model interaction, say $\cos(\nabla_i\gamma) + \delta\cos(2\nabla_i\gamma)$, the mean-

FIG. 7.19.   Specific heat of the $D = 3$ XY model, obtained via the self-consistent Hartree-Fock method, compared with the Monte Carlo data. The agreement is now not so good under the right-hand shoulder of the peak due to the absence of vortex contributions.
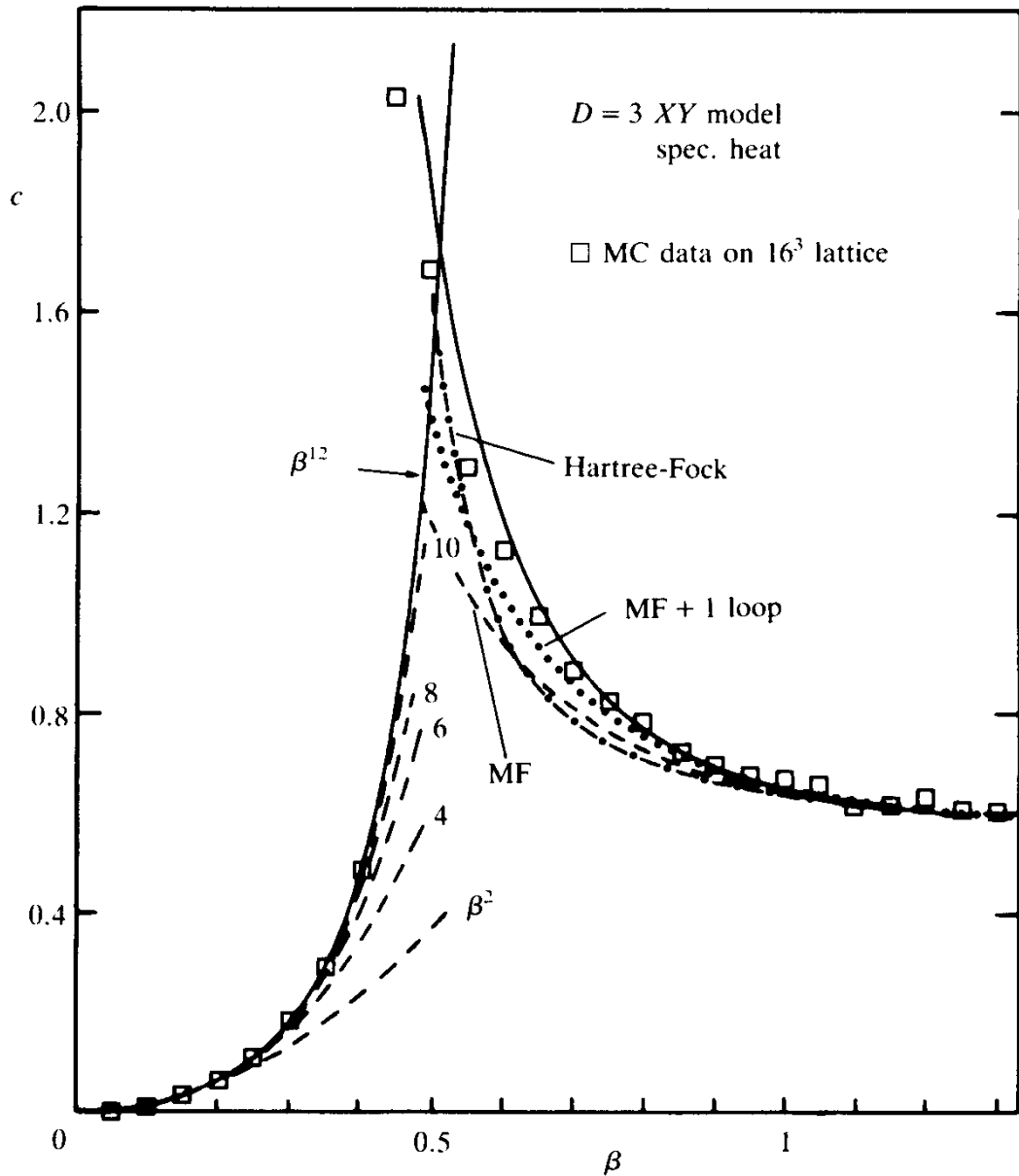
TABLE 7.6.   Proliferation of vortex loops of the XY model when passing the critical point $\beta_c \sim 0.454$ in a Monte Carlo simulation on an $8 \times 8 \times 8$ simple cubic lattice. The top entries are the numbers of loops of length 4, 6, 8, 10, ... The last column is the total length of all loops.

β	4	6	8	10	14	20	28	42	128	total
0.550	5	2	1	—	—	—	—	—	—	54
0.485	3	5	1	1	1	1	1	1	—	164
0.455	7	6	2	—	—	—	—	—	1	218

field calculations would have given a completely different behaviour for the low- and high-temperature regimes. If the transition is of second order, however, the physics in the immediate vicinity of the critical point would not be any different. The vortex lines of unit strength would condense whenever the softened stiffness becomes sufficiently weak, and this process would determine the critical indices. The most convincing evidence for this statement in Fig. 7.10 and Fig. 11.8, which show that the sharp rise in the specific heat at the low temperature side can be explained precisely by pure vortex contributions calculated within the Villain approximation to the XY model.

This leads us to conclude that the advantage of possessing a mean-field-plus-loop method is just an advantage with respect to a trivial model dependence and thus is of no physical value. Only very close to four dimensions (i.e., $D = 4 - \varepsilon$) or a resummation of such loop corrections via renormalization group methods can give correct results. As far as the critical regime is concerned, the Villain model itself is far preferable to the XY model. It has only a trivial $1/\beta$ expansion, namely the zeroth order term $Z_0 = (1/(\sqrt{2\pi\beta})^N)\det(-\bar{\nabla} \cdot \nabla)$. The knowledge of this is equivalent to knowing the mean field approximation with *all* its loop corrections in the XY model! In the Villain model, loop corrections of the perturbative kind are completely absent. All corrections come purely from *vortex loops* and thus carry only the important physical excitations which mediate the phase transition and determine the critical indices via the Villain approximation.

Of course, a real physical system always *has nonlinear interactions* which give rise to $1/\beta''$ dependent terms in the free energy. If such a system is to be studied away from the critical point, it does make sense to treat the known nonlinear energies perturbatively and to calculate the softening of the stiffness constants. Later, in crystal physics, we shall see that such effects are experimentally observable via the temperature behaviour of the elastic constants. However, as far as the phase transition is concerned there is no sense in burdening oneself with an additional purely model dependent softening. It is preferable to use a Villain description in which β_V is immediately identified with the *physical* perturbatively renormalized stiffness[d] of the γ-fluctuations determined either experimentally of by perturbation expansions. The renormalized β_V in

---

[d]How this can be extracted from experimental data will be seen in Chapter 7, Part III in the context of the thermal softening of crystals.

the self-consistent Hartree-Fock calculation was just an example of such a calculation.

When looking at the self-consistent Hartree-Fock equation

$$\beta^R = \beta\, e^{-1/(2\beta^R D)}$$

one may observe that it has a solution only for $\beta D > e/2 = 1.359$. For $D = 3$ this bound is almost equal to the correct critical value

$$\beta_c D = \frac{3}{2.2} \approx 1.36.$$

This coincidence should, however, not induce us to believe that the equation can really give access to the superfluid phase transition. First of all, the argument breaks down quantitatively for $D = 2$ for which $\beta_c D = 2/0.89 = 2.247$. But more severely, for $D > 3$, the breakdown occurs *far before* the critical point which has the large D behaviour $\beta_c D \to 1$. From the above discussion we know that the phase transition is driven by *vortices* and any singularities obtained after a partial resummation of infinitely many perturbation diagrams is due to the particular selection of these diagrams and does not necessarily reflect the physics of the transition. This should be kept in mind when attempting lightheartedly to make identifications[e] of a singular point of this equation with a phase transition, if it merely happens to have the correct order of magnitude. We shall come back to this issue once more in the context of the melting transition in Part III, Chapter 7.

APPENDIX 7A. THE LOW TEMPERATURE EXPANSION OF THE VILLAIN APPROXIMATION

In order to apply Eqs. (7.35) we have to expand $\beta_V = -[2\log(I_1/\beta)/ I_0(\beta)]^{-1}$, $R_V(\beta) = I_0(\beta)\sqrt{2\pi\beta_V}$ as follows (here a dot will denote differentiation, i.e., $\dot{} \equiv d/d\beta$):

$$\beta_V = \beta - \frac{1}{2} - \frac{5}{24\beta} - \frac{25}{96}\frac{1}{\beta^2} - \cdots, \tag{7A.1}$$

---

[e]See the paper by Samuel (referred to in the Notes and References), for example.

$$\dot{\beta}_V = 1 + \frac{5}{24\beta^2} + \frac{25}{48}\frac{1}{\beta^3} + \ldots , \tag{7A.2}$$

$$\dot{\beta}_V/\beta_V = \frac{1}{\beta} + \frac{1}{2\beta^2} + \frac{2}{3\beta^3} + \frac{39}{32\beta^4} + \ldots , \tag{7A.3}$$

$$\ddot{\beta}_V = -\frac{5}{12\beta^3} - \frac{25}{16}\frac{1}{\beta^4} - \ldots . \tag{7A.4}$$

$$\ddot{\beta}_V/\beta_V = -\frac{5}{12\beta^4} - \frac{85}{48\beta^5} - \ldots , \tag{7A.5}$$

$$\frac{\dot{R}}{R} = \frac{\dot{\beta}_V}{2\beta_V} + \frac{I_1(\beta)}{I_0(\beta)} = 1 + \frac{1}{8\beta^2} + \frac{5}{24\beta^3} + \frac{53}{128\beta^4} + \ldots , \tag{7A.6}$$

$$\frac{\ddot{R}}{R} - \left(\frac{\dot{R}}{R}\right)^2 = \frac{1}{2}\left[\frac{\ddot{\beta}_V}{\beta_V} - \left(\frac{\dot{\beta}_V}{\beta_V}\right)^2\right] + 1 - \frac{1}{\beta}\frac{I_1}{I_0} - \left(\frac{I_1}{I_0}\right)^2$$

$$= -\frac{1}{4\beta^3} - \frac{5}{8\beta^4} - \frac{53}{32\beta^5} - \ldots \tag{7A.7}$$

Using $u_{VM} = 1/2\beta_V$, $c_{VM} = 1/2$ we find the high-β_V expansions stated in the text.

NOTES AND REFERENCES

The Villain approximation is due to
J. Villain, *J. Phys.* (Paris) **36** (1977) 581.
The improvement of the Villain approximation is described in
W. Janke and H. Kleinert, *Nucl. Phys.* **B270** [FS16] (1986) 135.
A different improvement was proposed by
J. Jersák, T. Neuhaus and P.M. Zerwas, *Phys. Lett.* **133B** (1985) 103,
which we believe to be less reliable than ours as can be seen in Fig. 7.15 (the agreement close to the maximum is much worse).
The rigorous bound for β_c in (7.87) was derived by
R.J. Myerson, *Phys. Rev.* **B16** (1977) 3203.

The low temperature expansion and the quality of the Villain approximation were studied in collaboration with W. Janke, whose doctoral dissertation (Free University, Berlin, 1985) contains more details. See also

W. Janke and H. Kleinert, *Nucl. Phys.* **B270** [FS16] (1986) 399 and *Phys. Rev. Lett.* **56** (1986) 11

An experimental study of rotons is found in

S. Balibar, J. Buechner, B. Castaing, C. Laroche, A. Libchaber, *Phys. Lett.* **60A** (1977) 135,

which gives $E_{rot} \approx 9.6 \pm 0.2$ K. For larger mechanically generated vortex loops see the references in Chapter 1. The original theoretical discussions are found in

L.D. Landau, *J. Phys. USSR* **5** (1941) 71,

R.P. Feynman, *Phys. Rev.* **91** (1953) 1291, 1302; **92** (1954) 262.

For an experimental investigation of two-roton bound states, via Raman scattering of light, in superfluid ^{4}He, see

T.J. Greytak, in *Quantum Liquids*, eds. J. Ruvalds and T. Regge [North-Holland, Amsterdam, 1978] p. 121,

and theoretically in

A. Zawadowski, *ibid.*, p. 293.

The references for the data given in Table 7.3 are from

J. Tobochnik and G.V. Chester, *Phys. Rev.* **B20** (1979) 3761,

S. Samuel and F.G. Yee, *Nucl. Phys.* **B257** [FS14] (1985) 85,

W.J. Shugard, J.D. Weeks and G.H. Gilmer, *Phys. Rev. Lett.* **41** (1978) 1399, 1577,

J. Villain, *J. Phys.* (Paris) **36** (1975) 581,

M. Ferer, M.A. Moore and M. Wortis, *Phys. Rev.* **B8** (1973) 5205,

C. Dasgupta and B.I. Halperin, *Phys. Rev. Lett.* **47** (1981) 1556l,

B. Lautrup and M. Nauenberg, *Phys. Lett.* **95B** (1980) 631,

G. Bhanot, *Phys. Rev.* **D24** (1981) 461,

D.G. Caldi, *Nucl. Phys.* **B220** (FS8) (1983) 48,

T.A. DeGrand and D. Touissant, *Phys. Rev.* **D22** (1980) 2478, **D24** (1980) 466.

The study of the phase transition of the XY model via the Hartree-Fock self-consistency condition was advocated by

S. Samuel, *Phys. Rev.* **B25**, (1982) 1755, *Nucl. Phys.* **B191** (1981) 381

See also:

J. Bricomt, J.-R. Fontaine, J.L. Lebowitz, E.L. Lieb and T. Spencer, *Commun. Math. Phys.* **78** (1981) 545,

and

N.D. Hari Dass and A. Patkos *Nucl. Phys.* **B210** (1982) 529.

A more recent analysis can be found in

S. Ami and H. Kleinert, *Phys. Rev.* **B33** (1986) 4692.

Questions related to different orders of the phase transions in XY models are discussed in

W. Janke and H. Kleinert, *Nucl. Phys.* **B270** (1986) 399, *Phys. Rev. Lett.* **57** (1986) 279.

See also

H. Kleinert, *Phys Rev. Lett.* **56** (1986) 1441,

for related aspects on $U(1)$ lattice gauge theory.

GAUGE FIELDS OF VORTEX LINES

Up to now, we have dealt only with one type of gauge field, namely, the gauge field which describes superflow via a curl relation,

$$v_s \propto \bar{\nabla} \times \mathbf{A}. \tag{8.1}$$

This gauge field was introduced in order to ensure that the b_i field lines are closed. They are the rings of superflow arising in the disordered phase due to fluctuations which carry the liquid toward the ordered state. In the vortex-line representation of the XY model, we encountered another set of closed lines, namely, those of vortex lines. Vortex lines give rise to a second important gauge structure which we are now going to discuss.

8.1. VORTEX-GAUGE FIELD AND VORTEX-GAUGE INVARIANCE

Suppose we want to really execute a sum over closed vortex lines

$$\sum_{\{\ell_i(\mathbf{x})\}} \delta_{\bar{\nabla} \cdot \ell, 0} \, e^{2\pi i \sum_\mathbf{x} \ell_i(\mathbf{x}) A_i(\mathbf{x})}, \tag{8.2}$$

say on a computer. Then the constraint $\bar{\nabla} \cdot \ell(\mathbf{x}) = 0$ is not easy to

fulfill. The simplest way to circumvent this problem is to introduce integer-valued gauge field $n_i(\mathbf{x})$ for the closed ℓ-lines. We simply write

$$\ell_i(\mathbf{x}) = (\nabla \times \mathbf{n})_i(\mathbf{x}) \equiv \varepsilon_{ijk}\nabla_j n_k(\mathbf{x} + \mathbf{i}) \qquad (8.3)$$

and have automatically $\bar{\nabla} \cdot \boldsymbol{\ell}(\mathbf{x}) = 0$ for *any* choice of $n_i(\mathbf{x})$. The decomposition (8.3) is invariant under all integer-valued gauge transformations

$$n_i(\mathbf{x}) \to n_i(\mathbf{x}) + \nabla_i N(\mathbf{x}). \qquad (8.4)$$

This property is what we will refer to as *vortex-gauge invariance*. The field $n_i(\mathbf{x})$ will be called *vortex-gauge field*.

In order that this field be related to the $\ell_i(\mathbf{x})$ fields in a one-to-one way, we have to impose a gauge condition, such as

$$n_3(\mathbf{x}) = 0, \qquad (8.5)$$

together with the boundary conditions

$$n_2(x_1, x_2, 0) = 0, \qquad (8.6)$$
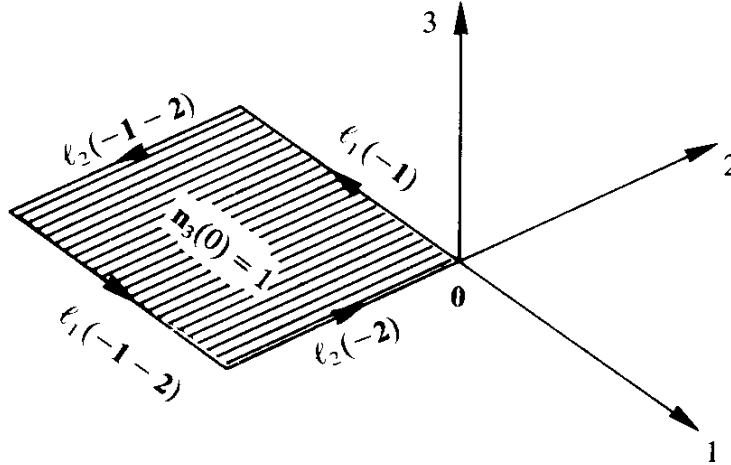
$$n_1(x_1, 0, 0) = 0, \qquad (8.7)$$

just as in the representation (6.5) of $b_i(\mathbf{x})$ in terms of the integer fields $a_i(\mathbf{x})$, where the analogous conditions were (6.15), (6.22). After fixing the gauge, it is easy to perform sums like (8.2). We merely have to let $n_1(\mathbf{x})$, $n_2(\mathbf{x})$ run over *all unconstrained* integer values, subject merely to the boundary condition (8.6), (8.7). Formula (8.3) then produces the associated vortex lines.

8.2. PHYSICAL MEANING OF VORTEX-GAUGE INVARIANCE

The question arises as to the physical meaning of vortex gauge invariance. In order to understand this it is useful to picture the integer numbers $n_i(\mathbf{x})$ as occupation numbers of plaquettes whose normals are given by the links i as shown in Fig. 8.1. When looking at a set of these occupation numbers, they may be further thought of as arising from a superposition of sheets of unit occupation. In this picture, the $\boldsymbol{\ell}(\mathbf{x})$ vectors, which are calculated from $\mathbf{n}(\mathbf{x})$ via the lattice curl $\nabla \times \mathbf{n}(\mathbf{x})$, have a simple

FIG. 8.1.   Elementary vortex loop associated with the vortex gauge field $n_3(\mathbf{x}) = \delta_{\mathbf{x},0}$.

geometric interpretation: they represent the oriented boundary lines of these sheets of unit occupation. Take, for example, $n_3(\mathbf{x}) = \delta_{\mathbf{x},0}$ which corresponds to the elementary plaquette drawn in Fig. 8.1 and whose normal is the link i at the origin. If we form the lattice curl we find the integers

$$\ell_1(\mathbf{x}) = \nabla_2 n_3(\mathbf{x} + \mathbf{1}) = \delta_{\mathbf{x}+\mathbf{1}+\mathbf{2},0} - \delta_{\mathbf{x}+\mathbf{1},0},$$

$$\ell_2(\mathbf{x}) = -\nabla_1 n_3(\mathbf{x} + \mathbf{2}) = -\delta_{\mathbf{x}+\mathbf{1}+\mathbf{2},0} + \delta_{\mathbf{x}+\mathbf{2},0},$$

$$\ell_3(\mathbf{x}) = 0. \tag{8.8}$$

These can be pictured as a unit current flowing along the links surrounding the plaquette. The general case follows by superposition.

Obviously there remains great freedom in choosing a surface for a given boundary. Consider now a vortex-gauge transformation

$$n_i(\mathbf{x}) \to n_i'(\mathbf{x}) = n_i(\mathbf{x}) + \nabla_i N(\mathbf{x}), \tag{8.9}$$

and take, for example,
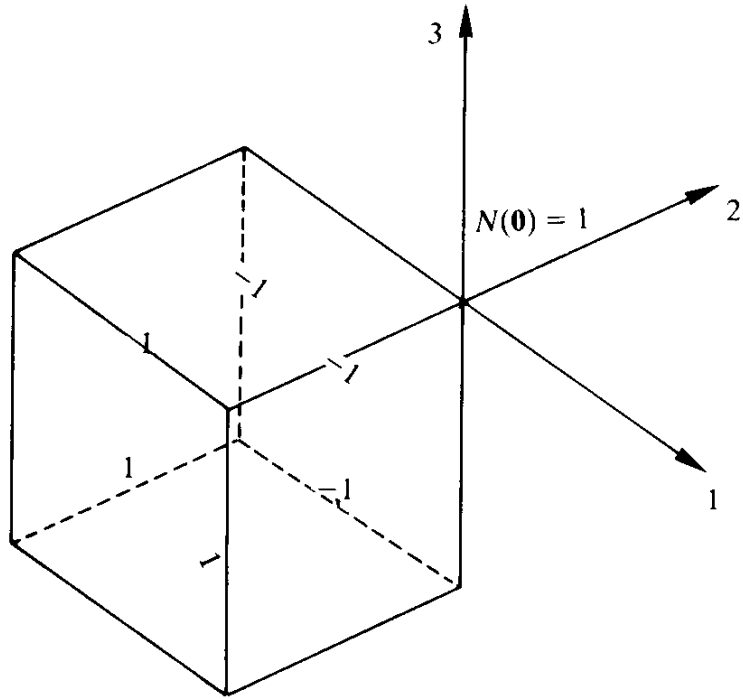
$$N(\mathbf{x}) = \delta_{\mathbf{x},0}. \tag{8.10}$$

This gives

$$\nabla_i N(\mathbf{x}) = \delta_{\mathbf{x}+i,0} - \delta_{\mathbf{x},0}. \tag{8.11}$$

When interpreted as plaquette occupation numbers, $\nabla_i N(\mathbf{x})$ amount to the faces of a unit cube being occupied by $n_i = -1$ for the coordinate planes and by $n_i = +1$ for the opposite ones (see Fig. 8.2). If we give the plaquettes an orientation with respect to the cube, say outward, all

FIG. 8.2. Closed surface associated with the pure vortex gauge field $n_i(\mathbf{x}) = \nabla_i N(\mathbf{x})$.

occupation numbers acquire the same sign, -1, and

$$n_i(\mathbf{x}) = -\nabla_i N(\mathbf{x}),$$

describes properly these numbers including the orientation. They are the normal vectors of the surface elements of the unit cube. Generalizing (8.10) to an arbitrary integer field $N(\mathbf{x})$, it can be pictured as a superposition of volume elements with unit occupation, and the operation $-\nabla_i N(\mathbf{x})$ changes this into closed oriented surfaces around each of these volume elements, all with unit occupation. When adding $\nabla_i N(\mathbf{x})$ to the gauge field $n_i(\mathbf{x})$ we see that this can have two effects: either it adds disjoint closed surfaces, or it deforms the surface $n_i(\mathbf{x})$. In both cases it maintains whatever boundary $\boldsymbol{\ell} = \nabla \times \mathbf{n}$ is present.

This observation is the key to the physical interpretation of the vortex-gauge transformations. We recall that the vortex lines may be thought of as the boundary lines of a surface S across which the angular field variable $\gamma(\mathbf{x})$ jumps by 2π. The position of the jumping surface is physically unimportant. Only the boundary line is relevant. Vortex-gauge invariance is a manifestation of precisely this fact. Gauge transformations do nothing but move the irrelevant surface around in space while maintaining the boundary line. In addition, they may create new disjoint and closed surfaces which correspond to no vortex line at all and are devoid of physical content.

8.3. CONTINUUM DESCRIPTION

It is useful to see what happens to this vortex-gauge invariance in the continuum limit. Recall that there the vortex lines were described by the vortex density, defined in (1.78),

$$\alpha_i(\mathbf{x}) = \varepsilon_{ijk} \, \partial_j \, \partial_k \, \gamma(\mathbf{x}). \tag{8.12}$$

A line of unit strength along L is given by

$$\alpha_i(\mathbf{x}) = 2\pi \, \delta_i(L). \tag{8.13}$$

Since regular gradients of $\gamma(\mathbf{x})$ do not contribute to (8.12), $\alpha_i(\mathbf{x})$ can be thought of as arising from a singular gradient

$$(\partial_k \gamma)^S(\mathbf{x}) = 2\pi \, \delta_k(S), \tag{8.14}$$

where

$$\delta_k(S) \equiv \int_S dS'_k \, \delta^{(3)}(\mathbf{x} - \mathbf{x}') \tag{8.15}$$

[short for $\delta_k(\mathbf{x}_i S)$] is the δ-function on a surface S which satisfies

$$\int dx_k \, \delta_k(S) = 1, \tag{8.16}$$

if the contour of integration pierces the surface S (see Fig. 1.9). Then $\gamma(\mathbf{x}) = \int dx_k (\partial_k \gamma)^S$ does indeed have a jump of 2π across the surface S.

The equivalence of (8.13) and (8.14) follows from Stokes' theorem. It can be expressed in terms of δ-functions as follows

$$\varepsilon_{ijk} \, \partial_j \, \delta_k(S) = \delta_i(L), \tag{8.17}$$

where L is the boundary line around S. The proof of (8.17) is given by multiplying both sides by an arbitrary smooth test function $f(\mathbf{x})$ and integrating over $\mathbf{x}$ whereupon the left-hand side becomes

$$\int d^3x \int_S dS'_k \, \varepsilon_{ijk} \, \partial_i \delta(\mathbf{x} - \mathbf{x}')f(\mathbf{x}) = \varepsilon_{ijk} \int_S dS_k \, \partial_i f(\mathbf{x})$$

$$= \oint_L dx_i f(\mathbf{x}) = \int d^3x \, \delta_i(L)f(\mathbf{x}),$$

which is equal to the right-hand side of (8.17).

Using (8.17) we have, indeed

$$\alpha_i(\mathbf{x}) = \varepsilon_{ijk} \, \partial_j(\partial_k \gamma)^S = 2\pi \delta_i(L). \tag{8.18}$$

Comparing Eq. (8.18) with (8.3) we recognize that, up to a factor -2π, the vortex density $\alpha_i(\mathbf{x})$ is the continuum analogue of the $\ell_i(\mathbf{x})$ field, while the singular gradients $(\partial_k \gamma)^S(\mathbf{x})$ are the analogues of the jumping numbers $n_k(\mathbf{x})$.

Let us now see what the vortex-gauge transformations become in the continuum. Since they correspond to changing the surface S to another one, S', with the same boundary, $(\partial_k \gamma)^S$ must change as follows

$$(\partial_k \gamma)^S \rightarrow (\partial_k \gamma)^S + 2\pi(\delta_k(S') - \delta_k(S)). \tag{8.19}$$

The fact that the boundaries of S and S' are the same means that $S - S'$ is a closed surface. Let V be the volume enclosed by it. Then we can make use of Gauss' law. It can be expressed in terms of δ-functions as follows: If S is a closed surface enclosing V, then $\delta_k(S)$ can be written as a pure gradient

$$\delta_k(S) = -\partial_k \delta(V), \tag{8.20}$$

where

$$\delta(V) \equiv \int_V d^3x' \, \delta^{(3)}(\mathbf{x} - \mathbf{x}') \tag{8.21}$$

is the δ-function which is singular over the volume V and satisfies

$$\int_{V'} d^3x \, \delta(V) = \int_{V' \cap V} d^3x.$$

The proof of (8.20) follows again by multiplying both sides by a test

function $f(\mathbf{x})$ and integrating over $\mathbf{x}$. This gives, on the left-hand side,

$$\int d^3x\, \delta_k(S) f(\mathbf{x}) = \int_S dS_k f(\mathbf{x}) = \int d^3x\, \delta_k f(\mathbf{x}) = -\int d^3x\, \partial_k \delta(V) f(\mathbf{x}),$$

which is again equal to the right-hand side. Applying formula (8.20) to the closed surface $S - S'$ in (8.19) we find that $(\partial_k \gamma)^S$ changes according to

$$(\partial_k \gamma)^S(\mathbf{x}) \rightarrow (\partial_k \gamma)^S(\mathbf{x}) - 2\pi \partial_k \delta(V). \tag{8.22}$$

Here we recognize the continuum version of the vortex-gauge transformation (8.4) with $N(\mathbf{x}) \triangleq \delta(V)$ (up to a factor -2π).

8.4. VORTEX GAUGE THEORY FOR THE VILLAIN MODEL-DOUBLE GAUGE THEORY

In the Villain model, there exists a derivation of the vortex-line representation which makes the vortex gauge structure more transparent than the one given previously in Sections 6.2 and 7.3.

Consider the partition function in the form (7.29)

$$Z_{VM} = \prod_{\mathbf{x}} \left[\int_{-\pi}^{\pi} \frac{d\gamma(\mathbf{x})}{2\pi} \right] \sum_{\{n_i(\mathbf{x})\}} e^{-(\beta v/2)\Sigma_\mathbf{x}(\nabla_i \gamma - 2\pi n_i)^2}. \tag{8.23}$$

We now observe that the sum over $n_i(\mathbf{x})$ and the integrals over $\gamma(\mathbf{x})$ are not independent of each other. It is possible to remove from $n_i(\mathbf{x})$ a pure lattice gradient, say,

$$n_i(\mathbf{x}) = n_i^0(\mathbf{x}) + \nabla_i N(\mathbf{x}), \tag{8.24a}$$

where $N(\mathbf{x})$ runs through *all* integers, and absorb these integers into the variables $\gamma(\mathbf{x})$, thus forming

$$\gamma^0(\mathbf{x}) = \gamma(\mathbf{x}) - 2\pi N(\mathbf{x}). \tag{8.24b}$$

The new variables $\gamma^0(\mathbf{x})$ range from minus infinity to plus infinity. The remaining $n_i^0(\mathbf{x})$, on the other hand, are no longer independent but require some specification.

For example, we can take

$$n_3^0(\mathbf{x}) = 0, \quad n_2^0(x_1, x_2, 0) = 0, \quad n_1^0(x_1, 0, 0) = 0. \qquad (8.25\text{a,b,c})$$

Indeed, this specification allows us to separate $N(\mathbf{x})$ out uniquely (up to a trivial overall constant). First of all, $N(\mathbf{x})$ must satisfy

$$N(\mathbf{x}) = \left(\frac{1}{\nabla_3} n_3\right)(\mathbf{x}) + f(x_1, x_2), \qquad (8.26)$$

where $((1/\nabla_3) n_3)(\mathbf{x})$ denotes the sum $\displaystyle\sum_{x_3' = -1}^{x_3 - 1} n(x_1, x_2, x_3')$, which satisfies the boundary condition

$$\left(\frac{1}{\nabla_3} n_3\right)(x_1, x_2, 0) = 0. \qquad (8.27)$$

The function $f(x_1, x_2)$ stands for an arbitrary integer "constant of integration." With this $N(\mathbf{x})$, $n_3^0(\mathbf{x})$ vanishes identically. The integers $f(x_1, x_2)$ can be further adjusted such that

$$n_2^0(x_1, x_2, 0) = n_2(x_1, x_2, 0) - \nabla_2 f(x_1, x_2)$$

vanishes. This fixes[a]

$$f(x_1, x_2) = \frac{1}{\nabla_2} n_2(x_1, x_2, 0) + g(x_1). \qquad (8.28)$$

The remaining integer constants of integration $g(x_1)$ can be chosen to fulfill the last condition (8.25c)

$$n_1^0(x, 0, 0) = n_1(x_1, 0, 0) - \nabla_1 g(x_1) = 0,$$

apart from a trivial constant. Thus the integer function

$$N(\mathbf{x}) = \frac{1}{\nabla_3} n_3(\mathbf{x}) + \frac{1}{\nabla_2} n_2(x_1, x_2, 0) + \frac{1}{\nabla_1} n_1(x_1, 0, 0) + n \qquad (8.29)$$

has the property that if $n_i(\mathbf{x})$ runs through all integers, $N(\mathbf{x})$ does too

---

[a]We are dropping the parenthesis around $((1/\nabla_2)f)(\mathbf{x})$ for brevity.

(apart form the overall constant n), and the subtracted integers

$$n_i^0(\mathbf{x}) = n_i(\mathbf{x}) - \nabla_i N \tag{8.30}$$

satisfy the conditions (8.25). Hence we can rewrite the partition function of the Villain model (8.23) in the equivalent form

$$Z_{VM} = \prod_{\mathbf{x}} \left[\int_{-\infty}^{\infty} \frac{d\gamma(\mathbf{x})}{2\pi} \right] \sum_{\{n_i(\mathbf{x})\}} \delta_{n_3,0}\, e^{-(\beta_v/2)\Sigma_{\mathbf{x}}(\nabla_i\gamma - 2\pi n_i)^2}, \tag{8.31}$$

where the symbol $\delta_{n_3,0}$ is supposed to imply also the boundary conditions (8.25b, c).

This form directly exhibits vortex-gauge invariance: the expression in the brackets is the partition function of a set of vortex lines described by the jumping numbers $n_i(\mathbf{x})$. The modified gradients

$$\nabla_i \gamma(\mathbf{x}) - 2\pi n_i(\mathbf{x}) \tag{8.32}$$

are invariant under arbitrary transformations

$$n_i(\mathbf{x}) \rightarrow n_i(\mathbf{x}) + \nabla_i N(\mathbf{x}), \quad \gamma(\mathbf{x}) \rightarrow \gamma(\mathbf{x}) + 2\pi N(\mathbf{x}), \tag{8.33}$$

moving around the irrelevant surface over which the phase angle $\gamma(\mathbf{x})$ jumps by 2π. With respect to this gauge invariance, the Kronecker delta $\delta_{n_3,0}$ in (8.31) may be considered as a *gauge-fixing factor* which is needed to remove the gauge degeneracy in the sum over all $n_i(\mathbf{x})$. It plays the same role as the gauge-fixing factor $\delta_{a_3,0}$ in (6.23) [which also implies the boundary conditions $a_2(x_1, x_2, 0) = 0$, $a_1(x_1, 0, 0) = 0$].

It is instructive to derive once more the vortex-line representation from the form (8.31). As in (7.16) we can introduce auxiliary variables $B_i(\mathbf{x})$ and rewrite Z_{VM} as

$$Z_{VM} = \prod_{\mathbf{x},i} \left[\int_{-\infty}^{\infty} \frac{dB_i(\mathbf{x})}{\sqrt{2\pi\beta_V}} \right] \prod_{\mathbf{x}} \left[\int_{-\pi}^{\pi} \frac{d\gamma(\mathbf{x})}{2\pi} \right] \sum_{\{n_i(\mathbf{x})\}} \delta_{n_3,0}\, e^{-(1/2\beta_V)\Sigma_{\mathbf{x}}B_i^2(\mathbf{x}) + i\Sigma_{\mathbf{x}}B_i(\nabla_i\gamma - 2\pi n_i)}. \tag{8.34}$$

Notice that with the modified gradients $\nabla_i \gamma(\mathbf{x}) - 2\pi n_i(\mathbf{x})$, the variables $b_i(\mathbf{x})$ are also vortex-gauge invariant quantities. Since the $\gamma(\mathbf{x})$ variables are now running over the entire real axis, they can be integrated out and yield

$$\bar{\nabla}_i B_i(\mathbf{x}) = 0. \tag{8.35}$$

Notice that [in contrast to the integer fields $b_i(\mathbf{x})$ of Eq. (7.18)] these fields are now *continuous*. They can be written as

$$B_i(\mathbf{x}) = (\bar{\nabla} \times \mathbf{A})_i(\mathbf{x}) = \varepsilon_{ijk}\bar{\nabla}_j A_k(\mathbf{x} - \mathbf{k}), \tag{8.36}$$

where $A_k(\mathbf{x})$ is a continuous gauge field. Unlike the previous integer field $a_i(\mathbf{x})$ in (7.19), we can now choose *any* gauge we please, in particular, the transverse gauge $\nabla \cdot \mathbf{A}(\mathbf{x}) = 0$ allows us to write

$$Z_{VM} = \frac{1}{(\sqrt{2\pi\beta_V})^{3N}}\prod_{\mathbf{x},i}\left[\int_{-\infty}^{\infty} dA_i(\mathbf{x})\right]\Phi[\mathbf{A}]$$

$$\times \sum_{\{n_i(\mathbf{x})\}} \delta_{n_3,0}\, e^{-(1/2\beta_V)\Sigma_{\mathbf{x}}(\bar{\nabla}\times\mathbf{A})^2 - 2\pi i\Sigma_{\mathbf{x}}(\bar{\nabla}\times\mathbf{A})\cdot\mathbf{n}}, \tag{8.37}$$

where $\Phi[\mathbf{A}] = \Pi_{\mathbf{x}}\delta(A_3(\mathbf{x}))$ or $\det(-\bar{\nabla}\cdot\nabla)\Pi_{\mathbf{x}}\delta(\bar{\nabla}_i A_i(\mathbf{x}))$, just as in (6.49), (6.56). Notice that (8.37) constitutes a double gauge theory, involving two gauge fields A_i of superflow and n_i of vortex lines. The energy is invariant under the gauge transformations (6.48) of A_i and (8.33) of n_i. The second exponent can be partially integrated on the lattice as follows:

$$e^{-2\pi i\Sigma_{\mathbf{x}}\varepsilon_{ijk}\bar{\nabla}_j A_k(\mathbf{x}-\mathbf{k})n_i(\mathbf{x})} = e^{-2\pi i\Sigma_{\mathbf{x}}A_k(\mathbf{x})\varepsilon_{kij}\nabla_i n_j(\mathbf{x}+\mathbf{k})}. \tag{8.38}$$

The numbers

$$\ell_k(\mathbf{x}) \equiv (\nabla \times \mathbf{n})_k(\mathbf{x}) \equiv \varepsilon_{kij}\nabla_i n_j(\mathbf{x}+\mathbf{k}) \tag{8.39}$$

satisfy precisely the relation (8.3) with the jump numbers $n_i(\mathbf{x})$ playing the role of the vortex gauge fields $n_i(\mathbf{x})$ introduced there. The ℓ_i's run through all integer *divergenceless* numbers so that the sum over $n_i(\mathbf{x})$ can be rewritten as

$$\sum_{\{n_i(\mathbf{x})\}} \delta_{n_3,0}\, e^{-2\pi i\Sigma_{\mathbf{x}}A_k(\mathbf{x})(\nabla\times\mathbf{n})_k(\mathbf{x})} = \sum_{\{\ell_i(\mathbf{x})\}} \delta_{\bar{\nabla}_i\ell_i,0}\, e^{-2\pi i\Sigma_{\mathbf{x}}A_k(\mathbf{x})\ell_k(\mathbf{x})} \tag{8.40}$$

and (8.37) is seen to coincide with the representation (7.25).[b] This shows that the ℓ_i vectors defined in (8.39) are *identical* to those introduced in (7.25) for the purpose of changing the integer gauge fields $a_i(\mathbf{x})$ into

[b]Apart from the factor $R_V(\beta)^{3N}$ by which Z_{VM} differs from Z_V'.

continuous ones $A_i(\mathbf{x})$. It is the virtue of the present derivation that it establishes a direct relation between these numbers and the jumping numbers $n_i(\mathbf{x})$ in the Villain model. This relation remained hidden in the original derivation of (7.25).

The fact that the loop variables $\ell_i(\mathbf{x})$ are the lattice curl of the jumping numbers $n_i(\mathbf{x})$ which, in turn, are the gauge fields of the vortex lines introduced in (7.3) confirms once more our physical interpretation of vortex gauge transformations given in Section 7.2: gauge transformations of $n_i(\mathbf{x})$ by a pure gradient $\nabla_i N(\mathbf{x})$ correspond to deformations of the jumping surfaces at fixed vortex lines and this does not change the superflow around the vortex lines described by $\ell_i(\mathbf{x}) = (\nabla \times \mathbf{n})_i$.

8.5. DERIVATION OF ENERGY OF VORTEX LINES FROM VORTEX-GAUGE FIELDS

The vortex gauge field is of great use in deriving interaction energies between vortex lines without invoking the gauge field of superflow.

The starting point is the Villain model (8.31). The exponent can be written explicitly, as

$$-\frac{\beta_V}{2} \sum_{\mathbf{x}} (\nabla_i \gamma - 2\pi n_i)^2 = -\frac{\beta_V}{2} \sum_{\mathbf{x}} ((\nabla_i \gamma)^2 - 4\pi \nabla_i \gamma n_i + 4\pi^2 n_i^2). \qquad (8.41)$$

A partial integration and a quadratic completion brings this to the form

$$-\frac{\beta_V}{2} \sum_{\mathbf{x}} \left(\gamma(\mathbf{x}) - \frac{2\pi}{-\bar{\nabla} \cdot \nabla} \bar{\nabla}_i n_i(\mathbf{x}) \right) (-\bar{\nabla} \cdot \nabla) \left(\gamma(\mathbf{x}) - \frac{2\pi}{-\bar{\nabla} \cdot \nabla} \bar{\nabla}_j n_j(\mathbf{x}) \right)$$

$$-\frac{\beta_V}{2} 4\pi^2 \sum_{\mathbf{x}} \left(n_i^2(\mathbf{x}) - \bar{\nabla}_i n_i(\mathbf{x}) \frac{1}{-\bar{\nabla} \cdot \nabla} \bar{\nabla}_j n_j(\mathbf{x}) \right) \qquad (8.42)$$

Reinserting this into (8.31), we can directly integrate out the γ fluctuations and arrive at

$$Z_{VM} = \frac{1}{(\sqrt{2\pi\beta_V})^N} \det(-\bar{\nabla} \cdot \nabla)^{-1/2} \sum_{\{n_i(\mathbf{x})\}} \delta_{n_i,0} \, e^{-(\beta_V/2)4\pi^2 \Sigma_\mathbf{x} n_i(\mathbf{x})(\delta_{ij} - \nabla_i \bar{\nabla}_j / \bar{\nabla} \cdot \nabla) n_j(\mathbf{x})}. \qquad (8.43)$$

The interaction[c] involves only the transverse part of the gauge field $n_j(\mathbf{x})$,

[c]The interaction is recognized as the dipole-dipole interaction energy (7.75) between elementary current loops described by $n_i(\mathbf{x})$ which we had introduced there to calculate the low temperature behaviour of the Villain model.

so that it is properly invariant under vortex-gauge transformations on $n_j(\mathbf{x})$,[d]

$$n_j(\mathbf{x}) \rightarrow n_j(\mathbf{x}) + \nabla_j N(\mathbf{x}).\tag{8.44}$$

Therefore, it can be expressed in terms of the gauge invariant curls

$$\ell_i(\mathbf{x}) = (\nabla \times \mathbf{n})_i(\mathbf{x}) = \varepsilon_{ijk}\nabla_j n_k(\mathbf{x} + \mathbf{i}).\tag{8.45}$$

Indeed, forming

$$\sum_{\mathbf{x}} \ell_i(\mathbf{x})^2 = \sum_{\mathbf{x}} \varepsilon_{ijk} \nabla_j n_k(\mathbf{x} + \mathbf{i})\, \varepsilon_{ij'k'} \nabla_{j'} n_{k'}(\mathbf{x} + \mathbf{i})$$

$$= \sum_{\mathbf{x}} \varepsilon_{ijk} \nabla_j n_k(\mathbf{x})\, \varepsilon_{ij'k'} \nabla_{j'} n_{k'}(\mathbf{x})$$

$$= \sum_{\mathbf{x}} \left(\nabla_j n_k(\mathbf{x}) \nabla_j n_k(\mathbf{x}) - \nabla_j n_k(\mathbf{x}) \nabla_k n_j(\mathbf{x}) \right)$$

$$= \sum_{\mathbf{x}} n_k(\mathbf{x})(-\bar{\nabla}_j \nabla_j)\, n_k(\mathbf{x}) - \bar{\nabla}_k n_k(\mathbf{x})\, \bar{\nabla}_j n_j(\mathbf{x})$$

$$= \sum_{\mathbf{x}} (-\bar{\nabla} \cdot \nabla) n_i(\mathbf{x}) \left(\delta_{ij} - \frac{\nabla_i \bar{\nabla}_j}{\bar{\nabla} \cdot \nabla} \right) n_j(\mathbf{x}),\tag{8.46}$$

we see that

$$\sum_{\mathbf{x}} n_i(\mathbf{x}) \left(\delta_{ij} - \frac{\nabla_i \bar{\nabla}_j}{\bar{\nabla} \cdot \nabla} \right) n_j(\mathbf{x}) = \sum_{\mathbf{x}} \ell_i(\mathbf{x}) \frac{1}{-\bar{\nabla} \cdot \nabla} \ell_i(\mathbf{x})\tag{8.47}$$

so that we obtain, once more, the Biot-Savart form (7.39),

$$Z_{VM} = \frac{1}{(\sqrt{2\pi}\beta_V)^N} \det(-\bar{\nabla} \cdot \nabla) \sum_{\{\ell_i(\mathbf{x})\}} \delta_{\ell_i,0}\, e^{-(\beta_V/2)4\pi^2 \sum_{\mathbf{x}} \ell_i(\mathbf{x})(1/-\bar{\nabla} \cdot \nabla)\ell_i(\mathbf{x})},\tag{8.48}$$

whose derivation there was somewhat more complicated. Notice that the calculation would be even shorter, if we were allowed to choose a transverse gauge

[d]Without the dipole interpretation of $n_i(\mathbf{x})$ this invariance reflects the ambiguity, in magneto-statics, of composing a current loop in terms of infinitesimal Ampère loops.

$$\overline{\nabla}_j n_j(\mathbf{x}) = 0. \tag{8.49}$$

Then the $\gamma(\mathbf{x})$ fluctuations in (8.41) would *decouple* from the defect gauge field and we would find immediately a Boltzmann factor

$$e^{-(\beta v/2)4\pi^2 \Sigma_x n_i^2(\mathbf{x})}. \tag{8.50}$$

From (8.47), on the other hand, we would obtain in the transverse gauge

$$\sum_\mathbf{x} n_i^2(\mathbf{x}) = \sum_\mathbf{x} \ell_i(\mathbf{x}) \frac{1}{-\overline{\nabla} \cdot \overline{\nabla}} \ell_i(\mathbf{x}), \tag{8.51}$$

which is again the proper Biot-Savart form.

Actually, as far as this calculation is concerned, the illegal nature of the gauge (8.49) is irrelevant. The reason lies in the fact that the $\gamma(\mathbf{x})$ fields in Z_{VM} are integrated out completely. Indeed, as long as we are calculating only the total partition function, without external sources for $\gamma(\mathbf{x})$,

$$Z_{VM} = \prod_\mathbf{x} \left[\int_{-\infty}^{\infty} \frac{d\gamma(\mathbf{x})}{2\pi} \right] \sum_{\{n_i(\mathbf{x})\}} \Phi[n] \, e^{-(\beta v/2)\Sigma_x(\nabla_i \gamma_i - 2\pi n_i)^2}. \tag{8.52}$$

This is invariant not only under the proper vortex-gauge transformations (8.33) but also under all non-integer transformations

$$n_i(\mathbf{x}) \rightarrow n_i(\mathbf{x}) + \nabla_i v(\mathbf{x}), \quad \gamma(\mathbf{x}) \rightarrow \gamma(\mathbf{x}) + 2\pi v(\mathbf{x}), \tag{8.53}$$

with *arbitrary, real* $v(\mathbf{x})$. The fact that $v(\mathbf{x})$ has to be integer and $\gamma(\mathbf{x})$ can be changed only by multiples of 2π will be of importance when calculating correlation functions of the fields $e^{i\gamma(\mathbf{x})}$. This will be done in the next chapter.

8.6. CONTINUUM LIMIT

It is useful to go through the same derivation once more in the continuum limit. There the bending energy of superflow is [recall (1.60)]

$$E = \frac{\sigma}{2} \int d^3x \, (\nabla \gamma)^2. \tag{8.54}$$

In the presence of vortex lines this has to be replaced by the continuous version of the exponent of (8.31). Using the singular gradients (8.14),

$$(\partial_i \gamma)^S = 2\pi \delta_i(S), \tag{8.55}$$

to specify the vortex lines as boundaries of jumping surfaces S, this amounts to the energy

$$E = \frac{\sigma}{2} \int d^3x (\partial_i \gamma - (\partial_i \gamma)^S)^2. \tag{8.56}$$

The energy density is invariant under changes of $S \to S'$, i.e., under the vortex-gauge transformations [see (8.19)]

$$(\partial_i \gamma)^S \to (\partial_i \gamma)^S - 2\pi \partial_i \delta(V), \quad \gamma \to \gamma - 2\pi \delta(V). \tag{8.57}$$

We now work out the square factor in (8.56) and write

$$E = \frac{\sigma}{2} \int d^3x ((\partial_i \gamma)^2 - 2\partial_i \gamma (\partial_i \gamma)^S + (\partial_i \gamma^S)^2). \tag{8.58}$$

Minimizing this in γ gives the interaction energy between the vortex lines,

$$E_{\text{int}} = \frac{\sigma}{2} \int d^3x \left[[(\partial_i \gamma)^S]^2 - (\partial_i \gamma)^S \frac{1}{-\nabla^2} (\partial_i \gamma)^S \right]. \tag{8.59}$$

This, in turn, can be re-expressed in terms of the vortex density $\alpha_i(\mathbf{x}) = \varepsilon_{ijk} \partial_j (\partial_k \gamma(\mathbf{x}))^S$ of (8.18). Since only the singular gradients contribute to $\alpha_i(\mathbf{x})$, we have directly

$$\int d^3x \left[[(\partial_i \gamma)^S]^2 - (\partial_i \gamma)^S \cdot \frac{\partial_i \partial_j}{\nabla^2} (\partial_j \gamma)^S \right] = \int d^3x \, \alpha_i(\mathbf{x}) \frac{1}{-\nabla^2} \alpha_i(\mathbf{x}). \tag{8.60}$$

Formally, we can use again the transverse vortex gauge

$$\partial_i (\partial_i \gamma)^S = 0, \tag{8.61}$$

in which case the mixed terms in (8.58) decouple and

$$E_{\text{int}} = \frac{\sigma}{2} \int d^3x \, [(\partial_i \gamma)^S]^2. \tag{8.62}$$

Although this gauge is incompatible with the underlying discrete lattice structure [only axial gauges like $(\partial_3 \gamma)^S = 0$ are], we can formally use this gauge for the reasons explained in the last section, and see that (8.60) gives

$$E_{\text{int}} = \frac{\sigma}{2} \int d^3x \, [(\partial_i \gamma)^S]^2 = \frac{\sigma}{2} \int d^3x \, \alpha_i(\mathbf{x}) \frac{1}{-\nabla^2} \alpha(\mathbf{x}), \tag{8.63}$$

and hence the correct Biot-Savart interaction energy.

CORRELATION FUNCTIONS

9.1. PATH-INTEGRAL REPRESENTATION

Let us now turn our attention to correlation functions. The order parameter which measures $\gamma(x)$ modulo 2π is $e^{i\gamma(x)}$ and the general correlation function is defined by

$$G^{(n,m)}(x_1, \ldots, x_n; x_1', \ldots, x_m') = \left\langle e^{i\gamma(x_1)} \cdot \ldots \cdot e^{i\gamma(x_n)} e^{-i\gamma(x_1')} \cdot \ldots \cdot e^{-i\gamma(x_m')} \right\rangle$$

$$= \frac{1}{Z'} \prod_x \left[\int_{-\pi}^{\pi} \frac{d\gamma(x)}{2\pi} \right] e^{\beta \Sigma_{x,i} \cos \nabla_i \gamma(x) + i \Sigma_x \gamma(x) Q(x)}$$

$$(9.1a)$$

in the *XY* model, and by

$$G^{(n,m)}(x_1, \ldots, x_n; x_1', \ldots, x_m') = \left\langle e^{i\gamma(x_1)} \cdot \ldots \cdot e^{i\gamma(x_n)} e^{-i\gamma(x_1')} \cdot \ldots \cdot e^{-i\gamma(x_m')} \right\rangle$$

$$= \frac{1}{Z_{VM}} \prod_x \left[\int_{-\pi}^{\pi} \frac{d\gamma(x)}{2\pi} \right] \sum_{\{n_i(x)\}}$$

$$\times e^{-(\beta_V/2)\Sigma_{x,i}(\nabla_i \gamma - 2\pi n_i)^2 + i\Sigma_x \gamma(x) Q(x)} \quad (9.1b)$$

in the Villain model, where we have introduced the abbreviation

$$Q(\mathbf{x}) = \sum_{i=1}^{n} \delta_{\mathbf{x}, \mathbf{x}_i} - \sum_{i=1}^{m} \delta_{\mathbf{x}, \mathbf{x}_i'}. \tag{9.2}$$

This may be interpreted as the "charge density" of a fixed set of external integer point sources to the $\gamma(\mathbf{x})$ field, positive for the phases $e^{i\gamma(\mathbf{x})}$, and negative for $e^{-i\gamma(\mathbf{x})}$.

Since the charges are all integer, the energy is invariant under all vortex gauge transformations[a] with integer $N(\mathbf{x})$

$$\gamma(\mathbf{x}) \to \gamma(\mathbf{x}) + 2\pi N(\mathbf{x}), \quad n_i(\mathbf{x}) \to n_i(\mathbf{x}) + 2\pi \nabla_i N(\mathbf{x}).$$

Let us see how the charges $Q(\mathbf{x})$ modify the high- and low-temperature expansions. For simplicity, we shall discuss explicitly the Villain model. It is trivial to carry over all our results to the XY model by simply replacing β_V, Z_{VM}, $e^{-(1/2\beta_V)b_i^2}$ by β, Z', $I_{b_i}(\beta)$, respectively. The auxiliary magnetic field $b_i(\mathbf{x})$ is introduced, as usual, and $G^{(n,m)}$ becomes

$$G^{(n,m)}(\mathbf{x}_1, \ldots, \mathbf{x}_n; \mathbf{x}_1', \ldots, \mathbf{x}_m')$$

$$= \frac{1}{Z_{VM}} \prod_{\mathbf{x}} \left[\int_{-\pi}^{\pi} \frac{d\gamma(\mathbf{x})}{2\pi} \right] \prod_{\mathbf{x},i} \left[\int_{-\infty}^{\infty} \frac{db_i(\mathbf{x})}{\sqrt{2\pi\beta_V}} \right] \sum_{\{n_i(\mathbf{x})\}}$$

$$\times e^{-(1/2\beta_V)\sum_{\mathbf{x}} b_i^2(\mathbf{x}) + i\sum_{\mathbf{x}}(Q(\mathbf{x}) - \nabla_i b_i(\mathbf{x}))\gamma(\mathbf{x}) - 2\pi i \sum_{\mathbf{x}} b_i(\mathbf{x}) n_i(\mathbf{x})}. \tag{9.3}$$

We now perform the sum over $n_i(\mathbf{x})$ which makes $b_i(\mathbf{x})$ integer. After this, we do the $\gamma(\mathbf{x})$ integrations and find an important new feature: the field lines $b_i(\mathbf{x})$ are no longer closed but satisfy the conservation law

$$\bar{\nabla}_i b_i(\mathbf{x}) = Q(\mathbf{x}). \tag{9.4}$$

Hence, within the magnetic analogy of the lines of superflow $b_i(\mathbf{x})$, the charges $Q(\mathbf{x})$ are *sources* of the magnetic field; they are integer, charged *magnetic monopoles*.

The condition (9.4) has an immediate consequence: summing over $\mathbf{x}$ gives $\sum_{\mathbf{x}} Q(\mathbf{x}) = 0$ so that $G^{(n,m)} \equiv 0$ unless $n = m$ and the monopoles form a neutral gas, i.e., the correlation functions (9.1) conserve monopole charge.

---

[a]Notice that in the presence of external point charges it is not possible to perform the illegal non-integer gauge transformations (8.53) which were useful in calculating the forces between vortex lines.

9.2.   MONOPOLE GAUGE FIELD-TRIPLE GAUGE THEORY

The presence of magnetic sources drastically changes the ensuing procedure in deriving the vortex-line representation. We can no longer write $b_i(\mathbf{x})$ as a curl of a vector potential alone but have to add a term whose divergence gives $Q(\mathbf{x})$. Let us call this term $m_i(\mathbf{x})$, i.e., let $m_i(\mathbf{x})$ be a fixed integer-valued field which satisfies

$$\bar{\nabla}_i m_i(\mathbf{x}) = Q(\mathbf{x}). \tag{9.5}$$

Note that any $m_i(\mathbf{x})$ which fulfills this condition is equally acceptable. The field $m_i(\mathbf{x})$ is obviously determined up to an arbitrary additional integer-valued curl, i.e., up to a transformation

$$m_i(\mathbf{x}) \to m_i(\mathbf{x}) + \varepsilon_{ijk}\bar{\nabla}_j M_k(\mathbf{x} - \mathbf{k}). \tag{9.6}$$

We shall call this result the *monopole gauge transformation* and refer to $m_i(\mathbf{x})$ as the *monopole gauge field*. A particular $m_i(\mathbf{x})$ can be pictured geometrically by a certain string of arrows connecting pairs of opposite charges (see Fig. 9.1). If we imagine magnetic monopoles as being realized in a laboratory via a limiting construction of infinitely thin coils, these strings are the coils which lead the magnetic field to an oppositely charged monopole (the so-called Dirac strings).

For instance, for a pair of monopoles at $\mathbf{x}_1 = 0$ and $\mathbf{x}_2 = \mathbf{X}_2$ on the 2-axis

$$Q(\mathbf{x}) = \delta_{x_1,0}\,\delta_{x_2,X_2} - \delta_{x_1,0}\,\delta_{x_2,0}, \tag{9.7a}$$

we may choose the string

$$m_i(\mathbf{x}) = \delta_{i2}(\delta_{x_1,0}\,\Theta_{x_2-X_2} - \delta_{x_1,0}\,\Theta_{x_2}), \tag{9.7b}$$

where

$$\Theta_x = \begin{cases} 1 \\ 0 \end{cases} \quad \text{for} \quad \begin{cases} x \geq 0 \\ x < 0 \end{cases} \tag{9.8}$$

is the lattice version of Heaviside's step function. In general we can set up $m_i(\mathbf{x})$ according to the following procedure. Suppose $G^{(m,n)}$ is an arbitrary non-zero correlation function. Since $Q(\mathbf{x})$ corresponds to a

neutral monopole gas, we can attach to each monopole a string and connect it to an imagined anti-monopole at one particular corner of the box, say (L, L, L) (see Fig. 9.2). Due to charge neutrality, the sum of all charges at this corner is zero. Hence we may imagine each monopole in the box to be connected with an equal and opposite counter charge at the corner (L, L, L) and, in this way, we have decomposed the system uniquely into a gas of monopole pairs. We can now construct a specific string connecting each pair.

FIG. 9.1. Two possible strings of "magnetic flux" connecting a monopole at X with an antimonopole at X' and satisfying (9.5). For simplicity we plot only a planar configuration.
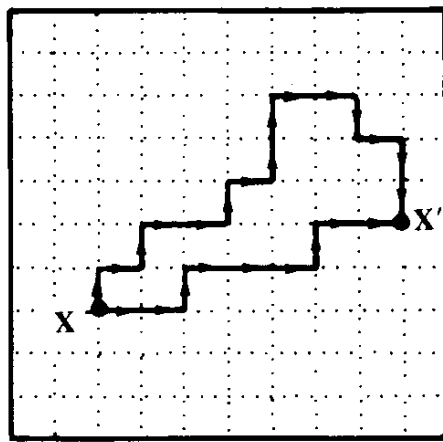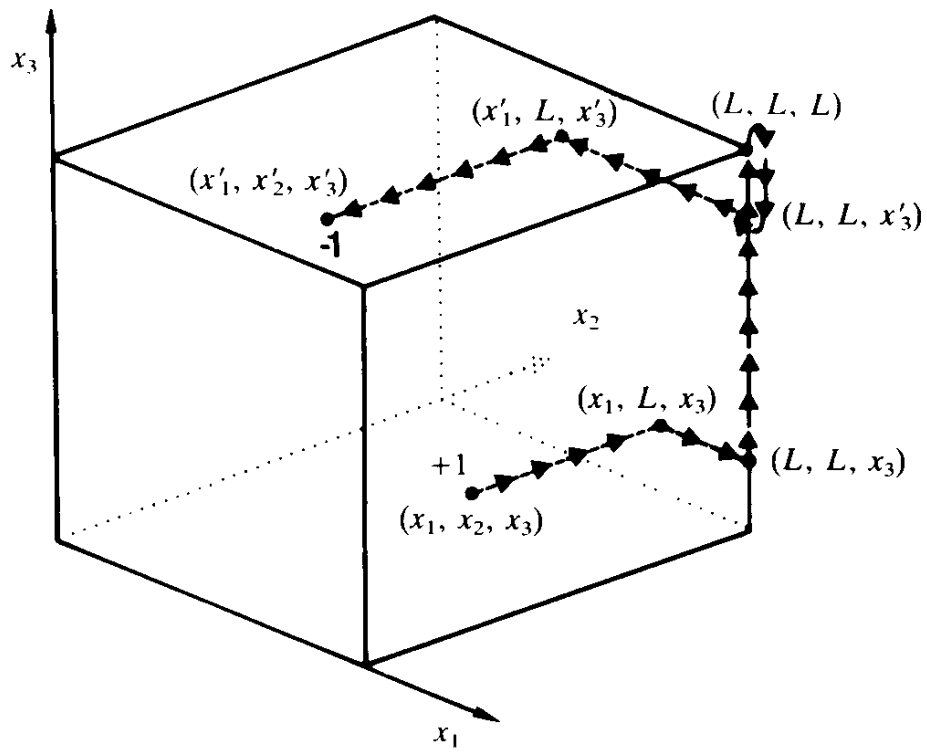
FIG. 9.2. Instead of connecting monopole and antimonopole pairs directly by a string we can place for each magnetic charge an oppositely charged partner at the corner (L, L, L) (say) of the box, and construct a certain standard string from each charges to the corner [using the gauge-fixing procedure of Eqs. (9.9)–(9.12)].

For this, we first apply the operation

$$m_2^{(0)}(x_1, x_2, x_3) = \frac{1}{\overline{\nabla}_2} \delta_{x_1, L} \, \delta_{x_2, L} \, \delta_{x_3, L},$$ (9.9)

where $1/\overline{\nabla}_2$ is the sum

$$\frac{1}{\overline{\nabla}_2} f(\mathbf{x}) \equiv \sum_{x_2' = 1}^{x_2} \delta(x_1, x_2', x_3).$$ (9.10)

This attaches a string to the corner (L, L, L) and carries it to the point (L, x_2, L). We then choose

$$m_1^{(1)}(x_1, x_2, x_3) = \frac{1}{\overline{\nabla}_1} \overline{\nabla}_2 m_2^{(0)}(x_1, x_2, x_3),$$ (9.11)

which carries a string further to (x_1, x_2, L). Finally, we arrive at

$$m_3(x_1, x_2, x_3) = \frac{1}{\overline{\nabla}_3} \overline{\nabla}_1 m_1^{(1)}(x_1, x_2, x_3),$$ (9.12)

which carries the string to the point $\mathbf{x}$.

If $m_i(\mathbf{x})$ is an arbitrary string emerging from the monopole running to the corner (L, L, L), we can always deform it into our standard string by means of a gauge transformation,

$$m_i(\mathbf{x}) \rightarrow m_i(\mathbf{x}) + \varepsilon_{ijk} \overline{\nabla}_j M_k(\mathbf{x} - \mathbf{k}).$$ (9.13)

That this is true follows directly from the fact that $\varepsilon_{ijk} \overline{\nabla}_j M_k(\mathbf{x} - \mathbf{k})$ is divergenceless and can be pictured as a set of *closed loops* of integer-valued strings. It is obvious that by adding closed loops, a fixed string can be deformed into an arbitrary shape (recall Ampère's construction of arbitrary current loops from infinitesimal loops in magnetostatics). Employing an arbitrary set of fixed strings, the magnetic field can be written as

$$b_i(\mathbf{x}) = \varepsilon_{ijk} \overline{\nabla}_j a_k(\mathbf{x} - \mathbf{k}) + m_i(\mathbf{x}).$$ (9.14)

The correlation function is then given by

$$G^{(n,n)}(\mathbf{x}_1, \ldots, \mathbf{x}_n; \mathbf{x}'_1, \ldots, x'_n)$$

$$= Z_{VM}^{-1} \frac{1}{(\sqrt{2\pi\beta_V})^{DN}} \sum_{\{a_i(\mathbf{x})\}} \delta_{a_3,0} \, e^{-(1/2\beta_V)\Sigma_{\mathbf{x}}(\bar{\nabla} \times \mathbf{a} + \mathbf{m})^2}. \tag{9.15}$$

We can now introduce the vortex lines as integer-valued non-backtracking closed lines $\ell_i(\mathbf{x})$ which make the vector potential a_k continuous. Thus,

$$G^{(n,n)}(\mathbf{x}_1, \ldots, \mathbf{x}_n; \mathbf{x}'_1, \ldots, \mathbf{x}'_n)$$

$$= Z_{VM}^{-1} \frac{1}{(\sqrt{2\pi\beta_V})^{DN}} \prod_{\mathbf{x}} \left[\int_{-\infty}^{\infty} dA_1 \, dA_2 \right]$$

$$\times \sum_{\{\ell_i(\mathbf{x})\}} \delta_{\bar{\nabla}_i \ell_i(\mathbf{x}),0} \, e^{-(1/2\beta_V)\Sigma_{\mathbf{x}}(\bar{\nabla} \times \mathbf{A} + \mathbf{m})^2 + 2\pi i \Sigma_{\mathbf{x}} A_i \ell_i}. \tag{9.16}$$

Since ℓ_i = integer this expression is monopole gauge invariant under

$$m_i(\mathbf{x}) \to m_i(\mathbf{x}) + \varepsilon_{ijk} \bar{\nabla}_j M_k(\mathbf{x} - \mathbf{k}), \quad A_i(\mathbf{x}) \to A_i(\mathbf{x}) + M_i(\mathbf{x}). \tag{9.17}$$

Notice that if we express ℓ_i in terms of the vortex-gauge field n_i, the present theory is a triple gauge theory, invariant under (6.48), (8.9) and (9.17).

9.3. OTHER REPRESENTATIONS OF CORRELATION FUNCTIONS IN THE VILLAIN MODEL

Up to this point, all formulas could be carried over directly to the XY model with the simple replacement $\beta_V \to \beta$, $Z_{VM} \to Z'$, $e^{-(1/2\beta_V)b_i^2} \to I_{b_i}(\beta)$. The Villain model has the advantage that its correlation functions allow for a few alternative representations which we are now going to discuss. They depend crucially on the quadratic nature of the field energy and are useful for a low temperature analysis of correlations.

Writing the exponent (9.16) as

$$-\frac{1}{2\beta_V} \sum_{\mathbf{x}} (\bar{\nabla} \times \mathbf{A})^2 - \frac{1}{2\beta_V} \sum_{\mathbf{x}} m_i^2(\mathbf{x})$$

$$+ 2\pi i \sum_{\mathbf{x}} A_k(\mathbf{x})(\ell_k(\mathbf{x}) + \frac{1}{2\pi\beta_V} i\varepsilon_{kij}\nabla_i m_j(\mathbf{x} + \mathbf{k}))$$

and going over to the transverse gauge $\nabla_i A_i \equiv 0$, the A_i field can be integrated with the result [compare (7.39)].

$$G^{(n,n)}(\mathbf{x}_1, \ldots, \mathbf{x}_n; \mathbf{x}_1', \ldots, \mathbf{x}_n')$$

$$= Z_{VM}^{-1} \frac{1}{(\sqrt{2\pi\beta_V})^N} \det(-\bar{\nabla} \cdot \nabla)^{-1/2} \sum_{\{\ell_i(\mathbf{x})\}} \delta_{\bar{\nabla}_i \ell_i, 0} \; e^{-(\beta_V/2)4\pi^2 \Sigma_\mathbf{x} \ell_i(\mathbf{x})(1/-\bar{\nabla} \cdot \nabla)\ell_i(\mathbf{x})}$$

$$\times \; e^{-(1/2\beta_V)\Sigma_\mathbf{x}(m_i^2 - (\nabla \times \mathbf{m})_i(1/\bar{\nabla} \cdot \nabla)(\nabla \times \mathbf{m})_i)} \; e^{-2\pi i \Sigma_\mathbf{x}(\nabla \times \mathbf{m})_i(1/-\bar{\nabla} \cdot \nabla)\ell_i}, \qquad (9.18)$$

where $(\nabla \times \mathbf{m})_i = \varepsilon_{ijk}\nabla_j m_k(\mathbf{x} + \mathbf{i})$, just as in (8.3).

The second exponential can be simplified by observing that

$$\sum_\mathbf{x} \left(m_i^2(\mathbf{x}) - \varepsilon_{ijk}\nabla_j m_k(\mathbf{x} + \mathbf{i})\frac{1}{-\bar{\nabla} \cdot \nabla}\varepsilon_{ij'k'}\nabla_{j'}m_{k'}(\mathbf{x} + \mathbf{i})\right)$$

$$= \sum_\mathbf{x} \left(m_i^2(\mathbf{x}) - \nabla_j m_k(\mathbf{x})\frac{1}{-\bar{\nabla} \cdot \nabla}\nabla_j m_k(\mathbf{x}) + \nabla_{k'}m_k(\mathbf{x})\frac{1}{-\bar{\nabla} \cdot \nabla}\nabla_k m_{k'}(\mathbf{x})\right)$$

$$= \sum_\mathbf{x} \bar{\nabla}_k m_k(\mathbf{x})\frac{1}{-\bar{\nabla} \cdot \nabla}\bar{\nabla}_{k'}m_{k'}(\mathbf{x}) = \sum_\mathbf{x} Q(\mathbf{x})\frac{1}{-\bar{\nabla} \cdot \nabla}Q(\mathbf{x}). \qquad (9.19)$$

This is manifestly invariant under the monopole gauge transformations. Also the third exponential in (9.18) has this invariance even though this is not immediately obvious. Under (9.17), it changes by a factor

$$e^{-2\pi i \Sigma_\mathbf{x}\varepsilon_{ijk}\varepsilon_{klm}\nabla_j\bar{\nabla}_l M_m(\mathbf{x} + \mathbf{i} - \mathbf{m})(1/-\bar{\nabla} \cdot \nabla)\ell_i(\mathbf{x})}$$

$$= e^{-2\pi i \Sigma_\mathbf{x}[\nabla_j\bar{\nabla}_i M_j(\mathbf{x} + \mathbf{i} - \mathbf{j})(1/-\bar{\nabla} \cdot \nabla)\ell_i(\mathbf{x}) - \nabla \cdot \bar{\nabla} M_i(\mathbf{x})(1/-\bar{\nabla} \cdot \nabla)\ell_i(\mathbf{x})]}. \qquad (9.20)$$

Using $\nabla_j\bar{\nabla}_i M_j(\mathbf{x} + \mathbf{i} - \mathbf{j}) = \bar{\nabla}_j\nabla_i M_j(\mathbf{x})$ and performing a partial integration, the first term in parentheses vanishes [due to $\bar{\nabla}_i \ell_i(\mathbf{x}) = 0$]. The second term leads to a phase $e^{-2\pi i \Sigma_\mathbf{x} M_i(\mathbf{x})\ell_i(\mathbf{x})}$, which, however, is just unity since M_i, ℓ_i are integers.

It is possible to bring the interaction factor in (9.18) to a more symmetric form by expressing $\ell_i(\mathbf{x})$ in terms of the vortex-gauge field $n_i(\mathbf{x})$ [using (8.3)] as

$$\ell_i(\mathbf{x}) = (\nabla \times \mathbf{n})_i = \varepsilon_{ijk}\nabla_j n_k(\mathbf{x} + \mathbf{i}).$$

The interaction factor now reads [cf. (8.43)]

$$\exp\left\{-4\pi^2\frac{\beta_V}{2}\sum_\mathbf{x}(\nabla \times \mathbf{n})_i\frac{1}{-\bar{\nabla} \cdot \nabla}(\nabla \times \mathbf{n})_i - \frac{1}{2\beta_V}\sum_\mathbf{x}(\bar{\nabla} \cdot \mathbf{m})\frac{1}{-\bar{\nabla} \cdot \nabla}(\bar{\nabla} \cdot \mathbf{m})\right.$$

$$\left. - 2\pi i \sum_\mathbf{x}(\nabla \times \mathbf{m})_i\frac{1}{-\bar{\nabla} \cdot \nabla}(\nabla \times \mathbf{n})_i\right\}, \qquad (9.21)$$

which displays manifestly vortex- and monopole-gauge invariances.

There exists yet another form for the third interaction term, which is dual to the third term in (9.18). In order to derive it we perform a partial integration so that it becomes equal to the third term in (9.21)

$$e^{-2\pi i \sum_x \epsilon_{ijk} \nabla_j m_k(x+i)(1/-\bar{\nabla}\cdot\nabla)\epsilon_{iln} \nabla_l n_n(x+i)} = e^{-2\pi i \sum_x m_k(x) n_k(x)} e^{2\pi i \sum_x \nabla_n m_n(x)(1/-\bar{\nabla}\cdot\nabla)\nabla_k n_k(x)}.$$

Since m_k, n_k are integers, the first factor is just unity. The second can be partially integrated to

$$e^{2\pi i \sum_x \bar{\nabla}_k m_k(x)(1/-\bar{\nabla}\cdot\nabla)\bar{\nabla}_n n_n(x)} = e^{2\pi i \sum_x Q(x)(1/-\bar{\nabla}\cdot\nabla)\bar{\nabla}\cdot\mathbf{n}(x)}, \qquad (9.22a)$$

which is the desired dual form.

In contrast to the third term in (9.18), which exhibited manifest vortex-gauge invariance, and produced a trivial unit phase under monopole-gauge transformations, this expression shows manifest monopole gauge invariance, and the vortex-gauge transformations $n_i(\mathbf{x}) \rightarrow n_i(\mathbf{x}) + \nabla_i N(\mathbf{x})$ produce a trivial unit phase

$$e^{2\pi i \sum_x Q(x)(1/-\bar{\nabla}\cdot\nabla)\bar{\nabla}\cdot\nabla N(\mathbf{x})} = e^{-2\pi i \sum Q(x)N(x)} = 1.$$

In order to interprete the interaction factor (9.22) geometrically we introduce a quantity,

$$\Omega(\mathbf{x}) = 4\pi \frac{1}{-\bar{\nabla}\cdot\nabla} \bar{\nabla}\cdot\mathbf{n}(\mathbf{x}) \qquad (9.23)$$

and write (9.22a) as

$$e^{(1/2)i \sum_x Q(x)\Omega(x)}. \qquad (9.22b)$$

We now convince ourselves that the quantity $\Omega(\mathbf{x})$ is nothing but the lattice version of the solid angle $\Omega(\mathbf{x})$ of Eq. (1.157) where the vortex loop $\ell_i(\mathbf{x})$ is seen from the point $\mathbf{x}$. Indeed, for long distances, $-1/\bar{\nabla}\cdot\nabla \sim 1/4\pi R$ and $\bar{\nabla}\cdot\mathbf{n} \sim \nabla\cdot\mathbf{n}$. Now, $n_i(\mathbf{x})$ is the description of the jumping surface, whose continuous form is

$$n_i(\mathbf{x}) \sim a\delta_i(S),$$

where a is the infinitesimal lattice spacing, so that

$$\bar{\nabla} \cdot \mathbf{n} \sim a^2 \partial_i \delta_i(S) \tag{9.24}$$

and (9.23) takes the limiting form

$$\Omega(\mathbf{x}) \rightarrow \partial_i \int d^3x' \frac{1}{R} \delta_i(S) = \partial_i \int dS'_i \frac{1}{R} = -\int dS'_i \partial'_i \frac{1}{R} = \int dS'_i R_i/R^3, \tag{9.25}$$

which is the same as (1.157). Thus the expression $(1/2)\Omega(\mathbf{x})$ is the magnetic potential caused by the vortex lines $\ell_i(\mathbf{x})$ at the position of the monopole, $\mathbf{x}$. The vortex-gauge transformation can change $\Omega(\mathbf{x})$ by at most multiples of 4π and this leaves the interaction (9.22b) invariant.

For symmetry reasons it may be useful to define a quantity which is dual to (9.23),

$$\Omega_i'''(\mathbf{x}) \equiv 2\pi \frac{1}{-\bar{\nabla} \cdot \nabla} (\nabla \times \mathbf{m})_i. \tag{9.26}$$

The interaction between monopoles and vortices takes the form

$$e^{(i/2)\Sigma_x Q(\mathbf{x})\Omega(\mathbf{x})} = e^{-i\Sigma_x \Omega_i'''(\mathbf{x})\ell_i(\mathbf{x})}. \tag{9.22c}$$

The proof follows by rewriting [see the equation above (9.22a)]

$$e^{(i/2)\Sigma_x Q(\mathbf{x})\Omega(\mathbf{x})} = e^{2\pi i \Sigma_x \bar{\nabla}_j m_i(\mathbf{x})(1/-\bar{\nabla}\cdot\nabla)\bar{\nabla}_n n_n(\mathbf{x})} = e^{2\pi i \Sigma_x (\nabla \times \mathbf{m})\cdot(1/-\bar{\nabla}\cdot\nabla)(\nabla \times \mathbf{n})} = e^{i\Sigma_x \Omega_i'''(\mathbf{x})\ell_i(\mathbf{x})}.$$

Let us close this section by remarking that the same results could have been derived by following the procedure outlined in Section 8.5. Then formula (9.1a) for the correlation function involves a sum not over all unconstrained jump numbers $n_i(\mathbf{x})$ but only over those with a fixed vortex gauge (say $n_3(\mathbf{x}) = 0$). This is compensated for by the fields $\gamma(\mathbf{x})$ running from $-\infty$ to ∞ instead of $-\pi, \pi$ [recall (8.31)]. Then the exponent can be written as

$$-\frac{\beta_V}{2}\sum_x \gamma(\mathbf{x})(-\bar{\nabla} \cdot \nabla)\gamma(\mathbf{x}) - \frac{\beta_V}{2} 4\pi^2 \sum_x n_i^2(\mathbf{x}) + i\sum_x \gamma(\mathbf{x})(Q(\mathbf{x}) - 2\pi i \beta_V \bar{\nabla}_i n_i),$$

so that integration over the γ fluctuations gives

$$G^{(n,n)}(\mathbf{x}_1, \ldots, \mathbf{x}_n; \mathbf{x}'_1, \ldots, \mathbf{x}'_n)$$

$$= Z_{VM}^{-1} \frac{1}{(\sqrt{2\pi\beta_V})^N} \det(-\bar{\nabla} \cdot \nabla)^{-1/2} e^{-(1/2\beta_V)\Sigma_x Q(x)(1/-\bar{\nabla}\cdot\nabla)Q(x)}$$

$$\times \sum_{\{n_i(\mathbf{x})\}} \delta_{n_3,0} \, e^{-(\beta_V/2)4\pi^2\Sigma_x(n_i^2 - \bar{\nabla}_i n_i(1/-\bar{\nabla}\cdot\nabla)\bar{\nabla}_i n_i) - 2\pi i \Sigma_x Q(x)(1/-\bar{\nabla}\cdot\nabla)\bar{\nabla}_i n_i}, \quad (9.27)$$

which is once more the same expression as (9.18) except for a slightly different arrangement of the interactions terms: the first and the last terms are the same as (9.19), (9.22a). The second term coincides with the first term in (9.18) after the calculation [cf. (8.46)]

$$\sum_x \ell_i \frac{1}{-\bar{\nabla} \cdot \nabla} \ell_i$$

$$= \sum_x (\bar{\nabla} \times \mathbf{n})_i \frac{1}{-\bar{\nabla} \cdot \nabla} (\bar{\nabla} \times \mathbf{n})_i$$

$$= \sum_x \left[\bar{\nabla}_i n_k(\mathbf{x} - \mathbf{k}) \frac{1}{-\bar{\nabla} \cdot \nabla} \bar{\nabla}_i n_k(\mathbf{x} - \mathbf{k}) - \bar{\nabla}_i n_k(\mathbf{x} - \mathbf{k}) \frac{1}{-\bar{\nabla} \cdot \nabla} \bar{\nabla}_k n_i(\mathbf{x} - \mathbf{i}) \right]$$

$$= \sum_x \left(n_k^2 - \bar{\nabla}_i n_i(\mathbf{x}) \frac{1}{-\bar{\nabla} \cdot \nabla} \bar{\nabla}_k n_k(\mathbf{x}) \right).$$

The expression (9.27) is easy to interprete physically. The first term is just the Boltzmann factor for the set of monopoles and antimonopoles at $\mathbf{x}_1, \ldots, \mathbf{x}_n$ and $\mathbf{x}'_1, \ldots, \mathbf{x}'_n$, respectively. This Boltzmann factor is multiplied by the partition function for an ensemble of vortex lines. They interact with each other via Biot-Savart-like forces, and with the monopoles via the standard magnetic energy. A similar interpretation holds for (9.18).

It is a gratefying property of the Villain model that, just as is the case with the partition function Z_{VM}, the correlation functions also factorize. If we use the factorization of Z_{VM} in the low temperature limit (7.40), (7.41), we can write the correlation function in the factorized form,

$$G^{(n,n)}(\mathbf{x}_1, \ldots, \mathbf{x}_n; \mathbf{x}'_1, \ldots, \mathbf{x}'_n)$$

$$= G_s^{(n,n)}(\mathbf{x}_1, \ldots, \mathbf{x}_n; \mathbf{x}'_1, \ldots, \mathbf{x}'_n) \, G_v^{(n,n)}(\mathbf{x}_1, \ldots, \mathbf{x}_n; \mathbf{x}'_1, \ldots, \mathbf{x}'_n),$$

$$(9.28)$$

where

$$G_s^{(n,n)}(\mathbf{x}_1, \ldots, \mathbf{x}_n; \mathbf{x}_1', \ldots, \mathbf{x}_n') = e^{-(1/2\beta_V)\sum_x Q(\mathbf{x})(1/-\bar{\nabla}\cdot\nabla)Q(\mathbf{x})} \qquad (9.29)$$

and

$$G_v^{(n,n)}(\mathbf{x}_1, \ldots, \mathbf{x}_n; \mathbf{x}_1', \ldots, \mathbf{x}_n')$$

$$= Z_v^{-1} \sum_{\{\ell_i(\mathbf{x})\}} \delta_{\bar{\nabla}_i \ell_i, 0} \, e^{-(\beta_V/2)4\pi^2 \sum_x \ell_i(\mathbf{x})(1/-\bar{\nabla}\cdot\nabla)\ell_i(\mathbf{x}) + (i/2)\sum_x Q(\mathbf{x})\Omega(\mathbf{x})}, \qquad (9.30)$$

Z_v being the partition function of the vortex loops which was given in (7.41). The subscript s stands for "spin-wave" since this correlation function accounts for the pure $\gamma(\mathbf{x})$ fluctuations without any vortex contributions. Of course the last term in (9.30) can be rewritten in any of the alternative forms (9.22a–c).

9.4. HIGH TEMPERATURE EXPANSION FOR THE TWO-POINT CORRELATION FUNCTION AND SUSCEPTIBILITY

We shall now use formula (9.3) and calculate the two-point correlation function at high temperatures. The integral over the connected part of the two-point correlation function is measurable directly as the *susceptibility* of the system

$$\chi(\beta) \equiv \frac{\beta}{2} \sum_{\mathbf{X}} G_c(\mathbf{X}, \mathbf{X}'). \qquad (9.31)$$

This name derives from the interpretation of the XY model as a system of planar spins. One imagines $\gamma(\mathbf{x})$ to be the aziumthal angles of spins attached to the sites of the lattice. They carry a magnetic moment. An external magnetic field would tend to orient the spins in its direction with an interaction energy given by

$$E = \sum_{\mathbf{x}} h \cos \gamma(\mathbf{x}).$$

Thus, the partition function of the spins in the external field reads

$$Z(h) = \prod_{\mathbf{x},i} \left[\int_{-\pi}^{\pi} \frac{d\gamma(\mathbf{x})}{2\pi} \right] e^{\beta \Sigma_{\mathbf{x},i} \cos \nabla_i \gamma + \beta h \Sigma_{\mathbf{x}} \cos \gamma(\mathbf{x})} \qquad (9.32)$$

[recall (5.11) and the discussion after it]. The magnetization u is defined as the expectation value [recall (5.16)]

$$u = \frac{1}{\beta} \frac{1}{N} \frac{\partial}{\partial h} \log Z(h) \equiv \langle \cos \gamma(\mathbf{x}) \rangle. \qquad (9.33)$$

The susceptibility is defined as the response of the magnetization to a change in the magnetic field,

$$\chi(\beta) = \frac{\partial}{\partial h} u = \frac{1}{\beta} \frac{1}{N} \frac{\partial^2}{\partial h^2} \log Z(h) = \beta \sum_{\mathbf{X}} (\langle \cos \gamma(\mathbf{X}) \cos \gamma(\mathbf{X}') \rangle - \langle \cos \gamma(\mathbf{X}) \rangle^2). \qquad (9.34)$$

Decomposing the cosines into exponentials, this becomes

$$\chi(\beta) = \frac{\beta}{2} \sum_{\mathbf{X}} (\langle e^{i\gamma(\mathbf{X})} e^{-i\gamma(\mathbf{X}')} \rangle - \langle e^{i\gamma(\mathbf{X})} \rangle^2) \qquad (9.35)$$

in agreement with the definition (9.32).

In writing down (9.36) we have used the fact that $\langle e^{i\gamma(\mathbf{X})} e^{-i\gamma(\mathbf{X}')} \rangle$ is a real function so that it is the same as $\langle e^{-i\gamma(\mathbf{X})} e^{i\gamma(\mathbf{X}')} \rangle$. We have also discarded the correlations $\langle e^{i\gamma(\mathbf{X})} e^{i\gamma(\mathbf{X}')} \rangle$, $\langle e^{-i\gamma(\mathbf{X})} e^{-i\gamma(\mathbf{X})} \rangle$ since two equally charged monopoles have field lines $b_i(\mathbf{x})$ extending to infinity [or to the point (L, L, L) in a finite box]. Thus they are accompanied by a zero [or a very small] Boltzmann factor and do not contribute (only for very small systems can they become significant). In order to establish contact with results given in the literature, we shall find it convenient to calculate directly the susceptibility. The graphical procedure to be followed will make it trivial to pick out the contributions to the correlation function at specific distances $\mathbf{X} - \mathbf{X}'$, if desired.

At high temperatures, the magnetization u vanishes and we can drop the suffix c in (9.31). The correlation function $G(\mathbf{X}, \mathbf{X}')$ becomes a sum over all oriented non-self-backtracking strings connecting the monopole at $\mathbf{X}$ with that at $\mathbf{X}'$ plus a sum over all closed loop contributions. This sum is to be divided by the partition function Z', for normalization. In

the Villain model the formula to be used is (9.15), which reads for the two-point function

$$G(\mathbf{X}, \mathbf{X}') = Z_{VM}^{-1} \frac{1}{(\sqrt{2\pi\beta_V})^{DN}} \sum_{\{a_i(\mathbf{x})\}} \delta_{a_3,0} \, e^{-(1/2\beta_V)\Sigma_\mathbf{x}(\bar{\nabla} \times \mathbf{a} + \mathbf{m})^2}, \qquad (9.36)$$

where $m_i(\mathbf{x})$ is the string field connecting the points $\mathbf{X}$ and $\mathbf{X}'$ (see Fig. 9.1), and satisfies

$$\bar{\nabla}_i m_i(\mathbf{x}) = \delta_{\mathbf{x},\mathbf{X}} - \delta_{\mathbf{x},\mathbf{X}'}.$$

The sum over the integer valued field a_i amounts to a sum over defect gauge transformations

$$m_i \rightarrow m_i + (\bar{\nabla} \times \mathbf{a})_i.$$

Graphically, they correspond to
1. changes in shape of the string, resulting from the insertions of closed loops which cancel part of the string via backtracking;
2. additional disconnected closed loops.

The disconnected closed loops are the same as those appearing in the strong-coupling series of the partition function itself,

$$Z_{VM} = \frac{1}{(\sqrt{2\pi\beta_V})^{DN}} \sum_{\{a_i(\mathbf{x})\}} \delta_{a_3,0} \, e^{-(1/2\beta_V)\Sigma_\mathbf{x}(\bar{\nabla} \times \mathbf{a})^2}.$$

In the XY model, the same formula holds after the replacements

$$\beta_V, \; Z_{VM}, \; e^{-(1/2\beta_V)b_i^2(\mathbf{x})} \rightarrow \beta, \; Z_{XY}', \; \frac{I_{b_i(\mathbf{x})}(\beta)}{I_0(\beta)}. \qquad (9.37)$$

It will be useful to define quantities in which the normalization factor is not yet divided out. Thus we define the sum

$$\bar{G}(\mathbf{X}, \mathbf{X}') \equiv \sum_{\{b_i(\mathbf{x})\}} \delta_{\bar{\nabla}_i b_i, 0} \prod_{\mathbf{x},i} \frac{I_{b_i(\mathbf{x})}(\beta)}{I_0(\beta)}, \qquad (9.38a)$$

to be divided by the "modified partition function", $Z'/[I_0(\beta)]^{Dn}$, which has a high temperature expansion of the form [compare with (4.19) and (4.46) for the true partition function]

$$\tilde{Z} = \frac{Z'}{(I_0(\beta))^{DN}}$$

$$= 1 + \xi_4 \left(\frac{I_1}{I_0}\right)^4 + \xi_6 \left(\frac{I_1}{I_0}\right)^6 + \xi_8^1 \left(\frac{I_1}{I_0}\right)^8 + \xi_8^2 \left(\frac{I_1}{I_0}\right)^6 \left(\frac{I_2}{I_0}\right) + \ldots \quad (9.38b)$$

Then the correlation function is given by

$$G(\mathbf{X}, \mathbf{X}') = \frac{1}{\tilde{Z}} \tilde{G}(\mathbf{X}, \mathbf{X}'). \quad (9.39)$$

and the susceptibility by the sum (9.31).

We will now count the different diagrams contributing to the susceptibility $\chi(\beta)$ according to their loop length.

The lowest non-trivial term is a line element across a single link

$$2D \quad \times\!\!-\!\!-\!\!-\!\!-\!\!\times \quad (9.40)$$

It can appear with $2D$ orientations.

Since $\tilde{Z}$ starts out with $1 + ND(D - 1)(I_1/I_0)^4$, division by $\tilde{Z}$ can be ignored to this order, and we find the lowest non trivial contribution to the susceptibility,

$$\chi(\beta) = \frac{\beta}{2} \left\{ 2D \frac{I_1(\beta)}{I_0(\beta)} \right\}. \quad (9.41)$$

The second order contribution is given by a line element across 2 links, of which there are two types:

$$N2D \quad \times\!\!-\!\!-\!\!\bullet\!\!-\!\!-\!\!\times$$

$$N2D(2D - 2) \quad \begin{array}{c} \times\!\!-\!\!-\!\!-\!\!-\!\!\bullet \\ | \\ | \\ \times \end{array} \quad (9.42)$$

Thus there are $N2D(2D - 1)$ diagrams which do not backtrack, so that

$$\tilde{G}^{(2)} = 2D(2D - 1)\left(\frac{I_1}{I_0}\right)^2 = 2\left(\binom{D}{1} + 4\binom{D}{2}\right)\left(\frac{I_1}{I_0}\right)^2. \quad (9.43)$$

The third order contribution contains, in addition to (9.42), the $(2D - 1)$ possibilities of adding a third line element which does not backtrack,

$$\bar{G}^{(3)} = 2D(2D - 1)^2 \left(\frac{I_1}{I_0}\right)^3 .$$

(9.44)

The forth order contribution contains one more factor $2D - 1$ but one has to subtract the $2D(2D - 2)$ possibilities that the fourth line element reaches the starting point and forms a closed loop:

$$\bar{G}^{(4)} = 2D[(2D - 1)^3 - (2D - 2)] \left(\frac{I_1}{I_0}\right)^4 .$$

(9.45)

Thus, up to this order, we find for the susceptibility

$$\chi(\beta) = \frac{\beta}{2} \left\{ 2D\frac{I_1}{I_0} + 2D(2D - 1)\left(\frac{I_1}{I_0}\right)^2 + 2D(2D - 1)^2\left(\frac{I_1}{I_0}\right)^3 \right.$$

$$\left. + 2D[(2D - 1)^3 - (2D - 2)]\left(\frac{I_1}{I_0}\right)^4 + \ldots \right\} .$$

(9.46)

In the Villain model, β and I_1/I_0 are replaced by β_V and $e^{-1/2\beta_V}$.

Within the curly brackets we may use the expansion $I_1/I_0 = \beta/2 - (1/2)(\beta/2)^3 + \ldots$ [see Table 4.8] and can immediately write down the expansion of $\chi(\beta)$ in powers of $\beta/2$ up to $(\beta/2)^5$, for all dimensions:

$$\chi(\beta) = \frac{\beta}{2} \left\{ 2D\left(\frac{\beta}{2}\right) + 2D(2D - 1)\left(\frac{\beta}{2}\right)^2 + [2D(2D - 1)^2 - D] \right.$$

$$\left. \times \left(\frac{\beta}{2}\right)^3 + 2D[(2D - 1)^3 - (2D - 2) - (2D - 1)]\left(\frac{\beta}{2}\right)^4 + \ldots \right\} .$$

(9.47)

The coefficients of this expansion are displayed in Table 9.1 (column sc). We have also given the higher order results and the corresponding numbers for different lattices, as they are available in the literature.

For higher order, the counting procedure becomes rapidly cumbersome due to the appearance of disconnected diagrams and the necessity of avoiding self-backtracking. The most convenient way of eliminating such forbidden configurations is to find first all *self-avoiding* graphs which are automatically non-self-backtracking. To these we add all disconnected self-avoiding graphs. Finally, we add all allowed graphs which have inter-

TABLE 9.1. High temperature expansion of the susceptibility for the $D = 3$ and $D = 2$ XY model for various lattices. The columns show the coefficients a_n:

$$\chi = \left(\frac{\beta}{2}\right) \sum_{n=1}^{\infty} a_n \left(\frac{\beta}{2}\right)^n.$$

In general, $a_0 = 1$, $a_1 = q$ = coordination number, $a_2 = q(q - 1)$.

n	$D = 3$			$D = 2$	
	fcc	bcc	sc	sc	triang
1	12	8	6	4	6
2	132	56	30	12	30
3	1398	388	147	34	135
4	14496	2592	696	88	570
5	148294	$17230\frac{2}{3}$	3275	$219\frac{1}{3}$	2306
6	1503063	$112843\frac{1}{3}$	$15171\frac{1}{2}$	529	$9041\frac{1}{2}$
7	$15132379\frac{1}{4}$	$736900\frac{1}{6}$	$70009\frac{1}{8}$	$1244\frac{5}{12}$	$34582\frac{1}{8}$
8	$151568185\frac{1}{6}$	$4773834\frac{1}{3}$	$320513\frac{1}{4}$	$2868\frac{1}{2}$	$129634\frac{1}{6}$
9				$6489\frac{8}{9}$	$477988\frac{1}{30}$
10				$14491\frac{2}{3}$	1138252.39166

sections or multiple lines. For simplicity, we shall illustrate the counting only for the special case of 2 dimensions.

To fifth order, there are 2×142 open-ended self-avoiding graphs with two orientations. To see this we take the 100 open-ended unoriented graphs of length four and extend each of them by one more link in three ways. This gives 150. There are, however, 8 graphs of the form where the extension violates the self-avoiding condition. By including the orientation factor 2 we arrive at the number 284.

Let us now turn to the disconnected pieces. They are still quite easy to count: the one-line graphs, of which there are 4, can be accompanied by $2N$ oriented loops of length four, four of which are not self-avoiding:

$$4 \; 2(N - 4) \quad \text{×——×} \quad \left(\square - \overset{\cdots}{\underset{\cdots}{\vdots}} \right) \tag{9.48}$$

The factor 2 accounts for the two possible orientations of the loop. Thus, to fifth order, we find in two dimensions,

$$\bar{G}^{(5)}: \quad (284 + 4\cdot 2(N-2))\left(\frac{I_1}{I_0}\right)^4. \tag{9.49}$$

We now turn to the allowed graphs with multiple lines. They occur with the same number as the ones which were omitted in (9.49), except that only one relative orientation is permissible (the other is self-back-tracking):

$$\tag{9.50}$$

Thus we find a further contribution

$$\bar{G}_2^{(5)}: \quad 4\cdot 2\left(\frac{I_1}{I_0}\right)^3\frac{I_2}{I_0}. \tag{9.51}$$

The fifth is the lowest order where division by

$$\bar{Z} = 1 + 2N\left(\frac{I_1}{I_0}\right)^4 + 4N\left(\frac{I_1}{I_0}\right)^6 + \ldots \tag{9.52}$$

needs to be taken in account. Indeed, together with the first two terms in the curly brackets of (9.46) it contributes to (9.49) and (9.51) the term

$$\bar{G}_3^{(5)}: \quad -8N\left(\frac{I_1}{I_0}\right)^5. \tag{9.53}$$

This cancels precisely the N part in (9.49) and we find for the fifth order susceptibility,

$$\chi^{(5)}(\beta) = \frac{\beta}{2}\left[(284 - 16)\left(\frac{I_1}{I_0}\right)^5 + 8\left(\frac{I_1}{I_0}\right)^3\left(\frac{I_2}{I_0}\right)\right]. \tag{9.54}$$

In the Villain model, this becomes

$$\chi_{VM}^{(5)}(\beta) = \frac{\beta_V}{2}[268e^{-5/2\beta_V} + 8e^{-7/2\beta_V}].$$

Inserting the expansion (4.54)

$$\frac{I_2}{I_0} = \frac{1}{2}\left(\frac{I_1}{I_0}\right)^2 + \frac{1}{6}\left(\frac{I_1}{I_0}\right)^4 + \frac{5}{48}\left(\frac{I_1}{I_0}\right)^6 + \ldots \tag{9.55}$$

into (9.54) this reads

$$\chi^{(5)}(\beta) = \frac{\beta}{2}\left[272\left(\frac{I_1}{I_0}\right)^5 + \frac{4}{3}\left(\frac{I_1}{I_0}\right)^7 + \ldots\right]. \tag{9.56}$$

To sixth order there are 2×390 self-avoiding open-ended oriented graphs. From these we have to subtract the disconnected graphs:

$$(9.57)$$

where the factor 2 accounts again for the two orientations. Hence we obtain the contribution

$$\bar{G}_1^{(6)}: \quad (780 + 24N - 80)\left(\frac{I_1}{I_0}\right)^6. \tag{9.58}$$

To this we have to add half of the subtracted graphs in which the orientation runs parallel to the open line, thereby doubling its strength

$$\bar{G}_2^{(6)}: \quad 32\left(\frac{I_1}{I_0}\right)^4\frac{I_2}{I_0} + 8\left(\frac{I_1}{I_0}\right)^2\left(\frac{I_2}{I_0}\right)^2. \tag{9.59}$$

The piece going with N in (9.58) drops out after dividing by $\bar{Z} = 1 + 2N(I_1/I_0)^4 + \ldots$ which, together with the second term in the curly brackets of (9.46) gives $-12N(I_1/I_0)^6$. Thus we are left with

$$\chi^{(6)}(\beta) = \frac{\beta}{2}\left[700\left(\frac{I_1}{I_0}\right)^6 + 32\left(\frac{I_1}{I_0}\right)^4\frac{I_2}{I_0} + 8\left(\frac{I_1}{I_0}\right)^2\left(\frac{I_2}{I_0}\right)^2\right] \tag{9.60}$$

and it is obvious how this translates to the Villain model. Inserting (9.55) we can expand to obtain

$$\chi^{(6)}(\beta) = \frac{\beta}{2}\left[780\left(\frac{I_1}{I_0}\right)^6 + \frac{20}{3}\left(\frac{I_1}{I_0}\right)^8\right]. \tag{9.61}$$

To seventh order there are 2×1086 open-ended oriented self-avoiding graphs. The subtracted configurations are shown in Fig. 9.3 Ignoring the terms which carry an extra factor N, since they will cancel when dividing in the end by $\tilde{Z}$, we find a contribution

$$\tilde{G}_1^{(7)}: \quad (2172 - 400)\left(\frac{I_1}{I_0}\right)^4. \tag{9.62}$$

To this we have to add half of the subtracted graphs in which the orientation is parallel to the open line. This gives

$$\tilde{G}_2^{(7)}: \quad (4 \cdot 6 + 8 \cdot 3 + 16 \cdot 4 + 8 \cdot 2 + 4 \cdot 6)\left(\frac{I_1}{I_0}\right)^5\left(\frac{I_2}{I_0}\right), \tag{9.63}$$
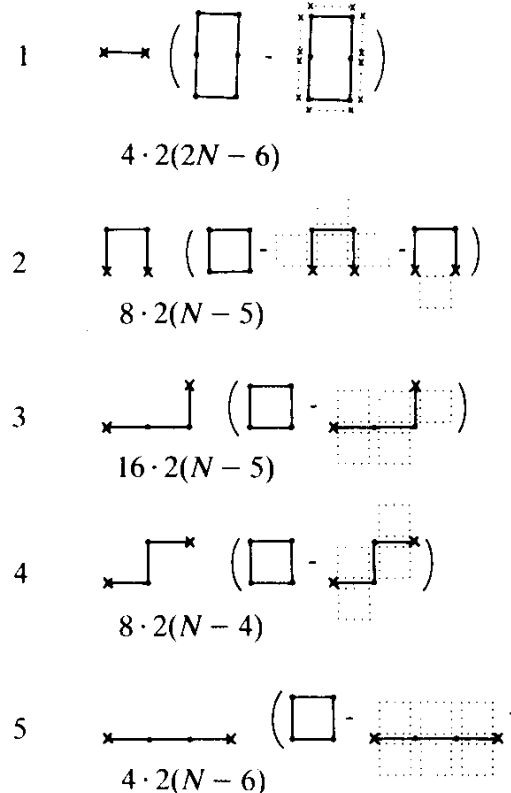
from graphs 1 and 5 plus

$$\tilde{G}_3^{(7)}: \quad (16 \cdot 1 + 8 \cdot 2)\left(\frac{I_1}{I_0}\right)^4\left(\frac{I_2}{I_0}\right)^2, \tag{9.64}$$

from graphs 3 and 4 plus

$$\tilde{G}_4^{(7)}: \quad 8 \cdot 1\left(\frac{I_1}{I_0}\right)\left(\frac{I_2}{I_0}\right)^3, \tag{9.65}$$

FIG. 9.3.   Susceptibility graphs of the seventh order.

from graphs 2. An exception occurs is the third subtracted graph in 2 which should not be added since it is already contained in 1.

In addition, there are 4 graphs for which a single line is touched by two oppositely oriented loops, i.e.,

$$4 \qquad \qquad \tag{9.66}$$

Thus we arrive at

$$\chi^{(7)}(\beta) = \frac{\beta}{2}\left[1776\left(\frac{I_1}{I_0}\right)^7 + 152\left(\frac{I_1}{I_0}\right)^5\left(\frac{I_2}{I_0}\right) + 32\left(\frac{I_1}{I_0}\right)^3\left(\frac{I_2}{I_0}\right)^2 + 8\frac{I_1}{I_0}\left(\frac{I_2}{I_0}\right)^3\right]. \tag{9.67}$$

Expanding I_2/I_0 à la (9.55) and recalling a corresponding term in (9.52) we find up to seventh order,

$$\chi(\beta) = \frac{\beta}{2}\left\{ 4\left(\frac{I_1}{I_0}\right) + 12\left(\frac{I_1}{I_0}\right)^2 + 36\left(\frac{I_1}{I_0}\right)^3 + 100\left(\frac{I_1}{I_0}\right)^4 + 272\left(\frac{I_1}{I_0}\right)^5 \right.$$

$$\left. + 718\left(\frac{I_1}{I_0}\right)^6 + 1862\frac{1}{3}\left(\frac{I_1}{I_0}\right)^7 + \ldots \right\}. \tag{9.68}$$

To eighth order, there are 2×2958 open-ended oriented self-avoiding graphs. According to Fig. 9.4 we have to subtract from them 1488 touching configurations:

$$\overline{G}_1^{(8)}: \quad 4428\left(\frac{I_1}{I_0}\right)^8. \tag{9.69a}$$

To these we have to add those in which lines are doubled. From Fig. 9.4a graphs 1–3 we read off

$$\overline{G}_2^{(8)}: \quad 32\left(\frac{I_1}{I_0}\right)^6\frac{I_2}{I_0} + 8\left(\frac{I_1}{I_0}\right)^4\left(\frac{I_2}{I_0}\right)^2 \qquad \text{graph 1,}$$

$$+48\left(\frac{I_1}{I_0}\right)^6\frac{I_2}{I_0} + 8\left(\frac{I_1}{I_0}\right)^4\left(\frac{I_2}{I_0}\right)^2 \qquad \text{graphs 2 and 3.} \tag{9.69b}$$

From Fig. 9.4b graphs 1 to 9 we find

FIG. 9.4a,b.   Susceptibility graphs of the eighth order.

FIG. 9.4.   continued

b7

16 2(N − 6)

b8

16 2(N − 7)

b9

4 2(N − 8)
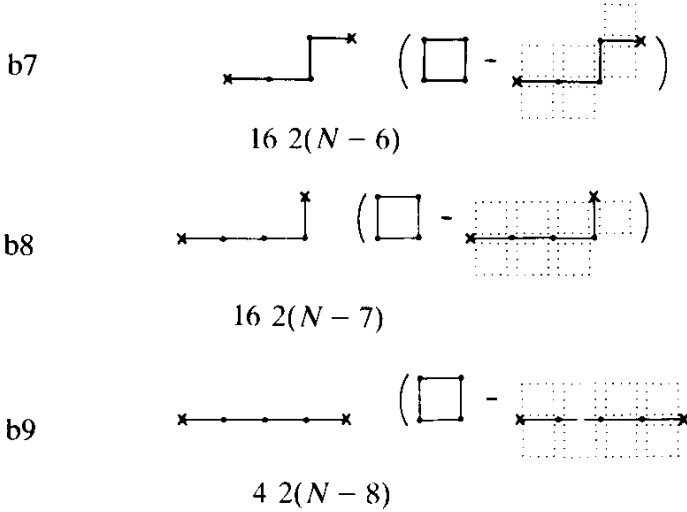
$$\bar{G}^{(8)}: \quad 80\left(\frac{I_1}{I_0}\right)^6\frac{I_2}{I_0} + 16\left(\frac{I_1}{I_0}\right)^2\left(\frac{I_2}{I_0}\right)^3, \ 32\left(\frac{I_1}{I_0}\right)^6\frac{I_2}{I_0} + 16\left(\frac{I_1}{I_0}\right)^4\left(\frac{I_2}{I_0}\right)^2,$$

$$48\left(\frac{I_1}{I_0}\right)^6\frac{I_2}{I_0} + 16\left(\frac{I_1}{I_0}\right)^4\left(\frac{I_2}{I_0}\right)^2 + 16\left(\frac{I_1}{I_0}\right)^2\left(\frac{I_2}{I_0}\right)^3,$$

$$16\left(\frac{I_1}{I_0}\right)^6\frac{I_2}{I_0} + 24\left(\frac{I_1}{I_0}\right)^4\left(\frac{I_2}{I_0}\right)^2, \ 32\left(\frac{I_1}{I_0}\right)^6\frac{I_2}{I_0} + 16\left(\frac{I_1}{I_0}\right)^4\left(\frac{I_2}{I_0}\right)^2,$$

$$48\left(\frac{I_1}{I_0}\right)^6\frac{I_2}{I_0} + 8\left(\frac{I_1}{I_0}\right)^4\left(\frac{I_2}{I_0}\right)^2, \ 64\left(\frac{I_1}{I_0}\right)^6\frac{I_2}{I_0} + 32\left(\frac{I_1}{I_0}\right)^4\left(\frac{I_2}{I_0}\right)^2,$$

$$96\left(\frac{I_1}{I_0}\right)^6\frac{I_2}{I_0} + 16\left(\frac{I_1}{I_0}\right)^4\left(\frac{I_2}{I_0}\right)^2, \ 32\left(\frac{I_1}{I_0}\right)^6\left(\frac{I_2}{I_0}\right) \tag{9.70}$$

Actually, in adding the touching configurations we have slightly overdone things. The 8 configurations

$$\tag{9.71}$$

in Fig. 9.4b, graph 1 and the 8 configuration

$$\tag{9.72}$$

in Fig. 9.4a, graphs 2 and 3 are really identical so that they should appear only once in the additional terms. Moreover, there are 8 exceptional graphs of the following form

$$4 \quad \boxed{\quad} \quad + 4 \quad \boxed{\quad} \quad \quad \quad \quad \quad \quad (9.73)$$

We can collect these into

$$\chi^{(8)}(\beta) = 4436\left(\frac{I_1}{I_0}\right)^8 + 528\left(\frac{I_1}{I_0}\right)^6\frac{I_2}{I_0} + 144\left(\frac{I_1}{I_0}\right)^4\left(\frac{I_2}{I_0}\right)^2 + 32\left(\frac{I_1}{I_0}\right)^2\left(\frac{I_2}{I_0}\right)^3.$$

$$(9.74)$$

Inserting the expansion (9.55) and including the $(I_1/I_0)^8$ term arising from $\chi^{(6)}$ we find in (9.68) the additional eighth order term

$$\chi^{(8)}(\beta): \quad \frac{\beta}{2}4746\frac{2}{3}\left(\frac{I_1}{I_0}\right)^8. \quad \quad \quad \quad (9.75)$$

We can now re-expand this series via Table 4.8 and obtain a power series in $\beta/2$. The result is given in Table 9.1. We have also listed higher order coefficients up to $(\beta/2)^{12}$ as obtained from a computer search of the allowed paths and quote results for other lattices for comparison.

9.5. RATIO TEST FOR THE SUSCEPTIBILITY EXPANSION

The susceptibility expansion has the advantage of exposing both even and odd coefficients. Thus, up to the same order in $(\beta/2)^n$, it yields twice as many coefficients. This makes it more suitable for an analysis via the ratio test than the expansion of the free energy.

The critical behaviour of the susceptibility can be parametrized experimentally via the critical index γ as follows:

$$\chi(\beta) \approx \beta(\beta - \beta_c)^{-\gamma}. \quad \quad \quad \quad (9.76)$$

Expanding this in a power series in β gives

$$\chi(\beta) = \beta\,\beta_c^{-\gamma}\sum_{n=0}^{\infty}\binom{-\gamma}{n}\frac{1}{\beta_c^n}\beta^n = \beta\,\beta_c^{-\gamma}\sum_{n=0}^{\infty}a_n\beta^n. \quad \quad (9.77)$$

Thus we see that the ratio of successive coefficients

$$R_n = \frac{a_n}{a_{n-1}} \qquad (9.78)$$

has the limiting behaviour [recall (4.60)]

$$R_n \to T_c\left(1 + \frac{\gamma - 1}{n}\right). \qquad (9.79)$$

From Table 9.1 we find the ratios

$$R_1 = \frac{1}{2}6 = 3, \qquad R_5 = \frac{1}{2}\frac{3275}{696} = 2.3527,$$

$$R_2 = \frac{1}{2}\frac{30}{6} = 2.5, \qquad R_6 = \frac{1}{2}\frac{15171.5}{3275} = 2.3162,$$

$$R_3 = \frac{1}{2}\frac{147}{30} = 2.45, \qquad R_7 = \frac{1}{2}\frac{70009.125}{15171.5} = 2.3072,$$

$$R_4 = \frac{1}{2}\frac{696}{147} = 2.367, \qquad R_8 = \frac{1}{2}\frac{320513.25}{70009.125} = 2.2891. \qquad (9.80)$$

In Fig. 9.5 we have plotted these as a function of $1/n$ and see that they converge well to

$$T_c \approx 2.2. \qquad (9.81)$$

The limiting slope gives[b]

$$\gamma \approx 1.4. \qquad (9.82)$$
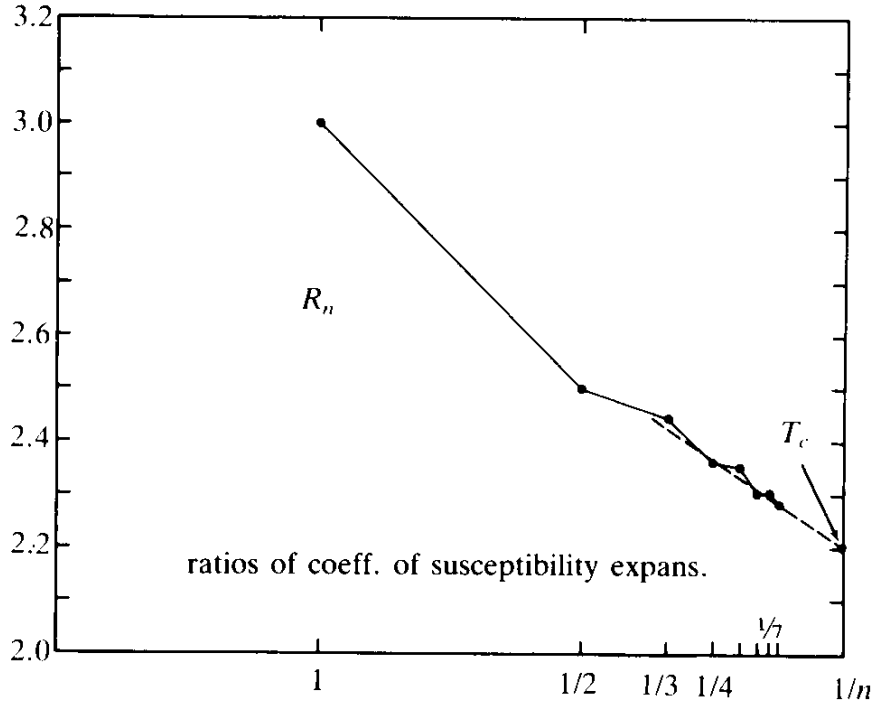
This is in good agreement with calculations via the renormalization group and ε-expansions which give $\gamma \sim 1.324$.[b]

9.6. ISOTROPY OF HIGH TEMPERATURE CORRELATION FUNCTIONS AT LARGE DISTANCES

At this juncture, a few comments are in order concerning another aspect of the correlation functions. When looking at the diagrams shown in Figs.

[b]See Table V in J C. Le Guillou and J. Zinn-Justin, *Phys. Rev.* **B21** (1980) 3976.

FIG. 9.5. The ratio test for the susceptibility expansion. The ratios R_n must converge towards $T_c(1 + (\gamma - 1)/n)$. We extract $T_c \sim 2.2$ and $\gamma \sim 1.4$.

9.1 to 9.4 the m_i-lines connecting the points $\mathbf{X}$, $\mathbf{X}'$ along the x- and y-axes and along the diagonal look quite different and one may wonder whether the correlation functions are isotropic in space for large separations.

At first sight, this does not appear to be so. Consider, for example, two points $\mathbf{X}$, $\mathbf{X}'$ separated by L links on the x-axis. The lowest contribution to (9.15) is due to a straight string m_i connecting the two points so that the small β_V expansion of the correlation function starts out with

$$G(\mathbf{X}, \mathbf{X}') \to e^{-(1/2\beta_V)|\mathbf{X} - \mathbf{X}'|}. \tag{9.83}$$

If, on the other hand, the points $\mathbf{X}$, $\mathbf{X}'$ are lying on the diagonal the string connecting them has $\sqrt{2}$ times as many links and the leading term is then

$$G(\mathbf{X}, \mathbf{X}') \to e^{-(1/2\beta_V)\sqrt{2}|\mathbf{X} - \mathbf{X}'|}. \tag{9.84}$$

Thus it appears as though G could not possibly become isotropic. In order to see that this argument is misleading, let us neglect for a moment the non-backtracking condition and consider the unrestricted random walks discussed in Part I, Chapter 6. With this approximation the expansion (9.38a) for the unrenormalized correlation function (9.38a), $\overline{G}(\mathbf{X}, \mathbf{X}')$ may be written

$$\widetilde{G}(\mathbf{X}, \mathbf{X}') = \sum_{\substack{\text{all random} \\ \text{chains from} \\ \mathbf{X} \text{ to } \mathbf{X}'}} e^{-L/2\beta_v}, \tag{9.85}$$

where the sum now runs over *all* random chains connecting $\mathbf{X}$ and $\mathbf{X}'$, including the backtracking ones, and L is the total number of links of the chain. Thus the statements (9.83), (9.84) are true here as well and one may again wonder about the question of asymptotic isotropy.

The advantage of the correlation function (9.85) is that the sum in it can be done by the techniques developed in Part I, Chapter 6. For this we introduce the Green function for a fixed number of links

$$\widetilde{G}(\mathbf{X}, \mathbf{X}', L) = e^{-L/2\beta_v} \sum_{\substack{\text{all paths} \\ \text{with } L \\ \text{links}}} 1, \tag{9.86}$$

and see that this satisfies the recursion relation (i = links)

$$\widetilde{G}(\mathbf{X}, \mathbf{X}', L) = e^{-1/2\beta_V} \sum_{\pm i} \widetilde{G}(\mathbf{X} + \mathbf{i}, \mathbf{X}', L - 1) \tag{9.87}$$

Subtracting on both sides $2De^{-1/2\beta_v}$ times $\widetilde{G}(\mathbf{X}, \mathbf{X}', L - 1)$, the sum on the right-hand side becomes the lattice Laplacian and we arrive at the difference equation

$$\widetilde{G}(\mathbf{X}, \mathbf{X}', L) - 2De^{-1/2\beta_v} \widetilde{G}(\mathbf{X}, \mathbf{X}', L - 1)$$

$$= e^{-(1/2\beta_V)} \sum_{\pm i} (\widetilde{G}(\mathbf{X} + \mathbf{i}, \mathbf{X}', L - 1) - \widetilde{G}(\mathbf{X}, \mathbf{X}', L - 1))$$

$$= e^{-1/2\beta_V} \overline{\nabla} \cdot \nabla \widetilde{G}(\mathbf{X}, \mathbf{X}', L - 1). \tag{9.88}$$

This can be rewritten as

$$\overline{\nabla}_L \widetilde{G}(\mathbf{X}, \mathbf{X}', L - 1) = e^{-1/2\beta_V}[\overline{\nabla} \cdot \nabla - (e^{1/2\beta_v} - 2D)] \widetilde{G}(\mathbf{X}, \mathbf{X}', L - 1)$$

$$\equiv \frac{1}{2M}[\overline{\nabla} \cdot \nabla - m^2] \widetilde{G}(\mathbf{X}, \mathbf{X}', L - 1), \tag{9.89}$$

where

$$m^2 \equiv e^{1/2\beta_v} - 2D \tag{9.90}$$

and[c]

$$M \equiv \tfrac{1}{2}(m^2 + 2D). \tag{9.91}$$

Using the initial condition

$$\widetilde{G}(\mathbf{X}, \mathbf{X}', 0) = \delta_{\mathbf{X}, \mathbf{X}'}, \tag{9.92}$$

this equation can be solved by the Fourier ansatz

$$\widetilde{G}(\mathbf{X}, \mathbf{X}', L) = \frac{1}{N} \sum_{L, \mathbf{k}} e^{-\Omega L} e^{i \mathbf{k} \cdot (\mathbf{X} - \mathbf{X}')}, \tag{9.93}$$

where

$$1 - e^{-\Omega} = \frac{1}{2M}(\overline{\mathbf{K}} \cdot \mathbf{K} + m^2). \tag{9.94}$$

We can now make use of this result and calculate $\widetilde{G}(\mathbf{X}, \mathbf{X}')$ as the sum over all $\widetilde{G}(\mathbf{X}, \mathbf{X}', L)$,

$$\widetilde{G}(\mathbf{X}, \mathbf{X}') = \frac{1}{N} \sum_{L} \sum_{\mathbf{k}} e^{-\Omega L} e^{i \mathbf{k} \cdot (\mathbf{X} - \mathbf{X}')}$$

$$= \frac{1}{N} \sum_{\mathbf{k}} \frac{1}{1 - e^{-\Omega}} e^{i \mathbf{k} \cdot (\mathbf{X} - \mathbf{X}')} = 2M \sum_{\mathbf{k}} \frac{1}{\overline{\mathbf{K}} \cdot \mathbf{K} + m^2} e^{i \mathbf{k} \cdot (\mathbf{X} - \mathbf{X}')}. \tag{9.95}$$

This is exactly the expression derived previously [in Eq. (6.47) of Part I] for the partition function $P(\mathbf{X}, \mathbf{X}')$ of a single random chain. Up to a factor, it is equal to the lattice Green's function $v_m(\mathbf{X} - \mathbf{X}')$ of mass m. In Eq. (6.119) of Part I, we showed that, for large distances, the lattice Green function converges to the Yukawa potential in the continuum

$$v_m(\mathbf{x}) \rightarrow \frac{1}{(4\pi)^{D/2}} \left(\frac{2m}{|\mathbf{x}|}\right)^{(D-2)/2} 2K_{D/2-1}(m|\mathbf{x}|). \tag{9.96}$$

It is gratifying to see that this is a completely isotropic function in spite of

[c]Notice that this is the $m \neq 0$ version of the parameter M in (I.6.20). Indeed, the recursion (9.87) reduces to (I.6.4) for $e^{-1/2\beta v} = 1/2D$ or $m = 0$.

the differences in the number of ways in which the two points **X**, **X**' can be connected along the different directions.

9.7. LOW TEMPERATURE EXPANSION OF THE CORRELATION FUNCTION IN THE VILLAIN MODEL

The factorized formulas (9.28)–(9.30) of Section 9.3 are useful in writing down the correlation function of the Villain model at low temperatures. In the limit $T \to 0$, the vortex lines are frozen out completely and the sum over $\ell_i(\mathbf{x})$ can be omitted. The same thing happens to the normalization factor Z_{VM}, which tends to unity. Thus $G^{(n,n)}$ reduces to the pure spin wave correlation function

$$G^{(n,n)}(\mathbf{x}_1, \ldots, \mathbf{x}_n; \mathbf{x}'_1, \ldots, \mathbf{x}'_n) \xrightarrow[T \to 0]{} G_s^{(n,n)}(\mathbf{x}_1, \ldots, \mathbf{x}_n; \mathbf{x}'_1, \ldots, \mathbf{x}'_n). \tag{9.97}$$

For increasing temperatures, vortex loops are excited in the same way as in the low temperature expansion of the partition function Z_{VM} and G_s gets multiplied by a vortex factor G_v [recall (9.29)].

To be specific, let us focus our attention upon the two-point function $G(\mathbf{X}, \mathbf{X}') \equiv G^{(1,1)}(\mathbf{X}, \mathbf{X}')$ for which the monopole charge density $Q(\mathbf{x})$ is $\delta_{\mathbf{x},\mathbf{X}'} - \delta_{\mathbf{x},\mathbf{X}'}$. The spin-wave correlation function form (9.30) becomes explicitly

$$G_s(\mathbf{X}, \mathbf{X}') = e^{-(1/2\beta v)\sum_\mathbf{x} Q(\mathbf{x})(1/-\bar{\nabla}\cdot\nabla)Q(\mathbf{x})} = e^{(1/\beta v)(r(\mathbf{X}-\mathbf{X}') - r(0))} = e^{1/\beta v)r(\mathbf{X}-\mathbf{X}')}. \tag{9.98}$$

In calculating the vortex correction (9.30), let us restrict ourselves to the smallest $\ell_i(\mathbf{x})$ loop. This may be represented by

$$\ell_i(\mathbf{x}) = \varepsilon_{ijk} \nabla_j n_k(\mathbf{x} + \mathbf{i}), \tag{9.99}$$

where $\mathbf{n}(\mathbf{x})$ is a unit vector at *one* point and vanishes everywhere else, i.e.,

$$n_i(\mathbf{x}) = \mathbf{i}\,\delta_{\mathbf{x},\mathbf{X}}. \tag{9.100}$$

The unit vector **i** can point in the x, y, or z directions.

The superflow (Biot-Savart-type) energy of this loop was calculated in (7.46),

$$V_4 = -2(v(1) - v(0)) = \tfrac{1}{3}.$$ (9.101)

Inserting (9.101) into (9.30) and using the $\Sigma_{\mathbf{x}}\Omega_i^m(\mathbf{x})\,\ell_i(\mathbf{x})$ form of the interactions [see (9.22c)], we may expand

$$G_v(\mathbf{X}, \mathbf{X'}) \approx Z_v^{-1}\left(1 + 2e^{-(\beta v/2)4\pi^2 V_4}\sum_{y,i}\cos[i\cdot(\bar{\nabla}\times\Omega^m)]\right)$$ (9.102)

where to the same order

$$Z_v \approx 1 + 6\sum_y e^{-(\beta v/2)4\pi^2 V_4},$$

so that

$$G_v(\mathbf{X}, \mathbf{X'}) \approx \exp\{2e^{2e^{-(\beta v/2)4\pi^2 V_4}\Sigma_{y,i}\{\cos[i\cdot(\bar{\nabla}\times\Omega^m)]-1\}}\}.$$ (9.103)

If we work out $\bar{\nabla}\times\Omega^m$ in more detail, we find [recall (9.26)]

$$\mathbf{i}\cdot(\bar{\nabla}\times\Omega^m) = 2\pi\mathbf{i}\cdot\frac{1}{-\bar{\nabla}\cdot\nabla}\bar{\nabla}\times(\nabla\times\mathbf{m}) = 2\pi m_i - 2\pi\nabla_i\frac{1}{-\bar{\nabla}\cdot\nabla}\bar{\nabla}\cdot\mathbf{m}$$

$$= 2\pi m_i - 2\pi\nabla_i\frac{1}{-\bar{\nabla}\cdot\nabla}Q.$$ (9.104)

Since m_i is an integer, it can be dropped inside the cosine. If $\mathbf{X}$ and $\mathbf{X'}$ are far apart, the curl $\bar{\nabla}\times\Omega^m$ is very small, and we can expand the cosine as

$$\cos[\mathbf{i}\cdot(\bar{\nabla}\times\Omega^m)] - 1 \sim -\frac{4\pi^2}{2}\left(\nabla_i\frac{1}{-\bar{\nabla}\cdot\nabla}Q\right)\left(\nabla_i\frac{1}{-\bar{\nabla}\cdot\nabla}Q\right).$$

Summing over $\mathbf{y}$ and all three $\mathbf{i}$ directions gives

$$\sum_{y,i}(\cos[\mathbf{i}\cdot\bar{\nabla}\times\Omega^m] - 1) \approx -\frac{4\pi^2}{2}\sum_{y,i}\left(\nabla_i\frac{1}{-\bar{\nabla}\cdot\nabla}Q(\mathbf{y})\right)\left(\nabla_i\frac{1}{-\bar{\nabla}\cdot\nabla}Q(\mathbf{y})\right).$$

Performing a partial integration, one of the Coulomb potentials cancels and we find the simple result

$$-\frac{4\pi^2}{2}\sum_y Q(\mathbf{y})\frac{1}{-\bar{\nabla}\cdot\nabla}Q(\mathbf{y}).$$

Thus

$$G_v(\mathbf{X}, \mathbf{X}') \approx e^{-2e^{-(\beta v/2)4\pi^2 V_4} \frac{4\pi^2}{2}} \sum_y Q(\mathbf{y}) \frac{1}{-\bar{\nabla} \cdot \nabla} Q(\mathbf{y}) = e^{4\pi^2 e^{-(\beta v/2)4\pi^2 V_4}} v'(\mathbf{X} - \mathbf{X}').$$

$$(9.105)$$

This has the same dependence on $\mathbf{X}$ and $\mathbf{X}'$ as the zero temperature limit (9.98). As a consequence, the effect of the vortex factor (9.105) can be accounted for by a renormalization of β_V^{-1}, i.e.,

$$(\beta_V^R)^{-1} = \beta_V^{-1} + 4\pi^2 e^{-(\beta v/2)4\pi^2 V_4},$$

$$(9.106)$$

where $V_4 = 1/3$ is the Coulomb energy of the smallest vortex loop $\square$ [see (7.46)]. One may say that a single randomly distributed fundamental vortex loop has precisely the same effect as a slight increase in the temperature of the system. The spin waves travel through the system with a small vortex loop freely just as they would at zero temperature. Only the stiffness of the $\gamma(\mathbf{x})$ fluctuations is reduced by the renormalization (9.106).

NOTES AND REFERENCES

There is a rich literature on magnetic monopoles starting with Dirac's original paper
P.A.M. Dirac, *Phys. Rev.* **74** (1948) 817,
J. Schwinger, *Phys. Rev.* **144** (1966) 1987,
D. Zwanziger, *Phys. Rev.* **D3** (1971) 880,
A. Jevicki and P. Senjanović, *Phys. Rev.* **D11** (1975) 860,
A.O. Barut, *J. Phys.* **A11** (1978) 2073,
T. Banks, E. Tomboulis, *Phys. Rev.* **D20** (1979) 501.
  The graphical analysis of the susceptibility was done in collaboration with H. Bruckmann whose thesis (Berlin, 1983) contains more details. Compare also with the high temperature expansions of
W.J. Camp and J.P. Van Dyke, *J. Phys.* **C8** (1975) 336.

GAS OF MONOPOLES

In the last chapters we showed that the calculation of correlation functions of the order parameter $e^{i\gamma(\mathbf{x})}$ amounts to calculating the behaviour of a fixed set of magnetic monopoles within an ensemble of vortex lines. It is worthwhile pointing out that the model can be enriched in a very simple manner to contain, from the outset, a whole *ensemble* of such monopoles. All we have to do is to discretize the angle $\gamma(\mathbf{x})$ so that it no longer covers the interval $[0, 2\pi)$ continuously but only the fractional angles

$$\gamma_\nu(\mathbf{x}) = \frac{2\pi}{n}\nu(\mathbf{x}), \quad \nu(\mathbf{x}) = 0, 1, \ldots, n-1. \tag{10.1}$$

The resulting model is called Z_n *spin model* or, in the Villain form, Z_n *Villain model*. A similar effect may be reached by modulating the γ dependence of the energy by an additional Boltzmann factor, which has pronounced maxima at these fractional angles, say,

$$(\sqrt{2\pi h n^2})^N e^{h\sum_x \cos n\gamma(\mathbf{x})}, \tag{10.2}$$

or its Villain form

$$(\sqrt{2\pi h})^N \sum_{\{v(\mathbf{x})\}} e^{-(h/2)\Sigma_{\mathbf{x}}(\gamma(\mathbf{x}) - (2\pi/n)v(\mathbf{x}))^2}. \tag{10.3}$$

For $n = 1$, the interaction (10.2) acts like an external magnetic field to the spin model, trying to align the angle to $\gamma \equiv 0$. For $n > 1$, the alignment can take place in n directions, $\gamma_v = (2\pi/n)v$, and we shall call (10.2), (10.3) a *generalized external magnetic field of order n*. Such $n > 1$ fields are quite common in crystalline spin systems, where they arise from symmetry breaking forces along certain crystal directions.

Let us now discuss the Z_n models in some detail.

10.1. Z_n VILLAIN MODEL

This model is defined by the partition function (using β for β_V)

$$Z_n = \frac{1}{n^N} \sum_{\{v(\mathbf{x})\}} \sum_{\{n_i(\mathbf{x})\}} e^{-(\beta/2)\Sigma_{\mathbf{x}}(\nabla_i \gamma_v(\mathbf{x}) - 2\pi n_i(\mathbf{x}))^2}. \tag{10.4}$$

The ensemble of magnetic monopoles is introduced by noticing that the fractional angles γ_v can be thought of as arising from an integral over a continuous variable $\gamma(\mathbf{x})$ coupled to a set of integer charges as follows:

$$\frac{1}{n} \sum_{v=0}^{n-1} = \int_{-\pi}^{\pi} \frac{d\gamma}{2\pi} \sum_{Q=-\infty}^{\infty} e^{inQ\gamma}. \tag{10.5}$$

This identity follows directly from Poisson's formula (6.37) since the sum over Q is

$$\sum_{Q=-\infty}^{\infty} e^{inQ\gamma} = \sum_{v} \delta\left(\frac{n\gamma}{2\pi} - v\right) = \frac{2\pi}{n} \sum_{v} \delta\left(\gamma - \frac{2\pi}{n}v\right). \tag{10.6}$$

Inserting (10.5) into (10.4) and performing the same manipulations as in the last chapter, we can rewrite Z_n in the following successive forms

$$Z_n = \prod_{\mathbf{x}} \left[\int_{-\pi}^{\pi} \frac{d\gamma(\mathbf{x})}{2\pi} \right] \sum_{\{n_i(\mathbf{x})\}} \sum_{\{Q(\mathbf{x})\}} e^{-(\beta/2)\Sigma_{\mathbf{x}}(\nabla_i \gamma(\mathbf{x}) - 2\pi n_i(\mathbf{x}))^2 + in\Sigma_{\mathbf{x}}Q(\mathbf{x})\gamma(\mathbf{x})}$$

$$= \sum_{\{n_i(\mathbf{x})\}} \sum_{\{Q(\mathbf{x})\}} \frac{1}{(\sqrt{2\pi\beta})^{3N}} \prod_{\mathbf{x},i} \left[\int_{-\infty}^{\infty} db_i(\mathbf{x}) \right]$$

$$\times \prod_{\mathbf{x}} \left[\int_{-\pi}^{\pi} \frac{d\gamma(\mathbf{x})}{2\pi} \right] e^{-(1/2\beta)\Sigma_\mathbf{x} b_i^2(\mathbf{x}) + i\Sigma_\mathbf{x} b_i(\nabla_i\gamma - 2\pi n_i) + in\Sigma_\mathbf{x} Q(\mathbf{x})\gamma(\mathbf{x})}$$

$$= \sum_{\{n_i(\mathbf{x})\}} \Phi[\mathbf{n}] \sum_{\{Q(\mathbf{x})\}} \frac{1}{(\sqrt{2\pi\beta})^{3N}}$$

$$\times \prod_{\mathbf{x},i} \left[\int_{-\infty}^{\infty} db_i(\mathbf{x}) \right] \delta(\bar\nabla_i b_i - nQ) e^{-(1/2\beta)\Sigma_\mathbf{x} b_i^2(\mathbf{x}) + 2\pi i\Sigma_\mathbf{x} b_i(\mathbf{x})n_i(\mathbf{x})}$$

$$= \frac{1}{(\sqrt{2\pi\beta})^{3N}} \sum_{\{Q_i(\mathbf{x})\}} \sum_{\{b_i(\mathbf{x})\}} \delta_{\bar\nabla_i b_i, nQ} \, e^{-(1/2\beta)\Sigma_\mathbf{x} b_i^2(\mathbf{x})}. \tag{10.7}$$

The magnetic field lines can again be generated from a vector potential coupled to vortex lines plus a monopole gauge field giving,

$$Z_n = \frac{1}{(\sqrt{2\pi\beta})^{3N}} \prod_{\mathbf{x}} \left[\int_{-\infty}^{\infty} dA_1(\mathbf{x}) dA_2(\mathbf{x}) \right] \sum_{\{\ell_i(\mathbf{x})\}} \delta_{\bar\nabla_i \ell_i, 0} \sum_{\substack{\{Q(\mathbf{x})\} \\ \nabla_i m_i^0(\mathbf{x}) = Q(\mathbf{x})}}$$

$$\times e^{-(1/2\beta)\Sigma_\mathbf{x}(\bar\nabla \times \mathbf{A})^2 + 2\pi i\Sigma_\mathbf{x} A_i(\mathbf{x})\ell_i(\mathbf{x})}$$

$$= \det(-\bar\nabla \cdot \nabla)^{-1/2} \frac{1}{(\sqrt{2\pi\beta})^N} \sum_{\{\ell_i(\mathbf{x})\}} \delta_{\bar\nabla_i \ell_i, 0}$$

$$\times \sum_{\{Q(\mathbf{x})\}} e^{-(4\pi^2\beta/2)\Sigma_\mathbf{x} \ell_i(\mathbf{x})(1/-\bar\nabla \cdot \nabla)\ell_i(\mathbf{x}) - (n^2/2\beta)\Sigma_\mathbf{x} Q(\mathbf{x})(1/-\bar\nabla \cdot \nabla)Q(\mathbf{x}) + 2\pi in\Sigma_\mathbf{x} Q(\mathbf{x})(1/-\bar\nabla \cdot \nabla)\bar\nabla_i n_i(\mathbf{x})}$$

$$= \det(-\bar\nabla \cdot \nabla)^{-1/2} \frac{1}{(\sqrt{2\pi\beta})^N} \sum_{\{\ell_i(\mathbf{x})\}} \delta_{\bar\nabla_i \ell_i, 0} \sum_{\{Q(\mathbf{x})\}}$$

$$\times e^{-(4\pi^2\beta/2)\Sigma_\mathbf{x} \ell_i(\mathbf{x})(1/-\bar\nabla \cdot \nabla)\ell_i(\mathbf{x}) - (n^2/2\beta)\Sigma_\mathbf{x} Q(\mathbf{x})(1/-\bar\nabla \cdot \nabla)Q(\mathbf{x}) + 2\pi in\Sigma_\mathbf{x}(\nabla \times \mathbf{m}^0)(1/-\bar\nabla \cdot \nabla)\ell(\mathbf{x})}.$$

$$\tag{10.8}$$

The last two lines describe indeed an ensemble of vortex lines coupled to a gas of monopoles of charges n.

For small $\beta < 1/3$ we know from Chapter 7 that the vortex lines condense. For large β, which turns out to be of the order of $\approx (1/10)n^2$, the monopoles proliferate. If n is sufficiently large (≥ 4), the two regions are clearly separated. If XY or Villain models are simulated on the computer, the variable $\gamma(\mathbf{x})$ is usually not taken to be a continuous variable but approximated by a number of discrete values ("Z_n

approximation"; recall, for instance, Table 7.2). Thus, such simulations always contain monopoles and display the second transition region at $\beta \approx (1/10)n^2$. This does not cause any problem since the second transition is easily distinguished from the superfluid transition by its n^2 dependence.

It should be stressed that in the representation in the third line of (10.8), the integer field $m_i^0(\mathbf{x})$, whose lattice divergence satisfies $\bar{\nabla}_i m_i^0(\mathbf{x}) = Q(\mathbf{x})$ is a *particular* one for every $Q(\mathbf{x})$ configuration. This is why we have added a superscript zero. We have seen in Chapter 9 that $m_i^0(\mathbf{x})$ is an integer valued gauge field for the magnetic charge. It is always possible to change it by the curl of an arbitrary integer valued field,

$$m_i^0(\mathbf{x}) \to m_i^0(\mathbf{x}) + (\bar{\nabla} \times \mathbf{M})_i(\mathbf{x}) \qquad (10.9)$$

and still maintain the property

$$\bar{\nabla}_i m_i(\mathbf{x}) = Q(\mathbf{x}).$$

This gauge freedom can be exploited to restrict the integrations over the $A_i(\mathbf{x})$ fields to the interval $(-\pi, \pi]$. Thus we can write

$$\bar{\nabla} \times \mathbf{A} = \bar{\nabla} \times \mathbf{A}^0 + \bar{\nabla} \times \mathbf{M} \qquad (10.10)$$

and absorb the $M(\mathbf{x})$ field into the magnetic monopole gauge field $m_i^0(\mathbf{x})$. This is then no longer a particular one satisfying $\bar{\nabla}_i m_i(\mathbf{x}) = Q(\mathbf{x})$ but runs through *all* integer values satisfying this condition. Moreover, once we sum over all $Q(\mathbf{x})$, the numbers $m_i(\mathbf{x})$ become completely unrestricted. In this way we arrive at the following alternative representation

$$Z_n = \frac{1}{(\sqrt{2\pi\beta})^{3N}} \prod_{\mathbf{x}} \left[\int_{-\pi}^{\pi} dA_1(\mathbf{x}) \int_{-\pi}^{\pi} dA_2(\mathbf{x}) \right] \sum_{\{\ell_i(\mathbf{x})\}} \delta_{\bar{\nabla}_i \ell_i, 0} \sum_{\{m_i(\mathbf{x})\}}$$

$$\times e^{-(1/2\beta)\Sigma_{\mathbf{x}}(\bar{\nabla} \times \mathbf{A} + \mathbf{m})^2 + 2\pi i \Sigma_{\mathbf{x}} A_i(\mathbf{x})\ell_i(\mathbf{x})}. \qquad (10.11)$$

10.2. VILLAIN MODEL IN A GENERALIZED EXTERNAL MAGNETIC FIELD

The same ensemble of vortex lines and monopoles is described by the Villain model in a generalized magnetic field of order n. Taking the Villain form (10.3) of the magnetic field and introducing in it an auxiliary integration over a variable $q(\mathbf{x})$ gives

$$\frac{1}{n^\nu} \sum_{\{\nu(\mathbf{x})\}} \prod_\mathbf{x} \left[\int dq(\mathbf{x}) \right] e^{-(1/2h)\Sigma_\mathbf{x} q^2(\mathbf{x}) + i\Sigma_\mathbf{x} q(\mathbf{x})(\gamma(\mathbf{x}) - (2\pi\nu(\mathbf{x})/n))}. \qquad (10.12)$$

Performing the sum over $\nu(\mathbf{x})$ produces δ-functions $\Sigma_{Q(\mathbf{x})} \delta(q(\mathbf{x})/n - Q(\mathbf{x}))$ so that (10.3) becomes

$$\sum_{\{Q(\mathbf{x})\}} e^{-(1/2h)\Sigma_\mathbf{x} n^2 Q^2(\mathbf{x}) + in\Sigma_\mathbf{x} Q(\mathbf{x})\gamma(\mathbf{x})}. \qquad (10.13)$$

Inserting this result into the partition function (10.4) and comparing with (10.7) we see that the only difference between a Z_n model and a Villain model in a generalized magnetic field of order n (of the Villain type) is an additional Boltzmann factor

$$e^{-(1/2h)\Sigma_\mathbf{x} n^2 Q^2(\mathbf{x})} \qquad (10.14)$$

accompanying the sum over the monopole charges $nQ(\mathbf{x})$. This may be considered as an extra core energy of the monopoles. It can be used to move the second transition to different values of β.

10.3. RELATION TO LATTICE GAUGE THEORY

The observation in the last paragraph opens up another road for studying the phase transitions of this model. When comparing (10.11) with the starting representation in (10.7) we observe a great similarity between the two. What the vortex lines are for $A_i(\mathbf{x})$, the monopoles are for $\gamma(\mathbf{x})$. The integer fields $n_i(\mathbf{x})$ describe the Volterra sheets in $\gamma(\mathbf{x})$, whose boundaries are the vortex lines. The fields $m_i(\mathbf{x})$ describe "Dirac strings" whose ends are the magnetic monopoles.

It is instructive to study the Villain model (10.11) without the vortex lines $\ell_i(\mathbf{x})$, but write it in the form[a]

$$\hat{Z} = \prod_\mathbf{x} \left[\int_{-\pi}^{\pi} d\hat{A}_1 \, d\hat{A}_2 \right] \sum_{\{m_{ij}(\mathbf{x})\}} e^{-(\beta/2)\Sigma_{\mathbf{x},i<j}(\nabla_i \hat{A}_j - \nabla_j \hat{A}_i - 2\pi m_{ij})^2}. \qquad (10.15)$$

This is obviously the same[b] as the $\ell_i(\mathbf{x}) = 0$ part of (10.11), if we identify

---

[a]Due to the its gauge invariance under the transformation $\hat{A}_i(\mathbf{x}) \to \hat{A}_i(\mathbf{x}) + \nabla_i \lambda(\mathbf{x})$, we could certainly have fixed the gauge in any other way. The present choice is the axial gauge $\hat{A}_3(\mathbf{x}) = 0$.

[b]Apart from a trivial overall factor $(\sqrt{2\pi\beta})^{3N}$.

$$m_{ij}(\mathbf{x}) \equiv \varepsilon_{ijk} m_k(\mathbf{x}), \qquad \hat{A}_i(\mathbf{x}) \equiv 2\pi A_i(\mathbf{x}),$$

and

$$\hat{\beta} \equiv \frac{1}{4\pi^2 \beta}. \tag{10.16}$$

The partition function (10.15) is an important model in its own right. It is the Villain form of what is known as *Abelian lattice gauge theory*. In it, $m_{ij}(\mathbf{x})$ may be considered as the gauge field of defects associated with the field $\hat{A}_i(\mathbf{x})$.

Notice that in the present case, the defining field $\hat{A}_i(\mathbf{x})$ happens to be a gauge field itself. Thus the Abelian lattice gauge theory has *three* gauge structures: that of the $\hat{A}_i(\mathbf{x})$ fields themselves *plus* the two gauge fields of stresses and defects which are the subject of this text.

Let us exhibit the gauge field of stresses. By the usual technique, the partition function can be rewritten in the form

$$\hat{Z} = \frac{1}{(\sqrt{2\pi\hat{\beta}})^{3N}} \prod_{\mathbf{x},i<j} \left[\int_{-\infty}^{\infty} df_{ij}(\mathbf{x}) \right] \prod_{\mathbf{x}} \left[\int_{-\pi}^{\pi} d\hat{A}_1(\mathbf{x})\, d\hat{A}_2(\mathbf{x}) \right]$$

$$\times \sum_{\{M_{ij}(\mathbf{x})\}} e^{-(1/2\hat{\beta})\Sigma_x f_{ij}^2 + i\Sigma_{\mathbf{x},i<j} f_{ij}(\nabla_i \hat{A}_j - \nabla_j \hat{A}_i - 2\pi M_{ij})}$$

$$= \frac{1}{(\sqrt{2\pi\hat{\beta}})^{3N}} \sum_{\{\bar{f}_{ij}(\mathbf{x})\}} \delta_{\bar{\nabla}_i \bar{f}_{ij}, 0} \, e^{-(1/2\hat{\beta})\Sigma_x \bar{f}_{ij}^2(\mathbf{x})}. \tag{10.17}$$

Geometrically, the sum over all integer valued antisymmetric tensors $\bar{f}_{ij}(\mathbf{x})$ satisfying $\bar{\nabla}_i \bar{f}_{ij} = 0$ can be viewed as the sum over oriented closed non-backtracking random surfaces. The high-temperature expansion of (10.17) amounts to an expansion into larger and larger such surfaces.[c]

Just as in the *XY* model, where we have generated integer valued closed magnetic fields by vortex loops, we may generate integer valued closed surfaces by introducing monopole charges for which the surfaces are the surfaces of equal magnetic potential. The magnetic potential is introduced by writing

$$\bar{f}_{ij}(\mathbf{x}) = \varepsilon_{ijk}\, \partial_k\, a(\mathbf{x}), \tag{10.18}$$

[c]For details see the review article on lattice gauge theory by J.M. Drouffe and J.P. Zuber, cited in the Notes and References.

which satisfies $\overline{\nabla}_i \overline{f}_{ij}(\mathbf{x}) = 0$ identically. The integer values of $a(\mathbf{x})$ are then produced by coupling $A(\mathbf{x})$ to integer valued magnetic charges $Q(\mathbf{x})$. In this way we find

$$\hat{Z} = \frac{1}{(\sqrt{2\pi\hat{\beta}})^{3N}} \sum_{\{Q(\mathbf{x})\}} \prod_{\mathbf{x}} \left[\int_{-\infty}^{\infty} dA(\mathbf{x}) \right] e^{-(1/2\hat{\beta})\Sigma_{\mathbf{x}}(\nabla A)^2 + 2\pi i \Sigma_{\mathbf{x}} Q(\mathbf{x}) A(\mathbf{x})}. \tag{10.19}$$

Integrating out the $A(\mathbf{x})$ fields gives

$$\hat{Z} = \frac{1}{(\sqrt{2\pi\hat{\beta}})^{3N}} \det(-\overline{\nabla} \cdot \nabla)^{-1/2} \sum_{\{Q(\mathbf{x})\}} e^{-(4\pi^2\hat{\beta}/2)\Sigma_{\mathbf{x}} Q(\mathbf{x})(1/-\overline{\nabla} \cdot \nabla) Q(\mathbf{x})}. \tag{10.20}$$

This is the same gas of magnetic monopoles which occurs in (10.7).

If the temperature $\hat{T} = 1/\hat{\beta}$ becomes sufficiently large, the monopoles start proliferating. For low temperatures, they are frozen out. There exists a transition region when $\hat{\beta}$ is of the order of 1/3. Note, however, that there is an important difference between the condensation of vortex lines and the proliferation of magnetic monopoles. For vortex lines, the condensation causes the screening of the gauge field A_i to which the lines are coupled via

$$e^{2\pi i \Sigma_{\mathbf{x}} \ell_i(\mathbf{x}) A_i(\mathbf{x})}. \tag{10.21}$$

If there are only a few small loops, the fact that they are closed and satisfy

$$\overline{\nabla}_i \ell_i(\mathbf{x}) = 0 \tag{10.22}$$

has the consequence that the additional field energy for the $A_i(\mathbf{x})$ field generated by the coupling (10.21) is always of the gradient type $(\overline{\nabla} \times \mathbf{A})^2$. This follows from Stokes' theorem (on the lattice) and was seen in detail in Chapter 3. For this reason, in the cold phase the $A_i(\mathbf{x})$ fluctuations retain their long-range nature and the range is not effected by a few vortex loops; only the gradient energies are (there is only a "wave function renormalization").

This situation changes drastically after the vortex lines condense. Then they become infinitely long and this does generate a mass term via the Meissner effect. It is as if the condition $\overline{\nabla}_i \ell_i(\mathbf{x}) = 0$ becomes irrelevant in

the condensed phase since there are pieces of lines everywhere. The mass term is then generated in the same way as in an unconstrained integral,

$$\prod_x \left[\int d\ell_i(\mathbf{x}) \right] e^{2\pi i \Sigma_x \ell_i(\mathbf{x}) A_i(\mathbf{x}) - (1/2)((2\pi)^2/m^2)\Sigma_x \ell_i^2(\mathbf{x})} \propto e^{-(m^2/2)\Sigma_x A_i^2(\mathbf{x})}. \quad (10.23)$$

For the magnetic monopoles coupled via $\Sigma_x Q(\mathbf{x}) A(\mathbf{x})$ in (10.19), the situation is entirely different. Here even the slightest appearance of monopoles, which are present at all temperatures except at $T = 0$, reduces the range of the $A(\mathbf{x})$ fluctuations to a finite value. This is best seen by removing, as usual, the natural core energy $v(0)$ in (10.19) and rewriting the partition function as

$$\widehat{Z} = \frac{1}{(\sqrt{2\pi\widehat{\beta}})^{3N}} \det(-\bar{\nabla} \cdot \nabla)^{-1/2} \det(-\bar{\nabla}' \cdot \nabla')^{1/2} \prod_x \left[\int_{-\infty}^{\infty} dA(\mathbf{x}) \right]$$

$$\times e^{-(1/2\widehat{\beta})\Sigma_x(\nabla'A)^2 + 2\pi i \Sigma_x Q(\mathbf{x})A(\mathbf{x})} \sum_{\{Q(\mathbf{x})\}} e^{-(4\pi^2\widehat{\beta}/2)\Sigma_x Q(\mathbf{x})(1/-\bar{\nabla}\cdot\nabla)Q(\mathbf{x})}, \quad (10.24)$$

where $\nabla' = \nabla(1 + \bar{\nabla} \cdot \nabla v(0))^{-1/2}$. For low temperature, this natural core energy makes $\langle Q \rangle$ so small that we can include only $Q(\mathbf{x}) = 0$, ± 1 and obtain

$$\sum_{\{Q(\mathbf{x})\}} e^{-(4\pi^2\widehat{\beta}/2)} {}^{(0)} e^{2\pi i \Sigma_x Q(\mathbf{x})A(\mathbf{x})} \sim 1 + 2e^{-(4\pi^2\widehat{\beta}/2)r(0)} \sum_A \cos 2\pi A(\mathbf{x})$$

$$\sim \exp[2e^{-(4\pi^2\widehat{\beta}/2)r(0)}\Sigma_x\cos 2\pi A(\mathbf{x})]. \quad (10.25)$$

Thus, for low temperature and long wavelengths, the field has the approximate energy density

$$\tfrac{1}{2}[(\nabla A)^2 + 4\widehat{\beta} e^{-(4\pi^2/2)\widehat{\beta}r(0)} \cos 2\pi A(\mathbf{x})]. \quad (10.26)$$

The $A^2(\mathbf{x})$ part in the cosine gives rise to a mass

$$m^2 = 4\widehat{\beta} \frac{4\pi^2}{2} e^{-(4\pi^2\widehat{\beta}/2)r(0)}. \quad (10.27)$$

Thus, for any non-zero density of monopoles, however small, there is

always screening of the magnetic potential $\varphi(\mathbf{x})$ down to a finite length scale $1/m$. This is the magnetic analogue of the screening of the electric fields in an electron gas which was first explained by Debye. It was noticed by Polyakov that a mechanism if this type could be invoked to explain the permanent confinement of electric charges in quark physics.

Having shown that compact magnetostatics is equivalent to a gas of magnetic monopoles alone we are now prepared to make final contact with the previous partition function of the Z_n Villain model. For this we restrict the field variables $\widehat{A}_i(\mathbf{x})$ in the same way to discrete values

$$\widehat{A}_{\nu_i}(\mathbf{x}) \equiv \frac{2\pi}{n} \nu_i(\mathbf{x}) \tag{10.28}$$

as we did before with the field variables $\gamma(\mathbf{x})$ in the spin model. This gives

$$\widehat{Z}_{\hat{n}} = \frac{1}{\hat{n}^{2N}} \sum_{\{\nu_1(\mathbf{x}), \nu_2(\mathbf{x})\}} \delta_{\nu_3, 0} \sum_{\{m_{ij}(\mathbf{x})\}} e^{-(\beta/2)\Sigma_\mathbf{x}(\nabla_i \widehat{A}_{\nu_j}(\mathbf{x}) - \nabla_j \widehat{A}_{\nu_i}(\mathbf{x}) - 2\pi m_{ij}(\mathbf{x}))^2}, \tag{10.29}$$

where we are working in the axial gauge (here $\nu_3(\mathbf{x}) \equiv 0$).

We may now introduce integer numbers $\ell_i(\mathbf{x})$ which enforce the discrete values of $\widehat{A}_{\nu_i}(\mathbf{x})$ via a sum

$$\frac{1}{\hat{n}^{2N}} \sum_{\{\hat{\nu}_1(\mathbf{x}), \hat{\nu}_2(\mathbf{x})\}} \delta_{\nu_3, 0} = \sum_{\{\ell_1(\mathbf{x}), \ell_2(\mathbf{x})\}} \delta_{\ell_3, 0} \prod_\mathbf{x} \left[\int d\widehat{A}_1(\mathbf{x}) d\widehat{A}_2(\mathbf{x}) \right] e^{i\hat{n}\Sigma_\mathbf{x} \ell_i(\mathbf{x}) \widehat{A}_i(\mathbf{x})},$$
$$\tag{10.30}$$

so that $\widehat{Z}_{\hat{n}}$ becomes

$$\widehat{Z}_{\hat{n}} = \sum_{\{\ell_i(\mathbf{x})\}} \delta_{\ell_3(\mathbf{x}), 0} \prod_\mathbf{x} \left[\int d\widehat{A}_1(\mathbf{x}) d\widehat{A}_2(\mathbf{x}) \right] e^{-(\beta/2)\Sigma_\mathbf{x}(\nabla_i \widehat{A}_j - \nabla_j \widehat{A}_i - 2\pi m_{ij})^2 + i\hat{n}\Sigma_\mathbf{x} \ell_i(\mathbf{x}) \widehat{A}_i(\mathbf{x})}. \tag{10.31}$$

Since $A_3(\mathbf{x})$ is zero, we can always complete the sum over $\ell_i(\mathbf{x})$ with $\ell_3(\mathbf{x}) \equiv 0$ to a sum over $\ell_i(\mathbf{x})$ which form closed loops with $\ell_3(\mathbf{x}) = -(1/\overline{\nabla}_3)(\overline{\nabla}_1 \ell_1 + \overline{\nabla}_2 \ell_2)$ [recall the discussion in Chapter 5 after Eq. (5.114)]. We may now integrate out the fields $\widehat{A}_1(\mathbf{x})$, $\widehat{A}_2(\mathbf{x})$ and obtain the following representation

$$\hat{Z}_{\hat{n}} = \det(-\bar{\nabla} \cdot \nabla)^{-1/2} \frac{1}{(\sqrt{2\pi\hat{\beta}})^{2N}} \sum_{\{Q(\mathbf{x})\}} \sum_{\{\ell_i(\mathbf{x})\}} e^{-(4\pi^2/2)\hat{\beta}\Sigma_\mathbf{x} Q(\mathbf{x})(1/-\bar{\nabla}\cdot\nabla)Q(\mathbf{x})}$$

$$\times \, e^{-(\hat{n}^2/2\hat{\beta})\Sigma_\mathbf{x}\ell_i(\mathbf{x})(1/-\bar{\nabla}\cdot\nabla)\ell_i(\mathbf{x}) + 2\pi i\hat{n}\Sigma_\mathbf{x}(\nabla\times\mathbf{m})_i(1/-\bar{\nabla}\cdot\nabla)\ell_i(\mathbf{x})}, \qquad (10.32)$$

where $Q(\mathbf{x}) = \bar{\nabla}_i m_i(\mathbf{x}) = (1/2)\nabla_i \varepsilon_{ijk} m_{jk}(\mathbf{x}).$[d]

This is the desired result. Apart from a smooth overall factor $(2\pi\hat{\beta})^N / (2\pi\beta)^{N/2}$, the partition functions Z_n and $\hat{Z}_{\hat{n}}$ are exactly the same sums over magnetic monopoles and vortex lines. The magnetic charges can be made equal by setting

$$\frac{n^2}{\beta} = 4\pi^2\hat{\beta}. \qquad (10.33)$$

The vortex lines have the same coupling strength by the identification

$$4\pi^2\beta = \frac{\hat{n}^2}{\hat{\beta}}. \qquad (10.34)$$

The two equations are solved uniquely by

$$n = \hat{n}, \qquad 4\pi^2\beta\hat{\beta} = n^2. \qquad (10.35)$$

Then

$$Z_n = \frac{n^{2N}}{(2\pi\beta)^{3N/2}}\hat{Z}_n = \frac{(2\pi\hat{\beta})^{3N/2}}{n^N}\hat{Z}_n, \qquad (10.36)$$

and we can conclude that the two models, the Z_n Villain spin model and the $\hat{Z}_n$ Villain form of the Abelian lattice gauge theory are completely equivalent.

This opens up a curious way of studying the vortex lines of the Villain model. We may simulate the $\hat{Z}_n$ model for larger n. This has, for low $\hat{\beta}$, a region below which monopoles proliferate. [For $D = 3$ this is not a proper phase transition. For $D = 4$ there is a second order phase transition at $\hat{\beta}_c \cong 0.63$; see Table 7.4.] For $\hat{\beta} \sim 0.076$ the model has a transition point above which the vortex lines proliferate. By studying this transition and plotting the thermodynamic functions over $\beta = n^2/(4\pi^2\hat{\beta})$ we must obtain

[d]The last Boltzmann factor can, of course, be rewritten as $e^{2\pi i\hat{n}\Sigma_\mathbf{x} Q(\mathbf{x})(1/-\bar{\nabla}\cdot\nabla)Q(\mathbf{x})}$ where $\ell_i(\mathbf{x}) = (\nabla \times \mathbf{n})_i(\mathbf{x}).$

the same result as we would by a direct simulation of the Villain model (if n is sufficiently large).

We conclude this section with the remark that instead of Z_n variables $\widehat{A}_{\nu_i}(\mathbf{x})$ we could, of course, have used continuous angular variables $A_i(\mathbf{x})$ and introduced the vortex loops $\ell_i(\mathbf{x})$ via a generalized magnetic field of order $\hat{n}$:

$$(\sqrt{2\pi\hat{n}})^{DN} \sum_{\{\nu_i(\mathbf{x})\}} e^{-(\hat{n}/2)\Sigma_\mathbf{x}(A_i(\mathbf{x}) - (2\pi/\hat{n})\nu_i(\mathbf{x}))^2}. \qquad (10.37)$$

Following the steps (10.12)–(10.14) this becomes

$$\sum_{\{\ell_i(\mathbf{x})\}} e^{-(1/2\hat{n})\Sigma_\mathbf{x}\ell_i^2(\mathbf{x}) + i\hat{n}\Sigma_\mathbf{x}\ell_i(\mathbf{x})A_i(\mathbf{x})}, \qquad (10.38)$$

which is the same as the coupling in (10.31) except for the Boltzmann factor due to an extra core energy

$$e^{-(1/2\hat{n})\Sigma_\mathbf{x}\ell_i^2(\mathbf{x})}.$$

Thus it is possible to study the proliferation of vortex lines *with different core energies* by looking at the Villain form of lattice gauge theory $\widehat{Z}_n$, investigating the behaviour of the transition at $\hat{\beta} \sim 0.076n^2$ for different magnetic fields $\hat{n}$, and plotting all the results as functions of $\beta = n^2/(4\pi^2\hat{\beta})$.

Conversely, one could study the lattice gauge theory by simulating the Z_n spin model in a magnetic field h^e and looking at the behaviour near $\beta \approx 0.04n^2$.

10.4. Z_n COSINE MODELS

The dual equivalence between the Z_n Villain model and the Z_n Villain form of lattice gauge theory can be found in a somewhat weaker form also for models with a cosine energy. Consider the Z_n spin model

$$Z_n' = \frac{1}{n^N} \sum_{\{\nu(\mathbf{x})\}} e^{\beta\Sigma_{\mathbf{x},i}\cos\nabla_i\gamma_\nu(\mathbf{x})}. \qquad (10.39)$$

Expanding the exponent in terms of modified Bessel functions gives

---

eThis is done in practice, see Bhanot and Creutz, cited in the Notes and References.

$$Z'_n = \frac{1}{n^N} \sum_{\{\nu(\mathbf{x})\}} \sum_{\{b_i(\mathbf{x})\}} I_{b_i(\mathbf{x})}(\beta) \, e^{i \Sigma_{\mathbf{x}} b_i(\mathbf{x}) \nabla_i \gamma_\nu(\mathbf{x})}. \tag{10.40}$$

We now observe that since $\nabla_i \gamma_\nu(\mathbf{x})$ are integer multiples of $2\pi/n$, the phase $\exp(ib_i \nabla_i \gamma_\nu)$ is periodic under the replacements

$$b_i(\mathbf{x}) \rightarrow b_i(\mathbf{x}) + n p_i(\mathbf{x}). \tag{10.41}$$

We may therefore execute the sum over these periods directly in the modified Bessel functions and define the periodic function in $b \in (0, p)$

$$I_b^n(\beta) \equiv \cdot \sum_{p=-\infty}^{\infty} I_{b+np}(\beta). \tag{10.42}$$

The explicit calculation of this sum proceeds via the integral representation

$$I_b^n(\beta) = \sum_p \int \frac{d\gamma}{2\pi} e^{\beta \cos \gamma + i(b + np)} = \frac{1}{n} \sum_{\nu=0}^{n-1} e^{\beta \cos \gamma_\nu} \cos b \gamma_\nu, \quad \gamma_\nu \equiv \frac{2\pi}{n} \nu. \tag{10.43}$$

Hence $I_b^n(\beta)$ are simply the Z_n versions of the Bessel integrals $\int_{-\pi}^{\pi} (d\gamma/2\pi) \exp(\beta \cos \gamma) \cos b\gamma$.

Using $I_b^n(\beta)$, Eq. (10.40) takes the form

$$Z'_n = \frac{1}{n^N} \sum_{\{\nu(\mathbf{x})\}} \sum_{b_i(\mathbf{x})=0}^{n-1} \prod_{\mathbf{x},i} I_{b_i(\mathbf{x})}^n(\beta) \, e^{-i \Sigma_{\mathbf{x}} \bar{\nabla}_i b_i(\mathbf{x}) \gamma_\nu(\mathbf{x})}. \tag{10.44}$$

Performing the sum over $\gamma_\nu(\mathbf{x})$ results in the conservation law

$$\bar{\nabla}_i b_i(\mathbf{x}) = n Q(\mathbf{x}) \tag{10.45}$$

with arbitrary integer field $Q(\mathbf{x})$. Without referring to $Q(\mathbf{x})$ we may also say

$$\bar{\nabla}_i b_i(\mathbf{x}) = 0 \quad \mathrm{mod} \ n. \tag{10.46}$$

Hence the partition function (10.40) becomes

$$Z'_n = \sum_{b_i(\mathbf{x})=0}^{n-1} \prod_{\mathbf{x},i} I_{b_i(\mathbf{x})}^n(\beta) \, \delta_{\bar{\nabla}_i b_i, 0 \, \mathrm{mod} \, n}. \tag{10.47}$$

The conservation law $\delta_{\bar{\nabla}_i b_i, 0 \bmod n}$ has the following effect: if we sum over $b_1(\mathbf{x})$, $b_2(\mathbf{x})$ independently, from 0 to $n - 1$, we may calculate a certain $b_3(\mathbf{x})$ which satisfies $\bar{\nabla}_i b_i(\mathbf{x})$ uniquely via $b_3(\mathbf{x}) = -(1/\bar{\nabla}_3)(\bar{\nabla}_i^{\perp} b_i^{\perp})$, using the boundary conditions explained in Section 4.3. In order to bring $b_3(\mathbf{x})$ into the interval $(-\pi, \pi]$, we have to shift it by an integer multiple of n after which it satisfies $\bar{\nabla}_i b_i(\mathbf{x}) = 0 \bmod n$. Since $I_b^n(\beta)$ are periodic in $b \to b + n$ we could alternatively write

$$Z_n' = \sum_{\substack{\{b_1(\mathbf{x}), b_2(\mathbf{x}) = 0, \ldots, n-1\} \\ b_3(\mathbf{x}) = -(1/\bar{\nabla}_3)(\bar{\nabla}_i^{\perp} b_i^{\perp})}} \prod_{\mathbf{x}, i} I_{b_i(\mathbf{x})}^n(\beta). \tag{10.48}$$

At this stage it is advantageous to introduce an integer valued gauge field $a_i(\mathbf{x})$ in the gauge $a_3(\mathbf{x}) = 0$. Setting

$$b_i(\mathbf{x}) = (\bar{\nabla} \times \mathbf{a})_i = \varepsilon_{ijk} \bar{\nabla}_j a_k(\mathbf{x} - \mathbf{k}), \tag{10.49}$$

we can reproduce the sum (10.48) by letting $a_1(\mathbf{x})$, $a_2(\mathbf{x})$ run from 0 to $n-1$. Hence the partition function takes the form

$$Z_n' = \sum_{\{a_i(\mathbf{x}) = 0, \ldots, n = 1\}} \Phi[\mathbf{a}] \prod_{\mathbf{x}, i} I_{(\bar{\nabla} \times \mathbf{a})_i(\mathbf{x})}(\beta), \tag{10.50}$$

where $\Phi[\mathbf{a}]$ is the gauge-fixing factor $\delta_{a_3, 0}$ (or any other).

Notice that the same manipulations can be effected in the Z_n Villain model in which case $I_b(\beta)$ is simply replaced by $e^{-(1/2\beta)b^2}$ and $I_b^n(\beta)$ by the periodic Gaussian $[e^{-(1/\beta)b^2}]^n = \Sigma_p e^{-(1/2\beta)(b + np)^2}$. Thus we arrive at the partition functions

$$Z_n = \sum_{\substack{\{b_1(\mathbf{x}), b_2(\mathbf{x}) = 0, \ldots, n-1\} \\ b_3(\mathbf{x}) = -(1/\bar{\nabla}_3)(\bar{\nabla}_i^{\perp} b_i^{\perp})}} \prod_{\mathbf{x}, i} [e^{-(1/2\beta)\Sigma_{\mathbf{x}} b_i(\mathbf{x})}]^n$$

$$= \sum_{\{a_i(\mathbf{x}) = 0, \ldots, n-1\}} \Phi[\mathbf{a}] \prod_{\mathbf{x}, i} [e^{-(1/2\beta)\Sigma_{\mathbf{x}}(\bar{\nabla} \times \mathbf{a})^2}]^n. \tag{10.51}$$

But let us continue with the Z_n spin model. Since $I_b^n(\beta)$ is periodic in $b \to b + n$, we can introduce a Boltzmann factor

$$I_{(n/2\pi)A}^n(\beta) \equiv e^{g_\beta(A)}, \tag{10.52}$$

for all A having discrete values of the form $(2\pi/n)v$ ($v =$ integer). This expression is periodic in $A \to A + 2\pi$ and with it, we may finally rewrite (10.50) as

$$Z'_n = \sum_{\{v_i(\mathbf{x})\}} \Phi[A_{v_i}] e^{\sum_{\mathbf{x},i<j} g_\beta(\nabla_i A_{v_j} - \nabla_j A_{v_i})}, \tag{10.53}$$

where $A_{v_i}(\mathbf{x}) = (2\pi/n) v_i(\mathbf{x})$ are discrete Z_n field variables on the unit circle, and $\Phi[A_{v_i}] = \delta_{v_i,0}$. We observe that this is a particular form of a Z_n lattice gauge theory.

The connection with the previous duality transformation is seen most directly by going to the large β limit in which case (10.39) takes the Villain form (apart from a trivial factor $e^{3\beta N}$) and (10.52) gives

$$e^{g_\beta(A)} \to \frac{e^\beta}{\sqrt{2\pi\beta}} \sum_{m=-\infty}^{\infty} e^{-(1/2\beta)(n^2/4\pi^2)(A - 2\pi m)^2}, \tag{10.54}$$

so that (10.52) has the limit

$$Z'_n \to \frac{n^{2N}}{(\sqrt{2\pi\beta})^{3N}} \left\{ \frac{1}{n^{2N}} \sum_{\{v_i(\mathbf{x})\}} \Phi[A_{v_i}] \sum_{m_{ij}(\mathbf{x})} e^{-(1/2\beta)(n^2/4\pi^2)\sum_{\mathbf{x},i<j}(\nabla_i A_{v_j} - \nabla_j A_{v_i} - 2\pi m_{ij})^2} \right\}, \tag{10.55}$$

in agreement with (10.29). It goes without saying that the cosine version of the lattice gauge theory,

$$\widehat{Z}_n = \frac{1}{n^{2N}} \sum_{\{v_i(\mathbf{x})\}} \Phi[A_{v_i}] e^{\beta \sum_{\mathbf{x},i<j}\cos(\nabla_i A_{v_j} - \nabla_j A_{v_i})}, \tag{10.56}$$

can be brought, by the same manipulations, to the dual form

$$\widehat{Z}_n = \sum_{\{\bar{f}_{ij}(\mathbf{x}) = 0,\ldots,n-1\}} \prod_{\mathbf{x},i<j} I^n_{\bar{f}_{ij}(\mathbf{x}),0}(\widehat{\beta})\, \delta_{\nabla_i \bar{f}_{ij},\,0 \bmod n}$$

$$= \sum_{\{a(\mathbf{x}) = 0,\ldots,n-1\}} \prod_{\mathbf{x}} I^n_{\varepsilon_{ijk}\nabla_k a(\mathbf{x})}(\widehat{\beta}) = \sum_{\{v(\mathbf{x})\}} e^{\sum_{\mathbf{x},i} g_{\widehat{\beta}}(\nabla_i \gamma_v)}, \tag{10.57}$$

which is a modified version of a Z_n spin model in which the energy $\beta \cos \nabla_i \gamma_v$ is replaced by the periodic function $g_\beta(\nabla_i \gamma_v)$ with the same period 2π.

10.5. HIGH TEMPERATURE SERIES OF Z_n MODELS

The high temperature series of Z_n Villain models cannot be performed on the basis of the vortex-line and monopole representations (10.7), (10.32) since one type of defects is always prolific.

The representations (10.51), however, are well suited for this purpose, and so is the corresponding series (10.48) for the Z_n spin models in the cosine form. We have to form all closed lines $b_i(\mathbf{x})$ using $b_1(\mathbf{x})$, $b_2(\mathbf{x})$ between 0 and $n - 1$ only and the weights $(e^{-(1/2\beta)b^2})^n$ or $I_b^n(\beta)$ for each element of these lines. Since the procedure is straightforward we will not go into details (see Table 4.1 for coming graphs).

10.6. Z_2 (ISING) MODEL, Z_3 (THREE-STATE POTTS) MODEL, Z_4 (ASHKIN-TELLER) MODEL

A special case of the Z_n cosine model, $n = 2$, is the best studied in statistical mechanics. It is known as the *Ising spin model*. Since its spin variables are $e^{i\gamma_v} = 1$, -1, it is usually stated in the form

$$Z_2' = \frac{1}{2^N} \sum_{\{s(\mathbf{x}) = \pm 1\}} e^{\beta \sum_{\mathbf{x},i} s(\mathbf{x})s(\mathbf{x}+i)}. \tag{10.58}$$

The high temperature expansion involves [see (10.43)]

$$I_0^2(\beta) = \tfrac{1}{2}(e^\beta + e^{-\beta}) = \cosh\beta, \qquad I_1^2(\beta) = \tfrac{1}{2}(e^\beta - e^{-\beta}) = \sinh\beta, \tag{10.59}$$

and reads

$$Z_2' = (\cosh\beta)^N \sum_{\{b_1(\mathbf{x}),b_2(\mathbf{x})=0,1\}} \prod_{\mathbf{x},i} \left(\frac{I_{b_i}^2(\beta)}{I_0^2(\beta)}\right) \delta_{\nabla_i b_i, 0 \bmod 2}. \tag{10.60}$$

Since $b_1(\mathbf{x}), b_2(\mathbf{x}) = 0, 1$ only, the ratios I_b^2/I_0^2 are 1 or $\tanh\beta$. The b_i lines are no longer oriented. In fact, we can verify that the sum involves all closed loops of unoriented lines which can occupy each link once at most. Each site can be crossed as many times (necessarily from different directions) as there are dimensions. The diagrams have been counted in Table 4.1 where $v = I_1^2/I_0^2 = \tanh\beta$ is the statistical weight of each occupied link.

The duality transformation relates Z_2' spin models to $\hat{Z}_2$ lattice gauge theories. If the lattice gauge theory has an energy $\hat{\beta}\cos(\nabla_i\hat{A}_{v_j} - \nabla_j\hat{A}_{v_i})$, the spin model has an energy [see (10.57)]

$$e^{g_{\hat{\beta}}(\gamma)} = \tfrac{1}{2}(e^{\hat{\beta}} + e^{-\hat{\beta}}\cos\gamma). \tag{10.61}$$

Since γ can only take values 0, π it is possible to express the Boltzmann factors (10.61) in terms of cosine energies,

$$R\,e^{\beta\cos\gamma} \equiv R(\cosh\beta + \sinh\beta\,\cos\gamma), \quad (\text{for } \gamma = 0,\,\pi), \tag{10.62}$$

where we have to identify

$$e^{\hat{\beta}} = 2R\,\cosh\beta, \qquad e^{-\hat{\beta}} = 2R\,\sinh\beta. \tag{10.63}$$

This shows that a $\hat{Z}_2$ gauge theory is dual to a Z_2' spin model with cosine energy if the inverse temperatures are related by

$$e^{-2\hat{\beta}} = \tanh\beta. \tag{10.64}$$

The three-dimensional Ising model is known to have a second order phase transition at

$$\beta_c = 0.22171 \quad (Z_2 \text{ spin model} = \text{Ising}). \tag{10.65}$$

This implies that the $\hat{Z}_2$ lattice gauge theory has a second order phase transition at

$$\hat{\beta} = 0.7613, \quad (\hat{Z}_2 \text{ lattice gauge theory}).$$

For the Z_3 lattice gauge theory one

$$e^{g_{\hat{\beta}}(\gamma)} = \tfrac{1}{2}(e^{\hat{\beta}} + e^{\hat{\beta}\cos 2\pi/3}\cos\gamma + e^{\hat{\beta}\cos 4\pi/3}\cos 2\gamma), \tag{10.66}$$

where γ can take the three values 0, $2\pi/3$, $4\pi/3$. The corresponding Boltzmann factors are

$$\tfrac{1}{2}(e^{\hat{\beta}} + 2e^{-\hat{\beta}/2}), \quad \gamma = 0, \tag{10.67}$$

and

$$\frac{1}{2}(e^{\hat{\beta}} - e^{-\hat{\beta}/2}), \quad \gamma = \frac{2\pi}{3}, \frac{4\pi}{3}. \tag{10.68}$$

These Boltzmann factors can also be reproduced in a Z_3 spin model with a cosine energy

$$Re^{\beta \cos \gamma}, \tag{10.69}$$

which takes the values

$$Re^{\beta} \quad \gamma = 0, \tag{10.70}$$

$$Re^{-\beta/2} \quad \gamma = \frac{2\pi}{3}, \frac{4\pi}{3}. \tag{10.71}$$

Hence we may make the identification

$$e^{-3\beta/2} = \frac{1 - e^{-3\hat{\beta}/2}}{1 + 2e^{-3\hat{\beta}/2}}. \tag{10.72}$$

The Z_3 spin model is equivalent to a three-state Pott's model and is known to have a first order phase transition at

$$\beta_c = 0.367 \quad (Z_3 \text{ spin model} = \text{three-state Potts}). \tag{10.73}$$

Hence we conclude that the Z_3 lattice gauge theory has a first order phase transition at

$$\hat{\beta}_c = 1.085 \quad (\hat{Z}_3 \text{ lattice gauge theory}). \tag{10.74}$$

Let us finally look at the Z_4 lattice gauge theory for which

$$e^{g_\beta(\gamma)} = \tfrac{1}{2}(e^{\hat{\beta}} + e^{\hat{\beta} \cos \pi/2} \cos \gamma + e^{\hat{\beta} \cos \pi} \cos 2\gamma + e^{\hat{\beta} \cos 3\pi/2} \cos 3\gamma), \tag{10.75}$$

which for $\gamma = 0, \pi/2, \pi, 3\pi/2$ takes the values

$$\frac{1}{2}(e^{\hat{\beta}} + 1 + e^{-\hat{\beta}} + 1) \quad \gamma = 0,$$

$$\frac{1}{2}(e^{\hat{\beta}} - e^{-\hat{\beta}}) \quad \gamma = \frac{\pi}{2},$$

$$\frac{1}{2}(e^{\hat{\beta}} - 1 + e^{-\hat{\beta}} - 1) \quad \gamma = \pi,$$

$$\frac{1}{2}(e^{\hat{\beta}} - e^{-\hat{\beta}}) \quad \gamma = \frac{3\pi}{2} \tag{10.76}$$

The Z_4 spin model with cosine energy, on the other hand, would have the values

$$Re^{\beta\cos\gamma} = \begin{cases} Re^{\beta} \\ R \\ Re^{-\beta} \\ R \end{cases} \text{ for } \gamma = \begin{cases} 0, \\ \dfrac{\pi}{2}, \\ \pi, \\ \dfrac{3}{2}\pi, \end{cases} \tag{10.77}$$

so that we can write

$$e^{2\beta} = \frac{\cosh\widehat{\beta} + 1}{\cosh\widehat{\beta} - 1} = \tanh^2(\widehat{\beta}/2). \tag{10.78}$$

The Z_4 spin model in three dimensions undergoes a second order phase transition at[f]

$$\beta_c = 2\beta_c(\text{Ising}) = 0.44342 \quad (Z_4 \text{ spin model} = \text{Ashkin-Teller model}), \tag{10.79}$$

so that the Z_4 lattice gauge theory has

$$\widehat{\beta}_c = 1.5226 \quad (Z_4 \text{ lattice gauge theory}). \tag{10.80}$$

The possibility of rewriting the partition function of the dual Z_2, Z_3, Z_4 spin models $Z = \prod_{\mathbf{x}} \left[\int_{-\pi}^{\pi} \dfrac{d\gamma(\mathbf{x})}{2\pi} \right] e^{\sum_{\mathbf{x},i} \beta_\beta(\nabla_i\gamma)}$ exactly in cosine form was a consequence of the fact that the Boltzmann factors can take only two different values which can be accounted for by $Re^{\beta\cos\nabla_i\gamma}$ with an appropriate choice of R and β.

It is clear that this is true for *any* field energy, as long as it is a periodic (non-trivial) function in $\nabla_i\gamma(\mathbf{x})$. For example, we can bring the Z_2, Z_3, Z_4 spin models to a Villain form

$$Z = R_V^{DN} \prod_{\mathbf{x}} \left[\int_{-\pi}^{\pi} \frac{d\gamma(\mathbf{x})}{2\pi} \right] \sum_{\{n_i(\mathbf{x})\}} e^{-(\beta_V/2)(\nabla_i\gamma - 2\pi n_i)}. \tag{10.81}$$

[f]The partition function can be shown to factorize $Z_4 = [Z_2(\text{Ising})]^2$; see M. Suzuki, *Prog. Theor. Phys.* **37** (1967) 770.

For Z_2 we merely have to equate

$$e^{\hat{\beta}} = R_V \sum_n e^{-(\beta_V/2)(2\pi n)^2} = R_V \frac{1}{\sqrt{2\pi\beta_V}} \sum_b e^{-(1/2\beta_V)b^2}, \qquad (10.82)$$

$$e^{-\hat{\beta}} = R_V \sum_n e^{-(\beta_V/2)(\pi - 2\pi n)^2} = R_V \frac{1}{\sqrt{2\pi\beta_V}} \sum_b (-)^b e^{-(1/2\beta_V)b^2}, \qquad (10.83)$$

which replaces (10.63). Observe that the latter result implies that these models have an *exact* "Villain approximation." Instead of writing the ansatz (7.1)

$$e^{\beta\cos\gamma} \approx R_V \sum_n e^{-(\beta_V/2)(\gamma - 2\pi n)^2}, \qquad (10.84)$$

performing the Fourier decomposition

$$\sum_b I_b(\beta) e^{ib\gamma} \approx R_V \frac{1}{\sqrt{2\pi\beta_V}} \sum_b e^{-(1/2\beta_V)b^2} e^{ib\gamma}, \qquad (10.85)$$

and equating only the lowest two terms, as Villain did [see (7.6), (7.7)] to obtain his approximation, we can now make both sides *identically equal* by the choice (10.63). In a similar way we can find the exact Villain forms of the Z_3 and Z_4 spin models, if desired.

NOTES AND REFERENCES

For Monte Carlo Studies of Z_n models see
G. Bhanot and M. Creutz, *Phys. Rev.* **B21** (1980) 2892.
Lattice gauge theories were introduced into quark physics by
K. Wilson, *Phys. Rev.* **D10** (1974) 2445.
   The monopole mechanism of permanent quark confinement (magnetic Debye screening) was proposed by
A. Polyakov, *Phys. Rev. Lett.* **59B** (1975) 82, *Nucl. Phys.* **B120** (1977) 429.
More details are worked out by
J.B. Bronzan and Ashok Das, *Phys. Rev.* **B26** (1982) 1415,
T. Banks, R. Myerson and J. Kogut, *Nucl. Phys.* **B129** (1977) 493.
   Further literature on discrete spin models are
S. Elitzur, R.B. Pearson and J. Shigemitsu, *Phys. Rev.* **D19** (1979) 3698.
M. Creutz, *Phys. Rev.* **D21** (1980) 1006.
   Discrete lattice gauge systems are discussed in

C.P. Korthals-Altes, *Nucl. Phys.* **B142** (1978) 315,

R. Savit, *Rev. Mod. Phys.* **52** (1980) 453

A. Ukawa, P. Windey and A.H. Guth, *Phys. Rev.* **D21** (1980) 1013.

The generalized external magnetic field is studied in the two-dimensional XY model by

J.V. José, L.P. Kadanoff, S. Kirkpatrick and D.R. Nelson, *Phys. Rev.* **B16** (1977) 1217.

For the critical values of β_c in the 3-D Ising model see

M. Fisher, D.S. Gaunt, *Phys. Rev.* **133** (1964) H225;

in the three-state Pott's model,

H.W.J. Blöte and R.H. Swendsen, *Phys. Rev. Lett.* **43** (1979) 799;

in the Z_n spin model,

M. Suzuki, *Prog. Theor. Phys.* **37** (1967) 770.

TWO-DIMENSIONAL CONSIDERATIONS

11.1. FILMS OF SUPERFLUID HELIUM

Since superfluid ^{4}He possesses extremely good wetting properties, it is possible to produce extended and rather uniform surface layers. An excellent adsorbent material is "grafoil" which is a commercial product of Union Carbide, New York (or equivalently "papyex" made by Lorraine, Paris). It consists of exfoliated natural graphite, rolled into flexible sheets and having adsorption areas of $20\,\mathrm{m^2/gram}$. The thickness of such layers can be reduced to a few Angströms which, close to the transition temperature, is much smaller than the coherence length $\xi(T)$. Such thin layers can be considered, to a certain approximation, as a two-dimensional superfluid and its critical properties should be described by the two-dimensional XY model, its Villain approximation or the Villain model.

The case of two dimensions is quite special since, if a system were to have long-range modes, the correlation function

$$\int \frac{d^2q}{(2\pi)^2} e^{i\mathbf{q}\cdot\mathbf{x}} \frac{1}{q^2} \qquad (11.1)$$

would diverge. It was observed a long time ago by Landau and Peierls that this would prevent the existence of a proper long-range order and

thus the formation of a condensate in which the order parameter takes a non-vanishing expectation value. Nevertheless, there does exist a continuous phase transition. This transition has been studied by many workers and its properties are now reasonably well understood.

For our purposes of developing gauge theories in various systems, the two-dimensional case is really not very interesting. It is degenerate in the sense that the gauge structure of superflow which is present in three (and more) dimensions is accidentally absent. The vortex gauge structure, however, is fully present and the comparison between the $D = 3$ and $D = 2$ cases is instructive.

11.2. HIGH TEMPERATURE EXPANSION OF $D = 2\,XY$ MODEL

The high temperature expansions in two and three dimensions differ very little. The partition functions (5.7), (6.23) of the XY model and their Villain approximations (7.15), (7.18) are

$$Z' = \prod_{\mathbf{x}} \left[\int_{-\pi}^{\pi} \frac{d\gamma(\mathbf{x})}{2\pi} \right] e^{\beta \Sigma_{\mathbf{x},i} \cos \nabla_i \gamma(\mathbf{x})} = I_0(\beta)^{2N} \sum_{\{b_i(\mathbf{x})\}} \delta_{\bar{\nabla}_i b_i, 0}\, e^{\Sigma_{\mathbf{x},i} \log(I_{b_i(\mathbf{x})}(\beta)/I_0(\beta))},$$

$$(11.2)$$

$$Z'_V = [R_V(\beta)]^{2N} Z_{VM} = [R_V(\beta)]^{2N} \prod_{\mathbf{x}} \left[\int_{-\pi}^{\pi} \frac{d\gamma(\mathbf{x})}{2\pi} \right] \sum_{\{n_i(\mathbf{x})\}} e^{-(\beta_V/2)\Sigma_{\mathbf{x},i}(\nabla_i \gamma - 2\pi n_i)^2}$$

$$= [R_V(\beta)]^{2N} \frac{1}{(\sqrt{2\pi\beta_V})^{2N}} \sum_{\{b_i(\mathbf{x})\}} \delta_{\bar{\nabla}_i b_i, 0}\, e^{-(1/2\beta_V)\Sigma_{\mathbf{x}} b_i^2(\mathbf{x})}, \qquad (11.3)$$

and the sum over integers $b_i(\mathbf{x})$ with $\bar{\nabla}_i b_i(\mathbf{x}) = 0$ is a sum over all unit valued, closed non-backtracking magnetic field lines. It can be performed just as before, the two-dimensional graphs being simpler to count. Since we have derived the expansion in Section 4.3 for general D, the free energy can directly be written down (see Tables 4.6 and 4.9)

$$-\beta f' = 2\log I_0(\beta) + 2\left(\frac{I_1(\beta)}{I_0(\beta)}\right)^4 + 4\left(\frac{I_1(\beta)}{I_0(\beta)}\right)^6 + \frac{49}{8}\left(\frac{I_1(\beta)}{I_0(\beta)}\right)^8$$

$$+ \frac{35}{6}\left(\frac{I_1(\beta)}{I_0(\beta)}\right)^{10} + \dots$$

$$= 2\left(\frac{\beta}{2}\right)^2 + \frac{3}{2}\left(\frac{\beta}{2}\right)^4 + \frac{2}{9}\left(\frac{\beta}{2}\right)^6 - \frac{31}{3 \cdot 2^5}\left(\frac{\beta}{2}\right)^8 - \frac{731}{300}\left(\frac{\beta}{2}\right)^{10} + \dots \quad (11.4)$$

It was plotted before in Fig. 4.5. Since for $D = 2$ the counting of diagrams is much simpler than in the general case it can be carried with not too much effort, up to $(I_1/I_0)^{12}$ (see Table 4.10)

$$-\beta f^{(12)} = -8\frac{485}{648}\left(\frac{I_1(\beta)}{I_0(\beta)}\right)^{12}. \tag{11.5}$$

This is equivalent to adding

$$-\beta f^{(12)} = -6\frac{3319}{4320}\left(\frac{\beta}{2}\right)^{12} \tag{11.5'}$$

to the $(\beta/2)^n$ expansion. Notice that the last three coefficients are negative so that it makes no sense to apply the ratio analysis in estimating the critical temperature. This anomalous behaviour indicates the absence of a usual singularity of the type $(\beta - \beta_c)^{-\alpha}$ in the specific heat in two dimensions.

For the free energy of the Villain model we have to replace $I_b(\beta)/I_0(\beta)$ by $e^{-b^2/(2\beta_V)}$ and the corresponding expansion is

$$-\beta f_{VM} = -\log(2\pi\beta_V) + 2e^{-4/2\beta_V} + 4e^{-6/2\beta_V} + 4e^{-8/2\beta_V}$$
$$- 4e^{-10/2\beta_V} - 33\tfrac{1}{4}e^{-12/2\beta_V} + \ldots \tag{11.6}$$
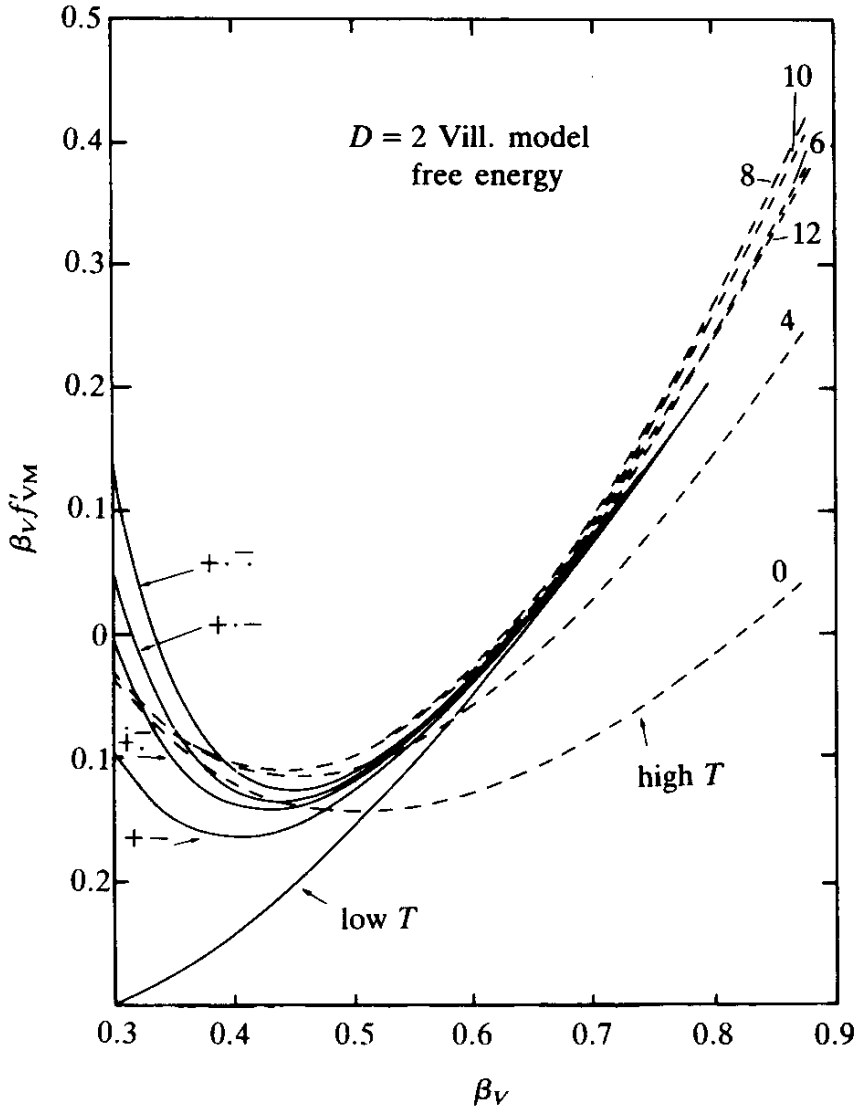
This is plotted in Fig. 11.1.[a] The expansions (11.4) and (11.6) make it trivial to calculate the internal energy and specific heat of the XY and the Villain models. The powers $(\beta/2)^n$ in (11.4), (11.5') become $-(n/2)(\beta/2)^{n-1}$, $n(n-1)(\beta/2)^n$ and the Boltzmann factors $e^{-a/(2\beta_V)}$ in (11.6) becomes $-(a/2\beta_V^2)e^{-a/2\beta_V}$, $(a^2/4\beta_V^2 - a/\beta_V)e^{-a/(2\beta_V)}$, respectively. When the resulting expressions are plotted and compared with data obtained from a Monte Carlo simulation (see Table 11.1, 11.2) they are found to be in excellent agreement with these, practically up to the peak in the specific heat near $\beta \approx 0.9$, $\beta_V \approx 0.5$ (see Figs. 11.2–11.5).

11.3. VORTEX REPRESENTATION IN TWO DIMENSIONS

In a thin layer, the superfluid vortex lines reduce to pointlike vortices. When considering the partition functions (11.2), (11.3), these vortices are introduced in a way completely analogous to the three-dimensional case.

[a]Actually, we plot $-\beta_V f'_{VM} = 2\beta_V - \beta_V f_{VM}$.

FIG. 11.1.   Free energy $-\beta_V f'_{VM} \equiv 2\beta_V - \beta_V f_{VM}$ of the $D = 2$ Villain model in the high-
and low-temperature expansions. The different curves show the various loop contributions.
The intersection of the two expansions lies at $\beta_{Vc} \sim 0.65$, to be compared with the
(hopefully) more precise value 0.73 obtained from Monte Carlo simulations of Shugard *et
al.* (1979) and renormalization group calculations [Eq. (11.160)].

The closed non-backtracking lines of the integer-valued magnetic field
$b_i(\mathbf{x})$ are expressed as a curl of an integer valued scalar field

$$b_i(\mathbf{x}) = \varepsilon_{ij} \overline{\nabla}_j a(\mathbf{x}), \tag{11.7}$$

where $\varepsilon_{12} = -\varepsilon_{21} = 1$. In constrast to the three-dimensional case [recall
(6.5)], this decomposition has no gauge degree of freedom left. The field
$a(\mathbf{x})$ corresponds to the third component of the three-dimensional vector
potential $a_i(\mathbf{x})$.

In terms of the integer valued field $a(\mathbf{x})$, the partition functions read

$$Z' = I_0(\beta)^{2N} \sum_{\{a(\mathbf{x})\}} \exp\left\{ \sum_{\mathbf{x},i} \log(I_{\varepsilon_{ij}\overline{\nabla}_j a}(\beta)/I_0(\beta) \right\}, \tag{11.8}$$
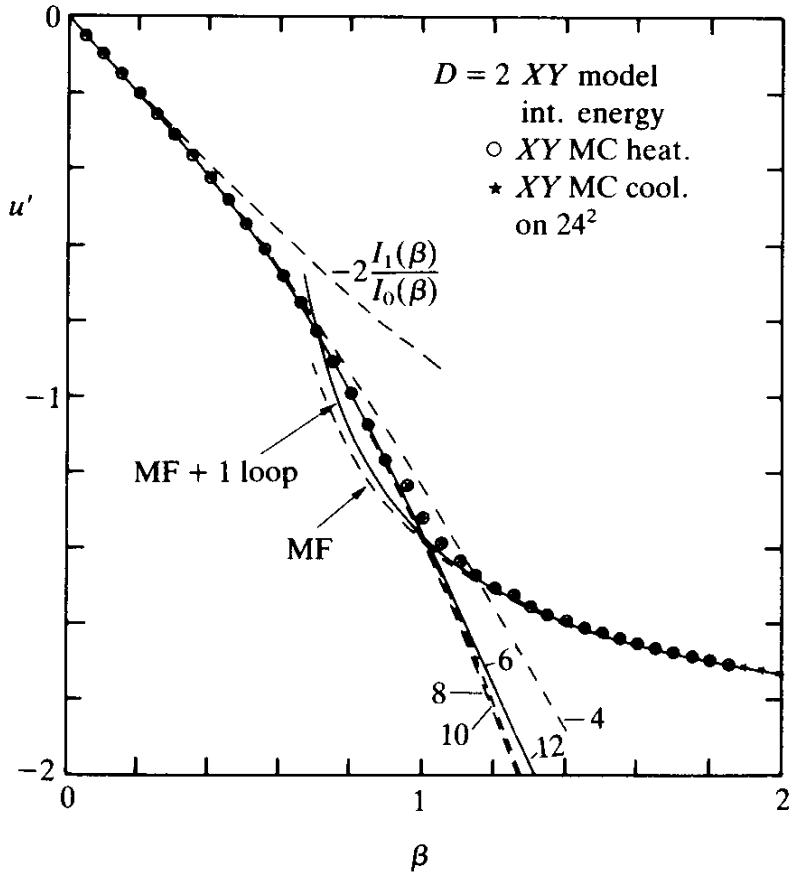
TABLE 11.1.   Monte Carlo data for the XY model in a 24^2 lattice, $U(1)$ approximated by $Z(16)$: equilibration 3500, mesurement 7000 sweeps. The words enclosed in parentheses, (heat), (cool), indicate the directions which the temperatures moves to during a cycle. The difference between the (heat) and (cool) values shows the distance from equilibrium.

β	u(cool)	u(heat)	c(cool)	c(heat)	$\langle \cos\theta \rangle$(cool)	$\langle \cos\varphi \rangle$(heat)
0.0000	1.9998	1.9996	0.0000	0.0000	0.0371	0.0369
0.0500	1.9501	1.9491	0.0026	0.0026	0.0387	0.0389
0.1000	1.8997	1.8998	0.0101	0.0098	0.0413	0.0409
0.1500	1.8490	1.8490	0.0231	0.0228	0.0433	0.0434
0.2000	1.7976	1.7964	0.0422	0.0427	0.0459	0.0463
0.2500	1.7436	1.7432	0.0678	0.0657	0.0493	0.0497
0.3000	1.6889	1.6898	0.0987	0.0966	0.0525	0.0524
0.3500	1.6335	1.6344	0.1398	0.1412	0.0568	0.0568
0.4000	1.5747	1.5749	0.1915	0.1827	0.0622	0.0624
0.4500	1.5148	1.5146	0.2622	0.2530	0.0679	0.0692
0.5000	1.4527	1.4531	0.3231	0.3278	0.0750	0.0745
0.5500	1.3863	1.3867	0.4115	0.4120	0.0847	0.0845
0.6000	1.3179	1.3179	0.5191	0.4941	0.0949	0.0977
0.6500	1.2442	1.2443	0.6153	0.6174	0.1083	0.1131
0.7000	1.1702	1.1695	0.7484	0.7431	0.1275	0.1316
0.7500	1.0938	1.0905	0.8828	0.9091	0.1576	0.1622
0.8000	1.0103	1.0061	1.0692	1.1092	0.2042	0.2112
0.8500	0.9185	0.9243	1.3267	1.2660	0.2846	0.2594
0.9000	0.8327	0.8359	1.4031	1.4431	0.3784	0.3592
0.9500	0.7416	0.8451	1.5022	1.5486	0.4970	0.4986
1.0000	0.6760	0.6677	1.3942	1.2346	0.5610	0.5866
1.0500	0.6127	0.6133	1.0591	1.1279	0.6416	0.6443
1.1000	0.5673	0.5687	0.9935	0.9740	0.6750	0.6723
1.1500	0.5312	0.5306	0.8810	0.9073	0.7009	0.6986
1.2000	0.5000	0.5008	0.8770	0.8450	0.7189	0.7154
1.2500	0.4719	0.4712	0.7876	0.7756	0.7390	0.7386
1.3000	0.4481	0.4487	0.7796	0.7792	0.7524	0.7466
1.3500	0.4272	0.4270	0.7332	0.7388	0.7609	0.7633
1.4000	0.4083	0.4076	0.7027	0.7246	0.7739	0.7723
1.4500	0.3905	0.3912	0.6916	0.6775	0.7863	0.7819
1.5000	0.3749	0.3753	0.6543	0.6773	0.7922	0.7937
1.5500	0.3610	0.3611	0.6495	0.6501	0.7980	0.7977
1.6000	0.3482	0.3475	0.6674	0.6527	0.8068	0.8085
1.6500	0.3361	0.3357	0.6282	0.6434	0.8117	0.8157
1.7000	0.3239	0.3242	0.6086	0.6453	0.8210	0.8205
1.7500	0.3133	0.3135	0.6237	0.6301	0.8254	0.8270
1.8000	0.3037	0.3035	0.6011	0.6061	0.8323	0.8380
1.8500	0.2947	0.2944	0.6259	0.5998	0.8342	0.8371
1.9000	0.2861	0.2859	0.6289	0.6126	0.8386	0.8418
1.9500	0.2774	0.2775	0.5994	0.6176	0.8478	0.8472
2.0000	0.2702	0.2694	0.6135	0.5981	0.8504	0.8527

TABLE 11.2. Internal energy and specific heat of the Villain model and the Villain approximation to the XY model: Monte Carlo data on 24^2 lattice, 3500 equil. + 7000 measuring sweeps.

β	β_V	u_{VM}(heat)	u_{VM}(cool)	c_{VM}(heat)	c_{VM}(cool)	u_V(heat)	u_V(cool)	c_V(heat)	c_V(cool)
0.05	0.1355	7.3772	7.3777	1.0010	1.0006	1.9492	1.9495	0.0026	0.0025
0.10	0.1668	5.9933	5.9926	0.9989	1.0016	1.8998	1.8993	0.0098	0.0101
0.15	0.1928	5.1830	5.1829	1.0038	1.0093	1.8489	1.8488	0.0228	0.0236
0.20	0.2167	4.6052	4.6069	1.0189	1.0113	1.7964	1.7972	0.0427	0.0414
0.25	0.2396	4.1549	4.1578	1.0218	1.0295	1.7431	1.7444	0.0657	0.0675
0.30	0.2620	3.7864	3.7876	1.0336	1.0523	1.6899	1.6904	0.0958	0.1007
0.35	0.2844	3.4701	3.4678	1.0703	1.0749	1.6346	1.6336	0.1388	0.1402
0.40	0.3069	3.1863	3.1861	1.0899	1.1002	1.5752	1.5751	0.1834	0.1870
0.45	0.3297	2.9325	2.9338	1.1577	1.1551	1.5149	1.5155	0.2533	0.2522
0.50	0.3529	2.7022	2.6990	1.1997	1.2007	1.4535	1.4519	0.3225	0.3231
0.55	0.3766	2.4835	2.4835	1.2419	1.2641	1.3875	1.3875	0.4008	0.4117
0.60	0.4008	2.2812	2.2797	1.2931	1.3211	1.3207	1.3199	0.4929	0.5081
0.65	0.4257	2.0837	2.0835	1.3572	1.3604	1.2485	1.2484	0.6034	0.6053
0.70	0.4512	1.8991	1.8995	1.4166	1.4696	1.1756	1.1758	0.7224	0.7565
0.75	0.4774	1.7214	1.7194	1.4820	1.4762	1.0999	1.0988	0.8574	0.8538
0.80	0.5044	1.5497	1.5526	1.5207	1.5492	1.0213	1.0229	0.9851	1.0059
0.85	0.5321	1.3938	1.3894	1.6053	1.5664	0.9457	0.9433	1.1573	1.1269
0.90	0.5605	1.2341	1.2336	1.6119	1.5782	0.8627	0.8625	1.2789	1.2500
0.95	0.5898	1.0959	1.0907	1.6135	1.6019	0.7873	0.7842	1.3971	1.3881
1.00	0.6199	0.9709	0.9732	1.3290	1.3392	0.7154	0.7168	1.2395	1.2487
1.05	0.6508	0.8766	0.8748	1.0487	1.0350	0.6588	0.6577	1.0491	1.0357
1.10	0.6826	0.8052	0.8088	0.9221	0.9678	0.6140	0.6163	0.9872	1.0350
1.15	0.7152	0.7483	0.7489	0.8109	0.7834	0.5768	0.5773	0.9241	0.8928
1.20	0.7486	0.7005	0.7018	0.7132	0.7229	0.5443	0.5452	0.8611	0.8719
1.25	0.7829	0.6603	0.6617	0.6678	0.6572	0.5159	0.5169	0.8481	0.8344
1.30	0.8180	0.6264	0.6271	0.6043	0.6323	0.4912	0.4917	0.8029	0.8383
1.35	0.8539	0.5946	0.5959	0.5899	0.5847	0.4674	0.4683	0.8140	0.8064
1.40	0.8907	0.5675	0.5673	0.5672	0.5640	0.4466	0.4464	0.8082	0.8040
1.45	0.9282	0.5434	0.5419	0.5571	0.5191	0.4277	0.4265	0.8143	0.7619
1.50	0.9666	0.5206	0.5197	0.5263	0.5362	0.4095	0.4088	0.7872	0.8022
1.55	1.0057	0.4983	0.4989	0.5116	0.5166	0.3915	0.3920	0.7796	0.7866
1.60	1.0456	0.4790	0.4790	0.5296	0.5222	0.3758	0.3758	0.8168	0.8054
1.65	1.0862	0.4604	0.4601	0.5155	0.5071	0.3605	0.3603	0.8031	0.7903
1.70	1.1276	0.4428	0.4434	0.5120	0.5098	0.3460	0.3465	0.8031	0.7992
1.75	1.1696	0.4271	0.4277	0.5061	0.5106	0.3330	0.3335	0.7962	0.8029
1.80	1.2123	0.4118	0.4121	0.4971	0.4887	0.3203	0.3206	0.7822	0.7683
1.85	1.2557	0.3978	0.3975	0.5127	0.5159	0.3087	0.3084	0.8064	0.8120
1.90	1.3997	0.3839	0.3842	0.4965	0.4915	0.2972	0.2975	0.7767	0.7680
1.95	1.3443	0.3711	0.3716	0.5041	0.4974	0.2866	0.2870	0.7851	0.7733
2.00	1.3994	0.3594	0.3590	0.5204	0.5031	0.2771	0.2767	0.8066	0.7774

FIG. 11.2. Internal energy of the two-dimensional XY model (in a Z_{16} approximation) from a Monte Carlo simulation on a square 24^2 lattice using a Z_{16} approximation and $3500 + 7000$ sweeps for equilibration and measurement, respectively. The low curves show the high-temperature expansion which agrees very well with the data. The high β curves show the mean field plus one-loop approximation.

$$Z_{VM} = \frac{1}{(\sqrt{2\pi\beta_V})^{2N}} \sum_{\{a(x)\}} e^{-(1/2\beta_V \Sigma_x)(\nabla a(x))^2}. \qquad (11.9)$$
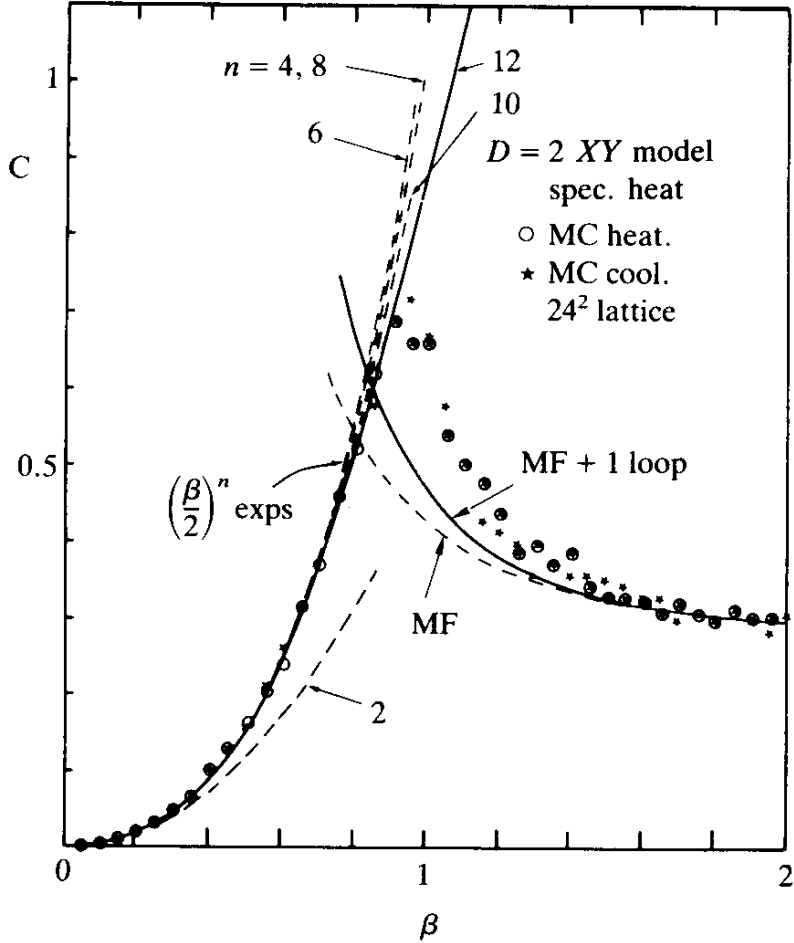
This representation shows that the two-dimensional Villain model is equivalent to another simple model of statistical mechanics,

$$Z_{DG} = \sum_{\{a(x)\}} e^{-(\beta_{DG}/2)\Sigma_x(a(x+i) - a(x))^2} = \sum_{\{a(x)\}} e^{-(\beta_{DG}/2)\Sigma_x(\nabla a)^2}, \qquad (11.10)$$

called the *discrete Gaussian model*. This model has been used to study the roughening transition of a solid-liquid interface. Because of its physical importance it will be discussed in some more detail later in Section 11.16.

Here we only remark that if the thermodynamic function $-\beta_{DG}f_{DG}$, u_{DG}, c_{DG} are extracted from Z_{DG} via the usual rules, they are obviously related to the corresponding quantities of the Villain model as follows:

FIG. 11.3.   Specific heat of the 2D XY model with the same curves and Monte Carlo run as in Fig. 11.2. Now there is considerable discrepancy between the mean field plus one-loop approximation and the data due to the neglect of vortices.
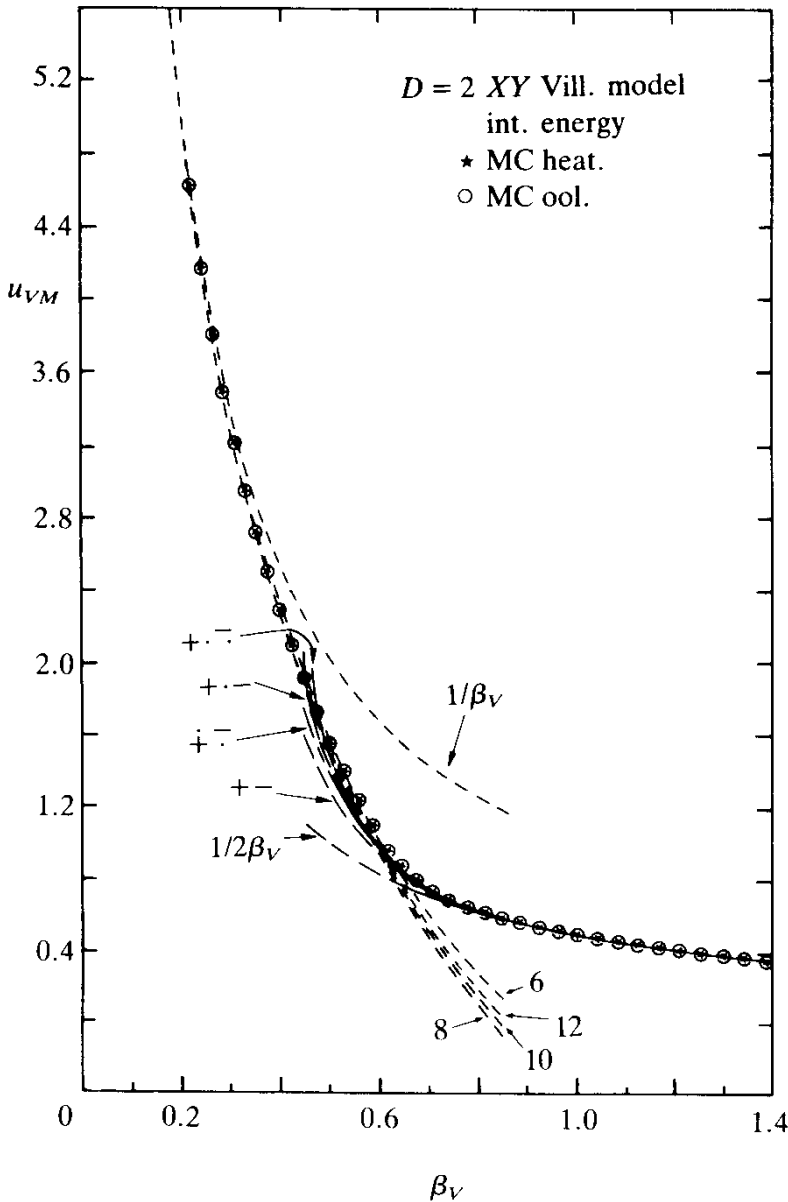
$$-\beta_V f_{VM} = -\log(2\pi\beta_V) - \beta_{DG}f_{DG}, \quad \beta_V = \frac{1}{\beta_{DG}},$$

$$u_{VM} = \frac{1}{\beta_V} - \beta_{DG}^2 u_{DG},$$

$$c_{VM} = 1 + c_{DG} - 2\beta_{DG}u_{DG}. \tag{11.11}$$

We now continue the discussion of the Villain model (11.9) along the lines of Section 7.3 and make use again of the fact that the integer field $a(\mathbf{x})$ can be changed into a continuous field by coupling it to an integer valued vortex field $\ell(\mathbf{x})$ (which corresponds to $\ell_3(\mathbf{x})$ in three dimensions). Integrating the field $a(\mathbf{x})$ out yields the vortex representation of the partition function [compare (7.39)]

$$Z_{VM} = \frac{1}{(\sqrt{2\pi\beta_V})^N}\det(-\bar{\nabla}\cdot\nabla)^{-1/2} \sum_{\{\ell(\mathbf{x})\}} e^{-(4\pi^2/2)\beta_V\Sigma_{\mathbf{x},\mathbf{x}'}\ell(\mathbf{x})v(\mathbf{x}-\mathbf{x}')\ell(\mathbf{x}')}. \tag{11.12}$$

FIG. 11.4. Internal energy of the Villain model from a Monte Carlo simulation on a 24^2 lattice using a Z_{16} approximation and 3500 + 7000 sweeps for equilibrium and measurement, respectively. The data are given in Table 11.2. The curves on the left come from a high-temperature expansion up to $e^{-1/2\,\beta_V}$ those on the right from a sum over vortex pairs of increasing distances. The agreement is excellent.
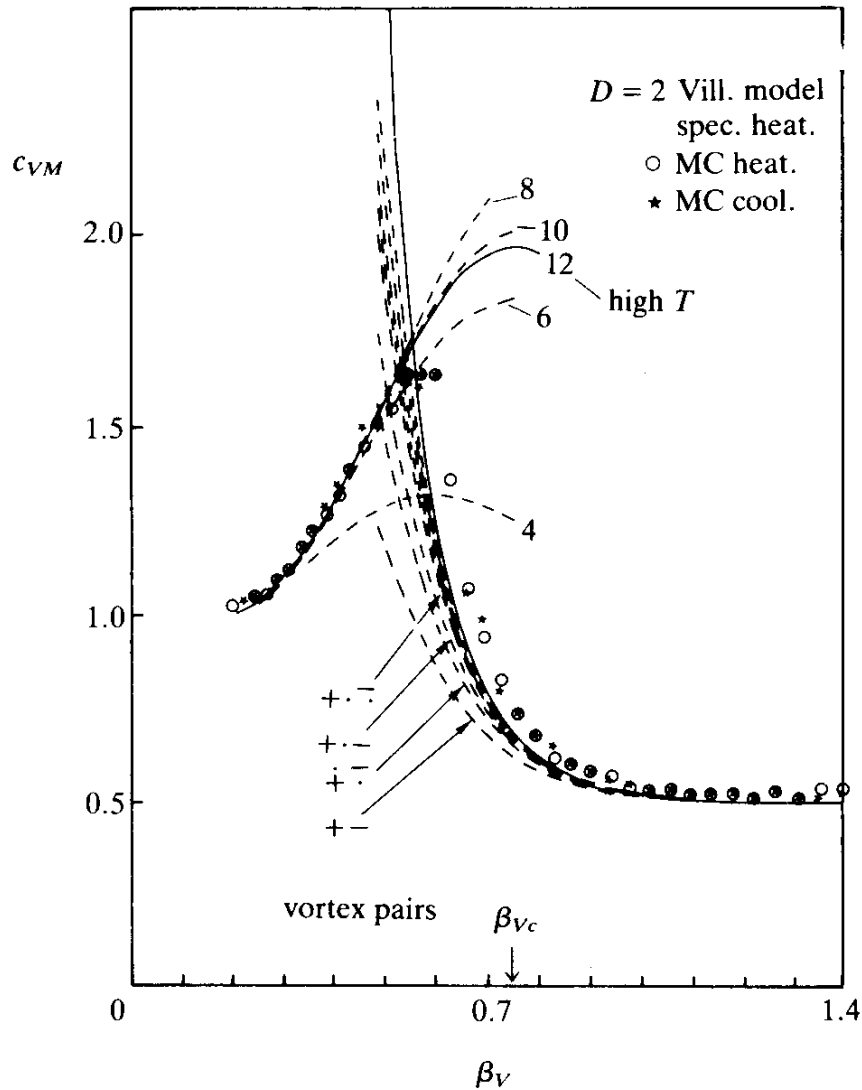
This is the partition function of a two-dimensional Coulomb gas with charges $q = 2\pi\sqrt{\beta_V}$. The potential $v(\mathbf{x})$ is divergent. We remove the infinity by a subtraction,

$$v(\mathbf{x} - \mathbf{x}') = v(0) + v'(\mathbf{x} - \mathbf{x}')$$

and the subtracted potential

$$v'(\mathbf{x} - \mathbf{x}') = v'(\mathbf{x} - \mathbf{x}') - v(0) = \int \frac{d^2k}{(2\pi)^2}(e^{i\mathbf{k}\cdot\mathbf{x}} - 1)\frac{1}{\overline{\mathbf{K}}\cdot\mathbf{K}} \qquad (11.13)$$

FIG. 11.5. Specific heat of the Villain model from the same Monte Carlo simulation of Fig. 11.4. The low β_V curve shows the high-temperature expansion up to loops of length twelve which is in good agreement with the data. The high β_V curves come from the sum of vortex pairs with increasing distances. The highest curve contains all pairs summed up for large separations via an integral of the type (11.27) plus the contribution of quadruplet $^{-}_{+}{}^{+}_{-}$ (which is the same as that of the pair $+\cdot-$).

is finite. It was calculated in (6.186) of Part I (see Table 6.6). Its asymptotic behavior is [see Eq. (I.6.202)]

$$v'(\mathbf{x}) \to -\frac{1}{2\pi}\log(|\mathbf{x}|2\sqrt{2}\,e^{\gamma}).$$
(11.14a)

This potential vanishes for $r_c = 1/(2\sqrt{2}\,e^{\gamma}) \approx 0.1985$, a length which is sometimes called the *core radius*. The inverse core radius

$$c = \frac{1}{r_c} = 2\sqrt{2}\,e^{\gamma} \approx 5.0376$$
(11.14b)

will be referred to as core parameter. If a small regulator mass m is

introduced and sent to zero at the end, the number $v(0)$ diverges like $-(1/4\pi)\log(m^2/32) \to +\infty$ [recall Eq. (6.204) in Part I. Inserting (11.13) into (11.12), the Boltzmann factor becomes

$$e^{-(\beta v/2)4\pi^2[v(0)(\Sigma_\mathbf{x}\ell(\mathbf{x}))^2 + \Sigma_{\mathbf{x}\neq\mathbf{x'}}\ell(\mathbf{x})v'(\mathbf{x}-\mathbf{x'})\ell(\mathbf{x'})]}.$$

As $m \to 0$, $v(0) \to \infty$ and only such charge configurations can contribute which have zero total charge[b]

$$\sum_\mathbf{x} \ell(\mathbf{x}) = 0. \tag{11.15}$$

It is often useful to rewrite the remaining sum in yet another way by removing from $v'(\mathbf{x})$ a further constant, namely, the value at the nearest neighbor $\mathbf{x} = 1$:

$$v'(1) = -\tfrac{1}{4}.$$

Let us call the new subtracted potential

$$v''(\mathbf{x}) \equiv v'(\mathbf{x}) - v'(1) = v(\mathbf{x}) - v(1). \tag{11.16a}$$

It behaves asymptotically almost like a pure logarithm,

$$v''(\mathbf{x}) \to -\frac{1}{2\pi}\log(|\mathbf{x}|2\sqrt{2}\,e^\gamma) + \frac{1}{4} = -\frac{1}{2\pi}\log|\mathbf{x}| - 0.0073. \tag{11.16b}$$

The advantage of this further subtraction lies in the fact that for $v''(\mathbf{x})$, the sum over the Coulomb interactions has no nearest neighbors but starts out with the next nearest neighbors. If we denote this property by a double prime on the summation symbol we can write

$$\sum_{\mathbf{x}\neq\mathbf{x'}} \ell(\mathbf{x})\,v'(\mathbf{x}-\mathbf{x'})\,\ell(\mathbf{x'}) = v'(1) \sum_{\mathbf{x}\neq\mathbf{x'}} \ell(\mathbf{x})\,\ell(\mathbf{x'}) + {\sum_{\mathbf{x}\neq\mathbf{x'}}}'' \ell(\mathbf{x})v''(\mathbf{x}-\mathbf{x'})\,\ell(\mathbf{x'}).$$

$$\tag{11.17}$$

This is useful since we know that starting from the next nearest

[b]On a finite lattice, the energy suppression is not complete since there

$$e^{-(\beta v/2)4\pi^2 v(0)(\Sigma_\mathbf{x}\ell)^2} = \left(\frac{1}{L}\right)^{\pi\beta v(\Sigma_\mathbf{x}\ell)^2}.$$

neighbour $\mathbf{x} = (1, 1)$, the lattice potential $v(\mathbf{x})$ is approximated quite well by its asymptotic form. Recall from Table 6.7 in Part I that at $\mathbf{x} = (1, 1)$, the exact value is $v'(1, 1) = -0.068$ as compared with the value from the asymptotic formula -0.0624.

Due to charge neutrality, the first term is simply

$$v'(1) \sum_{\mathbf{x}} \ell(\mathbf{x}) \sum_{\mathbf{x}' \neq \mathbf{x}} \ell(\mathbf{x}') = -v'(1) \sum_{\mathbf{x}} \ell^2(\mathbf{x}) = \frac{1}{4} \sum_{\mathbf{x}} \ell^2(\mathbf{x}). \quad (11.18)$$

Hence we can rewrite the partition function of the Villain model as the sum,

$$Z_{VM} = \frac{1}{(\sqrt{2\pi\beta_V})^N} \det(-\bar{\nabla}_i \nabla_i)^{-1/2}$$

$$\times \sum_{\{\ell(\mathbf{x})\}} \delta_{\Sigma_{\mathbf{x}} \ell(\mathbf{x}), 0} \, e^{-(\beta_V/2)4\pi^2(1/4)\Sigma_{\mathbf{x}} \ell(\mathbf{x})^2 - (\beta_V/2)4\pi^2 \Sigma''_{\mathbf{x} \neq \mathbf{x}'} \ell(\mathbf{x}) v''(\mathbf{x} - \mathbf{x}') \ell(\mathbf{x}')}. \quad (11.19)$$

The first term gives the *activation* or *core energy* for the creation of a single vortex. The quantity

$$z_1 = e^{-(\beta_V/2)4\pi^2(1/4)} \quad (11.20)$$

is usually referred to as the *fugacity*. At the critical value $\beta_{V_c} \approx 0.73$ to be determined later, this is of the order of

$$z_1 \sim 0.027. \quad (11.21)$$

Hence up to the neighbourhood of the critical temperature, the vortices are quite rare, due to their Coulomb self-energy.

11.4. LOW TEMPERATURE EXPANSION OF THE VILLAIN MODEL

For low temperatures, the Coulomb gas representation (11.19) can be expanded into the different configurations of charges $\ell(\mathbf{x})$. Such an expansion is similar to the expansion of the three-dimensional Villain model into vortex loops; here it is much simpler. The diagrams for this case consist of pairs of point charges of opposite signs which correspond to the intersections of the previous three-dimensional loops with the

xy-plane. We may imagine the two-dimensional model as being the limit of an anisotropic three-dimensional model, in which the coupling strength along the z direction becomes very large. Then the vortex loops are stretched out into pairs of straight "lines." Notice that the neutrality condition (11.15) is the $2D$ remnant of the closed loop condition $\overline{\nabla}_i \ell_i = 0.$[c]

The lowest diagrams come from a single pair of neighbouring charges (where the two straight lines would intersect the xy-plane). They are described by the $\ell(\mathbf{x})$ fields,

$$\ell(\mathbf{x}) = \pm(\delta_{\mathbf{x},0} - \delta_{\mathbf{x},1}), \qquad \ell(\mathbf{x}) = \pm(\delta_{\mathbf{x},0} - \delta_{\mathbf{x},2}) \qquad (11.22)$$

and will be pictured as $+-$. Their fugacity factor is

$$z_1^2 = e^{-\beta v \pi^2}. \qquad (11.23)$$

Since $v''(\mathbf{x})$ vanishes for nearest neighbors, their lowest contribution to Z_{VM} is found directly:

$$Z_{VM} = Z_0(1 + 4Ne^{-\beta v \pi^2} + \ldots), \qquad (11.24)$$
$$+ -$$

where

$$Z_0 = \frac{1}{(\sqrt{2\pi\beta_V})^N} \det(-\overline{\nabla} \cdot \nabla)^{-1/2} = \frac{1}{(\sqrt{2\pi\beta_V})^N} e^{-(N/2)1.16625} \qquad (11.25)$$

is the spin wave part of the partition function. The next contributions come from pairs in relative positions $(1, 1)$ and $(2, 0)$, $(2, 1), \ldots$ to be pictured as $\underset{+}{\cdot}\overline{\cdot}$, $+\cdot-$, $+\cdot\overline{\cdot}$, $\ldots$ Using the values of the Coulomb potential in Table 6.6 of Part I, we find

$$Z_{VM} = Z_0(1 + 4Ne^{-\beta v 4\pi^2/4} + 4Ne^{-\beta v 4\pi^2(1/\pi)} + 4Ne^{-\beta v 4\pi^2(1 - (2/\pi))}$$
$$+- \qquad\qquad \underset{+}{\cdot}\overline{\cdot} \qquad\qquad +\cdot-$$

$$+ 8Ne^{-\beta v 4\pi^2(2/\pi - 1/4)} + 4Ne^{-\beta v 4\pi^2(4/3\pi)} + 4Ne^{-\beta v 4\pi^2(17/4 - 12/\pi)})$$
$$+\cdot\overline{\cdot} \qquad\qquad +\cdot\overline{\cdot} \qquad\qquad +\cdots-$$

$$+ 8Ne^{-\beta v 4\pi^2(23/3\pi - 2)} + , \qquad (11.26)$$
$$+\cdots\overline{\cdot}$$

[c]On a finite lattice, (11.15) is violated [see the footnote to (11.15)] while $\overline{\nabla}_i \ell_i = 0$ is always still valid. The violation is due to closed loops which cross the boundary and involve periodic boundary conditions.

with the numerical values of the interaction energies being 1/4, 0.3183, 0.3634, 0.3866, 0.4244, 0.4303, 0.4408, respectively. For larger separations we can use the continuum approximation and integrate

$$N z_1^2 \, 2\pi \int_{r_0}^{\infty} dr \, r \, e^{-\beta_V 2\pi[\log(r 2\sqrt{2} e^{\gamma}) - \pi/2]} = N z_1^2 (2\sqrt{2} \, e^{\gamma} e^{-\pi/2})^{-2\pi\beta_V} \, 2\pi \int_{r_0}^{\infty} dr \, r^{(1-2\pi\beta_V)}$$

$$= N z_0^2 \, 2\pi \, \frac{r_0^{-(2\pi\beta_V - 2)}}{2\pi\beta_V - 2}, \qquad (11.27)$$

where r_0 is chosen such that the $1 + 4 + 4 + 4 + 8 + 4 + 4 + 8 = 37$ unit squares contained in the sum (11.26) are properly completed by the integral $2\pi \int_{r_0}^{\infty} dr \, r$ to a sum over the the full area of the system. Hence we have to take

$$r_0 \equiv \sqrt{\frac{37}{\pi}}.$$

The quantity z_0 is a modified fugacity,

$$z_0^2 \equiv z_1^2 (2\sqrt{2} \, e^{\gamma - \pi/2})^{-2\pi\beta_V} = (2\sqrt{2} \, e^{\gamma})^{-2\pi\beta_V} = c^{-2\pi\beta_V}, \qquad (11.28)$$

which appears naturally when separating the potential $v'(\mathbf{x})$ not into $v'(1) + v''(\mathbf{x})$ but into

$$v'(\mathbf{x}) = -\frac{1}{2\pi} \log(2\sqrt{2} e^{\gamma}) - \frac{1}{2\pi} \log|\mathbf{x}| = -v_c - \frac{1}{2\pi} \log|\mathbf{x}|, \qquad (11.29)$$

(recall (11.16)) i.e., into a constant $v_c \approx 0.2573$ and a piece which asymptotically has a *purely logarithmic* behaviour. Now v_c plays the role of the core energy and the modified fugacity reads

$$z_0 = c^{-\pi\beta_V} = e^{-(\beta_V/2) 4\pi^2 r_c}. \qquad (11.30)$$

Notice that all contributions to the partition function can be thought of as a superposition of pairs. In order to exclude double counting, all those configurations for which a plus and a minus charge fall on top of each other must be omitted (this corresponds to the previous non-backtracking

condition for the three-dimensional vortex loops). With the fugacity being rather small in the low temperature phase, the contribution of such forbidden configurations should be small as compared with the allowed ones. If this is so we can go to the grand canonical ensemble by simply exponentiating the series (11.26) for a single pair. For the free energy this amounts to the fugacity expansion

$$-\beta_V f_{VM} \approx -\frac{1}{2}\log(2\pi\beta_V) - \frac{1}{2}1.16625 + 4e^{-\beta_V\pi^2} + 4e^{-\beta_V 4\pi}$$
$$+ - \qquad + \stackrel{.}{\cdot}{}^{-}$$

$$+ 4e^{-\beta_V\pi^2(4 - 8/\pi)} + 8e^{-\beta_V\pi^2(8/\pi - 1)} + \ldots + z_0^2 2\pi \frac{r_0^{-(2\pi\beta_V - 2)}}{2\pi\beta_V - 2} + \ldots,$$
$$+ \cdot - \qquad\qquad + \cdot \stackrel{.}{\cdot}{}^{-}$$

$$(11.31)$$

and for the internal energy and specific heat to

$$u_{VM} = -\frac{\partial}{\partial\beta_V}(-\beta_V f_{VM})$$

$$\approx \frac{1}{2\beta_V} + 4\pi^2 e^{-\beta_V\pi^2} + 16\pi e^{-\beta_V 4\pi} + 4\pi^2\left(4 - \frac{8}{\pi}\right)e^{-\beta_V\pi^2(4 - 8/\pi)}$$
$$+ - \qquad\quad + \stackrel{.}{\cdot}{}^{-} \qquad\qquad + \cdot -$$

$$+ 8\pi^2\left(\frac{8}{\pi} - 1\right)e^{-\beta_V\pi^2(8/\pi - 1)} + \ldots$$

$$+ \cdot \stackrel{.}{\cdot}{}^{-}$$
$$+ z_0^2\frac{(2\pi)^2}{(2\pi\beta_V - 2)^2}[1 + (\log r_0 c)(2\pi\beta_V - 2)]r_0^{-(2\pi\beta_V - 2)} \qquad (11.32)$$

$$c_{VM} = -\beta_V^2\frac{\partial}{\partial\beta_V}u_{VM}$$

$$\approx \frac{1}{2} + \beta_V^2\left\{4\pi^4 e^{-\beta_V\pi^2} + 64\pi^2 e^{-\beta_V 4\pi} + 4\pi^4\left(4 - \frac{8}{\pi}\right)^2 e^{-\beta_V\pi^2(4 - 8/\pi)}\right.$$
$$+ - \qquad\qquad + \stackrel{.}{\cdot}{}^{-} \qquad\qquad + \cdot -$$

$$+ 8\pi^4\left(\frac{8}{\pi} - 1\right)^2 e^{-\beta_V\pi^2(8/\pi - 1)} + \ldots$$

$$+ \cdot \stackrel{.}{\cdot}{}^{-}$$

$$+ z_0^2 \frac{(2\pi)^3}{(2\pi\beta_V - 2)^3} [2 + 2\log(r_0 c)(2\pi\beta_V - 2)$$

$$+ [\log(r_0 c)]^2 (2\pi\beta_V - 2)^2] r_0^{-(2\pi\beta_V - 2)} \bigg\}.\tag{11.33}$$

These expressions will be referred to as *independent pair approximation* (IPA).

In Figs. 11.1, 11.4, 11.5 we have plotted these thermodynamic quantities and compared u_{VM}, c_{VM} with Monte Carlo data. The agreement is seen to be excellent for u_{VM} and reasonably good for c_{VM}.

Some of the discrepancy is due to neglecting, in the IPA, the binding energies between vortex pairs. In order to calculate these let us study the contribution of quadrupole configurations. The lowest quadrupole has the charges in nearest neighbour position and an $\ell(\mathbf{x})$ field

$$\begin{array}{c} - + \\ + - \end{array}\qquad\qquad \ell(\mathbf{x}) = \delta_{\mathbf{x},0} - \delta_{\mathbf{x},1} - \delta_{\mathbf{x},2} + \delta_{\mathbf{x},1+2}\tag{11.34}$$

This has the Coulomb energy

$$V\left(\begin{array}{c} - + \\ + - \end{array}\right) = \frac{1}{2} \sum_{\mathbf{x},\mathbf{x}'} \ell(\mathbf{x})\, v'(\mathbf{x} - \mathbf{x}')\, \ell(\mathbf{x}')$$

$$= \frac{1}{2}(4v'(0, 0) - 2v'(1, 0) - 2v'(0, 1) + 2v'(1, 1)$$

$$+ 2v'(1, 1) - 2v'(0, 1)$$

$$- 2v'(1, 0))$$

$$= -4v'(1, 0) + 2v'(1, 1) = 1 - \frac{2}{\pi} = 0.3634\tag{11.35}$$

(recall Table I.6.6). Comparison with (11.26) shows that this energy is the same as that of a charge pair in the second neighbour position $+ \cdot -$. Therefore the contribution of the lowest quadrupole to the partition function is of equal importance,

$$\Delta Z/Z_0 = N\ 2e^{-(\beta_V/2)4\pi^2(1 - 2/\pi)}.\tag{11.36}$$
$$\begin{array}{c} - + \\ + - \end{array}$$

Notice that also quadrupoles which are slightly excited can compete energetically with single pairs. For example, the configuration

$$\mp\!:\!\pm \qquad\qquad \ell(\mathbf{x}) = \delta_{\mathbf{x},0} - \delta_{\mathbf{x},2} - \delta_{\mathbf{x},2\cdot1} + \delta_{\mathbf{x},2\cdot1+2} \qquad (11.37)$$

$$\text{has}$$

$$V\!\left(\mp\!:\!\pm\right) = \tfrac{1}{2}(4v'(0,\,0) - 2v'(0,\,1) - 2v'(2,\,0) + 2v'(2,\,1)$$

$$+ 2v'(2,\,1) - 2v'(2,\,0)$$

$$- 2v'(0,\,1))$$

$$= -2v'(1,\,0) - 2v'(2,\,0) + 2v'(1,\,2)$$

$$= 3 - \frac{8}{\pi} = 0.4535 \qquad\qquad (11.38)$$

and contributes to Z the amount

$$\Delta Z/Z_0 = N\ 4e^{-4\pi^2\beta v(3\,-\,8/\pi)}, \qquad\qquad (11.39)$$
$$\mp\!:\!\pm$$

which is of the same size as $\Delta Z/Z_0$ for a single pair $+\cdot\overset{\raisebox{0.3ex}{\scriptsize$-$}}{}$. Other configurations are

$$+-+- \qquad\qquad \ell(\mathbf{x}) = \delta_{\mathbf{x},0} - \delta_{\mathbf{x},1} + \delta_{\mathbf{x},2\cdot1} - \delta_{\mathbf{x},3\cdot1}, \qquad (11.40)$$

$$V(+-+-) = -3v'(1,\,0) + 2v'(2,\,0) - v(3,\,0)$$

$$= 3 - \frac{8}{\pi} = 0.4535 \qquad\qquad (11.41)$$

which gives once more the same contribution as $\mp\!:\!\pm$, namely

$$\Delta Z/Z_0 = N\ 4e^{-4\pi^2\beta v(3\,-\,8/\pi)}. \qquad\qquad (11.42)$$
$$+-+-$$

Similarly

$$\overset{\displaystyle +}{\underset{\displaystyle +-}{}\;\mp} \qquad\qquad \ell(\mathbf{x}) = \delta_{\mathbf{x},0} - \delta_{\mathbf{x},1} - \delta_{\mathbf{x},2} + \delta_{\mathbf{x},1+2\cdot2} \qquad (11.43)$$

has the energy

$$V\left(\begin{smallmatrix} . & + \\ + & - \end{smallmatrix}\right) = -2v'(1, 0) + v'(2, 1) - v(2, 0) = \frac{7}{4} - \frac{4}{\pi} = 0.4768, \qquad (11.44)$$

which is somewhat more suppressed, giving

$$\Delta Z/Z_0 = N \; 8e^{-4\pi^2\beta v(7/4 \,-\, 8/\pi)}. \qquad (11.45)$$

$$\begin{smallmatrix} - & + & . \\ + & - & \end{smallmatrix}$$

The configuration

$$\begin{smallmatrix} . & + & - \\ - & + & . \end{smallmatrix} \qquad\qquad \ell(\mathbf{x}) = \delta_{\mathbf{x},0} - \delta_{\mathbf{x},-1} + \delta_{\mathbf{x},2} - \delta_{\mathbf{x},1+2} \qquad (11.46)$$

has

$$V\left(\begin{smallmatrix} . & + & - \\ - & + & . \end{smallmatrix}\right) = \tfrac{1}{2}(4v'(0, 0) - 2v'(1, 0) + 2v'(0, 1) - 2v'(1, 1)$$

$$- 2v'(1, 1) + 2v'(2, 1)$$

$$- 2v'(1, 0))$$

$$= -v'(1, 0) + 2v'(1, 1) + v'(2, 1)$$

$$= \tfrac{1}{2}, \qquad (11.47)$$

and contributes

$$\Delta Z/Z_0 = N \; 8e^{-4\pi^2\beta v(1/2)}, \qquad (11.48)$$

$$\begin{smallmatrix} . & + & - \\ - & + & . \end{smallmatrix}$$

which competes with a pair across $5 \cdot 1$ (i.e., $+ \ldots -$). Changing the signs of the upper two charges gives the same potential,

$$V\left(\begin{smallmatrix} . & - & + \\ - & + & . \end{smallmatrix}\right) = -3v'(1, 0) + 2v'(1, 1) - v'(2, 1) = \tfrac{1}{2} \qquad (11.49)$$

so that there is one more contribution,

$$\Delta Z/Z_0 = N 8e^{-4\pi^2\beta v(1/2)}. \qquad (11.50)$$

$$\begin{smallmatrix} . & - & + \\ - & + & . \end{smallmatrix}$$

Notice that the latter two energies are the same as the sum of the individual pairs, i.e., there is no binding energy between diagonal pairs. This can be understood in general terms by the same argument [recall (7.82)] as that which we used for two vortex loops stacked up along the space diagonal.

Knowing the binding energies between vortex pairs we can now estimate the error incurred when using the independent pair approximation. When exponentiating the free energy (11.31) of a single pair, the partition function contains quadrupoles in *all* configurations. Consider, for example, a configuration $\mp^{\pm}$. In the IPA it has the Boltzmann factor $e^{-4\pi^2\beta v2(1/4)}$ corresponding to the sum of the pair energies, i.e., the binding energy is neglected. If this energy is properly included, the Boltzmann factor should appear as

$$\Delta Z/Z_0 = N 4e^{-4\pi^2 2(1/4)(1-\delta)} \tag{11.51}$$

instead, with the relative binding energy

$$\delta\left(\mp^{\pm}\right) = \frac{4}{\pi} - 1 = 0.2732. \tag{11.52}$$

This gives a considerable enhancement of the quadrupole configuration as compared with its contribution in the IPA. In fact, those states which in the IPA have no binding energy, and weight factor ≥ 4, are practically ineffective in the plot of the specific heat in Fig. 11.5. As soon as the binding energy is taken into account the quadrupole moves the IPA curve a little bit up and reduces the discrepancy near the phase transition.

When exponentiating $-\beta f$ in (11.31) one finds 8 configurations of four charges in the next neighbour positions. There is a partner to $\mp^{\pm}_{+}$, namely $\mp_{+}$, which in a proper expansion carries the opposite sign in the binding energy and is so strongly suppressed that it can be completely neglected. In the IPA, however, it is included without binding energy, which is a gross exaggeration of its importance. The mistake is, fortunately, not serious since, as we mentioned before, even this reduced energy is too large to give a visible contribution to the graph in Fig. 11.5.

The conclusion of this discussion is that the close-lying quadruplet diagram with a large binding energy can be simply added to the free energy with only a very small numerical mistake due to double counting.

The other quadrupoles have a much smaller binding energy. In order to

find the corrections associated with them we can apply the reasoning of Section 7.6 [see the discussion after Eq. (7.60)].

A configuration like $\mp : \pm$ contributes

$$\Delta Z/Z_0 = N 4e^{-4\pi^2 \beta v (1/2)(1 - \delta)}, \tag{11.53}$$
$$\mp : \pm$$
$$+ : -$$

where

$$\delta = 1 - 6 + \frac{16}{\pi} = 0.093 \tag{11.54}$$

is the relative binding energy. There is also a quadrupole with the opposite relative charges $\mp : \mp$ with

$$\Delta Z/Z_0 = N 4e^{-4\pi^2 \beta v (1/2)(1 + \delta)}. \tag{11.55}$$
$$\mp : \mp$$
$$+ : +$$

Instead of the sum of these two, the IPA contains a piece

$$\Delta Z/Z_0 = N 8e^{-4\pi^2 \beta v (1/2)}. \tag{11.56}$$

Hence the partition must be corrected as follows:

$$Z = Z^{\text{IPA}} + N 4(e^{-4\pi^2 \beta v (1/2)(1 - \delta)} + e^{-4\pi^2 \beta v (1/2)(1 + \delta)} - 2)$$

$$= Z^{\text{IPA}} + N 8e^{-4\pi^2 \beta v (1/2)} 2\sinh^2(4\pi^2 \beta_V(\delta/2)). \tag{11.57}$$

Since the phase transition takes place at $\beta_V \sim 0.73$, the factor $\cosh(4\pi^2 \beta_V \delta/2) - 1$ for the quadrupoles $\mp : \pm$, $\mp : \mp$ is equal to

$$\cosh(4\pi^2 \beta_V(\delta/2)) - 1 \approx \cosh 1.339 - 1 = 1.0386, \tag{11.58}$$

which means that in the critical region, the 8 quadrupoles $\mp : \pm$, $\mp : \mp$ in the power series expansion $e^{-\beta f^{\text{IPA}}}$ are underestimated by a factor of about 2. The same result is true for the quadrupoles $+ - + -$ and $+ - - +$.

The other quadrupoles $\mp \, \dfrac{+}{-}$ and $\mp \, \dfrac{-}{+}$ give a factor

$$\cosh\left(4\pi^2\beta_V \frac{\delta}{2}\right) - 1 = \cosh 0.6686 - 1 \sim 0.2320, \qquad (11.59)$$

so that the corresponding term in $e^{-\beta f^{\rm IPA}}$ needs a 23% enforcement.

On the other hand, the quadrupoles consisting of pairs of dipoles stacked up along the diagonal need no correction since their binding energies vanish, just as was the case with three dimensions. The sum over all corrections of the free energy due to the binding energy of pairs with larger distance converges, although not very rapidly ($\sim \int dr\, r/r^4$) [cf. (7.85)].

Vortices which form larger "molecules" than quadrupoles can also have considerable binding energy so that they may be strongly enhanced with respect to the IPA. The most prominent example is

$$\begin{array}{c}- + - \\ + - +\end{array} \quad \ell(\mathbf{x}) = \delta_{\mathbf{x},0} - \delta_{\mathbf{x},2} - \delta_{\mathbf{x},1} + \delta_{\mathbf{x},1+2} + \delta_{\mathbf{x},2\cdot1} - \delta_{\mathbf{x},2\cdot1+2} \qquad (11.60)$$

with

$$V\left(\begin{array}{c}- + - \\ + - +\end{array}\right) = \tfrac{1}{2}(-2v'(1, 0) - 2v'(1, 0) + 2v'(1, 1) + 2v'(2, 0) - 2v(2, 1)$$

$$+ 2v'(1, 1) - 2v'(1, 0) - 2v'(1, 2) + 2v'(2, 0)$$

$$- 2v'(1, 0) - 2v'(1, 0) + 2v'(1, 1)$$

$$+ 2v'(1, 1) - 2v'(1, 0)$$

$$- 2v'(1, 0))$$

$$= -7v'(1, 0) + 4v'(1, 1) + 2v'(2, 0) - 2v'(1, 2)$$

$$= \frac{4}{\pi} - \frac{3}{4} = 0.5232, \qquad (11.61)$$

which corresponds to a relative binding energy

$$\delta = \left[\frac{3}{4} - \left(\frac{4}{\pi} - \frac{3}{4}\right)\right] \Big/ \frac{3}{4} = 0.3023$$

so that close to the critical point

$$\cosh(4\pi^2\beta_V \tfrac{3}{4}\delta) - 1 = \cosh 6.53 - 1 \approx 343,$$

implying that this term in the expansion is enhanced by a large factor.

The fact that this charge configuration's total contribution is extremely small saves us from making a gross mistake.

Let us now discuss another error inherent in the independent pair approximation. It concerns the summation over pair configurations which do not satisfy the "non-backtracking" condition. When forming the exponential $Z_{VM}^{IPA} = e^{-N\beta f_{VM}^{IPA}}$, there are pair configurations in which one $+$ and one $-$ charge fall on top of the other. For example, there can be chains of $+-$ pairs, in which one $+$ falls onto the next $-$ or these can occur in such a way that the open ends form again a next neighbour $+-$ pair; the smallest chain of this type is $\begin{smallmatrix} + & + \\ - & + \end{smallmatrix}$. These chains are certainly all forbidden in the correct sum. Fortunately, any chain of length more than three is suppressed by at least a Boltzmann factor

$$e^{-4\pi^2\beta_V(3/4)} < 4 \times 10^{-10} \quad \text{for} \quad \beta_V \gtrsim 0.73.$$

A danger arises, in principle, from the increasing configurational entropy of such spurious chains. This goes like $(2D)^n$ so that the sum behaves roughly like

$$\sum_{n=3} (2D)^n \, e^{-\cos^2\beta_V(n/4)} \tag{11.62}$$

and converges for

$$\beta_V > \frac{\log 2D}{\pi^2} \sim 0.14. \tag{11.63}$$

Fortunately, even near the critical point $\beta_{Vc} \sim 0.73$, this sum remains quite small.

11.5. DETERMINATION OF THE TRANSITION POINT

Using the low and high temperature expansions of the free energy of the XY and Villain models we can estimate the critical temperature. The result is not as trustworthy as in the three-dimensional case, since the fluctuations are much stronger. The omitted two-loop graphs are now merely suppressed by a factor of order $O(1/D^2) = O(1/4)$. This has the effect that the low- and high-temperature curves in the XY model plotted in Fig. 4.5 no longer intersect each other properly. They do, however,

approach each other very closely in the vicinity of the point

$$\beta_c \approx 1.05. \tag{11.64}$$

In the Villain model, there is an intersection around

$$\beta_{Vc} \approx 0.65 \tag{11.65}$$

as we can see in Fig. 11.1. The importance of fluctuations is illustrated by the fact that in the lowest approximation, neglecting high temperature loops and low temperature vortices, β_{Vc} should satisfy

$$-\log(2\pi\beta_V) \approx -\tfrac{1}{2}\log(2\pi\beta_V) - \tfrac{1}{2}1.1662, \tag{11.66}$$

i.e., gives a transition at

$$\beta_{Vc}^0 = \frac{1}{2\pi}e^{1.1662} = 0.5109, \tag{11.67}$$

to be compared with (11.65). We also realize that the point of intersection is not well determined but changes by a considerable amount if we add just one more term either to the low or to the high temperature series.

Looking at the Monte Carlo data for the specific heat in Fig. 11.5 we observe an important feature of the two-dimensional XY transition: the position of the peak lies significantly *above* the critical inverse temperature. In fact, contrary to the three-dimensional case, the peak in the specific heat cannot be used to estimate the transition point. If we perform an analysis of the finite size dependence of the peak we find that it is *almost independent* of the size, as soon as $N \gtrsim 24 \times 24$. This implies that the specific heat no longer diverges for $\beta_V \to \beta_{Vc}$. It is a smooth function of β_V containing only an essential singularity of the type $e^{-(\beta_V - \beta_{Vc})}$, as we will see in Section 11.9.

This smoothness is related to the previously observed feature of the high-temperature expansion, that of having anomalous signs for terms of large order. In Fig. 11.5 we saw that this had the effect of rounding the peak and flattening out any possible spike. Thus, if we want to use Monte Carlo techniques for a precise determination of the critical point we must take recourse to properties of the model other than the thermodynamic functions u and c.

It was pointed out by Kosterlitz and Thouless, and will be explained later in Section 11.8, that the most characteristic property of the critical point is a divergence in the dipole strength of the vortex pairs. One speaks of a *pair unbinding transition* (see Fig. 11.6). This is acompanied by a breakdown of the stiffness of the long-wavelength spin wave fluctuations. Anticipating a result which can only be understood after going through Section 11.9 we just quote some careful Monte Carlo studies of the stiffness which have led to the critical points

$$
\beta_c \sim \begin{cases} 1.12 & \text{(Tobochnik and Chester),[d]} \\ 1.19 \pm 0.02 & \text{(Samuel and Yee),[d]} \end{cases}
$$
$$
\beta_{Vc} \sim \begin{cases} 0.73, & \text{(Shugard et al.),[d]} \\ 0.738 \pm 0.01 & \text{(Janke and Kleinert),[d]} \end{cases}
$$

(11.68)

as the points where the stiffness jumps to zero. Although generally accepted, the precision of these values is not overly trustworthy since it depends on a quantitative fit of the theoretical correlation length (to be derived in Section 11.10) to lattice data which have strong finite-size effects.[e]

11.6. VILLAIN APPROXIMATION FOR $D = 2$

As in the three-dimensional case we can use the results for the Villain model, insert them into Eqs. (7.35), (7.37), and obtain the Villain approximation to the two-dimensional XY model. The resulting curves are shown in Figs. 11.7 and 11.8 for the internal energy and the specific heat. Just as in three dimensions, the approximation is seen to be excellent for small β including the critical regime. In the low temperature phase it is very bad except at extremely low temperatures where it becomes again good. The reason for the disagreement had been traced before (recall Fig. 7.12) and is of no surprise.

The critical value of β_V in the Villain model $\beta_{Vc} \approx 0.73$ has the Villain approximation (via $\beta_V = -[2\log(I_1(\beta)/I_0(\beta)]^{-1}]$ of

$$
\beta_c \approx 1.18.
$$

---

[d]Cited in the Notes and References.
[e]The collapse of stiffness is diagnosticized by the correlation length becoming shorter than the lattice size.

FIG. 11.6.   Spin configurations and vortex-antivortex pairs in the $2D$ Villain model. The parentheses indicate the initial configuration at the start (O.S. $\triangleq$ ordered start) and the number of sweeps after which the picture was taken. Notice the unbound pairs for $\beta_V < 0.7$.

$\beta_V = 0.5898$ (O.S.; 2000)

$\beta_V = 0.5898$ (O.S.; 7000)

$\beta_V = 0.6199$ (O.S.; 4000)

$\beta_V = 0.6508$ (O.S.; 7000)

$\beta_V = 0.7152$ (O.S.; 7000)

$\beta_V = 0.8180$ (O.S.; 7000)
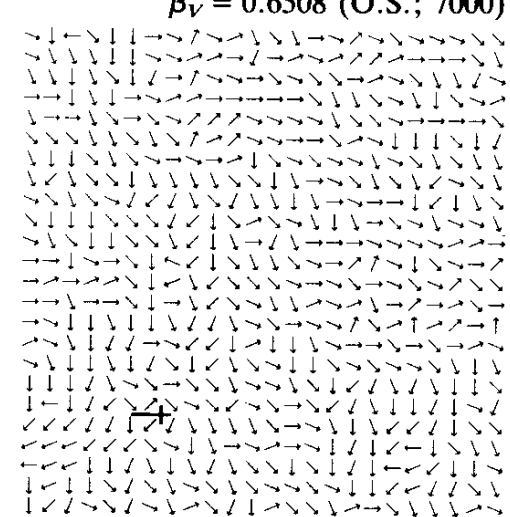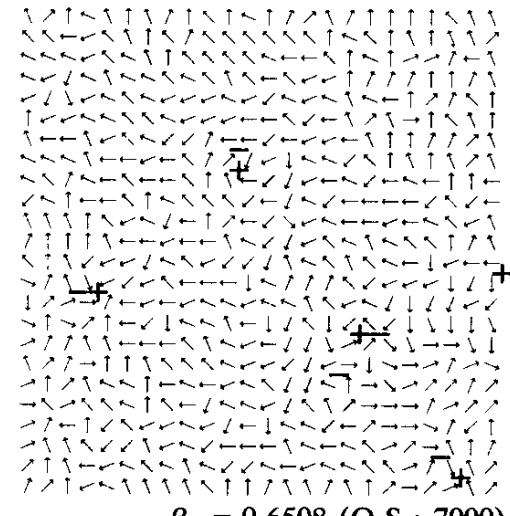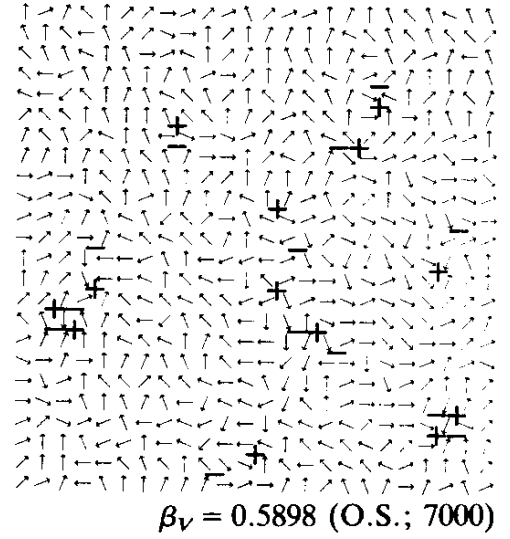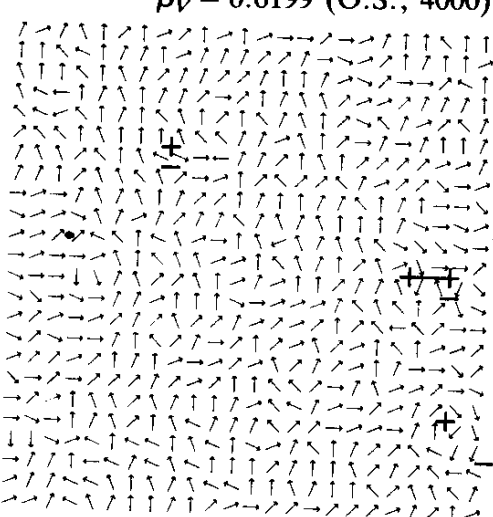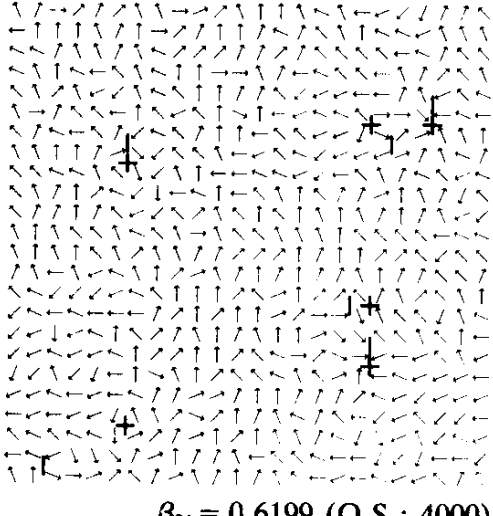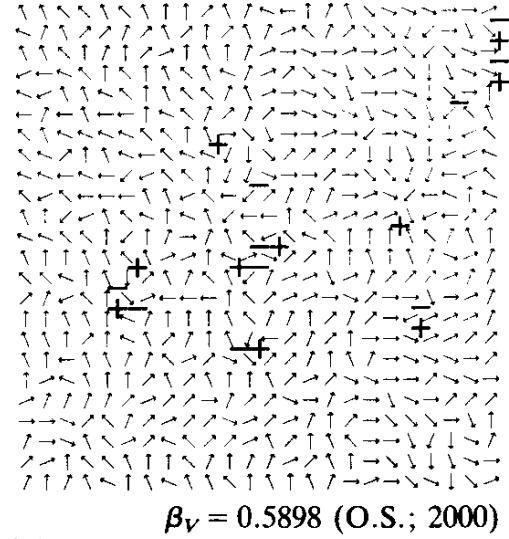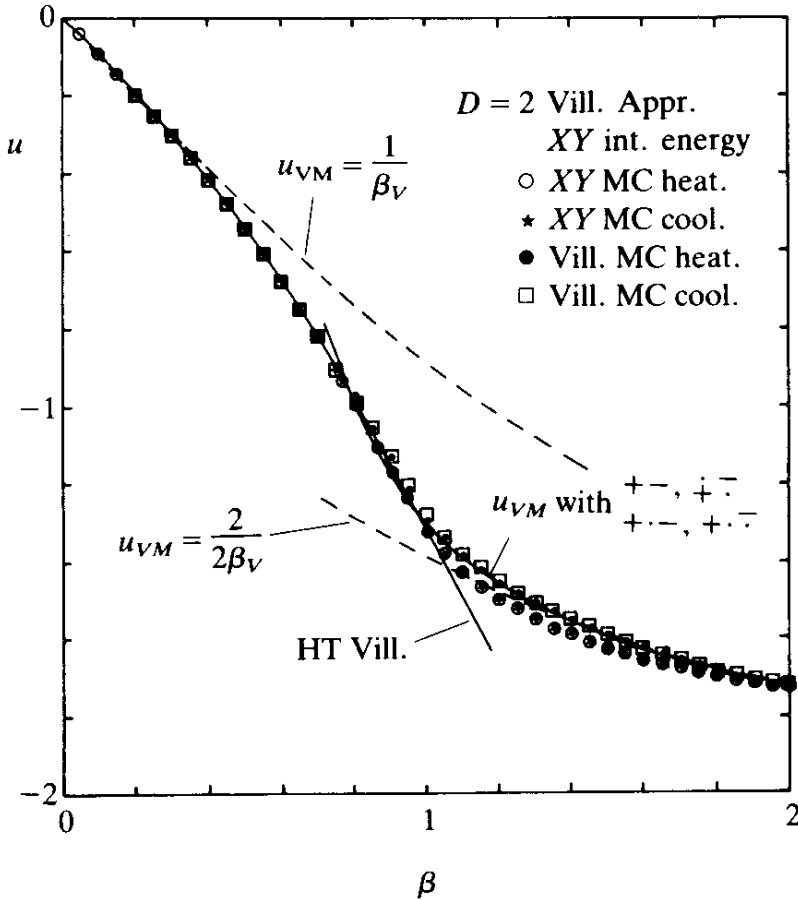
FIG. 11.7. Test of the Villain approximation to the 2D XY model internal energy. The squares and diamonds are the Villain Monte Carlo data of Table 11.2 transformed via (7.35) to XY coordinates. The curves are the low- and high-temperature approximations of the Villain model.
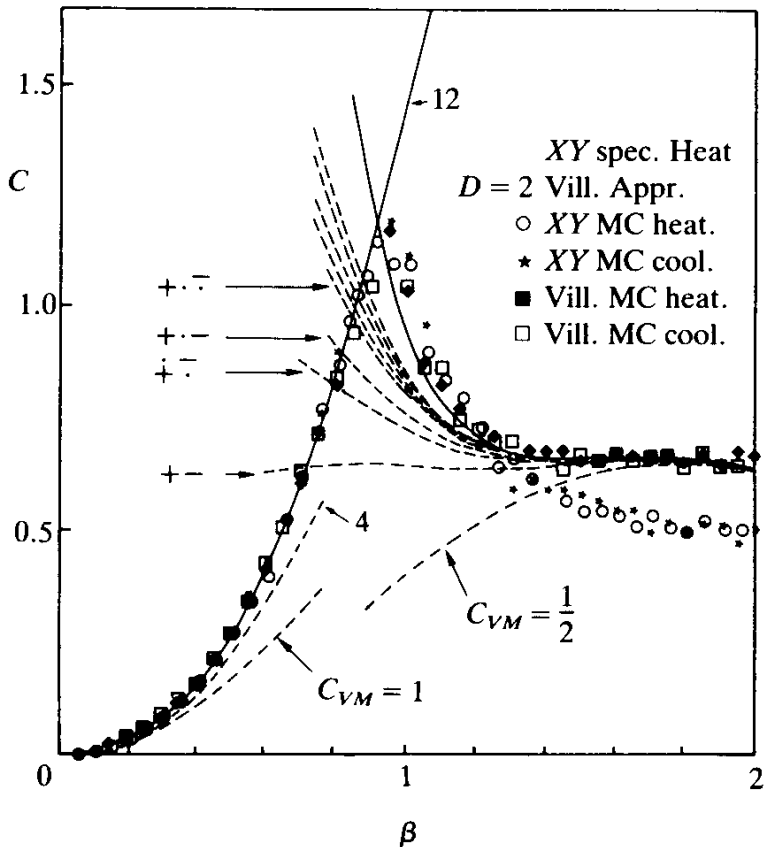
excellent agreement with the Monte Carlo value 1.19 ± 0.02 (see Table 7.4).

11.7. VORTEX CORRECTIONS IN $D = 2$ XY MODEL

With vortex corrections being so essential in understanding the behavior of the specific heat let us study their effects in the XY model. A look back at Fig. 11.3 shows how much the mean-field plus one-loop corrections fail to reproduce the increase in specific heat. Unfortunately, starting from the mean-field approach, it is very difficult to develop a systematic procedure to take the vortices into account. The reason is that within the $u(\mathbf{x})$ and $\alpha(\mathbf{x})$ field language, vortices are even more complicated solutions of nonlinear field equations than in the $\gamma(\mathbf{x})$ language. A rough heuristic estimate of their effect can be obtained by using the previous vortex expansion for the free energy of the Villain model and going through the Villain approximation. The result of such a calculation for

FIG. 11.8. The same test as in Fig. 11.6 but for the specific heat using the Monte Carlo data of Table 11.2 and Eq. (7.37).
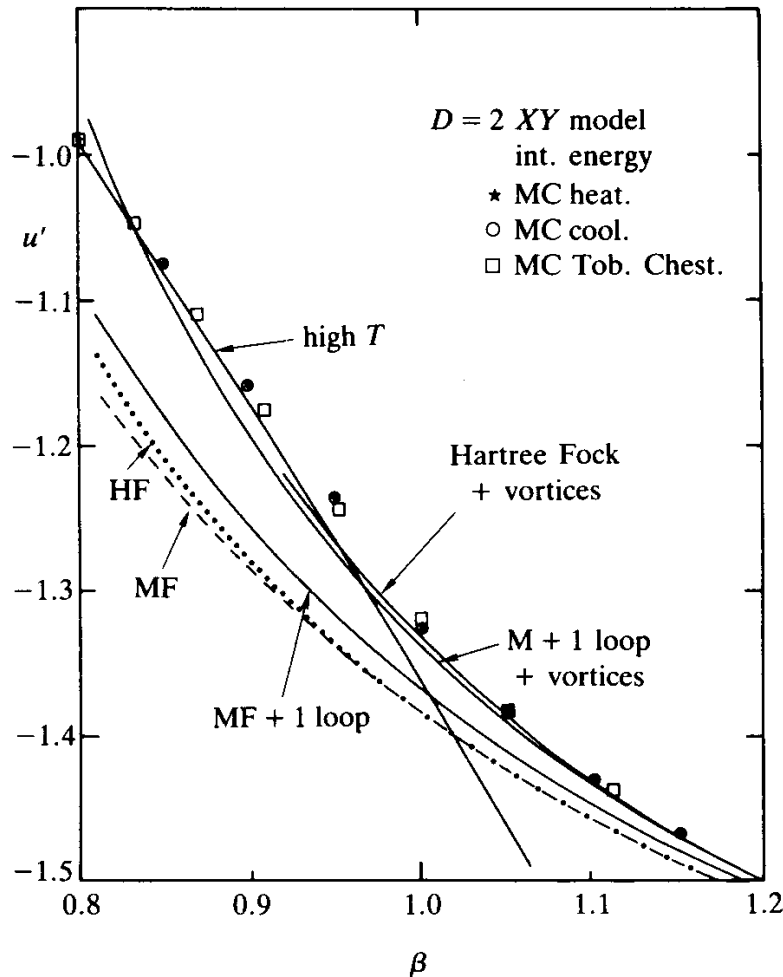
the internal energy and specific heat is shown in Figs. 11.7 and 11.8. We see that the correction has the right order of magnitude.

Within the XY model itself, a systematic calculation of vortex corrections can proceed along the lines of the perturbative approach that was described in Section 7.7. In principle, this gives the full expansion in powers of β^{-n} of the partition function. In Section 7.8 we saw that a large number of terms can be summed in one stroke by taking recourse to the self-consistent Hartree-Fock approximation. Indeed, the internal energy and specific heat of the $D = 3$ XY model came out in rather good agreement with Monte Carlo data. The only exception was in the immediate neighborhood of the transition. If we apply these results [which were derived there for general D, see Eqs. (7.152–7.156)] to the $D = 2$ case, we find the curves shown in Figs. 11.9 and 11.10 (labeled HF).

In order to calculate the vortex corrections we remember the representation (6.59) which reads, in two dimensions:

$$Z' = I_0(\beta)^{2N} \prod_{\mathbf{x}} \left[\int_{-\infty}^{\infty} dA(\mathbf{x}) \right] \exp(-\beta E[A]) \sum_{\{\ell(\mathbf{x})\}} \exp\left(2\pi i \sum_{\mathbf{x}} \ell(\mathbf{x}) A(\mathbf{x}) \right),$$

(11.69)

FIG. 11.9.   Internal energy of the $2D$ XY model as obtained from self-consistent Hartree-Fock methods plus vortex corrections. The remaining curves and data are as in Fig. 11.2.

where
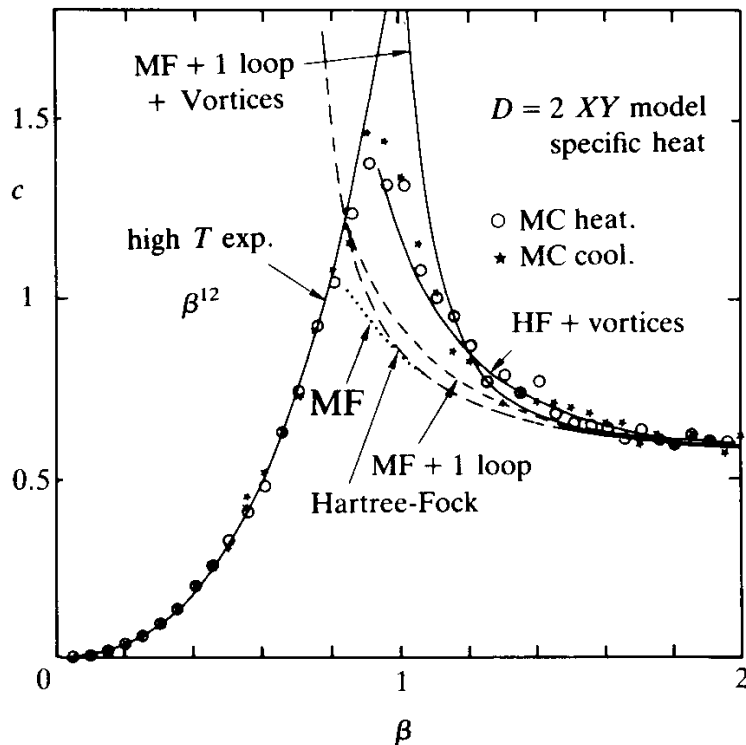
$$-\beta E[A] = \sum_{x,i} \log I_{B_i(x)}(\beta), \tag{11.70}$$

with the large β expansion

$$-\beta E[A] = \sum_p \sum_{x,i} \frac{G_c^{(p)}(\beta)}{(-2\beta)^p p!} [B_i^2(x)]^p \quad (B_i = \varepsilon_{ij} \overline{\nabla}_i A(x)), \tag{11.71}$$

represents the nonlinear field energy of the "vector potential" A (which in two dimensions is now a scalar). The coefficients $G_c^{(p)}(\beta)$ were calculated in Eqs. (6.33), (6.35). The first few coefficients were found to be [see Table 6.2]

FIG. 11.10.   Specific heat of the $2D$ XY model from self-consistent Hartree-Fock methods plus vortex corrections.

$$G_c^{(1)} = 1 + \frac{1}{2\beta} + \ldots, \quad G_c^{(2)} = \frac{1}{3\beta} + \ldots, \quad G_c^{(3)} = -\frac{3}{5\beta^2} + \ldots \quad (11.72)$$

In the absence of vortices, this partition function can be evaluated perturbatively. The "free field" term

$$-\beta E_0 = -\frac{G_c^{(1)}(\beta)}{2\beta} \sum_{\mathbf{x},i} (\nabla_i A(\mathbf{x}))^2 \quad (11.73)$$

gives the free correlation function

$$\langle A(\mathbf{x}) A(0) \rangle = \frac{2\beta}{G_c^{(1)}(\beta)} \frac{1}{-\bar{\nabla} \cdot \nabla} \quad (11.74)$$

and this can be used to perform all the Wick contractions in the remaining interaction terms.

The crucial observation is now that this perturbation series leads to the *same* β^{-n} series as that obtained by the method discussed in Section 7.7. In order to verify this we simply recall that the expansion (11.70) of $I_b(\beta)$ was derived from the asymptotic series of the Bessel functions

$$I_b(\beta) = \frac{e^\beta}{\sqrt{2\pi\beta}}\left(1 - \frac{(2b)^2 - 1}{8\beta} + \frac{((2b)^2 - 1)((2b)^2 - 9)}{2!(8\beta)^2} - \cdots \right). \qquad (11.75)$$

It is, however, well-known that this series is obtained precisely by calculating the defining integral

$$I_b(\beta) = \int_{-\pi}^{\pi} \frac{d\gamma}{2\pi} e^{\beta\cos\gamma + ib\gamma} \qquad (11.76)$$

perturbatively, i.e., by expanding

$$\cos\gamma = 1 - \frac{\gamma^2}{2} + \sum_{n=2}^{\infty} (-)^n \frac{(\gamma^2)^n}{(2n)!}, \qquad (11.77)$$

using γ^2 as a "free field energy" and treating the remainder as an "interaction energy." Thus the $\ell(\mathbf{x}) = 0$ part of the partition function (11.69) is indeed what we had already calculated in Section 7.7.

A systematic calculation of the vortex corrections can now be obtained by including the same basic $\ell(\mathbf{x})$ configurations as in the Villain model. The main difficulty in doing this is that as soon as vortices are present, it is no longer possible to treat the first term (11.73) in the energy (11.71) as a free-field part and the rest as a small interaction. In the absence of vortices, this was possible since the field A was of the order of $\sqrt{\beta}$ (since $\langle AA \rangle \propto \beta$). This assured the decreasing importance of the higher interaction terms. In the presence of vortices, however, the field is of order β. This is seen most easily by using the leading term (11.73) and minimizing the field energy in A, which gives

$$A(\mathbf{x}) \sim (-\bar{\nabla}\cdot\nabla)^{-1} \frac{\beta}{G_c^{(1)}(\beta)} 2\pi i\,\ell(\mathbf{x}). \qquad (11.78)$$

There does, however, exist a parameter of smallness for reasonably large β and this is the size of the fluctations around the field configurations of vortices. So we take refuge in a saddle-point approximation. First we minimize the energy and find the "classical fields" $A^{cl}(\mathbf{x})$, $b_i^{cl}(\mathbf{x})$ satisfying

$$\frac{\delta}{\delta A(\mathbf{x})}\left[-\beta E[A] + 2\pi i \sum_{\mathbf{x}} \ell(\mathbf{x}) A(\mathbf{x}) \right] = 0, \qquad (11.79)$$

where $E[A]$ is given by (11.70). Let us write $-\beta E[A] = \Sigma_{x,i} \log I_{B_i(x)}(\beta) = \Sigma_{x,i} W(B_i(x))$. Since $B_i = \varepsilon_{ij}\bar{\nabla}_j A$, Eq. (11.79) amounts to

$$-\varepsilon_{ij}\nabla_j W'(B_i(x)) + 2\pi i \,\ell(x) = 0. \tag{11.80}$$

Of course, for large β, this is satisfied by (11.78). It is useful to split off the large β limit and write

$$W(B_i) = \tfrac{1}{2} W''(0) B_i^2 + W_{int}(B_i) \tag{11.81}$$

where

$$W''(0) = -\frac{\displaystyle\int_{-\pi}^{\pi} \frac{d\gamma}{2\pi} \gamma^2 e^{\beta \cos \gamma}}{\displaystyle\int_{-\pi}^{\pi} \frac{d\gamma}{2\pi} e^{\beta \cos \gamma}} = -\frac{G_c^{(1)}}{2\beta}, \tag{11.82}$$

and

$$W_{int}(B_i) = \log I_{B_i(x)}(\beta) + \frac{G_c^{(1)}}{2\beta} B_i^2(x). \tag{11.83}$$

Then we can formally solve Eq. (11.80) by putting

$$A^{cl}(x) = -2\pi i \, W''(0)^{-1} \sum_{x'} v(x - x')(\ell(x') - q(x')), \tag{11.84}$$

$$B_i^{cl}(x) = -2\pi i \, W''(0)^{-1} \sum_{x'} \varepsilon_{ij} \bar{\nabla}_j v(x - x')(\ell(x') - q(x')), \tag{11.85}$$

where $v(x) = -1/\bar{\nabla} \cdot \nabla$ is the lattice Coulomb potential and
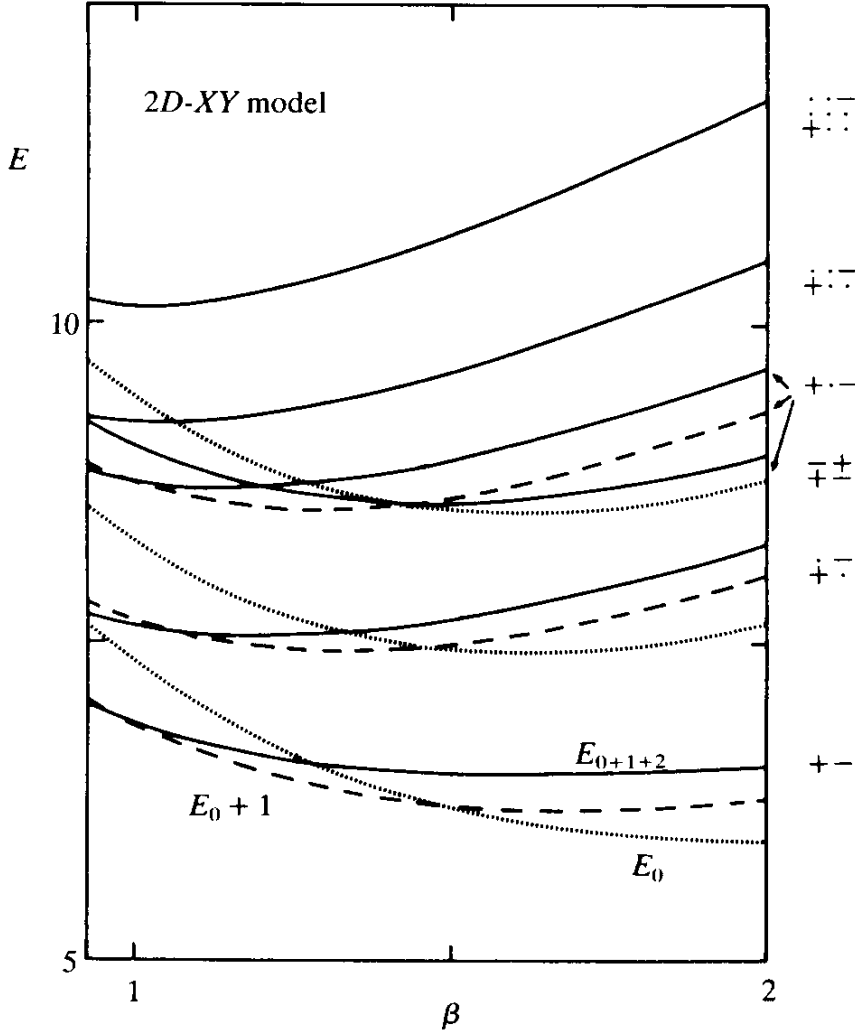
$$q(x) = \frac{1}{2\pi i} \sum_i \varepsilon_{ij} \nabla_j W'_{int}(B_i^{cl}(x)) \tag{11.86}$$

collects the effects of the nonlinearities of the problem. This quantity may be viewed as the *screening charge* which *reduces* the bare charge $\ell(x)$.

Equations (11.83), (11.85) may be solved by iteration. The convergence is quite rapid.

Inserting this solution back into the total energy of (11.70) we find

FIG. 11.11.   Loop expansion of bound vortex energies (zero loop E_0, up to 1-loop E_{0+1}, and up to 2-loop E_{0+1+2}) as a function of inverse temperature β.

$$-\beta E^{cl} = 4\pi^2 W''(0)^{-1} \frac{1}{2} \sum_{x,x'} (\ell(x) v(x - x') \ell(x') - q(x) v(x - x') q(x'))$$

$$+ \sum_{x,i} W_{int}(B_i^{cl}(x)). \tag{11.87}$$
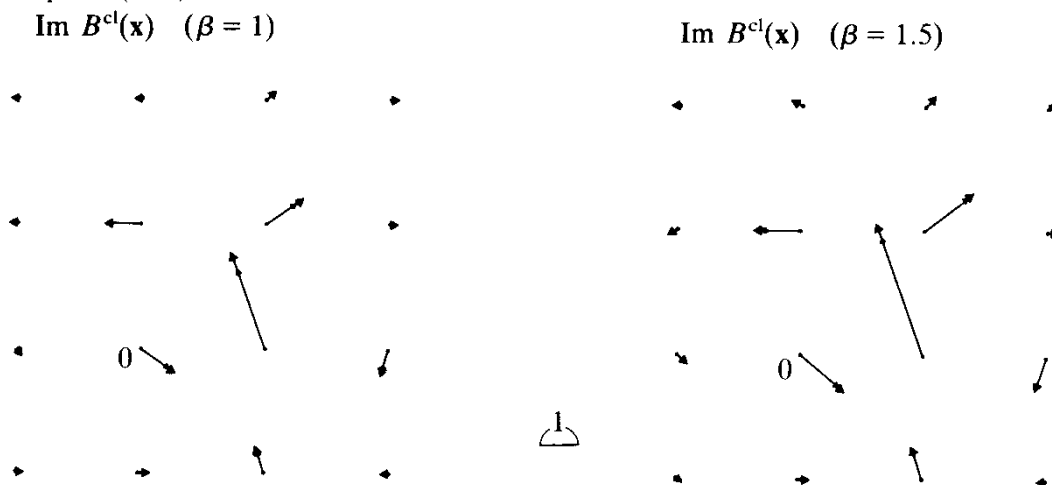
Notice that the pure $\ell v \ell$ term is the naive large β limit obtained by dropping all but the first term in (11.71). The nonlinearities lead to the extra q terms. They give a non-vanishing contribution even for large β. The rapid convergence allows us to stop after one iteration, i.e., after the $q(x) = 0$ field of (11.85) in $W''_{int}(B_i^{cl}(x))$ of (11.86) and (11.87).

Starting from the saddle point energy (11.87) we can calculate fluctuation corrections. The interested reader is referred to the original paper by Ami and Kleinert (1985) for more details. Here we only quote the result. The energies of the elementary vortex configurations including the screening charges acquire the β dependencies shown in Fig. 11.11.

FIG. 11.12. Screening charges (small arrows) caused by the nonlinearities as compared with the bare charges (large arrows) of an elementary vortex dipole $+-$ with $\beta = 1.5$ and $\beta = 1$.

$q(\mathbf{x})$ $(\beta = 1)$ $q(\mathbf{x})$ $(\beta = 1.5)$
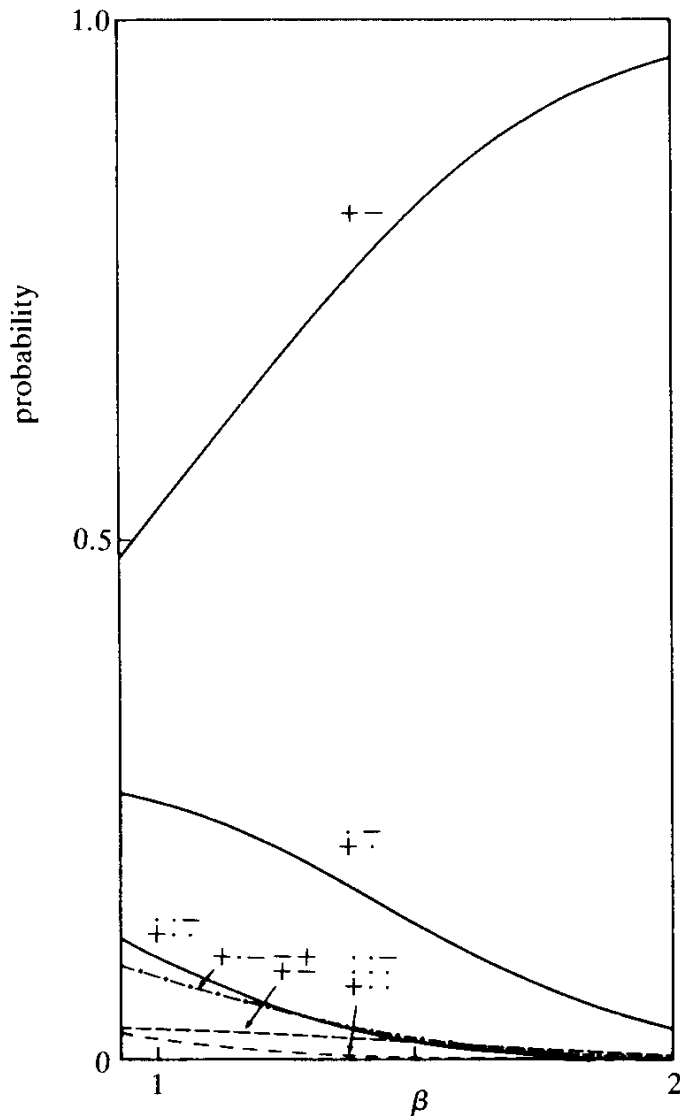
FIG. 11.13. Classical values for the imaginary magnetic fields Im $B_i^{cl}(\mathbf{x})$ (large arrows) as compared to those without the nonlinear screening charges $q(\mathbf{x})$ (small arrows) for the dipole pairs $(+-)$.

Im $B^{cl}(\mathbf{x})$ $(\beta = 1)$ Im $B^{cl}(\mathbf{x})$ $(\beta = 1.5)$

We see that even for large β the corrections are significant. (The E_0 curves are, of course, calculated with (11.73)). In order to give an idea of the size of the screening charge we have plotted the bare and the screening charge for the lowest vertex-antivortex part $+-$ at $\beta = 1.5$ and $\beta = 1$ in Fig. 11.12. We have also displayed the associated B_i^{cl} field (which is imaginary due to the coupling $2\pi i\,\ell A$) in Fig. 11.13. We see that the screening charge is quite small so that it is sufficient to iterate Eqs. (11.83)–(11.85) only once. The relative importance of the different vortex configurations is shown in Fig. 11.14. The final internal energy and specific heat including quadratic fluctuations, are plotted in Figs. 11.9 and 11.10: we see that the vortex corrections generally close the gap between the Hartree-Fock curves and the Monte Carlo data.

FIG. 11.14. The relative importance of various bound vortices, $e^{-\beta E}/\Sigma e^{-\beta E}$ as a function of inverse temperature β.
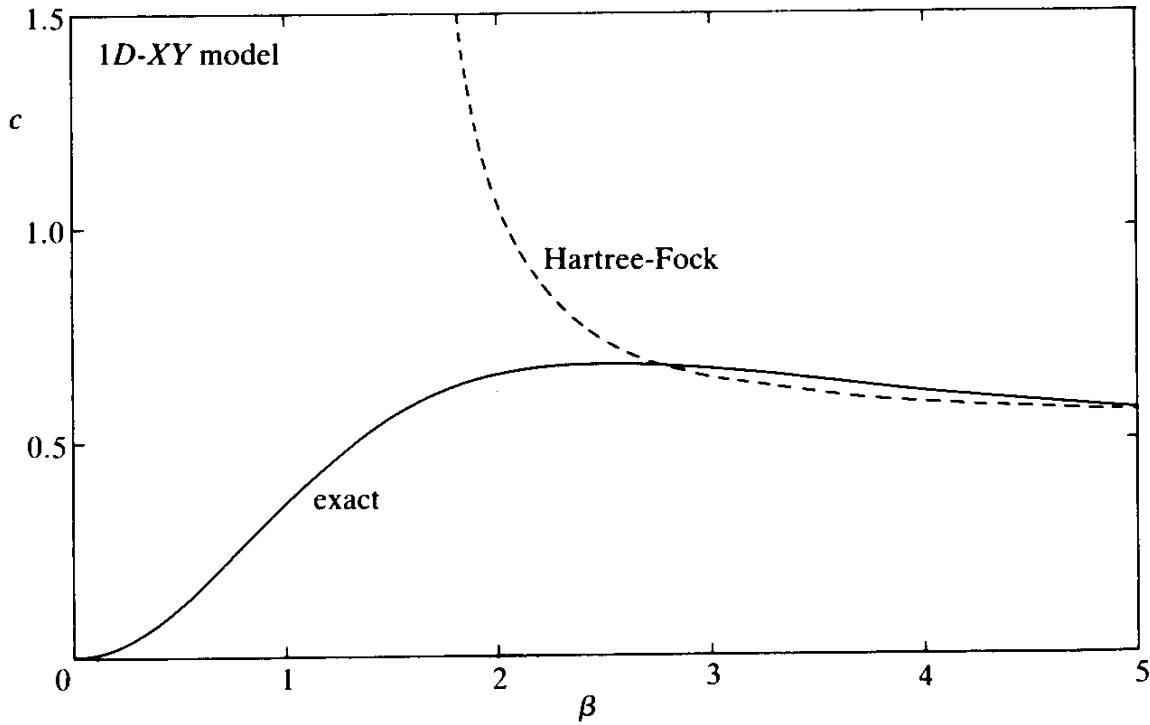
It should be mentioned, however, that the quality of these results is, in part, fortuitous. The Hartree-Fock approximation overestimates the specific heat near the phase transition. This is related to the fact, discussed earlier, that this approximation has a phase transition $\beta_c = e/4$ ≈ 0.68 [recall Fig. (7.17)] which the perturbative approach to the XY model should not really have.

This property of the approximation can be illustrated by looking at the Hartree-Fock approximation to the XY model in one dimension. For *open* boundary conditions, the partition function is simply

$$Z' = I_0(\beta)^N,$$

giving the specific heat

FIG. 11.15.   Exact and Hartree-Fock results for the heat capacity for the $1D$ XY model as functions of β.

$$c = \beta^2 \left(\frac{I_1(\beta)}{I_0(\beta)}\right)' = \beta^2 \left(1 - \frac{I_1(\beta)}{\beta I_0(\beta)} - \left(\frac{I_1(\beta)}{I_0(\beta)}\right)^2\right). \tag{11.88}$$

The Hartree-Fock approximation, on the other hand, including three-loop corrections gives

$$-\beta f^{\mathrm{HF}} = \beta^R + \frac{1}{2} - \frac{1}{2}\log(2\pi\beta^R) + \frac{1}{2\cdot 4!}\frac{1}{(\beta^R)^4} \tag{11.89}$$
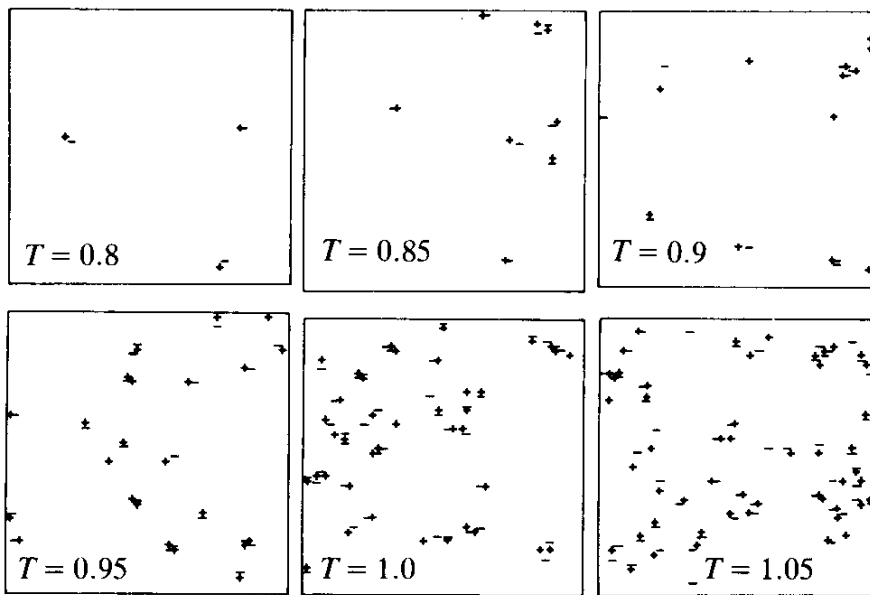
and therefore

$$u^{\mathrm{HF}} = -\frac{\beta^R}{\beta} + \frac{1}{3!}\frac{1}{\beta(\beta^R)^3(2\beta^R - 1)}, \tag{11.90}$$

$$c^{\mathrm{HF}} = \frac{1}{2\beta^R - 1}\left(\frac{1}{3!(\beta^R)^3} + \beta^R\right) + \frac{1}{(2\beta^R - 1)^2(\beta^R)^2} + \frac{2}{3\beta^R(2\beta^R - 1)^3}, \tag{11.91}$$

where $\beta^R = \beta e^{-1/2\beta^R}$. The comparison is shown in Fig. 11.15. For $\beta = e/2 \approx 1.35$ the Hartree-Fock curve diverges due to the unphysical phase

FIG. 11.16. Vortex-antivortex pairs in the XY model as given by Tobochnik and Chester (cited in the Notes and References).

transition. Certainly, it is this physically incorrect property of the approximation in our $D = 2$ approach which has (partly) helped in achieving the good agreement with the Monte Carlo data.

We close this section by plotting in Fig. 11.16 the distribution of vortex-antivortex pairs found by Tobochnik and Chester (1979) in Monte Carlo simulations. There is reasonable agreement with the probabilities of Fig. 11.14.

11.8. CORRELATION FUNCTIONS IN THE 2-DIMENSIONAL VILLAIN MODEL

Consider the correlation function of the order parameter for two different points $x' = X$ and $x' = X'$. In the Villain model it is given by [recall (9.1)]

$$G(X, X') = G(X - X') = \langle e^{i\gamma(X)} e^{-i\gamma(X')} \rangle$$

$$= \frac{1}{Z_{VM}} \prod_{x} \left[\int_{-\pi}^{\pi} \frac{d\gamma(x)}{2\pi} \right] \sum_{\{n_i(x)\}} e^{-(\beta v/2)\Sigma_{x,i}(\nabla_i\gamma - 2\pi n_i)^2 + i\Sigma_x\gamma(x)Q(x)}, \quad (11.92)$$

where we have introduced the quantity

$$Q(x) = \delta_{x,X} - \delta_{x,X'}, \quad (11.93)$$

which plays the role of an external charge distribution with a positive charge at X and a negative one at X' [compare (9.2)].

In the three-dimensional discussion we had interpreted the phase angle $\gamma(\mathbf{x})$ as a potential for the magnetic field. With this interpretation these charges had the character of magnetic monopoles. It will be useful to go to the vortex gauge [compare (8.5)–(8.7)]

$$n_2(\mathbf{x}) = 0, \qquad n_1(x_1, 0) = 0, \tag{11.94}$$

and extend the range of $\gamma(\mathbf{x})$ integrations from $(-\pi, \pi)$ to $(-\infty, \infty)$ so that [compare (8.31)]

$$G(\mathbf{X}, \mathbf{X}') = \frac{1}{Z_{VM}} \prod_{\mathbf{x}} \left[\int_{-\infty}^{\infty} \frac{d\gamma(\mathbf{x})}{2\pi} \right] \sum_{\{n_i(\mathbf{x})\}} \delta_{n_2,0} \, e^{-(\beta V/2)\Sigma_{\mathbf{x},i}(\nabla_i\gamma - 2\pi n_i)^2 + i\Sigma_{\mathbf{x}}\gamma(\mathbf{x})Q(\mathbf{x})}. \tag{11.95}$$

For very low temperatures, the jump numbers $n_i(\mathbf{x})$ are frozen out and we can calculate

$$G(\mathbf{X}, \mathbf{X}') \to \frac{1}{Z_{VM}} \prod_{\mathbf{x}} \left[\int_{-\infty}^{\infty} \frac{d\gamma(\mathbf{x})}{2\pi} \right] e^{-(\beta V/2)\Sigma_{\mathbf{x},i}(\nabla_i\gamma)^2 + i\Sigma_{\mathbf{x}}\gamma(\mathbf{x})Q(\mathbf{x})}$$

$$= \frac{1}{Z_{VM}} \prod_{\mathbf{x}} \left[\int \frac{d\gamma(\mathbf{x})}{2\pi} \right]$$

$$\times \, e^{-(\beta V/2)\Sigma_{\mathbf{x}}[\gamma(\mathbf{x}) + (i/\beta_V \bar{\nabla}\cdot\nabla)Q(\mathbf{x})](-\bar{\nabla}\cdot\nabla)[(\gamma + (i/\beta_V \bar{\nabla}\cdot\nabla)Q(\mathbf{x})]} e^{-(1/2\beta_V)\Sigma_{\mathbf{x}}Q(\mathbf{x})(-1/\bar{\nabla}\cdot\nabla)Q(\mathbf{x})}$$

$$= \frac{1}{Z_{VM}} \cdot \left(\frac{1}{2\pi} \sqrt{\frac{2\pi}{\beta_V}} \right)^N \det(-\bar{\nabla}_i\nabla_i)^{-1/2} \, e^{-(1/2\beta_V)\Sigma_{\mathbf{x}}Q(\mathbf{x})(1/-\bar{\nabla}\cdot\nabla)Q(\mathbf{x})}.$$

Since for small T, $Z_{VM} \sim (1/\sqrt{2\pi\beta_V})\det(\bar{\nabla}\cdot\nabla)^{-1/2}$ the prefactors cancel and, inserting (11.93), (11.13) we obtain the low temperature limit

$$G(\mathbf{X}, \mathbf{X}') \to G_{T\to 0}(\mathbf{X}, \mathbf{X}') \equiv G_{T\to 0}(\mathbf{X} - \mathbf{X}')$$

$$= e^{-(1/2\beta_V)\Sigma_{\mathbf{x}}Q(\mathbf{x})(-1/\bar{\nabla}\cdot\nabla)Q(\mathbf{x})} = e^{-(1/2\beta_V)\Sigma_{\mathbf{x}}Q(\mathbf{x})v(\mathbf{x} - \mathbf{x}')Q(\mathbf{x}')}$$

$$= e^{(1/\beta_V)(v(\mathbf{X} - \mathbf{X}') - v(0))} = e^{(1/\beta_V)v'(\mathbf{X} - \mathbf{X}')}. \tag{11.96}$$

Thus, the subtracted Coulomb potential $v'(\mathbf{x})$ gives directly the *exponent* of the low temperature correlations. For large distances we can use the asymptotic form (11.14) and find

$$G_{T \to 0}(\mathbf{x}) \to (|\mathbf{x}| 2\sqrt{2} \, e^{\gamma})^{-1/2\pi\beta_V}. \tag{11.97}$$

This power behavior is a manifestation of the Landau-Peierls observation that there is no proper order in two dimensions. If there were, the correlation function would tend towards a constant, namely, the square of the expectations of the individual order parameters,

$$G(\mathbf{X}, \mathbf{X}') = \langle e^{i\gamma(\mathbf{X})} e^{-i\gamma(\mathbf{X}')} \rangle,$$

$$G(\mathbf{X}, \mathbf{X}') \xrightarrow[|\mathbf{X} - \mathbf{X}'| \to \infty]{} |\langle e^{i\gamma(\mathbf{X})} \rangle|^2, \tag{11.98}$$

and the same type of cluster property would be found for all higher Green functions in accordance with the general connectedness structure of local field theories, as discussed in Part I, Section 4.3.

Let us now investigate the modifications of this low temperature correlation function brought about by the thermal activation of vortices. For this we rewrite the sum in (11.95) as follows:

$$\sum_{\{n_i(\mathbf{x})\}} \delta_{n_2, 0} \, e^{-(\beta_V/2)\Sigma_{\mathbf{x},i}(\nabla_i \gamma)^2 + i\Sigma_{\mathbf{x}} \gamma(\mathbf{x})(Q(\mathbf{x}) + 2\pi i \beta_V \bar{\nabla}_i n_i) - (\beta_V/2)4\pi^2 \Sigma_{\mathbf{x}} n_i^2(\mathbf{x})}. \tag{11.99}$$

Integrating out the $\gamma(\mathbf{x})$ field this becomes

$$G(\mathbf{X} - \mathbf{X}') = \frac{1}{Z_{VM}} \frac{1}{(\sqrt{2\pi\beta_V})^N} \sum_{\{n_i(\mathbf{x})\}} \delta_{n_2, 0} \, e^{-(\beta_V/2)4\pi^2 \Sigma_{\mathbf{x}}(n_i^2 - \bar{\nabla}_i n_i(-1/\bar{\nabla} \cdot \nabla)\bar{\nabla}_j n_j)}$$

$$\times e^{-2\pi i \Sigma_{\mathbf{x}} Q(\mathbf{x})(-1/\bar{\nabla} \cdot \nabla)\bar{\nabla}_i n_i(\mathbf{x})} G_{T \to 0}(\mathbf{X} - \mathbf{X}') \tag{11.100}$$

Recalling the relation between vortices and jumping numbers in three dimensions,

$$\ell_i(\mathbf{x}) = \varepsilon_{ijk} \nabla_j n_k(\mathbf{x} + \mathbf{i}),$$

we can now identify in two dimensions,

$$\ell(\mathbf{x}) = \varepsilon_{ij} \nabla_j n_k(\mathbf{x}) \tag{11.101}$$

with the boundary condition

$$n_1(x_1, 0) = 0$$

and see that the first Boltzmann factor under the sum over $n_i(\mathbf{x})$ is again the partition function of the two-dimensional Coulomb gas of vortices

$$e^{-(\beta v/2)4\pi^2 \Sigma_\mathbf{x} \ell(\mathbf{x})(-1/\bar{\nabla}\cdot\nabla)\ell(\mathbf{x})} \qquad (11.102)$$

Dividing out the normalization factor Z_{VM} we find that the presence of vortices modifies the low temperature correlation function multiplicatively by a correlation factor, i.e.,

$$G_r(\mathbf{X}, \mathbf{X}') = \frac{1}{Z_r} \sum_{\{\ell(\mathbf{x})\}} e^{-(\beta v/2)4\pi^2 \Sigma_\mathbf{x} \ell(\mathbf{x})(-1/\bar{\nabla}\cdot\nabla)\ell(\mathbf{x}) - 2\pi i \Sigma_\mathbf{x} Q(\mathbf{x})(-1/\bar{\nabla}\cdot\nabla)\bar{\nabla}_i n_i(\mathbf{x})}, \qquad (11.103)$$

where

$$Z_r \equiv \sum_{\{\ell(\mathbf{x})\}} e^{-(\beta v/2)4\pi^2 \Sigma_\mathbf{x} \ell(\mathbf{x})(-1/\bar{\nabla}\cdot\nabla)\ell(\mathbf{x})} \qquad (11.104)$$

is the partition function of the pure vortex ensemble [compare (9.30)]. The interaction in the second Boltzmann factor has the same kind of geometric interpretation as in the three-dimensional case. If $n_i(\mathbf{x})$ describes a vortex-antivortex pair, then

$$\Omega(\mathbf{x}) = 2\pi \frac{1}{-\bar{\nabla}\cdot\nabla} \bar{\nabla}_i n_i(\mathbf{x}) \qquad (11.105)$$

is the lattice version of the angle under which the pair is seen by the monopole at the point $\mathbf{x}$. This follows from the same sort of arguments used in Eqs. (9.23)–(9.25). Taking $\mathbf{x}$ far away from the vortex pair we can approximate

$$-\frac{1}{\bar{\nabla}\cdot\nabla}(\mathbf{x}) \to -\frac{1}{2\pi}\log|\mathbf{x}| + \text{const}, \qquad (11.106)$$

and $n_i(\mathbf{x}) \to \delta_i(S)$ where S is now a line connecting the pair. Formula (11.105) then becomes

$$\Omega(\mathbf{x}) \to -\int d^2x' \log R\, \partial_i' \delta_i(S) = \int d^2x'\, \partial_i' \log R\, \delta_i(S) = -\int dS_i'\, R_i/R,$$

$$(11.107)$$

which is precisely the angle described above. In terms of $\Omega(\mathbf{x})$, the vortex correlation (11.44) takes the simple form [compare with (9.30)]

$$G_v(\mathbf{x}_1, \mathbf{x}_1') = Z_v^{-1} \sum_{\{\ell(\mathbf{x})\}} e^{-(\beta v/2)4\pi^2\Sigma_x \ell(\mathbf{x})(-1/\bar\nabla\cdot\nabla)\ell(\mathbf{x}) + i\Sigma_x Q(\mathbf{x})\Omega(\mathbf{x})}. \quad (11.108)$$

An alternative form for the interaction is found by expressing $Q(\mathbf{x})$ in terms of a monopole gauge field $m_i(\mathbf{x})$ [recall (9.5)] whose lattice divergence is equal to

$$Q(\mathbf{x}) = \bar\nabla_i m_i(\mathbf{x}). \quad (11.109)$$

Inserting this, the last exponential in (11.108) becomes

$$e^{2\pi i \Sigma_x \bar\nabla_i m_i(\mathbf{x})(-1/\bar\nabla\cdot\nabla)\bar\nabla_i n_i(\mathbf{x})}. \quad (11.110)$$

This, in turn, can be rewritten as

$$e^{-2\pi i \Sigma_x(\nabla\times\mathbf{m})(-1/\bar\nabla\cdot\nabla)(\nabla\times\mathbf{n})}. \quad (11.111)$$

Working out the cross products and performing partial integrations, produces only a trivial factor $e^{-2\pi i \Sigma_x m_i(\mathbf{x})n_i(\mathbf{x})} = 1$. Now we can insert $\boldsymbol{\ell} = \nabla \times \mathbf{n}$ and we arrive at

$$e^{-2\pi i \Sigma_x(\nabla\times\mathbf{m})(-1/\bar\nabla\cdot\nabla)\ell(\mathbf{x})}. \quad (11.112)$$

This is the two-dimensional analogue of the last term in the interaction (9.18).

In two dimensions, this interaction has a similar but dual geometric interpretation as the interaction in (11.103). For a pair of oppositely charged monopoles, the monopole gauge field $m_i(\mathbf{x})$ may be represented as a string connecting the two. The field $m_k^\perp = \varepsilon_{k\ell} m_\ell(\mathbf{x} - \boldsymbol{\ell})$ is the set of normal vectors to this string. The expression (11.112) may also be written as

$$e^{-2\pi i \Sigma_x((1/-\bar{\nabla}\cdot\nabla)\bar{\nabla}_k m_k^\perp(x))\ell(x)}.$$ (11.113)

Comparison with (11.105) shows that the potential $\Omega^m(x) = 2\pi(-1/\bar{\nabla}\cdot\nabla)$ $\times \bar{\nabla}_k m_k^\perp$ is the angle under which the pair of monopoles at is seen by a vortex at x.

We arrive therefore at the following alternative form for the vortex correction to the correlation function,

$$G_v(\mathbf{X}, \mathbf{X}') = Z_v^{-1} \sum_{\{\ell(\mathbf{x})\}} e^{-(\beta v/2)4\pi^2 \Sigma_x \ell(\mathbf{x})(1/-\bar{\nabla}\cdot\nabla)\ell(\mathbf{x})} e^{i\Sigma_x \Omega^m(\mathbf{x})\ell(\mathbf{x})}.$$ (11.114)

11.9.   EXPLICIT CALCULATION OF THE TWO-POINT CORRELATION FUNCTION AT LOW TEMPERATURES

After these preliminaries, let us now actually calculate the vortex correction (11.114) in the limit of low temperature. In this limit β is so large that the sum over vortices is strongly suppressed, and we can resort to the independent pair approximation. The lowest contribution comes from a vortex-antivortex pair at $\mathbf{y}$ and $\mathbf{y}' \neq \mathbf{y}$, i.e., from the configurations

$$\ell(\mathbf{x}) = \delta_{\mathbf{x},\mathbf{y}} - \delta_{\mathbf{x},\mathbf{y}'}.$$ (11.115)

Summing over all positions $\mathbf{y} \neq \mathbf{y}'$, Eq. (11.114) becomes approximately equal to

$$G_v(\mathbf{X}, \mathbf{X}') \approx Z_v^{-1}\left[1 + \sum_{\mathbf{y}\neq\mathbf{y}'} e^{\beta v 4\pi^2 v'(\mathbf{y}-\mathbf{y}')}\cos(\Omega^m(\mathbf{y}) - \Omega^m(\mathbf{y}'))\right],$$

where

$$Z_v \approx 1 + \sum_{\mathbf{y}\neq\mathbf{y}'} e^{\beta v 4\pi^2 v'(\mathbf{y}-\mathbf{y}')}.$$ (11.116)

We may therefore write

$$G_v(\mathbf{X}, \mathbf{X}') \sim 1 + \sum_{\mathbf{y}\neq\mathbf{y}'} e^{\beta v 4\pi^2 v'(\mathbf{y}-\mathbf{y}')}[\cos(\Omega^m(\mathbf{y}) - \Omega^m(\mathbf{y}')) - 1]$$

$$\sim \exp\left(\sum_{\mathbf{y}\neq\mathbf{y}'} e^{\beta v 4\pi^2 v'(\mathbf{y}-\mathbf{y}')[\cos(\Omega^m(\mathbf{y})-\Omega^m(\mathbf{y}'))-1]}\right).$$ (11.117)

Notice that the final result can also be expressed in terms of the correlation function of the vortices. These are defined by

$$\langle \ell(\mathbf{y})\ell(\mathbf{y}')\rangle = Z_v^{-1} \sum_{\{\ell(\mathbf{x})\}} \ell(\mathbf{x})\ell(\mathbf{x}')\, e^{-(\beta v/2)4\pi^2 \Sigma_\mathbf{x} \ell(\mathbf{x})(1/-\bar{\nabla}\cdot\nabla)\ell(\mathbf{x})}, \qquad (11.118)$$

and may be cast within the same independent pair approximation as

$$\langle \ell(\mathbf{y})\ell(\mathbf{y}')\rangle \approx -2e^{-\beta v 4\pi^2 v'(\mathbf{y}-\mathbf{y}')}. \qquad (11.119)$$

For large separations, this is equal to [see also (11.28)]

$$\langle \ell(\mathbf{y})\ell(\mathbf{y}')\rangle \xrightarrow[|\mathbf{y}-\mathbf{y}'|\to\infty]{} -2(|\mathbf{y}-\mathbf{y}'|2\sqrt{2}\,e^{\gamma})^{-2\pi\beta v} = -2z_0^2|\mathbf{y}-\mathbf{y}'|^{-2\pi\beta v}. \qquad (11.120)$$

This has the same type of power behaviour as the correlation function $G_{T\to 0}(\mathbf{y}-\mathbf{y}')$ in (11.97), the main difference being that the two powers are reciprocals of each other. For small T, $G_{T\to 0}$ is almost a constant while the correlation function (11.120) falls off very rapidly.

For $\mathbf{y}=\mathbf{y}'$ we can use charge neutrality and calculate $\langle \ell^2(\mathbf{y})\rangle$ from

$$\langle \ell^2(\mathbf{y})\rangle = -\sum_{\mathbf{y}'\neq\mathbf{y}} \langle \ell(\mathbf{y})\ell(\mathbf{y}')\rangle = 2z_0^2 \int_0^\infty dR\, R^{3-2\pi\beta v}. \qquad (11.121)$$

In terms of (11.119), the vortex correction can be written as

$$G_v(\mathbf{X},\,\mathbf{X}') \approx e^{-(1/2)\Sigma_{\mathbf{y}\neq\mathbf{y}'}\langle \ell(\mathbf{y})\ell(\mathbf{y}')\rangle[\cos(\Omega^m(\mathbf{y})-\Omega^m(\mathbf{y}'))-1]}. \qquad (11.122)$$

Suppose Ω^m were small. Then the exponent would have the expansion

$$G_v(\mathbf{X},\,\mathbf{X}') \approx e^{(1/2)\Sigma_{\mathbf{y}\neq\mathbf{y}'}\langle \ell(\mathbf{y})\ell(\mathbf{y}')\rangle[(1/2)(\Omega^m(\mathbf{y}))^2+\Omega^m(\mathbf{y}')^2)-\Omega^m(\mathbf{y})\Omega^m(\mathbf{y}')]}, \qquad (11.123)$$

which, by charge neutrality, would be equal to

$$e^{-(1/2)\Sigma_{\mathbf{y}\neq\mathbf{y}'}\langle \ell(\mathbf{y})\ell(\mathbf{y}')\rangle\,\Omega^m(\mathbf{y})\Omega^m(\mathbf{y}')}. \qquad (11.124)$$

This formula has been used in the literature (by José et al., see the Notes and References), since it looks like an obvious approximation to (11.122). Unfortunately, the assumption of small $\Omega^m(\mathbf{y})$ is not applicable here since Ω^m contains jumps by 2π whenever $\mathbf{x}$ passes across the string connecting

the monopoles. The mistake, however, was cancelled against another one so that their final result is (almost) correct. Proceeding further in the calculation of (11.122) we shall assume that the positions $\mathbf{X}$, $\mathbf{X}'$ of the monopoles to be several lattice spacings apart such that the fast power falloff of $\langle \ell(\mathbf{y})\ell(\mathbf{y}')\rangle$ permits us to use the approximation that $\Omega^m(\mathbf{y})$ and $\Omega^m(\mathbf{y}')$ differ very little from each other, apart from possible jumps by 2π. Therefore we introduce the center of mass position $\bar{\mathbf{y}} = (\mathbf{y} + \mathbf{y}')/2$ of the vortices and expand,

$$\Omega^m(\mathbf{y}) \approx \Omega^m(\bar{\mathbf{y}}) - \tfrac{1}{2}\Delta y_i \bar{\nabla}_i \Omega^m(\bar{\mathbf{y}})$$

$$\Omega^m(\mathbf{y}') \approx \Omega^m(\bar{\mathbf{y}}) + \tfrac{1}{2}\Delta y_i \bar{\nabla}_i \Omega^m(\bar{\mathbf{y}}) \qquad (11.125)$$

where $\Delta \mathbf{y} = \mathbf{y}' - \mathbf{y}$ is the distance between the vortices. The gradient of Ω^m is calculated as follows,[f]

$$\bar{\nabla}_i \Omega = -\varepsilon_{ij}\varepsilon_{jk}\bar{\nabla}_k \Omega = -2\pi\,\varepsilon_{ij}\varepsilon_{jk}\bar{\nabla}_k \frac{1}{-\bar{\nabla}\cdot\nabla}(\nabla \times \mathbf{m})$$

$$= -2\pi\,\varepsilon_{ij}\frac{1}{-\bar{\nabla}\cdot\nabla}\varepsilon_{jk}\varepsilon_{n\ell}\bar{\nabla}_k \nabla_n m_\ell$$

$$= -2\pi\,\varepsilon_{ij}\frac{1}{-\bar{\nabla}\cdot\nabla}\bar{\nabla}_\ell m_\ell - 2\pi\,\varepsilon_{ij}m_j. \qquad (11.126)$$

Now since $\bar{\nabla}_\ell m_\ell = Q(\mathbf{x})$ we write

$$\cos(\Omega^m(\mathbf{y})) - \Omega^m(\mathbf{y}')) - 1 \sim \cos(\Delta y_i \nabla_i \Omega(\bar{\mathbf{y}})) - 1$$

$$= \cos\left(-2\pi\Delta y_i \varepsilon_{ij}\nabla_j \frac{1}{-\bar{\nabla}\cdot\nabla}Q(\bar{\mathbf{y}})\right) - 1. \qquad (11.127)$$

[f] Notice that for large distances from the monopoles at $\mathbf{X}$, $\mathbf{X}'$,

$$\Omega^m(\mathbf{x}) \sim \tan^{-1}\frac{x_2 - X_2}{x_1 - X_1} - \tan^{-1}\frac{x_2 - X_2'}{x_1 - X_1'}.$$

Therefore

$$\partial_i \Omega^m(\mathbf{x}) \sim -\varepsilon_{ij}\left(\frac{x_j - X_j}{|\mathbf{x} - \mathbf{X}|^2} - \frac{x_j - X_j'}{|\mathbf{x} - \mathbf{X}'|^2}\right) + \text{jumps} = -\varepsilon_{ij}\partial_j(\log|\mathbf{x} - \mathbf{X}| - \log|\mathbf{x} - \mathbf{X}'|) + \text{jumps}.$$

The gradients describe the magnetic field around electric currents piercing the plane at $\mathbf{X}$ and $\mathbf{X}'$.

Inside the cosine the integer jump numbers m_j of (11.126) are irrelevant so that we can expand, for small distances

$$\cos(\Omega^m(\mathbf{y}) - \Omega^m(\mathbf{y}')) - 1 \sim -\frac{4\pi^2}{2}\Delta y_i \nabla y_j \nabla_i \frac{1}{-\bar{\nabla}\cdot\nabla}Q(\bar{\mathbf{y}})\nabla_j\frac{1}{-\bar{\nabla}\cdot\nabla}Q(\bar{\mathbf{y}}).$$

$$(11.128)$$

With this we rewrite (11.122) as follows:

$$G_v(\mathbf{X}, \mathbf{X}') \sim e^{\pi^2\Sigma_{\Delta y\neq 0}\langle\ell(\Delta y)\ell(0)\rangle\Delta y_i\Delta y_j\Sigma_{\bar{y}}\nabla_i(1/-\bar{\nabla}\cdot\nabla)Q(\bar{y})\nabla_j(1/-\bar{\nabla}\cdot\nabla)Q(\bar{y})}.$$

$$(11.129)$$

We now perform an average over the two spatial directions, replacing $\Delta y_i\Delta y_j$ by $(1/2)\delta_{ij}$. After this, a partial integration of ∇_i removes one of the lattice Coulomb potentials and we are left with

$$G_v(\mathbf{X}, \mathbf{X}') \sim e^{(\pi^2/2)\Sigma_{\Delta y}\langle\ell(\Delta y)\ell(0)\rangle(\Delta y)^2\Sigma_{\bar{y}}Q(\bar{y})(1/-\bar{\nabla}\cdot\nabla)Q(\bar{y})}.$$

$$(11.130)$$

Inserting the monopole charge distribution (11.93) this gives[g]

$$G_v(\mathbf{X}, \mathbf{X}') \sim e^{-\pi^2\Sigma_{\Delta y}\langle\ell(\Delta y)\ell(0)\rangle(\Delta y)^2 v'(\mathbf{X} - \mathbf{X}')}.$$

$$(11.131)$$

Comparison with the limiting form (11.96) shows that the corrected correlation function can once more be written in the same form,

$$G(\mathbf{X}, \mathbf{X}') = G_{T\to 0}(\mathbf{X}, \mathbf{X}')\, G_v(\mathbf{X}, \mathbf{X}') \approx e^{(1/\beta_V^R)v'(\mathbf{X}-\mathbf{X}')},$$

$$(11.132)$$

with the only modification that β_V is replaced by a renormalized value β_V^R which is calculated from β_V via the simple second moment sum rule[h]

---

[g]Notice that there is a factor 2 in the exponent as compared with the result of José *et al.* Those authors apparently forgot the last term in the expansion

$$\Omega^m(\mathbf{y})\Omega^m(\mathbf{y}') = \Omega^m\left(\bar{\mathbf{y}}+\frac{\Delta\mathbf{y}}{2}\right)\Omega^m\left(\bar{\mathbf{y}}-\frac{\Delta\mathbf{y}}{2}\right) = \Omega^m(\bar{\mathbf{y}})^2 - \left(\frac{\Delta\mathbf{y}}{2}\right)^2\Omega^m(\bar{\mathbf{y}})'^2 + \frac{(\Delta\mathbf{y})^2}{4}\Omega^m(\bar{\mathbf{y}})\,\Omega^m(\bar{\mathbf{y}})'',$$

which by partial integration in the sum over $\bar{\mathbf{y}}$ doubles the second term.

[h]Actually, one can prove quite *generally*, i.e., *without* the fugacity expansion, that the stiffness of phase fluctuations, which is observable via the superfluid density, is renormalized by

$$\beta^R = \beta + \pi^2\lim_{\mathbf{k}\to 0}\frac{1}{k^2}\langle\ell(\mathbf{k})\ell(\mathbf{k})\rangle$$

(to be shown in Section 11.12). This reduces to (11.133) at low fugacity.

$$(\beta_V^R)^{-1} = \beta_V^{-1} - \pi^2 \sum_{\Delta y} \langle \ell(\Delta y)\,\ell(0)\rangle (\Delta y)^2 = \beta_V^{-1} + 2\pi^2 \sum_{\Delta y} e^{\beta_V 4\pi^2 v'(\Delta y)} (\Delta y)^2.$$

(11.133)

This means that a rare ensemble of vortex pairs changes the effective bending energy of the field at long wavelengths from $(1/2)\beta_V(\nabla_i\gamma)^2$ to $(1/2)\beta_V^R(\nabla_i\gamma)^2$.

Using (11.120), the sum in (11.133) can be calculated approximately with the result

$$(\beta_V^R)^{-1} \sim \beta_V^{-1} + 4\pi^3(2\sqrt{2}\,e^{\gamma})^{-2\pi\beta_V} \int_1^\infty \frac{dR}{R} R^{4-2\pi\beta_V} = \beta_V^{-1} + 4\pi^3 z_0^2 \frac{1}{2\pi\beta_V - 4}.$$

(11.134)

Notice that the presence of a vortex pair *reduces* the bending energy (as should have been expected).

As β_V approaches $2/\pi$, the reduction becomes dramatic but there the approximation is no longer reliable. Still, since $4\pi^3 z_0^2 \beta_V = 2/\pi = 4\pi^3(2\sqrt{2}\,e^{\gamma})^{-4} \sim 0.2$ is reasonably small, we can carry β_V up to a percent below $2/\pi$ until the approximation breaks down. Hence we obtain the lowest estimate

$$\beta_V^c \sim \frac{2}{\pi} = 0.637$$

(11.135)

for the critical inverse temperature (to be compared with the true value of 0.73).

The approximation obtained by replacing the sum by an integral has the largest error when the temperature is small, i.e., for large β_V. There only nearest neighbours contribute and

$$(\beta_V^R)^{-1} \to \beta_V^{-1} + 2\pi^2 4 e^{-\beta_V 4\pi^2(1/4)}$$

in contrast to (11.134) which gives

$$(\beta_V^R)^{-1} \to \beta_V^{-1} + 2\pi^2(2\sqrt{2}\,e^{\gamma})^{-2\pi\beta_V} \frac{2\pi}{2\pi\beta_V - 4}.$$

While the exponential falloff is rather similar, due to

$$c^{-2\pi\beta_V} = (2\sqrt{2}\,e^\gamma)^{-2\pi\beta_V} = e^{-1.6167 \times 2\pi\beta_V} \sim e^{-\pi^2\beta_V} = e^{-1.5708 \times 2\pi\beta_V}$$

[compare (11.14)], the algebraic factor is quite different.

Incidentally, the large β_V behaviour at the right-hand side can be improved by treating the next nearest neighbour pair separately and writing

$$\sum_{\Delta y} e^{\beta_V 4\pi^2 v'(\Delta y)}\,(\Delta y)^2 \approx 4e^{-\beta_V 4\pi^2(1/4)} + (2\sqrt{2}\,e^\gamma)^{-2\pi\beta_V}\,2\pi \int_{(5/\pi)^{1/2}}^{\infty} dR\, R^{3-2\pi\beta_V}$$

$$= 4e^{-\beta_V 4\pi^2(1/4)} + (2\sqrt{2}\,e^\gamma)^{-2\pi\beta_V}\frac{2\pi}{2\pi\beta_V - 4}\left(\frac{5}{\pi}\right)^{2-\pi\beta_V},$$

$$(11.136)$$

where the radius of integration $(5/\pi)^{1/2}$ is chosen in analogy to r_0 of Eq. (11.27) in such a way that the 5 closest unit squares are properly completed to an integral over the entire system. This approximation is valid for all $\beta_V > 2/\pi$ with an error of less than 1%.

11.10. THE RENORMALIZATION GROUP

It is possible to explore the critical region more accurately by taking recourse to a resummation of infinitely many diagrams via the renormalization group. In the present case, the procedure is simple enough to be included in this text. The resummation is based on the following argument: in the correlation function $G(\mathbf{X}, \mathbf{X}')$, the presence of a few vortices softens the stiffness of the $\gamma(\mathbf{x})$ fluctuations from β_V to $\beta_V^R < \beta$. When calculating the effect on β_V of a gas of independent pairs in (11.134), the result can be improved by taking this softening into account self-consistently. This implies that in the correction term of (11.134), the renormalized β_V^R should be used rather than β. A first improved equation is therefore

$$(\beta_V^R)^{-1} = \beta_V^{-1} + 4\pi^3 z_R^2 \int_1^\infty \frac{dR}{R} R^{4-2\pi\beta_V^R} = \beta_V^{-1} - 4\pi^3 z_R^2 \frac{1}{4 - 2\pi\beta_V^R}, \qquad (11.137)$$

where we have introduced the quantity

$$z_R = c^{-\pi\beta_V^R}, \qquad (11.138)$$

which is the renormalized version of z_0 in (11.28).

For $\beta_V^R < 2/\pi$ there is a solution. For $\beta_V^R \lesssim 2/\pi$, the approximation again breaks down since the correction term becomes comparable with the original value of β_V. In order to find out more reliably what happens in the immediate vicinity of $\beta_V^R \lesssim 2/\pi$ we must employ a better infinite resummation procedure. It is suggested by the fact that the renormalization of β_V^{-1} in (11.134),

$$(\beta_V^R)^{-1} = \beta_V^{-1} + 2\pi^2 \sum_{\Delta y} (\Delta y)^2 \, e^{4\pi^2 \beta_V v'(\Delta y)} = \beta_V^{-1} + 4\pi^3 z_0^2 \int_1^\infty \frac{dR}{R} R^{4-2\pi\beta_V},$$

$$(11.139)$$

which gives the softening of the stiffness constant due to vortex and antivortex pairs, is *additive* with respect to pairs of different sizes. It is therefore possible to define a partially renormalized stiffness $\beta_V(\lambda)$ which contains only the effect of pairs with separation smaller than λ:

$$\beta_V^{-1}(\lambda) = \beta_V^{-1} + 4\pi^3 z_0^2 \int_1^\lambda \frac{dR}{R} R^{4-2\pi\beta_V}. \qquad (11.140)$$

This equation can now be made self-consistent. We remember that the stiffness β_V contained in z_0 and β on the right-hand side had its origin in the Boltzmann factor $e^{4\pi^2 \beta_V v'(x)}$ where $v'(x)$ is the subtracted Coulomb potential on the lattice. The potential, in turn, may be viewed as the energy resulting from separating the charges against the local force $\beta_V d|x|/|x|$ the nearest neighbour potential being $-v_c = -(1/2\pi)\log c$. Thus

$$\beta_V v'(x) = -\frac{\beta_V}{2\pi}\left(\log c + \int_1^{|x|} \frac{dr'}{r'} \right), \qquad (11.141)$$

where $c = 2\sqrt{2}\, e^\gamma \approx 5.0376$ is the inverse core radius [see (11.29)]. If we want to work self-consistently, this local force has to be calculated using the local stiffness $\beta_V(r)$ rather than β_V. Thus we have to replace $\beta_V v'(x)$ in the Boltzmann factor, by the integral

$$-\frac{1}{2\pi}\left(\beta_V \log c + \int_0^{|x|} \frac{dr}{r} \beta_V(r) \right)$$

and we arrive at the following self-consistent version of (11.140)

$$\beta_V^{-1}(\lambda) = \beta_V^{-1} + 4\pi^3 z_0^2 \int_0^{\log \lambda} d\log R \, e^{4\log R - 2\pi \int_0^{\log R} d\log r \, \beta_V(r)}. \qquad (11.142)$$

In this way, the algebraic equation (11.137) is turned into an *integral equation*. For $\lambda = 1$, $\beta_V(\lambda)$ is equal to the bare stiffness β_V. In the limit, $\lambda \to \infty$, it gives the fully renormalized stiffness:

$$\beta_V^R = \lim_{\lambda \to \infty} \beta_V(\lambda). \qquad (11.143)$$

In order to solve this it is useful to introduce an auxiliary fugacity[j] for a pair separated by a distance λ,

$$z(\lambda) = z_0 e^{2\log\lambda - \pi \int_0^{\log\lambda} d\log\lambda \, \beta_V(\lambda)} \qquad (11.144)$$

and write the integral equation as

$$\beta_V^{-1}(\lambda) = \beta_V^{-1} + 4\pi^3 \int_0^{\log \lambda} d\log R \, z^2(R). \qquad (11.145)$$

It is now straightforward to convert the pair of equations (11.144), (11.145) into a pair of differential equations

$$\frac{dz(\lambda)}{d\log\lambda} = (2 - \pi\beta_V(\lambda)) z(\lambda), \qquad (11.146)$$

$$\frac{d\beta_V^{-1}(\lambda)}{d\log\lambda} = 4\pi^3 z^2(\lambda). \qquad (11.147)$$

These are commonly referred to as the *renormalization group equations* of the Villain model. The initial conditions are

$$\beta_V(1) = \beta_V, \qquad z(1) = z_0 = c^{-\pi\beta_V}, \qquad c = 2\sqrt{2}\,e^\gamma \approx 5.0376.$$

The equations can easily be solved; for each initial $\beta_V(1)$, $z(1)$, they provide us with a trajectory in the β_V, z plane.

---

[j]It reduces to the ordinary fugacity z_0 of (11.28) times $\lambda^{2 - \pi\beta_V}$ if $\beta_V(\lambda)$ does not depend on λ.

For the calculation it is useful to introduce reduced quantities

$$x \equiv \frac{2}{\pi} \beta_V^{-1} - 1, \qquad y \equiv 2\pi z \qquad (11.148)$$

and to define

$$\ell \equiv \log \lambda. \qquad (11.149)$$

Then Eqs. (11.146) and (11.147) take the simpler form ($' \equiv d/d\ell$)

$$y' = 2xy, \qquad x' = 2y^2. \qquad (11.150)$$

There are obviously two trivial solutions, the straight lines

$$y = \pm x. \qquad (11.151)$$

Along these straight lines, the trajectories move, as a function of ℓ, as follows:

$$x_- = \frac{-|x_0|}{1 + \frac{1}{2}|x_0|\ell}, \qquad y_- = \frac{|x_0|}{1 + \frac{1}{2}|x_0|\ell},$$

$$x_+ = \frac{x_1}{1 - \frac{x_1}{2}\ell}, \qquad y_+ = \frac{x_1}{1 - \frac{1}{2}x_1(\ell - \ell_1)}, \qquad (11.152)$$
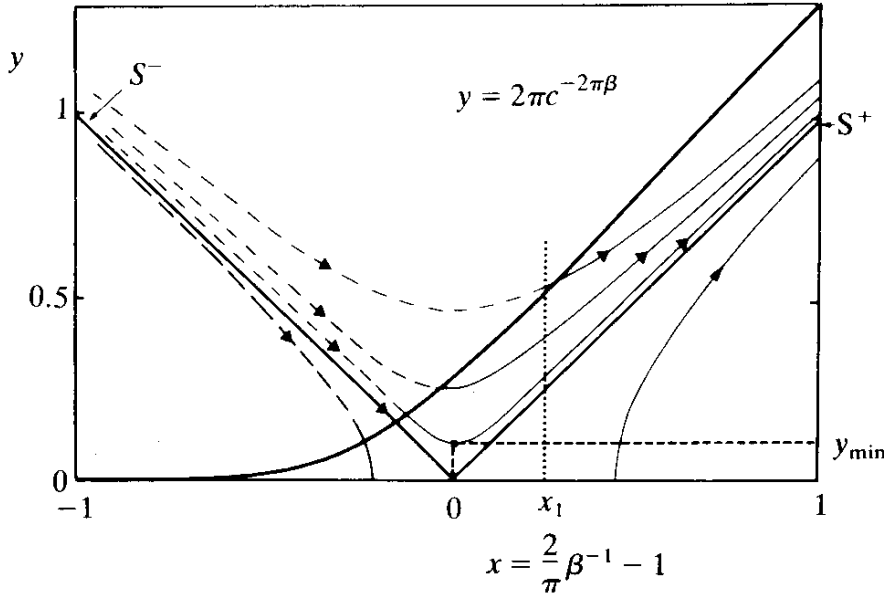
where $x_-(\ell)$, $y_-(\ell)$ are equal to x_0, y_0 for $\ell = 0$ and $x_+(\ell)$, $y_+(\ell)$ are equal to x_1, y_1 for $\ell = \ell_1$. The two trajectories will be called S_-, S_+, respectively (see Fig. 11.17). For increasing ℓ, S_- moves downwards, towards that axis. For decreasing ℓ, S_+ moves upwards.

It is not hard to find the remaining trajectories. Dividing the two equations (11.150) by one another gives

$$\frac{dy}{dx} = \frac{x}{y}, \qquad (11.153)$$

or

FIG. 11.17.   Renormalization group trajectories of the 2D Villain model. The solid curve is the fugacity relation $y_0 = 2\pi c^{-2/(1+x)}$. The intercept with the separatrix S_- gives the critical point x_c, y_c.

$$y = \sqrt{x^2 + \kappa^2}. \tag{11.154}$$

The connection with ℓ is given by

$$\ell = \frac{1}{2} \int dx \frac{1}{x^2 + \kappa^2} = \frac{1}{2} \frac{1}{\kappa} \tan^{-1} \frac{x}{\kappa} \qquad \kappa^2 > 0,$$

$$= \frac{1}{4\sqrt{-\kappa^2}} \log \frac{x - \sqrt{-\kappa^2}}{x + \sqrt{-\kappa^2}} \quad \kappa^2 < 0. \tag{11.155}$$

We can now distinguish three regimes in the xy-plane.

1. $\kappa^2 < 0$, $x_0 < 0$. The trajectories lie left of S_- and move towards the x-axis for increasing ℓ, intercepting it at $x_0^R = \kappa$.

2. $\kappa^2 > 0$, $x_0 > 0$. The trajectories lie to the right of S_+ and move away from the x-axis with increasing ℓ, starting from $\bar{x}_0^R = \kappa$.

3. $\kappa^2 > 0$. If $x_0 < 0$, the trajectories move first toward the x-axis, pass through a minimum at,

$$x_{min} = 0, \quad y_{min} = \kappa,$$

after which they move again away from the x-axis. Since the trajectories S_- and S_+ separate these three regimes, they are called *separatrices*.

According to (11.147), the Villain model itself is specified by the initial fugacity curve

$$z_0 = c^{-\pi\beta_V}, \qquad c \approx 2\sqrt{2}\,e^{\gamma} \approx 5.0376. \tag{11.156}$$

In terms of the present variables, this amounts to

$$y_0 = 2\pi c^{-2/(1+x_0)}, \tag{11.157}$$

and is indicated by the solid curve in Fig. 11.17. What the trajectories tell us is that for sufficiently low temperatures, and as long as $x_0 \ll 0$, the Villain model is equivalent to a Coulomb gas in which the fugacity is infinite, i.e., in which the charges are really absent, with renormalized stiffness β_V^R given by the intercept of the corresponding trajectory with the β_V^{-1} axis. For $x_0 > 0$, the trajectories run off eventually to infinity and this is no longer true. Somewhere for small $x_0 < 0$ the model undergoes a phase transition.

It is then easy to identify the critical value β_{Vc}. It is given by the intersection point of the dashed line with the left-hand separatrix S_-. Thus, under the assumption that the Villain value of z_0 is sufficiently small to justify the fugacity expansion, the critical value β_{Vc} is obtained from the equation

$$y_c = -x_c = 2\pi c^{-2/(1+x_c)}, \qquad c = 2\sqrt{2}\,e^{\gamma} \approx 5.0376. \tag{11.158}$$

This is solved by

$$x_c \approx -0.1438, \tag{11.159}$$

so that

$$\beta_{Vc} = \frac{2}{\pi}\frac{1}{1+x_c} \approx 0.7436. \tag{11.160a}$$

From Monte Carlo simulations, the critical point is found to lie at

$$\beta_{Vc} \approx 0.73,$$

in good agreement with this number. The deviation is of the same order as that resulting from writing the approximation $1/(1+x_c) \sim 1 - x_c$ at $x_c \approx -0.14$ (i.e., $\lesssim 2\%$) which is the typical error inherent in the fugacity expansion.

It is instructive to calculate the renormalized stiffness β_V^R as a function of β_V. It follows from a combination of (11.157) and (11.54), giving

$$x_0^R = \kappa = -[x_0^2 - 4\pi^2 c^{-4/(1+x_0)}]^{1/2}. \tag{11.161}$$

Translating x_0 to β_V, Eq. (11.48) gives the discrete function, plotted in Fig. 7.7. At very low temperatures, there is only an exponentially small renormalization due to finite activation energy of the vortices. Close to the transition, β_V^R turns downward sharply and ends at the critical point

$$\beta_{V_c}^R = \frac{2}{\pi}.$$ (11.160b)

11.11. COHERENCE LENGTH

The renormalization group equations (11.146), (11.147) can be used to tell us more than just the location of the critical point. As noticed by Kosterlitz, they also give valuable information on the behaviour of experimental quantities in the neighbourhood of this critical point. One of these quantities is the coherence length ξ of the spin waves. In the entire low temperature phase, spin waves are massless modes and of infinite range. As soon as the Villain model line crosses the left-hand separatrix, the coherence length becomes finite and decreases rapidly with temperature. In three-dimensional systems, the behavior close to the critical point is usually given by a power law

$$\xi(\tau) \propto \tau^{-\nu},$$

where $\tau \equiv T/T_c - 1$.

The two-dimensional Villain model, however, does not obey this general law. As we shall demonstrate immediately, it has the following anomalous critical behavior

$$\xi(\tau) \propto e^{\mathrm{const}/\tau^{1/2}}.$$ (11.162)

This can be derived from the renormalization group as follows. Consider a trajectory through a point x_0, y_0 on the initial fugacity curve $y = 2\pi c^{-2/(1+x)}$, just above the critical temperature. When increasing the scale parameter $\ell = \log \lambda$, the trajectory follows closely the separatrix S_- towards the x-axis. Thus, upon including larger and larger vortex pairs, the fugacity decreases just as it does in the ordered phase. The system acts in a completely coherent fashion. The length scale is related to the change of x by Eq. (11.155). Hence it satisfies

$$\ell = \frac{1}{2} \int_{x_0}^{x} \frac{dx}{y^2}.$$ (11.163)

Inserting the trajectory (11.154) gives

$$\ell = \frac{1}{2} \int_{x_0}^{x} \frac{dx}{x^2 + y_{\min}^2} = \frac{1}{2y_{\min}} \left(\tan^{-1} \frac{x}{y_{\min}} - \tan^{-1} \frac{x_0}{y_{\min}} \right).$$ (11.164)

Close to the minimum of the trajectory at $x = 0$, $y = y_{\min}$, the scale $\lambda = e^{\ell}$ can increase by several orders of magnitude with only very little change in x and y. Once x has passed through the minimum, the increase slows down. The function $\ell(x)$ becomes almost constant if x, y move toward larger positive values.

Let us follow the renormalization group trajectory (11.154) as a function of ℓ [as given by (11.164)] for several initial points x_0, $y_0 = 2\pi e^{-2/(1 + x_0)}$ on the fugacity curve of the Villain model. These points are a smooth function of τ. For $\tau = 0$, $x_0 \leqslant x_c$, $y_0 = y_c = -x_c$ lies on the separatrix. Suppose now that we select the final points x, y on the trajectory to have all a common $x_1 > 0$ which is large enough so that the temperature lies above the peak in the specific heat of the Villain model, but with y small enough to justify working with the fugacity expansion. The coherence length $\xi(x, y)$ at $x = x_1$ is then a smooth function of x_0, y_0 and thus of τ. For dimensional reasons, the coherence length of the initial Villain model with parameters x_0, y_0 is related to this coherence length $\xi(x, y)$ by the scale factor $\lambda = e^{\ell}$, i.e., we can calculate

$$\xi(x_0, y_0) = \xi(x, y)\, e^{\ell} = \xi(x, y)\, e^{(1/2)\int_{x_0}^{x}(dx/y^2)}$$

$$= \xi(x, y)\, e^{(1/2y_{\min})[\tan^{-1}(x/y_{\min}) - \tan^{-1}(x_0/y_{\min})]}. \qquad (11.165)$$

Inspecting Fig. 11.17, we decide to choose the final parameters x, y to be

$$x = x_1 = 0.25, \qquad y = y_1 = \sqrt{x_1^2 + y_{\min}^2}. \qquad (11.166)$$

This choice satisfies the above requirements. It is large enough to be well beyond the peak of the specific heat in the Villain model which lies around $x \sim 0$ as seen in Fig. 11.5, and thus within the disordered phase, and y_1 is small enough to justify the fugacity expansion.

We now have to express the parameters x_0, y_0 in terms of the temperature of the Villain model. For this we introduce the reduced temperature

$$\tau \equiv \frac{2}{\pi}(\beta^{-1} - \beta_c^{-1}), \qquad (11.167)$$

so that x increases directly with τ as it passes the critical point, and we can write

$$x_0 = x_c + \tau. \qquad (11.168)$$

The critical value y_0 has to lie on the fugacity curve

$$y_0 = 2\pi c^{-2/(1+x_0)}, \qquad c = 2\sqrt{2}\,e^{\gamma} \approx 5.0376.$$

For small τ it may be expanded as

$$y_0 = y_c + \alpha\tau = -x_c + \alpha\tau, \tag{11.169}$$

where α is the slope of (11.157) at the critical point,

$$\alpha \equiv \frac{\partial y_0}{\partial x_0}\bigg|_{x_c} = \frac{2\log c\, y_c}{(1+x_c)^2} = \frac{-2\log c\, x_c}{(1+x_c)^2}. \tag{11.170a}$$

Eliminating the core parameter via Eq. (11.157), this can be expressed entirely in terms of x_c

$$\alpha = \frac{x_c}{1+x_c}\log\frac{|x_c|}{2\pi} \approx 0.635. \tag{11.170b}$$

The parameter $y_{\min}$ of the renormalization group trajectory is now determined by the condition that the trajectory passes through x_0, y_0, i.e.,

$$-x_c + \alpha\tau \approx \sqrt{(x_c + \tau)^2 + y_{\min}^2}.$$

This gives

$$y_{\min} \approx \sqrt{(x_c - \alpha\tau)^2 - (x_c + \tau)^2}$$

$$\approx \sqrt{2|x_c|(\alpha + 1)}\,\tau^{1/2} \equiv \bar{y}_{\min}\,\tau^{1/2} \approx 0.686\,\tau^{1/2}. \tag{11.171}$$

Thus, for small τ, $y_{\min}$ vanishes as $\tau^{1/2}$. Inserting this into Eq. (11.165) we find

$$\xi(\tau) \propto \xi(x_1, y_1)\exp\left\{\frac{1}{2\bar{y}_{\min}\tau^{1/2}}\left(\tan^{-1}\frac{x_1}{\bar{y}_{\min}\tau^{1/2}} + \tan^{-1}\frac{|x_c| - \tau}{\bar{y}_{\min}\tau^{1/2}}\right)\right\} \cdot \tag{11.172}$$

For very small τ, the parenthesis approaches smoothly the value π so that we find the critical behavior

$$\xi(\tau) \underset{\tau\to 0}{\propto} e^{(\pi/2\bar{y}_{\min})(1/\tau^{1/2})} \approx e^{2.29(1/\tau^{1/2})}. \tag{11.173a}$$

This critical behavior is a distinguishing feature of the pair unbinding transition in two dimensions and it is therefore desirable to confirm it, either experimentally or by Monte Carlo simulations. Unfortunately, this is very hard to do. The reason is that unless τ is much smaller than $(|x_c|/\bar{y}_{\min})^2 \approx 5 \times 10^{-2}$, the τ dependence of the expression in parentheses of (11.172) can obscure completely the leading $\tau^{1/2}$ dependence. In order to see this most easily we calculate the lowest two corrections to the leading $\tau^{-1/2}$ behavior in the exponent. This gives

$$\xi(\tau) \underset{\tau \to 0}{\overset{\propto}{\sim}} \left\{ \frac{\pi}{2\bar{y}_{\min}\tau^{1/2}} - \frac{1}{2|x_c|}\left(1 + \frac{\tau}{|x_c|}\right) - \frac{1}{2x_1} + \frac{1}{6}\bar{y}_{\min}^2\left(\frac{1}{x_1^3} + \frac{1}{|x_c|^3}\right)\tau + \ldots \right\}$$

$$\approx \exp\left\{ \frac{2.29}{\tau^{1/2}} - 5.47 - 24.2\tau + 32.4\tau - \ldots \right\} . \tag{11.173b}$$

If the first term is to dominate it has to be 10 times larger than the others. This gives $\tau \lesssim 10^{-2}$. Unless τ is driven to such small values, a best fit of $\xi(\tau) \sim a e^{b/\tau^{\nu}}$ to the experimental data will result in an apparently *larger* critical index ν. It is therefore not astonishing that Tobochnik and Chester (1979), when trying to fit the coherence length of the XY model, obtained in a Monte Carlo simulation on a 100×100 lattice, find for the best functional form (see Fig. 11.18)

$$\xi \sim 0.5 e^{0.9/(T/T_c - 1)^{0.7}} .$$

At their smallest value of $T/T_c - 1 = 0.12$, ξ is equal to 25 and, due to the finite size of their system, it is impossible for them to invade into the regime where the index ν can be resolved. Real laboratory experiments encounter a similar problem, since a two-dimensional system can only be prepared by adsorption on a smooth surface and it is hard to prevent inhomogeneities beyond a few hundred Ångstroms.

The most recent Monte Carlo data are shown in Figs. 11.8b–d.

11.12. UNIVERSALITY OF THE CRITICAL STIFFNESS

It should be noted that in obtaining for the renormalized stiffness constant β_{vc}^R the value $2/\pi$ we did not recessarily have to deal only with the particular Villain model, as it stands, but could just as well have considered an entire family of models with different fugacities. In the vortex representation this family is described by the partition functions,

FIG. 11.18.(a)   Monte Carlo data of the coherence length of the XY model in the range $T[\epsilon(1.0, 1.3)$ as obtained first by Tobochnik and Chester (1979). They fitted the small circles with $\xi \approx 0.5\exp[0.9/(T/0.89 - 1)^{0.7}]$. Their results were improved recently by Samuel and Yee (1985) whose best fit, $\xi \propto \exp[\mathrm{const.}/(T/0.85 - 1)^{0.45}]$, is shown as a dotted curve. The solid curve shows an alternative power fit $\xi \propto (T/0.93 - 1)^{-1.46}$ which demonstrates how hard it is to resolve a Kosterlitz-Thouless behavior. Equally good fits were obtained with $T_c \in (0.82, 0.85)$ and $\nu \in (0.45, 0.65)$ (and with $T_c \in (0.91, 0.96)$, $\nu \in (1.2, 1.65)$ for the power fit].
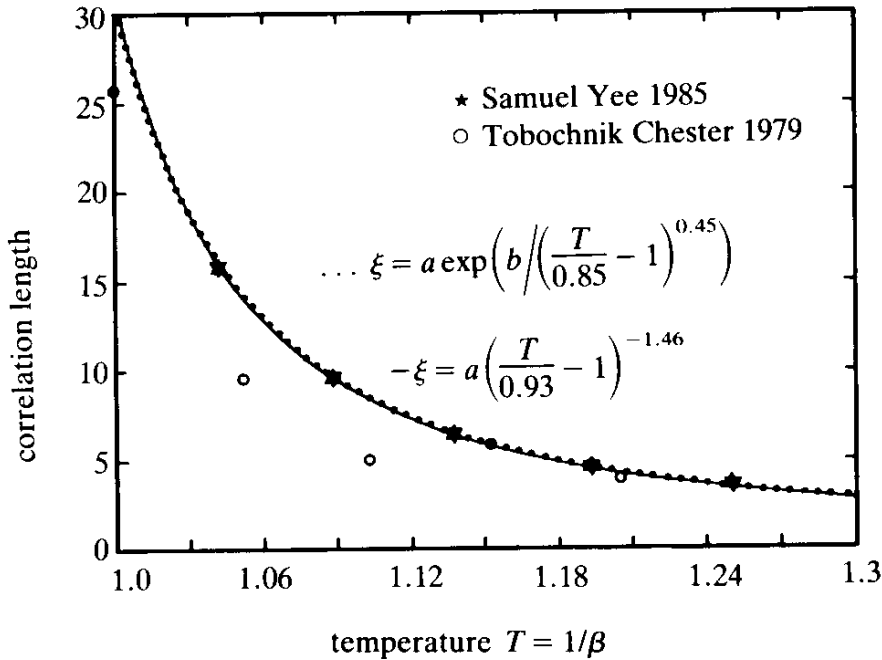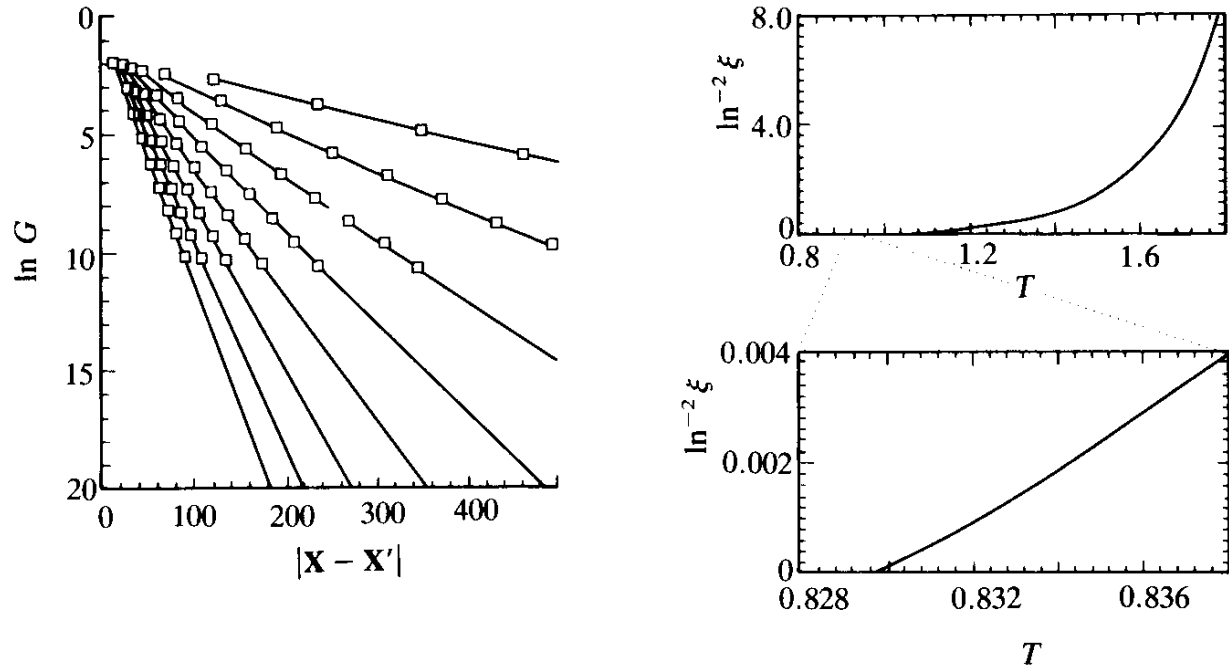
FIG. 11.18.(b), (c), (d)   The most recent determination of the coherence length by S. Heinekamp, R.A. Pelcovits. They perform the linear fits (to the logarithm of the correlation function $G(\mathbf{X} - \mathbf{X}')$ of the Villain model on a square lattice) shown on the left. The reduced temperature $(T - T_c)/T_c$ associated with the straight lines are, from left to right, (6, 6.4, 7, 7.3, 7.7, 8, 8.7, 9.2) $\times 10^{-2}$, respectively. The slopes yield the almost straight line (c) in the immediate neighborhood of the critical point shown on the bottom right. The Kosterlitz-Thouless theory requires a strictly linear fit with slope 1/2. The top right shows the behavior of the larger neighborhood of T_c.

$$Z_{VM} = \det(-\bar{\nabla} \cdot \nabla)^{-1/2} \frac{1}{(\sqrt{2\pi\beta_V})^N} \sum_{\{\ell(\mathbf{x})\}} e^{-(4\pi^2/2)\beta_V \Sigma_\mathbf{x} \ell(\mathbf{x})(1/\bar{\nabla} \cdot \nabla)\ell(\mathbf{x}) - \beta_V(4\pi^2/2)e_c\Sigma_\mathbf{x}\ell^2(\mathbf{x})},$$

$$(11.174)$$

where e_c is an arbitrary extra core energy. Indeed, after the usual subtraction, the vortex sum is equal to

$$\sum_{\{\ell(\mathbf{x})\}} e^{-(4\pi^2/2)\beta_V(\Sigma_{\mathbf{x},\mathbf{x}'}\ell(\mathbf{x})v'(\mathbf{x}-\mathbf{x}')\ell(\mathbf{x}') + (e_c + 1/2)\Sigma_\mathbf{x}\ell^2(\mathbf{x}))}$$

and the renormalization of β now follows from the formula

$$(\beta_V^R)^{-1} = \beta_V^{-1} + 2\pi^2 z_0^2 \int_1^\infty \frac{dR}{R} R^{4-2\pi\beta_V} \qquad (11.175)$$

with fugacity [compare (11.28), (11.29)]

$$z_0 = e^{-(4\pi^2\beta_V/2)e_c}(2\sqrt{2}\,e^\gamma)^{-\pi\beta_V} = (e^{-2\pi e_c}c)^{-\pi\beta_V} = e^{-2\pi(e_c + v_c)\pi\beta_V}.$$

The important point to realize is that the renormalization group analysis provides us with a *universal* statement concerning the critical stiffness of this whole family of models. Whatever the initial value of z_0, at the critical point the values z_c, β_{Vc}^{-1} have to lie on one and the same renormalization group trajectory which passes through the point $z = 0$, $\beta_V = 2/\pi$. This is the lowest value which the renormalized stiffness β_V^R can have. Above the critical temperature, the stiffness collapses immediately to zero.

The universal stiffness can be measured in the laboratory. In general, due to fluctuation corrections, the experimentally observable bending energy contains higher gradient effects and the effective energy density in momentum space has the form [compare Eq. (1.60)]

$$e(\mathbf{k}) = \frac{\rho_s(\mathbf{k})}{2} \frac{\hbar^2}{M^2} \mathbf{k}^2 |\gamma(\mathbf{k})|^2. \qquad (11.176)$$

The superfluid current is defined as the response of the energy with respect to changes in the superfluid velocity $\mathbf{v}_s = (\hbar/M)\mathbf{k}\,\gamma(\mathbf{k})$,

$$\mathbf{j}_s(\mathbf{k}) = \frac{\partial e(\mathbf{k})}{\partial \mathbf{v}_s} = \rho_s(\mathbf{k}) \frac{\hbar}{M} \mathbf{k}\,\gamma(\mathbf{k}). \qquad (11.177)$$

Its correlations are

$$\langle j_{si}(\mathbf{k}) j_{sj}(\mathbf{k}') \rangle = T\rho_s(\mathbf{k})\left(\delta_{ij} - \frac{k_i k_j}{\mathbf{k}^2} \right) \delta^{(2)}(\mathbf{k} - \mathbf{k}'). \qquad (11.178)$$

The quantity $\rho_s(0)$, observed in the limit of long wavelength, is the physical superfluid density. In the Villain model, the bending energy density of long wavelength excitations in the presence of vortices is $\beta_V^R(\nabla_i \gamma)^2/(2a^2)$. Hence ρ_s is related to the dimensionless stiffness parameter β_V^R via

$$\frac{\rho_s}{T}\frac{\hbar^2}{M^2} = \beta_V^R. \qquad (11.179)$$

Since the critical value of β_V^R is $2/\pi$, one concludes that the experimental data for $\rho_s(0)$, when plotted as a function of the critical temperature T_c should lie on a straight line,

$$\rho_s(0)_c = \frac{M^2}{\hbar^2}\frac{2}{\pi}T_c = 3.52 \times 10^{-9}\frac{\text{g}}{\text{cm}^2}\left(\frac{T_c}{\text{K}}\right). \qquad (11.180)$$

What is observed in the laboratory is the superfluid mass (and dissipation) in a thin film of superfluid ^{4}He, adsorbed on a torsional oscillator. The shift in period is proportional to the superfluid density. Some theoretical analysis is necessary to account for the dynamic effect. The resulting curves beautifully fall on the straight line (11.180) (see Fig. 11.19).
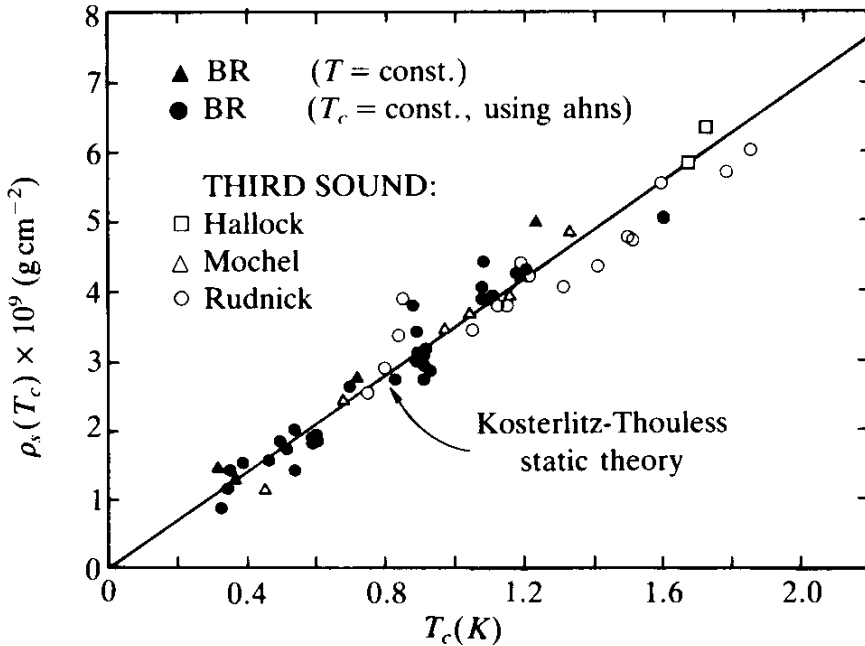
11.13. EXACT FORMULA FOR THE RENORMALIZATION OF SUPERFLUID DENSITY BY VORTICES

Having observed the universality of the renormalized stiffness it is useful to realize that there exists a very general derivation of the renormalization effects for the stiffness β_V which gives an *exact* formula *independent* of the small fugacity assumption. We now give this derivation.

Using the superfluid currents in Eq. (11.177), the hydrodynamic energy is given by

$$\int d^2x \, e(\mathbf{x}) = \int d^2x \frac{\rho_s}{2}v_s^2 = \int d^2x \frac{1}{2\rho_s}\mathbf{j}_s^2. \qquad (11.181)$$

FIG. 11.19. Comparison of experimental stiffness of phase fluctuations in films of superfluid ^{4}He with the universality formula (11.180) of Kosterlitz and Thouless (from Bishop and Reppy, cited in the Notes and References).

Comparing this with the corresponding form in our Villain model

$$\sum_x \frac{\beta_V}{2}(\nabla_i \gamma)^2 = \sum_x \frac{1}{2\beta_V}b_i^2, \tag{11.182}$$

we find the relations

$$\rho_s = \frac{M^2}{\hbar^2}\beta_V k_B T, \tag{11.183}$$

$$\mathbf{j}_s = \rho_s \mathbf{v}_s = \rho_s \frac{\hbar}{M}\frac{1}{a}\nabla\gamma = \frac{\rho_s}{\beta_V}\frac{\hbar}{M}\frac{1}{a}\mathbf{b} = \frac{M}{\hbar}k_B T\frac{1}{a}\mathbf{b}. \tag{11.184}$$

Thus, the superfluid density can be determined from the correlation function of the $\mathbf{b}(\mathbf{x})$ field as

$$\langle b_i^*(\mathbf{k})\,b_j(\mathbf{k})\rangle = \frac{\hbar^2}{M^2}\frac{a^2}{(k_B T)^2}\langle j_{si}^*(\mathbf{k})j_{sj}(\mathbf{k})\rangle = \frac{\hbar^2}{M^2}\frac{\rho_s(\mathbf{k})}{k_B T}\left(\delta_{ij} - \frac{k_i k_j}{\mathbf{k}^2}\right). \tag{11.185}$$

In the Villain model, these correlations are easily calculated by inserting an external source λ_i into the partition function,

$$Z_{VM} = \frac{1}{(\sqrt{2\pi\beta_V})^N} \sum_{\{\ell(\mathbf{x})\}} \prod_{\mathbf{x}} \left[\int_{-\infty}^{\infty} \frac{dA(\mathbf{x})}{\sqrt{2\pi\beta_V}} \right] e^{-(1/2\beta_V)\Sigma_{\mathbf{x}} b_i^2 \ + \ \Sigma_{\mathbf{x}} \lambda_i b_i \ + \ 2\pi i \Sigma_{\mathbf{x}} \ell(\mathbf{x})A(\mathbf{x})},$$

(11.186)

where $b_i = \varepsilon_{ij}\bar{\nabla}_j A$. Integrating out the $A(\mathbf{x})$ fields gives

$$Z_{VM} = \frac{1}{(\sqrt{2\pi\beta_V})^N} \det(-\bar{\nabla} \cdot \nabla)^{-1/2}$$

$$\times \sum_{\{\ell(\mathbf{x})\}} e^{-(1/2)4\pi^2\beta_V\Sigma_{\mathbf{x},\mathbf{x}'}(\ell \ - \ (i/2\pi)\varepsilon_{ij}\nabla_i\lambda_j)(1/-\bar{\nabla} \cdot \nabla)(\ell \ - \ (i/2\pi)\varepsilon_{ij}\nabla_i\lambda_j)}. \quad (11.187)$$

If we differentiate this twice with respect to λ_i, divide by Z_{VM} and set $\lambda_i = 0$ in the end, we obtain

$$\langle b_i(\mathbf{x}) b_j(\mathbf{x}') \rangle$$

$$= \beta_V \left(\delta_{ij} - \frac{\nabla_i \bar{\nabla}_j}{\bar{\nabla} \cdot \nabla} \right) \left[\delta_{\mathbf{x},\mathbf{x}'} - 4\pi^2\beta_V \left\langle \ell(\mathbf{x}) \frac{1}{-\bar{\nabla} \cdot \nabla}(\mathbf{x}, \mathbf{x}') \ell(\mathbf{x}') \right\rangle \right]. \quad (11.188)$$

In momentum space, this becomes

$$\langle b_i^*(\mathbf{k}) b_j(\mathbf{k}) \rangle = \beta_V \left(\delta_{ij} - \frac{K_i \bar{K}_j}{\bar{K} \cdot K} \right) \left[1 - 4\pi^2\beta_V \frac{1}{\bar{K} \cdot K} \langle \ell^\dagger(\mathbf{k}) \ell(\mathbf{k}) \rangle \right] \quad (11.189)$$

This is to be compared with the correlation function in the absence of vortices,

$$\langle b_i^*(\mathbf{k}) b_j(\mathbf{k}) \rangle = \beta_V \left(\delta_{ij} - \frac{\bar{K}_i \bar{K}_j}{\bar{K} \cdot K} \right) \quad \text{(no vortices).} \quad (11.190)$$

Thus we see that the vortices change the superfluid density as follows,

$$\frac{\rho_s(\mathbf{k})}{\rho_s^0(\mathbf{k})} = 1 - \beta_V \frac{4\pi^2}{\bar{K} \cdot K} \langle \ell^\dagger(\mathbf{k}) \ell(\mathbf{k}) \rangle. \quad (11.191)$$

For $\mathbf{k} \to 0$, $\rho_s(\mathbf{k})/\rho_s^0(\mathbf{k})$ has to be identified with the β_V^R/β_V. This exact formula has to be compared with the previous approximate equation (11.133). It follows from the present one by going to the limit of small fugacity in which case the vortex correction is very small and $\rho_s(\mathbf{0})/\rho_s^0(\mathbf{0})$ can be inverted approximately as

$$\frac{(\beta_V^R)^{-1}}{\beta_V^{-1}} = \left(\frac{\rho_s(0)}{\rho_s^0(0)}\right)^{-1} \approx 1 + \beta_V \lim_{\mathbf{k}\to 0} \frac{4\pi^2}{k^2} \langle \ell^\dagger(\mathbf{k})\ell(\mathbf{k})\rangle. \qquad (11.192)$$

That the limit $\langle \ell^*(\mathbf{k})\ell(\mathbf{k})\rangle/k^2$ is the same as $\Sigma_{\Delta y}(\Delta y)^2 \langle \ell(\Delta y)\ell(0)\rangle$ follows from the charge neutrality of $\ell(\Delta y)$, which therefore has no $\mathbf{k} = 0$ content in its Fourier decomposition $[\Sigma_{\Delta y}\ell(\Delta y) = 0$ with $\ell(\mathbf{k} = 0) = 0]$. Thus, if we expand

$$\langle \ell(\Delta y)\ell(0)\rangle = \sum_{\mathbf{k}} e^{i\mathbf{k}\cdot\Delta y} f(\mathbf{k}), \qquad (11.193)$$

then $f(\mathbf{k})$ starts out, for small $\mathbf{k}$, as $k^2 f_2 + O(k^4)$. The limit of $\langle \ell^*(\mathbf{k})\ell(0)\rangle/k^2$ for $\mathbf{k}\to 0$ picks up precisely the leading term f_2. The second moments in (11.133), on the other hand, correspond to applying a derivative $-(\partial/\partial k_1)^2 - (\partial/\partial k_2)^2$ to $f(\mathbf{k})$ after which the sum over Δy enforces $\mathbf{k} = 0$. This leads to $-4f_2$ such that (11.192) indeed reduces to the expression (11.133). In general, we now have the *exact* renormalization formula

$$\beta_V^R = \beta_V + \pi^2\beta_V^2 \sum_{\Delta y} \langle \ell(\Delta y)\ell(0)\rangle(\Delta y)^2. \qquad (11.194)$$

Within the Coulomb gas of vortices, the renormalized superfluid density can be interpreted as having modified the Coulomb potential $-(1/\overline{\nabla}\cdot\nabla)$ by a factor $\rho_s(\mathbf{k})/\rho_s$. Thus we may attribute to the gas a dielectric constant

$$\varepsilon(\mathbf{k}) = \rho_s^0(\mathbf{k})/\rho_s(\mathbf{k}), \qquad (11.195)$$

and the exact formula (11.191) can also be written as

$$\frac{1}{\varepsilon(\mathbf{k})} = 1 - \beta_V \frac{4\pi^2}{k^2}\langle \ell^*(\mathbf{k})\ell(\mathbf{k})\rangle \qquad (11.196)$$

so that

$$\frac{1}{\varepsilon(0)} = 1 + \beta_V \pi^2 \sum_{\Delta y} \langle \ell(\Delta y)\ell(0)\rangle(\Delta y)^2. \qquad (11.197)$$

In the limit of small fugacity the exact formula (11.194) leads to precisely the same result as formula (11.133). Thus the conclusions remain the same as those described in the last section, in particular the formula for the universal jump,

$$\rho_s(0)_c = \frac{M^2}{\hbar^2}\beta_{Vc}^R T_c = \frac{M^2}{\hbar^2}T_c\frac{2}{\pi}. \tag{11.198}$$

11.14. EQUIVALENCE OF THE VILLAIN MODEL TO THE LIMITING CASE OF THE SINE-GORDON MODEL

It is useful to realize that the Villain model can be looked upon as a limiting case of a *Sine-Gordon model* on the lattice. This is defined by a partition function

$$Z = \prod_{\mathbf{x}}\left[\int_{-\infty}^{\infty}\frac{d\varphi(\mathbf{x})}{\sqrt{2\pi\beta_V}}\right]e^{-(1/\beta_V)\Sigma_{\mathbf{x}}[(1/2)(\nabla\varphi)^2 - h\cos(2\pi\varphi)]}. \tag{11.199}$$

The limit in question is that of large h. In this limit, the exponential of the cosine has a Villain approximation

$$e^{(h/\beta_V)\cos(2\pi\varphi)} \rightarrow e^{h/\beta_V}\sum_n e^{-(h/2\beta_V)2\pi(\varphi - n)^2}. \tag{11.200}$$

This, in turn, can be rewritten as

$$e^{h/\beta_V}\int\frac{d\ell}{\sqrt{2\pi h/\beta_V}}e^{-(\beta_V/2h)\ell^2 + i\ell 2\pi(\varphi - n)}, \tag{11.201}$$

which, after summing over all n and using Poisson's formula, becomes

$$e^{h/\beta_V}\frac{1}{\sqrt{2\pi h/\beta_V}}\sum_\ell e^{-(\beta_V/2h)\ell^2 + 2\pi i\ell\varphi}. \tag{11.202}$$

Inserting this into (11.199), we have the limiting form,

$$Z \xrightarrow[h\to\infty]{} e^{N(h/\beta_V)}\frac{1}{(\sqrt{2\pi h/\beta_V})^N}\prod_{\mathbf{x}}\left[\int_{-\infty}^{\infty}\frac{d\varphi(\mathbf{x})}{\sqrt{2\pi\beta_V}}\right]$$

$$\times e^{-(1/2\beta_V)\Sigma_{\mathbf{x}}(\nabla\varphi)^2 + 2\pi i\Sigma_{\mathbf{x}}\ell(\mathbf{x})\varphi(\mathbf{x})}e^{-(\beta_V/2h)\Sigma_{\mathbf{x}}\ell^2(\mathbf{x})}. \tag{11.203}$$

Integrating out the $\varphi(\mathbf{x})$ field, this becomes

$$Z \xrightarrow[h \to \infty]{} e^{N(h/\beta_V)} \frac{1}{(\sqrt{2\pi h/\beta_V})^N} \sum_{\{\ell(\mathbf{x})\}} e^{-(4\pi^2\beta_V/2)\Sigma_\mathbf{x}\ell(\mathbf{x})(1/-\bar{\nabla}\cdot\nabla)\ell(\mathbf{x}) - (\beta_V/2h)\Sigma_\mathbf{x}\ell^2(\mathbf{x})}. \tag{11.204}$$

Apart from the trivial prefactor, this is just a Coulomb gas of the same type as (11.12). The only difference lies in the presence of an extra Boltzmann factor

$$e^{-\beta_V\cdot(1/2h)\Sigma_\mathbf{x}\ell^2(\mathbf{x})}, \tag{11.205}$$

which corresponds to an extra core energy. For very large h, this Boltzmann factor can be neglected and the partition functions coincide (apart from the trivial overall factor).

Contact with the Villain model is now established by noticing that, in the limit $h \to \infty$, the sum over $\ell(\mathbf{x})$ squeezes the field $\varphi(\mathbf{x})$ to integer numbers and Z becomes a sum, i.e.,

$$Z \xrightarrow[h \to \infty]{} e^{h/\beta_V} \frac{1}{2\pi\sqrt{h}} \sum_{\{\varphi(\mathbf{x})\}} e^{-(1/2\beta_V)\Sigma_\mathbf{x}(\nabla\varphi)^2}. \tag{11.206}$$

It consists of a single *discrete* variable $\varphi(\mathbf{x})$, with nearest-neighbour coupling, performing purely Gaussian fluctuations. Apart from a trivial prefactor, this is precisely the *discrete Gaussian model* obtained in Eqs. (11.9), (11.10) from the Villain model. Actually, the above calculations show that the equivalence in the limit $h \to \infty$ can be generalized to the entire class of models describing a Coulomb gas with an additional core energy.

Defining the extended Villain model by

$$Z_{VMext} = \prod_\mathbf{x} \left[\int_{-\infty}^{\infty} \frac{d\gamma(\mathbf{x})}{2\pi} \right] \sum_{\{n_i(\mathbf{x})\}} e^{-(\beta_V/2)\Sigma_{\mathbf{x},i}(\nabla_i\gamma - 2\pi n_i)^2 - \beta_V(4\pi^2/2)e_c\Sigma_\mathbf{x}(\epsilon_{ij}\nabla_i n_j)^2}, \tag{11.207}$$

we can show, via the usual manipulations, that it is equivalent to a Coulomb gas with additional core energy [see (11.174)],

$$Z_{VMext} = \frac{1}{(\sqrt{2\pi\beta_V})^N} \det(-\bar{\nabla}\cdot\nabla)^{-1/2}$$

$$\times \sum_{\{\ell(\mathbf{x})\}} e^{-\beta_V(4\pi^2/2)\Sigma_\mathbf{x}\ell(\mathbf{x})(1/-\bar{\nabla}\cdot\nabla)\ell(\mathbf{x})} e^{-\beta_V(4\pi^2/2)e_c\Sigma_\mathbf{x}\ell^2(\mathbf{x})}. \tag{11.208}$$

The same Coulomb gas is obtained from the partition function

$$Z = \prod_{x} \left[\int_{-\infty}^{\infty} \frac{d\varphi(x)}{\sqrt{2\pi\beta_V}} \right] e^{-(1/\beta_V)\Sigma_x[(1/2)(\nabla\varphi)^2 - h\cos_V(2\pi\varphi)]}, \qquad (11.209)$$

where $\cos_V\gamma$ is a short-hand notation for the Villain version of the cosine, i.e.,

$$e^{(h/\beta_V)\cos_V(2\pi\varphi)} \equiv e^{h/\beta_V} \sum_{n} e^{-(h/2\beta_V)(2\pi\varphi - 2\pi n)^2}, \qquad (11.210)$$

which can also be rewritten as

$$e^{(h/\beta_V)\cos_V(2\pi\varphi)} \equiv e^{h/\beta_V} \sqrt{\frac{\beta_V}{2\pi h}} \int d\ell \sum_{n} e^{-(\beta_V/2h)\ell^2 + i\ell 2\pi(\varphi - 2\pi n)}$$

$$= e^{h/\beta_V} \sqrt{\frac{\beta_V}{2\pi h}} \sum_{\ell} e^{-(\beta_V/2h)\ell^2 + 2\pi i\ell\varphi}. \qquad (11.211)$$

This implies that Z is equal to

$$Z = \frac{e^{Nh/\beta_V}}{(2\pi\sqrt{h})^N} \prod_{x} \left[\int_{-\infty}^{\infty} d\varphi(x) \right] \sum_{\{\ell(x)\}} e^{-(1/2\beta_V)\Sigma_x(\nabla\varphi)^2 + 2\pi i\Sigma_x\ell(x)\varphi(x) - (\beta_V/2h)\Sigma_x\ell^2(x)}$$

$$= \frac{e^{Nh/\beta_V}}{(\sqrt{2\pi h})^N} \left(\sqrt{\frac{\beta_V}{2\pi}} \right)^N \sum_{\{\ell(x)\}} e^{-\beta_V(4\pi^2/2)\Sigma_x\ell(x)(1/-\vec{\nabla}\cdot\vec{\nabla})\ell(x) - (\beta_V/2h)\Sigma_x\ell^2(x)} \qquad (11.212)$$

and this is the same as (11.208), apart from a trivial overall factor, if we make the identification

$$\frac{1}{h} = 4\pi^2 e_c. \qquad (11.213)$$

11.15. ESTIMATE OF THE CRITICAL TEMPERATURE IN THE SINE-GORDON MODEL

The equivalence of the Villain model to the sine-Gordon model for large h opens up another possibility of estimating the transition temperature. For this we continue the theory from Euclidean two-dimensional space

into a time dependent quantum field theory in a single space dimension. The classical limit of this model describes a chain of pendula hanging from a rubber band. The sine-Gordon model has been studied in great detail in order to understand the movement of topological non-trivial field configurations, the so-called kinks or solitons. These are the places where the pendula make a complete turn by 2π. A simple way of estimating the stability of the quantum field theory was found by Coleman when he proved that the sine-Gordon theory is further equivalent to a theory of self-interacting massive fermions in 2 dimensions. Adapting his method to our situation let us to consider a field theory on an infinitesimally fine spatial lattice of spacing $a \rightarrow 0$ with Lagrangan density

$$\mathcal{L} = \frac{1}{2}(\partial_t \bar{\varphi})^2 - \frac{1}{2}(\nabla_x \bar{\varphi})^2 + \frac{h}{\beta}\cos(2\pi\sqrt{\beta}\,\bar{\varphi}), \qquad (11.214)$$

so that our φ equals $\sqrt{\beta}\,\bar{\varphi}$. This leads to a Hamiltonian density

$$\mathcal{H} = \frac{1}{2}\bar{\pi}^2 + \frac{1}{2}(\partial_x \bar{\varphi})^2 - \frac{h}{\beta}\cos(2\pi\sqrt{\beta}\,\bar{\varphi}), \qquad (11.215)$$

where

$$\bar{\pi}(\mathbf{x}) = \partial_x \bar{\varphi}(\mathbf{x}) \qquad (11.216)$$

is the canonical momentum of the $\bar{\varphi}(\mathbf{x})$ field, which satisfies the quantum mechanical commutation rules

$$[\bar{\pi}(x), \varphi(x')] = -i\delta_{x,x'}. \qquad (11.217)$$

Coleman attempted to find a good ground state by expanding $\bar{\varphi}(x)$ into free particles of momentum k with an unknown trial mass m

$$\bar{\varphi}(x, t) = \int_{-\pi/a}^{\pi/a} \frac{dk_1}{2\pi\sqrt{2k_0}}[e^{ik_1x}a(k_1, m) + e^{-ik_1x}a^\dagger(k_1, m)] \qquad (11.218)$$

where k_1 are the spatial momenta and $k_0 = \sqrt{K_1 K_1 + m^2}$. The commutation rules (11.218) imply that $a(k_1, m)$, $a^\dagger(k_1, m)$ satisfy

$$[a(k_1, m), a^\dagger(k_1', m)] = 2\pi\delta^{(1)}(k_1 - k_1'). \qquad (11.219)$$

The ground state $|0\rangle$ is defined by the state with no particle, i.e.,

$$a(k_1, m)|0\rangle = 0. \tag{11.220}$$

Such a ground state would be the exact eigenstate of a free field Hamiltonian density

$$\mathcal{H}_0 = \frac{1}{2}\tilde{\pi}^2 + \frac{1}{2}(\partial_x \tilde{\varphi})^2 + \frac{m^2}{2}\tilde{\varphi}^2, \tag{11.221}$$

with energy

$$E_0 = \int_{-\pi/a}^{\pi/a} \frac{dk_1}{2\pi} \frac{\frac{k_0^2 + \overline{K}_1 K_1}{2} + \frac{m^2}{2}}{2k_0} = \int_{-\pi/a}^{\pi/a} \frac{dk_1}{2\pi} \frac{\overline{K}_1 K_1 + m^2}{2k_0} = \int_{-\pi/a}^{\pi/a} \frac{dk_1}{2\pi} \frac{k_0}{2}. \tag{11.222}$$

This energy diverges for small lattice spacing and we have to perform a subtraction of $-\int_{-\pi a}^{\pi/a} \frac{dk_1}{2\pi} \frac{k_1}{2}$ to obtain a finite result.

The full Hamiltonian density (11.216) may be viewed as $\mathcal{H}_0$ plus an interaction density

$$\mathcal{H}_{\text{int}} = -\frac{h}{\beta}\cos(2\pi\sqrt{\beta}\tilde{\varphi}) - \frac{m^2}{2}\tilde{\varphi}^2. \tag{11.223}$$

Let us calculate the expectation value of this expression in the ground state $|0\rangle$ defined by (11.220). For $-(m^2/2)\tilde{\varphi}^2$ this is trivial and gives $-\int(dk_1/2\pi)((m^2/2)/2k_0)$. For the cosine term, it is useful to write

$$\cos(2\pi\sqrt{\beta}\tilde{\varphi}) = \frac{1}{2}(e^{i2\pi\sqrt{\beta}(\tilde{\varphi}^+ + \tilde{\varphi}^-)} + e^{-i2\pi\sqrt{\beta}(\tilde{\varphi}^+ + \tilde{\varphi}^-)}), \tag{11.224}$$

where $\tilde{\varphi}^+$ denotes the $a^\dagger$ part and $\tilde{\varphi}^-$ the a part of the field $\tilde{\varphi}$ in (11.218). In order to calculate the expectation value in the state $|0\rangle$ it is advantageous to reorder these exponentials such that the a parts all stand to the right of the $a^\dagger$ parts. This is done by means of the Baker-Hausdorff formula which says that, if the commutator $[A, B]$ is a c-number, then

$$e^{A + B} = e^{-(1/2)[A, B]} e^A e^B. \tag{11.225}$$

Now

$$[\tilde{\varphi}^-(x, t), \tilde{\varphi}^+(x, t)] = \int_{-\pi/a}^{\pi/a} \frac{dk_1}{2\pi} \frac{1}{2k_0} = \int \frac{dk_1 dk_0}{(2\pi)^2} \frac{1}{k_0^2 + \bar{K}_1 K_1 + m^2}.$$
(11.226)

If we assume the mass m to be very small (compared to $1/a^2$) this can be approximated by [recall (6.204) of Part I]

$$[\tilde{\varphi}^-(x, t), \tilde{\varphi}^+(x, t)] \xrightarrow[a \to 0]{} -\frac{1}{4\pi} \log(m^2 a^2/c^2),$$
(11.227)

where $c^2 = 32$. This leads to

$$e^{i2\pi\sqrt{\beta}(\tilde{\varphi}^+ + \tilde{\varphi}^-)} \xrightarrow[a \to 0]{} e^{(\pi\beta/2)\log(m^2 a^2/c^2)} e^{i2\pi\sqrt{\beta}\tilde{\varphi}^+} e^{i2\pi\sqrt{\beta}\tilde{\varphi}^-}$$

$$= \left(\frac{m^2 a^2}{c^2}\right)^{\pi\beta/2} e^{i2\pi\sqrt{\beta}\tilde{\varphi}^+} e^{i2\pi\sqrt{\beta}\tilde{\varphi}^-}.$$
(11.228)

The expectation value of this expression is $(m^2 a^2/c^2)^{\pi\beta/2}$. Adding all terms together, including the subtractions, this leads to a vacuum expectation value for the energy of

$$E_0^{\text{sub}} = \int \frac{dk_1}{2\pi} \frac{\bar{K}_1 K_1 + m^2}{2k_0} - \frac{h}{\beta}\left(\frac{m^2 a^2}{c^2}\right)^{(\pi/2)\beta} - \frac{m^2}{2} \int \frac{dk_1}{2\pi} \frac{1}{2k_0} - \int \frac{dk_1}{2\pi} \frac{|k_1|}{2}.$$
(11.229)

The integrals give

$$\int \frac{dk_1}{2\pi} \frac{|k_1|}{2} = \frac{1}{8\pi} k_1^2$$

$$\int \frac{dk_1}{2\pi} \frac{\bar{K}_1 K_1 + m^2}{2k_0} \xrightarrow[a \to 0]{} \frac{1}{2\pi} \frac{k_1 \sqrt{k_1^2 + m^2}}{4} + \frac{m^2}{2} \int \frac{dk_1}{2\pi} \frac{1}{2k_0},$$
(11.230)

so that

$$E_0^{\text{sub}} = \frac{1}{8\pi} \frac{2\pi}{a} \sqrt{\left(\frac{\pi}{a}\right)^2 + m^2} - \frac{h}{\beta}\left(\frac{m^2 a^2}{c^2}\right)^{(\pi/2)\beta} - \frac{1}{8\pi} 2\left(\frac{\pi}{a}\right)^2.$$
(11.231)

With the previous assumption that the lattice spacing a is very small (compared to $1/m$), this becomes

$$E_0^{\text{sub}} = \frac{1}{8\pi} m^2 - \frac{h}{\beta} \left(\frac{m^2 a^2}{c^2} \right)^{(\pi/2)\,\beta} \tag{11.232}$$

Here we see that the limit of small lattice spacing can be non-trivial only if we let the magnetic field h vary with a as follows,

$$h = h^{\text{ren}} \left(\frac{\mu^2 a^2}{c^2} \right)^{-(\pi/2)\beta}, \tag{11.233}$$

where μ is some arbitrary mass scale and h^{ren} is a renormalized magnetic field which is finite in the continuum limit. The resulting finite energy is then

$$E_0^{\text{sub}} = \frac{1}{8\pi} m^2 - \frac{h^{\text{ren}}}{\beta} \left(\frac{m^2}{\mu^2} \right)^{(\pi/2)\beta} \tag{11.234}$$

If we now vary the mass m of the trial state we observe that E_0^{sub} is bounded from below only as long as

$$\beta < \frac{2}{\pi} \tag{11.235}$$

If β exceeds this value, the sine-Gordon model has no ground state and thus no sensible continuum limit. This is the field theoretic version of the phase transition.

11.16. SELF-CONSISTENT APPROXIMATION TO THE COHERENCE LENGTH OF THE XY AND SINE-GORDON MODELS

A very similar argument can be employed to study the behaviour of the coherence length of the XY, Villain and sine-Gordon models for small β, i.e., for the hot disordered spin system. This coherence length is finite and must grow to infinity as the spin system enters the cold ordered phase. At the usual critical points, this occurs with a power-like behaviour,

$$\xi \sim \frac{1}{(\beta_c - \beta)^\nu}.$$ (11.236)

The two-dimensional system is special. As we had shown earlier in Section 11.8 via renormalization group arguments, the behaviour is not this but rather

$$\xi \sim e^{\text{const}/\sqrt{\beta_c - \beta}}.$$ (11.237)

In this section we shall employ self-consistent methods and estimate the behaviour of ξ in another way. Since these methods are not as reliable as the renormalization group technique, they merely lead to the approximate statement

$$\xi \sim e^{-\text{const}/(\beta_c - \beta)}.$$ (11.238)

The most convenient starting point for this is the sine-Gordon model (11.199)

$$Z = \prod_x \left[\int \frac{d\varphi(x)}{\sqrt{2\pi\beta}} \right] e^{-(1/2\beta)\Sigma_x[(\nabla\varphi)^2 - 2h\cos(2\pi\varphi)]}.$$ (11.239)

where we have dropped the subscript V of β_V. By rewriting the exponent as

$$\frac{h}{\beta} - \frac{1}{2\beta} \sum_x [(\nabla\varphi)^2 + 4\pi^2 h \, \varphi^2] + \frac{h}{\beta} \sum_x \left[\cos(2\pi\varphi) - 1 + \frac{1}{2}(2\pi\varphi)^2 \right],$$ (11.240)

this partition function is seen to correspond to the theory of a field of mass

$$m = 2\pi\sqrt{h}$$ (11.241)

with interactions

$$h \sum_{n=2}^{\infty} \frac{(-1)^n}{(2n)!} (2\pi\varphi)^{2n}.$$ (11.242)

The correlation function is

$$\langle \varphi(\mathbf{x})\,\varphi(\mathbf{y}) \rangle = \beta \int \frac{d^2k}{(2\pi)^2} \frac{e^{i\mathbf{k}\cdot(\mathbf{x}-\mathbf{y})}}{\mathbf{K}\cdot\bar{\mathbf{K}} + m^2} \beta v_m(\mathbf{x}-\mathbf{y}). \qquad (11.243)$$

This shows that for small β, perturbation theory is applicable. The coherence length of the free quanta is equal to

$$\xi_0 = m^{-1} = \frac{1}{\sqrt{4\pi^2 h}}. \qquad (11.244)$$

The interactions will renormalize this quantity.

In order to sum up an infinite number of renormalization diagrams we invoke the Hartree-Fock resummation technique explained in Section 7.7. We attribute to the φ field an unknown mass m_R and normally order the interaction with respect to the free field fluctuations. Then we write

$$e^{-(1/2\beta)\sum_x(\nabla\varphi)^2 + (h/\beta)\sum_x\cos(2\pi\varphi)}$$

$$= \exp\left\{ -\frac{1}{2}\beta \sum_x (\nabla\varphi)^2 + \frac{h}{\beta}e^{-(4\pi)(\varphi)R} \sum_x \,:\cos\,(2\pi\varphi):\right\}$$

$$= \exp\left\{ N\frac{h}{\beta}e^{-(4\pi^2/2)\langle\varphi^2\rangle_R}\left(1 + \frac{4\pi^2}{2}\langle\varphi^2\rangle_R\right)\right.$$

$$-\frac{1}{2\beta}\sum_x [(\nabla\varphi)^2 + 4\pi^2 h\,e^{-(4\pi^2/2)\langle\varphi^2\rangle_R}\varphi^2]$$

$$\left. +\frac{h}{\beta}e^{-(4\pi^2/2)\langle\varphi^2\rangle_R} \sum_x \,:\cos(2\pi\varphi) - 1 + \frac{1}{2}4\pi^2\varphi^2:\right\} \qquad (11.245)$$

and see that the renormalized mass satisfies the equation

$$m_R^2 = m^2\,e^{-(4\pi^2/2)\langle\varphi^2\rangle_R} = m^2\,e^{-(4\pi^2\beta/2)v_{m_R}(0)}, \qquad (11.246)$$

where $v_{m_R}(0)$ is the free lattice Green's function (11.244) of mass m_R at the origin. From Part I, Eq. (6.204), we take $v_{m_R}(0) = -(1/4\pi)$ $\times \log(m_R^2/32)$ and obtain

$$m_R^2 = 4\pi^2 h\,e^{(\pi\beta/2)\log(m_R^2/32)} \qquad (11.247)$$

or

$$1 = \frac{4\pi^2 h}{32}\,e^{(\pi\beta/2 - 1)\log(m_R^2/32)}. \qquad (11.248)$$

For very small β, this is solved by

$$m_R^2 = 4\pi^2 h \left(1 + \frac{\pi\beta}{2} \log \frac{4\pi^2 h}{32} + \ldots \right). \tag{11.249}$$

Now, as long as the parameter h is smaller than

$$h_{\max} = \frac{32}{4\pi^2} \approx 0.81 \tag{11.250}$$

(which corresponds to a certain minimal core energy of the vortices, i.e., to a certain maximal fugacity), the renormalization lowers the mass. This goes on until β hits the critical value

$$\beta_c = \frac{2}{\pi}, \tag{11.251}$$

which is the same value found before for β^R in the Villain model. Using β_c we can rewrite (11.248) as

$$\xi_R = \frac{1}{\sqrt{m_R^2}} = \frac{1}{\sqrt{32}} e^{(1/2)\log(32/4\pi^2 h)(1/(1 - \beta/\beta_c))}, \tag{11.252}$$

which shows the increase of the correlation length announced in (11.239). Due to the crudeness of the resummation, the square root in the exponent is missed (which was obtained by the more accurate but also more elaborate renormalization group procedures of Section 11.10).

11.17. SURFACE ROUGHENING AND CRYSTAL GROWTH

The knowledge of the solid-liquid interface is of importance if one wants to predict the outcome of crystal-growth processes in a supersaturated melt. The interest in such processes dates back a few thousand years, in the context of producing salt crystals. Apart from a few attempts in the seventeenth century, this ancient knowledge was not expanded since interest focused more on understanding the structure of existing crystals rather than on the process of their formation.

For regular crystals,[j] the important milestone in our structural understanding was the derivation of the seven point groups giving rise to seven

crystal systems and the classification into 14 types of simple lattices by A. Bravais in 1845. The work was completed by Schoenflies who extended Bravais' results to general lattices with a basis and found the 230 space groups into which all regular crystals can be classified.[j] The crystal structure can be seen in Bragg scattering by which one can identify crystal planes. These are characterized by reciprocal lattice vectors and labelled by their components, the Miller indices.
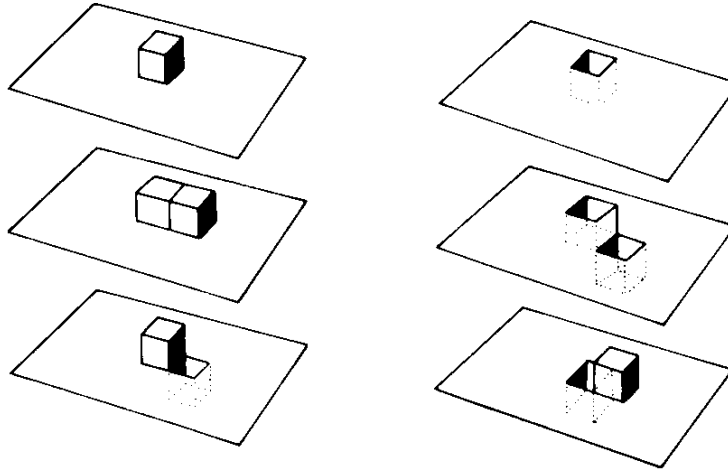
In a crystal-growth process, crystal faces always form along such planes. But only a few of them can really appear depending on the strength of couplings to the nearest neighbours lying *within* the planes. If these are sufficiently strong, the growth proceeds by a step mechanism, either via spiral growth, as described first by Burton, Cabrera and Frank, or via two-dimensional nucleation, for example by the Birth-Spread mechanism. These growth mechanisms do not occur if a crystal plane is of high order, i.e., if it has large Miller indices in which case an atom has only very few nearest neighbours within the plane, or if the nearest neighbours in a low order plane are only weakly bound. The reason for this is found by studying the fluctuations of the atoms in the plane itself. When doing this one finds that every plane possesses a critical temperature above which it becomes rough. This gives the criterion for the possibility of crystal growth. If the roughening temperature lies below the formation temperature the plane can never appear as a crystal face.

In order to study the roughening process in a plane, a simple model was proposed by Kossel and Stranski and later by Chiu and Weeks. They represent the fluctuations on the surface on a solid by a set of unit boxes, piling up on top of each other. These boxes represent the atoms (see Fig. 11.20). In such an approach, crystalline vibrations are completely neglected. The step configurations can be parametrized by an integer field $a(x)$ measuring the number of boxes on top of each place. If the energy is assumed to be quadratic in neighboring height difference,[k] we obtain the

[j]We have to use the word *regular* since in the last ten years it has become apparent that there exists a wide variety of crystal structures which does not fit into this scheme, the so-called *modulated crystals*. They are not completely periodic but the atomic positions (or charge distributions or compositions) show periodic deviations from the regular array (as if they contained a frozen phonon wave). For a review see A. Janner, T. Janssen, P.M. de Wolff, *Europhys. News.* 13 (1982) 1.

[k]Actually, in crystal roughening one usually takes $|a(x + i) - a(x)|$ rather than $(a(x + i) - a(x))^2$. Near the phase transition, this does not really matter since the one-step excitations are dominant.

FIG. 11.20. Excessive atoms or vacancies in the surface of the discrete Gaussian roughening model contribution.

partition function (R stands for "roughening model")

$$Z = \prod_{\mathbf{x}} \left(\sum_{a(\mathbf{x})} \right) e^{-(1/T_R)\Sigma_{\mathbf{x},i}(a(\mathbf{x}+i) - a(\mathbf{x}))^2}. \tag{11.253}$$

This is precisely the discrete Gaussian model of Eq. (11.10) with the identification $1/T_R \equiv 1/2T_{DG} = 1/2\beta_V$. The relation between the box graphs and the high temperature expansion of the Villain model is quite obvious. Since $a(\mathbf{x})$ is the potential for the closed magnetic field lines

$$b_i = \varepsilon_{ij} \bar{\nabla}_j a(\mathbf{x}), \tag{11.254}$$

the boundary lines of the boxes, as seen from above the plane, coincide with these magnetic field lines. A change in orientation means going from an additional atom to a missing atom (see Fig. 11.20). Since we already performed a complete counting of all non-self-backtracking loops, there is no need to repeat the equivalent counting for the box fluctuations. The pile up of boxes neglects fluctuations in which the surface overhangs. This is why the model is called the SOS model (solid-on-solid).

The SOS model has been simulated by Monte Carlo techniques by Shugard, Weeks and Gilmer and by Swendsen. The first authors find good agreement with the universality statements of the Kosterlitz-Thouless theory. The second author compares the simulation with high- and low-temperature expansions of the Villain model and finds not too good agreement below the critical regime. The mistake lies in the high-temperature expansion for which Swendson uses the false eighth and

FIG. 11.21. Internal energy of the discrete Gaussian model from low- and high-temperature series and comparison with Monte Carlo data.
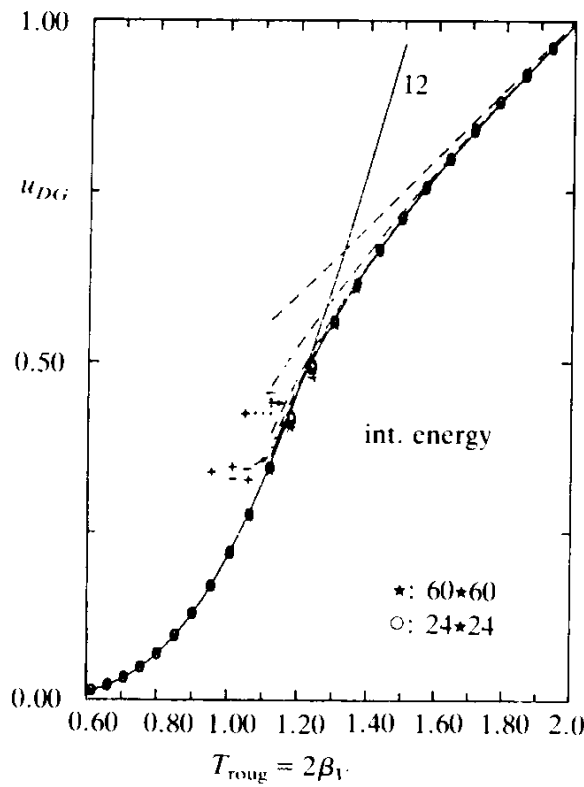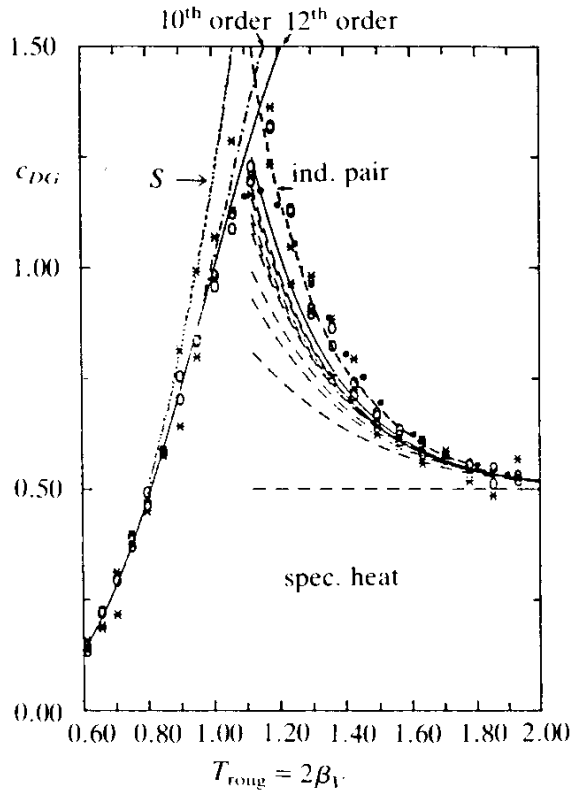
FIG. 11.22. Specific heat of the same discrete Gaussian model as in Fig. 11.10. The agreement is excellent except in the immediate vicinity of the critical point. The dotted curve shows the fit of Swendson's much quoted 1978 paper which unfortunately gave an erroneous low T expansion.

tenth order terms $8e^{-8/2\beta v} + 16e^{-10/2\beta v}$, to be compared with the proper expansion (11.6). After correcting his errors, the agreement is excellent (see Figs. 11.21–11.22).

NOTES AND REFERENCES

Early experiments on the superfluid transition in thin films are due to
H.P.R. Frederikse, *Physica* **15** (1949) 860,
M. Bretz, *Phys. Rev. Lett.* **31** (1973) 1447.
The work up to 1978 is reviewed by
J.F. Dash, in *Quantum Liquids*, eds. J. Ruvalds and T. Regge (North-Holland, Amsterdam, 1978).
For the best experimental evidence of the Kosterlitz-Thouless transition in thin films of superfluid ^{4}He see
D.J. Bishop and J.D. Reppy, *Phys. Rev. Lett.* **40** (1978) 1727,
who give an experimental test of the universality relation of Kosterlitz and Thouless. For recent experiments see, for instance,
J. Maps and R.B. Hallock, in *Ordering in Two Dimensions*, ed. S.K. Sinha (North-Holland, Amsterdam, 1980).
For theoretical arguments on (the absence of) long-range order in two-dimensional systems see
L.D. Landau and E.M. Lifshitz, *Theory of Elasticity* (Pergamon Press, London, 1959),
R.E. Peierls, *Helv. Phys. Acta* 7, Suppl. II (1939) 81, *Ann. Inst. Henri Poincaré* 5 1935 177,
D. Mermin and H. Wagner, *Phys. Rev. Lett.* **22** (1966) 1133,
P.C. Hohenberg, *Phys. Rev.* **158** (1967) 383.
The two-dimensional XY model is discussed in
V.L. Berezinskii, *Sov. Phys. JETP* **32** (1970) 493,
J.M. Kosterlitz and D.J. Thouless, *J. Phys.* **C6** (1973) 1181, *Prog. Low Temp. Phys.* **7B** (1978) 371,
J.M. Kosterlitz, *J. Phys.* **C7** (1974) 1046.
See also
D.J. Amit, Y. Goldschmidt and G. Grinstein, *J. Phys.* **A13** (1980) 585,
P. Minhagen and G.G. Warren, *Phys. Rev.* **B24** (1981) 2526, 6758,
J.V. José, L.P. Kadanoff, S. Kirkpatrick and D.R. Nelson, *Phys. Rev.* **B15** (1977) 1217,
T. Ohta, D. Jasnow, *Phys. Rev.* **B20** (1979) 139,
J. Cardy and N. Praga, *J. Phys.* **C13** (1980) 571.
For a controversial, opposing view see
J. Zittartz, *Z. Phys.* **B23** (1976) 55, 63,
J. Zittartz and B.A. Hubermann, *Solid State Commun.* **18** (1976) 1373.
The field theoretic variational arguments in Section 11.14 are due to
S. Coleman, *Phys. Rev.* **11** (1976) 2088.
Monte Carlo simulations of the $2D$ XY model were done by
Jan Tobochnik and G.V. Chester, *Phys. Rev.* **B20** (1979) 3761,
S. Heinekamp and R.A. Pelcovitz, *Phys. Rev.* **B32** (1986) 4528.
Our data comes from
W. Janke, FU Berlin Dissertation, 1985.
The most recent determination of the behaviour of the coherence length is due to
S. Samuel and F.G. Yee, *Nucl. Phys.* **B257** [FS14] (1985) 85.

Monte Carlo data of the Villain model were first obtained in the dual roughening model by
W.J. Shugard, J.D. Weeks, G.H. Gilmer, *Phys. Rev. Lett.* **41** (1979) 1399, (E) 1577.
   For a review on crystal growth, see
F. Bennema, in *Surface Mobilities on Solid Materials*, ed. V. Thieu Bhin (Plenum Press,
New York, 1983).
The spiral growth mechanism is discussed in
W.K. Burton, N. Cabrera and F.C. Frank, *Phil. Trans. Roy. Soc.* **A234** (1951) 299,
the Birth-Spread mechanism in
W.B. Hillig, *Acta Met.* **14** (1966) 1968.
See also:
M. Ohara and R.C. Reid, *Modelling Crystal Growth Rates from Solutions* (Prentice Hall,
Englewood, N.J., 1973) and
F. Bennema and J.P. van der Eerden, *J. Cryst. Growth* **42** (1977) 201.
   For the role of the roughening transition in crystal growth see
J.P. van der Eerden, *Phys. Re* . **B13** (1976) 4942 and
J.P. van der Eerden, P. Bennema and T.A. Cheropanova, *Progr. Cryst. Growth Charact.* **1**
(1978) 219.
The roughening transition was studied via the SOS model by
S.T. Chiu and J.D. Weeks, *Phys. Lett.* **39** (1977) 768,
R.H. Swendsen, *Phys. Rev.* **B18** (1978) 492.
See also
H.J. Knops, *Phys. Rev. Lett.* **39** (1977) 768.
Further references on roughening see:
H. Van Beijern, *Phys. Rev. Lett.* **38** (1977) 992, *Comman. Math. Phys.* **40** (1975) 1,
R.L. Dobrushin, *Theor. Prob. App.* **17** (1972) 582,
K.A. Jackson, *J. Cryst. Growth* **24/25** (1976) 130,
H.J. Leamy and G.H. Gilmer, *J. Cryst. Growth* **24/25** (1976) 499.

LATTICE DERIVATION OF DISORDER FIELD THEORY

12.1. EQUIVALENCE OF THE XY MODEL TO A LATTICE SUPERCONDUCTOR

In Chapter 6 we studied the XY model via a vortex-line representation in which the system appears as a grand canonical ensemble of non-back-tracking random loops, with a Biot-Savart type long-range interaction. The exact representation in the gauge $A_3 = 0$ [see (6.59)] was

$$Z'_{XY}(\beta) = I_0(\beta)^{3N} \prod_{\mathbf{x}} \left[\int_{-\infty}^{\infty} dA_1(\mathbf{x})\, dA_2(\mathbf{x}) \right] e^{\sum_{\mathbf{x},i}\sum_{p=1}^{x}[G_c^{(p)}(\beta)/(-2\beta)^p p!](\bar{\nabla} \times \mathbf{A})_i^{2p}}$$

$$\times \sum_{\{\ell_i(\mathbf{x})\}} \delta_{\bar{\nabla}_i \ell_i, 0}\, e^{2\pi i \sum_{\mathbf{x}} \ell_i(\mathbf{x}) A_i(\mathbf{x})}. \tag{12.1}$$

Within the Villain approximation [see (7.25)], this was equal to

$$Z'_{XY} \sim Z'_V = I_0(\beta)^{3N} \prod_{\mathbf{x}} \left[\int_{-\infty}^{\infty} dA_1(\mathbf{x})\, dA_2(\mathbf{x}) \right] e^{-\sum_{\mathbf{x}}(1/2\beta v)(\bar{\nabla} \times \mathbf{A})^2}$$

$$\times \sum_{\{\ell_i(\mathbf{x})\}} \delta_{\bar{\nabla}_i \ell_i, 0}\, e^{-2\pi i \sum_{\mathbf{x}} \ell_i(\mathbf{x}) A_i(\mathbf{x})}, \tag{12.2}$$

where $\beta_V = -(1/2)[\log(I_1(\beta)/I_0(\beta))]^{-1}$. In this chapter we shall make use of these lattice expressions and show that they can serve for a proper *derivation* of a disorder-field theory of the type found by more qualitative arguments in Sections 2.1, 2.4. We shall proceed in a sequence of steps.

First we observe that a sum over closed random lines of the type $\Sigma_{\{\ell_i(\mathbf{x})\}} \, \delta_{\nabla_i\ell_i,0}$ was encountered before in the strong coupling expansion of the XY model, (4.19), or its Villain approximation, (7.18). There we arrived at the sum

$$
\begin{aligned}
\bar{Z}'_{XY} &= \prod_{\mathbf{x}} \left[\int_{-\pi}^{\pi} \frac{d\bar{\gamma}(\mathbf{x})}{2\pi} \right] e^{\bar{\beta}\Sigma_{\mathbf{x},i}\cos\nabla_i\bar{\gamma}} \\
&\approx \bar{Z}'_V = \bar{R}_V^{3N} \prod_{\mathbf{x}} \left[\int_{-\pi}^{\pi} \frac{d\bar{\gamma}(\mathbf{x})}{2\pi} \right] \sum_{\{\bar{n}_i(\mathbf{x})\}} e^{-(\bar{\beta}_V/2)\Sigma_{\mathbf{x}}(\nabla_i\bar{\gamma}-2\pi\bar{n}_i)^2} \\
&= \bar{R}_V^{3N} (2\pi\bar{\beta}_V)^{-3N/2} \sum_{\{\bar{b}_i(\mathbf{x})\}} \delta_{\nabla_i\bar{b}_i,0} \, e^{-(1/2\bar{\beta}_V)\Sigma_{\mathbf{x}}\bar{b}_i(\mathbf{x})^2}.
\end{aligned}
\tag{12.3}
$$

We have ornamented all quantities with a wiggle in order to distinguisch this XY model, which we shall call "auxiliary," from the original XY model. In the original model, the right-hand side was interpreted as a sum over non-backtracking closed integer-valued "magnetic field lines." Each loop appears with a Boltzmann-type factor $e^{-(1/2\bar{\beta}_V)\Sigma_{\mathbf{x}}\bar{b}_i(\mathbf{x})^2}$. In the limit $\bar{\beta}_V \to \infty$ (zero auxiliary temperature $\bar{T}$), all loops occur with equal probability. Comparison with (12.1), (12.2) suggests the identification of the "magnetic loops" $\bar{b}_i(\mathbf{x})$ of the auxiliary model with the vortex loops $\ell_i(\mathbf{x})$ of the original XY model. For this to be useful we must be able to include the coupling of the loops $\ell_i(\mathbf{x})$ to the vector potential, $\exp(2\pi i \Sigma_{\mathbf{x}} \ell_i(\mathbf{x}) A_i(\mathbf{x}))$. This is easily done. All we have to do is enter the vector potential into the argument of the cosine function in (12.3). Indeed, let us perform the usual steps, leading to the vortex-line representation of this modified auxiliary XY model whose partition function will be called $\bar{Z}'^A_{XY}$.

First we have to do the Villain approximation:

$$
\bar{Z}'^A_{XY}(\bar{\beta}) = \prod_{\mathbf{x}} \left[\int_{-\pi}^{\pi} \frac{d\bar{\gamma}(\mathbf{x})}{2\pi} \right] e^{\bar{\beta}\Sigma_{\mathbf{x},i}\cos(\nabla_i\bar{\gamma}-2\pi A_i)}
$$

$$
\sim \bar{Z}'^A_V(\bar{\beta}) = \bar{R}_V^{3N} \sum_{\{\bar{n}_i(\mathbf{x})\}} \prod_{\mathbf{x}} \left[\int_{-\pi}^{\pi} \frac{d\bar{\gamma}(\mathbf{x})}{2\pi} \right] e^{-(\bar{\beta}_V/2)\Sigma_{\mathbf{x},i}(\nabla_i\bar{\gamma}-2\pi\bar{n}_i-2\pi A_i)^2}.
$$

$$
\tag{12.4}
$$

Then we follow the steps (7.15)–(7.18) and rewrite this as an integral over auxiliary magnetic fields,

$$\overline{Z}_V'^{\mathbf{A}} = \overline{R}_V^{3N} \prod_{\mathbf{x}} \left[\int_{-\pi}^{\pi} \frac{d\overline{\gamma}}{2\pi} \right] \prod_{\mathbf{x},i} \left[\int \frac{d\overline{B}_i(\mathbf{x})}{\sqrt{2\pi\overline{\beta}_V}} \right] e^{-(1/2\overline{\beta}_V)\Sigma_\mathbf{x}\overline{B}_i^2(\mathbf{x})}$$

$$\times \sum_{\{\overline{n}_i(\mathbf{x})\}} e^{-i\Sigma_\mathbf{x}\overline{B}_i(\mathbf{x})(\nabla_i\overline{\gamma} - 2\pi\overline{n}_i - 2\pi A_i)}.$$

$$(12.5)$$

Executing the sum over $\overline{n}_i(\mathbf{x})$ makes the magnetic fields $\overline{B}_i(\mathbf{x})$ integer, say $\overline{b}_i(\mathbf{x})$, and integrating out the $\overline{\gamma}(\mathbf{x})$ fields leaves

$$\overline{Z}_V'^{\mathbf{A}} = I_0(\overline{\beta})^{3N} \sum_{\{\ell_i(\mathbf{x})\}} \delta_{\overline{\nabla}_i\ell_i,0}\, e^{-(1/2\overline{\beta}_V)\Sigma_\mathbf{x}\ell_i(\mathbf{x})^2 + 2\pi i\Sigma_\mathbf{x}\ell_i(\mathbf{x})A_i(\mathbf{x})},$$

$$(12.6)$$

where we have renamed the integer magnetic fields $\overline{b}_i(\mathbf{x})$ as $\ell_i(\mathbf{x})$, in accordance with the new vortex-line interpretation. For $\overline{\beta} \to \infty$, this is precisely the required sum over $\ell_i(\mathbf{x})$ in (12.1), (12.2). Therefore we arrive at the following form for the vortex-line representation of the XY model:

$$Z'_{XY} = I_0(\beta)^{3N} \prod_{\mathbf{x}} \left[\int_{-\infty}^{\infty} dA_1(\mathbf{x})\,dA_2(\mathbf{x}) \right] e^{-\beta E[\mathbf{A}]}\, \overline{Z}_{XY}'^{\mathbf{A}} / (I_0(\overline{\beta}))^{3N}\big|_{\overline{\beta}\to\infty}, \quad (12.7a)$$

with the auxiliary XY model coupled to the vector potential $\mathbf{A}(\mathbf{x})$,

$$\overline{Z}_{XY}'^{\mathbf{A}} = \prod_{\mathbf{x}} \left[\int_{-\pi}^{\pi} \frac{d\overline{\gamma}(\mathbf{x})}{2\pi} \right] e^{\overline{\beta}\Sigma_{\mathbf{x},i}\cos(\nabla_i\overline{\gamma} - 2\pi A_i)}.$$

$$(12.7b)$$

The energy $E[\mathbf{A}]$ is the hydrodynamic energy of the superflow

$$-\beta E[\mathbf{A}] = \sum_{\mathbf{x},i} \sum_{p=1}^{\infty} \frac{G_c^{(p)}(\beta)}{(-2\beta)^p p!} (\overline{\nabla} \times \mathbf{A})_i^{2p} \quad \text{(asymptotic expansion)}, \quad (12.7c)$$

or

$$-\beta E[\mathbf{A}] = -\frac{1}{2\beta_V} \sum_{\mathbf{x}} (\overline{\nabla} \times \mathbf{A})^2 \quad \text{(Villain approximation)}. \quad (12.7d)$$

Recall that in the limit $\bar{\beta} \to \infty$, the factor $I_0(\bar{\beta})^{-3N}$ tends to $\sqrt{2\pi\bar{\beta}_V}^{3N} e^{-3N\bar{\beta}}$. Before doing the limit, i.e., for a general finite $\bar{\beta}$, the partition function on the right-hand side of (12.7) is often called a *lattice superconductor*. The reason for this name will become clear in the next section. Since the limit $\bar{\beta} \to \infty$ corresponds to zero auxiliary temperature $\bar{T}$, one may say that the XY model is equivalent to a "frozen" lattice superconductor (where "frozen" refers only to the $\bar{\gamma}$-field).

Notice that due to (12.6), the general "unfrozen" lattice superconductor is *also* equivalent to an ensemble of vortex lines. This has the following partition function and Villain approximations:

$$Z_{XY}^{'C} \approx \left(\frac{I_0(\beta)}{I_0(\bar{\beta})}\right)^{3N} \prod_x \left[\int dA_1(x)\, dA_2(x)\right] e^{-\beta E[A]} \, \tilde{Z}_{XY}^{'A}$$

$$\approx Z_V^{'C} = I_0(\beta)^{3N} \prod_x \left[\int dA_1(x)\, dA_2(x)\right] e^{-(1/2\beta_V)\Sigma_x (\nabla \times A)^2}$$

$$\times \sum_{\{\ell_i(x)\}} \delta_{\nabla_i \ell_i, 0} \, e^{-(1/2\bar{\beta}_V)\Sigma_x \ell_i^2(x) + 2\pi i \Sigma_x \ell_i A_i(x)}. \tag{12.8}$$

This differs from the vortex representation of the original XY model (12.2) only by the additional factor $e^{-(1/2\bar{\beta}_V)\Sigma_x \ell_i^2(x)}$. Such a term makes vortex lines more difficult to form. It plays the role of an additional core energy. Thus we see that the general "unfrozen" lattice superconductor is equivalent to an XY model with an additional core energy in the vortex lines. This is why we have named this partition function $Z_{XY}^{'C}$. The superscript stands for core energy.

12.2. FROM LATTICE SUPERCONDUCTOR TO GINZBURG-LANDAU THEORY

The lattice superconductor representation (12.7) brings us very close to our goal of deriving the disorder field theory. All we have to do is treat the auxiliary XY model with the same field theoretic techniques which we used to analyze the original XY model Section 5.2. These permitted re-expressing the XY model in terms of a single or two complex fields. There is no problem in following the same procedure here in the presence of the additional vector potential. Only minor modifications are necessary. Instead of Eq. (5.34) we write

$$\cos(\nabla_i \bar{\gamma} - 2\pi A_i) = \tfrac{1}{2}(e^{i(\bar{\gamma}(\mathbf{x}+\mathbf{i}) - \bar{\gamma}(\mathbf{x}) - 2\pi A_i(\mathbf{x}))} + \text{c.c.})$$

$$= \tfrac{1}{2}(U^\dagger(\mathbf{x})\, U(\mathbf{x}+\mathbf{i})\, e^{-2\pi i A_i(\mathbf{x})} + \text{c.c.})$$

$$= \tfrac{1}{2}[U^\dagger(\mathbf{x})(U(\mathbf{x}+\mathbf{i})\, e^{-2\pi i A_i(\mathbf{x})} - U(\mathbf{x}))$$

$$+ U^\dagger(\mathbf{x})\, U(\mathbf{x}) + \text{c.c.}],$$

$$(12.9)$$

where $U(\mathbf{x}) \equiv e^{i\bar{\gamma}(\mathbf{x})}$ is a complex field with $U_a = (\cos\bar{\gamma}, \sin\bar{\gamma})$ being the analogue of the two-component field (5.35). It is useful to introduce a *covariant lattice derivative* of the complex field,

$$D_i U(\mathbf{x}) = U(\mathbf{x}+\mathbf{i})\, e^{-2\pi i A_i(\mathbf{x})} - U(\mathbf{x})$$

$$= (e^{-2\pi i A_i(\mathbf{x})}\, \nabla_i + e^{-2\pi i A_i(\mathbf{x})} - 1)\, U(\mathbf{x}).$$

$$(12.10)$$

The name characterizes the simple transformation properties under the gauge transformations:

$$U(\mathbf{x}) \rightarrow e^{2\pi i \Lambda(\mathbf{x})}\, U(\mathbf{x}), \quad A_i(\mathbf{x}) \rightarrow A_i(\mathbf{x}) + \nabla_i \Lambda(\mathbf{x}).$$

$$(12.11a)$$

Indeed,

$$D_i U(\mathbf{x}) = U(\mathbf{x}+\mathbf{i})\, e^{-2\pi i A_i(\mathbf{x})} - U(\mathbf{x}) \rightarrow e^{2\pi i \Lambda(\mathbf{x}+\mathbf{i})}\, U(\mathbf{x}+\mathbf{i})\, e^{-2\pi i A_i(\mathbf{x}) - 2\pi i \nabla_i \Lambda(\mathbf{x})}$$

$$-e^{2\pi i \Lambda(\mathbf{x})}\, U(\mathbf{x})$$

$$= e^{2\pi i \Lambda(\mathbf{x})} D_i U(\mathbf{x}).$$

$$(12.11b)$$

Thus $D_i U(\mathbf{x})$ transforms in the same way as $U(\mathbf{x})$ itself in spite of involving two $U(\mathbf{x})$ fields at the nearest neighbour sites $\mathbf{x}$ and $\mathbf{x}+\mathbf{i}$. The difference in the transformation laws of $U(\mathbf{x})$ and $U(\mathbf{x}+\mathbf{i})$ is made up for by the gauge transformation on the vector potential $A_i(\mathbf{x})$.

It is easy to see that in the continuum limit, as discussed in Eq. (2.4) in Part I, the covariant lattice derivative reduces to the ordinary covariant derivative. If we want to do this limit we have to go to dimensionful $A_i(\mathbf{x})$ fields, replacing $A_i(\mathbf{x})$ by $aA_i(\mathbf{x})$ where a is the lattice constant. Then, for $a \rightarrow 0$, the hydrodynamic Boltzmann factor in (12.7a) acquires the continuous form [recall (4.6)].

$$e^{-((\rho\hbar^2/M^2)/2T)\int d^3x(\nabla \times \mathbf{A})^2}.$$

For general $a \neq 1$, the covariant lattice derivative (12.10) is

$$D_i U(\mathbf{x}) = \frac{1}{a}(U(\mathbf{x} + \mathbf{i})\, e^{-2\pi i a A_i(\mathbf{x})} - U(\mathbf{x})).$$

For $a \to 0$, this reduces to

$$D_i U(\mathbf{x}) \to (\partial_i - 2\pi i A_i)\, U(\mathbf{x}), \qquad (12.12)$$

and therefore coincides with the covariant derivative D_i introduced in (2.4), Part I.

In previous lattice calculations we saw that the derivative ∇_i always occurs together with a partner $\bar{\nabla}_i$ which arises via the lattice analogue of partial integration. Let us see what this partner is for the covariant derivative D_i of (12.10). Consider two arbitrary complex fields $u(\mathbf{x})$ and $v(\mathbf{x})$. Then

$$\sum_{\mathbf{x}} u^\dagger(\mathbf{x})\, D_i v(\mathbf{x}) = \sum_{\mathbf{x}} u^\dagger(\mathbf{x})(v(\mathbf{x} + \mathbf{i})\, e^{-2\pi i A_i(\mathbf{x})} - v(\mathbf{x}))$$

$$= \sum_{\mathbf{x}} (u^\dagger(\mathbf{x})\, e^{-2\pi i A_i(\mathbf{x})}\, v(\mathbf{x} + \mathbf{i}) - u^\dagger(\mathbf{x})\, v(\mathbf{x}))$$

$$= -\sum_{\mathbf{x}} (u^\dagger(\mathbf{x}) - u^\dagger(\mathbf{x} - \mathbf{i})\, e^{-2\pi i A_i(\mathbf{x} - \mathbf{i})})\, v(\mathbf{x}). \qquad (12.13)$$

Thus we will be able to do partial integrations with covariant drivatives if we define the right-hand side as

$$-\sum_{\mathbf{x}} (\bar{D}u)^\dagger(\mathbf{x})\, v(\mathbf{x}),$$

with the identification

$$\bar{D}_i u(\mathbf{x}) = u(\mathbf{x}) - u(\mathbf{x} - \mathbf{i})\, e^{2\pi i A_i(\mathbf{x} - \mathbf{i})}$$

$$= (e^{2\pi i A_i(\mathbf{x} - \mathbf{i})}\, \bar{\nabla}_i + 1 - e^{2\pi i A_i(\mathbf{x} - \mathbf{i})})\, u(\mathbf{x}). \qquad (12.14)$$

This is the covariant version of $\bar{\nabla}_i$. In the continuum limit, it reduces to $\partial_i - 2\pi i A_i$ just as was the case with D_i.

Using these covariant derivatives, we can rewrite (12.7b) in a form very similar to the $A_i = 0$ case. First we see that by definition of D_i

$$\sum_{\mathbf{x}} \cos(\nabla_i \bar{\gamma} - 2\pi A_i) = \frac{1}{2} \sum_{\mathbf{x}} U^\dagger(\mathbf{x})(1 + D_i)\, U(\mathbf{x}) + \text{c.c.} \qquad (12.15)$$

Second we observe that, since (12.9) is to be summed over all **x**, we can rearrange the U fields as follows:

$$\frac{1}{2} \sum_{\mathbf{x}} U^\dagger(\mathbf{x} + \mathbf{i})\, U(\mathbf{x})\, e^{2\pi i A_i(\mathbf{x})} + \text{c.c.}$$

$$= \frac{1}{2} \sum_{\mathbf{x}} (U^\dagger(\mathbf{x})(U(\mathbf{x} - \mathbf{i})\, e^{2\pi i A_i(\mathbf{x} - \mathbf{i})} - U(\mathbf{x})) + U^\dagger(\mathbf{x})\, U(\mathbf{x})]$$

$$= \frac{1}{2} \sum_{\mathbf{x}} U^\dagger(\mathbf{x})(1 - \bar{D}_i)\, U(\mathbf{x}). \qquad (12.16)$$

And third we notice that

$$(D_i - \bar{D}_i)\, U(\mathbf{x})$$

$$= U(\mathbf{x} + \mathbf{i})\, e^{-2\pi i A_i(\mathbf{x})} - U(\mathbf{x}) - U(\mathbf{x}) + U(\mathbf{x} - \mathbf{i})\, e^{2\pi i A_i(\mathbf{x} - \mathbf{i})} \qquad (12.17\text{a})$$

is the same as

$$\bar{D}_i(U(\mathbf{x} + \mathbf{i})\, e^{-2\pi i A_i(\mathbf{x})} - U(\mathbf{x})) = \bar{D}_i D_i\, U(\mathbf{x}) = D_i \bar{D}_i\, U(\mathbf{x}). \qquad (12.17\text{b})$$

The property $D_i - \bar{D}_i = \bar{D}_i D_i = D_i \bar{D}_i$ will be very useful for the next step. Recall that in (5.37) we already profited from this property for $A_i = 0$, $\nabla_i - \bar{\nabla}_i = \bar{\nabla}_i \nabla_i = \nabla_i \bar{\nabla}_i$. Now using (12.15)–(12.17), we can rewrite the auxiliary model (12.7b) in the presence of an A_i field in a way completely analogous to (5.39):

$$\bar{Z}_{XY}^{\prime A} = \prod_{\mathbf{x}} \left[\int_{-\pi}^{\pi} \frac{d\bar{\gamma}(\mathbf{x})}{2\pi} \right] e^{D\tilde{\beta} \Sigma_{\mathbf{x}} U^\dagger(\mathbf{x})(1 + \bar{D}_i D_i/2D)\, U(\mathbf{x})}. \qquad (12.18)$$

This model can be transformed directly into a complex field theory of the type (5.44), i.e.,

$$\bar{Z}_{XY}^{\prime A} = \prod_{\mathbf{x}} \left[\int \frac{d\varphi_1(\mathbf{x})\, d\varphi_2(\mathbf{x})}{4\pi \beta D} \right] e^{-\bar{\beta} \bar{E}[\varphi,\, \varphi^\dagger,\, A]}, \qquad (12.19)$$

where the only difference with respect to the energy (5.44b) is the

appearance of the covariant derivatives $\bar{D}_i D_i$ instead of $\bar{\nabla}_i \nabla_i$ in the operator

$$\mathcal{D} = 1 + \frac{\bar{D}_i D_i}{2D} \tag{12.20}$$

of (5.40). The field theory has a Landau expansion [see (5.45)].

$$\bar{\beta E}[\varphi, \varphi^\dagger, \mathbf{A}] = \sum_{\mathbf{x}} \left\{ \frac{1}{8D}(\bar{D}_i\varphi)^\dagger(D_i\varphi) + \frac{1}{4}\left(\frac{1}{\bar{\beta}D} - 1\right)|\varphi|^2 + \frac{1}{64}|\varphi|^4 + \dots \right\}.$$
$$\tag{12.21}$$

Inserting $Z_{XY}^{\prime A}$ into the partition function (12.7a) we arrive at the proper disorder theory of vortex lines in the XY model,

$$Z_{XY}' = \lim_{\bar{\beta}\to\infty} \left(\frac{I_0(\beta)}{I_0(\bar{\beta})}\right)^{3N} \prod_{\mathbf{x}} \left[\int_{-\infty}^{\infty} dA_1(\mathbf{x})\, dA_2(\mathbf{x}) \right] e^{-\beta E[\mathbf{A}]}$$

$$\times \prod_{\mathbf{x}} \left[\int_{-\infty}^{\infty} \frac{d\varphi_1(\mathbf{x})\, d\varphi_2(\mathbf{x})}{4\pi\bar{\beta}D} \right] e^{-\bar{\beta}E[\varphi,\,\varphi^\dagger,\,\mathbf{A}]}. \tag{12.22}$$

12.3. COMPARISON WITH APPROXIMATE DISORDER THEORY

In order to compare this result with the continuum form (2.7) which was derived from more approximate considerations we have to go to dimensionful fields, replacing A_i by aA_i and φ by $a^{D/2-1}\varphi$. Then the energy in (12.21) reads

$$\int d^D x \left\{ \frac{1}{8D}(\bar{D}_i\varphi)^\dagger(D_i\varphi) + \frac{1}{4a^2}\left(\frac{1}{\bar{\beta}D} - 1\right)|\varphi|^2 + \frac{a^{D-4}}{64}|\varphi|^4 + \dots \right\}. \tag{12.23}$$

The higher powers, $|\varphi|^{2n}$, appear with a factor $a^{n(D-2)-D}$. Any higher lattice derivative D_i carries an extra factor a, and so does any additional power in A_i.

This field theory has a continuum limit only in the neighborhood of the critical temperature where $1/(\bar{\beta}D) - 1$ approaches zero with a^2, say $1/(\bar{\beta}D) - 1 = a^2\tau \to 0$ at a fixed $\tau = (\bar{T}_c/T - 1)$. In the limit $a \to 0$, all higher powers in φ and A_i and all higher derivatives D_i become irrelevant

and the disorder theory takes the Ginzburg-Landau form (2.7) derived before in a qualitative way. An important result within this specific model which was not available in the qualitative derivation of (2.7), is the size of the unrenormalized quartic coupling. After a renormalization $\varphi \to \sqrt{4D}\,\varphi$ we make the identification

$$g = D^2 a^{D-4} \tag{12.24}$$

In three dimensions this is equal to $9/a$ which is a large coupling strength.

Let us now compare the coupling of the vector potential with that in (2.7). In order to do so we renormalize the A_i field in the Villain expression (12.7d) by $\sqrt{\beta_V}$ (i.e., $A_i \to \sqrt{\beta_V} A_i$). Then the field energy has the form $\Sigma_{\mathbf{x}}(1/2)(\nabla \times \mathbf{A})^2$ and the coupling to the random loops is $\exp(-2\pi\sqrt{\beta_V}\,i\Sigma_{\mathbf{x}}\ell_i A_i(\mathbf{x}))$. In the disorder field theory, the covariant derivative becomes

$$D_i \varphi(\mathbf{x}) = \varphi(\mathbf{x} + \mathbf{i})\,e^{-2\pi\sqrt{\beta_V}\,iA(\mathbf{x}+\mathbf{i})} - \varphi(\mathbf{x})$$

with the continuum limit

$$D_i \to \partial_i - 2\pi\sqrt{\beta_V}\,iA_i(\mathbf{x}). \tag{12.25}$$

Comparison with (2.7) leads us to identify the charge of the disorder field as

$$q = 2\pi\sqrt{\beta_V}. \tag{12.26}$$

It is gratifying to note that this charge is the same as the one derived in (2.8) from the more qualitative arguments. For this we recall that in the lattice formulation, β was the inverse temperature measured in units of

$$\sigma = \rho\frac{\hbar^2}{M^2}a \sim 1\,\mathrm{K}$$

and that

$$\beta = \sigma/T, \tag{12.27}$$

and we can rewrite (12.26) in terms of proper physical units as follows,

$$q = \frac{1}{\sqrt{T}} \sqrt{\frac{\beta_V}{\beta}} \sqrt{\rho}\, \frac{\hbar}{M} 2\pi. \qquad (12.28)$$

This agrees with the charge (2.8) if the identification is performed at sufficiently low temperatures, for which

$$\sqrt{\frac{\beta_V}{\beta}} \sqrt{\rho} \sim \sqrt{\rho_s}.$$

12.4. NATURAL CORE ENERGIES

We had seen before that, in the XY model (12.2), the vortex loops have no extra core energy from the outset. The disorder partition function has to be evaluated at $\tilde{\beta} = \infty$ ("frozen" superconductor) which implies the absence of a Boltzmann factor $\exp(-(1/2\tilde{\beta}_V)\Sigma_{\mathbf{x}}\ell_i^2(\mathbf{x}))$ in (12.6). Thus it appears, at first, as though the vortex lines proliferate, due to their overwhelming entropy. This is not true though. The reason lies in the fact that the superflow around a vortex line makes it hard to create such a line. It gives rise to a self energy which acts just like a core energy. In order to see this explicitly, let us consider the vortex-line representation in the Villain approximation (7.26) after integrating out the A_i field

$$Z'_{XY} \sim Z'_V = I_0(\beta)^{3N} (\sqrt{2\pi\beta_V})^{2N} \det(-\overline{\nabla}_i\nabla_i)^{-1/2}$$

$$\times \sum_{\{\ell_i(\mathbf{x})\}} \delta_{\overline{\nabla}_i\ell_i,0}\, e^{-\beta_V(4\pi^2/2)\Sigma_{\mathbf{x},\mathbf{x}'}\,\ell_i(\mathbf{x})\,v(\mathbf{x}-\mathbf{x}')\ell_i(\mathbf{x}')}. \qquad (12.29)$$

The Coulomb Green function $v(\mathbf{x})$ can be split into

$$v(\mathbf{x}) = v(0)\,\delta_{\mathbf{x},0} + v'(\mathbf{x}) \sim 0.253\,\delta_{\mathbf{x},0} + v'(\mathbf{x}). \qquad (12.30)$$

In this way we can separate out the self energy of each link, i.e.,

$$e^{-\beta_V(4\pi^2/2)[v(0)\Sigma_{\mathbf{x}}\ell_i^2(\mathbf{x})\, +\, \Sigma_{\mathbf{x},\mathbf{x}'}\,\ell_i(\mathbf{x})v'(\mathbf{x}-\mathbf{x}')\ell_i(\mathbf{x}')]}. \qquad (12.31)$$

The subtracted Coulomb Green function has the form

$$v'(\mathbf{x}) = \left[\frac{1}{-(\overline{\nabla}_i \nabla_i)} - v(\mathbf{0})\right]\delta_{\mathbf{x},\mathbf{0}}. \tag{12.32}$$

It can be thought of as arising from a vector potential with energy

$$\beta E[\mathbf{A}] = -\frac{1}{2\beta_V}\sum_{\mathbf{k}}\frac{\overline{K}_i K_i}{1 - v(\mathbf{0})\overline{K}_i K_i}|A_i(\mathbf{k})|^2. \tag{12.33}$$

Introducing the symbol

$$\nabla_i' \equiv \frac{1}{\sqrt{1 + v(\mathbf{0})\overline{\nabla}_i \nabla_i}}\nabla_i, \tag{12.34}$$

we shall write this energy in $\mathbf{x}$ space as

$$-\beta E[\mathbf{A}] = -\frac{1}{2\beta_V}\sum_{\mathbf{x}}(\nabla' \times \mathbf{A})^2. \tag{12.35}$$

By undoing the A_i integration from (12.2) to (12.29), the partition function takes the alternative form

$$Z'_{XY} \sim Z'_V = I_0(\beta)^{3N}\det(1 + v(\mathbf{0})\overline{\nabla}_i \nabla_i)^{-1}\prod_{\mathbf{x},i=1,2}\left[\int_{-\infty}^{\infty}dA_1(\mathbf{x})\right]e^{-(1/2\beta_V)\Sigma_\mathbf{x}(\overline{\nabla}' \times \mathbf{A})^2}$$

$$\times \sum_{\{\ell_i(\mathbf{x})\}}\delta_{\overline{\nabla}_i\ell_i,0}\,e^{-\beta_V(4\pi^2/2)v(\mathbf{0})\Sigma_\mathbf{x}\ell_i^2(\mathbf{x}) + 2\pi i\Sigma_\mathbf{x}\ell_i(\mathbf{x})A_i(\mathbf{x})}. \tag{12.36}$$

This is a vortex-line representation which displays explicitly the core energies $\beta_V(4\pi^2/2)v(\mathbf{0})\sum_\mathbf{x}\ell_i^2(\mathbf{x})$ caused by the superflow. These will be referred to as *natural core energies*. Just as before, the sum over closed vortex lines can now be performed by means of an auxiliary XY model (12.4). Comparing with (12.6) we see that we can identify $\overline{\beta}_V$ as follows:

$$\overline{\beta}_V = \frac{1}{\beta_V 4\pi^2 v(\mathbf{0})}. \tag{12.37}$$

With this result we find the representation (12.8); here however the "magnetic field energy" of the vector potential $\beta E[\mathbf{A}]$ is to be replaced by

$$\beta E'[\mathbf{A}] = \frac{1}{2\beta_V}\sum_{\mathbf{x}}(\overline{\nabla}' \times \mathbf{A})^2. \tag{12.38}$$

This modification changes only the short distance behavior of the A_i correlation functions, not, however, the superflow in the far zone around the vortex lines.

Explicitly we find that the partition function of the XY model in the Villain approximation has the following disorder representation as a lattice superconductor with finite temperature $\bar{T}_V \equiv \bar{\beta}_V^{-1} = 4\pi^2 \beta_V v(0)$:

$$Z'_{XY} = \left(\frac{I_0(\beta)}{I_0(\bar{\beta})}\right)^{3N} \det(1 + v(0)\bar{\nabla}_i \nabla_i)^{-1} \prod_{\mathbf{x}} \left[\int dA_1(\mathbf{x})\, dA_2(\mathbf{x})\right] e^{-(1/2\beta_V)\Sigma_{\mathbf{x}}(\bar{\nabla}' \times \mathbf{A})^2}$$

$$\times \prod_{\mathbf{x}} \left[\int_{-\pi}^{\pi} \frac{d\bar{\gamma}(\mathbf{x})}{2\pi}\right] e^{\bar{\beta}\Sigma_{\mathbf{x}}\cos(\nabla_i\bar{\gamma} - 2\pi A_i)}. \tag{12.39}$$

We can now go through all the steps indicated in Section 12.2 and arrive at the disorder field theory (12.22), with the field energy (12.38) and $\bar{\beta}$ determined from (12.37). The natural core energy supplies us with a mass term in (12.23),

$$\frac{1}{4a^2}\left(\frac{1}{\bar{\beta}D} - 1\right)|\varphi|^2. \tag{12.40}$$

As an application of (12.39) let us calculate the transition temperature of the three-dimensional XY model. First at the mean field level where at $\bar{\beta} = 1/D$ the mass term changes sign and vortex lines proliferate. From Fig. 7.1 we see that this corresponds to

$$\bar{\beta}_{Vc} = 0.275. \tag{12.41}$$

Inserting this value into (12.37) we find

$$\beta_{Vc} = \frac{1}{4\pi^2 v(0)\,\bar{\beta}_{Vc}} = 0.361, \tag{12.42}$$

corresponding to (see again Fig. 7.1)

$$\beta_c = 0.52. \tag{12.43}$$

This is a bit too high (recall the proper $\beta_c \sim 0.46$).

It is easy to include corrections due to fluctuations of the φ field, but neglecting the fluctuations of the vector potential. From the analysis of

the original XY model we know that this moves the transition from $\bar{\beta}_c = 1/3$ to $\bar{\beta}_c = 0.45$. This corresponds to $\bar{\beta}_{Vc} = 0.33$. Inserting this value into (12.37) we have

$$\beta_{Vc} = \frac{1}{4\pi^2 v(0)\bar{\beta}_{Vc}} = 0.30, \qquad (12.44)$$

which corresponds to (see Fig. 7.1)

$$\beta_c = 0.39. \qquad (12.45)$$

This value is now too low. Still considering the crudeness of our considerations, in particular the neglect of the A_i fluctuations, the agreement between the various numbers is surprisingly good.

Let us conclude this section by summarizing the physics inherent in this disorder theory. In the previous chapter, the phase transition of the XY model was described as a condensation of closed integer-valued vortex lines. For low temperatures, there are no such lines. As the temperature is increased, a few small closed loops, the rotons, are thermally excited. Close to the transition point, the loops become larger and larger and at T_c their average length becomes infinite. Above T_c, the system is a condensate of vortex lines. The awakening of the vortex loops was seen explicitly in the energy (7.26) which showed the contribution of the different vortex loops to the free energy. It is these loops which correspond to the Feynman graphs of the disorder theory. When passing T_c, the proliferation process can no longer be followed by counting such individual graphs. In fact, the high $\bar{\beta}$ series is no longer convergent. The disorder field theory, however, succeeds in summing the infinity of such graphs by the simple property $|\varphi| \neq 0$. We had noticed before in Chapter 4 that the awakening of vortex loops upon heating is completely analogous and is dual to the awakening of closed lines of superflow upon cooling in the high temperature expansion of (7.18) or (7.19). The order field theory $\psi(\mathbf{x})$ sums up the closed superflow lines (in a loop expansion via Feynman diagrams). The main difference between the loop systems is that the lines of superflow have *only a core energy* while the vortex lines $\ell_i(\mathbf{x})$ are surrounded by superflow which gives them, in addition, a long range interaction. The presence of the superflow around vortex lines is accounted for by the gauge field A_i which makes the disorder field theory in $\varphi(\mathbf{x})$ a gauge theory of the Ginzburg-Landau form while the order field theory describing superflow lines contains only a ψ field.

12.5. TYPE-I OR TYPE-II DISORDER THEORY

With the disorder field theory being of the Ginzburg-Landau form the question arises as to the type of this theory. The disordered phase of the XY model displays a Meissner effect and is characterized by two length scales, λ and ξ_{size}. The first measures how far the superflow, described by the vector potential $\mathbf{A}$, can invade into a disordered part of the fluid. The second gives the distance over which the vortex density, carried by the disorder field $\varphi(\mathbf{x})$, changes rapidly at a superfluid-normal boundary. In analogy with the definition of type-I and type-II superconductors we shall speak of *type-I or type-II disorder theories* depending on whether λ is smaller or larger than ξ_{size}.

In the previous qualitative discussion of Section 2.4 the length scales were arbitrary parameters such that the theory could be of either type. The present specific disorder theory derived from the XY model has the advantage that the quantities λ and ξ_{size} are completely determined and can, in principle, be calculated. From (12.21) we see that, at the mean field level,

$$\xi_{\text{size}}^2 = \frac{1}{4D} \frac{1}{\dfrac{1}{\overline{\beta}D} - 1}.$$
(12.46)

The magnetic penetration depth λ can be read off the quadratic energy of A_i in the exponent of (12.22),

$$\frac{1}{2\beta_V}(\nabla \times \mathbf{A})^2 + \frac{1}{8D} 4\pi^2 \mathbf{A}^2 |\varphi|^2,$$
(12.47)

such that the penetration depth is given by

$$\lambda^2 = \frac{4D}{4\pi^2 \beta_V |\varphi|^2}.$$
(12.48)

Inserting the size of the disorder parameter,

$$|\varphi|^2 = 8\left(\frac{1}{\overline{\beta}D} - 1\right),$$
(12.49)

we find a ratio

$$\kappa = \frac{\lambda}{\sqrt{2}\xi_{size}} = \frac{D}{\sqrt{4\pi^2\beta_V}}.$$

(12.50)

In fact, on recalling the charge (12.26), this equation takes the simple form

$$\kappa = D/q.$$

(12.51)

At the critical point, $\beta_V \sim 0.33$, so that

$$\kappa \sim 0.83 \sim 1.18/\sqrt{2}.$$

(12.52)

Hence we conclude that, at the mean field level the disorder field theory of the XY model is of type II. The penetration depth of the superflow into the disordered phase is larger than the scale over which the vortex lines vary. An immediate consequence of this conclusion is the following: it is impossible to improve upon the mean field calculation of Eqs. (12.40)–(12.45) by simply integrating out the gauge field fluctuations and looking at the effective potential for constant $|\varphi|$. We saw in the discussion of the Ginzburg-Landau theory of superconductivity (Section 3.11) that this would produce a cubic term in $|\varphi|$ which leads to a first order phase transition if taken seriously. The superfluid transition is known to be of second order. Therefore, the assumption of a smooth $|\varphi|$ which underlies this procedure must be false. A type-II superconductor has too large size fluctuations to justify this assumption. The disorder field theory of vortex lines of superfluid ^{4}He is an important example which illustrates the danger of integrating out zero-mass fluctuations in a background field if this does not happen to be sufficiently smooth (as it is in an extreme type-I superconductor).

In the next chapter we shall see how it is nevertheless possible to study the case of large size fluctuations, namely, by going into the opposite direction as in Section 12.4, that is, by developing a disorder theory for the vortex lines of the Ginzburg-Landau theory. In this way we shall be able to estimate a κ value at which the transition does become first order.

12.6. QUANTUM VORTEX DYNAMICS IN FILMS OF SUPERFLUID HELIUM

Before ending this chapter we must comment on the extension of our theory to dynamic aspects of superfluidity and disorder. Up until recently, the main work on this subject was due to Nelson and Fisher (1977) and Ambegaokar, Nelson and Siggia (1980). These authors formulated a theory of moving vortices in a film of superfluid helium. Structurally, their theory is equivalent to the Maxwell-Lorentz theory of electromagnetic fields and electrons in two dimensions, apart from dissipative forces: the gauge theory of time-dependent superflows in a plane has the same form as that of electromagnetic fields. The vortices move through the superfluid as a function of time just as electrons (without spin) would move through space-time. Using similar techniques as in the Maxwell-Lorentz theory it is possible to calculate, for instance, the renormalization of the superfluid density (the analogue of the inverse dielectric constant) due to the presence of a grand canonical ensemble of moving vortices. It is obvious that such a theory shares all the well-known shortcomings of the Maxwell-Lorentz theory of electrons. It is therefore necessary to find a quantum field theory of moving vortices which provides the same extension to the previous theory as quantum electrodynamics (QED) does to the Maxwell-Lorentz theory of the electron. Such a theory was developed in 1985. Because of its analogy with QED we have named it *quantum vortex dynamics (QVD)*. The starting point is the action of time dependent phase fluctuations in a film of superfluid helium at low temperature,

$$\mathscr{A}_0 = \frac{T_0}{2} \int dt \, d^2x \left[\frac{1}{c^2} (\partial_t \gamma)^2 - (\nabla \gamma)^2 \right], \tag{12.53}$$

where c is the velocity of (third) sound ($\approx 18.2 \mathrm{K} \cdot \text{Å}$) and $T_0 \equiv \rho \hbar^2 / M^2$. The partition function may be defined on a stack of square lattices with spacing a and stacking distance ε along the imaginary time axis $\tau = x_0 \equiv it$ as [recall the general discussion in Section I.1.7],

$$Z_0 \equiv \prod_{x,\tau} \left[\int_{-\infty}^{\infty} \frac{d\gamma(x, \tau)}{\sqrt{2\pi\varepsilon c^2/T_0 a^2}} \right] \exp\left\{ -\frac{T_0}{2} \frac{a^2}{\varepsilon c^2} \sum_{x,\tau} \left[(\nabla_0 \gamma)^2 + c^2 \frac{\varepsilon^2}{a^2} (\nabla_i \gamma)^2 \right] \right\}, \tag{12.54}$$

where

$$\nabla_0 \gamma(\mathbf{x}, \tau) = \gamma(\mathbf{x}, \tau + \varepsilon) - \gamma(\mathbf{x}, \tau),$$

$$\nabla_i \gamma(\mathbf{x}, \tau) = \gamma(\mathbf{x} + i a, \tau) - \gamma(\mathbf{x}, \tau), \qquad (12.55)$$

are the lattice derivatives. If $K_i = (e^{ik_i a} - 1)/i$ and $K_0 = \Omega \equiv (e^{i\omega\varepsilon} - 1)/i$ (with $\omega = \omega_n \equiv (2\pi/\beta)n$) denote their eigenvalues, the integrals over $\gamma(\mathbf{x}, \tau)$ give [recall (6.247), Part I]

$$Z_0 = \exp\left\{ -\frac{N}{2} \int_{-\pi/a}^{\pi/a} \frac{d^2 k a^2}{(2\pi)^2} \sum_n \log(\Omega_n \bar{\Omega}_n + c^2 \varepsilon^2 \mathbf{K} \cdot \bar{\mathbf{K}}/a^2) \right\}, \qquad (12.56)$$

where N is the total number of spatial sites on the square lattice.

At the end, we have to take the limits $\varepsilon \to 0$, $a \to 0$ in which case Z_0 reduces to the expression

$$Z_0 \to \exp\left\{ -\frac{N}{2T} \int \frac{d^2 k a^2}{(2\pi)^2} [c|\mathbf{k}| + T \log(1 - e^{-c|\mathbf{k}|})] \right\}. \qquad (12.57)$$

This can easily be calculated. It has the same form as the partition function of free phonons in a crystal and forms the basis of the Debye theory of the specific heat of solids. Since we shall review that theory in detail in Part III, Section 7.3, we shall refrain from calculating the temperature dependence of the thermodynamic quantities in this chapter. Here the only relevant point is that there exists a Debye temperature

$$\Theta_D = \sqrt{4\pi} \frac{c}{a}, \qquad (12.58)$$

which separates the classical from the quantum regime. For $T \ll \Theta_D$, the specific heat has the quantum behavior [see Eq. (7.185), Part III]

$$C \xrightarrow[T \ll \Theta_D]{} N \cdot 12 \cdot \xi(3) \cdot \left(\frac{T}{\Theta_D}\right)^2. \qquad (12.59)$$

For $T \gg \Theta_D$, the system behaves classically and C obeys the Dulong-Petit law, according to which C is equal to 1/2 times the total sum of kinetic and potential degrees of freedom, i.e.,

$$C \xrightarrow[T \gg \Theta_D]{} N. \tag{12.60}$$

Moving vortices can now be introduced into the system along the lines of Section 8.1. We simply go over from the Gaussian partition function (12.54) to the periodic Gaussian

$$Z = \prod_{\mathbf{x}, \tau} \left[\int \frac{d\gamma(\mathbf{x}, \tau)}{\sqrt{2\pi}} \right] \sum_{\{n_\mu(\mathbf{x}, \tau)\}} \Phi[n_\mu] \exp \left\{ -\frac{1}{2} \frac{T_0}{T} \frac{1}{N_\tau} \right.$$

$$\left. \times \sum_{\mathbf{x}, \tau} \left[N_\tau^2 \left(\frac{T}{T_D} \right)^2 (\nabla_0 \gamma - 2\pi n_0)^2 + (\nabla_i \gamma - 2\pi n_i)^2 \right] \right\}, \tag{12.61}$$

where $\Phi[n_\mu]$ is a gauge-fixing functional of the jump numbers $n_\mu = (n_0, n_1, n_2)$ and we have introduced $N_\tau \equiv 1/T\varepsilon$ and $T_D \equiv c/a$. The latter quantity is related to the Debye temperature Θ_D via $T_D = (1/\sqrt{4\pi}) \Theta_D \approx 0.282 \Theta_D$. From $c = 18.2 \text{K} \cdot \text{Å}$ we calculate $T_D \approx 5.08$, $\Theta_D \approx 18.02$. The superfluid transition, on the other hand, takes place at $T_c \approx 2.2\text{K}$. Thus it lies well within the T^2 quantum regime of the specific heat, Eq. (12.59).

The two space plus one time dimensional partition function (12.61) is completely equivalent to the Villain model of three-dimensional superfluid helium *without* dynamics. The only difference is that the third axis is rescaled and reinterpreted as a time axis, which is of finite length $1/T$, with periodic boundary conditions, and that the lattice spacings are different along the 1,2 and the 3 directions. We can therefore proceed as in Sections 7.2 and 12.1. After introducing auxiliary variables B^0, B^i, the partition function takes the form

$$Z = \prod_{\mathbf{x}, \tau} \left[\int \frac{dB^0(\mathbf{x}, \tau)}{\sqrt{2\pi\beta/\hat{c}^2 N_\tau}} \right] \prod_{\mathbf{x}, \tau, i} \left[\int \frac{dB^i(\mathbf{x}, \tau)}{\sqrt{2\pi\beta/N_\tau}} \right] \prod_{\mathbf{x}, \tau} \left[\int \frac{d\gamma(\mathbf{x}, \tau)}{\sqrt{2\pi\hat{c}^2 N_\tau}} \right]$$

$$\times \sum_{\{n_\mu\}} \Phi[n_\mu] e^{-(N_\tau/\beta)\Sigma_{\mathbf{x}, \tau}(\hat{c}^2 B^{02} + B^{i2}) + i\Sigma_{\mathbf{x}, \tau} B^\mu(\nabla_\mu \gamma - 2\pi n_\mu)}, \tag{12.62}$$

where we have used the Greek index μ to label $\mu = 0, 1, 2$, and set

$$\beta \equiv \frac{T_0}{T}, \qquad \hat{c} = \frac{T_D}{T} \frac{1}{N_T}. \tag{12.63}$$

The integration over $\gamma(\mathbf{x}, \tau)$ enforces $\bar{\nabla}_\mu B^\mu = 0$ so that one can write [compare Eq. (6.5)]

$$B^{\mu}(\mathbf{x}) = \varepsilon^{\mu\nu\lambda}\bar{\nabla}_{\nu}A_{\lambda}(x - \lambda), \tag{12.64}$$

where we have denoted the three-vectors $(\mathbf{x}, \tau)$ by x. The $\Sigma_{\mathbf{x},\tau}(\hat{c}^2 B^{02} + B^{i2})$ part of the exponent takes the same form as $2 + 1$-dimensional electromagnetism. The field B^0 is the magnetic field (which has to be imagined as pointing orthogonally to the plane). The fields B^1, B^2 correspond to the two *electric* field components within the plane. In order to see this we notice that, in two dimensions, the components A^1, A^2 are vector potentials while A^0 plays the role of the Coulomb potential. Thus, writing (12.64) out in component form,

$$B^0(\mathbf{x}) = \bar{\nabla}_1 A_2(\mathbf{x} - \mathbf{2}) - \bar{\nabla}_2 A_1(\mathbf{x} - \mathbf{1}),$$

$$B^1(\mathbf{x}) = \bar{\nabla}_2 A_0(\mathbf{x} - \mathbf{0}) - \bar{\nabla}_0 A_2(\mathbf{x} - \mathbf{2}),$$

$$B^2(\mathbf{x}) = \bar{\nabla}_0 A_1(\mathbf{x} - \mathbf{1}) - \bar{\nabla}_1 A_0(\mathbf{x} - \mathbf{0}), \tag{12.65}$$

we can identify the electric fields as

$$E_1(\mathbf{x}) = B^2(\mathbf{x}), \qquad E_2(\mathbf{x}) = -B^1(\mathbf{x}), \tag{12.66}$$

i.e.

$$E_i(\mathbf{x}) = \varepsilon_{ij} B^j(\mathbf{x}). \tag{12.67}$$

The fields associated with a given $\ell^{\mu}(\mathbf{x}, \tau)$ configuration are found by minimizing the energy. It is useful to introduce the metric

$$g_{\mu\nu} = \begin{pmatrix} \hat{c}^2 & 0 & 0 \\ 0 & 1 & 0 \\ 0 & 0 & 1 \end{pmatrix}, \tag{12.68}$$

to lower the indices of B^{μ} and write the energy as

$$-\frac{N_{\tau}}{2\beta}\sum_{\mathbf{x},\tau} B_{\mu} B^{\mu} + 2\pi i \sum_{\mathbf{x},\tau} A_{\mu} \ell^{\mu}. \tag{12.69}$$

This leads directly to the field equation

$$\varepsilon^{\lambda\mu\nu}\nabla_{\mu}B_{\nu}(x + \lambda) = 2\pi i \ell^{\lambda}, \tag{12.70}$$

or, in component form, omitting the shifts in the arguments of $B_\mu(x - \mu)$,

$$\nabla_1 B_2 - \nabla_2 B_1 = 2\pi i \ell^0, \quad \nabla_2 B_0 - \nabla_0 B_2 = 2\pi i \ell^1, \quad \nabla_0 B_1 - \nabla_1 B_0 = 2\pi i \ell^2.$$
$$(12.71)$$

After inserting (12.66), these read

$$\nabla_i E^i = 2\pi i \ell^0,$$

$$\hat{c}^2 \nabla_2 B^0 - \nabla_0 E^1 = 2\pi i \ell^1,$$

$$-\hat{c}^2 \nabla_1 B^0 - \nabla_0 E^2 = 2\pi i \ell^2. \qquad (12.72)$$

The first equation is the Euclidean version of Coulomb's law. If we define

$$(\nabla \times \mathbf{B})^i \equiv \varepsilon^{ij} \nabla_j B^0, \qquad (12.73)$$

the remaining two equations can be rewritten as

$$\hat{c}^2 (\nabla \times \mathbf{B}) - \nabla_0 \mathbf{E} = 2\pi i \boldsymbol{\ell}. \qquad (12.74)$$

In this form we recognize the Euclidean lattice version of the Maxwell equations in two dimensions. The link vectors ℓ^0, ℓ^i play the role of a charge density ℓ^0 and a current density ℓ^i for the electric and magnetic fields E^i, B^0, respectively.

In the transverse gauge $\nabla_i A_i = 0$ the partition function takes the form

$$Z = \det(-\bar{\nabla}_i \nabla_i) \frac{1}{(\sqrt{2\pi\beta/N_\tau})^{2N}} \prod_{\mathbf{x}} \left[\int_{-\infty}^{\infty} d^3 A_\mu \, \delta(\nabla_i A_i) \right] \sum_{\{n_\mu\}} \Phi[n_\mu]$$

$$\times \exp\left\{ -\frac{N_\tau}{2\beta} \sum_{\mathbf{x},\tau} [\hat{c}^2 (\bar{\nabla}_i A_j)^2 + (\bar{\nabla}_0 A_j)^2 + (\bar{\nabla}_i A_0)^2] + 2\pi i \sum_{\mathbf{x},\tau} A_\mu \ell^\mu \right\}.$$
$$(12.75)$$

We now integrate out the A_0, A_i fields. This leads to the partition function

$$Z = Z_0 \cdot Z_v, \qquad (12.76)$$

where Z_0 is the partition function (12.56) of the harmonic phase fluctuations and Z_v collects the effect of the vortices:

$$Z_v = \sum_{\{\ell^\mu(\mathbf{x},\tau)\}} \delta_{\bar\nabla_\mu \ell^\mu, 0} \exp\left\{ -\frac{4\pi^2\beta}{2N_\tau} \sum_k \left[\ell^0(k)^* \ell^0(k) \frac{1}{K_\ell \bar{K}_\ell} \right.\right.$$
$$\left.\left. + \ell^i(k)^* \ell^j(k)\left(\delta_{ij} - \frac{K_i \bar{K}_j}{K_\ell \bar{K}_\ell}\right) \frac{1}{K_0 \bar{K}_0 + \hat{c}^2 K_i \bar{K}_i} \right]\right\} \qquad (12.77)$$

where k stands for $(\omega_n, \mathbf{k})$. Since the world lines of vortices $\ell^\mu(\mathbf{x}, \tau)$ are closed, we can replace $\bar{K}_i \ell^i$ by $\bar{K}_0 \ell^0$ and find,

$$Z_v = \sum_{\{\ell^\mu(\mathbf{x},\tau)\}} \delta_{\bar\nabla_\mu \ell^\mu, 0} \exp\left\{ -\frac{4\pi^2\beta}{2N_\tau} \sum_k \ell^\mu(k)^* \ell_\mu(k) \frac{1}{K_0 \bar{K}_0 + \hat{c}^2 K_i \bar{K}_i} \right\}$$
$$= \sum_{\{\ell^\mu(\mathbf{x},\tau)\}} \delta_{\bar\nabla_\mu \ell^\mu, 0} \exp\left\{ -\frac{4\pi^2\beta}{2N_\tau} \sum_{\mathbf{x},\tau;\mathbf{x}',\tau'} \ell^\mu(\mathbf{x},\tau)\, v(\mathbf{x}-\mathbf{x}', \tau-\tau')\, \ell_\mu(\mathbf{x}',\tau') \right\},$$
$$(12.78)$$

where

$$v(\mathbf{x}, \tau) = \frac{1}{N_\tau} \sum_n \int \frac{d^2k}{(2\pi)^2} a^2 e^{-i(\omega_n T - \mathbf{k}\cdot\mathbf{x})} \frac{1}{\Omega_n \bar\Omega_n + \hat{c}^2 K_i \bar{K}_i} \qquad (12.79)$$

is the zero-mass Green function on the anisotropic $2 + 1$-dimensional lattice.

It is possible to add, in the exponent of (12.75), an extra core energy term

$$\frac{e_c}{T} \sum_{\mathbf{x},\tau} (\hat{c}^2 \ell^0(\mathbf{x}, \tau)^2 + \ell^i(\mathbf{x}, \tau)^2) \qquad (12.80)$$

and go through the same development as in the formalism of Section 12.2. The result is a disorder field theory of the Ginzburg-Landau type which now lives in two space and one time dimensions rather than three space dimensions and in the continuum limit has a partition function

$$Z = \prod_{\mathbf{x}, \tau} \left[\int d\varphi(\mathbf{x}, \tau) d\varphi^{\dagger}(\mathbf{x}, \tau) \right] \prod_{\mathbf{x}, \tau} \left[\int d^3 A_i \Phi[A_i] \right]$$

$$\times \exp\left\{ -\frac{1}{T} \int d\tau \, d^2 x \frac{1}{2} B_{\mu}^2 - \frac{1}{2} \int d\tau \, d^2 x \left[\frac{1}{2} |D_{\mu} \varphi|^2 \right. \right.$$

$$\left. \left. + \frac{m^2}{2} |\varphi|^2 + \frac{g}{4} |\varphi|^4 + \ldots \right] \right\},$$ (12.81)

where $B_{\mu}^2 \equiv c^2 B^{02} + B'^2$, $D_{\mu} \equiv \partial_{\mu} - ieA_{\mu}$, and $|D_{\mu}\varphi|^2 = (1/c^2)(D_0\varphi)^*$ $(D_0\varphi) + (D_i\varphi)^*(D_i\varphi)$ are appropriately rescaled continuum versions of the corresponding lattice quantities.

This theory is renormalizable and can be used to calculate the radiative corrections to all dynamical phenomena. In contrast to the previous theory of the Maxwell-Lorentz type, it allows for a straightforward description of the regime *above* the critical temperature. The field theory must only be evaluated in the neighborhood of the appropriate non-zero expectation value of the disorder field $\varphi(\mathbf{x}, \tau)$. For more details, the reader is referred to the original paper by the author (quoted in the Notes and References).

NOTES AND REFERENCES

The observation that an *XY* model is equivalent to a frozen lattice superconductor was first made by
M. Peskin, *Ann. Phys.* **113** (1978) 122.
See also
T. Banks and E. Rabinovici, *Nucl. Phys.* **B160** (1979) 349,
P.R. Thomas and M. Stone, *Nucl. Phys.* **B144** (1978) 513.
   The dynamical aspects of vortices in films of superfluid ^{4}He were discussed by
D.R. Nelson and D.S. Fisher, *Phys. Rev.* **B16** (1977) 4945,
V. Ambegaokar, B.I. Halperin, D.R. Nelson and E.D. Siggia, *Phys. Rev.* **B21** (1980) 9806,
V. Ambegaokar and S. Teitel, *Phys. Rev.* **B19** (1984) 1667,
D.L. Huber, *Phys. Rev.* **B26** (1982) 3758,
A.V. Nikitorov and E.B. Sonin, *Sov. Phys. JETP* **58** (1984) 373,
R. Coté and A. Griffin, *Phys. Rev. B* (in press).
Incidentally, the dual system is the two-dimensional superconductor. From Chapter 13, we know that there the dynamics of vortices is given by a pure $|\psi|^4$ theory. A discussion at the "Maxwell-Lorentz" level was given by
B.I. Halperin and D.R. Nelson, *J. Low Temp. Phys.* **36** (1979) 599.
A full-fledged quantum field theory of two-dimensional vortices was formulated in
H. Kleinert, *Int. J. Engng. Sci.* **23** (1985) 927.

VORTEX LINES IN THE GINZBURG-LANDAU THEORY AND THEIR DISORDER FIELD THEORY

13.1. GENERAL DISCUSSION

In the last chapter we derived and studied the disorder field theory which describes the vortex lines in a superfluid. These vortex lines are closed loops with long-range Biot-Savart type interactions. The disorder field theory is a complex field theory coupled to a gauge potential. It is of the Ginzburg-Landau type. Previously, in Chapter 3 we discussed this theory in the context of superconductivity and found that it also contained vortex lines of its own, although of an entirely different nature from those in the superfluid. The vortex lines in the Ginzburg-Landau theory are macroscopic fluctuations involving the size $|\varphi|$ of the complex field and the magnetic field. Each of these deviates from its equilibrium value only within a small range around the vortex line. In a type-II superconductor, the range λ over which the magnetic field varies extends beyond the range ξ_{size} over which the scalar field varies. The "magnetic core" is larger than the "scalar core." In a type-I superconductor, the opposite is true. It can be shown that for two parallel vortex lines the force due to the magnetic field is repulsive, that due to the size field is attractive. For antiparallel lines (which are hard to produce in a superconductor) the magnetic force would reverse sign and the total force would always be attractive. At any

rate, the range of the forces is always short, since the long-range phase fluctuations of the scalar field are unphysical gauge modes, and thus unobservable, and the magnetic field is screened by the Meissner effect.

The question arises whether it is not possible to make use of what we have learned about the superfluid and treat also the superconductor as a statistical ensemble of *its* vortex lines. There should exist a disorder field theory also for this ensemble. Its loop expansion would give direct pictures of the loops contained in this ensemble. Let us derive such a disorder theory. It would, of course, be possible to proceed as we did in the case of the superfluid (Chapter 1). We could discuss an individual line according to core region and far zone, analyze the small field fluctuations coupled to it, find the forces between the lines, and set up an approximate $|\varphi|^4$ disorder field theory. One immediate conclusion would be that due to the existence of only short-range forces, the disorder field theory of vortex lines in the Ginzburg-Landau theory has *no* gauge field coupled to it. It is a pure complex field theory with short range, steric interactions only. We shall not, however, go through these qualitative arguments in detail, since in the last chapters starting from Chapter 4, we learned that it is much more useful to perform all operations on a specific lattice model where they are well defined. This is what we shall now do.

13.2. VORTEX-LINE REPRESENTATION OF A GENERAL LATTICE SUPERCONDUCTOR

The starting point is the partition function of the lattice superconductor in (12.7) which we shall write in the form,

$$Z_{LS}(\bar{\beta}, \beta) = \det(-\bar{\nabla}_i \nabla_i)^{1/2} \prod_{\mathbf{x}} \left[\int_{-\infty}^{\infty} \frac{dA_1(\mathbf{x}) \, dA_2(\mathbf{x})}{(q/2\pi)^2} \right] e^{-(4\pi^2/2q^2)\Sigma_{\mathbf{x}}(\bar{\nabla} \times \mathbf{A})^2}$$

$$\times \prod_{\mathbf{x}} \left[\int_{-\pi}^{\pi} \frac{d\bar{\gamma}(\mathbf{x})}{2\pi} \right] e^{\bar{\beta}\Sigma_{\mathbf{x},i}\cos(\nabla_i \bar{\gamma} - 2\pi A_i)}, \tag{13.1}$$

where q is the charge defined in (12.26),

$$q = 2\pi\sqrt{\beta_V}. \tag{13.2}$$

The partition function of the *XY* model at temperature $1/\beta$, from which it was derived, is given by the zero $\bar{T}$ temperature limit:

$$Z_{XY}(\beta) = \lim_{\bar{\beta} \to 0} \frac{I_0(\beta)^{3N}}{I_0(\bar{\beta})^{3N}} \left(\frac{q}{2\pi}\right)^{2N} \det(-\bar{\nabla}_i \nabla_i)^{-1/2} Z_{LS}(\bar{\beta}, \beta). \quad (13.3)$$

For $q \to 0$, the lattice superconductor reduces trivially to another XY model involving $\bar{\beta}$ and $\bar{\gamma}$ and the normalization factor in (13.1) is chosen such that this happens without an extra overall factor [recalling the result of the integrations over A_1, A_2 in (6.64), (6.72)]. By a rescaling $A_i \to (q/2\pi)A_i$, the partition function (13.1) takes the generic form

$$Z_{LS} = \det(-\bar{\nabla}_i \nabla_i)^{1/2} \prod_{\mathbf{x}} \left[\int_{-\infty}^{\infty} dA_1(\mathbf{x}) dA_2(\mathbf{x}) \right] e^{-(1/2)\Sigma_{\mathbf{x}}(\bar{\nabla} \times \mathbf{A})^2}$$

$$\times \prod_{\mathbf{x}} \left[\int_{-\pi}^{\pi} \frac{d\bar{\gamma}}{2\pi} \right] e^{\bar{\beta} \Sigma_{\mathbf{x},i} \cos(\nabla_i \bar{\gamma} - qA_i)}, \quad (13.4)$$

which shows explicitly the role of the charge q as a coupling strength to the A_i fluctuations. In the present chapter we shall study the lattice superconductor for all parameters q, $\bar{\beta}$, i.e., without assuming (13.2).

Before proceeding it is useful to remember the method of (12.29)–(12.36) for extracting the natural core energy of the vortex loops by modifying the propagation of the vector potential from $-1/\bar{\nabla}_i \nabla_i$ to $-1/\bar{\nabla}_i' \nabla_i' = (-1/-\bar{\nabla}_i \nabla_i)(1 + v(0)\bar{\nabla} \cdot \nabla)$. This permits us to write, alternatively,

$$Z_{LS} = \det(1 + v(0)\bar{\nabla} \cdot \nabla)^{-1} \det(-\bar{\nabla} \cdot \nabla)^{1/2}$$

$$\times \prod_{\mathbf{x}} \left[\int_{-\infty}^{\infty} dA_1(\mathbf{x}) dA_2(\mathbf{x}) \right] e^{-(1/2)\Sigma_{\mathbf{x}}(\bar{\nabla}' \times \mathbf{A})^2}$$

$$\times \prod_{\mathbf{x}} \left[\int \frac{d\bar{\gamma}(\mathbf{x})}{2\pi} \right] e^{\bar{\beta}' \Sigma_{\mathbf{x}} \cos(\nabla_i' \bar{\gamma} - qA_i)}. \quad (13.5)$$

We may check that this reduces again to the XY model for $q \to 0$ [since the integrations over A_i give $\det(-\bar{\nabla}_3' \nabla_3')^{-1/2} \det(-\bar{\nabla}' \cdot \nabla')^{-1/2} = \det(1 + v(0)\bar{\nabla} \cdot \nabla) \det(-\bar{\nabla} \cdot \nabla)^{-1/2}$, recalling (6.64)–(6.72). The derivatives ∇_i' are defined, as in (12.34), by $\nabla_i' \equiv (1 + v(0)\bar{\nabla} \cdot \nabla)^{-1/2} \nabla_i$].

The parameter $\bar{\beta}'$ now is the inverse Villain transform

$$\bar{\beta}_V' = (\bar{\beta}_V^{-1} + 4\pi^2 \beta_V v(0))^{-1} = (\bar{\beta}_V^{-1} + q^2 v(0))^{-1}. \quad (13.6)$$

With respect to (12.39) there is the extra core energy $\bar{\beta}_V^{-1}$ added to the natural one $q^2 v(0)$. This additivity follows directly from the Villain approximation,

$$\prod_{\mathbf{x}} \left[\int_{-\pi}^{\pi} \frac{d\tilde{\gamma}}{2\pi} \right] e^{\tilde{\beta}\Sigma_{\mathbf{x},i}\cos(\nabla_i\tilde{\gamma} - qA_i)}$$

$$= R_V(\tilde{\beta})^{3N} \prod_{\mathbf{x}} \left[\int_{-\pi}^{\pi} \frac{d\tilde{\gamma}}{2\pi} \right] e^{-(\tilde{\beta}_V/2)\Sigma_{\mathbf{x}}(\nabla_i\tilde{\gamma} - qA_i - 2\pi n_i)^2}$$

$$= (I_0(\tilde{\beta}))^{3N} \sum_{\{\ell_i(\mathbf{x})\}} \delta_{\bar{\nabla}_i \ell_i, 0}\, e^{-(1/2\tilde{\beta}_V)\Sigma_{\mathbf{x}}\ell_i(\mathbf{x})^2 + iq\Sigma_{\mathbf{x}}\ell_i(\mathbf{x})A_i(\mathbf{x})},$$

with which the integration of the vector potential in (13.5) produces the exponential

$$\det(-\bar{\nabla}_3\nabla_3)^{-1/2}\det(-\bar{\nabla}_i\nabla_i)^{-1/2}\, e^{-(1/2)(\tilde{\beta}_V^{-1} + q^2 v(0))\Sigma_{\mathbf{x}}\ell_i^2(\mathbf{x}) - (q^2/2)\Sigma_{\mathbf{x},\mathbf{x}'}\ell_i(\mathbf{x})v'(\mathbf{x} - \mathbf{x}')\ell_i(\mathbf{x}')}.$$

Undoing these operations for the $v'(\mathbf{x} - \mathbf{x}')$ part leads directly to (13.5) and (13.6). The Ginzburg-Landau theory associated with the general lattice superconductor is obtained by using the identity (12.18) or (12.19) which allows us to write (13.4) in the form

$$Z_{LS} = \det(-\bar{\nabla}\cdot\nabla)^{1/2}\prod_{\mathbf{x}}\left[\int_{-\infty}^{\infty} dA_1(\mathbf{x})dA_2(\mathbf{x})\right] e^{-(1/2)\Sigma_{\mathbf{x}}(\bar{\nabla}\times\mathbf{A})^2}\, \bar{Z}_{XY}^{\prime\mathbf{A}}$$

$$= \det(-\bar{\nabla}\cdot\nabla)^{1/2}\prod_{\mathbf{x}}\left[\int_{-\infty}^{\infty} dA_1(\mathbf{x})dA_2(\mathbf{x})\right] e^{-(1/2)\Sigma_{\mathbf{x}}(\bar{\nabla}\times\mathbf{A})^2}$$

$$\times \prod_{\mathbf{x}}\left[\int_{-\infty}^{\infty} \frac{d\varphi_1(\mathbf{x})d\varphi_2(\mathbf{x})}{4\pi\tilde{\beta}D} \bullet\right] e^{-\tilde{\beta}'E[\varphi,\,\varphi^\dagger,\,\mathbf{A}]}, \tag{13.7a}$$

while (13.5) becomes

$$Z_{LS} = \det(1 + v(0)\,\bar{\nabla}\cdot\nabla)^{-1}\det(-\bar{\nabla}\cdot\nabla)^{1/2}$$

$$\times \sum_{\mathbf{x}}\left[\int_{-\infty}^{\infty} dA_1(\mathbf{x})dA_2(\mathbf{x})\right] e^{-(1/2)\Sigma_{\mathbf{x}}(\bar{\nabla}'\times\mathbf{A})^2}$$

$$\times \prod_{\mathbf{x}}\left[\int \frac{d\varphi_1(\mathbf{x})d\varphi_1^\dagger(\mathbf{x})}{4\pi\tilde{\beta}'D}\right] e^{-\tilde{\beta}'E'[\varphi,\,\varphi^\dagger,\,\mathbf{A}]}. \tag{13.7b}$$

In the first case (13.7a)

$$\tilde{\beta}E = \sum_{\mathbf{x}}\left\{\frac{1}{8D}|D_i\varphi|^2 + \frac{1}{4}\left(\frac{1}{\overline{\beta}D} - 1\right)|\varphi|^2 + \frac{1}{64}|\varphi|^4 + \ldots\right\}. \tag{13.8}$$

In the second case, (13.7b), E is replaced by E' and $\bar\beta$ by $\bar\beta'$ which is related to $\bar\beta$ via (13.6a):

$$\bar\beta'_V = (\bar\beta_V^{-1} + q^2 v(0))^{-1},$$

or, more explicitly,

$$-2\log\frac{I_1(\bar\beta')}{I_0(\bar\beta')} = -2\log\frac{I_1(\bar\beta)}{I_0(\bar\beta)} + q^2 v(0).$$

Equation (13.7b) is the Ginzburg-Landau theory whose vortex lines will now be studied via the lattice superconductor (13.1).

In the lattice superconductor, the vortex lines can be displayed in the same way as those in the original XY model: instead of interpreting the $\ell_i(\mathbf{x})$ fields as vortex lines of the XY model, we remember their original meaning, namely, that of the closed "magnetic field lines" of the auxiliary XY model [remember that we had called them $\bar b_i(\mathbf{x})$ in (12.3) before changing the notation to $\ell_i(\mathbf{x})$ in (12.6) for the purpose of calling them vortex lines]. Therefore, it is quite easy to find the vortex lines of the auxiliary XY model. All we have to do is follow the procedure after Eq. (6.5) or (8.3) and express $\ell_i = \bar b_i$ in terms of an auxiliary integer-valued vector potential $\bar a_i(\mathbf{x})$, in the gauge $\bar a_3(\mathbf{x}) = 0$, writing

$$\ell_i(\mathbf{x}) = \bar b_i(\mathbf{x}) = (\bar\nabla \times \bar a)_i(\mathbf{x}) = \varepsilon_{ijk}\bar\nabla_j \bar a_k(\mathbf{x} - \mathbf{k}). \tag{13.9}$$

Notice that $\bar a_i(\mathbf{x})$ is the "stress gauge field" of the auxiliary XY model while being the "vortex gauge field" of the lattice superconductor.

The introduction of $\bar a_i(\mathbf{x})$ brings the lattice superconductor (13.4) to the form

$$Z_{LS} = \det(-\bar\nabla \cdot \nabla)^{1/2}\prod_{\mathbf{x}}\left[\int_{-\infty}^{\infty} dA_1(\mathbf{x})\,dA_2(\mathbf{x})\right] e^{-(1/2)\Sigma_\mathbf{x}(\bar\nabla \times \mathbf{A})^2} I_0(\bar\beta)^{3N}$$

$$\times \sum_{\{\bar a_i(\mathbf{x})\}} \delta_{\bar a_3,0}\, e^{-(1/2\bar\beta_V)\Sigma_\mathbf{x}(\bar\nabla \times \bar a)^2 + iq\Sigma_\mathbf{x}(\bar\nabla \times \bar a)\cdot\mathbf{A}}. \tag{13.10}$$

It is here where the vortex lines of the superconductor are introduced as sources thereby permitting us to make the auxiliary gauge field $\bar a_i(\mathbf{x})$ continuous, i.e., we write, in analogy with (6.41),

$$\sum_{\bar{a}_i(\mathbf{x})} \delta_{\bar{a}_3, 0} = \int_{-\infty}^{\infty} d\bar{A}_1(\mathbf{x}) \, d\bar{A}_2(\mathbf{x}) \sum_{\{\bar{\ell}_i(\mathbf{x})\}} \delta_{\bar{\nabla}_i \bar{\ell}_i, 0} \, e^{2\pi i \Sigma_{\mathbf{x}} \bar{\ell}_i(\mathbf{x}) \bar{A}_i(\mathbf{x})}. \tag{13.11}$$

The closed non-backtracking integer lines $\bar{\ell}_i(\mathbf{x})$ are the *vortex lines of the lattice superconductor*. With these, the partition function (13.10) becomes

$$Z_{LS} = \det(-\bar{\nabla} \cdot \nabla)^{1/2} I_0(\widetilde{\beta})^{3N} \prod_{\mathbf{x}} \left[\int_{-\infty}^{\infty} dA_1(\mathbf{x}) \, dA_2(\mathbf{x}) \int_{-\infty}^{\infty} d\bar{A}_1(\mathbf{x}) \, d\bar{A}_2(\mathbf{x}) \right]$$

$$\times \sum_{\{\bar{\ell}_i(\mathbf{x})\}} \delta_{\bar{\nabla}_i \bar{\ell}_i, 0} \exp\left\{ -\frac{1}{2} \sum_{\mathbf{x}} (\bar{\nabla} \times \mathbf{A})^2 + iq \sum_{\mathbf{x}} (\bar{\nabla} \times \bar{\mathbf{A}}) \cdot \mathbf{A} \right.$$

$$\left. -\frac{1}{2\widetilde{\beta}_V} \sum_{\mathbf{x}} (\bar{\nabla} \times \bar{\mathbf{A}})^2 + 2\pi i \sum_{\mathbf{x}} \bar{\ell}_i(\mathbf{x}) \bar{A}_i(\mathbf{x}) \right\}. \tag{13.12}$$

Now, in this expression, the A_i field is coupled just as in (6.38) except that $2\pi\ell_i(\mathbf{x})$ is replaced by $q(\bar{\nabla} \times \bar{\mathbf{A}})$. It can therefore be integrated out in the same way as was done there with the result

$$\det(-\bar{\nabla} \cdot \nabla)^{-1/2} e^{-(q^2/2)\Sigma_{\mathbf{x},\mathbf{x}'} (\bar{\nabla} \times \bar{\mathbf{A}})(\mathbf{x}) v(\mathbf{x} - \mathbf{x}') \cdot (\bar{\nabla} \times \bar{\mathbf{A}})(\mathbf{x}')}. \tag{13.13}$$

Hence the partition function (13.12) becomes

$$Z_{LS} = I_0(\widetilde{\beta})^{3N} \prod_{\mathbf{x}} \left[\int_{-\infty}^{\infty} d\bar{A}_1(\mathbf{x}) \, d\bar{A}_2(\mathbf{x}) \right] e^{-(1/2\widetilde{\beta}_V)\Sigma_{\mathbf{x}}[(\bar{\nabla} \times \bar{\mathbf{A}})^2 + q^2 \widetilde{\beta}_V (\bar{\nabla} \times \bar{\mathbf{A}})(-\bar{\nabla} \cdot \nabla)^{-1} \cdot (\bar{\nabla} \times \bar{\mathbf{A}})]}$$

$$\times \sum_{\{\bar{\ell}_i(\mathbf{x})\}} \delta_{\bar{\nabla}_i \bar{\ell}_i, 0} \, e^{-2\pi i \Sigma \bar{\ell}_i(\mathbf{x}) \bar{A}_i(\mathbf{x})}. \tag{13.14}$$

For $q = 0$ this is the same as the vortex-line representation (12.6), as it should (apart from the wiggles), since then the lattice superconductor coincides with an *XY* model.

Let us now study the properties of (13.14) for $q \neq 0$. In order to see best what happens, it is useful to take advantage of the gauge invariance

$$\bar{A}_i(\mathbf{x}) \rightarrow \bar{A}_i(\mathbf{x}) + \nabla_i \bar{\Lambda}(\mathbf{x}) \tag{13.15}$$

of the partition function and change the gauge-fixing functional from

$$\Phi[\widetilde{\mathbf{A}}] = \prod_{\mathbf{x}} \delta(\widetilde{A}_3) \tag{13.16}$$

as it is in (13.14) [compare (6.64) and (6.75)] to

$$\Phi[\widetilde{\mathbf{A}}] = \det(-\bar{\nabla} \cdot \nabla) \prod_{\mathbf{x}} \delta(\bar{\nabla}_i \widetilde{A}_i). \tag{13.17}$$

Since both satisfy (6.55), this cannot change the integral. The advantage is that, in this gauge, the second term in (13.14) becomes a simple mass term

$$\sum_{\mathbf{x}} (\nabla \times \widetilde{\mathbf{A}}) \cdot (-\bar{\nabla} \cdot \nabla)^{-1} (\nabla \times \widetilde{\mathbf{A}})$$

$$= \sum_{\mathbf{x}} (\bar{\nabla}_k \widetilde{A}_\ell (-\bar{\nabla} \cdot \nabla)^{-1} \bar{\nabla}_k \widetilde{A}_\ell - \bar{\nabla}_k \widetilde{A}_k (-\bar{\nabla} \cdot \nabla)^{-1} \bar{\nabla}_\ell \widetilde{A}_\ell)$$

$$= \sum_{\mathbf{x}} \bar{\nabla}_k \widetilde{A}_\ell (-\bar{\nabla} \cdot \nabla)^{-1} \bar{\nabla}_k \widetilde{A}_\ell$$

$$= -\sum_{\mathbf{x}} \widetilde{A}_\ell (-\bar{\nabla} \cdot \nabla)^{-1} \nabla_k \bar{\nabla}_k \widetilde{A}_\ell = \sum_{\mathbf{x}} \widetilde{A}_\ell^2(\mathbf{x}).$$

Similarly, the gradient term becomes $(\bar{\nabla} \times \widetilde{\mathbf{A}})^2 = \Sigma_{i,j}(\bar{\nabla}_i \widetilde{A}_j)^2$ so that the energy of the $\widetilde{\mathbf{A}}$ field is simply

$$\frac{1}{2\widetilde{\beta}_V} \sum_{\mathbf{x}} [(\nabla_i \widetilde{A}_j)^2 + m_A^2 \widetilde{A}_i^2] = \frac{1}{2\widetilde{\beta}_V} \sum_{\mathbf{k}} \widetilde{A}_i^\dagger(\mathbf{k})(\bar{K}_i K_i + m_A^2) \widetilde{A}_i(\mathbf{k}) \tag{13.18}$$

with a mass

$$m_A^2 \equiv q^2 \widetilde{\beta}_V = 4\pi^2 \beta_V \widetilde{\beta}_V. \tag{13.19}$$

Hence we see that the vortex-line representation of the lattice superconductor differs from that of the XY model only in that the vector potential has a short range

$$\lambda = \frac{1}{m_{\widetilde{A}}} = \frac{1}{\sqrt{q^2 \widetilde{\beta}_V}}. \tag{13.20}$$

This is, of course, the lattice superconductor's version of the Meissner effect. The fluctuations of the $\bar{A}_i$ field can be integrated out just as in (6.73)[a] with the result

$$Z_{LS} = I_0(\bar{\beta})^{3N}(\sqrt{2\pi\bar{\beta}_V})^{2N}\det(-\bar{\nabla}_i\nabla_i)^{1/2}\det(-\bar{\nabla}_i\nabla_i + m_A^2)^{-1}$$

$$\times \sum_{\{\bar{\ell}_i(\mathbf{x})\}} \delta_{\nabla_i\tilde{\ell}_i,0}\, e^{-\bar{\beta}_V(4\pi^2/2)\Sigma_{\mathbf{x},\mathbf{x}'}\bar{\ell}_i(\mathbf{x})v_{m_{\bar{A}}}(\mathbf{x}-\mathbf{x}')\bar{\ell}_i(\mathbf{x}')}, \qquad (13.21)$$

where

$$v_m(\mathbf{x}) = \frac{1}{N}\sum_{\mathbf{k}} e^{i\mathbf{k}\cdot\mathbf{x}}\frac{1}{\overline{K}_iK_i + m^2} \qquad (13.22)$$

is the Yukawa potential on the lattice for the screened vector potential. The partition functions (13.14) and (13.21) are the desired vortex-line representations of the lattice superconductor. For $q = 0$, they reduce to those of the XY model [see (7.25), (7.26)].

13.3. DISORDER FIELD THEORY OF VORTEX LINES IN LATTICE SUPERCONDUCTORS

We are now prepared to convert the sum over closed non-backtracking vortex lines in (13.14) into a disorder field theory of the lattice superconductor. For this it is useful to separate out again a natural core energy by splitting the Yukawa potential as follows

$$v_m(\mathbf{x}) = v_m(\mathbf{0})\,\delta_{\mathbf{x},0} + v'(\mathbf{x}). \qquad (13.23)$$

Then (13.14) can be rewritten as

[a]The inverse of the matrix between $A_i^\dagger(\mathbf{k})$ and $A_j(\mathbf{k})$ is now

$$\left[(\overline{K}\cdot K + m_A^2)\,\delta_{ij} + \frac{1}{\varepsilon}\overline{K}\cdot\overline{K}\cdot\frac{K_iK_j}{\overline{K}\cdot K}\right]^{-1}$$

$$= \left[(\overline{K}\cdot K + m_A^2)\left(\delta_{ij} - \frac{K_i\overline{K}_j}{\overline{K}\cdot K}\right) + \left(\overline{K}\cdot K + m_A^2 + \frac{1}{\varepsilon}\overline{K}\cdot K\right)\frac{K_i\overline{K}_j}{\overline{K}\cdot K}\right]^{-1}$$

$$= \frac{1}{\overline{K}\cdot K + m_A^2}\left(\delta_{ij} - \frac{K_i\overline{K}_j}{\overline{K}\cdot K}\right) + \frac{\varepsilon}{\overline{K}\cdot K}\frac{K_i\overline{K}_j}{\overline{K}\cdot K}\right]$$

which produces $\det(-\bar{\nabla}\cdot\nabla)^{-1/2}\cdot\det(-\bar{\nabla}\cdot\nabla + m_A^2)^{-1}$ and leads to (13.21), by current conservation.

$$Z_{LS} = I_0(\bar{\beta})^{3N} \det(-\bar{\nabla}_i \nabla_i) \det(v_{m_A^-}/v'_{m_A^-})$$

$$\times \prod_{\mathbf{x},i} \left[\int_{-\infty}^{\infty} d\bar{A}_i(\mathbf{x}) \right] \delta(\bar{\nabla}_i \bar{A}_i) \, e^{-(1/2\bar{\beta}_V)\Sigma_{\mathbf{x},\mathbf{x}'} \bar{A}_i(\mathbf{x}) v'^{-1}_{m_A^-}(\mathbf{x},\,\mathbf{x}') \bar{A}_i(\mathbf{x}')}$$

$$\times \sum_{\{\bar{\ell}_i(\mathbf{x})\}} \delta_{\bar{\nabla}_i \bar{\ell}_i, 0} \, e^{-(1/2)4\pi^2 \bar{\beta}_V \, v_{m_A^-}(0)\Sigma_{\mathbf{x}} \bar{\ell}_i^2(\mathbf{x}) \, + \, 2\pi i \Sigma_{\mathbf{x}} \bar{\ell}_i(\mathbf{x}) \bar{A}_i(\mathbf{x})}, \tag{13.24}$$

where

$$v'^{-1}_{m_A^-}(\mathbf{x},\,\mathbf{x}') = \frac{1}{N} \sum_{\mathbf{k}} e^{i\mathbf{k}\cdot(\mathbf{x}-\mathbf{x}')}(\bar{K}_i K_i + m_A^2)/[1 - v_{m_A^-}(0)(\bar{K}_i K_i + m_A^2)]. \tag{13.25}$$

Let us denote the core energy by $(1/2\beta'_V)\Sigma \bar{\ell}_i^2$, i.e.,

$$\beta'_V \equiv \frac{1}{4\pi^2 \bar{\beta}_V v_{m_A^-}(0)}. \tag{13.26}$$

The sum over closed $\bar{\ell}_i(\mathbf{x})$ lines can be re-expressed (after a Villain approximation) in the form

$$\sum_{\{\bar{\ell}(\mathbf{x})\}} \delta_{\bar{\nabla}_i \bar{\ell}_i, 0} \, e^{-(1/2\beta'_V)\Sigma_{\mathbf{x}} \bar{\ell}_i^2(\mathbf{x})} = (I_0(\beta'))^{-3N} \prod_{\mathbf{x}} \left[\int_{-\pi}^{\pi} \frac{d\gamma'}{2\pi} \right] e^{\beta' \Sigma_{\mathbf{x},i} \cos \nabla_i \gamma'}, \tag{13.27}$$

where β' is related to β'_V of (6.25) in the usual way $[\beta'^{-1}_V = (-2\log(I_1(\beta')/I_0(\beta')))]$ This brings Z_{LS} to the following form,

$$Z_{LS} = \left(\frac{I_0(\bar{\beta})}{I_0(\beta')} \right)^{3N} \det(-\bar{\nabla}_i \nabla_i) \det(v_{m_A^-}/v'_{m_A^-}) \prod_{\mathbf{x},i} \int_{-\infty}^{\infty} d\bar{A}_i(\mathbf{x}) \, \delta(\bar{\nabla}_i \bar{A}_i)$$

$$\times e^{-(1/2\bar{\beta}_V)\Sigma_{\mathbf{x},\mathbf{x}'} \bar{A}_i(\mathbf{x}) v'^{-1}_{m_A^-}(\mathbf{x},\,\mathbf{x}') \bar{A}_i(\mathbf{x}')} \prod_{\mathbf{x}} \left[\int_{-\pi}^{\pi} \frac{d\gamma'}{2\pi} \right] e^{\beta' \Sigma_{\mathbf{x},i} \cos(\nabla_i \gamma' - 2\pi \bar{A}_i)}. \tag{13.28}$$

This looks again like a lattice superconductor except that the vector potential is now screened.

The γ' integrals can now be transformed to a complex disorder field theory

$$\prod_{\mathbf{x}} \left[\int \frac{d\gamma'}{2\pi} \right] e^{\beta' \Sigma_{\mathbf{x},i} \cos(\nabla_i \gamma' - 2\pi \bar{A}_i)} = \prod_{\mathbf{x}} \left[\int \frac{d\psi \, d\psi^\dagger}{4\pi\beta'} \right] e^{-(1/4\beta' D)\Sigma_{\mathbf{x}} |\psi(\mathbf{x})|^2 \, + \, \Sigma_{\mathbf{x}} \log I_0(|\psi|)},$$

$$\tag{13.29a}$$

where

$$\widehat{\psi}(\mathbf{x}) \equiv \sqrt{1 + \frac{\overline{\overline{D}}_i \overline{D}_i}{2D}}\, \psi(\mathbf{x}).$$

with the obvious notation

$$\overline{D}\psi(\mathbf{x}) = \psi(\mathbf{x} + \mathbf{i})\, e^{-2\pi i \overline{A}(\mathbf{x} + \mathbf{i})} - \psi(\mathbf{x}).$$

Sometimes, the two-field version will be more useful and we shall write, instead of (13.28),

$$\prod_{\mathbf{x}} \left[\int \frac{d\gamma'}{2\pi} \right] e^{\beta' \Sigma_{\mathbf{x},i} \cos(\nabla_i \gamma' - 2\pi A_i)}$$

$$= \prod_{\mathbf{x}} \left[\int_{-\infty}^{\infty} \frac{d\alpha_1\, d\alpha_2}{(2\pi i)^2} \int_{-\infty}^{\infty} d\tilde{u}_1\, d\tilde{u}_2 \right] e^{D\beta'\, \Sigma_{\mathbf{x}} \tilde{u}^\dagger (1 + (\overline{\overline{D}}_i \overline{D}_i / 2D)) \tilde{u} - (1/2)\Sigma_{\mathbf{x}}(\alpha^\dagger \tilde{u} + \text{c.c.}) + \Sigma_{\mathbf{x}} \log I_0(|\alpha|)}.$$

$$(13.29b)$$

For a constant $\tilde{u}$ field, the vector potential in the covariant derivatives [see (12.17)] appears as follows:

$$\sum_{\mathbf{x}} \tilde{u}^\dagger \left(1 + \frac{\overline{\overline{D}}_i \overline{D}_i}{2D} \right) \tilde{u} = \sum_{\mathbf{x}} |\tilde{u}|^2 \left(1 + \frac{1}{D} \sum_i (\cos 2\pi \overline{A}_i - 1) \right)$$

$$= \sum_{\mathbf{x}} |\tilde{u}|^2 \left(1 - \frac{4\pi^2}{2D} \mathbf{A}^2 + \ldots \right).$$

In either case, the disorder field theory has a Landau expansion

$$-\overline{\beta}E = -\frac{1}{2\overline{\beta}_V} \sum_{\mathbf{x},i} \overline{A}_i(\mathbf{x}) v_{m_A}^{-1}(\mathbf{x}, \mathbf{x}') \overline{A}_i(\mathbf{x}')$$

$$- \sum_{\mathbf{x}} \left\{ \frac{1}{8D} |\overline{D}_i \psi|^2 - \frac{1}{4}\left(\frac{1}{\beta' D} - 1 \right)|\psi|^2 - \frac{1}{64}|\psi|^4 - \ldots \right\}, \qquad (13.30)$$

where $\overline{D}_i \psi(\mathbf{x}) \approx (\partial_i - 2\pi i \overline{A}_i) \psi(\mathbf{x})$. Recall that β' is related to $\overline{\beta}_V$ via β'_V of Eq. (13.26) and that $v_{m_A}(0)$ contains the second parameter of the model, β, via $m_A^2 = 4\pi \beta_V \overline{\beta}_V$ of Eq. (13.19).

13.4. LIMITING CASES

In order to understand the physical content of the disorder version of the lattice superconductor (13.24) or its field theoretic versions (13.29), it is useful to look at a few particularly simple limiting cases.

First, there is a trivial case, namely $q = 0$, in which the lattice superconductor is really an XY model. Inserting $q = 0$ into (13.28), the potentials $v_{m_{\tilde{A}}}$ and $v'_{m_{\tilde{A}}}$ become $(-\bar{\nabla} \cdot \nabla)^{-1}$ and $v'(\mathbf{x})$, respectively; the parameter β'_V becomes

$$\beta'_V \rightarrow (4\pi^2 \bar{\beta}_V v(0))^{-1} \tag{13.31}$$

and Z_{LS} reduces to

$$Z_{LS}^{q=0} = \left(\frac{I_0(\tilde{\beta})}{I_0(\beta')}\right)^{3N} (\det v')^{-1} \prod_{\mathbf{x},i} \left[\int_{-\infty}^{\infty} d\tilde{A}_i(\mathbf{x}) \right] \delta(\bar{\nabla}_i \tilde{A}_i) e^{-(1/2\bar{\beta}_V)(\nabla' \times \tilde{A})^2}$$

$$\times \prod_{\mathbf{x}} \left[\int_{-\pi}^{\pi} \frac{d\gamma'}{2\pi} \right] e^{\beta' \cos(\nabla_i \gamma' - 2\pi \tilde{A}_i)}. \tag{13.32}$$

If we replace $\tilde{\beta}$ by β and β' by $\tilde{\beta}$ this is precisely the lattice superconductor which was found in (12.39) as a disorder version of the XY model,

$$(\det v')^{-1} \prod_{\mathbf{x},i} \left[\int d\tilde{A}_i \right] \delta(\bar{\nabla}_i \tilde{A}_i)$$

$$= \det(1 + v(0) \bar{\nabla}_i \nabla_i)^{-1} \det(-\bar{\nabla}_i \nabla_i) \prod_{\mathbf{x},i} \left[\int d\tilde{A}_i \right] \delta(\bar{\nabla}_i \tilde{A}_i)$$

$$= \det(1 + v(0) \bar{\nabla}_i \nabla_i)^{-1} \prod_{\mathbf{x}} \left[\int d\tilde{A}_1(\mathbf{x}) d\tilde{A}_2(\mathbf{x}) \right]. \tag{13.33}$$

The replacement $\tilde{\beta} \rightarrow \beta$, $\beta' \rightarrow \tilde{\beta}$ is necessary since the roles of order and disorder of the two theories are reversed.

A more interesting case is obtained in the limit $\tilde{\beta} \rightarrow \infty$. There the potential $v_{m_{\tilde{A}}}$ becomes local,

$$v_{m_{\tilde{A}}}(\mathbf{x}) \rightarrow \frac{1}{m_{\tilde{A}}^2} \delta_{x,0} = \frac{1}{q^2 \bar{\beta}_V} \delta_{x,0} \rightarrow 0. \tag{13.34}$$

Therefore, the subtracted potential

$$v'_m(\mathbf{x}) = \frac{1}{N} \sum_{\mathbf{k}} e^{i\mathbf{k}\cdot\mathbf{x}} \left(\frac{1}{\overline{K_\ell K_\ell} + m^2} - \frac{1}{N} \sum_{\mathbf{k}} \frac{1}{\overline{K_\ell K_\ell} + m^2} \right) \qquad (13.35)$$

vanishes identically. The $\overline{A}_i$ integral can be performed with the result

$$(\det v'_{m_{\overline{A}}})^{-1} \prod_{\mathbf{x},i} \left[\int d\overline{A}_i(\mathbf{x}) \right] \delta(\overline{\nabla}_i \overline{A}_i) \, e^{-(1/2\widetilde{\beta}_V)\Sigma_{\mathbf{x},\mathbf{x}'} \overline{A}_i(\mathbf{x}) v'_{m_{\overline{A}}}(\mathbf{x}, \mathbf{x}')^{-1} \overline{A}_i(\mathbf{x}')}$$

$$= \det(-\overline{\nabla}\cdot\nabla)^{-1/2} \sqrt{2\pi\widetilde{\beta}_V}^{2N}, \qquad (13.36)$$

such that Z_{LS} becomes an XY model, up to a factor:

$$Z_{LS} \xrightarrow[\widetilde{\beta}_V \to \infty]{} \left(\frac{I_0(\widetilde{\beta})}{I_0(\beta')} \right)^{3N} (\sqrt{2\pi\widetilde{\beta}_V})^{2N} \left(\frac{1}{q^2\widetilde{\beta}_V} \right)^N \det(-\overline{\nabla}_i\nabla_i)^{1/2}$$

$$\times \prod_{\mathbf{x}} \left[\int_{-\pi}^{\pi} \frac{d\gamma'(\mathbf{x})}{2\pi} \right] e^{\beta' \Sigma_{\mathbf{x},i} \cos \nabla_i \gamma'}. \qquad (13.37)$$

Since $q = 2\pi\sqrt{\beta_V}$, $(\sqrt{2\pi\widetilde{\beta}_V})^{2N}(1/q^2\widetilde{\beta}_V)^N = 1/\sqrt{\beta_V}^{2N} = (q/2\pi)^{-2N}$, we see that the XY model coincides with the XY model we started out with. In fact, looking at (13.26) we see that in the limit $\widetilde{\beta}_V \to \infty$,

$$\beta'_V \to \frac{1}{4\pi^2\widetilde{\beta}_V \dfrac{1}{q^2\widetilde{\beta}_V}} = \frac{q^2}{4\pi^2} \qquad (13.38)$$

so that β'_V is indeed the same as β_V in (13.2).

Thus we have the following remarkable situation: according to Section 12.1–12.5 there exists a disorder field theory of the XY model which is the theory of its vortex lines with long range interactions. It is of the Ginzburg-Landau type with the complex field representing the vortex lines and the vector potential the long-range forces between the lines. This Ginzburg-Landau disorder theory has vortex lines of its own. They have only short-range interactions due to the Meissner effect. We have set up a further disorder theory for these vortex lines of the disorder theory. This disorder theory turns out to coincide with the *original XY model* and its complex *order* field theory. Thus there is no intrinsic meaning to the concept of disorder field. It is a relative concept. From the point of view of the order field theory of the XY model, the Ginzburg-Landau theory is a disorder theory, and vice versa. Such theories will be

called *dual* to each other and the transition from one to the other will be called a *duality transformation*.

Recall that the disorder theory of the XY model (12.22) was derived for a specific Ginzburg-Landau theory which is associated with the lattice superconductor (13.1) at $\bar{\beta} = \infty$. The general Ginzburg-Landau theory is characterized by a field energy (13.7) or, after removing core energies, by

$$\bar{\beta}'E' = \sum_x \left\{ \frac{1}{8D}|D_i\varphi|^2 + \frac{1}{4}\left(\frac{1}{\bar{\beta}'D} - 1\right)|\varphi|^2 + \frac{1}{64}|\varphi|^4 + \ldots + \frac{1}{2}(\nabla' \times \mathbf{A})^2 \right\}.$$

(13.39)

The XY model corresponds to the limit $\bar{\beta} \to \infty$ for which $1/\beta' \to q^2 v(0)$, [see (13.6)]. In Section 12.5 we showed that at the mean field level, the Ginzburg-Landau theory (13.39) is characterized by a ratio of the two length scales [see (12.50), (12.51)],

$$\kappa = \frac{\lambda}{\sqrt{2}\,\xi_{size}} = \frac{D}{2\pi\sqrt{\beta_V}} = \frac{D}{q}.$$

(13.40)

For $\bar{\beta} = \infty$ we know from the XY model that the transition occurs at $\beta_V \sim 0.33$ so that $q^2 = 4\pi^2\beta_V = 13.03$ and

$$\kappa \sim 1.18/\sqrt{2} > \frac{1}{\sqrt{2}},$$

(13.41)
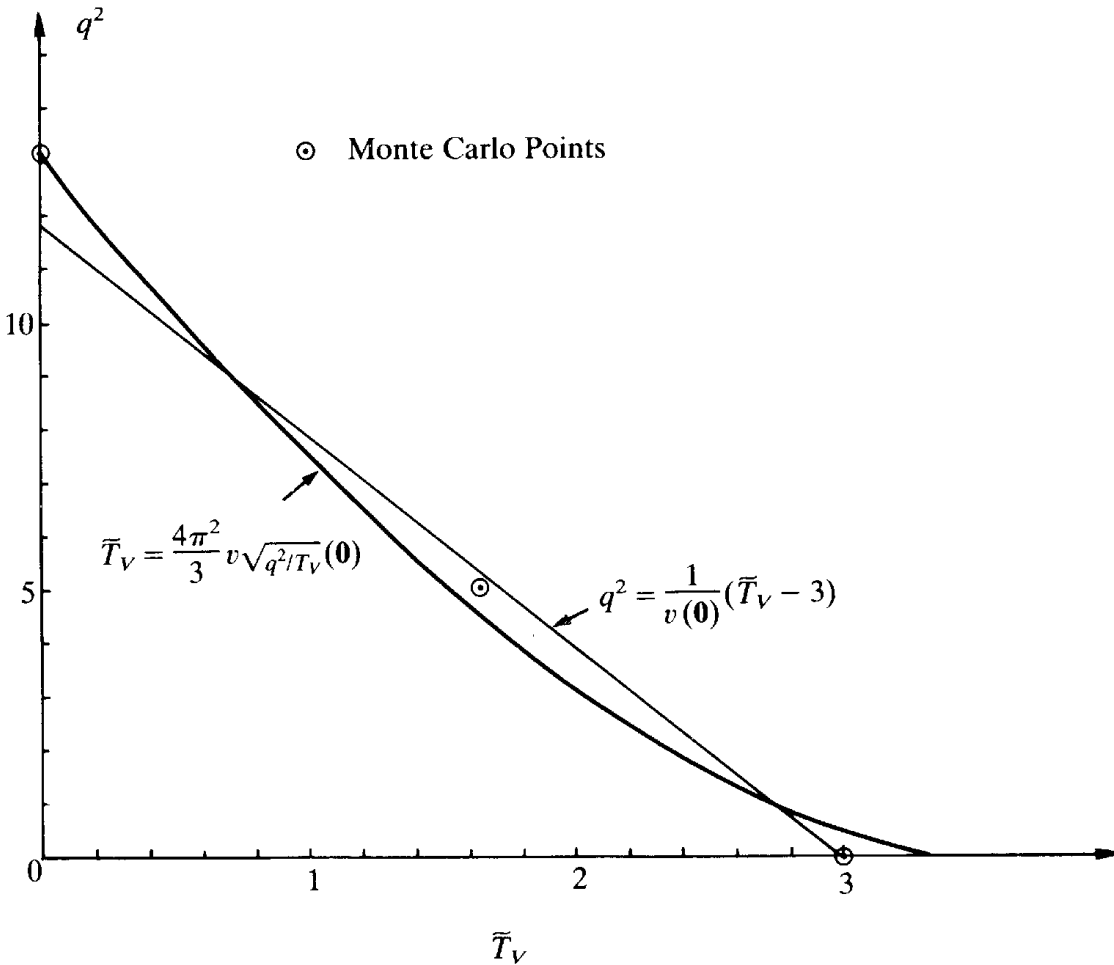
which made the XY model dually equivalent to a Ginzburg-Landau theory of type II with a specific charge $q \approx 3.61$ and a specific parameter $\kappa = 1.18/\sqrt{2}$.

The field energy (13.39) puts us in a position to study the phase transition of the general lattice superconductors (13.1) via its disorder theory (13.28), (13.30), that is, an XY model coupled to a *massive* vector meson $\bar{A}_i$. This is a great advantage. The problems encountered with loop calculations of the Ginzburg-Landau theory in Section 3.11 were all due to the masslessness of the vector potential A_i: this was what made the quantity

$$\text{tr}\log(-\nabla^2 + q^2|\psi|^2)$$

(13.42a)

in (3.104) so sensitive to the zeroes of ψ. This quantity was responsible for the decisive cubic term in $|\psi|$. In the presence of a mass term

FIG. 13.1. Phase boundaries of the lattice superconductor (LSC), Eq. (13.1): The thin straight line is from the mean field approximation to (13.39). The fact vurve is from the mean field approximation to the disorder field theory (13.30) of the LSC [from Kleinert (1982)]. The Monte Carlo points are from Dasgupta and Halperin (1981).

$(-\nabla^2 \rightarrow -\nabla^2 + m^2)$, this sensitivity disappears and a trace log of the form

$$\text{tr} \log(-\nabla^2 + m^2 + q^2|\psi|^2) \qquad (13.42b)$$

can be easily expanded in powers of $|\psi|^2$. This feature will be explored to argue that there exists a tricritical length ratio κ in the Ginzburg-Landau theory and to estimate is value.

13.5. PHASE TRANSITIONS IN LATTICE SUPERCONDUCTORS

Let us now study the general lattice superconductor (13.1) which, according to (13.39) corresponds to a Ginzburg-Landau energy

$$\overline{\beta'}E' = \frac{1}{2}(\nabla' \times \mathbf{A})^2 + \frac{1}{8D}|D_i\varphi|^2 + \frac{1}{4}\left(\frac{1}{\overline{\beta'}D} - 1\right)|\varphi|^2 + \frac{1}{64}|\varphi|^4 + \ldots, \quad (13.43)$$

with $D_i\varphi(\mathbf{x}) = \varphi(\mathbf{x} + \mathbf{i})e^{-iqA_i(\mathbf{x})} - \varphi(\mathbf{x})$. The mass term changes sign at

$\tilde{\beta}'_c = 1/D$ such that, at the mean field level, Eq. (13.6) yields a line of second order phase transitions in the $\bar{T}_V$, q^2 plane described by $\bar{T}_V = (\beta'_{cV})^{-1} - q^2 v(0)$, where β'_{cV} is shorthand for $-2\log(I_0(\tilde{\beta}'_c)/I_1(1/D))$ [see (7.11b)]. Fluctuations in the φ field change $\tilde{\beta}'$ to 1/2.2 [see Fig. 4.4]. This corresponds to $\tilde{\beta}'_{cV} \approx 1/3$ (see Fig. 7.1) so that the line is shifted to

$$\bar{T}_V \approx 3 - q^2 v(0). \tag{13.44}$$

This is true as long as A_i fluctuations are negligible, which is the case for small q. Indeed, at $q = 0$ it gives the correct transition temperature $\bar{T}_V = 3$ of the XY model (see Fig. 7.1).

For increasing q, the critical temperature decreases due to the destructive influence of the A_i fluctuations upon the order of the XY model. There exists a critical q_c, where order is completely destroyed even at zero temperature $\bar{T}_V$. According to (13.44) this happens at

$$q_c^2 = \frac{3}{v(0)} = \frac{3}{0.2527} \approx 11.87. \tag{13.45}$$

The characteristic ratio $\kappa = \lambda/\sqrt{2}\,\xi_{\text{size}}$ which defines the type of the superconductor (13.43),

$$\kappa = \frac{D}{q} = \frac{3}{q}, \tag{13.46}$$

ranges from $\kappa = 1.23/\sqrt{2}$ at $q^2 = 11.87$ to $\kappa \to \infty$ for $q^2 = 0$. Hence the Ginzburg-Landau theory (13.43) covers a large portion of the type-II regime. For the whole regime, the Ginzburg-Landau theory possesses a disorder field theory of its vortex lines whose partition function is given by the modified XY model (13.28) or its field formulation (13.25)–(13.30).

Let us examine the phase transition within this disorder formulation. For $\bar{T} = 0$, we already saw that (13.28) reduces to a pure XY model, i.e., (13.30) to a pure $|\psi|^4$ field theory. Its phase transition lies at $\beta' = 1/D$ in the mean field approximation and at $\beta' \sim 1/2.2$ after including fluctuation corrections [see once more Fig. 4.4]. This corresponds to $\beta'_V \sim 3$. By (13.38), this gives the phase transition at the proper value $q^2 = 4\pi^2\beta'_V = 13.16$. The discrepancy with the approximation (13.45) is about 13%. In fact, this discrepancy is astonishingly small. When calculating the phase transition line of the lattice superconduction (13.43) we included only $\varphi(\mathbf{x})$ field fluctuations but neglected $A_i(\mathbf{x})$ fluctuations. These are

expected to lower the reliability of (13.44) for increasing q. Thus we are lucky to find that even at the point of largest $q^2 \sim 13.16$, the error is not larger than 13%.

Let us now see where the disorder field theory predicts the phase transition of the lattice superconductor for $\bar{T}_V > 0$ should lie. In this case, its disorder theory (13.28) is no longer a pure XY model but is modified by $\bar{A}_i(\mathbf{x})$ fluctuations which increase with $\bar{T}_V$. For small $\bar{T}_V$, we can use the harmonic approximation and expand the disorder field $\hat{\psi}$ in (13.29a) as

$$\hat{\psi}(\mathbf{x}) = \psi - \frac{1}{2D} 4\pi^2 \bar{A}_i^2 \psi + \ldots, \tag{13.47}$$

so that

$$\log I_0(|\hat{\psi}|) \sim \log I_0(|\psi|) - \frac{I_1(|\psi|)}{I_0(|\psi|)} |\psi| \frac{4\pi^2}{4D} A_i^2. \tag{13.48}$$

Thus the combined gauge field action, quadratic in $\bar{A}_i$, may be cast as

$$-\frac{1}{2\bar{\beta}_V} \sum_{\mathbf{x},\mathbf{x}'} \bar{A}_i(\mathbf{x}) \left(v'_{m_{\bar{A}}}(\mathbf{x}, \mathbf{x}')^{-1} + \frac{I_1(|\psi|)}{I_0(|\psi|)} |\psi| \frac{4\pi^2 \bar{\beta}_V}{2D} \delta_{\mathbf{x},\mathbf{x}'} \right) \bar{A}_i(\mathbf{x}'), \tag{13.49}$$

where we recall that

$$v'_{m_{\bar{A}}}(\mathbf{k})^{-1} \equiv \frac{\bar{K}_\ell K_\ell + m_{\bar{A}}^2}{1 - v_{m_{\bar{A}}}(0)(\bar{K}_\ell K_\ell + m_{\bar{A}}^2)}, \qquad v_{m_A}(0) \equiv \frac{1}{N} \sum_{\mathbf{k}} \frac{1}{\bar{K}_\ell K_\ell + m^2}. \tag{13.50}$$

Let us denote the quantity $(I_1(|\psi|)/I_0(|\psi|))|\psi|(4\pi^2\bar{\beta}_V/2D)$ by μ^2. Then we can perform the A integral as follows:

$$\det(1/v'_{m_{\bar{A}}}) \prod_{\mathbf{x},i} \left[\int d\bar{A}_i(\mathbf{x}) \right] \delta(\bar{\nabla}_i \bar{A}_i) \, e^{-(1/2\bar{\beta}_V)\Sigma_{\mathbf{x},\mathbf{x}'} \bar{A}_i(\mathbf{x})(v'^{-1}_{m_{\bar{A}}} + \mu^2 \delta_{\mathbf{x},\mathbf{x}'})\bar{A}_i(\mathbf{x}')}$$

$$= (\sqrt{2\pi\bar{\beta}_V})^{2N} e^{-\Sigma_{\mathbf{k}}\log(1 + v'_{m_{\bar{A}}}(\mathbf{k})\mu^2)}. \tag{13.51}$$

In this way, the disorder field theory has become a theory of a simple complex ψ field.

In the neighborhood of the critical point, $|\psi|$ is small so that the logarithm can be expanded in powers of μ^2. The lowest order term vanishes since $\Sigma_{\mathbf{k}} v'_{m_{\bar{A}}}(\mathbf{k}) = v'_{m_{\bar{A}}}(0) = 0$, by construction. Hence the line of phase transition is given by

$$\beta_V' \approx 1/3 \approx \frac{1}{4\pi^2 \bar{\beta}_V v_{m_{\bar{A}}}(0)} \cdot \qquad (13.52)$$

Using the result of Chapter 6, Part I, this can be written as a power series (hopping series) in $1/(m_{\bar{A}}^2 + 2D)$:

$$\bar{T}_V \approx \frac{4\pi^2}{3} v_{m_{\bar{A}}}(0) = \frac{4\pi^2}{3} \int \frac{d^3k}{(2\pi)^3} \frac{1}{\bar{K}_\ell K_\ell + m_{\bar{A}}^2}$$

$$= \frac{4\pi^2}{3} \sum_{n=0,2,4,\ldots} \frac{H_n}{(m_{\bar{A}}^2 + 2D)^{n+1}} \cdot \qquad (13.53)$$

Remembering that [by (13.19)]

$$m_{\bar{A}}^2 = q^2/\bar{T}_V, \qquad (13.54)$$

this determines the phase transition line in the $\bar{T}_V$, q^2 plane as a function of the parameter $m_{\bar{A}}^2$.

The result is plotted in Fig. 13.1 and compared with (13.44) and Monte Carlo calculations. The agreement is perfect at $\bar{T} = 0$ and is expected to get worse for increasing $\bar{T}$ due to the neglected anharmonic A_i fluctuations. It is gratifying to note that at the Monte Carlo point $q^2 \approx 5$, $\bar{T}_V \sim 1.65$, the agreement is still quite good. Notice that this point is about equally far away from the end points $\bar{T}_V = 0$ and $\bar{T}_V = 3$ where the disorder and order formulations have pure XY model transitions, respectively, and one or the other of the two lines in Fig. 13.1 is more reliable. In fact, the distance of this point from either line is of the same order of magnitude. At $q = 0$, Eqs. (13.53), (13.54) gives $\bar{T}_V \approx (4\pi^2/3)v(0)$ ≈ 3.325 which differs from the true value $\bar{T}_V \sim 3$ only by $\sim 11\%$.

As far as the Monte Carlo points are concerned it should be mentioned that the partition function of the lattice superconductor (13.1) has not been studied as it stands but in the form

$$Z_{LS} = \det(-\bar{\nabla} \cdot \nabla)^{1/2} I_0(\bar{\beta})^{3N} \left[\left(\frac{q}{2\pi} \right)^N \sum_{\{\bar{a}(\mathbf{x})\}} e^{-(1/2\bar{\beta}_V)\Sigma_\mathbf{x}(\nabla \times \bar{a})^2} \right.$$

$$\times \prod_\mathbf{x} \left[\int_{-\pi}^{\pi} \frac{d\gamma(\mathbf{x})}{2\pi} \right] e^{-(1/2)(q^2/4\pi^2)\Sigma_\mathbf{x}(\nabla_i \gamma - 2\pi\bar{a}_i)^2} \right]. \qquad (13.55)$$

That this is identical to (13.1) can be proven through the following two steps.

(1) Instead of the sum over *all* $\bar{a}(x)$ we go over to the restricted sum with $\bar{a}_3 = 0$ but extend the range of the γ fields from $(-\pi, \pi)$ to $(-\infty, \infty)$. This does not produce any change since we can always write $\bar{a}_3(x) \equiv \nabla_3 n(x)$, with an integer field $n(x)$, and absorb $n(x)$ into $\gamma(x)$ such that $\gamma(x) + n(x)$ covers the entire real axis.

(2) We introduce the auxiliary field $b_i(x)$ and write the exponential as

$$\sum_{\{\bar{a}(x)\}} \delta_{\bar{a}_3, 0} \prod_{x}\left[\int_{-\infty}^{\infty} \frac{d\gamma}{2\pi}\right] \prod_{x,i}\left[\int_{-\infty}^{\infty} \frac{db_i(x)}{q/2\pi}\right] e^{-(4\pi^2/2q^2)\Sigma_x b_i^2(x) + i\Sigma_x b_i(\nabla_i\gamma - 2\pi\bar{a}_i) - (1/2\bar{\beta}_V)\Sigma_x(\nabla\times\bar{a})^2}.$$

$$(13.56)$$

The integrals $\int_{-\infty}^{\infty} d\gamma(x)/2\pi$ enforce $\bar{\nabla}_i b_i = 0$ and we arrive at

$$\sum_{\{\bar{a}(x)\}} \delta_{\bar{a}_3, 0} \prod_{x,i}\left[\int \frac{db_i(x)}{q/2\pi}\right] \delta(\bar{\nabla}_i b_i) e^{-(4\pi^2/2q^2)\Sigma_x b_i^2 - 2\pi i\Sigma_x b_i\bar{a}_i - (1/2\bar{\beta}_V)\Sigma_x(\nabla\times\bar{a})^2}.$$

$$(13.57)$$

On setting $b_i \equiv (\nabla \times A)_i$, with $A_3(x) \equiv 0$, this becomes

$$\sum_{\{a(x)\}} \delta_{\bar{a}_3, 0} \frac{1}{(1/2\pi)^N} \prod_{x}\left[\int_{-\infty}^{\infty} \frac{dA_1(x) dA_2(x)}{(q/2\pi)^2}\right]$$

$$\times e^{-(4\pi^2/2q^2)\Sigma_x(\bar{\nabla}\times A)^2 - 2\pi i\Sigma(\bar{\nabla}\times A)_i\bar{a}_i - (1/2\bar{\beta}_V)\Sigma_x(\nabla\times\bar{a})^2}, \qquad (13.58)$$

where we have integrated out $b_3(x)$ via the identity

$$\int db_3 \, \delta(\bar{\nabla}_i b_i) = (\det \bar{\nabla}_3)^{-1} = 1, \qquad (13.59)$$

and used the fact that in the gauge $A_3 = 0$,

$$b_1 = -\nabla_3 A_2, \qquad b_2 = \nabla_3 A_1. \qquad (13.60)$$

These lead to

$$\prod_{x} [db_1(x) db_2(x)] = \det \nabla_3^2 \prod_{x}\left[\int dA_1(x) \, dA_2(x)\right] = \prod_{x}\left[\int dA_1(x) \, dA_2(x)\right].$$

$$(13.61)$$

A change of the A_i field to $(q/2\pi)A_i$ establishes the equality of (13.61) with (13.10) which, in turn, is the same as (13.1) after a Villain approximation.

Let us now also look at the first nontrivial correction to the disorder field theory, obtained by expanding the loop integral (13.51) up to μ^4,

$$(\sqrt{2\pi\bar{\beta}_V})^{2N} e^{(N/2)\alpha_4\mu^4}, \tag{13.62}$$

where

$$\alpha_4 = \int \frac{d^3k}{(2\pi)^3} \left(\frac{1}{\overline{K}_\ell K_\ell + m^2} - v_m(0) \right)^2 = \int \frac{d^3k}{(2\pi)^3} \frac{1}{(\overline{K}_\ell K_\ell + m^2)^2} - v_m^2(0)$$

$$= -\frac{\partial}{\partial m^2} v_m(0) - v_m^2(0), \tag{13.63}$$

to be evaluated at $m^2 = m_A^2 = q^2/\overline{T}_V = 4\pi^2\beta_V\bar{\beta}_V$. For small $\overline{T}_V$, m^2 becomes large and the evaluation can proceed via the hopping series,

$$v_m(0) = \int \frac{d^3k}{(2\pi)^3} \frac{1}{\overline{K}_\ell K_\ell + m^2} = \int \frac{d^3k}{(2\pi)^3} \frac{1}{2D + m^2 - 2\sum_i \cos k_i}$$

$$= \sum_{n=0}^{\infty} \frac{1}{(2D + m^2)^{n+1}} H_n,$$

$$-\frac{\partial}{\partial m^2} v_m(0) = \sum_{n=0}^{\infty} \frac{(n+1)}{(2D + m^2)^{n+2}} H_n, \tag{13.64}$$

with H_n given in Part I, Eq. (6.126) and Table 6.2. It follows that

$$\alpha_4 = \frac{1}{(2D + m^2)^2} \left[\sum_{n=0}^{\infty} \frac{(n+1)H_n}{(2D + m^2)^n} - \left(\sum_{n=0}^{\infty} \frac{H_n}{(2D + m^2)^n} \right)^2 \right]$$

$$= \frac{1}{(2D + m^2)^2} \sum_{n=2}^{\infty} \frac{(n+1)H_n - H_n'}{(2D + m^2)^n}, \tag{13.65}$$

where the coefficients H_n' satisfy

$$H_0' = 1, \qquad H_n' = \frac{1}{n} \sum_{k=2,4,\ldots}^{n} (3k - n) H_k H_{n-k}', \tag{13.66}$$

i.e., for $D = 3$:

$$H_2' = 12, \qquad H_4' = 216, \qquad H_6' = 4800, \ldots \tag{13.67}$$

The leading behavior is given by

$$\alpha_4 \sim \frac{1}{(6 + m^2)^4}\left(6 + 234\frac{1}{(6 + m^2)^2} + 8220\frac{1}{(6 + m^2)^4} + \dots\right)$$

$$\alpha_4 = 6\frac{\bar{T}_V^4}{q^8} + 90\frac{\bar{T}_V^6}{q^{10}} + 3252\frac{\bar{T}_V^8}{q^{12}} + \dots \tag{13.68}$$

For small fields $\mu^2 \sim (4\pi^2 \bar{\beta}_V/4D)|\psi|^2$, so that the correction (13.62) has the effect of reducing the quartic term of the disorder field theory from $(1/64)|\psi|^4$ to

$$\left[\frac{1}{64} - \frac{\alpha_4}{2}\left(\frac{4\pi^2\bar{\beta}_V}{4D}\right)^2\right]|\psi|^4 \sim \left[\frac{1}{64} - 3\left(\frac{4\pi^2}{12q^4}\right)^2\bar{T}_V^2\right]|\psi|^4$$

$$\xrightarrow[q^2 \to 4\pi^2/3]{} \frac{1}{64}\left[1 - \frac{27}{4\pi^4}\bar{T}_V^2\right]|\psi|^4 \tag{13.69}$$

Notice once more the important difference between the one-loop correction (13.51) and that of the Ginzburg-Landau theory in (3.104). There we arrived at an integral

$$\int \frac{d^3k}{(2\pi)^3}\log(k^2 + q^2|\psi|^2). \tag{13.70}$$

For $|\psi| \sim 0$, the logarithm was singular so that the result could not be given as a power series in $|\psi|^2$. The cubic term

$$-\frac{1}{6\pi}q^3(|\psi|^2)^{3/2}$$

shows this fact explicitly. This is why the result depended crucially on the constancy of the $|\psi|$ field. In the present case, this is no longer true. Instead of (13.70) we now have a fluctuation integral

$$\int \frac{d^3k}{(2\pi)^3}\log\left(1 + \left(\frac{1}{\mathbf{K} \cdot \mathbf{K} + m^2} - v_m(0)\right)\mu^2\right). \tag{13.71}$$

As long as $m^2 \neq 0$ this does have a well-behaved power series in μ^2. In contrast to (13.70), the calculated fluctuation correction is therefore more reliable.

13.6. TRICRITICAL POINT IN A SUPERCONDUCTOR

In Section 3.11 we discussed fluctuation corrections to the Ginzburg-Landau theory. In particular, we showed that the "blackbody" energy of the gauge-field fluctuations

$$-\beta \Delta f = -\int \frac{d^3k}{(2\pi)^3} \log(\mathbf{k}^2 + q^2|\varphi|^2) \tag{13.72}$$

generates a cubic term in the order parameter

$$-\frac{1}{6\pi} q^3|\varphi|^3, \tag{13.73}$$

suggesting that the transition is of first order. In order to evaluate the integral in (13.72) it was necessary to assume that the size of the order parameter $|\varphi|$ is approximately constant. This could be justified as long as the parameter κ, which distinguishes type-I and type-II superconductors, is very far below $1/\sqrt{2}$ (deep type I). As κ moves towards the type-II regime, the fluctuations of $|\varphi|$ increase due to the formation of vortex lines and correspondence with experiments disappears at some point κ_t, the transition will become continuous. This is a tricritical point and we now set out to determine it approximately. Since it is the vortex lines which invalidate the assumption $|\varphi| \approx$ const., we expect a disorder field theory of vortex lines to provide for the simplest estimate of κ_t.

The starting point is the lattice superconductor (13.1) which is equivalent to a Ginzburg-Landau theory (3.95) with a charge

$$q = 2\pi\sqrt{\beta_V}. \tag{13.74}$$

At the mean field level, the Ginzburg-Landau theory is given by (13.43). In order to establish the connection with the Ginzburg-Landau partition function (3.95) we have to renormalize the gradient term to the form

$$\tfrac{1}{2}|D_i\varphi|^2,$$

which amounts to replacing $|\varphi|^2$ by $4D|\varphi|^2$. This brings the quartic coupling to $(g/4)|\varphi|^4$ with

$$g = D^2. \tag{13.75}$$

The parameter κ is given by [see (13.46)]

$$\kappa = \sqrt{\frac{g}{q^2}} = \frac{D}{q}.$$

(13.76)

In three dimensions, the quartic coupling is $g = 9$ and hence extremely large, much larger than it would be in any physical superconductor. The charge, on the other hand, can be varied from $q^2 = 4\pi^2/3 = 13.159$ to zero depending on the place on the critical curve in the q^2, $\widetilde{T}_V$ plane. We noticed in the last section that along this curve, the parameter κ varies from

$$\kappa = \frac{D}{\sqrt{4\pi^2/D}} \approx 0.827 \approx 1.17/\sqrt{2},$$

(13.77)

to infinity so that at the mean field approximation level, the lattice superconductor is always of type II.

Using the result of the last section we can now convince ourselves that for small $\widetilde{T}_V$, the transition is always of second order. For $\widetilde{T}_V = 0$ this is obvious since the $\bar{A}_i$ fields are completely frozen and the disorder theory becomes a pure XY model [see (13.37)]. For $\widetilde{T}_V \neq 0$, but small, we saw in Eq. (13.69) that the fluctuation corrections weaken the quartic term by a very small amount. As long as $\widetilde{T}_V \lesssim 1$, say, this term is comfortably positive and the transition is that of a $|\psi|^4$ theory which is of second order.

Hence we conclude that a superconductor with large charge $q^2 = 4\pi\beta_V \lesssim 13.159$, large $g \sim 9$, and $\kappa \gtrsim 1.18/\sqrt{2}$ always undergoes a *second order* transition. In this regime, the fluctuation corrections (13.72) to the Ginzburg-Landau theory as derived in Section 3.11 is unreliable due to vortex fluctuations. Physical superconductors have *small* charges and *small* quartic couplings. It is therefore desirable to extend the result into that regime. One extention is rather straightforward, namely, toward smaller quartic coupling g. This goes as follows.

Consider the mass term of the Ginzburg-Landau version (13.8b) of the lattice superconductor,

$$\frac{1}{4}\left(\frac{1}{\bar{\beta}'D} - 1\right)|\varphi|^2.$$

(13.78)

For small $\widetilde{T}$, $\bar{\beta}'$ and $\bar{\beta}'_V$ become equal and (13.6) leads to

$$\frac{1}{4D}(\tilde{T}_V + q^2 v(\mathbf{0}) - D)|\varphi|^2. \tag{13.79}$$

This suggests a simple way of generating a smaller quartic coupling. We simply consider the temperature variable $\tilde{T}_V$ not as a constant but as a space dependent fluctuating field variable $\tilde{t}(\mathbf{x})$, which fluctuates in a Gaussian way around the true temperature $\tilde{T}_V$. This implies that the partition function (13.8a) receives a "smearing" factor

$$\prod_{\mathbf{x}} \left[\int \frac{d\tilde{t}(\mathbf{x})}{\sqrt{2\pi\Delta^2}} \right] e^{-(1/2\Delta^2)\Sigma_{\mathbf{x}}(\tilde{t}(\mathbf{x}) - \tilde{T}_V)^2}, \tag{13.80}$$

where Δ is some width parameter. Applying this to the mass term (13.79) in the exponential gives

$$\prod_{\mathbf{x}} \left[\int \frac{d\tilde{t}_V(\mathbf{x})}{\sqrt{2\pi\Delta^2}} \right] e^{-(1/2\Delta^2)\Sigma_{\mathbf{x}}(\tilde{t}_V(\mathbf{x}) - \tilde{T}_V)^2} e^{(1/4D)\Sigma_{\mathbf{x}}(\tilde{t}(\mathbf{x}) + q^2 v(\mathbf{0}) - D)|\varphi|^2}$$

$$= e^{\Sigma_{\mathbf{x}}[(1/4D)(\tilde{T}_V + q^2 v(\mathbf{0}) - D)|\varphi|^2 + (1/2)(\Delta^2/16D^2)|\varphi|^4]}. \tag{13.81}$$

The additional term *reduces* the original quartic coupling from $(1/64)|\varphi|^2$ to

$$\frac{1}{64}\left(1 - \frac{2\Delta^2}{D^2}\right)|\varphi|^4. \tag{13.82}$$

Thus, by increasing the width of the $\tilde{t}(\mathbf{x})$ fluctuations to $\Delta = 2.12$, the quartic coupling can be reduced down to zero (for $D = 3$). This happens at fixed q^2. Since $\kappa = \sqrt{g/q^2}$, this implies that the resulting superconductor can be carried deep into the type-I regime. This result is only little changed by fluctuation corrections since, as we saw in the last section, the one-loop result left only a 13% discrepancy at the critical point $q_c^2 = 4\pi^2/3$, $\tilde{T}_{Vc} = 0$.

In order to study what happens to the order of the phase transition let us now do the same operation on the disorder theory. Its mass term was [see (13.30)]

$$\frac{1}{4}\left(\frac{1}{\beta'D} - 1\right)|\psi|^2. \tag{13.83}$$

Remember that β' was given by its Villain version [see (13.26)]

$$\beta'_V = [4\pi^2 \bar{\beta}_V v_{m_{\tilde{A}}}(0)]^{-1}, \tag{13.84}$$

where

$$v_{m_{\tilde{A}}}(0) = \int \frac{d^3k}{(2\pi)^3} \frac{1}{\bar{K}_\ell K_\ell + q^2 \bar{\beta}_V} \tag{13.85}$$

was the Yukawa potential on the lattice at the origin. For small T_V, $q^2 \sim q_c^2$ and $1/\beta'_V D$ can be expanded as follows:

$$\frac{1}{\beta'_V D} = \frac{4\pi^2}{q^2 D}\left(1 - \frac{\bar{T}_V}{q^2}\int \frac{d^3k}{(2\pi)^3} K_\ell \bar{K}_\ell + \ldots \right)$$

$$= \frac{4\pi^2}{q^2 D}\left(1 - 6\frac{\bar{T}_V}{q^2} + \ldots \right) \sim \left[1 - \frac{1}{q_c^2}(\delta q^2 + 6\bar{T}_V) + \ldots \right]. \tag{13.86}$$

At $\bar{T}_V = 0$, the phase transition is that of an XY model and takes place at $\beta'_c D \sim 1$. Corrections due to $|\psi|$ fluctuations change this point to $\beta'_c \sim 0.45$ or

$$\beta'_c D \sim 1.35. \tag{13.87}$$

We can roughly account for this effect by replacing the mass term (13.84) by

$$\approx \frac{1}{4}\left(\frac{1}{\beta' D} - \frac{1}{\beta'_c D}\right)|\psi|^2. \tag{13.88}$$

We are now ready to apply the temperature-smearing operation (13.80) to the disorder theory. In the neighborhood of the transition point we expand (13.88) as,

$$\approx \frac{1}{4}\left[\frac{1}{(\beta'_c + \delta\beta')D} - \frac{1}{\beta'_c D}\right]|\psi|^2 \sim \frac{1}{4}\left[\frac{1}{\beta'_c D}\left(1 - \frac{\delta\beta'}{\beta'_c}\right) - 1\right]|\psi|^2$$

$$\sim -\frac{1}{4\beta'_c D}\frac{\delta\beta'}{\beta'_c}|\psi|^2. \tag{13.89}$$

From (13.86) we know that

$$\frac{\delta \beta_V'}{\beta_{V_c}'} = \frac{1}{q_c^2}(\delta q^2 + 6\widetilde{T}_V).$$ (13.90)

Using the Villain relation $\beta_V'^{-1} = -2\log(I_1(\beta')/I_0(\beta'))$ we find

$$\frac{\beta'}{\beta_V'}\frac{d\beta_V'}{d\beta'} \equiv r = 2\beta_V'\beta'\,[2\sinh(1/2\beta_V) - 1/\beta'].$$ (13.91)

For $T_V' \sim 3$, $T' \sim 2.2$, we calculate the right-hand side (or consult Fig. 4.1 and read off the slope)

$$\frac{d\beta_V'}{d\beta'} \sim 0.46,$$ (13.92)

so that, $r \sim 0.63$ and hence

$$\frac{\delta \beta'}{\beta_c'} = \frac{\delta \beta_V'}{\beta_{V_c}'}\frac{1}{0.63}.$$ (13.93)

Therefore we can rewrite the mass term (13.78) in the neighborhood of the critical point $q_c^2 = 4\pi^2/3$, $\widetilde{T}_{V_c} = 0$ as

$$\frac{1}{4\beta_c' D}\frac{1}{0.63}\frac{1}{q_c^2}(\delta q^2 + 6\widetilde{T}_V)|\psi|^2.$$ (13.94)

This mass term is to be compared with the fluctuation corrected mass term (13.79) of the Ginzburg-Landau theory. Observe an important difference: while the Ginzburg-Landau theory had a $\widetilde{T}_V$ dependence given by

$$\frac{1}{12}\widetilde{T}_V|\varphi|^2,$$ (13.95)

the disorder version has the stronger $\widetilde{T}_V$ dependence,

$$0.134\,\widetilde{T}_V|\psi|^2 \sim \frac{1.6}{12}\widetilde{T}_V|\psi|^2.$$ (13.96)

Thus, when subjected to the same temperature smearing as the Ginzburg-Landau theory in (13.81), it generates a quartic term which is larger by a factor $(1.6)^2 \approx 2.5$. Hence, while the quartic term in the Ginzburg-Landau theory was reduced to (13.82),

$$\frac{1}{64}\left(1 - \frac{2}{9}\Delta^2\right)|\psi|^4,$$

(13.97)

that of the disorder field is reduced to

$$\approx \frac{1}{64}\left(1 - 2.5\frac{2}{9}\Delta^2\right)|\psi|^4.$$

(13.98)

At

$$\Delta \approx \sqrt{9/5},$$

(13.99)

the quartic term of the disorder theory vanishes. We now recall that in the disorder theory, the $\overline{A}_i$ field had been integrated out. The theory has therefore become a pure $\psi(\mathbf{x})$ field theory. In such a theory, the point of vanishing quartic coupling is well known to be a tricritical point. Beyond this point, the phase transition becomes first order. Since this theory is the dual equivalent of the Ginzburg-Landau theory we conclude that the order of the Ginzburg-Landau theory also changes from second to first.

What is its quartic coupling at this point? Inserting (13.97) into (13.99) we see that the quartic coupling is reduced to

$$\sim \frac{3}{5 \cdot 64}|\psi|^4.$$

(13.100)

The charge at the transition is still $q^2 = q_c^2 = 4\pi^2/3 = 13.159$. This implies that the value κ which characterizes the type of the superconductor, $\kappa = \sqrt{g/q^2}$, is reduced, at the tricritical point, by a factor $\sqrt{3/5} = 0.77$ with respect to the pure XY model's value (13.40), (13.41). Hence

$$\kappa_t \sim 0.9/\sqrt{2}.$$

(13.101)

This value lies just within the type-I regime. Considering the crudeness of our approximations it is possible that the tricritical point coincides with

the separation point $\kappa = 1/\sqrt{2}$ between type-I and type-II supercon-
ductivity. Unfortunately, this result is not yet applicable to actual super-
conductors. Although there are many superconductors with this value of
κ, none of them has a charge as large as that of the present model,
$q^2 \sim 13.16$. It will therefore be important to extend the present discussion
into the region of small q which amounts to large $\tilde{T}_V \lesssim 3$. This has not yet
been done since for large $\tilde{T}_V$, the $\bar{A}_i$ fluctuations acquire a longer and
longer range and the corrections to the disorder field theory are less
reliable.

Shortly after these estimates became available,[b] Monte Carlo
simulations were performed which confirmed the existence of a tricritical
point for small values of u. On the basis of these results the question was
raised whether there exist tricritical points in four dimensions. This has
triggered a large number of Monte Carlo investigations most of which
find evidence for such a point (see the Notes & References in Chapter 3).

NOTES AND REFERENCES

The phase diagram of the lattice superconductor via the disorder field theory of its vortex
lines was first studied by
H. Kleinert, *Lett. Nuovo Cimento* **35** (1982) 405.
This led to the prediction of a tricritical point. Such a tricritical point was confirmed in
Monte Carlo simulations by
J. Bartholomew, *Phys. Rev.* **B28** (1983) 5378
and later by
Y. Muneshisa, *Phys. Lett.* **155B** (1985) 159.
In the related transition smectic-nematic liquid crystal it was found experimentally by
J. Thoen, M. Maynissen and W. Van Dael, *Phys. Rev. Lett.* **52** (1984) 204.
The Monte Carlo points in Fig. 13.1 were obtained by
C. Dasgupta and B. Halperin, *Phys. Rev. Lett.* **47** (1981) 1556.
The possibility of a tricritical point in four dimensions was proposed by
H. Kleinert, *Phys. Lett.* **B128** (1983) 69, *Phys. Rev. Lett.* **56** (1986) 1441.
See also the Notes & References of Chapter 3.

[b]See H. Kleinert, referred to in the Notes and References.

INDEX